British Journal of Pharmacology

April 1995

Volume 114 Number 8 pages 1523–1750

Dr S J Coker
Department of Pharmacology
University of Liverpool
P.O. Box 147
LIVERPOOL L69 3BX

British Journal of Pharmacology (1995) 114, 1523-1524 © 1995 Stockton Press All rights reserved 0007-1188/95 $12.00

SPECIAL REPORT

Interaction of clozapine with the histamine H_3 receptor in rat brain

*,†,[1]A. Alves Rodrigues, †F.P. Jansen, †R. Leurs, [2],†H. Timmerman & *G.D. Prell

*Department of Pharmacology, Mount Sinai School of Medicine of the City University of New York, New York, N.Y. 10029, U.S.A. and †Leiden/Amsterdam Center for Drug Research, Department of Pharmacochemistry, Faculty of Chemistry, Vrije Universiteit, De Boelelaan 1083, 1081 HV Amsterdam, The Netherlands

We examined possible interactions between neuroleptics and the histamine H_3 receptor and found an interaction of clozapine with this receptor. In competition binding experiments, using the H_3 antagonist, [^{125}I]-iodophenpropit, we observed a K_i of 236 ± 87 nM. Functionally, clozapine was studied on the H_3-mediated inhibition of [^{3}H]-5-hydroxytryptamine ([^{3}H]-5-HT) release from rat brain cortex slices. Clozapine acts as an antagonist with an apparent K_B value of 79.5 nM.

Keywords: Histamine H_3 receptor; clozapine; neuroleptic; rat brain slices; [^{125}I]-iodophenpropit; [^{3}H]-5-HT release

Introduction Recent studies suggest that histamine may be involved in schizophrenia. In treatment-resistant patients, the mean level of *tele*-methylhistamine (t-MH) in cerebrospinal fluid, an index of histaminergic activity, was 2.6 fold higher than in controls (Prell *et al.*, 1995). Cerebrospinal fluid levels of t-MH correlated positively with those of other neurotransmitters metabolites, and with severity of schizophrenic symptoms (Prell *et al.*, 1995). Consonant with increased histaminergic activity are a reduction in densities of H_1 receptors in *postmortem* frontal cortex (Nakai *et al.*, 1991) and the reported therapeutic actions of famotidine, an H_2 antagonist in schizophrenic patients (Kaminski *et al.*, 1990; Deutsch *et al.*, 1993). Evidence for elevated histaminergic activity suggests possible functional anomalies in H_3 receptors. H_3 autoreceptors regulate release of histamine as well as other neurotransmitters (H_3 heteroreceptors), that may be involved in schizophrenia (e.g. 5-hydroxytryptamine (5-HT) and dopamine) (Fink *et al.*, 1990). Therefore, we examined the effects of neuroleptics on H_3 receptors, giving particular attention to clozapine.

Methods *Binding assays* Competition binding experiments were performed according to the method fully described by Jansen *et al.* (1994).

Functional assays (Based on Van der Werf *et al.*, 1987). [^{3}H]-5-hydroxytryptamine (5 μCi, 11 Ci mmol^{-1}) in 2 ml Krebs Ringer buffer was used to preload the rat neocortex slices. Loaded slices were perfused at 0.3 ml min^{-1}. Six 10 min fractions were collected, tritium overflow was evoked by electrical stimulation (rectangular pulses, 30 mA and 2 ms, 1 Hz) during the second fraction. Lastly, the slices were perfused with 0.1 N HCl to extract the remaining tritium in the tissue.

Results *Binding studies* Displacement of 0.25 nM [^{125}I]-iodophenpropit binding by clozapine (Figure 1a) fitted best to a one site model ($P<0.05$) using the non-linear curve fitting programme LIGAND, resulting in a K_i value of 236 ± 87 nM ($n = 6$, mean ± s.e.mean). Fitting data to a sigmoidal curve yielded a slope equal to 0.80 ± 0.05. Other neuroleptics studied showed relatively low affinity for [^{125}I]-iodophenpropit binding (Table 1).

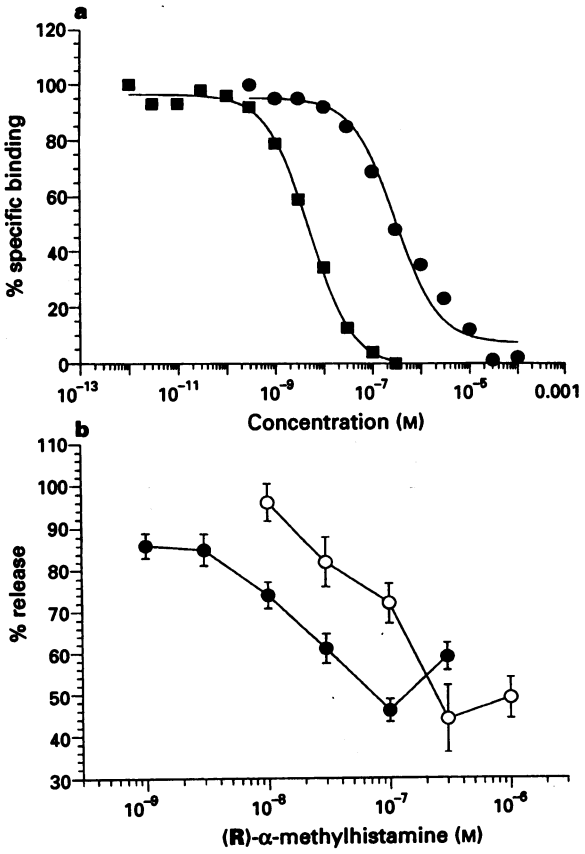

Figure 1 (a) Inhibition of [^{125}I]-iodophenpropit binding (0.25 nM) by the H_3 receptor antagonist, thioperamide (■) and clozapine (●). Data are expressed as % specific binding, determined using 0.3 μM thioperamide and represented 55%-65% of the total binding. The curves show one site fittings of a single representative experiment ($n = 6$) with triplicate determinations. (b) Inhibition by (R)-α-methylhistamine of the electrically stimulated [^{3}H]-5-HT release from rat neocortex slices in the absence (●) and presence (○) of 1 μM clozapine. Each point represents mean ± s.e.mean of three or four different experiments performed in duplicate. The EC_{50} values are determined from the mean values according to the equation $E = 100 - (100 - E_{max})/(1 + (EC_{50}/[A])$ where E represents the effect observed at any agonist concentration of [A], EC_{50} represents the agonist concentration that produces half-maximal effect, and E_{max} the maximal effect. The dissociation constant (K_B) was calculated from the equation $[A']/[A] = 1 + [B]/K_B$, where [A] is the concentration of the agonist that produces half-maximal effect, [A'] is the concentration of the agonist that produces half-maximal effect in the presence of the antagonist concentration [B].

[1] †is present address.
[2] Author for correspondence.

Table 1 Affinity of H_3 receptor agonists and antagonists and of several neuroleptics [RBI] for [^{125}I]-iodophenpropit binding sites to rat cortex compared with their functional potency (apparent values of K_B and K_i are shown, based on competitive antagonism)

Ligand	*Inhibition of [^{3}H]-5-HT release*	*[^{125}I]-iodophenpropit binding*
Histamine	EC_{50} = 48.2 nM (3)	K_{iH} = 38 ± 10 nM (4)[a]
(R)-α-methylhistamine	EC_{50} = 6.0 nM (4)	K_{iH} = 3.5 ± 1.2 nM (4)[a]
Thioperamide	K_B = 1.1 nM (3)	K_i = 4.3 ± 1.6 nM (7)[a]
Impromidine	K_B = 19.5 nM (3)	K_i = 51 ± 9 nM (3)[a]
Clozapine	K_B = 79.5 nM (4)	K_i = 236 ± 87 (6)
Chlorpromazine	ND	IC_{50} > 10 μM (2)
Haloperidol	ND	IC_{50} > 10 μM (2)
Spiperone	ND	IC_{50} > 10 μM (2)

For the binding studies data shown are mean ± s.e.mean. The values in parentheses represent the number of independent experiments. Functional data represent the value obtained from the fitting of mean data (3–4 experiments) as described in detail in the legend of Figure 1b.
ND: Not determined. [a]Jansen *et al.*, 1994.

Functional studies The electrically evoked tritium overflow was inhibited in a concentration-dependent manner by histamine and the H_3 agonist, (R)-α-methylhistamine (Table 1, Figure 1b). H_3-antagonists inhibited the (R)-α-methylhistamine effect with potencies comparable to their affinity for the [^{125}I]-iodophenpropit binding sites (Table 1). Clozapine (1 μM) shifted the (R)-α-methylhistamine concentration-response curve to the right (Figure 1b) yielding an apparent K_B value of 79.5 nM. Clozapine, itself, did not affect the stimulated (104 ± 1%; n = 3, mean ± s.e.mean) or the basal release of [^{3}H]-5-HT (100 ± 2%; n = 3, mean ± s.e.mean).

Discussion Clozapine, an atypical neuroleptic, has therapeutic efficacy in the treatment of drug-resistant schizophrenia (Baldessarini & Frankenburg, 1991). High affinity interactions of clozapine with 5-hydroxytryptamine 5-HT_2 and 5-HT_3 receptors, α_1- and α_2-adrenoceptors, histamine H_1, dopamine D_1 and D_4, and muscarinic receptors have been reported (Baldessarini & Frankenburg, 1991). Yet, in comparison to the typical neuroleptics, clozapine shows lower *in vitro* affinity for striatal dopamine D_2 receptors.

In the present work, we observed an intriguing interaction of clozapine with the histamine H_3 receptor, where clozapine acts as an H_3 antagonist. Other neuroleptics showed low affinity for the H_3 receptor.

The interaction of the non-imidazole compound, clozapine with the H_3 receptor is striking, since the imidazole moiety was thought to be required for high affinity H_3 binding.

In man, plasma concentrations of clozapine associated with clinical responses are approximately 0.6–1.2 μM (Baldessarini & Frankenburg, 1991). In rat, with doses higher than 5 mg kg^{-1} and within the therapeutic range in man, clozapine levels in the brain averaged 29 fold higher than corresponding serum drug levels (Balderassini *et al.*, 1993). Assuming total serum levels of 0.9 μM and 95% protein bound, total brain levels of 1.1 μM can be obtained. If the K_i value for clozapine at the rat H_3 receptor is similar for its human counterpart, brain clozapine concentrations might be high enough for a functional interaction with the H_3 receptor under clinical conditions. In conclusion: clozapine, showed a higher affinity for the histamine H_3 receptor than several other neuroleptics. Functionally, it revealed an antagonistic behaviour.

References

BALDESSARINI, R.J. & FRANKENBURG, F.R. (1991). Clozapine-A novel antipsychotic agent. *N. Engl. J. Med.*, **324**, 746–754.

BALDESSARINI, R.J., CENTORRINO, F., FLOOD, J.G., VOLPICELLI, S.A., HOUSTON-LYONS, D. & COHEN, B.M. (1993). Tissue concentrations of clozapine and its metabolites in the rat. *Neuropsychopharmacol.*, **9**, 117–124.

DEUTSCH, S.I., ROSSE, R.B., KENDRICK, K., FAY-McCARTHY, M., COLLINS, J.P. & WYATT, R.J. (1993). Famotidine adjunctive pharmacotherapy of schizophrenia: Preliminary data. *Clin. Neuropharmacol.*, **6**, 518–524.

FINK, K., SCHLICKER, E., NEISE, A. & GOTHERT. (1990). Involvement of presynaptic H3 receptors in the inhibitory effect of histamine on serotonin release in the rat brain cortex. *Naunyn-Schmied. Arch. Pharmacol.*, **342**, 513–519.

JANSEN, F.P., WU, T.S., VOSS, H.P., STEINBUSCH, H.W.M., VOLLINGA, R.C., RADEMAKER, B., BAST, A., & TIMMERMAN, H. (1994). Characterization of the binding of the first selective radiolabelled histamine H_3-receptor antagonist, [^{125}I]-iodophenpropit, to rat brain. *Br. J. Pharmacol.*, **113**, 355–362.

KAMINSKI, R., MORIARTY, T.M., BODINE, J. & DAVIDSON, M. (1990). Effect of famotidine on deficit symptoms of schizophrenia. *Lancet*, **335**, 1351–1352.

NAKAI, T., KITAMURA, N., HASHIMOTO, T., KAJIMOTO, Y., NISHINO, N., MITA, T. & TAKANA, C. (1991). Decreased histamine H_1 receptors in the frontal cortex of brains from patients with chronic schizophrenia. *Biol. Psychiat.*, **30**, 349–356.

PRELL, G.D., GREEN, J.P., KAUFMANN, C.A., KHANDELWAL, J.K., MORRISHOW, A.M., KIRCH, D.G., LINNOILA, M. & WYATT, R.J. (1995). Histamine metabolites in cerebrospinal fluid of patients with chronic schizophrenia: their relationships to levels of other aminergic transmitters and ratings of symptoms. *Schiz. Res.*, **14**, 93–104.

VAN DER WERF, J.F., BAST, A., BIJLOO, G.J., VAN DER VLIET, A. & TIMMERMAN, H. (1987). HA autoreceptor assay with superfused slices of rat brain cortex and electrical stimulation. *Eur. J. Pharmacol.*, **138**, 199–206.

(Received January 12, 1995
Accepted January 20, 1995)

British Journal of Pharmacology (1995) 114, 1525–1527 © 1995 Stockton Press All rights reserved 0007–1188/95 $12.00

SPECIAL REPORT

Functional evidence for a 5-HT_{2B} receptor mediating contraction of longitudinal muscle in human small intestine

[1]R.A. Borman & D.E. Burleigh

Department of Pharmacology, Queen Mary and Westfield College, Mile End Road, London E1 4NS

Application of 5-hydroxytryptamine induces contraction of longitudinal muscle strips from human terminal ileum. The response was resistant to antagonism by ketanserin, ondansetron or DAU6285, but was non-surmountably antagonized by methysergide. The selective 5-$HT_{2B/2C}$ receptor antagonist, SB 200646A evoked a concentration-dependent, parallel and dextral displacement of the concentration-response curve to 5-HT, yielding a pA_2 estimate of 7.17. Application of yohimbine, a 5-HT_1 and 5-HT_{2B} receptor antagonist, also induced a rightward shift of the response curve to 5-HT, yielding a pA_2 estimate of 8.10. In conclusion, it appears that a 5-HT_{2B} receptor mediates the contractile response of the longitudinal muscle of human small intestine to 5-HT.

Keywords: Human ileum; longitudinal muscle; contraction; 5-HT_{2B} receptor; SB 200646A; yohimbine

Introduction Physiological and pharmacological studies have indicated that 5-hydroxytryptamine (5-HT) may possess a pivotal role in mediating sensory and reflex responses in the gastrointestinal tract of various species, including man. It has been shown to induce secretory processes in the small and large intestine (Borman & Burleigh, 1993; 1994a), and to influence motility in the human colon (Borman & Burleigh, 1994a). Due to the lack of selective antagonists, previous studies in human small intestine have failed to characterize fully the receptors responsible for the contractile effects of 5-HT (Baxter *et al.*, 1991; Borman & Burleigh, 1994b). In the present study, we have used selective antagonists to classify the receptor responsible for 5-HT-induced contraction in the longitudinal muscle layer of human small intestine.

A preliminary report of these findings was presented to the Autumn 1994 meeting of the British Pharmacological Society in Sunderland.

Methods Human terminal ileum (within 30 cm of the ileocaecal junction) was obtained from specimens of human intestine removed at operation for carcinoma or Crohn's disease. Tissue removed from specimens with Crohn's disease was judged to be macroscopically normal by a Consultant Histopathologist. Tissue was transported in Dulbecco's Modified Eagle's Medium (DMEM; with 3.70 g l^{-1} sodium bicarbonate and 25 mM HEPES buffer, without glutamine) plus Ham's F12 Medium (with 1.24 g l^{-1} phenol red and 1.176 g l^{-1} sodium bicarbonate, without glutamine, 1:1 with DMEM) with 10% foetal bovine serum added, and placed in gassed Krebs solution within 60 min of removal from the patient. Some tissue was stored overnight in Krebs solution at 4°C before use. This treatment did not significantly alter responses to applied agonists.

After removal of mucosa and submucosa by sharp dissection, strips of longitudinal muscle (1.5–2.5 × 15 mm) were prepared from the muscularis externa, and were suspended under isotonic conditions and a preload of 1 g, in gassed (5% CO_2 in oxygen) Krebs solution at 37°C. After 60 min equilibration, 5-HT was applied to the tissue in a cumulative manner, with a 3 min contact time for each concentration. After a further 60 min, the challenge to 5-HT was repeated in the absence (control) or presence of antagonist (incubated for 30 min). The response to 5-HT was expressed as a % of the maximum contraction induced by a supramaximal concentration of acetylcholine (30 μM), applied at the end of each experiment. EC_{50} values for 5-HT were determined graphically from individual concentration-response curves. Concentration-ratios were calculated as the ratio of EC_{50} values between two successive response curves in the same preparation and expressed as geometric mean with 95% confidence limits (95% CL). All other data are given as arithmetic mean ± s.e.mean. Statistical comparisons used the Mann-Whitney U-test, with $P<0.05$ being taken to represent a significant difference.

Compounds used were 5-hydroxytryptamine creatinine sulphate (Sigma), acetylcholine chloride (Sigma), ondansetron hydrochloride (GR38032F, Glaxo), methysergide hydrogen maleate (Sandoz), yohimbine hydrochloride (Sigma), ketanserin tartrate (Janssen) and DAU6285 (1H-benzimidazole-1-carboxylic acid,2,3-dihydro-6-methoxy-2-oxo-8-methyl-8-azabicyclo (3,2,1) oct-3-yl ester chloridate, Boehringer Ingelheim Italia). DMEM, Ham's F12 Medium and foetal bovine serum were obtained from ICN Flow Laboratories, Cat. No. 12-331-54, 12-422-54 and 29-101-54 respectively. SB 200646A (N-(1-methyl-1*H*-indol-5-yl)-*N'*-(3-pyridyl) urea hydrochloride) was generously donated by SmithKline Beecham Pharmaceuticals. All these compounds were dissolved in distilled water and diluted in Krebs solution of the following composition (mM): NaCl 118, $NaHCO_3$ 25, KCl 4.7, $MgSO_4$ 1.2, KH_2PO_4 1.2, $CaCl_2$ 2.5 and glucose 11.5.

Results Cumulative application of 5-HT produced a contraction of longitudinal muscle strips of human terminal ileum. The maximum response to 5-HT was 41.4 ± 2.8% of the response to acetylcholine, with an EC_{50} for 5-HT of 34.9 nM (95% CL 26.3–46.2). The response to 5-HT showed desensitization on repetition of the challenge, with a significant dextral shift of the second control concentration-response curve, but with no alteration of the maximum response. This led to a concentration-ratio between successive control response curves of 2.3 (95% CL 1.5–3.7).

The contractile response to 5-HT was shown to be insensitive to antagonism by ketanserin (1 μM; 5-HT_{2A} receptor antagonist), ondansetron (1 μM; 5-HT_3 receptor antagonist) or DAU6285 (1 μM; 5-HT_4 receptor antagonist; Schiavone *et al.*, 1992) ($n \geq 4$ all treatments). The response was, however, antagonized in a non-surmountable manner by methysergide (10 pM to 1 nM; Figure 1a).

Application of SB 200646A (0.3 to 3 μM; a 5-$HT_{2B/2C}$ receptor antagonist; Baxter *et al.*, 1994) or yohimbine (30 to 300 nM; a 5-HT_1 and 5-HT_{2B} receptor antagonist) evoked

[1] Author for correspondence.

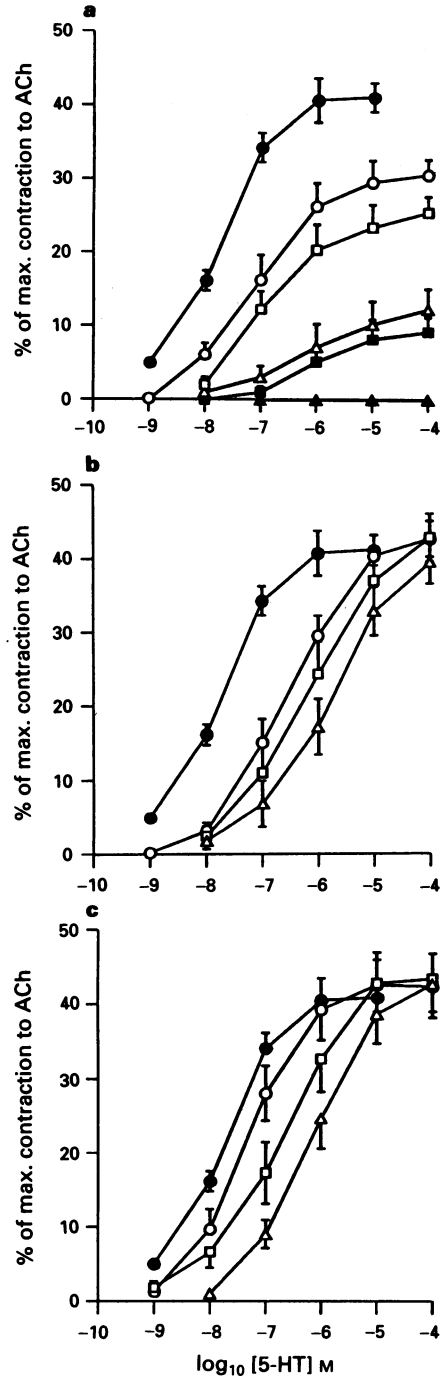

Figure 1 Effect of antagonists on the contractile response to 5-hydroxytryptamine (5-HT) of the longitudinal muscle of human small intestine. Results shown as % of maximum contraction to acetylcholine (ACh). Figure shows a second concentration-response curve to 5-HT in the absence (●) and presence of (a) methysergide at concentrations of 1pM (○), 10 pM (□), 100 pM (△), 1nM (■) and 10 nM (▲); (b) SB 200646A at concentrations of 0.3 μM (○), 1 μM (□) and 3 μM (△), and (c) yohimbine at concentrations of 30 nM (○), 100 nM (□) and 300 nM (△). Data are mean ± s.e.mean for $n \geqslant 6$ determinations

concentration-dependent dextral shifts of the second concentration-response curve to 5-HT, with no alteration of the maximum response (Figure 1b and 1c respectively). Schild analysis of the antagonism produced by SB 200646A yielded a Schild plot with a slope of 0.96 (95% CL 0.66–1.25) and an apparent pA_2 estimate of 7.17 ± 0.16. For yohimbine, Schild analysis produced a plot with a slope of 1.10 (95% CL 0.78–1.42) and a pA_2 estimate of 8.10 ± 0.06 (slope constrained to unity for both pA_2 estimates).

Discussion The 5-HT_{2B} receptor has been shown to mediate the contractile effect of 5-HT in the rat stomach fundus (Baxter *et al.*, 1994). The receptor mRNA transcript has subsequently been identified in the rat (Kursar *et al.*, 1992), mouse (Loric *et al.*, 1992) and more recently, in the human small intestine (Kursar *et al.*, 1994). The receptor has proved difficult to classify definitively due to the lack of selective antagonists, with few compounds able to differentiate clearly between receptor sub-types. The close similarity of the 5-HT_{2B} receptor with both the 5-HT_{2C} receptor, and the 5-HT_{1D} receptor (the two receptors share a comparable tryptamine fingerprint) has further complicated investigations. Of those compounds which do show some selectivity, yohimbine and rauwolscine have proved most useful in differentiating 5-HT_{2B} receptors from the closely related 5-HT_{2C} receptor. Both of these compounds, however, have been shown to have effects at other 5-HT receptor sub-types, as well as at other non-5-HT receptors. More recently, the discovery of a novel 5-$HT_{2B/2C}$ receptor antagonist, SB 200646A (Baxter *et al.*, 1994), has greatly facilitated the characterization of the 5-HT_{2B} receptor.

In the longitudinal muscle of human small intestine, both yohimbine and SB 200646A were shown to antagonize competitively the contractile response to 5-HT, with pA_2 estimates similar to those reported at the rat 5-HT_{2B} receptor (Baxter *et al.*, 1994). Although yohimbine is not uniquely selective for the 5-HT_{2B} receptor and has been shown to antagonize responses at 5-HT_1 receptors as well as α_2-adrenoceptors, the relative selectivity of SB 200646A for the 5-HT_{2B} receptor over these other subtypes ($pK_i < 5.0$; Kennett *et al.*, 1994), and the lack of effect of yohimbine at the 5-HT_{2C} receptor ($pK_i < 6.0$; Baxter *et al.*, 1994), provides firm evidence for the involvement of a 5-HT_{2B} receptor in the contractile response to 5-HT of human small intestinal longitudinal muscle. This confirms the results of Kursar *et al.* (1994), whose studies revealed 5-HT_{2B} receptor mRNA to be expressed in human small intestine, and provides the first functional evidence for a human 5-HT_{2B} receptor.

We would like to express our gratitude to the surgeons at several hospitals for their cooperation in providing tissue specimens; and in particular to Mr M Henry (Central Middlesex), Mr G Lord (Newham General), Mr J Rogers (Royal London) and Mr P Thomas (Whips Cross Hospital). We are also grateful to SmithKline Beecham Pharmaceuticals for their kind donation of SB 200646A, and to Dr G.S. Baxter for helpful discussions.

References

BAXTER, G.S., MURPHY, O.E. & BLACKBURN, T.P. (1994). Further characterization of 5-hydroxytryptamine receptors (putative 5-HT_{2B}) in rat stomach fundus longitudinal muscle. *Br. J. Pharmacol.*, **112**, 323–331.

BAXTER, G.S., PRITIKIN, J., YOUNG, H. & CLARKE, D.E. (1991). 5-HT receptors in human ileum and colon. *Br. J. Pharmacol.*, **102**, 163P.

BORMAN, R.A. & BURLEIGH, D.E. (1993). Evidence for the involvement of a 5-HT_4 receptor in the secretory response of human small intestine to 5-HT. *Br. J. Pharmacol.*, **110**, 927–928.

BORMAN, R.A. & BURLEIGH, D.E. (1994a). Heterogeneity of 5-HT receptors in human sigmoid colon. *Br. J. Pharmacol.*, **112**, 558P.

BORMAN, R.A. & BURLEIGH, D.E. (1994b). Comparison of 5-HT receptors mediating contraction of circular and longitudinal muscle in human small intestine. *Br. J. Pharmacol.*, **113**, 141P.

KENNETT, G.A., WOOD, M.D., GLEN, A., GREWAL, S., FORBES, I., GADRE, A. & BLACKBURN, T.P. (1994). *In vivo* properties of SB 200646A, a 5-$HT_{2C/2B}$ receptor antagonist. *Br. J. Pharmacol.*, **111**, 797–802.

KURSAR, J.D., NELSON, D.L., WAINSCOTT, D.B., COHEN, M.L. & BAEZ, M., (1992). Molecular cloning, functional expression, and pharmacological characterization of a novel serotonin receptor (5-hydroxytryptamine$_{2F}$) from rat stomach fundus. *Mol. Pharmacol.*, **42**, 549–557.

KURSAR, J.D., NELSON, D.L., WAINSCOTT, D.B. & BAEZ, M. (1994). Molecular cloning, functional expression, and mRNA tissue distribution of the human 5-hydroxytryptamine$_{2B}$ receptor. *Mol. Pharmacol.*, **46**, 227–234.

LORIC, S., LAUNAY, J.M., COLAS, J.F. & MAROTEAUX, L. (1992). New mouse 5-HT_2-like receptor, expression in brain, heart and intestine. *Fed. Eur. Biochem. Soc.*, **312**, 203–207.

SCHIAVONE, A., GIRALDO, E., GIUDICI, L., TURCONI, M. & SAGRADA, A. (1992). DAU 6285: a novel antagonist at the putative 5-HT_4 receptor. *Life Sci.*, **51**, 583–592.

(Received January 18, 1995
Accepted January 24, 1995)

British Journal of Pharmacology (1995) 114, 1529–1540 © 1995 Stockton Press All rights reserved 0007–1188/95 $12.00

Pharmacological evidence for the presence of three distinct functional endothelin receptor subtypes in the rabbit lateral saphenous vein

Stephen A. Douglas, George R. Beck, Jr., *John D. Elliott & [1]Eliot H. Ohlstein

Departments of Cardiovascular Pharmacology and *Medicinal Chemistry, SmithKline Beecham Pharmaceuticals, 709 Swedeland Road, P.O. Box 1539, King of Prussia, Pennsylvania 19406-0939, U.S.A.

1 Contraction of the rabbit isolated saphenous vein is mediated by a heterogeneous endothelin (ET) receptor population. This study has characterized these receptor subtypes by use of several pharmacologically distinct ET receptor agonists and antagonists.

2 ET-1, ET-3, sarafotoxin S6c (STXc) and [Ala^{3,11}]ET-1 produced biphasic, concentration-dependent contractions of the saphenous vein, responses which were best fitted by a two-site model comprised of a high (pM) and a low (nM) affinity site. In contrast, IRL 1620 only recognized one of these sites. $ET_{(16-21)}$ was devoid of contractile activity. ET-1, ET-3 and STXc were equipotent at the high affinity site (pD_2s of 12.0 ± 0.2, 12.2 ± 0.2 and 12.3 ± 0.3) indicating that this site had the characteristics of an ET_B receptor. In contrast, the low affinity site had the functional characteristics of an ET_C receptor since the pD_2s for ET-3 (10.2 ± 0.3) and STXc (10.6 ± 0.3) were significantly greater than that for ET-1 (9.1 ± 0.1). These contractile responses were insensitive to BQ-123, confirming that ET_A receptors were not involved in mediating this effect.

3 SB 209670 differentially antagonized the high affinity phases of the isopeptide concentration-response curves in a fashion dependent on the competing agonist: relative to the K_B obtained against STXc (0.15 nM). SB 209670 was 10 fold less potent when ET-1 was used as the competing agonist. This differential effect was not evident at the low affinity site (K_B = 38 nM). SB 209670 produced parallel, concentration-dependent rightward shifts in the concentration-response curve to STXc Ro 47-0203 was approximately 1 to 2 orders of magnitude less potent than SB 209670 at inhibiting the high affinity component of the concentration-response curve to STXc, whereas BQ-788 and Ro 46-2005 were approximately 3 orders of magnitude less potent than SB 209670. In addition to RES-701 and BQ-123, the high affinity site was insensitive to PD 142893 suggesting that it may represent an ET_{B2} receptor. Ro 47-0203 and SB 209670 were equipotent at inhibiting the low affinity component of the STXc concentration-response curve. Although Ro 46-2005, BQ-788, PD 142893 and RES-701 produced significant antagonism at the low affinity site, they were at least ten fold less potent than SB 209670.

4 ET-1, ET-3 and STXc produced endothelium-dependent vasorelaxation in the precontracted saphenous vein. Antagonist IC_{50}s were approximated as being: SB 209670, 3 nM; BQ-788 and RES 701, 300 nM; Ro 46-2005 and PD 142893, 3 μM; BQ-123, ⩾ 10 μM, consistent with vasorelaxation being mediated by an ET_{B1} receptor.

5 In summary, three pharmacologically distinct ET receptor subtypes have been identified in the rabbit saphenous vein. Two contractile receptors are present on the vascular smooth muscle, a high affinity site with the characteristics of an ET_{B2} receptor and a distinct lower affinity site with the characteristics of an ET_C receptor. In addition, an ET_{B1} receptor is present on the endothelium which mediates the vasodilator actions of this peptide family.

Keywords: Endothelin receptors; saphenous vein; SB 209670; Ro 47-0203; bosentan; Ro 46-2005; PD 142893; BQ-123; BQ-788; RES-701

Introduction

Two major subtypes of mammalian endothelin (ET) receptor have been cloned, the ET_A receptor, which exhibits selectivity for ET-1 over ET-3 and sarafotoxin S6c (STXc), and the ET_B receptor, which is non-isopeptide selective (Arai *et al.*, 1990; Sakurai *et al.*, 1990; Masaki *et al.*, 1994). Although a putative ET_C receptor (selective for ET-3 over ET-1) has been cloned from the dermal melanophores of *Xenopus laevis* (Karne *et al.*, 1993), a mammalian homologue has not been identified. Initial structure-activity studies suggested that the primary role of the ET_A receptor was to mediate smooth muscle contraction and that this response was modulated indirectly by ET_B receptor-mediated nitric oxide release (Warner *et al.*, 1989; Douglas & Hiley, 1990; 1991a; Emori *et al.*, 1990). Subsequently, however, ET_B receptors have also been shown to mediate vasoconstriction (Douglas & Hiley, 1991a,b; Bigaud & Pelton, 1992; Clozel *et al.*, 1992; Harrison *et al.*, 1992; Panek *et al.*, 1992; Sumner *et al.*, 1992; James *et al.*, 1993; Gardiner *et al.*, 1994; Godfraind, 1994a,b; Seo *et al.*, 1994; Teerlink *et al.*, 1994). It has now been proposed that multiple ET_B receptors exist within the mammalian cardiovascular system (Warner *et al.*, 1993a,b; Douglas *et al.*, 1994b; Ohlstein *et al.*, 1994a). Warner *et al.* (1993a,b) have described the presence of 'ET_{B1}' and 'ET_{B2}' receptors which are distinguished by their anatomical location (endothelium *versus* smooth muscle), function (vasodilatation *versus* vasoconstriction) and pharmacological profile (sensitivity to PD 142893).

ET_B receptor-mediated vasoconstriction is of particular importance in the control of vascular tone in low pressure conduit vessels (Moreland *et al.*, 1994) such as those found in the venous and pulmonary circulations. One such vessel, the saphenous vein, is extremely sensitive to the vasoconstrictor actions of the ET isopeptides, responses mediated by a

[1] Author for correspondence.

heterogeneous receptor population (Komori & Vanhoutte, 1989; Miller *et al.*, 1989; Berti *et al.*, 1990; Moreland *et al.*, 1992; Webb *et al.*, 1993; Gray *et al.*, 1994). Until recently it has only been possible to characterize this heterogeneous receptor population by use of agonists (Auguet *et al.*, 1993; Bax *et al.*, 1993; White *et al.*, 1994). However, several novel ET receptor antagonists have been described recently. In addition to the well characterized ET_A-selective antagonist, BQ-123 (Ihara *et al.*, 1991; Moreland, 1994) and the $ET_{A/B}$ antagonist PD 142893 (Doherty *et al.*, 1993), such antagonists include the nonpeptide $ET_{A/B}$ receptor antagonists SB 209670 (Ohlstein *et al.*, 1994b), Ro 47-0203 (bosentan) and Ro 46-2005 (Clozel *et al.*, 1993; 1994) and several peptidic ET_B-selective antagonists including BQ-788 and RES-701 (Ishikawa *et al.*, 1994; Tanaka *et al.*, 1994). Of these antagonists, SB 209670 is the most potent, exhibiting K_is at the human cloned ET_A and ET_B receptors of 0.4 and 18 nM (Nambi *et al.*, 1994b). The use of this antagonist in experimental disease models has identified a role for ET-1 in the aetiology of a variety of pathological processes including hypertension, renal failure, restenosis and cerebral vasospasm and neurodegeneration (Brooks *et al.*, 1994; Douglas *et al.*, 1994a,b, 1995; Ohlstein *et al.*, 1994a,b; Willette *et al.*, 1994). In the present study these ET receptor antagonists have been used to characterize the receptors responsible for mediating the constrictor and dilator actions of the ET isopeptides in the rabbit saphenous vein.

Methods

The lateral saphenous vein was excised from New Zealand White male rabbits (2–3 kg) following sodium pentobarbitone overdose (100 mg kg^{-1} via the central ear vein), cleaned of adherent tissue and cut into 4 mm rings. Rings were suspended under optimal resting tension (5 mN) in 10 ml organ baths (37 ± 1°C, aerated wtih 95% O_2/5% CO_2) containing Krebs-bicarbonate solution (mM): NaCl 112, KCl 4.7, KH_2PO_4 1.2, $MgSO_4$ 1.2, $CaCl_2$ 2.5, $NaHCO_3$ 25, dextrose 11 and indomethacin 0.01. Changes in isometric tension were recorded with Grass FTO3c force-displacement transducers linked to Beckman R-611 dynographs. Where appropriate, the endothelium was removed by rubbing the intimal surface of vessel with a stainless steel rod. Endothelium-intact and -denuded tissues were defined as those which, when exposed to acetylcholine (1 μM) in the presence of tone induced by noradrenaline (1 μM), responded with a relaxant response of either > 50% or < 10% relaxation, respectively. Tissues were allowed a 90 min equilibration period prior to any experimentation.

ET isopeptide-induced vasoconstriction in the rabbit isolated saphenous vein

Thirty min following the addition of vehicle, concentration-response curves to either ET-1, ET-3, STXc, [$Ala^{3,11}$]ET-1, IRL 1620 or $ET_{(16-21)}$ were constructed in the endothelium-intact tissues. Responses were expressed as a percentage of the contractile response elicited by 60 mM KCl determined at the beginning of each experiment. An individual ring preparation was used once to construct a single concentration-response curve. Concentration-response curves were analysed by fitting the experimental data to one of the following logistic equations by nonlinear least squares regression (Douglas *et al.*, 1994c):

$$\text{(i) One site fit } R = \frac{R_{max} \cdot C^n}{EC_{50}{}^n + C^n}$$

where R is the response, C the concentration of agonist, EC_{50} the concentration of agonist required to produce a half maximal response, n the Hill coefficient and R_{max} the maximal response or:

$$\text{(ii) Two site fit } R = \frac{R_{maxH} \cdot C^n{}_H}{EC_{50H}{}^n{}_H + C^n{}_H} + \frac{R_{maxL} \cdot C^n{}_L}{EC_{50H}{}^n{}_H + C^n{}_H}$$

where R is the response, C the concentration of agonist, EC_{50H} and EC_{50L} the concentration of agonist required to produce a half maximal response at a high and low affinity site, n_H and n_L the Hill coefficients at a high and low affinity site and R_{maxH} and R_{maxL} the maximal responses at a high and low affinity site, respectively.

The contractile actions of ET-1, ET-3 and STXc were also assessed in endothelium-denuded tissues in the presence either of vehicle, SB 209670 (1 μM) or BQ-123 (10 μM). In order to perform a more accurate determination of SB 209670 potency by Schild analysis, cumulative concentration-response curves were constructed to STXc either in the presence of vehicle or in the presence of increasing concentrations of SB 209670. So that the potency of a series of chemically and pharmacologically diverse ET receptor antagonists could be compared with SB 209670, cumulative concentration-response curves were also constructed to STXc in the presence of 10 μM Ro 46-2005, Ro 47-0203, PD 142893, BQ-788 or RES-701.

ET isopeptide-induced vasorelaxation in the rabbit isolated saphenous vein

Following a 90 min equilibration period, endothelium-intact saphenous vein rings were precontracted with 1 μM noradrenaline. Once a sustained contraction had been obtained, tissues were exposed to a single concentration of either ET-1, ET-3 or STXc in order to determine the degree of peptide-induced vasorelaxation (expressed as a percentage reversal of the induced tone).

In a separate series of experiments, tissues were precontracted with noradrenaline and exposed to 1 nM ET-3. Once the ensuing 'control' relaxant response had been recorded, the tissue was washed and subsequently incubated with either vehicle or SB 209670, BQ-788, Ro 46-2005, RES 701, PD 142893 or BQ-123 for 30 min period. Tissues were then recontracted with noradrenaline and exposed to a 'secondary' administration of ET-3. The degree of antagonist-induced inhibition was determined by comparing the degree of relaxation obtained to the 'control' and 'secondary' additions of 1 nM ET-3.

Materials

All solutions were made freshly each day and stored on ice in a light tight container. ET-1, ET-3, STXc, IRL 1620 (Namby *et al.*, 1994a) (Suc[Glu9;Ala11,15]-endothelin-1(8-21)) $ET_{(16-21)}$, [$Ala^{3,11}$]ET-1 and BQ-123 (cyclo(D-Trp-D-Asp-Pro-D-Val-Leu); Ihara *et al.*, 1991) were from American Peptide Co. (Santa Clara, CA, U.S.A.). SB 209670 (+)-(1S,2R,3S)-3-(2-carboxymethoxy-4-methoxyphenyl)-1-(3,4-methylenedioxyphenyl)-5-(prop-1-yloxy)indane-2-carboxylic acid; Ohlstein *et al.*, 1994b), PD 142893 (Ac-D-Dip-Leu-Asp-Ile-Ile-Trp; Doherty *et al.*, 1993), BQ-788 (N-*cis*-2,6-dimethylpiperidinocarbonyl-L-γ-MeLeu-D-Trp (1-CO_2Me) -D-Nle; Ishikawa *et al.*, 1994), Ro 46-2005 (4-tert-butyl-N-[6-(2-hydroxy)-ethoxy))-5-(3-methoxyphenoxy)pyrimidin-4-yl]-benzene sulphonamide) and Ro 47-0203 (4-tert-butyl-N-[6-(2-hydroxy)-ethoxy)-5-(2-methoxyphenoxy)-2,2′-bipyrimidin-4-yl]-benzene sulphonamide) (Clozel *et al.*, 1993; 1994) were synthesized in the Department of Medicinal Chemistry, SmithKline Beecham. RES-701 (Gly-Asn-Trp-His-Gly-Thr-Ala-Pro-Asp-Trp-Phe-Phe-Asn-Tyr-Tyr-Trp; Tanaka *et al.*, 1994) was the generous gift of Kyowa Hakko Kogyo Co., Ltd. (Tokyo, Japan). All antagonists solution were made using dimethylsulphoxide (DMSO) as the diluent. DMSO, acetylcholine bromide, noradrenaline bitartrate (stock solution in 1 mg ml^{-1} ascorbate)

and indomethacin were from Sigma Chemical Co. (St Louis, MO, U.S.A.). All other reagents were analytical grade.

Statistics

Values are expressed as the mean ± s.e.mean and n represents the number of tissues studied in a particular group. Statistical comparisons were made by analysis of variance (ANOVA; Fisher's protected least squares difference) where $P<0.05$ was accepted as being significant.

Results

ET isopeptide-induced vasoconstriction in the rabbit isolated saphenous vein

ET-1, ET-3 and STXc produced concentration-dependent contractions of the endothelium-intact saphenous vein over a broad concentration-range of approximately 5 log units (Figure 1). The concentration-response curves generated were biphasic and best fitted to a two site model consisting of a high (pM) and low (nM) affinity site (Table 1). Removal of the endothelium did not have a significant effect on these contractile actions (Table 1). The contractile potencies of ET-3 and STXc at the high affinity site were not significantly different from that of ET-1. In contrast, however, STXc and ET-3 were significantly more potent than ET-1 at the low affinity site. Relative to ET-1, ET-3 and STXc were full agonists at the high affinity site and partial agonists at the low affinity site. Furthermore, relative to the low affinity site, the high affinity site appeared to be a 'lower efficacy site', contributing approximately 40% towards the overall contractile response to ET-1. The concentration-response curve for the contractile actions of [Ala^{3,11}]ET-1 was also biphasic and, similarly, was best fitted to a two site model (Figure 1). This analogue was 87 and 12 fold less potent than ET-1 at the high and low affinity sites, respectively (Table 1), but differed from ET-3 and STXc, in that, relative to ET-1, it was a full agonist at both sites. In contrast, the concentration-response curve generated to IRL 1620 was obtained over a much narrower concentration-range of approximately 3 log units

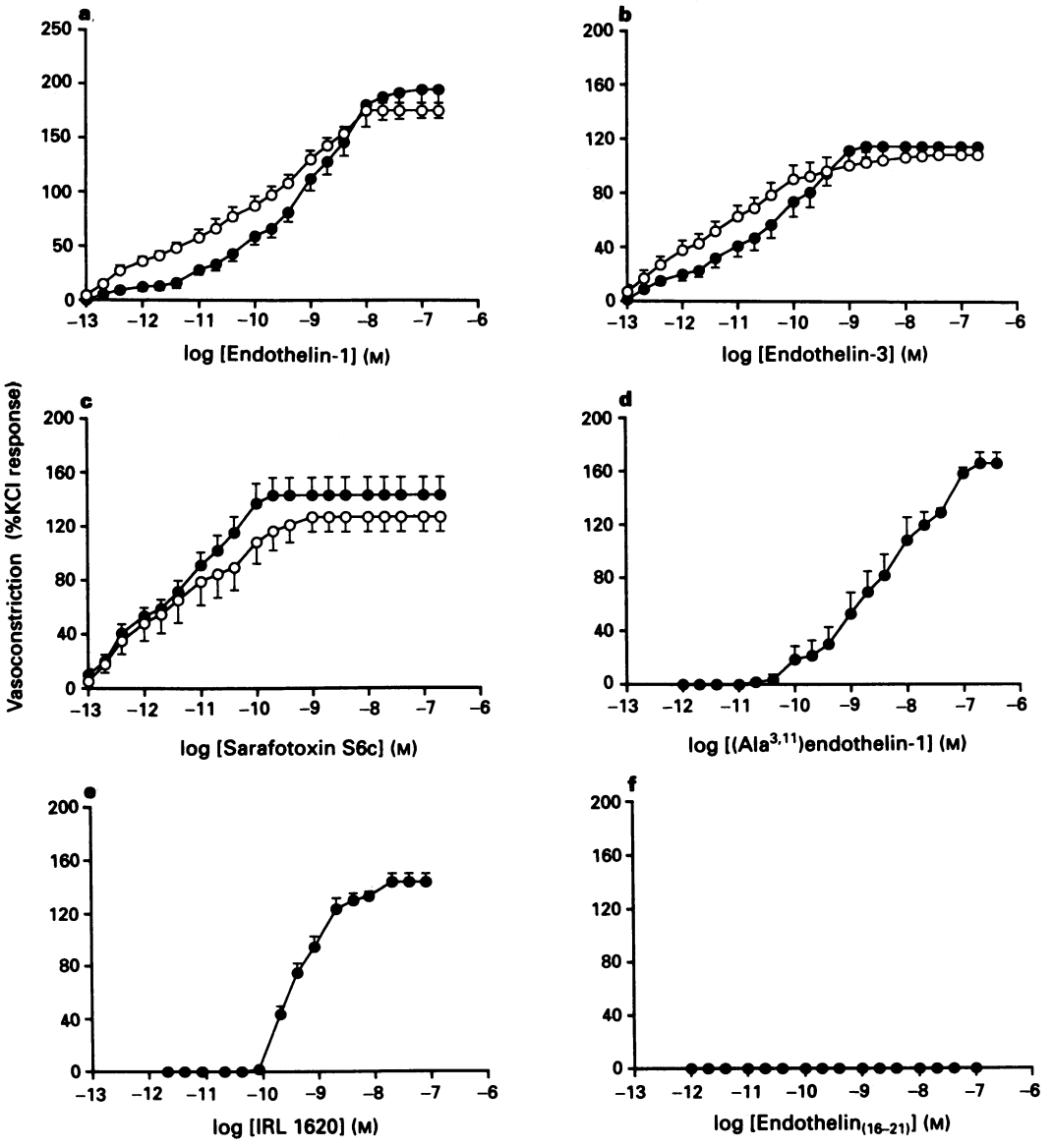

Figure 1 Cumulative concentration-response curves obtained in endothelium-intact (●) and endothelium-denuded (○) rabbit isolated saphenous vein rings in response to the addition of either (a) ET-1 ($n=7$ and 8, respectively), (b) ET-3 ($n=9$ and 8, respectively), (c) STXc (both $n=5$), (d) [Ala^{3,11}]ET-1 ($n=3$), (e) IRL 1620 ($n=3$) or (f) the C-terminal hexapeptide ET$_{(16-21)}$ ($n=3$). Values are the mean ± s.e.mean and n represents the number of tissues studied in a particular group. The corresponding pD_2 and R_{max} values are shown in Table 1. For abbreviations, see text.

(Figure 1) and, consequently, was best fitted to a one site model (Table 1). $ET_{(16-21)}$ was devoid of contractile activity (Figure 1, Table 1).

Effect of specific ET isopeptide agonists on antagonistic actions of 1 μM SB 209670 and 10 μM BQ-123 in the endothelium-denuded rabbit isolated saphenous vein

The contractile actions of ET-1, ET-3 and STXc were not significantly altered by BQ-123 (Figure 2, Table 2). In contrast, SB 209670 (1 μM) inhibited both components of the biphasic concentration-response curve to STXc producing parallel, 6918 and 28 fold rightward displacements of the high and low affinity components of this curve, respectively (Figure 2, Table 2). SB 209670 also inhibited the high and low affinity components of biphasic concentration-response curve to both ET-1 and ET-3 (Figure 2, Table 2) producing parallel, 646 and 22 fold rightward displacements in the high and low affinity components of the ET-1-response curve and 1259 and 74 fold rightward displacements in the high and low affinity components of the ET-3-response curve, respectively. Thus, SB 209670 differentially antagonized the high affinity component of the concentration-response curve dependent on the agonist used (a similar differential effect did not occur at the low affinity site).

Effect of SB 209670 on STXc-induced contraction of the endothelium-denuded rabbit isolated saphenous vein

SB 209670 (100 nM–3 μM) produced parallel, concentration-dependent rightward shifts in both components of biphasic

Table 1 Curve fitted parameters obtained for the contractile actions of some endothelin (ET) isopeptides in the rabbit isolated saphenous vein

	High affinity site		*Low affinity site*		
Agonist	pD_2	R_{max} (%KCl)	pD_2	R_{max} (%KCl)	n
ET-1					
Endothelium intact	11.27 ± 0.32	50 ± 11	8.87 ± 0.09	154 ± 30	7
Endothelium denuded	11.98 ± 0.25	74 ± 13	9.08 ± 0.14	105 ± 11	8
STXc					
Endothelium intact	12.44 ± 0.21*	64 ± 9	10.70 ± 0.14***	74 ± 15*	5
Endothelium denuded	12.35 ± 0.26	53 ± 9	10.63 ± 0.26**	74 ± 10*	5
ET-3					
Endothelium intact	11.60 ± 0.22	51 ± 9	9.84 ± 0.14***	65 ± 7**	9
Endothelium denuded	12.19 ± 0.21	54 ± 8	10.23 ± 0.32**	56 ± 9**	8
IRL 1620					
Endothelium intact	–	–	9.27 ± 0.16	142 ± 6	3
Endothelium denuded	ND	ND	ND	ND	–
[Ala^{3,11}]ET-1					
Endothelium intact	9.33 ± 0.59***	76 ± 37	7.79 ± 0.55***	95 ± 31	3
Endothelium denuded	ND	ND	ND	ND	–
$ET_{(16-21)}$					
Endothelium intact	<7	–	<7	–	3
Endothelium denuded	ND	ND	ND	ND	–

Values are the mean ± s.e.mean; *n* represents the number of animals used in a particular group. Parameters are derived by fitting the concentration-response data (Figure 1) to a logistic equation (see Methods). Statistical comparisons: $*P<0.05$, $**P<0.01$ and $***P<0.001$ (ANOVA; Fisher's Protected least squares difference) compared to values obtained to ET-1 in corresponding endothelium-intact or -denuded tissue. Endothelial denudation did not alter the concentration-response curves to ET-1, ET-3 or STXc. Unlike ET-1, ET-3, STXc and [Ala^{3,11}]ET-1, IRL 1620 was shown to fit best a one-site model. ND = values not determined in endothelium-denuded tissues. $ET_{(16-21)}$ (≤ 0.1 μM) was devoid of contractile activity in endothelium-intact tissues.

Table 2 Relative potencies of SB 209670 and BQ-123 at inhibiting endothelin (ET) isopeptide-induced contraction of the endothelium-denuded rabbit isolated saphenous vein

	High affinity site			*Low affinity site*			
Agonist	pD_2	K_B (nM)	pK_B	pD_2	K_B (nM)	pK_B	n
ET-1							
Control	11.98 ± 0.24			9.08 ± 0.14			8
BQ-123 10 μM	12.13 ± 0.23	NS	NS	8.30 ± 0.50	NS	NS	5
SB 209670 1 μM	9.17 ± 0.20***	1.55	8.81	7.74 ± 0.32**	48	7.32	5
ET-3							
Control	12.19 ± 0.21			10.23 ± 0.32			9
BQ-123 10 μM	12.05 ± 0.25	NS	NS	10.14 ± 0.27	NS	NS	7
SB 209670 1 μM	9.09 ± 0.10***	0.79	9.01	8.36 ± 0.07***	14	7.87	8
STXc							
Control	12.35 ± 0.26			10.63 ± 0.26			5
BQ-123 10 μM	12.35 ± 0.24	NS	NS	11.19 ± 0.42	NS	NS	4
SB 209670 1 μM	8.51 ± 0.11***	0.15	9.84	9.19 ± 0.17**	38	7.42	5

Values are the mean ± s.e.mean; *n* represents the number of animals used in a particular group. Parameters are derived by fitting the concentration-response data (Figure 2) to a logistic equation (see Methods). Statistical comparisons: $**P<0.01$ and $***P<0.001$ (ANOVA; Fisher's Protected least squares difference) compared to values obtained to a particular agonist in corresponding control tissues (which are from Table 1 and are included for ease of comparison). Since 10 μM BQ-123 failed to produce a significant inhibition of the agonist-induced contractile responses (NS), no K_B (or, therefore, pK_B) value could be determined.

concentration-response curve to STXc (Figure 3, Table 3). SB 209670 did not significantly alter the maximal contractile effects of STXc at either the high or the low affinity site, indicative of competitive antagonism. This was confirmed by Schild analysis where SB 209670 antagonized both the high and low affinity components of the biphasic concentration-response curve to STXc with regression slopes of 1.13 and 1.06, respectively (r^2 values of 0.97 and 0.99, respectively). SB 209670 was determined as having pA_2 values of 7.88 and 7.24 at the high and low affinity sites, respectively.

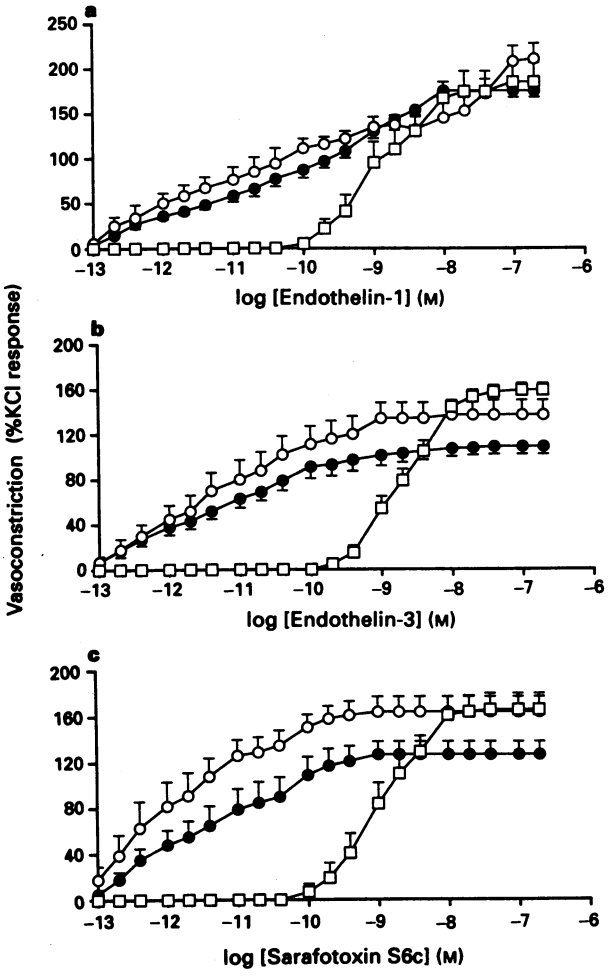

Figure 2 Cumulative concentration-response curves obtained in endothelium-denuded rabbit isolated saphenous vein rings in response to the addition of (a) ET-1, (b) ET-3 and (c) STXc in the presence of either vehicle (●; $n = 8$, 9 and 5, respectively), 10 μM BQ-123 (○; $n = 5$, 7 and 4, respectively) or 1 μM SB 209670 (□; $n = 5$, 8 and 5, respectively). Values are the mean ± s.e.mean and n represents the number of tissues studied in a particular group. Control values obtained to ET-1, ET-3 and STXc in the presence of vehicle are from Figure 1 and are included for ease of comparison. The corresponding pD_2 values determined for each agonist in the presence or absence of antagonist are shown in Table 2 along with the corresponding antagonist K_B and pK_B values. For abbreviations, see text.

Effect of 10 μM Ro 46-2005, Ro 47-0203, PD 142893, BQ-788 and RES-701 on the contractile actions of STXc in the endothelium-denuded rabbit isolated saphenous vein

Ro 47-0203, Ro 46-2005 and BQ-788, all at 10 μM concentrations, produced significant 832, 36 and 91 fold shifts in the

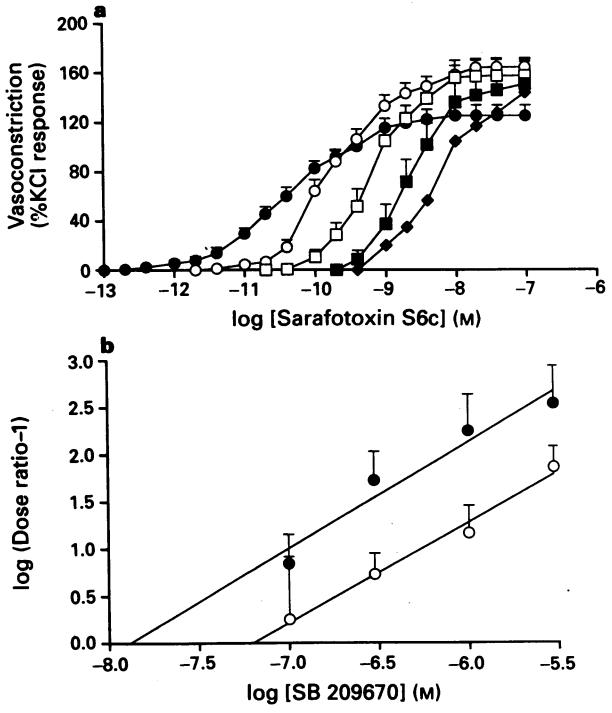

Figure 3 Panel (a) demonstrates the concentration-dependent inhibition by SB 209670 of the contractile responses observed in endothelium-denuded rabbit isolated saphenous vein rings in response to the addition of STXc; (●; $n = 6$) represents control responses, obtained in the presence of vehicle. Responses obtained in the presence of SB 209670 are as follows: 100 nM (○; $n = 6$); 300 nM (□; $n = 6$); 1 μM (■; $n = 6$); 3 μM (◆; $n = 6$). The corresponding pD_2 and R_{max} values obtained in the presence or absence of SB 209670 are shown in Table 3. Panel (b) represents the Schild analysis of these data which demonstrates that SB 209670 is a potent, competitive functional antagonist of both the high (○; $pA_2 = 7.88$; regression slope = 1.13; $r^2 = 0.97$) and low (●; $pA_2 = 7.24$; regression slope = 1.06; $r^2 = 0.99$) affinity components of the biphasic contractile response to STXc. Values are the mean ± s.e.mean and n represents the number of tissues studied in a particular group. For abbreviations, see text.

Table 3 Effect of SB 209670 on the STXc-induced contraction of the endothelium-denuded rabbit isolated saphenous vein

	High affinity site		*Low affinity site*		
	pD_2	R_{max} (%KCl)	pD_2	R_{max} (%KCl)	n
[SB 209670]					
Control	11.04 ± 0.33	76 ± 17	9.60 ± 0.24	50 ± 17	6
0.1 μM	10.09 ± 0.11**	73 ± 13	9.13 ± 0.25	92 ± 15	6
0.3 μM	9.30 ± 0.12***	96 ± 16	8.75 ± 0.19**	61 ± 15	6
1 μM	8.78 ± 0.23***	71 ± 9	8.38 ± 0.09***	80 ± 13	6
3 μM	8.50 ± 0.17***	97 ± 6	7.71 ± 0.22***	49 ± 10	6

Values are the mean ± s.e.mean; n represents the number of animals used in a particular group. Parameters are derived by fitting the concentration-response data (Figure 3) to a logistic equation (see Methods). Statistical comparisons: **$P < 0.01$ and ***$P < 0.001$ (ANOVA; Fisher's Protected least squares difference) compared to values obtained to STXc in the absence of antagonist ('Control').

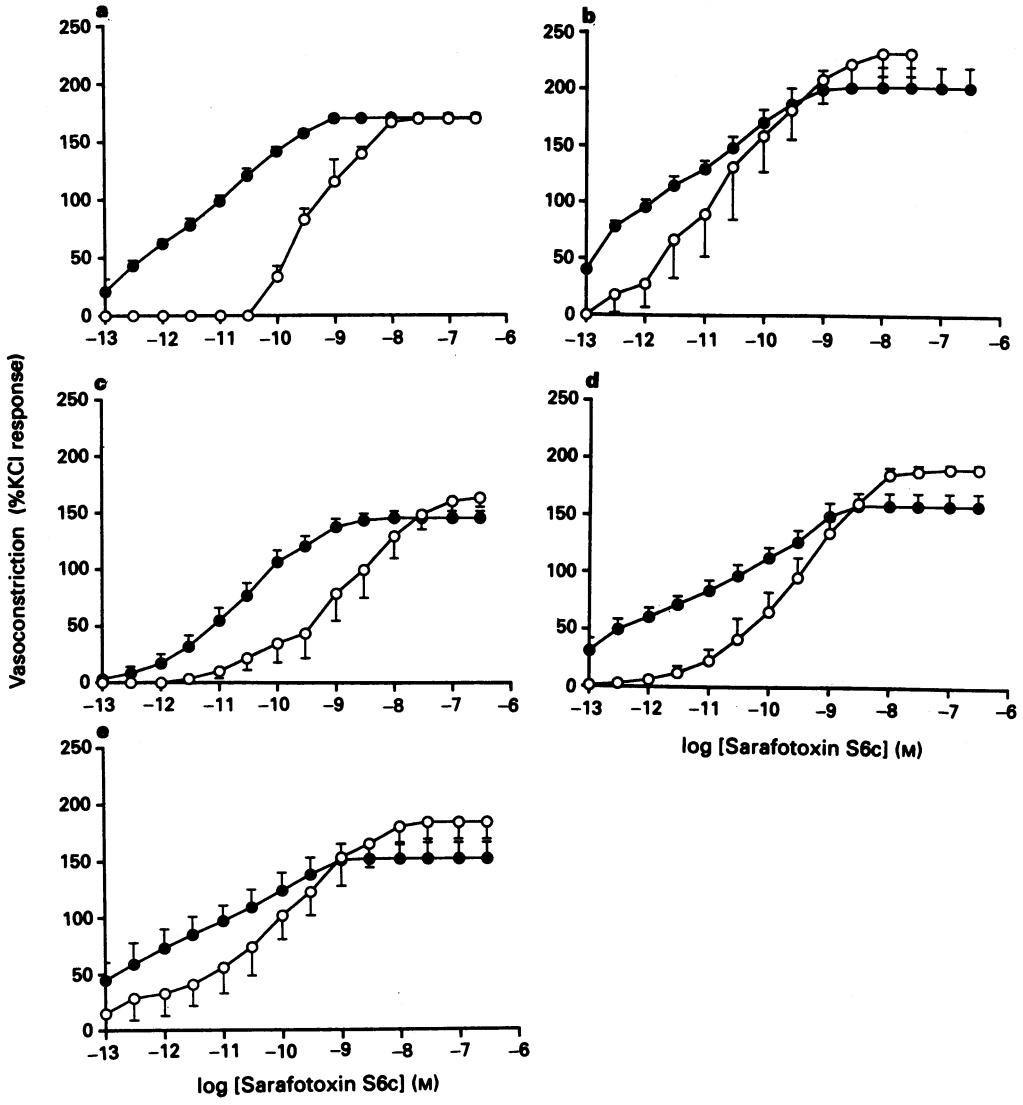

Figure 4 Cumulative concentration-response curves obtained to STXc in endothelium-denuded rabbit isolated saphenous vein rings in the presence of either (●) vehicle or (○) 10 μM concentrations of (a) Ro 47-0203 (both $n = 3$), (b) Ro 46-2005 ($n = 6$ and 3, respectively), (c) BQ-788 (both $n = 8$), (d) PD 142893 (both $n = 6$) and (e) RES-701 (both $n = 4$). Values are the mean ± s.e.mean and n represents the number of tissues studied in a particular group. The corresponding pD_2 values determined for STXc in the presence or absence of each individual antagonist are shown in Table 4 along with the corresponding antagonist K_B and pK_B values. For abbreviations, see text.

Table 4 Effect of various endothelin (ET) receptor antagonists at inhibiting the STXc-induced contraction of the endothelium-denuded rabbit isolated saphenous vein

	High affinity site				*Low affinity site*				
Antagonist	pD_2	K_B (nM)	pK_B	*Rank order*	pD_2	K_B (nM)	pK_B	*Rank order*	n
Control	12.70 ± 0.20				10.61 ± 0.19				3
Ro 47-0203 10 μM	9.78 ± 0.09***	14	7.85	97	8.38 ± 0.17***	62	7.21	2	3
Control	11.28 ± 0.26				9.74 ± 0.25				8
BQ-788 10 μM	9.32 ± 0.44**	110	6.96	758	8.54 ± 0.33*	673	6.17	18	8
Control	12.82 ± 0.08				10.42 ± 0.09				6
Ro 46-2005 10 μM	11.26 ± 0.48**	283	6.55	1,950	9.40 ± 0.43*	585	6.23	15	3
Control	12.66 ± 0.38				10.15 ± 0.29				6
PD 142893 10 μM	11.28 ± 0.71	NS	NS	69,183	9.08 ± 0.20*	1,710	5.77	45	6
Control	12.64 ± 0.38				10.11 ± 0.14				4
RES-701 10 μM	11.71 ± 0.68	NS	NS	69,183	9.24 ± 0.11**	2,023	5.69	54	4
Control	12.35 ± 0.26				10.63 ± 0.26				5
BQ-123 10 μM	12.35 ± 0.24	NS	NS	69,183	11.19 ± 0.42	NS	NS	263	4

Values are the mean ± s.e.mean; n represents the number of animals used in a particular group. Parameters are derived by fitting the concentration-response data (Figure 4) to a logistic equation (see Methods). Statistical comparisons: *$P<0.05$, **$P<0.01$ and ***$P<0.001$ (ANOVA; Fisher's Protected least squares difference) compared to corresponding control values obtained to STXc in the absence of antagonist ('Control'). Where a 10 μM concentration of antagonist failed to produce a significant inhibition of the contractile actions of STXc (NS), no K_B (and, therefore, pK_B) value could be determined. The rank order of antagonist potency was approximated based on the pK_B values determined in this Table (using a 10 μM concentration of antagonist) and those determined for SB 209670 against STXc (using a 1 μM concentration, Table 2).

high affinity portion of the STXc concentration-response curve (Figure 4). Thus, based on the K_B values determined for SB 209670, Ro 47-0203 was 1 to 2 orders of magnitude less potent than SB 209670 at this site, whereas Ro 46-2005 and BQ-788 were 3 orders of magnitude less potent (Table 4). However, 10 μM concentrations of PD 142893 and RES-701 failed to inhibit this portion of the concentration-response curve to STXc. In contrast, 10 μM concentrations of Ro 47-0203, Ro 46-2005, BQ-788, PD 142893 and RES-701 caused significant rightward shifts in the low affinity portion of the biphasic STXc concentration-response curve (170, 10, 16, 12 and 7 fold shifts, respectively). Therefore, Ro 47-0203 was equipotent with SB 209670 at this low affinity site, whereas Ro 46-2005, BQ-788, PD 142893 and RES-701 were 1 to 2 orders of magnitude less potent. SB 209670, BQ-788, Ro 47-0203 and Ro 46-2005 appeared to be 1 to 2 orders of magnitude less potent at the low affinity site relative to the high affinity site.

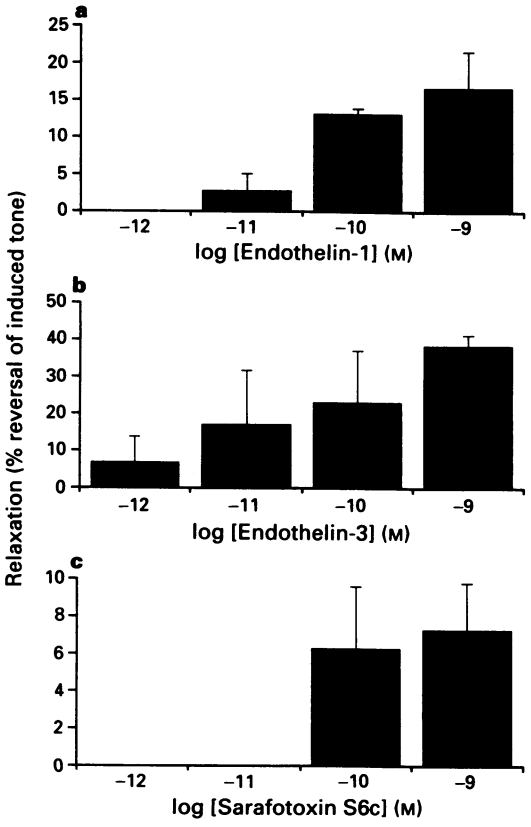

Figure 5 Concentration-dependent relaxant responses obtained in precontracted (1 μM noradrenaline) rabbit isolated saphenous vein rings with endothelium-intact following the addition of single concentration of either (a) ET-1 ($n = 3$), (b) ET-3 ($n = 7$) or (c) STXc ($n = 3$). Values are the mean ± s.e.mean and n represents the number of tissues studied in a particular group.

Vasodilator actions of the ET isopeptides

ET-3 produced concentration-dependent vasorelaxation in saphenous vein preparations precontracted with noradrenaline (Figure 5), an action dependent on the presence of a functional endothelium (Figure 6). At concentrations greater than 1 nM, the relaxant response to ET-3 was overwhelmed by a concomitant contractile response. The relaxant responses to ET-1 and STXc were qualitatively smaller than those obtained with ET-3 (Figures 5 and 7). As with ET-3, such responses were also superceded by vasoconstriction at agonist concentrations of greater than 1 nM (such that sigmoidal concentration-response curves, and, therefore, a rank order of relaxant potency, could not be determined).

Effect of ET receptor antagonists on the vasodilator actions of ET-3

SB 209670 was the most potent antagonist studied at inhibiting the relaxant actions of ET-3 (Figures 8 and 9) with significant inhibition being observed at antagonist concentrations as low as 1 nM. BQ-788 and RES-701 were also effective at inhibiting this response at concentrations of 1 μM, whereas Ro 46-2005 and PD 142893 only produced a significant (albeit virtually complete) inhibition at 10 μM concentrations. Although BQ-123 (10 μM) also produced significant antagonism of ET-3-induced relaxation, inhibition was incomplete. Since tissues were used to study the effects of a single concentration of antagonist against a single concentration of agonist, concentration-response curves could not

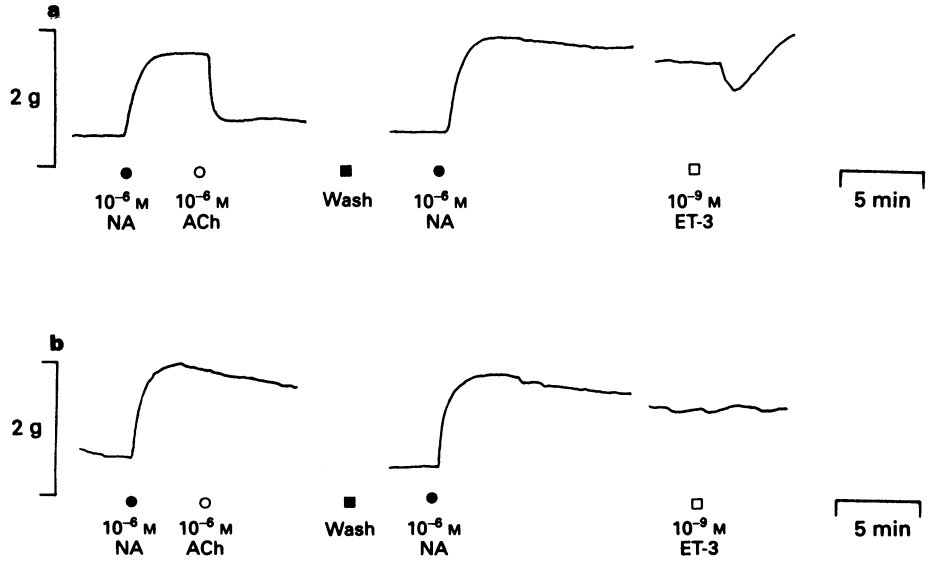

Figure 6 Representative experimental trace illustrating that, in rabbit isolated saphenous vein rings preconstricted with 1 μM noradrenaline (●; 10^{-6} M NA), the vasorelaxant actions of either 1 μM acetylcholine (○; 10^{-6} M ACh) or 1 nM ET-3 (□; 10^{-9} M) are obtained only in the presence of an intact functional endothelium (a). Panel (b) shows that when the endothelium is physically destroyed by gently rubbing the intimal surface of the saphenous vein with a stainless steel rod, the vasorelaxant activity of both acetylcholine and ET-3 are abolished. (■; Wash) represents where the tissue was washed in between exposure to acetylcholine and ET-3.

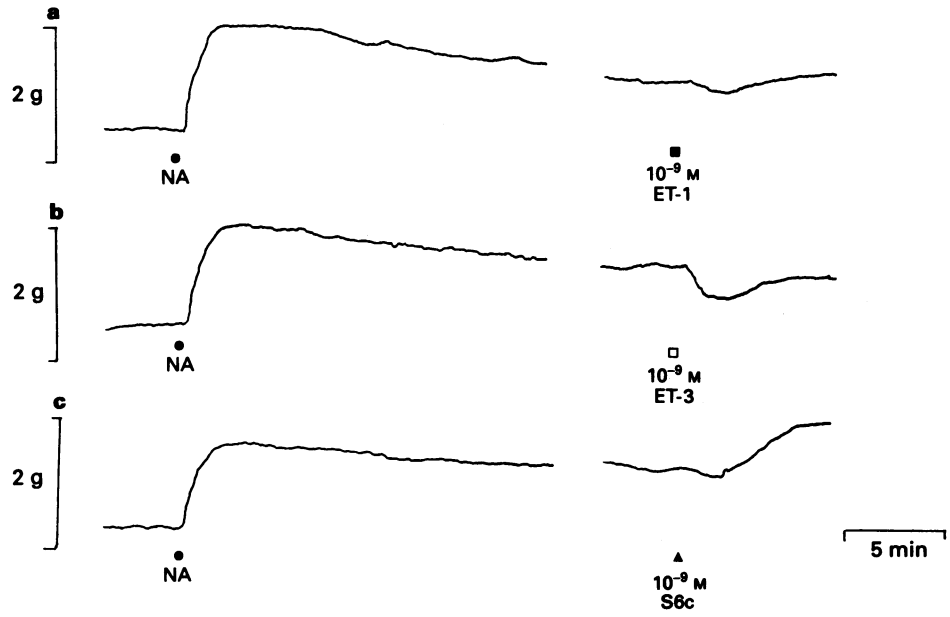

Figure 7 Representative experimental trace comparing the vasorelaxant activities of 1 nM concentrations of (a) endothelin-1 (ET-1; ■; 10^{-9} M), (b) endothelin-3 (ET-3, □; 10^{-9} M) and (c) sarafotoxin S6c (S6c, ▲; 10^{-9} M) in rabbit isolated, endothelium-intact saphenous vein rings preconstricted with 1 μM noradrenaline (●; NA).

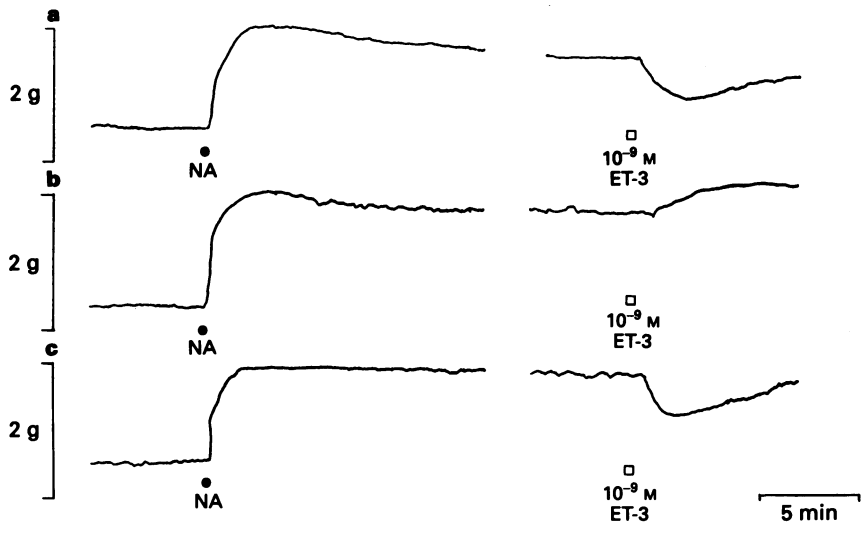

Figure 8 Representative experimental trace comparing the vasorelaxant activities of 1 nM concentrations of endothelin-3 (ET-3, □; 10^{-9} M) in rabbit isolated, endothelium-intact saphenous vein rings preconstricted with 1 μM noradrenaline (●; NA) in (a) control tissues (pretreated with vehicle) or those pretreated with either (b) 0.1 μM SB 209670 or (c) 10 μM BQ-123. The figure demonstrates that SB 209670 completely abolishes the vasorelaxant actions of ET-3, a response that is relatively insensitive to the ET_A-selective ET receptor antagonist, BQ-123 (see Figure 9).

be fitted to a logistic equation. Nevertheless, IC_{50}s were approximated as being: SB 209670, 3 nM; BQ-788 and RES 701, 300 nM; Ro 46-2005 and PD 142893, 3 μM; BQ-123, $\geqslant$ 10 μM.

Discussion

Contraction of the rabbit saphenous vein is mediated by a heterogeneous population of ET receptors (Auguet *et al.*, 1993; Bax *et al.*, 1993; Webb *et al.*, 1993; White *et al.*, 1994). In accord with Gray *et al.* (1994), the present study demonstrated that ET-1, ET-3, STXc produced biphasic contractions of the rabbit saphenous vein over a broad concentration-range, suggestive of negative cooperativity. Curve-fitting identified two distinct sites of high (pM) and low (nM) affinity. Significant contractile responses could be detected with agonist concentrations as low as 0.2 pM, a value similar to that required for ET-1 to elicit a positive inotropic response in rabbit papillary muscle (Kasai *et al.*, 1994). The rank order of contractile potency at the high affinity site was consistent with this being an ET_B receptor-mediated response (ET-1 = ET-3). In contrast, however, based on the definitions adopted by the IUPHAR Committee on Receptor Nomenclature (Masaki *et al.*, 1994), the low affinity site had the characteristics of an ET_C receptor since ET-3 and STXc were 14 and 35 fold more potent than ET-1 at this site. This is in accord with previous reports where STXc was a more potent vasoconstrictor than ET-1 in rabbit and human saphenous veins and pulmonary arteries (Moreland *et al.*, 1992; LaDoucer *et al.*, 1993; White *et al.*, 1994).

Further support for the hypothesis that contraction of the rabbit saphenous vein is mediated by two non-ET_A receptors comes from the observation that neither component of the

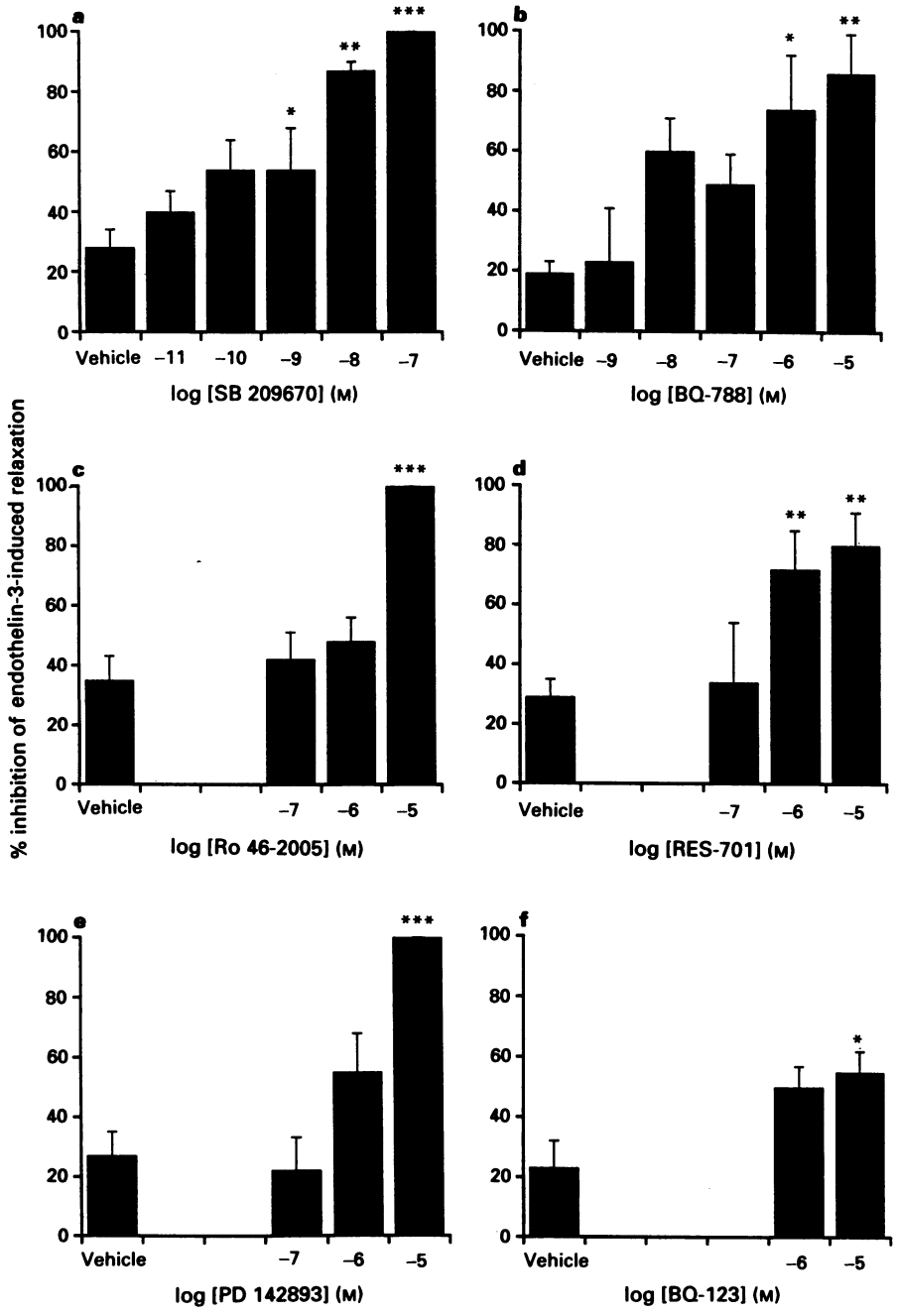

Figure 9 Inhibitory action of ET receptor antagonists on the vasodilator responses obtained to 1 nM ET-3 in endothelium-intact isolated saphenous vein rings of rabbit preconstricted with 1 μM noradrenaline. Responses were obtained in the presence of (a) SB 209670 (10 pM–100 nM; $n = 5$), (b) BQ-788 (1 nM–10 μM; $n = 3$), (c) Ro 46-2005 (0.1–10 μM; $n = 4$), (d) RES-701 (0.1–10 μM; $n = 6$), (e) PD 142893 (0.1–10 μM; $n = 5$) or (f) BQ-123 (1–10 μM; $n = 4$). Values are the mean ± s.e.mean and n represents the number of tissues studied in a particular group and statistical significance: $^*P < 0.05$, $^{**}P < 0.01$ and $^{***}P < 0.001$ for values obtained in the presence of antagonist compared to control values obtained in the presence of vehicle alone (ANOVA; Fisher's protected least squares difference). For abbreviations, see text.

biphasic contractile response to ET-1, ET-3 or STXc is inhibited by BQ-123. Similar findings have been reported by Moreland *et al.* (1992, 1994) and Sudjarwo *et al.* (1993) where ET-induced contractions of rabbit, monkey and porcine isolated saphenous veins were insensitive to the ET_A-selective antagonists, BQ-123 and FR 139317. Indeed, whilst several investigators have demonstrated weak inhibition of peptide-induced contraction of isolated saphenous veins by BQ-123, the pA_2 determined for this antagonist (approximately 6) is not consistent with this being the result of ET_A receptor occupation (Auguet *et al.*, 1992; Bax *et al.*, 1993; White *et al.*, 1994). The present findings are, in part, consistent with radioligand binding studies where [^{125}I]-ET-3 recognizes a high and low affinity form of an ET_B receptor in the rabbit saphenous vein (Webb *et al.*, 1993; Gray *et al.*, 1994). However, radioligand binding studies clearly demonstrate the presence of BQ-123-sensitive [^{125}I]-ET-1 binding sites and ET_A receptor mRNA in this tissue (Webb *et al.*, 1993; Gray *et al.*, 1994). Indeed, Gray *et al.* (1994) have demonstrated that 20% of the contractile response to the ET isopeptides was mediated by a BQ-123-sensitive, low affinity receptor. The reason for the disparity between the current data and the findings of Gray *et al.* (1994) is unclear but may reflect differences in the strains of rabbit used (Burgandy *versus* New Zealand White) or, alternatively, may be a function of the segment of saphenous vein studied (lateral *versus* medial

saphenous vein). Subtle differences in the precise anatomical origin of the vein may be of pharmacological significance since the relative contribution of specific ET receptor subtypes to peptide-induced vasoconstriction varies as one progresses along a vascular tree (Godfraind, 1994a,b; MacLean *et al.*, 1994). Unfortunately, the precise anatomical origin of the saphenous veins used by Gray *et al.* (1994) and Webb *et al.* (1994) was not stated.

Multiple functional ET_B receptors are present within the mammalian cardiovascular system: Warner *et al.* (1993a,b) have identified an ET_{B1} receptor (linked to endothelium-dependent vasodilatation in the rat mesentery) and an ET_{B2} receptor (which mediates contraction of the rat stomach strip and rabbit pulmonary artery). In addition to their anatomical and functional distinctions, the ET_{B1} and ET_{B2} receptors differ pharmacologically since only the ET_{B1} receptor is sensitive to PD 142893 (Warner *et al.*, 1993a,b). Since the high affinity site described in this study is insensitive PD 142893, it may correspond to an ET_{B2} subtype. This hypothesis is supported by the observation that [$Ala^{3,11}$]-ET-1, a peptide which is inactive at the ET_{B1} (Douglas & Hiley, 1990; 1991a; Topouzis *et al.*, 1991), recognizes the high affinity site in the saphenous vein. The contractile ET_{B2} and ET_C receptors were further distinguished by use of a variety of ET receptor antagonists. SB 209670 was a potent, competitive antagonist at both the high and low affinity sites and was one to two orders of magnitude and equipotent with Ro 47-0203 at these two sites, respectively. In addition, both Ro 46-2005 and BQ-788 inhibited the high and low affinity sites. In contrast, however, not only was the ET_{B2} receptor insensitive to BQ-123 and PD 142893, but it was also insensitive to RES-701. This contrasts the low affinity ET_C site which, although insensitive to BQ-123, was inhibited by both PD 142893 and RES-701.

In accord with Poli *et al.* (1991), $ET_{(16-21)}$ was ineffective as a vasoconstrictor in this tissue. Thus, in contrast to the original reports by Maggi *et al.* (1989), and in support of subsequent radioligand binding studies (Tschirhart *et al.*, 1991; Buchan *et al.*, 1994), $ET_{(16-21)}$ does not act as an agonist at the ET receptors responsible for mediating contraction of the rabbit saphenous vein.

SB 209670 differentially antagonized the high (but not the low) affinity phase of the concentration-response curve to ET-1, ET-3 and STXc in a fashion dependent on the competing agonist. Whilst this phenomenon contradicts conventional drug-receptor theory, a similar finding has been reported for SB 209670 in the rat pulmonary artery (ET_{B2} receptor-mediated contraction; Ohlstein *et al.*, 1994a) and has also been observed with BQ-123 and PD 142893 in numerous vascular preparations (Bax *et al.*, 1993; 1994; Warner *et al.*, 1993a; Kasai *et al.*, 1994; Smith *et al.*, 1994). The mechanism underlying this type of phenomenon is unknown, although it has been suggested that ET-3 and STXc interact with an additional site present on ET receptors which is inaccessible to ET-1 (Hiley *et al.*, 1992; Smith *et al.*, 1994).

The endothelium attenuates the contractile actions of the ET isopeptides by stimulating the release of nitric oxide (Warner *et al.*, 1989; Douglas & Hiley, 1990; 1991a). In the present study, both components of the biphasic concentration-response curves to ET-1, ET-3 and STXc were shifted by approximately 3 fold following endothelial destruction, consistent with previous observations made in human, canine and rabbit saphenous veins (Berti *et al.*, 1990; Poli *et al.*, 1991; Simonet *et al.*, 1992; Auguet *et al.*, 1993; Akar *et al.*, 1994). Indeed, in the presence of active tone, ET-3 produced endothelium-dependent vasorelaxation in this tissue. Vasorelaxation was also observed with ET-1 and STXc, although, in accord with Auguet *et al.* (1993), such responses were quantitatively less pronounced than those to ET-3. Based on the threshold concentration of peptide required to elicit a dilator response, vasorelaxation appeared to be mediated by a non-ET_A receptor subtype. Indeed, relaxation was insensitive to 1 μM BQ-123. Antagonist IC_{50}s were approximated as being: SB 209670, 3 nM; BQ-788 and RES 701, 300 nM; Ro 46-2005 and PD 142893, 3 μM; BQ-123, $\geqslant$ 10 μM. Since ET-3-induced vasorelaxation was antagonized by PD 142893, this response appeared to be mediated by an ET_{B1} receptor.

In summary, three pharmacologically distinct, functional ET receptor subtypes have been identified in the rabbit saphenous vein. Two contractile receptors are present on the vascular smooth muscle: a high affinity, low efficacy ET_{B2} receptor (i.e. STXc = ET-3 = ET-1; SB 209670 > Ro 47-0203 > BQ-788 > Ro 46-2005; insensitive to PD 142893, RES-701 and BQ-123) and a distinct lower affinity, high efficacy ET_C receptor (i.e. STXc $\geqslant$ ET-3 > ET-1; SB 209670 $\geqslant$ Ro 47-0203 > Ro 46-2005 and BQ-788 > RES 701 and PD 142893; insensitive to BQ-123). In addition, an ET_{B1} receptor is present on the endothelium which mediates the relaxant actions of the ET isopeptides (i.e. ET-3 $\geqslant$ ET-1 $\geqslant$ STXc; SB 209670 $\geqslant$ BQ-788 = RES 701 $\geqslant$ Ro 46-2005 and PD 142893; insensitive to BQ-123). However, although the available pharmacological data suggest the presence heterogeneous, functional receptor subtypes in this tissue, confirmation by conventional protein purification/molecular cloning is necessary before their existence can be firmly established. It is appropriate to note, however, that low stringency homology screening has only been able to identify mRNA transcripts in the rabbit saphenous vein which appear to correspond to the known cloned ET_A and ET_B receptors (Webb *et al.*, 1993). If novel mRNA species are present in this tissue, they are likely to either (i) differ markedly from those encoding for the known ET_A and ET_B receptors or (ii) be so similar to the known cloned receptors that it is readily mistaken for a known subtype during homology screening. To this end, it is interesting that a single nucleotide point mutation of the codon for residue Tyr^{129} present in the wild type human cloned ET_A receptor (e.g. from TAT [Tyr^{129}] to TTT [Phe^{129}]) can dramatically alter the pharmacological characteristics of the mutant receptor such that, essentially, it resembles an ET_B subtype (Lee *et al.*, 1994). Alternatively, it is conceivable that the high and low affinity sites linked to saphenous vein contraction are derived from a single gene product, differing only by the extent to which they are subject to post translational modification (e.g. proteolytic maturation or glycosylation).

The authors would like to thank A. Lago, J. Lee, J. Leber, A. Gao, R. Cousins and J. Sutiphong for the synthesis of some of the ET receptor antagonists used in this study and for their helpful discussions during the preparation of this manuscript.

References

AKAR, F., UYDES, B.S., AYRANCIOGLU, K., YENER, A., ASLAMACI, A., ARSAN, M., TOURNER, A. & KANZIK, I. (1994). Endothelial function on human gastropiploic artery in comparison with saphenous vein. *Cardiovasc. Res.*, **28**, 500–504.

ARAI, H., HORI, S., ARAMORI, I., OHKUBO, H. & NAKANISHI, S. 1990). Cloning and expression of a cDNA encoding an endothelin receptor. *Nature*, **348**, 730–732.

AUGUET, M., DELAFLOTTE, S., CHABRIER, P.E. & BRAQUET, P.C. (1993). Characterization of endothelin receptors mediating contraction and relaxation in rabbit saphenous artery and vein. *Can. J. Physiol. Pharmacol.*, **71**, 818–823.

BAX, W.A., BOS, E. & SAXENA, P.R. (1993). Heterogeneity of endothelin/sarafotoxin receptors mediating contractions of the human isolated saphenous vein. *Eur. J. Pharmacol.*, **239**, 267–268.

BAX, W.A., PETTERSON, R.W.G., INAN, T., BOS, E. & SAXENA, P.R. (1994). Heterogeneity of endothelin/sarafotoxin receptors mediating contractions of the human isolated coronary artery. *Br. J. Pharmacol.*, **111**, 15P.

BERTI, F., ROSSONI, G., BIASI, G., BUSCHI, A., MANDELLI, V. & TONDO, C. (1990). Defibrotide, by enhancing prostacyclin generation, prevents endothelin-1 induced contraction in human saphenous veins. *Prostaglandins*, **40**, 337–350.

BIGAUD, M. & PELTON, J.T. (1992). Discrimination between ETA- and ETB-receptor-mediated effects of endothelin-1 and [Ala^{1,3,11,15}]endothelin-1 by BQ-123 in the anaesthetized rat. *Br. J. Pharmacol.*, **107**, 912–918.

BROOKS, D.P., DEPALMA, P.D., GELLAI, M., NAMBI, P., OHLSTEIN, E.H., ELLIOTT, J.D., GLEASON, J. & RUFFOLO, R.R. (1994). Nonpeptide endothelin receptor antagonists. III: Effect of SB 209670 and BQ-123 on acute renal failure in anesthetized dogs. *J. Pharmacol. Exp. Ther.*, **271**, 769–775.

BUCHAN, K.W., ALLDUS, C., CHRISTODOULOU, C., CLARK, K.L., DYKES, C.W., SUMNER, M.J., WALLACE, D.M., WHITE, D.G. & WATTS, I.S. (1994). Characterization of three non-peptide endothelin receptor ligands using human cloned ET_A and ET_B receptors. *Br. J. Pharmacol.*, **112**, 1251–1257.

CLOZEL, M., BREU, V., BURRI, K., CASSAL, J.-M., FISCHLI, W., GRAY, G.A., HIRTH, G., LÖFFLER, B.-M., MÜLLER, M., NIEDHART, W. & RAMUZ, H. (1993). Pathophysiological role of endothelin revealed by the first orally active endothelin receptor antagonist. *Nature*, **365**, 759–761.

CLOZEL, M., BREU, V., GRAY, G.A., KALINA, B., LÖFFLER, B.-M., BURRI, K., CASSAL, J.-M., HIRTH, G., MÜLLER, M., NIEDHART, W. & RAMUZ, H. (1994). Pharmacological characterization of bosentan, a new potent orally active nonpeptide endothelin receptor antagonist. *J. Pharmacol. Exp. Ther.*, **270**, 228–235.

CLOZEL, M., GRAY, G.A., BREU, V., LÖFFLER, B.-M. & OSTERWALDER, R. (1992). The endothelin ET_B receptor mediates both vasodilation and vasoconstriction *in vivo*. *Biochem. Biophys. Res. Commun.*, **186**, 867–873.

DOHERTY, A.M., CODY, W.L., HE, J.X., DEPUE, P.L., CHENG, X.-M., WELCH, K.M., FLYNN, M.A., REYNOLDS, E.E., LADOUCEUR, D.M., DAVIS, L.S., KEISER, J.A. & HALEEN, S.J. (1993). In vitro and in vivo studies with a series of hexapeptide endothelin antagonists. *J. Cardiovasc. Pharmacol.*, **22** (Suppl. 8), S98–S102.

DOUGLAS, S.A., EDWARDS, R.M., ELLIOTT, J.D. & OHLSTEIN, E.H. (1995). *In vivo* pharmacological characterization of the non-peptide endothelin receptor antagonist SB 209670. *Br. J. Pharmacol.*, **114**, 405–413.

DOUGLAS, S.A. & HILEY, C.R. (1990). Endothelium-dependent vascular activities of endothelin-like peptides in the isolated superior mesenteric arterial bed of the rat. *Br. J. Pharmacol.*, **101**, 81–88.

DOUGLAS, S.A. & HILEY, C.R. (1991a). Endothelium-dependent mesenteric vasorelaxant effects and systemic actions of endothelin (16–21) and other endothelin-related peptides in the rat. *Br. J. Pharmacol.*, **104**, 311–320.

DOUGLAS, S.A. & HILEY, C.R. (1991b). Responses to endothelin-1, human proendothelin (1–38) and porcine proendothelin (1–39) in the rat on intravenous administration and in the blood perfused mesentery. *Neurochem. Int.*, **18**, 445–454.

DOUGLAS, S.A., LOUDEN, C., VICKERY-CLARK, L.M., STORER, B.L., HART, T., FEUERSTEIN, G.Z., ELLIOTT, J.D. & OHLSTEIN, E.H. (1994a). A role for endogenous endothelin-1 in neointimal formation following rat carotid artery balloon angioplasty: protective effects of the novel nonpeptide endothelin receptor antagonist SB 209670. *Circ. Res.*, **75**, 190–197.

DOUGLAS, S.A., MEEK, T.D. & OHLSTEIN, E.H. (1994b). Novel receptor antagonists welcome a new era in endothelin biology. *Trends Pharmacol. Sci.*, **15**, 313–316.

DOUGLAS, S.A., VICKERY-CLARK, L.M. & OHLSTEIN, E.H. (1994c). Functional evidence that balloon angioplasty results in transient nitric oxide synthase induction. *Eur. J. Pharmacol.*, **255**, 81–89.

EMORI, T., HIRATA, Y. & MARUMO, F. (1990). Specific receptors for endothelin-3 in cultured bovine endothelial cells and its cellular mechanism of action. *FEBS Lett.*, **263**, 261–264.

GARDINER, S.M., KEMP, P.A., MARCH, J.E., BENNETT, T., DAVENPORT, A.P. & EDVINSSON, L. (1994). Effects of an ET_A-receptor antagonist, FR 139317, on regional haemodynamic responses to endothelin-1 and [Ala^{11,15}]Ac-endothelin-1 (6–21) in conscious rats. *Br. J. Pharmacol.*, **112**, 477–486.

GODFRAIND, T. (1994a). Endothelin receptors in human coronary arteries. *Trends Pharmacol. Sci.*, **15**, 136.

GODFRAIND, T. (1994b). Evidence for heterogeneity of endothelin receptor distribution in human coronary artery. *Br. J. Pharmacol.*, **110**, 1201–1205.

GRAY, G.A., LÖFFLER, B.M. & CLOZEL, M. (1994). Characterization of the endothelin receptors mediating contraction of the rabbit saphenous vein. *Am. J. Physiol.*, **266**, H959–H966.

HARRISON, V.J., RANDRIANTSOA, A. & SCHOEFFER, P. (1992). Heterogeneity of endothelin-sarafotoxin receptors mediating contraction of pig coronary artery. *Br. J. Pharmacol.*, **105**, 511–513.

HILEY, C.R., MCSTAY, M.K.G., BOTTRILL, F.E. & DOUGLAS, S.A. (1992). Cross-desensitization studies with endothelin isopeptides in the rat isolated superior mesenteric arterial bed. *J. Vasc. Res.*, **29**, 135.

IHARA, M., NOGUCHI, K., SAEKI, T., FUKURODA, S., TSUCHIDA, S., KIMURA, T., FUKAMI, K. & YANO, M. (1991). Biological profiles of highly potent novel endothelin antagonists selective for the ET_A receptor. *Life Sci.*, **50**, 247–255.

ISHIKAWA, K., IHARA, M., NOGUCHI, K., MASE, T., MINO, N., SAEKI, T., FUKURODA, T., FUKAMI, T., OZAKI, S., NAGASE, T., NISHIKIBE, M. & YANO, M. (1994). Biochemical and pharmacological profile of a potent and selective endothelin B-receptor antagonist, BQ-788. *Proc. Natl. Acad. Sci. U.S.A.*, **91**, 4892–4896.

JAMES, A.F., URADE, Y., WEBB, R.L., KARAKI, H., UMEMURA, I., FUJITANI, Y., ODA, K., OKADA, T., LAPPE, R.W. & TAKAI, M. (1993). IRL 1620, succinyl-[Glu^{9},Ala^{11,15}]-endothelin (8–21), a highly specific agonist of the ET_B receptor. *Cardiovasc. Drug Rev.*, **11**, 253–270.

KARNE, S., JAYAWICKREME, C.K. & LERNER, M.R. (1993). Cloning and characterization of an endothelin-3 specific receptor (ET_C receptor) from *Xenopus laevi* dermal melanophores. *J. Biol. Chem.*, **268**, 19126–19133.

KASAI, H., TAKANASHI, M., TAKASAKI, C. & ENDOH, M. (1994). Pharmacologic properties of endothelin receptor subtypes mediating positive inotropic effects in rabbit heart. *Am. J. Physiol.*, **266**, H2220–H2228.

KOMORI, K. & VANHOUTTE, P.M. (1989). Effects of SIN-1 on electrical responses of smooth muscle of the canine saphenous vein. *J. Cardiovasc. Pharmacol.*, **14** (Suppl. 11), S62–S66.

LADOUCER, D.M., FLYNN, M.A., KEISER, J.A., REYNOLDS, E. & HALEEN, S.J. (1993). ET_A and ET_B receptors coexist on rabbit pulmonary artery vascular smooth muscle mediating contraction. *Biochem. Biophys. Res. Commun.*, **196**, 209–215.

LEE, J.A., ELLIOTT, J.D., SUTIPHONG, J.A., FRIESEN, W.J., OHLSTEIN, E.H., STADEL, J.M., GLEASON, J.G. & PEISHOFF, C.E. (1994). Tyr-129 is important to the peptide ligand affinity and selectivity of human endothelin type A receptor. *Proc. Natl. Acad. Sci. U.S.A.*, **91**, 7164–7168.

MACLEAN, M.R., MCCULLOCH, K.M. & BAIRD, M. (1994). Endothelin ET_A- and ET_B-receptor-mediated vasoconstriction in rat pulmonary arteries and arterioles. *J. Cardiovasc. Pharmacol.*, **23**, 838–845.

MAGGI, C.A., GIULIANI, S., PATACCHINI, R., SANTICIOLI, P., ROVERO, P., GIACHETTI, A. & MELI, A. (1989). The C-terminal hexapeptide, endothelin (16–21) discriminates between different endothelin receptors. *Eur. J. Pharmacol.*, **166**, 121–122.

MASAKI, T., VANE, J.R. & VANHOUTTE, P.M. (1994). V. International Union of Pharmacology nomenclature of endothelin receptors. *Pharmacol. Rev.*, **46**, 137–142.

MILLER, V.M., KOMORI, K., BURNETT, J.C., Jr. & VANHOUTTE, P.M. (1989). Differential sensitivity to endothelin-1 in canine arteries and veins. *Am. J. Physiol.*, **257**, H1127–H1131.

MORELAND, S. (1994). BQ-123, a selective endothelin ET_A receptor antagonist. *Cardiovasc. Drug Rev.*, **12**, 48–69.

MORELAND, S., MCMULLEN, D., ABBOA-OFFEI, B. & SEYMOUR, A. (1994). Evidence for a differential location of vasoconstrictor endothelin receptors in the vasculature. *Br. J. Pharmacol.*, **112**, 704–708.

MORELAND, S., MCMULLEN, D.M., DELANEY, C.L., LEE, V.G. & HUNT, J.T. (1992). Venous smooth muscle contains vasoconstrictor ET_B-like receptors. *Biochem. Biophys. Res. Commun.*, **184**, 100–106.

NAMBI, P., PULLEN, M. & SPIELMAN, W. (1994a). Species differences in the binding characteristics of [^{125}I]-IRL 1620, a potent agonist for endothelin-B receptors. *J. Pharmacol. Exp. Ther.*, **268**, 202–207.

NAMBI, P., WU, H.L., PULLEN, M., ELSHOURBAGY, N., OHLSTEIN, E.H., BROOKS, D.P., ELLIOTT, J.D., GLEASON, J. & RUFFOLO, R.R., Jr. (1994b). Non-peptide endothelin receptor antagonists. I: Effects on binding and signal transduction in human ET_A and ET_B receptors. *J. Pharmacol. Exp. Ther.*, **271**, 755–761.

OHLSTEIN, E.H., BECK, G., DOUGLAS, S.A., NAMBI, P., GLEASON, J.G., RUFFOLO, R.R., Jr., FEUERSTEIN, G.Z. & ELLIOTT, J.D. (1994a). Non-peptide endothelin receptor antagonists. II: Pharmacological characterization of SB 209670. *J. Pharmacol. Exp. Ther.*, **271**, 762–768.

OHLSTEIN, E.H., NAMBI, P., DOUGLAS, S.A., EDWARDS, R.M., GELLAI, M., LAGO, A., LEBER, J.D., COUSINS, R.D., GAO, A., FRAZEE, J.S., PEISHOFF, C.E., BEAN, J.W., EGGLESTON, D.S., ELSHOURBAGY, N.A., KUMAR, C., LEE, J.A., BROOKS, D.P., RUFFOLO, R.R., Jr., FEUERSTEIN, G.Z., WEINSTOCK, J., GLEASON, J.G. & ELLIOTT, J.D. (1994b). SB 209670, a rationally designed potent nonpeptide endothelin receptor antagonist. *Proc. Natl. Acad. Sci. U.S.A.*, **91**, 8052–8056.

PANEK, R.L., MAJOR, T.C., HINGORANI, G.P., DOHERTY, A.M., TAYLOR, D.G. & RAPUNDALO, S.T. (1992). Endothelin and structurally related analogs distinguish between endothelin receptor subtypes. *Biochem. Biophys. Res. Commun.*, **184**, 566–571.

POLI, E., CASOLI, C., SPAGGIARI, I., STARCICH, R. & BERTACCINI, G. (1991). Contractile effect of endothelin-2 on the isolated human saphenous vein. *Arch. Int. Pharmacodyn. Ther.*, **313**, 108–119.

SAKURAI, T., YANAGISAWA, M., TAKUWA, Y., MIYAZAKI, H., KIMURA, S., GOTO, K. & MASAKI, T. (1990). Cloning of a cDNA encoding a non-isopeptide selective subtype of the endothelin receptor. *Nature*, **348**, 732–735.

SEO, B., OEMAR, B.S., SIEBENMANN, R., VON SEGESSER, L. & LÜSCHER, T.F. (1994). Both ET_A and ET_B receptors mediate contraction to endothelin-1 in human blood vessels. *Circulation*, **89**, 1203–1208.

SIMONET, S., BONHOMME, E., LAUBIE, M., THURIEAU, C., FAUCHERE, J.L. & VERBEUREN, T.J. (1992). Venous and arterial endothelial cells respond differently to thrombin and its endogenous receptor agonist. *Eur. J. Pharmacol.*, **216**, 135–137.

SMITH, C.F.C., BAKER, C., REDMOND, L., STOGGALL, S., WRIGHT, N. & WILSON, C. (1994). Are different antagonist pA_2 values against endothelin-1 and endothelin-3 due to different ET_A receptor subtypes in guinea-pig, rat and rabbit vascular tissue? *Br. J. Pharmacol.*, **112**, 550P.

SUDJARWO, S.A., HORI, M., TANAKA, T., MATSUDA, Y., OKADA, T. & KARAKI, H. (1994). Subtypes of endothelin ET_A and ET_B receptors mediating venous smooth muscle contraction. *Biochem. Biophys. Res. Commun.*, **200**, 627–633.

SUMNER, M.J., CANNON, T.R., MUNDIN, J.W., WHITE, D.G. & WATTS, I.S. (1992). Endothelin ETA and ETB receptors mediate vascular smooth muscle contraction. *Br. J. Pharmacol.*, **107**, 858–860.

TANAKA, T., TSUKUDA, E., NOZAWA, M., NONAKA, H., OHNO, T., KASE, H., YAMADA, K. & MATSUDA, Y. (1994). RES-701-1, a novel, potent, endothelin type B receptor-selective antagonist of microbial origin. *Mol. Pharmacol.*, **45**, 724–730.

TEERLINK, J.R., BREU, V., SPRECHER, U., CLOZEL, M. & CLOZEL, J.-P. (1994). Potent vasoconstriction mediated by ET_B receptors in canine coronary arteries. *Circ. Res.*, **74**, 105–114.

TOPOUZIS, S., HUGGINS, J.P., PELTON, J.T. & MILLER, R.C. (1991). Modulation by endothelium of the responses induced by endothelin-1 and some of its analogues in the rat isolated aorta. *Br. J. Pharmacol.*, **102**, 545–549.

TSCHIRHART, E.J., DRIJFHOUT, J.W., PELTON, J.T., MILLER, R.C. & JONES, C.R. (1991). Endothelins: functional and autoradiographic studies in the guinea-pig trachea. *J. Pharmacol. Exp. Ther.*, **258**, 381–387.

WARNER, T.D., ALLCOCK, G.H., CORDER, R. & VANE, J.R. (1993a). Use of the endothelin antagonists BQ-123 and PD 142893 to reveal three endothelin receptors mediating smooth muscle contraction and the release of EDRF. *Br. J. Pharmacol.*, **110**, 777–782.

WARNER, T.D., ALLCOCK, G.H., MICKLEY, E.J., CORDER, R. & VANE, J.R. (1993b). Comparative studies with endothelin receptor antagonists BQ-123 and PD 142893 indicate at least three endothelin receptors. *J. Cardiovasc. Pharmacol.*, **22** (Suppl. 8), S117–S120.

WARNER, T.D., DE NUCCI, G. & VANE, J.R. (1989). Rat endothelin is a vasodilator in the isolated perfused mesentery of the rat. *Eur. J. Pharmacol.*, **159**, 325–326.

WEBB, M.L., LIU, E.C., MOSHIZADEGAN, H., CHAO, C.C., LYNCH, J., FISHER, S.M. & ROSE, P.M. (1993). Expression of endothelin receptor subtypes in rabbit saphenous vein. *Mol. Pharmacol.*, **44**, 959–965.

WHITE, D.G., GARRATT, H., MUNDIN, J.W., SUMNER, M.J., VALLANCE, P.J. & WATTS, I.S. (1994). Human saphenous vein contains both ETA and ETB contractile receptors. *Eur. J. Physiol.*, **257**, 307–310.

WILLETTE, R.N., ZHANG, H., MITCHELL, M.P., SAUERMELCH, C.F., OHLSTEIN, E.H. & SULPIZIO, A.C. (1994). Nonpeptide endothelin antagonist: cerebrovascular characterization and effects on delayed cerebral vasospasm. *Stroke*, 2450–2455.

(Received November 3, 1994
Revised December 5, 1994
Accepted December 15, 1994)

British Journal of Pharmacology (1995) 114, 1541-1548 © 1995 Stockton Press All rights reserved 0007-1188/95 $12.00

Modulation by nicotinamide adenine dinucleotide of sympathetic and sensory-motor neurotransmission via P_1-purinoceptors in the rat mesenteric arterial bed

Vera Ralevic

Department of Anatomy and Developmental Biology, University College London, Gower Street, London WC1E 6BT

1 The pharmacological actions of the purine nucleotides β-nicotinamide adenine dinucleotide (NAD), β-nicotinamide adenine dinucleotide phosphate (β-NADP), adenosine 5'-diphosphoribose (ADP-ribose), the vitamin nicotinamide and structural analogues of NAD and NADP were tested in the isolated perfused mesenteric arterial bed of the rat. Prejunctional effects of NAD were tested against sympathetic vasoconstriction at basal tone, and against sensory-motor vasodilatation at raised tone.

2 NAD and NADP had no vasoconstrictor action but were weak vasodilators of the raised-tone mesenteric arterial bed. A rank order of vasodilator potency of ADP >> ADP-ribose >> NADP ≥ NAD = adenosine was observed. The P_1-purinoceptor antagonist, 8-*para*-sulphophenyltheophylline (8-*p*SPT; 3 μM) inhibited vasodilator responses to NAD (pK_B of 6.61 ± 0.21, $n = 7$) and adenosine (pK_B of 5.78 ± 0.14, $n = 6$), but not those elicited by NADP, ADP and ADP-ribose. Nicotinamide, and analogues of NAD and NADP, namely nicotinamide-1,N^6-ethenoadenine dinucleotide phosphate, β-nicotinamide mononucleotide, nicotinamide hypoxanthine dinucleotide phosphate, nicotinamide hypoxanthine dinucleotide, nicotinamide guanine dinucleotide, and nicotinamide-1,N^6-ethenoadenine dinucleotide had no vasoconstrictor or vasodilator actions (at doses of up to 50 nmol).

3 At basal tone, electrical field stimulation (EFS) (32 Hz, 1 ms, 90 V, 5 s) at 2 min intervals elicited reproducible vasoconstrictor responses due to activation of sympathetic nerves. NAD and adenosine (10-100 μM) inhibited these responses in a concentration-dependent manner with similar potencies. Nicotinamide had no effect on sympathetic vasoconstriction at concentrations of up to 0.1 mM. Postjunctional effects of NAD (100 μM), as tested on constrictor responses to NA (5 nmol), accounted for approximately 60% inhibition at this concentration.

4 In preparations in which tone had been raised with methoxamine (10-40 μM), EFS (8 Hz, 0.1 ms, 60 V, for 30 s) elicited vasodilatation due to activation of sensory-motor nerves. This vasodilatation was inhibited by NAD and adenosine (0.1-100 μM) in a similar concentration-dependent manner: pD_2 values were 6.2 ± 0.10 ($n = 11$) and 6.1 ± 0.15 ($n = 6$) for NAD and adenosine respectively. Nicotinamide had no effect on sensory-motor vasodilatation at concentrations of up to 0.1 mM.

5 Inhibition of sympathetic constriction by NAD and adenosine was antagonized by 8-*p*SPT (3 μM). Inhibitory effects of NAD and adenosine on sensory-motor vasodilatation were similarly antagonized by 8-*p*SPT (1 μM), pK_B values were 6.72 ± 0.21 for NAD and 6.36 ± 0.22 for adenosine, resulting in parallel rightward shifts in the concentration-inhibitory effect curves.

6 The adenosine deaminase inhibitor, pentostatin (1 μM), augmented the inhibitory effects of NAD and adenosine. Concentration-inhibitory effect curves for NAD and adenosine on sympathetic vasoconstriction and sensory-motor vasodilatation were shifted to the left without a change in the maximum.

7 It is concluded that NAD can act as a modulator of sympathetic and sensory-motor transmission in rat mesenteric arteries via P_1-purinoceptors possibly via direct actions but with a contribution of adenosine formed following breakdown of NAD or released pre- and/or postjunctionally. Structure-activity relationships of NAD, NADP, ADP and ADP-ribose showed that the P_1-purinoceptor activity of NAD is abolished after removal of nicotinamide, or ribose plus nicotinamide, to yield the structurally-related ADP-ribose and ADP respectively, or when there is phosphorylation of the 2'-hydroxyl group of NAD to yield NADP.

Keywords: Nicotinamide adenine dinucleotide; purinoceptors; rat mesenteric arterial bed; sympathetic transmission; sensory-motor transmission

Introduction

Extracellular purine nucleosides and nucleotides influence many biological process via P_1- and P_2-purinoceptors (Drury & Szent-Gyorgyi, 1929; Green & Stoner, 1950; Burnstock, 1978; Ralevic & Burnstock, 1991a). At present there are five well-established divisions of the P_2-purinoceptor: P_{2X}, P_{2Y}, P_{2Z}, P_{2T} and P_{2U} (synonymous with P_{2N}) (Burnstock & Kennedy, 1985; Gordon, 1986; Hoyle, 1992; Abbracchio & Burnstock, 1994); however, in a revision of purine receptor taxonomy 'P2X' and 'P2Y' will comprise extended families incorporating these receptors based on whether they function as receptor-operated ion channels, or are coupled to G-proteins, respectively (Abbracchio & Burnstock, 1994; Fredholm *et al.*, 1994). The term P_{2Z} purinoceptor will be retained since this mediates responses to ATP^{4-} by the opening of a nonselective ion pore. P_1-purinoceptors are activated by adenosine > adenosine 5'-monophosphate (AMP) > adenosine 5'-diphosphate (ADP) > adenosine-5'-triphosphate (ATP), and are antagonized by methylxanthines such as caffeine, theophylline and 8-phenyltheophylline; P_2-purinoceptors are selectively activated by ATP or ADP and are not antagonized by methylxanthines (Burnstock & Kennedy, 1985; Hoyle, 1992; Abbracchio & Burnstock, 1994). P_1-purinoceptors have been further subdivided into A_1, A_2 and A_3 classes, and antagonists with a degree of selectivity have been developed (see

Burnstock & Buckley, 1985; Cooper & Londos, 1988; Kennedy, 1990; Abbracchio *et al.*, 1993).

The coenzyme β-nicotinamide adenine dinucleotide (NAD), together with its phosphorylated and reduced forms, belongs to the family of naturally occurring adenine dinucleotides which are attracting considerable recent interest because of their potent and diverse actions as extracellular signal molecules (Hoyle, 1990; Ogilvie, 1992; Schluter *et al.*, 1994). In many tissues adenine dinucleotides act through nucleoside and nucleotide receptors; however, in some cases they appear to act via their own distinct dinucleotide receptors (see Hoyle, 1990). In the brain NAD-binding sites, distinct from those reported for adenosine, have been visualized autoradiographically (Candy *et al.*, 1984; Snell *et al.*, 1985). In the periphery and in the central nervous system the actions of NAD appear to be very similar to those of adenosine, for example: causing hyperpolarization and relaxation of the smooth muscle of the guinea-pig taenia coli (Romanenko, 1980; Romanenko *et al.*, 1980; Burnstock & Hoyle, 1985), causing prejunctional inhibition of sympathetic neuromuscular transmission in the vas deferens (Stone, 1981) and inhibiting synaptic transmission by decreasing glutamate release in rat hippocampal slices (Galarreta *et al.*, 1993). NAD may be partially degraded to adenosine, which subsequently acts on P_1-purinoceptors (Bruns, 1980a; Burnstock & Hoyle, 1985), or it may evoke release of adenosine from the tissue and activate P_1-purinoceptors via this mechanism (Stone, 1981). Phosphorylation of the 2'-hydroxyl group of NAD yields NADP which acts like a P_2-purinoceptor agonist (Burnstock & Hoyle, 1985).

Adenosine 5'-diphosphoribose (ADP-ribose) is an ADP moiety with a second ribose sugar attached to the β-phosphate via an esteric linkage. ADP-ribose is chemically related to NAD and NADP; NAD can be regarded as ADP-ribose covalently attached to the vitamin nicotinamide by a high energy β-N-glycosidic bond. Although its intracellular roles have been widely studied (Hayaishi & Ueda, 1977; Ueda & Hayaishi, 1985; Hussain *et al.*, 1989) information about the actions of ADP-ribose on extracellular receptors is limited. Hoyle & Edwards (1992) showed that ADP-ribose has a mixed pharmacological profile in the guinea-pig taenia coli, evoking both P_1 (A_2)- and P_{2Y}-purinoceptor-mediated responses, while being inactive at P_{2X}-purinoceptors in the guinea-pig vas deferens. To our knowledge, the extracellular actions of ADP-ribose in blood vessels have not been investigated.

The main aim of the present study was to examine the extracellular actions of NAD in the rat mesenteric arterial bed to see whether it acts at a specific class of adenine dinucleotide receptor or mimics the actions of adenosine at the P_1-purinoceptor. The study also aimed to examine the pharmacological profiles of the structurally related NADP, ADP and ADP-ribose. To this end, prejunctional effects of NAD and nicotinamide on sympathetic and sensory-motor transmission were tested. In rat mesenteric arteries noradrenaline (NA) is the principal sympathetic transmitter, and calcitonin gene-related peptide (CGRP) and principal vasodilator transmitter released from sensory nerves (Kawasaki *et al.*, 1988). Postjunctional actions of NAD, NADP, nicotinamide, ADP, ADP-ribose and analogues of NAD and NADP were also examined.

Methods

Isolated mesenteric arterial bed preparation

Male Wistar rats (300–350 g) were killed by asphyxiation with CO_2. Mesenteric beds were isolated and set up for perfusion as described previously (Ralevic *et al.*, 1994). The abdomen was opened and the superior mesenteric artery exposed and cannulated with a hypodermic needle. The superior mesenteric vein was severed, the gut dissected away and the preparation mounted on a stainless steel grid (7 × 5 cm) in a humid chamber (custom made at University College London). The preparation was perfused at a constant flow rate of 5 ml min^{-1} with a peristaltic pump (model 7554–30, Cole-Parmer Instrument Co., Chicago, Illinois, U.S.A.). The perfusate was Krebs solution of the following composition (mM): NaCl 133, KCl 4.7, NaH_2PO_4 1.35, $NaHCO_3$ 16.3, $MgSO_4$ 0.61, $CaCl_2$ 2.52 and glucose 7.8, gassed with 95% O_2:5% CO_2 and maintained at 37°C. Responses were measured as changes in perfusion pressure (mmHg) with a pressure transducer (model P23XL, Viggo-Spectramed, Oxnard, CA, U.S.A.) on a side arm of the perfusion cannula, and recorded on a polygraph (model 7D, Grass Instrument Co., Quincy, Mass, U.S.A.). Preparations were allowed to equilibrate for 30 min prior to experimentation.

Assessment of direct actions at basal and raised tone

The direct effects of agents were assessed at basal and raised tone by injecting 50 μl of these agents at doses of up to 1.5 μmol into a rubber septum proximal to the preparation. Vasodilator responses were examined in mesenteric arterial bed preparations in which the tone had been raised by continuous perfusion with methoxamine (10–50 μM).

Assessment of neuromodulatory effects on perivascular sympathetic and sensory-motor nerves

At basal tone intermittent pulses of EFS (32 Hz, 90 V, 1 ms for 5 s) were given at 2 min intervals to elicit vasoconstrictor responses due to activation of perivascular sympathetic nerves. These responses could be blocked by guanethidine (5 μM) or by prazosin (1 μM). In separate preparations guanethidine (5 μM) was added to the perfusate to block sympathetic transmission and methoxamine added to raise the tone of the preparations. EFS (8 Hz, 60 V, 0.1 ms for 30 s) elicited vasodilatation due to activation of sensory-motor nerves. These responses are blocked by tetrodotoxin (1 μM) or by capsaicin (Ralevic *et al.*, 1994). The effects of each of adenosine, NAD and nicotinamide on sympathetic vasoconstriction and sensory-motor vasodilatation were examined by adding these to the perfusate cumulatively (0.03–100 μM). Postjunctional effects of NAD (10, 30 and 100 μM) were tested against constrictions to repeated doses of NA (5 nmol in 50 μl) applied at 5 min intervals. These responses were reproducible for the duration of the experiment and produced a similar magnitude of constriction as EFS. Each concentration of NAD was in contact with the tissue for 10 min separated by at least 10 min washout, which allowed two applications of NA to be tested per concentration of NAD. Postjunctional effects of NAD at raised tone were tested against relaxation to CGRP (15 pmol). Pentostatin (1 μM) and 8-*p*SPT (1-10 μM) were added to the perfusate either after an initial control stimulation of sensory-motor nerves or at the onset of the experiments for sympathetic transmission, but always allowing 20 min incubation with the drug. Preliminary studies showed that 1 μM 8-*p*SPT produced a significant reversal of inhibition of sensory-motor neurotransmission, whereas 3 μM was required to reverse NAD- and adenosine-induced inhibition of sympathetic neurotransmission.

Drugs used

Drug dilutions were made up daily from stock solutions of 10 or 100 mM (concentrates stored frozen) in distilled water. The following drugs were obtained from Sigma: adenosine 5'-diphosphate (sodium salt), adenosine 5'-diphosphoribose (sodium salt), adenosine hemisulphate, β-nicotinamide adenine dinucleotide, β-nicotinamide adenine dinucleotide phosphate (sodium salt), nicotinamide-1,N^6-ethenoadenine dinucleotide

phosphate, β-nicotinamide mononucleotide, nicotinamide hypoxanthine dinucleotide phosphate (disodium salt), niacinamide, nicotinamide hypoxanthine dinucleotide (sodium salt), nicotinamide-1,N^6-ethenoadenine dinucleotide, nicotinamide guanine dinucleotide, noradrenaline bitartrate, 8-(*para*-Sulphophenyl) theophylline was from Research Biochemicals International. Pentostatin (2'-deoxycoformycin) was a generous gift from Parke-Davis, Ann Arbor, MI, U.S.A.

Data analysis

Vasodilator responses were measured as changes in perfusion pressure (mmHg) and evaluated as a percentage of the methoxamine-induced tone. Inhibition of sympathetic vasoconstriction by NAD or adenosine was evaluated as a percentage of the preceding control stimulation in the absence of these agents. Inhibition of sensory-motor vasodilatation was evaluated as a percentage of the control vasodilatation (calculated as a percentage of the methoxamine-induced increase in tone) in the absence of drugs. Results are presented as means ± s.e.mean, followed by the number of observations in parentheses (n). pD_{20} and pD_{30} are defined as the negative log of the dose (in mol) that evokes a decrease in perfusion pressure of 20 and 30 mmHg respectively. pD_2 is defined as the negative log of the dose or concentration (as appropriate) of agonist required to produce 50% of the maximal response. pK_B was evaluated from the formula $K_B = [B]/(DR-1)$, where B = concentration of agonist and DR (dose-ratio) = the difference between pD_2 values in the absence and presence of antagonist. Differences between means were determined by Student's unpaired or paired t test and were considered significant when $P<0.05$.

Results

Direct actions of NAD, NADP, nicotinamide, adenosine, ADP, ADP-ribose and analogues of NAD and NADP

At basal tone NAD, NADP, nicotinamide, ADP-ribose and analogues of NAD and NADP had no vasoconstrictor actions. In experiments with raised tone, methoxamine (10–50 μM) increased the tone of the preparations by 60.85 ± 3.17 from a basal tone of 37.64 ± 1.21 mmHg (n = 14). Nucleotides elicited vasodilatation with a potency order of ADP >> ADP-ribose >> NADP > NAD = adenosine (Figure 1). pD_2 values were 10.33 ± 0.12 (n = 8) for ADP, 8.20 ± 0.14 for ADP-ribose (n = 7) and 7.59 ± 0.06 for NADP (n = 12). There was no significant difference between the pD_{30} values for NAD and adenosine, which were 6.73 ± 0.07 (n = 7) and 6.91 ± 0.14 (n = 8) respectively. Maximum vasodilatation to NADP, 35.49 ± 3.72% at 0.5 μmol (n = 12), was significantly smaller than that of the other vasodilators, and was less than half of the maximum vasodilatation to ADP, 84.20 ± 2.80% (n = 8). At the highest dose of NADP, vasoconstriction following the initial relaxation was sometimes observed. Nicotinamide had no vasodilator actions. None of the analogues of NAD and NADP had vasodilator actions at doses of up to 50 nmol; at the highest dose tested (500 nmol) only nicotinamide hypoxanthine dinucleotide, nicotinamide hypoxanthine dinucleotide phosphate and nicotinamide-1,N^6-ethenoadenine dinucleotide elicited weak vasodilatation in two of four preparations.

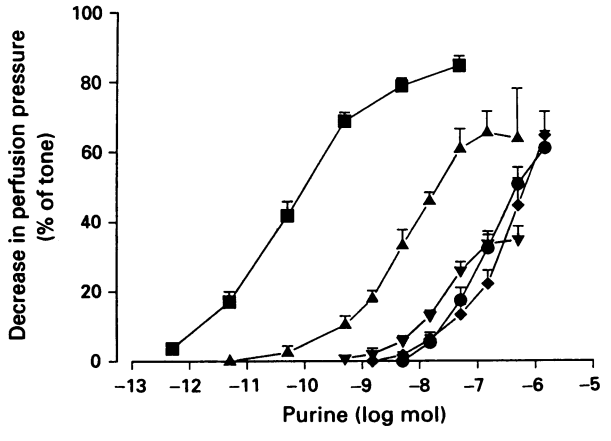

Figure 1 Dose-response curves showing vasodilator responses of the rat mesenteric arterial bed to ADP (■, n = 8), ADP-ribose (▲, n = 8), NADP (▼, n = 12), NAD (◆, n = 8) and adenosine (●, n = 8). Responses are shown as percentage decrease in methoxamine-evoked tone. Data are given as means ± s.e.mean. For abbreviation in this and subsequent figures, see text.

*Effect of 8-*para*-sulphophenyltheophylline (8-pSPT) on vasodilator responses*

Addition of the P_1-purinoceptor antagonist 8-*p*SPT (3 μM) to the perfusate caused a tendency for the tone of the preparations to increase; by reducing the methoxamine concentration the increase in tone (66.75 ± 6.60 mmHg, n = 12) was not statistically different from that in the absence of 8-*p*SPT. 8-*p*SPT (3 μM) antagonized responses to NAD and adenosine, shifting to the right the dose-response curves (Figure 2). pD_{20} values for adenosine were 7.22 ± 0.17 and 6.78 ± 0.14 (n = 6) in the absence and presence of 8-*p*SPT ($P<0.05$). pD_{20} values for NAD were 7.07 ± 0.12 and 5.93 ± 0.24 (n = 7) in the absence and presence of 8-*p*SPT ($P<0.001$). In the presence, but not in the absence, of 8-*p*SPT there was a significant difference between the pD_{20} values for adenosine and NAD ($P<0.05$). pK_B values for the effect of 8-*p*SPT on adenosine, 5.78 ± 0.14 (n = 6), and NAD, 6.61 ± 0.21 (n = 7), were also significantly different ($P<0.01$). Vasodilatations due to NADP, ADP and ADP-ribose were not antagonized by 8-*p*SPT (Figure 2).

Effect of NAD and adenosine on sympathetic vasoconstriction

At basal tone intermittent pulses of EFS (32 Hz, 1 ms, 90 V for 5 s) at 2 min intervals elicited constrictor responses due to activation of sympathetic nerves (Figure 3a). These averaged 26.1 ± 2.7 mmHg (n = 42) at the start of experimentation and were relatively stable being 27.5 ± 2.0 mmHg (n = 42) at the end of the experiment. Vasoconstrictor responses were attenuated in a concentration-dependent manner by NAD and adenosine (10–100 μM) (Figures 3a, b and 4). The concentration-inhibitory effect curves to NAD and adenosine were superimposable. There was no significant difference between inhibition of sympathetic vasoconstriction by NAD and adenosine at any concentration. Inhibition attained at the highest concentration tested (100 μM) was 63.54 ± 9.0% (n = 8) and 56.55 ± 3.69% (n = 7) for NAD and adenosine respectively. Nicotinamide had no effect on sympathetic vasoconstriction at concentrations of up to 100 μM.

The inhibitory effects of 10 μM NAD and adenosine were abolished by 8-*p*SPT (3 μM), and were significantly antagonized, by approximately 70% at 30 μM NAD and adenosine (Figure 4). At 100 μM NAD responses were significantly antagonized, by approximately 50%, by 8-*p*SPT ($P<0.01$); inhibition by NAD was 68.49 ± 8.03% (n = 4) and 32.58 ± 4.84% (n = 8) in the absence and presence of 8-*p*SPT respectively. In contrast, inhibition by 100 μM adenosine was unaffected by 8-*p*SPT; inhibition was 56.55 ± 3.69% (n = 4) and 58.99 ± 6.0% (n = 8) in the absence and presence of 8-*p*SPT respectively.

Inhibition of adenosine deaminase with pentostatin augmented the inhibitory effects of both NAD and adenosine,

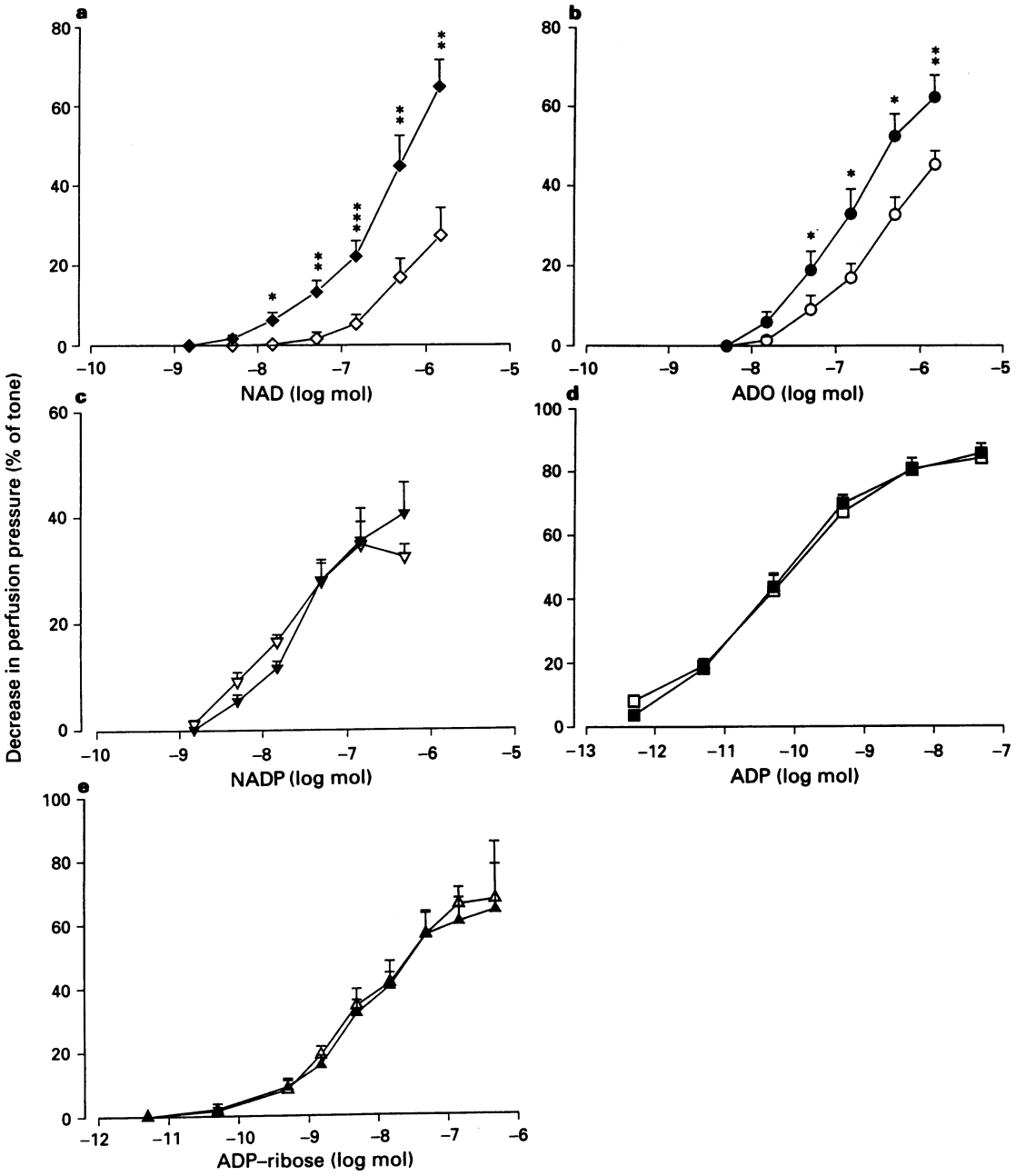

Figure 2 Dose-response curves showing vasodilator responses of purine compounds in the rat mesenteric arterial bed in the absence (closed symbols) and presence of 8-*para*-sulphophenyltheophylline (3 μM) (open symbols): (a) NAD (◆, $n = 8$); (b) adenosine (●, $n = 6$); (c) NADP (▼, $n = 6$); (d) ADP (■, $n = 7$); (e) ADP-ribose (▲, $n = 8$). Data are given as mean ± s.e.mean.

lowering the threshold for inhibition to approximately 3 μM without changing the maximum (Figure 4).

Exogenously applied doses of NA (5 nmol) elicited vasoconstriction of 25.71 ± 2.33 mmHg under control conditions in eight preparations. NAD inhibited these responses by 5.49 ± 1.92% (10 μM NAD), 24.33 ± 3.42% (30 μM NAD) and 38.11 ± 3.77% (100 μM NAD).

Effect of NAD and adenosine on sensory-motor vasodilatation

Methoxamine raised the tone of the preparations by 48.25 ± 2.0 mmHg from 33.32 ± 0.6 mmHg ($n = 47$). EFS (8 Hz, 0.1 ms, 60 V, 30 s) elicited frequency-dependent vasodilatation of the mesenteric arterial bed preparations. Mean vasodilatation in the absence of agents was 48.4 ± 2.3% ($n = 47$). In the presence of NAD or adenosine (0.1–100 μM) vasodilator responses were attenuated in a concentration-dependent manner (Figures 3b and 5). There was no significant difference in the maximum inhibition, approximately 67.73 ± 6.42% ($n = 6$) and 71.81 ± 9.32% ($n = 10$) inhibition by 30 μM adenosine and NAD respectively. Relaxation to 15 pmol CGRP in the presence of 10 μM NAD was 42.09 ± 8.99% ($n = 6$), which is similar to that obtained in the absence of NAD (Ralevic *et al.*, 1994). Above 30 μM, NAD and adenosine had some postjunctional effects causing the tone of the preparation to drop. Nicotinamide had no inhibitory effects on sensory-motor vasodilatation.

8-*p*SPT (1 and 10 μM) blocked the inhibitory effects of NAD and adenosine, shifting to the right the inhibitory-effect curves. The pD_2 of NAD was significantly decreased from 6.20 ± 0.1 ($n = 11$) in control conditions to 5.40 ± 0.18 ($n = 6$) and 5.08 ± 0.13 ($n = 4$) in the presence of 1 μM 8-*p*SPT ($P < 0.01$) and 10 μM 8-*p*SPT ($P < 0.001$). The pD_2 of adeno-

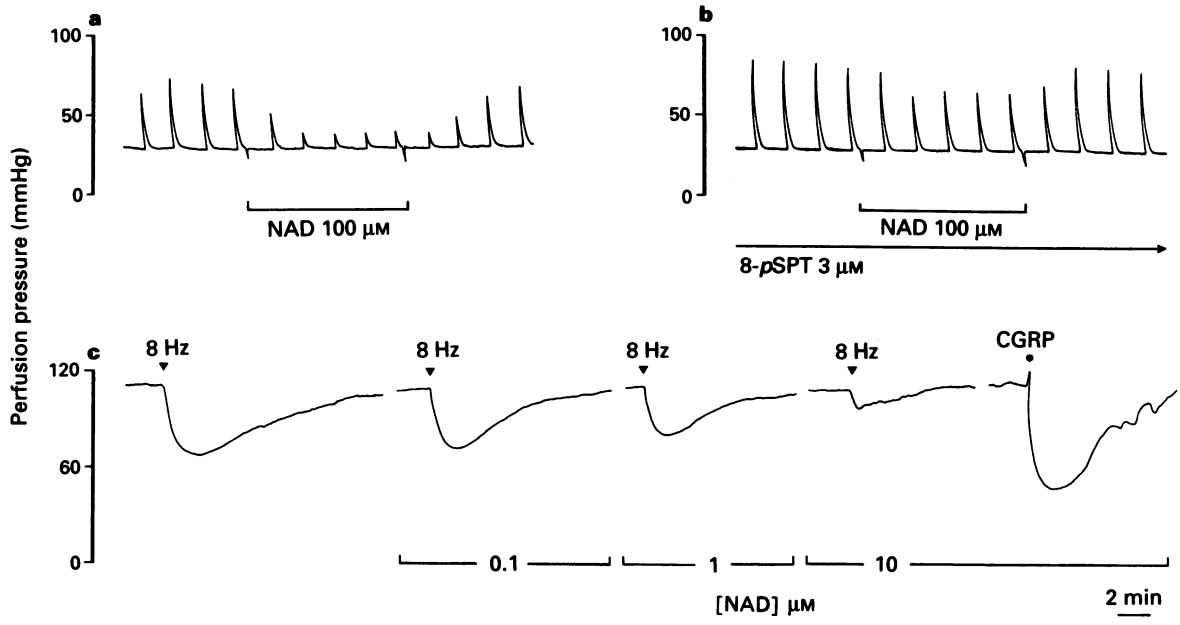

Figure 3 Representative traces showing effect of nicotinamide adenine dinucleotide (NAD) on responses of the rat isolated mesenteric arterial bed to electrical field stimulation (EFS) at basal tone (a,b) and at raised tone (tone raised with methoxamine) in the presence of guanethidine (c). (a) Inhibition of sympathetic constriction to EFS (32 Hz, 90 V, 1 m, 5 s) by 100 μM NAD, (b) reversal of sympathetic inhibition by 100 μM NAD with 8-*para*-sulphophenyltheophylline (8-*p*SPT, 3 μM), (c) concentration-dependent inhibition of sensory-motor vasodilatation to EFS (8 Hz, 60 V, 0.1 ms, 30 s) by NAD (0.1, 1 and 10 μM) and lack of effect of 10 μM NAD on relaxation to a dose of calcitonin gene-related peptide (CGRP, 15 pmol).

sine was significantly decreased from 6.10 ± 0.15 (n = 6) to 5.58 ± 0.16 (n = 6) in the presence of 1 μM 8-*p*SPT (P < 0.05) (Figure 5). There was no significant difference in pK_B values (mean ± 95% confidence limits) for 8-*p*SPT with adenosine, 6.36 ± 4.14, 8.59, and NAD, 6.72 ± 4.59, 8.85.

Pentostatin (1 μM) potentiated the effects of NAD and adenosine (Figure 5), producing a parallel shift to the right of the concentration-inhibitory effect curves without affecting the maximum. In the presence of pentostatin the pD_2 of NAD increased to 6.51 ± 0.17 (n = 7) and of adenosine to 6.31 ± 0.1 (n = 5), although these differences did not reach statistical significance.

Discussion

The results of this study show that NAD mimics the actions of adenosine in rat mesenteric arteries; it can act as a prejunctional modulator of sympathetic and sensory-motor neurotransmission and is also a relatively weak postjunctional vasodilator. Attenuation of pre- and postjunctional effects of NAD by 8-*p*SPT indicates an action at P_1-purinoceptors, while potentiation of inhibitory neuromodulation by the adenosine deaminase inhibitor, pentostatin, suggests that at least part of the effect of NAD is mediated via adenosine. The structurally related NADP and ADP-ribose were both vasodilators but were functionally dissimilar to NAD since they did not act at P_1-purinoceptors.

Several possibilities are considered for the mechanism(s) by which NAD elicits its pre- and postjunctional effects: it may act directly at nucleoside, nucleotide or dinucleotide receptors; it may act via adenosine following breakdown; finally, NAD may act via adenosine released from neural or other tissues (Stone, 1981; Stone & Perkins, 1981). Distinct receptors for the adenine dinucleotides have been described for NAD in the central nervous system (Richards *et al.*, 1983a,b; Snell *et al.*, 1985), and for certain of the α,ω-polyphosphates in some peripheral and central tissues (Hilderman *et al.*, 1991; Pintor *et al.*, 1993). To date there is no evidence for distinct adenine dinucleotide receptors in rat mesenteric arteries. Postjunctional effects of α,ω-polyphosphates in these vessels have been shown to be mediated via nucleotide receptors (Ralevic *et al.*, 1995); vasoconstriction is via P_{2X}-purinoceptors on the smooth muscle; vasodilatation is via P_{2Y}-purinoceptors on endothelial cells (Ralevic & Burnstock, 1988; 1991b).

The results of the present study show that P_1-purinoceptors are implicated in the effects of NAD because of antagonism by 8-*p*SPT. NAD was equipotent with adenosine with respect to pre- and postjunctional effects, suggesting that it acts directly at P_1-purinoceptors. However, potentiation of the effects of NAD by pentostatin indicates that at least part of its actions are mediated by adenosine. Further experiments are required to determine to what extent degradation or induction of adenosine release from postjunctional sources is involved. Breakdown of NAD to adenosine would be due to the enzyme 5'-nucleotidase, located exclusively on the extracellular face of the plasma membrane. Breakdown of adenosine in rat tissues is known to be an extremely rapid process and is potentiated markedly by inhibitors of adenosine deaminase such as pentostatin (Henderson *et al.*, 1977; Padua *et al.*, 1990; Klohs & Kraker, 1992). Burnstock & Hoyle (1985) reported a significant degradation of NAD to adenosine during passage over a preparation of the guinea-pig taenia coli. In that preparation, as in the present study, NAD was found to act at P_1-purinoceptors at least partly following breakdown to adenosine, while the actions of NADP were similar to those of a P_2-purinoceptor agonist (Burnstock & Hoyle, 1985). In the guinea-pig taenia coli, dipyridamole, a purine nucleoside uptake inhibitor, markedly potentiated responses to NAD, confirming an involvement of adenosine (Burnstock & Hoyle, 1985). Dipyridamole could not be used in the present study since it caused direct relaxation of the mesenteric arterial vasculature at operant concentrations. A necessity for NAD to be broken down to adenosine before acting on P_1-purinoceptors has been claimed in human fibroblasts (Bruns, 1980a). On the other hand, compared to the mononucleotides, adenine dinucleotides are known to have relatively long half-lives in plasma and in physiological solu-

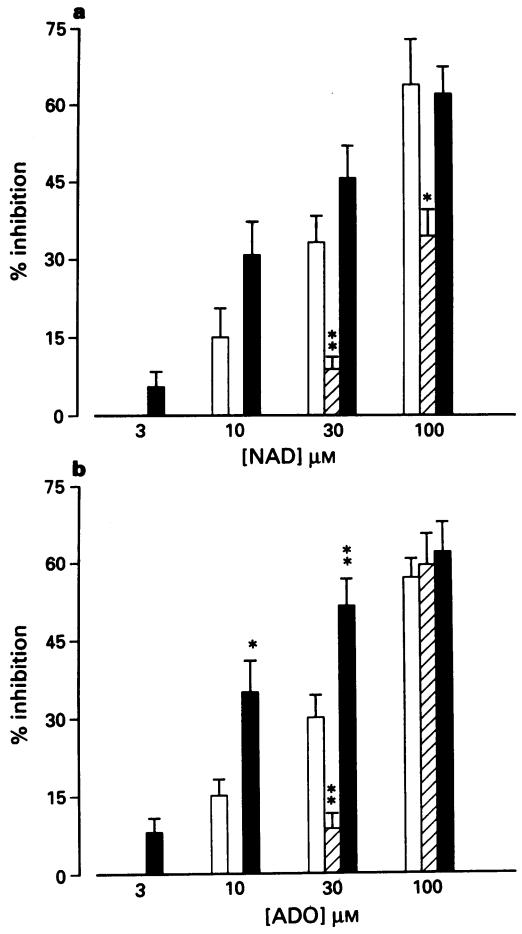

Figure 4 Graphs showing inhibitory effects of (a) nicotinamide adenine dinucleotide (NAD, $n = 4-8$) and (b) adenosine (ADO, $n = 4-8$) on vasoconstriction to electrical field stimulation of the rat mesenteric arterial bed at basal tone. There was no inhibition of sympathetic constrictor responses by NAD and adenosine at 3 μM in the absence of pentostatin and at 10 μM in the presence of 8-*para*-sulphophenyltheophylline (8-*p*SPT). Open columns, NAD or adenosine alone; hatched columns, NAD or adenosine in the presence of 8-*p*SPT (3 μM); solid columns, NAD or adenosine in presence of pentostatin (1 μM).

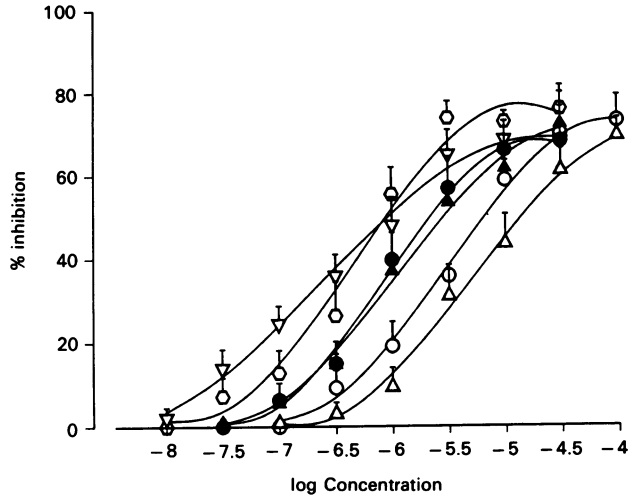

Figure 5 Concentration-dependent inhibition of sensory-motor vasodilatation of the rat mesenteric arterial bed in the presence of: nicotinamide adenine dinucleotide (NAD) alone (▲, $n = 10$); adenosine alone (●, $n = 6$); NAD in the presence of 8-*para*-sulphophenyltheophylline (8-*p*SPT) (3 μM) (△, $n = 6$); adenosine in the presence of 8-*p*SPT (3 μM) (○, $n = 6$); NAD in the presence of pentostatin (1 μM) (▽, $n = 7$); adenosine in the presence of pentostatin (1 μM) (○ $n = 5$).

tion (Luthjie & Ogilvie, 1988; Busshardt *et al.*, 1989; Ogilvie, 1992). Until more comprehensive data on NAD breakdown are available it is not possible to determine to what extent the action of NAD is dependent on the formation versus the release of adenosine in rat mesenteric arteries.

Interestingly, 8-*p*SPT was a more potent antagonist of NAD than adenosine both for postjunctional vasodilatation and for inhibition of sympathetic constriction at 100 μM of these purine compounds. These results suggest that NAD and adenosine are acting on different receptors. One possibility is that NAD may be acting on a distinct dinucleotide receptor, which would still be classified as a P_1-purinoceptor by virtue of antagonism by 8-*p*SPT. It is also possible that NAD and adenosine are acting at different currently recognised subtypes of the P_1-purinoceptor. A greater antagonism by 8-PT of responses to NAD compared to those of adenosine has been reported previously in the guinea-pig taenia coli, where the relative antagonism of NAD was an order of magnitude greater than that of adenosine (Burnstock & Hoyle, 1985; Hoyle & Edwards, 1992). The data from those studies showed an even greater difference in the inhibitory effect of 8-PT on NAD and adenosine than seen with 8-*p*SPT in the present study, supporting the concept of activation of different receptors. Postjunctional actions of NAD contributed significantly to its inhibitory effect on sympathetic constriction, and it is likely that this is also the case for adenosine which was equipotent as a vasodilator. The greater inhibition of NAD-mediated compared to adenosine-mediated sympathetic inhibition by 8-*p*SPT may be a reflection of the greater inhibition by 8-*p*SPT of the postjunctional effects of NAD.

Both NAD and adenosine were relatively weak vasodilators of the rat mesenteric arterial bed and it is likely that their more important extracellular role in rat mesenteric vessels is prejunctional modulation of sympathetic and sensory-motor neurotransmission. The greater potency of NAD and adenosine as inhibitors of sensory-motor compared to sympathetic neurotransmission (10 μM of these agents was approximately threshold for inhibition of sympathetic neurotransmission, but caused maximum inhibition of sensory-motor neurotransmission) may be because higher parameters of stimulation were used to elicit sympathetic vasoconstriction compared to sensory-motor nerve-mediated vasodilatation. This would also explain why a higher concentration of 8-*p*SPT was required to produce a significant attenuation of the inhibitory effects of adenosine and NAD on sympathetic compared to sensory-motor neurotransmission. Sensory-motor vasodilatation of the rat mesenteric arterial bed is mediated by the release of CGRP from capsaicin-sensitive afferents (Kawasaki *et al.*, 1988). Prejunctional modulation of sympathetic and sensory-motor neurotransmission by adenosine is mediated via P_1-purinoceptors of the A_1-subtype (Jackson, 1987; Rubino *et al.*, 1994); however, it is possible that different subtypes of A_1-purinoceptors are present on sympathetic and sensory-motor nerve terminals, or that different prejunctional inhibitory transduction mechanisms are involved.

Within the cell, ADP-ribose may regulate the activities of a number of enzymes, either by covalent attachment to, or by physical association with these enzymes (Hussain *et al.*, 1989). ADP-ribosylation of specific proteins is thought to occur in almost all forms of life and almost all compartments of the cell, and has been implicated in the control of a number of biological events (Hayaishi & Ueda, 1977; Ueda & Hayaishi, 1985). However, the extracellular actions of ADP-ribose, particularly on vascular preparations, have received little attention. This study shows that this molecule can act as

as a vasodilator, possibly at P_2-purinoceptors of the P_{2Y} subtype, but not at P_1-purinoceptors since vasodilatation was not inhibited by 8-*p*SPT. In contrast to rat mesenteric arteries, relaxant effects of ADP-ribose in the guinea-pig taenia coli are mediated by both P_1 (A_2)- and P_{2Y}-purinoceptors (Hoyle & Edwards, 1992). ADP-ribose does not appear to be an agonist at P_{2X}-purinoceptors (it did not cause constriction), in agreement with results obtained in the vas deferens (Fedan *et al.*, 1986; Hoyle & Edwards, 1992). It was not possible to test directly the involvement of P_2-purinoceptors since available compounds with P_{2Y}-purinoceptor antagonist activity (for instance suramin and reactive blue 2) (Burnstock & Warland, 1987; Dunn & Blakeley, 1988) produce a substantial drop in tone of the raised-tone mesenteric arterial preparation at operant concentrations.

The length of the polyphosphate chain and hence its negative charge (each phosphate carries a single negative charge) has been proposed as crucial for postjunctional activity of adenine dinucleotides; four or more phosphates/negative charges are required for vasoconstrictor activity while three or less phosphates/negative charges are required for vasodilator action (Ralevic *et al.*, 1995). According to the criteria established in that study of structure-activity relationships of the adenine dinucleotides (Ralevic *et al.*, 1995), NAD, having a pyrophosphate chain and two negative charges, qualifies as a vasodilator and not a vasoconstrictor, as was indeed found. Further support for the hypothesis that it is the charge carried by the molecule which is crucial for activity, rather than the number of phosphates *per se*, is the fact that ADP-ribose, carrying a maximum of two negative charges, is a vasodilator but not a vasoconstrictor, whereas ADP, having the same number of phosphates but carrying a maximum of three negative charges is a vasoconstrictor via P_{2X}-purinoceptors as well as being a potent vasodilator. However, steric hindrance presented by the ribose moiety may also be implicated in the weaker potency of ADP-ribose as a vasodilator compared to ADP.

Some interesting observations can be made from the structure-activity relationships of ADP, ADP-ribose and NAD, which highlight an important role of the ribose and nicotinamide moieties in determining the pharmacological profile of the molecule. Addition of ribose to ADP abolishes the P_{2X}-purinoceptor activity inherent in ADP and the resulting compound, ADP-ribose, is also less potent than ADP as a vasodilator at P_{2Y}-purinoceptors. The pharmacology of ADP-ribose is also different from that of ATP, from which it differs only in that the terminal phosphate is replaced by a ribose moiety, since ATP is a vasoconstrictor as well as a vasodilator at P_{2X}- and P_{2Y}-purinoceptors respectively. Further addition of nicotinamide, which had no actions *per se*, to ADP-ribose has a dramatic effect on agonist profile since it produces NAD, having P_1-, but not P_2-purinoceptor activity. Hence, moieties which are inert themselves, can crucially determine agonist potency as well as subtype of purine receptor that is activated by the molecule into which they are substituted. Mechanism(s) by which nicotinamide and/or ribose substitutions can produce profound effects on agonist profile may include steric hindrance at the receptor binding site or alterations in the strength and distribution of the negative charge of the pyrophosphate chain.

Vasodilatation by NADP was not mediated via P_1-purinoceptors since it was not antagonized by 8-*p*SPT, and is likely to be via P_2-purinoceptors, as in the guinea-pig taenia coli (Burnstock & Hoyle, 1985). These findings indicate that NAD and NADP act on separate classes of receptors with different mechanisms of action and is consistent with the fact that phosphorylation of the 2'-hydroxyl group is essential for P_1-purinoceptor activation (Londos & Wolff, 1977; Bruns, 1980b). Further, the 2'-phosphate group renders NADP resistant to cleavage by 5'-nucleotidase (Burger & Lowenstein, 1970). P_{2Y}-purinoceptors may be involved since vasodilatation to NADP is dependent on an intact endothelium (Ralevic *et al.*, 1995). An implication of the lack of P_1-purinoceptor activity of NADP is that it is unlikely to be able to modulate prejunctionally sympathetic or sensory-motor neurotransmission.

Nicotinamide mononucleotide was ineffective as a vasodilator, whereas AMP, equivalent to NAD without nicotinamide mononucleotide, is a weak vasodilator of the rat mesenteric arterial bed (unpublished observations), indicating that the purine moiety is important for vasodilator activity. None of the remaining analogues of NAD and NADP had significant postjunctional vasoconstrictor or vasodilator actions, which indicates that structural modifications of these molecules can profoundly affect their pharmacological actions.

In conclusion, these results show that in rat mesenteric arteries NAD can act prejunctionally as an inhibitory modulator of sympathetic and sensory-motor neurotransmission via P_1-purinoceptors, partly via adenosine. It is also a weak postjunctional vasodilator. In contrast, P_1-purinoceptor activity was absent in ADP-ribose (equivalent to NAD without nicotinamide) which was a relatively potent vasodilator, probably at P_2-purinoceptors. Additional studies are warranted to examine whether these molecules, traditionally associated with intracellular events, are released from cells under physiological or pathophysiological conditions to locally modulate vascular tone.

The support of the British Heart Foundation is gratefully acknowledged. Prof. G. Burnstock and Dr C.H.V. Hoyle are thanked for comments on the manuscript.

References

ABBRACCHIO, M. & BURNSTOCK, G. (1994). Purinoceptors: are there families of P2X and P2Y purinoceptors? *Pharmacol. Ther.*, **64**, 445–475.

ABBRACCHIO, M.P., CATTABENI, F., FREDHOLM, B.B. & WILLIAMS, M. (1993). Purinoceptor nomenclature: a status report. *Drug. Dev. Res.*, **28**, 207–213.

BRUNS, R.F. (1980a). Adenosine receptor activation by adenine dinucleotides requires conversion of the nucleotides to adenosine. *Naunyn-Schmied. Arch. Pharmacol.*, **315**, 5–13.

BRUNS, R.F. (1980b). Adenosine receptor activation in human fibroblasts: nucleoside agonists and antagonists. *Can. J. Physiol. Pharmacol.*, **58**, 673–691.

BURGER, R.M. & LOWENSTEIN, J.M. (1970). Preparation and properties of 5'-nucleotidase from smooth muscle of small intestine. *J. Biol. Chem.*, **245**, 6274–6280.

BURNSTOCK, G. (1978). A basis for distinguishing two types of purinergic receptor. In *Cell Membrane Receptors for Drugs and Hormones: a Multidisciplinary Approach*, ed. Straub, R.W. & Bolis, L. pp. 107–118. New York: Raven Press.

BURNSTOCK, G. & BUCKLEY, N.J. (1985). The classification of receptors for adenosine and adenine nucleotides. In *Methods Used in Adenosine Research (Methods in Pharmacology Series)*. ed. Paton, D.M. pp. 193–212. New York: Plenum Press.

BURNSTOCK, G. & HOYLE, C.H.V. (1985). Actions of adenine dinucleotides in the guinea-pig taenia coli: NAD acts indirectly on P_1-purinoceptors; NADP acts like a P_2-purinoceptor agonist. *Br. J. Pharmacol.*, **84**, 825–831.

BURNSTOCK, G. & KENNEDY, C. (1985). Is there a basis for distinguishing two types of P_2-purinoceptor? *Gen. Pharmacol.*, **16**, 433–440.

BURNSTOCK, G. & WARLAND, J.J.I. (1987). P_2-purinoceptors of two subtypes in rabbit mesenteric artery: RB2 selectively inhibits responses mediated via the P_{2y}- but not the P_{2x}-purinoceptor. *Br. J. Pharmacol.*, **90**, 383–391.

BUSSHARDT, E., GEROK, W. & HAUSSINGER, D. (1989). Regulation of hepatic parenchymal and non-parenchymal cell function by diadenine nucleotides Ap_3A and Ap_4A. *Biochim. Biophys. Acta*, **1010**, 151–159.

CANDY, J.M., SNELL, C.R. & SNELL, P.H. (1984). Autoradiographic localization of nicotinamide adenine dinucleotide binding sites in the rat brain. *Br. J Pharmacol.*, **82**, 311P.

COOPER, D.M.F. & LONDOS, C. (1988). *Receptor Biochemistry and Methodology*, Vol. II. *Adenosine Receptors*. New York: Alan R. Liss.

DRURY, A.N. & SZENT-GYORGYI, A. (1929). The physiological activity of adenine compounds with special reference to their action upon mammalian heart. *J. Physiol.*, **68**, 213–237.

DUNN, P.M. & BLAKELEY, A.G. (1988). Suramin: a reversible P_2-purinoceptor antagonist in the mouse vas deferens. *Br. J. Pharmacol.*, **93**, 243–245.

FEDAN, J.S. HOGABOOM, G.K. & O'DONNELL, J.P. (1986). Further comparison of the contractions of the smooth muscle of the guinea-pig isolated vas deferens induced by ATP and related compounds. *Eur. J. Pharmacol.*, **129**, 279–291.

FREDHOLM, B.B., ABBRACCHIO, M.P., BURNSTOCK, G., DALY, J.W., HARDEN, T.K., JACOBSON, K.A., LEFF, P. & WILLIAMS, M. (1994). Nomenclature and classification of purinoceptors. *Pharmacol. Rev.*, **46**, 143–156.

GALARRETA, M., SOLIS, J.M., MENENDEZ, N., CONEJERO, C. & MARTIN DEL RIO, R. (1993). Nicotinamide adenine dinucleotides mimic adenosine inhibition on synaptic transmission by decreasing glutamate release in rat hippocampal slices. *Neurosci. Lett.*, **159**, 55–58.

GORDON, J.L. (1986). Extracellular ATP: effects, sources and fate. *Biochem. J.*, **233**, 309–319.

GREEN, H.N. & STONER, H.B. (1950). *Biological Actions of the Adenine Nucleotides*. London: Lewis.

HAYAISHI, O. & UEDA, K. (1977). Poly (ADP-ribose) and ADP-ribosylation of proteins. *Annu. Rev. Biochem.*, **46**, 95–116.

HENDERSON, J.F., BROX, L., ZOMBOR, G., HUNTING, D. & LOMAX, C.L. (1977). Specificity of adenosine deaminase inhibitors. *Biochem. Pharmacol.*, **26**, 1967–1972.

HILDERMAN, R.H., MARTIN, M., ZIMMERMAN, J.K. & PIVORUN, E.B. (1991). Identification of a unique membrane receptor for adenosine 5′,5‴-P_1,P_4-tetraphosphate. *J. Biol. Chem.*, **266**, 6915–6918.

HOYLE, C.H.V. (1990). Pharmacological activity of adenine dinucleotides in the periphery: possible receptor classes and transmitter function. *Gen. Pharmacol.*, **21**, 827–831.

HOYLE, C.H.V. (1992). Transmission: purines. In *Autonomic Neuroeffector Mechanisms*. ed. Burnstock, G. & Hoyle, C.H.V. pp. 367–407. Reading: Harwood Academic.

HOYLE, C.H.V. & EDWARDS, G.A. (1992). Activation of P_1- and P_{2Y}-purinoceptors by ADP-ribose in the guinea-pig taenia coli, but not of P_{2X}-purinoceptors in the vas deferens. *Br. J. Pharmacol.*, **107**, 367–374.

HUSSAIN, M.Z., GHANI, Q.P. & HUNT, T.K. (1989). Inhibition of propylhydroxylase by poly (ADPR) and phosphoribosyl-AMP. *J. Biol. Chem.*, **264**, 7850–7855.

JACKSON, E.K. (1987). Role of adenosine in noradrenergic neurotransmission in spontaneously hypertensive rats. *Am. J. Physiol.*, **253**, H909–H918.

KAWASAKI, H., TAKASAKI, K., SAITO, A. & GOTO, K. (1988). Calcitonin gene-related peptide acts as a novel vasodilator neurotransmitter in mesenteric resistance vessels of rat. *Nature*, **335**, 165–167.

KENNEDY, C. (1990). P_1- and P_2-purinoceptor subtypes – an update. *Arch. Int. Pharmacodyn.*, **303**, 30–50.

KLOHS, W. & KRAKER, A.J. (1992). Pentostatin: future directions. *Pharmacol. Rev.*, **44**, 459–477.

LONDOS, C. & WOLFF, J. (1977). Two distinct adenosine-sensitive sites on adenylate cyclase. *Proc. Natl. Acad. Sci. U.S.A.*, **74**, 5482–5486.

LUTHJE, J. & OGILVIE, A. (1988). Catabolism of Ap_4A and Ap_3A in whole blood. The dinucleotides are long-lived signal molecules in blood ending up as intracellular ATP in erythrocytes. *Eur. J. Biochem.*, **173**, 241–245.

OGILVIE, A. (1992). Extracellular functions for Ap_nA. In *Ap_4A and other Dinucleoside Polyphosphates*. ed. McLennan, A.G. pp. 229–273. Boca Raton: CRC Press.

PADUA, R., GEIGER, J.D., DAMBOCK, S. & NAGY, J.J.I. (1990). 2′-Deoxycoformycin inhibition of adenosine deaminase in rat brain: in vivo and in vitro analysis of specificity, potency, and enzyme recovery. *J. Neurochem.*, **54**, 1169–1178.

PINTOR, J., DIAZ-REY, A. & MIRAS-PORTUGAL, T. (1993). Ap_4A and ADP-β-S binding to P_2 purinoceptors present on rat brain synaptic terminals. *Br. J. Pharmacol.*, **108**, 1094–1099.

RALEVIC, V. & BURNSTOCK. G. (1988). Actions mediated by P_2-purinoceptor subtypes in the isolated perfused mesenteric bed of the rat. *Br. J. Pharmacol.*, **95**, 637–645.

RALEVIC, V. & BURNSTOCK. G. (1991a). Roles of P_2-purinoceptors in the cardiovascular system. *Circulation*, **84**, 1–14.

RALEVIC, V. & BURNSTOCK. G. (1991b). Effects of purines and pyrimidines on the rat mesenteric arterial bed. *Circ. Res.*, **69**, 1583–1590.

RALEVIC, V., HOYLE, C.H.V. & BURNSTOCK. G. (1995). Pivotal role of phosphate chain length in vasoconstrictor *versus* vasodilator actions of adenine nucleotides in rat mesenteric arteries. *J. Physiol.*, (in press).

RALEVIC, V., RUBINO, A. & BURNSTOCK. G. (1994b). Prejunctional modulation of sensory-motor nerve-mediated vasodilatation of the rat mesenteric arterial bed by opioid peptides. *J. Pharmacol. Exp. Ther.*, **268**, 772–778.

RICHARDS, C.D., SNELL, C.R. & SNELL, P.H. (1983a). Nicotinamide adenine dinucleotide (NAD) suppresses excitatory synaptic transmission in the dentate gyrus of the guinea-pig. *J. Physiol.*, **336**, 63–64P.

RICHARDS, C.D., SNELL, C.R. & SNELL, P.H. (1993b). Nicotinamide adenine dinucleotide depresses synaptic transmission in the hippocampus and has specific binding sites on the synaptic membranes. *Br. J. Pharmacol.*, **79**, 553–564.

ROMANENKO, A.V. (1980). Vitamin PP, nicotinamide nucleotides and nerve muscular transmission in guinea-pig caecum longitudinal muscle (taenia coli). *Ukrainskii Biochimicheskii Zhurnal (Kiev)*, **52**, 624–627.

ROMANENKO, A.V., BAIDAN, L.V., KHALMURADOV, A.G. & SHUBA, M.F. (1980). The mechanism of action of vitamin PP and nicotinamide nucleotides on nerve muscle transmission in taenia coli of guinea-pig. *Doklady Akad. Nauk. USSR*, **243**, 493–496.

RUBINO, A., RALEVIC, V. & BURNSTOCK, G. (1994). The P_1-purinoceptors that mediate the prejunctional effect of adenosine on capsaicin-sensitive non-adrenergic non-cholinergic neurotransmission in the rat mesenteric arterial bed are of the A_1 subtype. *J. Pharmacol. Exp. Ther.*, **267**, 1100–1104.

SCHLUTER, H., OFFERS, E., BRUGGEMANN, G., VAN DER GIET, M., TEPEL, M., NORDHOFF, E., KARAS, M., SPIEKER, C., WITZEL, H. & ZIDEK, W. (1994). Diadenosine phosphates and the control of blood pressure. *Nature*, **367**, 186–188.

SNELL, P.H., SNELL, C.R. & RICHARDS, C.D. (1985). Stereospecific binding sites for [^{3}H]nicotinamide adenine dinucleotide in the rat brain. *Eur. J. Pharmacol.*, **116**, 121–127.

STONE, T.W. (1981). Actions of adenine dinucleotides on the vas deferens, guinea-pig taenia caeca and bladder. *Eur. J. Pharmacol.*, **75**, 93–102.

STONE, T.W. & PERKINS, M.N. (1981). Adenine dinucleotide effects on rat cortical neurones. *Brain Res.*, **229**, 241–245.

UEDA, K. & HAYAISHI, O. (1985). ADP-ribosylation. *Annu. Rev. Biochem.*, **54**, 73–100.

(Received August 31, 1994
Revised December 21, 1994
Accepted December 22, 1994)

British Journal of Pharmacology (1995) 114, 1549–1556 © 1995 Stockton Press All rights reserved 0007–1188/95 $12.00

Mechanisms of bradykinin-induced contraction of the guinea-pig gallbladder *in vitro*

Daniela A. Cabrini, Ana M. Silva & [1]João B. Calixto

Department of Pharmacology, Centre of Biological Sciences, Universidade Federal de Santa Catarina, Rua Ferreira Lima, 82, 88015-420, Florianópolis, SC, Brazil

1 The mechanisms underlying bradykinin (BK)-mediated contractions in strips of guinea-pig gallbladder (GPG) were examined by use of selective bradykinin (BK) receptor agonists and antagonists.

2 Addition of BK and related kinins (0.1 pM–10 μM) after 2 h of equilibration of the preparation caused graded contractions characterized by two distinct phases: high affinity (0.1 pM–1 nM) and low affinity (3 nM–10 μM). The rank order of potency for the first phase (mean EC_{50}, pM) was: BK (1.36) = Hyp^3-BK (1.44) = Lys-BK (1.54) > Tyr^8-BK (2.72) > Met-Lys-BK (4.30). The rank order of potency for the second phase (mean EC_{50}, nM, at concentration producing 50% of the contraction caused by 80 mM KCl) was: Hyp^3-BK (8.95) > Met-Lys-BK (12.78) > Tyr^8-BK (33.75) > Lys-BK (60.92) > BK (77.35). The contractile responses (g of tension) to 3 μM of BK (the highest concentration tested) were: Hyp^3-BK, 1.76 ± 0.09; BK, 1.65 ± 0.12; Lys-BK, 1.45 ± 0.13; Tyr^8-BK, 1.36 ± 0.15 and Met-Lys-BK, 1.36 ± 0.15. The selective B_1 agonist, des-Arg^9-BK, caused only a weak contraction with maximal response (0.21 ± 0.05 g), which corresponded to approximately 10% of that induced by BK.

3 BK-induced contraction in GPG was inhibited by indomethacin (3 μM) or ibuprofen (30 μM), and was partially reduced by phenidone (30 μM), but was not affected by atropine (1 μM), nicardipine (1 μM), Ca^{2+}-free medium plus EGTA, dazoxiben (30 nM), L-655,240 (10 nM, a selective receptor antagonist of thromboxane A_2), MK-571 (0.1 μM, a selective leukotriene D_4 receptor antagonist), tetrodotoxin (0.3 μM), CP 96,345 (0.3 μM, a NK_1 receptor antagonist), mepyramine (1 μM), glibenclamide (1 μM), H-7 (3 μM), staurosporine (100 nM), or phorbol 12-myristate 13-acetate (1 μM). However, BK-induced contractions in GPG maintained in Ca^{2+}-free medium were markedly attenuated by ryanodine (10 μM).

4 Prostaglandin E_2, prostaglandin $F_{2\alpha}$ or U46619 (0.1 nM to 100 μM), caused concentration-dependent contractions in GPG with mean EC_{50}s of 3.1 μM; 1.7 μM and 0.47 nM and maximal responses of 1.36 ± 0.15; 1.32 ± 0.20 and 0.96 ± 0.09 g, respectively.

5 The selective B_2 receptor antagonists, Hoe 140, NPC 17731 and NPC 17761 (0.01–1 μM), caused concentration-dependent displacements to the right of the contractile concentration-response curve for BK. The selective B_1 receptor antagonist, des-Arg^9-[Leu^8]-BK (1 μM), did not affect BK-induced GPG contraction.

6 These data suggest that both high and low affinity BK responses in GPG are mediated by activation of B_2 receptors, and that BK-mediated contraction in GPG depends on the release of intracellular Ca^{2+} sources sensitive to ryanodine. In addition, BK-induced contraction in GPG is mediated by release of proinflammatory eicosanoid(s) derived from the cyclo-oxygenase pathway from arachidonic acid metabolism unrelated to thromboxane A_2, and seems not to be coupled to activation of a protein kinase C-dependent mechanism.

Keywords: Guinea-pig gallbladder; bradykinin; kinin; B_1 and B_2 bradykinin agonists and antagonists; prostanoids; calcium

Introduction

Bradykinin (BK) is a nonapeptide generated in plasma by the action of plasma and glandular kallikreins on both high and low molecular weight kininogens (Regoli & Barabé, 1980; Bhoola *et al.*, 1992). Kinins are widely recognized as participants in many physiological and pathological states. Thus, kinins are known to promote contraction or relaxation responses in vascular or non-vascular smooth muscles. Although most BK responses are indirectly mediated by release of eicosanoid products derived from the arachidonic acid pathway (Gaginella & Kachur, 1989; Hall, 1992), studies on the structure-activity relationship of several analogues, and the use of potent and selective BK receptor antagonists, have led to the characterization of two classes of BK membrane receptors, denoted as B_1 and B_2 (Regoli & Barabé, 1980; Burch *et al.*, 1990; Marceau & Regoli, 1991; Bhoola *et al.*, 1992). The B_1 receptors exhibit higher affinity for kinin metabolites, des-Arg^9-BK and des-Arg^{10}-kallidin (Lys-BK), and are selectively and competitively antagonized by the B_1 receptor antagonists, des-Arg^9-[Leu^8]-BK or des-Arg^{10}-[Leu^8]-LBK. However, most of the physiological and pathological actions of BK are mediated by activation of B_2 receptors which seem to be widely distributed throughout the peripheral and central nervous system. In contrast to B_1 receptors, B_2 receptors exhibit high affinity for BK and kallidin (Lys-bradykinin), but a low affinity for the B_1 agonist des-Arg^9-BK (Regoli & Barabé, 1980; Burch *et al.*, 1990; Bathon & Proud, 1991).

In the present study we have attempted to investigate the mechanisms underlying BK-mediated contractile responses in the guinea-pig gallbladder (GPG) *in vitro* by using kinin-selective receptor agonists and antagonists. Some of these results were presented at the Meeting of KININ 93 (Silva *et al.*, 1993).

Methods

Tissue preparation

Guinea-pigs of either sex (300–400 g) were anaesthetized with ether and killed with a blow on the neck followed by

[1] Author for correspondence.

cervical dislocation. Usually, 4 strips of each guinea-pig gallbladder (10–15 mm long, 3–4 mm wide) were isolated and each preparation was set up in a 5 ml glass organ bath containing Krebs-Henseleit solution of the following composition (mM): NaCl 118.0, KCl 4.4, $MgSO_4$ 1.1, $CaCl_2$ 2.5, $NaHCO_3$ 25.0, KH_2PO_4 1.2 and glucose 11.0, maintained at 37°C and pH of 7.4, gassed with 95% O_2 and 5% CO_2. Isometric tension changes were recorded by means of an F-60 force transducer (Narco-Biosystem or Letica 6006) under a continuous basal tension of 0.5 g. Preparations were allowed to equilibrate for at least 2 h before drug addition, during which the bath solution was changed every 20 min. Usually, four to six baths were used in parallel.

Concentration-response curves (CRCs) for bradykinin and related peptides

Following the equilibration period of 2 h, and in order to confirm the viability of the tissues, preparations were exposed to high potassium concentration (KCl 80 mM, prepared by equimolar substitution of 74.4 mM NaCl by KCl) as a standard stimulus. After washout, replacement with normal medium and return to the original baseline (about 30 min), CRCs were obtained for BK and related peptides. The CRCs for all studied agonists were performed by means of the cumulative method (Van Rossum, 1963). Each concentration of the agonist was added when the effect of the preceding addition had reached its maximum. To ascertain whether BK-induced contraction in GPG underwent desensitization, in preliminary experiments ($n = 5$), several CRCs for BK (1 pM to 10 μM) were carried out on the same preparation at 60 min intervals between curves, following 30, 60 or 120 min of equilibration period. No significant desensitization was observed for at least two consecutive CRCs for BK, when experiments were performed 120 min after setting up the preparation. Accordingly, no more than two CRCs for BK and related peptides were carried out on the same strip. Each preparation was exposed to only one agonist. All experiments with BK and analogues were carried out in the presence of captopril (3 μM), to prevent the action of kininase II.

Influence of calcium on bradykinin-induced contraction

To confirm the possible involvement of extracellular Ca^{2+} in BK-induced contractile responses to GPG, after 2 h of equilibration, preparations were transferred to Krebs solution without Ca^{2+}, containing 1 mM EGTA, for 20 min, during which the bath solution was renewed every 5 min. The tissues then remained in Ca^{2+}-free solution plus EGTA for 10 min, and responses to BK were subsequently obtained (Calixto & Medeiros, 1991). In another set of experiments, GPG preparations were allowed to equilibrate for 2 h in normal medium and a CRC was obtained for BK (0.1 pM–10 μM) either in the absence or presence of nicardipine (1 μM, incubated 20 min beforehand). After obtaining a CRC for BK in Ca^{2+}-free medium, some preparations were incubated for 20 min with ryanodine (10 μM, a neutral alkaloid which affects either opening or closing of the sarcoplasmic reticulum Ca^{2+} channels) (Jenden & Fairburt, 1969; Meissner, 1986), and another CRC for BK was subsequently obtained in Ca^{2+}-free Krebs solution.

Effect of prostanoid and protein kinase C in bradykinin-induced contraction

To assess whether prostanoids were involved in the contractile response elicited by BK, following 2 h equilibration, CRCs were obtained for BK (0.1 pM–10 μM) in the absence or in the presence of the following drugs added 20 min before addition of BK: indomethacin (3 μM), ibruprofen (30 μM) (both cyclo-oxygenase inhibitors), phenidone (30 μM, a lipoxygenase inhibitor), dazoxiben (30 nM, an inhibitor of thromboxane A_2 (TxA_2)-synthase), or MK-571 (100 nM, a leukotriene D_4 selective receptor antagonist). In separate experiments, CRCs for PGE_2 (0.1 nM–100 μM), $PGF_{2\alpha}$ (0.1 nM–100 μM) or for TxA_2, prostaglandin H_2-mimetic U46619 (0.1 nM–1 μM) were also carried out by means of the cumulative method. To avoid desensitization, only one CRC was obtained in each preparation.

Another three sets of experiments were designed to assess the possible role of protein kinase C-dependent mechanisms in mediating responses to BK in GPG, by analysing the effects of staurosporine (0.1 μM), H-7 (3 μM) (two protein kinase C antagonists) or phorbol 12-myristate 13-acetate (1 μM, an activator of protein kinase C). Drugs were added to the preparations 30 min before construction of the CRC for BK, except for phorbol 12-myristate 13-acetate which was added 60 min prior to BK.

Effect of B_1 and B_2 bradykinin receptor antagonists on bradykinin-induced contraction

Following 2 h of equilibration, CRCs were obtained for BK (0.1 pM–10 μM), in the absence or presence of Hoe-140, NPC 17761 or NPC 17731 (three selective B_2 receptor antagonists, 0.01–1 μM), or for the selective B_1 receptor antagonist, des-Arg^9-[Leu^8]-BK (1 μM). All antagonists were added to the preparations for at least 10 min before challenge with the agonist. In order to achieve the best period of equilibration for antagonist with the receptor, we evaluated the effect of different preincubation periods (e.g. 5 to 30 min). Longer periods of incubation with the antagonist (up to 30 min) did not afford further inhibition compared to that achieved after 10 min (data not shown). Thus, a 10 min antagonist preincubation period was used in the present study. Control experiments for BK were always carried out in parallel in the presence of phosphate-buffered solution (PBS), (concentration: NaCl 137 mM; KCl 2.7 mM, and phosphate buffer 10 mM), in order to correct for any time-dependent changes in responsiveness to BK.

To evaluate further the mechanism of action of BK, following 2 h of equilibration, single or cumulative CRCs for BK were obtained in the absence or in the presence of each of the following drugs, added to the bath 10 to 30 min prior to BK: mepyramine (1 μM, an H_1-histamine receptor antagonist); atropine (1 μM, a muscarinic receptor antagonist); prazosin (0.1 μM, α_1-adrenoceptor-blocker); tetrodotoxin (0.3 μM, a Na^+ channel blocker); glibenclamide (1.0 μM, an ATP-sensitive K^+-channel blocker), CP 96,345 (0.3 μM, a NK_1 tachykinin receptor antagonist) or WEB 2086 (100 nM, a selective PAF receptor antagonist).

Statistical analysis

Most data are presented as mean ± s.e.mean. The EC_{50} values are given as geometric means accompanied by their respective 95% confidence limits. Tests for statistical significance were performed either by using Student's paired or unpaired t test or by analysis of variance followed by Dunnett's multicomparison test when appropriate. $P < 0.05$ or less was considered as indicative of significance. The corresponding tests used are indicated below each figure or table. The contractile response for kinin and other agonists are expressed in absolute tension (g) developed per preparation.

The apparent EC_{50} values for the second phase of BK and related kinin-induced responses, i.e. the concentration of agonists required to elicit 50% response relative to that caused by 80 mM KCl, were determined from individual experiments from agonist CRCs using the least-squares methods (Guimarães *et al.*, 1992). The EC_{50}s for the first phase were calculated as a function of their own respective maximal response. The contractile responses induced by kinins (10 μM), the highest concentration used, were also compared.

Drugs

Drugs used were: phorbol 12-myristate 13-acetate, H-7 (5 isoquinolinyl sulphonyl-2 methyl piperazine), staurosporine, Hyp^3-BK, BK, Lys-BK, Tyr^8-BK, Met-Lys-BK, des-Arg^9-BK, captopril, indomethacin, ibuprofen, phenidone, nicardipine, tetrodotoxin, mepyramine hydrochloride, atropine sulphate, prostaglandin E_2 and prostaglandin $F_{2\alpha}$ (all from Sigma Chemical Company, St. Louis, MO, U.S.A.), prazosin (Pfizer, New York, U.S.A.), glibenclamide (Hoechst, Somerville, NJ, U.S.A.), MK-571 (3-(3-(2-(7-chloro-2-quinolinyl) ethenyl)phenyl ((3-dimethyl amino-3-oxo-propyl)thio)methyl) propanoic acid; kindly provided by Merck Frosst, Canada), Hoe 140 (D-Arg^0-[Hyp^3,Thi^5,D-Tic^7,Oic^8]-BK; kindly supplied by Hoechst, Frankfurt, Main, Germany), NPC 17731 (D-Arg^0 [Hyp^3, D-HypE (transpropyl)^7, Oic^8]-BK) and NPC 17761 (D-Arg^0 [Hyp^3,D-HypE (*trans* thiophenyl)^7, Oic^8]-BK) (kindly supplied by Scios Nova, Baltimore, U.S.A.). WEB 2086 (3-[4-)2-chlorophenyl-9-methyl-6H-thieno [3,2-f] [1,2,4] triazolo-4, 3-a) (1, 4]-diazepin-2-yl)-1-(4-morpholinyl)-1-propanon) (Boehringer Ingelheim, Germany), U46619 (9,11-dideoxy-92, 11α-methanoepoxy prostaglandin $F_{2\alpha}$, UpJohn Co, Kalamazoo, MI, U.S.A.), ryanodine and CP 96,345 ((25,35)-cis-2-(diphenylmethyl)-N-[(2-methoxyphenyl)-methyl]-1-azabicyclo[2,2,2]octan-3-amine) (Research Biochemicals Incorporated RBI, Natick, MA, U.S.A.), des-Arg^9-[Leu^8]-BK and L-655,240 (3-[1-(4-chlorobenzyl)-5-fluoro-3-methylindol-2yl]2,2-dimethylpropanoic acid) (kind gifts from Dr P. D'Orleans-Juste and Dr Pierre Sirois, Department of Pharmacology, University of Sherbrooke, Sherbrooke, Canada), dazoxiben (Pfizer, Kent, UK). The stock solution for all peptides used was prepared in PBS (1–10 mM) and kept in siliconized plastic tubes, maintained in a freezer at −18°C. Stock solutions of prazosin, indomethacin, nicardipine, glibenclamide, phorbol 12-myristate 13-acetate, staurosporine, L-655,240 and U46619 were made in absolute ethanol. All other drugs were dissolved in PBS just before use at the desired concentration. The final bath concentration of ethanol did not exceed 0.05% and did not affect the CRC for BK.

Results

Concentration-response relationships of bradykinin and related peptides

The results in Figure 1 show that BK (0.1 pM–10 μM) caused a concentration-dependent contractile response in GPG characterized by two distinct phases: the first phase, plateauing at 1 nM, and a second phase above 10 μM. The results in Figure 1a also show the CRCs for BK (0.1 pM–10 μM) in GPG performed at 2, 3, 4 and 5 h after the equilibration period. As may be observed, the first phase of the contractile response elicited by BK increased significantly when preparations remained 4 h in equilibration. As shown in Figure 1b, all the kinins that were studied (0.1 pM–10 μM) when added to GPG after 2 h of equilibration caused reproducible and concentration-dependent contractile responses. The relative rank order of potency for the first phase was: BK = Hyp^3-BK = Lys-BK> Tyr^8-BK> Met-Lys-BK, and for the second phase was: Hyp^3-BK> Met-Lys-BK> Tyr^8-BK> Lys-BK> BK. The contractions (g of tension) caused by 10 μM of these peptides (the maximal tested concentration) in GPG were also similar (Table 1). The BK-mediated contraction of GPG appears to be mediated by the B_2 receptor subtype, because des-Arg^9-BK, a selective B_1 agonist, up to 1 μM, caused only a very weak contraction in this preparation (0.21 ± 0.05 g) which corresponds approximately to 10% of that caused by BK (Figure 1b).

Influence of extra- and intracellular calcium on bradykinin-mediated contraction

Preincubation of strips of GPG with nicardipine 20 min beforehand only partially attenuated the first (but not the second) phase of the contractile response elicited for BK ($P<0.05$, unpaired t test) (Figure 2a). The contractile response to BK of GPG was not significantly affected when the experiments were performed in Ca^{2+}-free medium containing EGTA (1 mM) (Figure 2b). In contrast, pre-incubation of GPG maintained in Ca^{2+}-free medium plus ryanodine (10 μM) markedly attenuated both phases of the BK-induced contraction (Figure 2c).

Influence of protein kinase C inhibitors and activator

Pre-incubation of GPG with the protein kinase C inhibitors, staurosporine (0.1 μM) or H-7 (3 μM) or with the protein kinase C activator, phorbol 12-myristate 13-acetate (1 μM), did not change the tonus of the preparation and also failed to affect BK-induced contraction significantly (Figure 3a, b and c).

Influence of prostanoids

The data in Figure 4a and b show that both phases of the BK-induced contraction in GPG were markedly antagonized

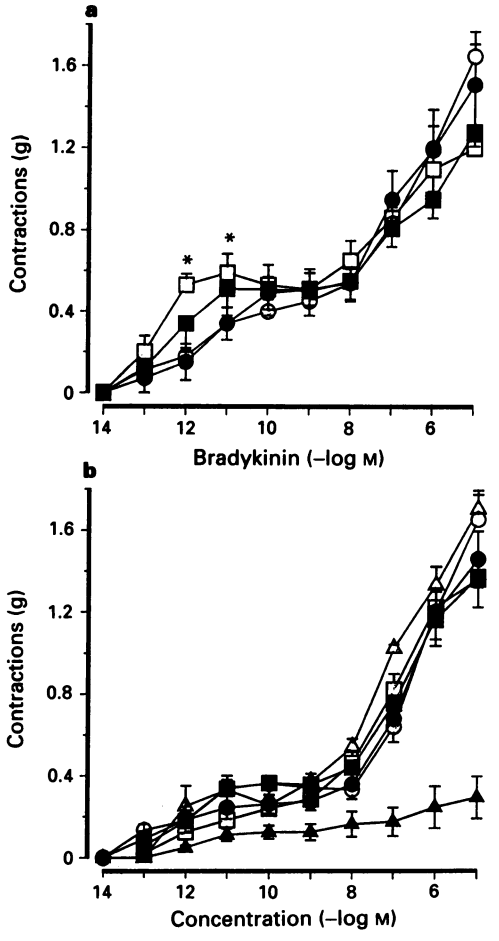

Figure 1 (a) Concentration-response curves for bradykinin in strips of the guinea-pig gallbladder performed in the same tissue at 2 (○); 3 (●), 4 (□) or 5 (■) h after setting up each preparation. Each preparation was exposed to consecutive increases in BK concentration and cumulative-response curves were constructed. The first curve was carried out at 2 h and the second curve was performed at 3, 4 or 5 h following the equilibration period of the preparation. (b) Mean concentration-response curves for bradykinin (○); Lys-BK (●); Met-Lys-BK (□); Tyr^8-BK (■); [Hyp^3]-BK (△) and des-Arg^9-BK (▲) in the guinea-pig isolated gallbladder carried out 2 h after setting up the preparations. Only one concentration-response curve was performed for each peptide per preparation. Each point represents the mean with s.e.mean of 6 to 9 experiments. In some cases the error bars are hidden within the symbols. Significant differences from respective control values where $*P<0.05$ (Student's unpaired t test).

by indomethacin (3 μM) or by ibuprofen (30 μM). However, the BK-induced contraction in GPG was only partially attenuated by phenidone (30 μM) and was not affected by dazoxiben (30 nM), L-655,240 (10 nM) or MK-571 (0.1 μM) (Figures 5 and 6). The results in Figure 7 (a, b and c) show that prostaglandin $F_{2\alpha}$, prostaglandin E_2 and U46619 (0.1 nM to 100 μM) all caused a concentration-dependent contraction of the GPG. The EC_{50}s (and 95% confidence limits) were: $PGF_{2\alpha}$ 1.7 (0.4–7.4) μM; PGE_2 3.1 (0.9–10.7) μM and U46619 0.48 (0.1–1.5) nM. The maximal contractile responses in g of tension were 1.32 ± 0.20 for $PGF_{2\alpha}$; 1.36 ± 0.15 for PGE_2 and 0.96 ± 0.09 for U46619.

Analysis of the antagonism of Hoe 140, NPC 17761 or NPC 17731 to the BK-induced contraction

The selective B_2 receptor antagonists, Hoe 140, NPC 17761 and NPC 17731 (0.01–1 μM) did not affect the basal tone of the strips but caused a concentration-dependent displacement to the right of the BK-induced contraction in GPG (Figure 8a, b and c). Because BK concentrations higher than 10 μM were not tested, it was not possible to determine whether the actions of BK antagonists were surmountable, thus making difficult the estimation of the pA_2 values. Preincubation of

Table 1 Responsiveness of guinea-pig gallbladder to bradykinin and related kinins

	EC_{50}			
Agonists	*First phase* (pM)	*Second phase* (nM)	*Contraction*[b] (g)	n
KCl (80 mM)	–	–	1.50 ± 0.17	20
BK	1.35 (0.63–2.89)[a]	77.35 (26.23–228.07)	1.65 ± 0.12	10
Hyp^3-BK	1.44 (0.41–5.08)	8.95 (4.04–19.86)	1.76 ± 0.09	5
L-BK	1.54 (0.25–9.26)	60.92 (21.69–171.07)	1.45 ± 0.13	9
Tyr^8-BK	2.72 (0.45–16.33)	33.75 (5.85–194.82)	1.36 ± 0.15	8
Met-L-BK	4.30 (0.52–35.25)	12.78 (2.51–64.89)	1.36 ± 0.15	5

[a]95% confidence limits; [b]Responses to 80 mM KCl or 3 μM of agonists (highest concentration tested) are reported as mean ± s.e.mean. Results were analysed by means of analysis of variance followed by Dunnett's multiple comparison test.

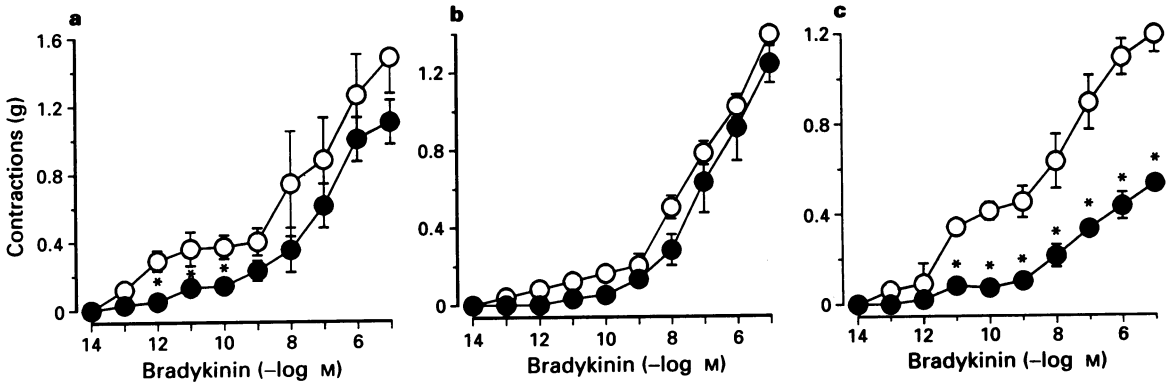

Figure 2 Concentration-response curves for bradykinin in the guinea-pig isolated gallbladder in the absence (○) or presence of (a) nicardipine (●, 0.1 μM), (b) in calcium-free Krebs plus EGTA (●, 1 mM), or (c) in the presence of calcium-free Krebs plus ryanodine (●, 10 μM). Each point represents the mean ± s.e.mean of 6 to 7 experiments. Significant differences from respective control values where $*P<0.05$ (Student's unpaired t test).

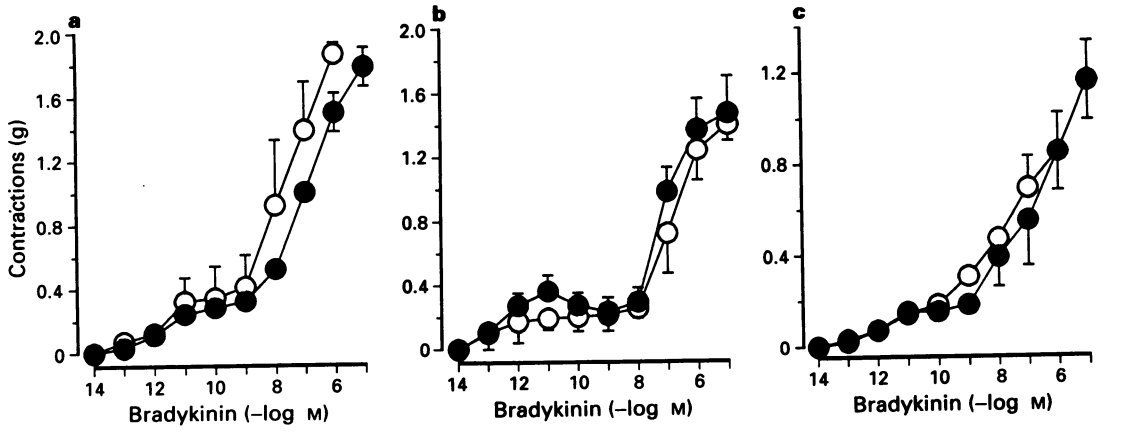

Figure 3 Concentration-response curves for bradykinin in the guinea-pig isolated gallbladder in the absence (○) or in the presence of (a) staurosporine (●, 0.1 μM), (b) H-7 (●, 3 μM), or (c) phorbol 12-myristate 13-acetate (●, 1 μM). Each point represents the mean ± s.e.mean of 5 to 6 experiments.

GPG with the selective B_1 receptor antagonist, des-Arg^9-[Leu^8]-BK (1 μM) did not affect the CRC for BK (Figure 9).

Effect of several classes of drugs on BK-induced contraction

Preincubation of GPG preparations with tetrodotoxin (0.3 μM), glibenclamide (1.0 μM), mepyramine (1 μM), atropine (1 μM), prazosin (0.1 μM), CP 96,345 (0.3 μM) and WEB 2086 (0.1 μM) did not significantly affect the contractile responses induced by BK (Figure 6c for WEB 2086 alone, Table 2).

Discussion

In the present study we have demonstrated that BK and related kinins cause concentration-dependent contractions of GPG *in vitro*, characterized by two distinct phases, and that these effects are likely to be mediated by activation of B_2

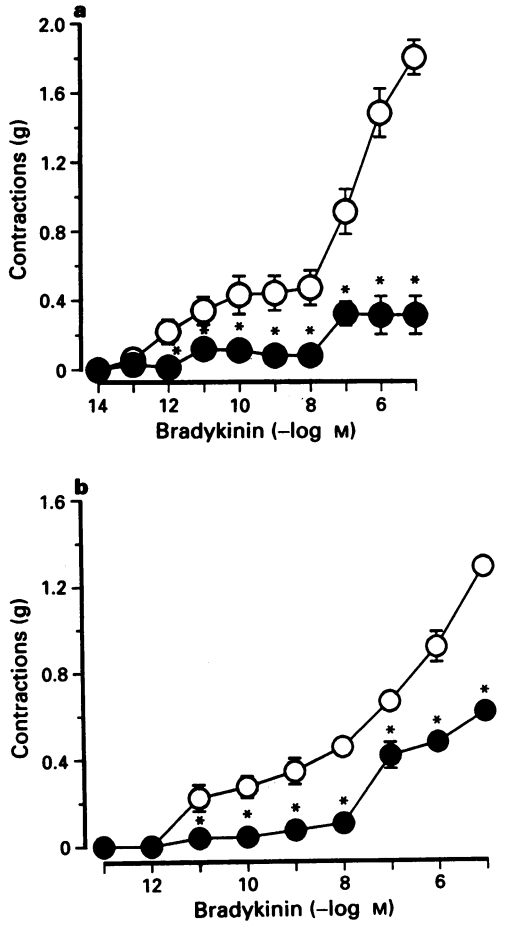

Figure 4 Concentration-response curves for bradykinin in the guinea-pig isolated gallbladder obtained in the absence (○) or in the presence of (a) indomethacin (●, 3 μM), (b) ibuprofen (●, 30 μM). Each point represents the mean ± s.e.mean of 6 to 7 experiments. Significant differences from respective control values where $*P<0.05$ (Student's unpaired t test).

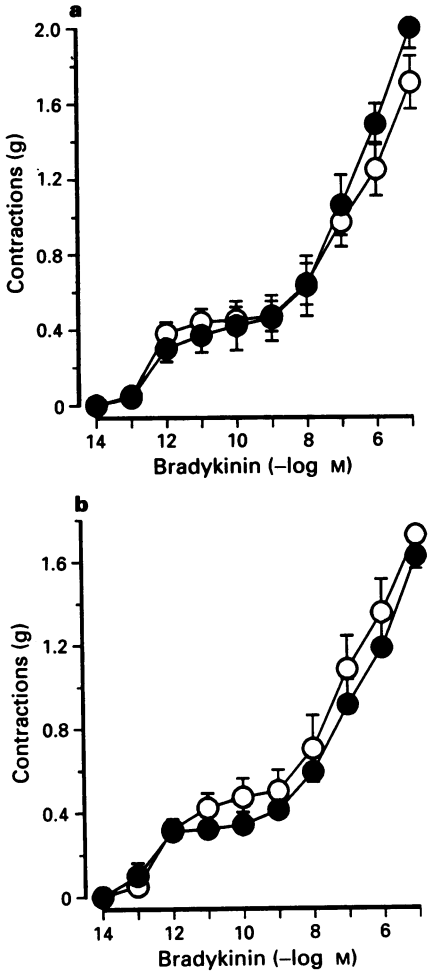

Figure 5 Concentration-response curves for bradykinin in the guinea-pig isolated gallbladder obtained in the absence (○) or the presence of (a) dazoxiben (●, 30 μM) or (b) L655,240 (●, 10 nM). Each point represents the mean ± s.e.mean of 5 to 6 experiments.

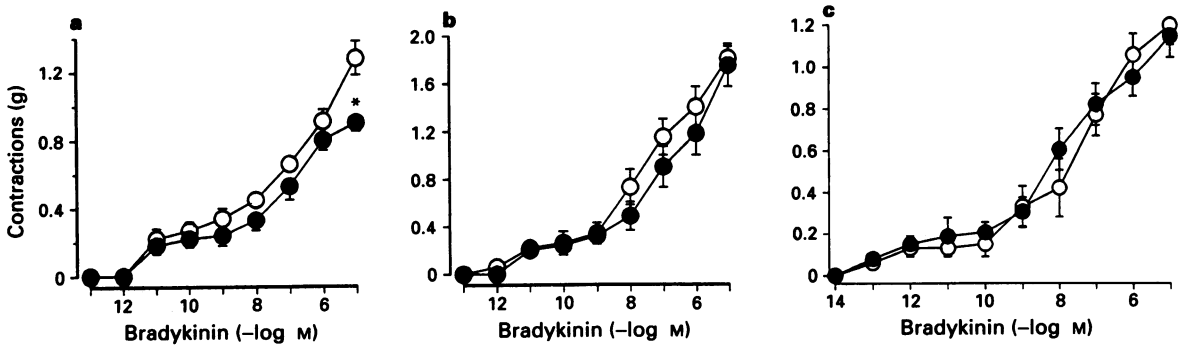

Figure 6 Concentration-response curves for bradykinin in the guinea-pig isolated gallbladder in the absence (○) or the presence of (a) phenidone (●, 30 μM), (b) MK-571 (●, 0.1 μM) or (c) WEB 2086 (●, 0.1 μM). Each point represents the mean ± s.e.mean of 5 to 6 experiments. Significant differences from respective control values where $*P<0.05$ (Student's unpaired t test).

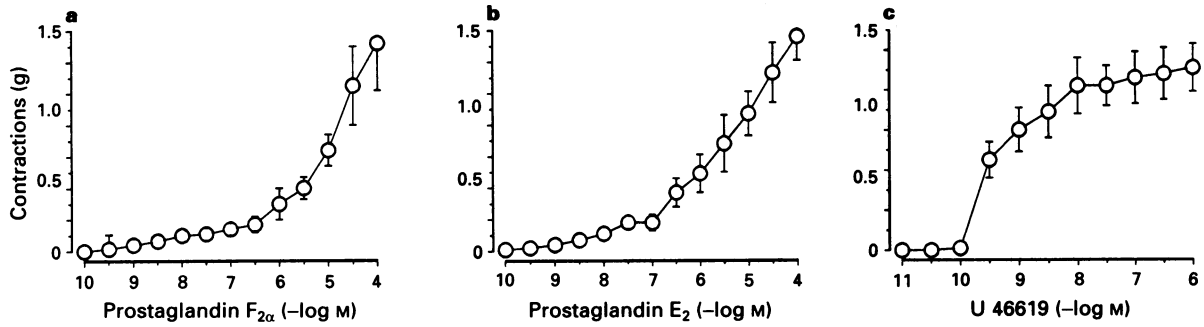

Figure 7 Concentration-response curves for prostaglandin $F_{2\alpha}$ (a), prostaglandin E_2 (b) or U46619 (c) in the guinea-pig isolated gallbladder. Each point represents the mean ± s.e.mean of 6 experiments.

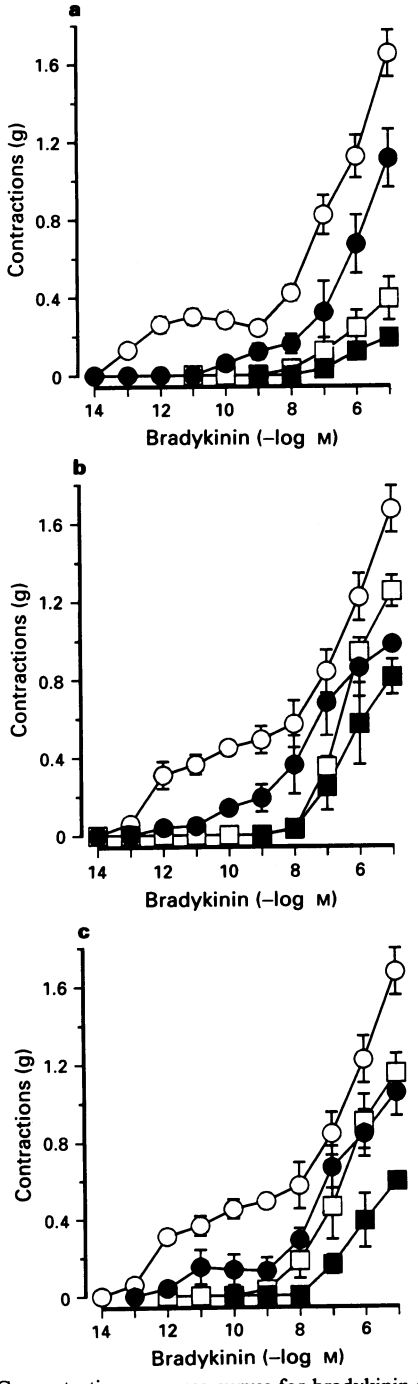

Figure 8 Concentration-response curves for bradykinin in the guinea-pig isolated gallbladder in the absence (○) or in the presence of increasing concentrations of (a) Hoe 140 (μM): 0.01 (●), 0.1 (□) and 1 (■); (b) NPC 17761 (μM): 0.01 (●), 0.1 (□) and 1 (■) or (c) NPC 17731 (in μM): 0.01 (●), 0.1 (□) and 1 (■). Each point represents the mean ± s.e.mean of 5 to 6 experiments. In some cases the error bars are hidden within the symbols.

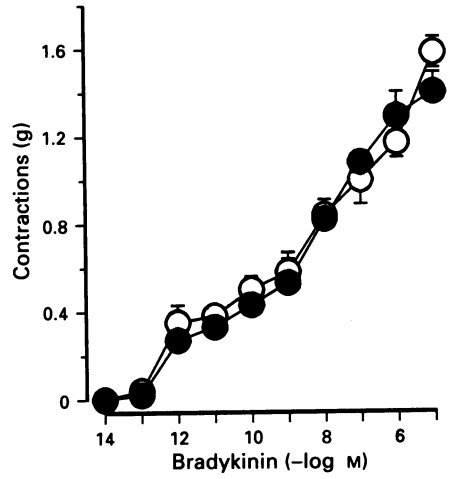

Figure 9 Concentration-response curves for bradykinin in the guinea-pig isolated gallbladder in the absence (○) or in the presence of des-Arg^9-[Leu^8]-bradykinin (●, 1 μM). Each point represents the mean ± s.e.mean of 5 to 6 experiments. In some cases the error bars are hidden within the symbols.

receptors at the smooth muscle. This evidence is substantiated by the following observations. First, the order of potency of the kinins studied in GPG is compatible with the action of kinins acting at B_2 receptors (Regoli & Barabé, 1980). Secondly, the selective B_1 receptor agonist des-Arg^9-BK, up to 1 μM, had very weak agonist activity, and the selective B_1 receptor antagonist, des-Arg^9-[Leu^8]-BK, up to 1 μM, failed to inhibit the contractile response induced by BK in GPG. In addition, the potent and selective B_2 receptor antagonists, Hoe 140, NPC 17731 and NPC 17761, caused a concentration-dependent displacement to the right of the BK-induced contraction. However, our results do not allow us to ascertain whether or not the interaction between BK with the B_2 receptors in GPG involves a competitve mechanism, because the maximal contractile response for BK in the presence of the B_2 antagonists was not obtained, due to the limited concentration of BK used.

Results of this study also demonstrated that BK-induced contraction in GPG is largely mediated indirectly by release of prostanoid metabolite(s) derived from the cyclo-oxygenase pathway as BK response was inhibited by indomethacin or ibuprofen. Similar results have been reported for kinin-induced contraction in the GPG (Woods & Baird, 1991) and for BK-stimulated electrogenic bicarbonate secretion in mucosal and serosal GPG (Baird & Margolius, 1989). The fact that BK-induced contraction in this preparation was not affected by dazoxiben, a selective inhibitor of TxA_2 synthesis (Randall *et al.*, 1981), or by L-655,240, a competitive receptor antagonist of TxA_2 (Hall *et al.*, 1987; Girard *et al.*, 1989), strongly suggests that the cyclo-oxygenase metabolites released by BK in GPG are probably unrelated to TxA_2. We

Table 2 Effect of several classes of drugs on bradykinin (100 nM)-induced contraction in guinea-pig gallbladder

Agents	Concentration (μM)	Contraction (g) Control	Antagonist
Tetrodotoxin	0.3	0.69 ± 0.09	0.80 ± 0.01
Glibenclamide	1.0	0.55 ± 0.15	0.55 ± 0.12
Mepyramine	1.0	0.69 ± 0.10	0.71 ± 0.11
Atropine	1.0	0.65 ± 0.08	0.51 ± 0.03
CP 96,345	0.3	1.01 ± 0.06	1.03 ± 0.07
Prazosin	0.1	1.08 ± 0.08	1.08 ± 0.11

Each group represents the mean ± s.e.mean of 4 to 6 experiments.
Results were analysed by means of Student's paired *t* test.

and others have previously shown that B_2 receptors mediating relaxation in guinea-pig trachea, in circular muscle from guinea-pig ileum as well as the B_1 and B_2 receptor-mediated contraction for BK in rat portal vein rings, are also indirectly mediated by release of a cyclo-oxygenase product derived from the arachidonic acid pathway (Bramley *et al.*, 1990; Calixto & Medeiros, 1991; Schlemper & Calixto, 1994; Campos & Calixto, 1994). While the B_2 receptor mediates BK-induced relaxation in the trachea and gut which depends on the release of prostaglandin E_2, the contractile responses elicited by either BK or des-Arg^9-BK in rat portal vein are mediated by release of TxA_2. At this stage of our study it is difficult to ascertain the nature of prostanoid released by BK in GPG. However, based on the potencies of the prostanoids tested, it is probable that the cyclo-oxygenase derived metabolite released by BK in the GPG is PGE_2. A similar conclusion was suggested for BK-stimulated electrogenic bicarbonate secretion in GPG (Baird & Margolius, 1989). In addition, BK-induced contraction in GPG was also partially attenuated by phenidone, suggesting some role of a lipo-oxygenase metabolite from arachidonic acid in its contractile responses. However, pre-incubation of GPG with MK-571, a selective leukotriene D_4 receptor antagonist (Jones *et al.*, 1989), which has been shown to antagonize competitively leukotriene D_4-induced contractions in GPG (Freedman *et al.*, 1993), failed to affect BK-mediated contraction in GPG. These results suggest that leukotriene D_4 is unable to mediate BK-induced contractions in this preparation. However, additional biochemical studies are required to clarify this point.

Concerning the sources of Ca^{2+} necessary for BK-mediated contraction in GPG, although dihydropyridine L-type Ca^{2+} channels are present in GPG (Renzetti *et al.*, 1990) our data indicate that the contractile response elicited by this peptide is dependent on the release of Ca^{2+} from intracellular stores. This conclusion is based on the fact that even at higher concentrations nicardipine (a voltage-sensitive L-type Ca^{2+} channel antagonist) failed to affect BK-induced contraction in GPG. Furthermore, the contraction in response to BK in GPG was not modified in Ca^{2+}-free medium plus EGTA. The contractile response elicited by BK in GPG maintained in Ca^{2+}-free solution was markedly attenuated by ryanodine. In contrast with the results reported for BK-induced contraction in circular muscle from the guinea-pig ileum (Calixto & Medeiros, 1991), rabbit aorta and jugular vein (Calixto & Medeiros, 1992) and rat portal vein (Campos & Calixto, 1994) which are largely dependent on the activation of protein kinase C-dependent mechanisms, BK-induced contractions in GPG were not affected by high concentrations of either staurosporine or H-7, two putative protein kinase C antagonists (for review see Hidaka & Kobayashi, 1992).

The contractile responses induced by BK in GPG were not affected by tetrodotoxin, glibenclamide, mepyramine, atropine, CP 96,345, WEB 2086 or prazosin, indicating that BK has a direct myogenic effect on GPG, excluding the participation of action potential-dependent neural release of histamine, acetylcholine, noradrenaline, tachykinins (NK_1 receptor), or PAF or by activation of ATP-sensitive K^+ channels.

Falcone *et al.* (1993) reported that [^{3}H]-BK and related kinins bind with high affinity (K_i 0.45 nM) to a B_2 receptor in GPG. In addition, the authors also demonstrated that BK caused a graded increase of polyphosphoinositide hydrolysis in GPG cells, and that the BK responses were competitively and noncompetitively antagonized by NPC 17731 and Hoe 140, respectively. Also, the B_2 receptor antagonists, NPC 567, NPC 17731, NPC 17761 and Hoe 140 behaved as pure competitive antagonists against BK-induced contraction in GPG, yielding pK_b values of 5.0; 7.2; 7.7 and 8.5, respectively. Similar values of pK_b for these antagonists were observed in the presence of indomethacin, which as reported here, significantly decreased both the potency and the efficacy of BK in GPG. Interestingly, Falcone *et al.* (1993) did not find the higher affinity site for BK reported in the present study. However, there are marked methodological differences between these studies, such as the duration of equilibrium period, the basal tension of the preparations, the presence of different drugs in bath medium, and the frequent use of capsaicin to reduce the release of calcitonin gene-related peptide. Such differences make it difficult to compare studies.

In summary, we present functional evidence that both high and low affinity contractions induced by BK in GPG are mediated by activation of B_2 receptors, and that this contraction depends on the release of Ca^{2+} from intracellular stores sensitive to ryanodine. In addition, part of this BK-induced contraction is probably mediated indirectly by release of a cyclo-oxygenase derived product from the arachidonic acid pathway unrelated to TxA_2, and that the contractions are not coupled to activation of a protein kinase C-dependent mechanism. Considering the cyclo-oxygenase metabolites play an important role in inflammatory processes affecting the gallbladder and the biliary systems (Kaminski & Deshpande, 1980; Thornell *et al.*, 1981; Kaminski *et al.*, 1985; Kaminski, 1989; Myers & Bartula, 1992), and also the fact that BK has an important proinflammatory action (Marceau *et al.*, 1983; Proud & Kaplan, 1988) which can release eicosanoids and stimulate electrogenic bicarbonate secretion in GPG (Baird & Margolius, 1989) it seems probable that kinins have a physiopathological role in the GPG.

The authors are grateful to Elizabet Ramos Ganzer for secretarial help in preparing this manuscript. This work was supported by grants from CNPq and FINEP. We thank the pharmaceutical companies for the kind donation of drugs used in this work. D.A.C. is an M.Sc. student and A.M.S. is an undergraduate Medical student receiving a grant from CNPq (Brazil).

References

BAIRD, A.W. & MARGOLIUS, H.S. (1989). Bradykinin stimulates electrogenic bicarbonate secretion by the guinea pig gallbladder. *J. Pharmacol. Exp. Ther.*, **248**, 268–272.

BATHON, J.M. & PROUD, D. (1991). Bradykinin antagonists. *Annu. Rev. Pharmacol. Toxicol.*, **31**, 129–162.

BHOOLA, K.D., FIGUEROA, C.D. & WORTHY, K. (1992). Bioregulation of kinins: kallikreins, kininogens, and kininases. *Pharmacol. Rev.*, **44**, 1–80.

BRAMLEY, A.M., SAMHOUN, M.N. & PIPER, P.J. (1990). The role of epithelium in modulating the responses of guinea-pig trachea induced by bradykinin *in vitro*. *Br. J. Pharmacol.*, **99**, 762–766.

BURCH, R.M., FARMER, S.G. & STERANKA, L.R. (1990). Bradykinin receptor antagonists. *Med. Res. Rev.*, **10**, 237–269.

CALIXTO, J.B. & MEDEIROS, Y.S. (1991). Characterization of bradykinin mediating pertussis toxin-insensitive biphasic response in circular muscle of the isolated guinea pig ileum. *J. Pharmacol. Exp. Ther.*, **259**, 659–665.

CALIXTO, J.B. & MEDEIROS, Y.S. (1992). Effect of protein kinase C and calcium on bradykinin-mediated contractions of rabbit vessels. *Hypertension*, **19**, II87–II93.

CAMPOS, A.H. & CALIXTO, J.B. (1994). Mechanisms involved in the contractile responses of kinins in rat portal vein rings: mediation by B_1 and B_2 receptors. *J. Pharmacol. Exp. Ther.*, **268**, 902–909.

FALCONE, R.C., STEPHEN, J., HUBBS, S.J., VANDERLOO, J.D., PROSSER, J.C., LITTLE, J., GOMES, B., AHARONY, D. & KRELL, R.D. (1993). Characterization of bradykinin receptors in guinea pig gallbladder. *J. Pharmacol. Exp. Ther.*, **266**, 1291–1299.

FREEDMAN, S.M., WALLACE, J.L. & SHAFFER, E.A. (1993). Characterization of leukotriene-induced contraction of the guinea pig gallbladder *in vitro*. *Can. J. Physiol. Pharmacol.*, **71**, 145–150.

GAGINELLA, T.S. & KACHUR, J.F. (1989). Kinins as mediator of intestinal secretion. *Am. J. Physiol.*, **256**, G1–G15.

GIRARD, Y., YOAKIM-RANCOURT, C., HAMEL, P., GILLARD, J.W., GUINDON, Y., LETTS, G., EVANS, J., LÉVEILLÉ, C., ETHIER, D., LORD, A., JONES, T., MASSON, P., FORD-HUTCHINSON, A.W. & ROKACH, J. (1989). Tetrahydrocarbazol-1-acetic acids: New class of thromboxane receptor antagonists. In *Prostaglandins in Clinical Research: Cardiovascular System*. pp. 585–589. New York: Alan R. Liss, Inc.

GUIMARÃES, C.L., CALIXTO, J.B. & RAE, G.A. (1992). Potent constrictor actions of endothelin-1, endothelin-2 and endothelin-3 in rat isolated portal vein. *Hypertension*, **19**, II79–II86.

HALL, J.M. (1992). Bradykinin receptors: pharmacological properties and biological roles. *Pharmacol. Ther.*, **56**, 131–190.

HALL, R.A., GILLARD, J., GUINDON, Y., LETTS, G., CHAMPION, E., ETHIER, D., EVANS, J., FORD-HUTCHINSON, A.W., FORTIN, R., JONES, T.R., LORD, A., MORTON, H.E., ROKACH, J. & YOAKIM, C. (1987). Pharmacology of L-655,240 (3-[1-(4-chlorobenzyl)-5-fluoro-3-methyl-indol-2-yl]2,2-dimethylpropanoic acid), a potent, selective thromboxane/prostaglandin endoperoxide antagonist. *Eur. J. Pharmacol.*, **135**, 193–201.

HIDAKA, H. & KOBAYASHI, R. (1992). Pharmacology of protein kinase C inhibitors. *Annu. Rev. Pharmacol. Toxicol.*, **32**, 377–397.

JENDEN, D.J. & FAIRBURST, A.S. (1969). The pharmacology of ryanodine. *Pharmacol. Rev.*, **21**, 1–25.

JONES, T.R., ZAMBONI, R., BELLEY, M., CHAMPION, L., CHARETTE, L., FORD-HUTCHINSON, A.W., FRENETTE, R., GAUTHIER, J.-Y., LEGER, S., MASSON, P., MCFARLANE, C.S., PIECHUTA, H., ROKACH, J., WILLIANS, H., YOUNG, R.N., DEHAVEN, R.N. & PONG, S.S. (1989). Pharmacology of L-600, 711 (MK-571): a novel potent and selective leukotriene D_4 receptor antagonist. *Can. J. Physiol. Pharmacol.*, **67**, 17–28.

KAMINSKI, D.L. (1989). Arachidonic acid metabolites in hepatobiliary physiology and disease. *Gastroenterology*, **97**, 781–792.

KAMINSKI, D.L. & DESHPANDE, Y.G. (1980). Evaluation of the F prostaglandins in canine bile flow. *Prostaglandins*, **20**, 367–372.

KAMINSKI, D.L., DESHPANDE, Y.G., QUALY, J. & THOMAS, L. (1985). The role of prostaglandins in feline experimental cholecystitis. *Surgery*, **98**, 760–768.

MARCEAU, F., LUSSIER, A., REGOLI, D. & GIROUD, G.P. (1983). Pharmacology of kinins: their relevance to tissue injury and inflammation. *Gen. Pharmacol.*, **14**, 209–241.

MARCEAU, F. & REGOLI, D. (1991). Kinin receptors of the B_1 type and their antagonists. In *Bradykinin Antagonists: Basic and Clinical Research*. ed. Burch, R.M. pp. 33–49. New York: Marcel Dekker Inc.

MEISSNER, G. (1986). Ryanodine activation and inhibition of the Ca^{2+} release channel of sarcoplasmic reticulum. *J. Biol. Chem.*, **261**, 6300–6306.

MYERS, S.I. & BARTULA, L. (1992). Human cholecystitis is associated with increased gallbladder prostaglandin I_2 and prostaglandin E_2 synthesis. *Hepatology*, **16**, 1176–1179.

PROUD, D. & KAPLAN, A.P. (1988). Kinin formation: mechanisms and role in inflammatory disorders. *Annu. Rev. Immunol.*, **6**, 49–83.

RANDALL, M.J., PARRY, M.J., HAWKESWOOD, E., CROSS, P.E. & DICKINSON, R.P. (1981). UK-37,248, a novel, selective thromboxane synthetase inhibitor with platelet anti-aggregatory and antithrombotic activity. *Thromb. Res.*, **23**, 145–162.

REGOLI, D. & BARABÉ, J. (1980). Pharmacology of bradykinin and related kinins. *Pharmacol. Rev.*, **32**, 1–46.

RENZETTI, L.M., WANG, M.B. & RYAN, J.P. (1990). Contribution of intracellular calcium to gallbladder smooth muscle contraction. *Am. J. Physiol.*, **259**, G1–G5.

THORNELL, E., JANSON, R. & SVANVIK, J. (1981). Indomethacin intravenously. A new way for effective relief of bilary pain: a double blind study in man. *Surgery*, **90**, 468–473.

SCHLEMPER, V. & CALIXTO, J.B. (1994). Nitric oxide pathway-mediated relaxant effect of bradykinin in the guinea pig isolated trachea. *Br. J. Pharmacol.*, **111**, 83–88.

SILVA, A.M., CABRINI, D.A. & CALIXTO, J.B. (1993). Characterization of the response induced by bradykinin in the isolated guinea pig gallbladder. *Proc. KINN, Meeting, Brazil.* 65P.

VAN ROSSUM, J.M. (1963). Cumulative dose-response curves. II. Techniques for making a dose-response curve in isolated organs and the evaluation of drug parameters. *Arch. Int. Pharmacodyn. Ther.*, **143**, 299–330.

WOODS, M. & BAIRD, A.W. (1991). Increased responsiveness of guinea-pig gallbladder to kinin. *Br. J. Pharmacol.*, **104**, 141P.

(Received April 5, 1994
Revised December 19, 1994
Accepted December 22, 1994)

British Journal of Pharmacology (1995) 114, 1557–1562 © 1995 Stockton Press All rights reserved 0007–1188/95 $12.00

The biphasic response of rat vesical smooth muscle to ATP

Chiara Bolego, Christian Pinna, Maria P. Abbracchio, Flaminio Cattabeni & [1]Lina Puglisi

Institute of Pharmacological Sciences, University of Milan, Via Balzaretti, 9 20133 Milan, Italy

1 Adenosine-5'-triphosphate (ATP) is known to exert a variety of biological effects via the activation of either ionotropic P_{2X}- or G-protein coupled P_{2Y}-purinoceptor subtypes. In this study the effects induced by ATP and ATP analogues on rat bladder strips were characterized at resting tone and in carbachol-prestimulated tissues.

2 ATP exerted a clear concentration-dependent biphasic response, which was maximal at 1 mM concentration and was characterized by an immediate and transient contraction, followed by a slower sustained relaxation. The receptor mediating contraction was susceptible to desensitization by ATP and by the ATP analogue, α,β-methyleneATP (α,β-meATP) showing the typical features of the P_{2X}-purinoceptor; conversely, ATP-evoked relaxation did not undergo tachyphylaxis following either ATP or α,β-meATP.

3 The slower and sustained relaxant phase seemed to be due to activation of P_{2Y}-purinoceptors, based on responses obtained with the P_{2Y} agonist, 2-methyl-thioATP (2-meSATP) and, more importantly, based on the clear involvement of the G-proteins. In fact, the G-protein activator, guanosine 5'-O-(3-thiotriphosphate) (GTPγS) significantly potentiated and the G-protein blocking agent, guanosine 5'-O-(2-thio-diphosphate) (GDPβS) completely abolished the ATP-induced relaxation. No effects were exerted by these two G-protein modulators on the ATP-induced contraction.

4 The relaxant component of the ATP response of bladder tissue was not significantly influenced by nitro-benzyl-thioinosine (NBTI) or by 8-phenyltheophylline (8-PT), suggesting that the contribution of the ATP metabolite adenosine to this response was negligible. Moreover, relaxation evoked by ATP and by the adenosine analogue, 5'-N-ethylcarboxamidoadenosine (NECA) was additive.

5 Suramin was unable to modify either the relaxant or the contractile responses of bladder strips to ATP. However, when tested on the concentration-response curve to the slowly hydrolysable P_{2X}-agonist α,β-meATP, a rightward shift was detected, suggesting that ATP contractile responses are mediated by suramine-sensitive P_{2X}-purinoceptors.

6 Uridine-5'-triphosphate (UTP) only induced a rapid and concentration-dependent contraction of the rat bladder preparation, which was not desensitized by pre-exposure to α,β-meATP, suggesting that UTP responses were not mediated by the 'classical' P_{2X}-purinoceptor.

7 It is therefore concluded that both P_{2X}- and P_{2Y}-purinoceptors, which mediate ATP-induced contraction and relaxation, respectively, are present in rat bladder. Moreover, removal of epithelium did not affect ATP-elicited contraction, whereas ATP-induced relaxation was significantly augmented. These data suggest that P_{2X}- and P_{2Y}- purinoceptors are localized in smooth muscle cells and that the relaxant response is probably modulated by excitatory factor(s) released by epithelial cells.

Keywords: ATP; rat urinary bladder; P_2-purinoceptors

Introduction

The actions of purines as neurotransmitters/neuromodulators have been studied in various smooth muscle preparations (Kennedy, 1990). These actions are mediated via receptors which have been classified as P_1-and P_2-purinoceptors, preferentially recognizing adenosine and adenosine-5'-triphosphate (ATP), respectively (Burnstock, 1978). Largely on the basis of the different structure-activity relationships of ATP analogues, P_2-purinoceptors on smooth muscle have been subdivided into P_{2X}- and P_{2Y}-purinoceptors, generally associated with contraction and relaxation, respectively (Burnstock & Kennedy, 1985). However, it has been proposed recently that the agonist-potency order cannot be taken as an absolute parameter for P_2-purinoceptor classification, but that information on transduction mechanisms and molecular structure has also to be taken into account. This has led to the proposal of the existence of two P_2-purinoceptor families: the ionotropic P_{2X}-purinoceptor family, mediating fast and transient responses to ATP, and the metabotropic P_{2Y}-purinoceptor family, mediating slower responses through G-proteins (Abbracchio & Burnstock, 1994; Barnard *et al.*, 1994; Fredholm *et al.*, 1994).

Among its many biological effects, ATP is known to affect bladder function. Non-cholinergic, non-adrenergic, nerve-mediated contraction of the detrusor involving ATP as neurotransmitter has been known for many years (Langley & Anderson, 1985), whereas few studies suggest a possible role for ATP in the non-cholinergic, non-adrenergic, nerve-mediated relaxation of the detrusor (Klarskov, 1987a,b). In particular, in mouse carbachol-prestimulated bladder, ATP induced a biphasic force response: a marked contraction followed by a sustained relaxation (Boland *et al.*, 1993). The nature of the P_2-purinoceptor(s) mediating these functional effects still needs to be fully characterized.

The aim of the present study was to investigate the response(s) induced by ATP (and ATP analogues) in rat bladder at resting tone and in the carbachol prestimulated bladder strips, in order to confirm a possible role of ATP in nerve-mediate detrusor relaxation and tentatively define the purinoceptor subtype(s) involved in this response and their localization.

Methods

Muscle preparation

Male Sprague-Dawley rats weighing 175–200 g were used for all experiments. The animals were killed by cervical disloca-

[1] Author for correspondence.

tion. The abdomen was opened and the entire urinary bladder cut below the trigone, rapidly removed and opened along its longitudinal axis. The organ was placed in a 10 ml or 20 ml organ bath, perfused (rate: 60 ml h^{-1}) with Krebs solution at 37°C continuously bubbled with a 95% O_2 and 5% CO_2 mixture. The Krebs solution had the following composition (mM): NaCl 113, KCl 4.7, $CaCl_2$-$6H_2O$ 2.5, KH_2PO_4 1.2, $NaHCO_3$ 25, $MgSO_4$-$7H_2O$ 1.2, glucose 11.5, pH 7.4.

A resting load of 2 g (19.6 milliNewton, mN) was applied, and the preparation was allowed to equilibrate for 60 min before the start of the experiment. The effects of ATP and related compounds were examined both in the resting bladder and in the bladder prestimulated with carbachol. When studying the role of epithelial cells in the action of the drugs under investigation, the epithelium was removed by treatment with a 0.15% (w/v) collagenase Krebs solution for 3 min as previously described (Pinna *et al.*, 1992). The integrity of smooth muscle was evaluated with 1 μM acetylcholine.

Force was recorded by means of an isometric microdynamometer consisting of a strain gauge transducer, a high-gain amplifier and a galvanometer (2-channel recorder Gemini, 7070, Basile, Italy). Concentration-response curves to ATP and related compounds were obtained by a cumulative increase in the total concentration of agonist tested in 1 μM carbachol-precontracted tissues. Because of its desensitizing effect, the concentration-response curves to α,β-methyleneATP (α,β-meATP) were not cumulative. In this case suramin was added in perfusion. After the pharmacological evaluation, the tissue was carefully dessicated by means of a vacuum-dessicator and the dry weight determined. Each response was expressed either as mN force per mg dry weight (d.wt.) or as % of control response.

Materials

Acetylcholine chloride (ACh), adenosine (ADO), adenosine-5'-triphosphate (ATP), α,β-methyleneATP (α,β-meATP), carbachol, guanosine 5'-O-(2-thio-diphosphate) (GDPβS), guanosine 5'-O-(3-thiotriphosphate) (GTPγS), 2-methylthioATP (2-meSATP), 5'-N-ethyl-carboxamidoadenosine (NECA), nitrobenzyl-thioinosine (NBTI), 8-phenyl-theophylline (8-PT) and uridine-5'-triphosphate (UTP) were from Sigma. Suramin was a kind gift from Bayer. All drugs were dissolved in Krebs solution (except for 8-PT which was dissolved in 80% methanol containing 0.2 M NaOH) and added to the smooth muscle bath in volumes of 0.15 ml or less. All other chemicals were reagent grade and were obtained from Sigma.

Statistical analysis

The data in the test are expressed as mean ± standard error of 4–36 experiments. Statistical analysis of the data was performed with Student's *t* test. A probability value of $P<0.05$ was considered statistically significant.

Results

Figure 1a shows the effects of ATP on rat urinary bladder resting tone, At 1 mM concentration, ATP exerted a clear biphasic effect, consisting of a rapid and transient contraction (0.76 ± 0.06 mN mg^{-1} d.wt., $n=36$), followed by a slower sustained relaxation (0.10 ± 0.02 mN mg^{-1} d.wt., $n=36$, Figure 1a(i)). After washing the tissue twice, the second application of 1 mM ATP, 10 min after the first challenge, was characterized by a marked reduction of contraction (residual response was 43 ± 3% of initial response, $P<0.01$), whereas relaxation did not seem to be affected (Figure 1a(ii)). A complete restoration of the biphasic response to ATP could be obtained after 1 h (Figure 1a(iii)). To demonstrate the relaxation phase more clearly, a concentration-response curve was performed on the carbachol (1 μM) prestimulated bladder (Figure 1b). Under these experimental conditions the relaxant response was also detectable at 30 μM ATP (0.04 ± 0.007 mN mg^{-1} d.wt., $n=15$) and was maximal at 1 mM (0.5 ± 0.05 mN mg^{-1} d.wt., $n=15$). No further relaxation was obtained with 3 mM ATP (data not shown).

The possible desensitizing effect of the P_{2X}-purinoceptor agonist, α,β-methyleneATP (α,β-meATP) was tested in experiments shown in Figure 2. Application of the selective P_{2X}-agonist at 5 μM concentration resulted in a marked reduction

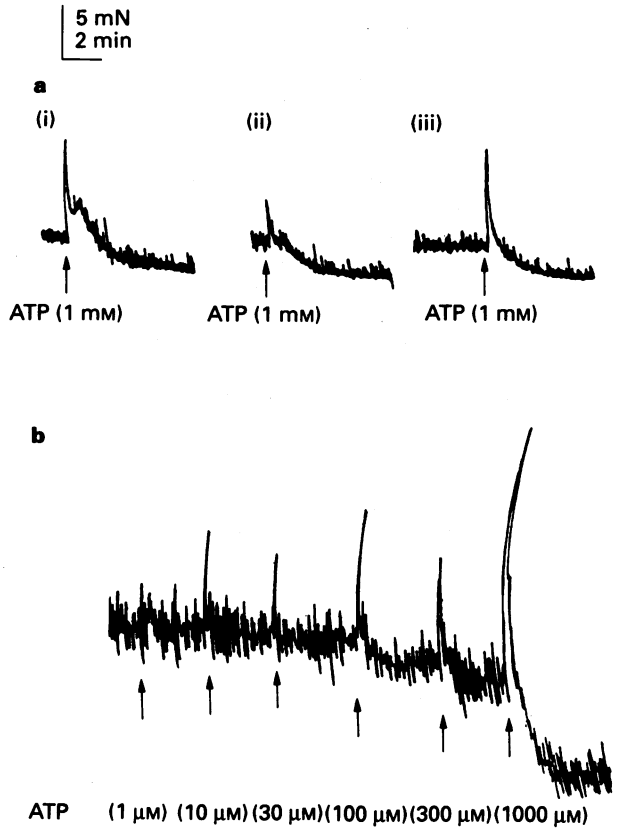

Figure 1 ATP induces a biphasic response in rat urinary bladder. (a) Original tracing showing contraction and relaxation induced by ATP in rat urinary bladder preparation at resting tone. The intervals between the first (i) and the second (ii) challenge and between the second and the third (iii) challenge with agonist were 10 and 60 min, respectively. (b) Original tracing showing the contractile and relaxant responses to ATP in tissue prestimulated with 1 μM carbachol.

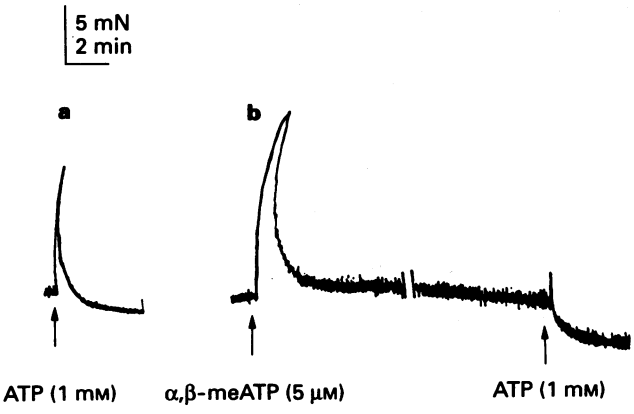

Figure 2 Representative tracing showing desensitization induced by α,β-methylene ATP (α,β-meATP) on the ATP contractile response of rat urinary bladder. The interval between the first ATP challenge (a) and the α,β-meATP treatment (b) was 60 min. The α,β-meATP contact time was 20 min. The second ATP challenge was performed after a further 30 min.

of the tissue contraction to ATP (compare contraction in Figure 2b with Figure 2a), without affecting the relaxant response. Interestingly and consistent with its selectivity on P_{2X}-receptors, α,β-meATP produced only a sustained monophasic contractile response (1.41 ± 0.08 mN mg^{-1} d.wt., n = 21) which was significantly higher than the ATP-induced contraction ($P<0.001$).

Conversely as shown in Figure 3a, the P_{2Y}-purinoceptor agonist, 2-methyl-thio-ATP (2-meSATP), induced a concentration-related relaxation on carbachol prestimulated strips. Consistent with its apparent selectivity for P_{2Y}-purinoceptors, a high concentration (1 mM) of this agonist mediated a significantly greater relaxation with respect to ATP (0.50 ± 0.05 vs 0.89 ± 0.014 mN mg^{-1} d.wt., $n = 4$). Since it has been reported that P_{2Y}-purinoceptors are linked to G-protein activation (Kennedy, 1990; Abbracchio & Burnstock, 1994), we have assessed whether G-proteins are involved in any of the ATP-induced effects by utilizing G-protein modulators, such as guanosine 5'-O-(3-thiotriphosphate) (GTPγS) (which is known to permanently activate G-proteins) and 5'-O-(2-thio-diphosphate) (GDPβS) (which conversely stabilizes G-proteins in their inactive state). Results are shown in Figure 3b. GTPγS (10 μM) amplified ATP-induced relaxation without affecting the contractile phase ($n = 3$, Figure 3b(i)). Conversely, 100 μM GDPβS completely inhibited only ATP-induced relaxation (Figure 3b(ii)), further confirming that G-protein coupling is involved only in the later ATP-dependent relaxing phase.

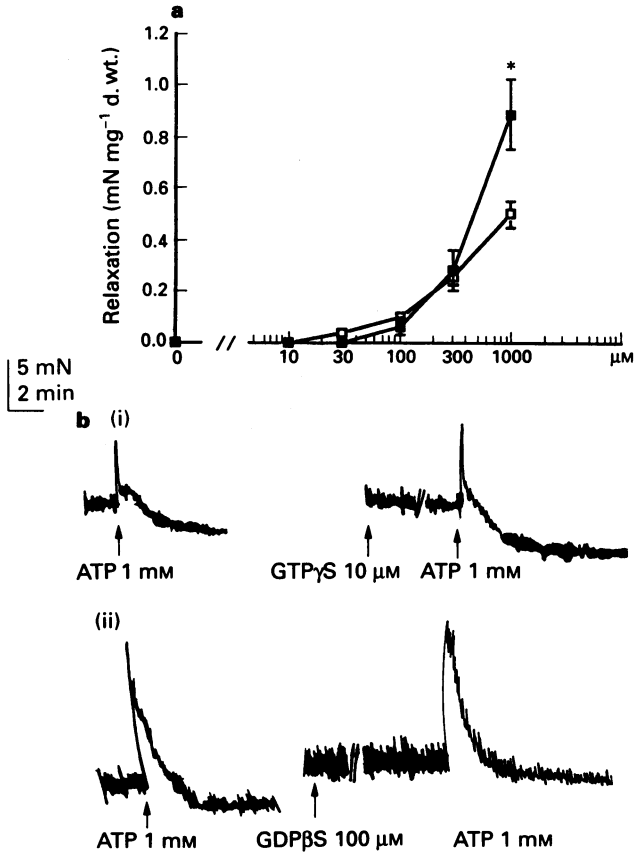

Figure 3 Involvement of P_{2Y}-purinoceptors in ATP-induced relaxation of rat bladder. (a) Concentration-response curves for relaxation to ATP (□) and 2-methyl-thioATP (2-meSATP) (■) in rat urinary bladder strips precontracted with 1 μM carbachol. Values represent the mean ± s.e.mean of 4 separate experiments. (b) Representative trace showing the effect of guanosine 5'-O-(3-thiotriphosphate) (GTPγS) (i) and guanosine 5'-O-(2-thio-diphosphate) (GDPβS) (ii) on ATP-induced responses. Rat urinary bladder preparations at resting tone were exposed to either GTPγS or GDPβS for 20 min before application of the second ATP challenge.

Since ATP is known to be quickly hydrolyzed to adenosine (Cusack & Hourani, 1984), in order to investigate the possible contribution of this metabolite to the detected responses (and to ATP-induced relaxation in particular), we have performed experiments in the presence of modulators of adenosine effects, such as the adenosine uptake inhibitor, nitrobenzyl-thioinosine (NBTI) and the adenosine receptor antagonist, 8-phenyltheophylline (8-PT). As shown in Figure 4a(i), NBTI did not significantly affect either the basal resting tone or ATP-induced responses. In the presence of NBTI, the ATP-induced relaxation was not significantly different from that obtained in the absence of the uptake inhibitor, apparently ruling out any significant contribution of adenosine to the detected response. Conversely, NBTI significantly potentiated the relaxation induced by exogenously added adenosine (Figure 4a(ii)). In fact, in NBTI-pretreated bladder strips, adenosine-induced relaxation was 250 ± 20% of the relaxation measure in the absence of the uptake inhibitor ($P<0.001$). In the presence of 8-PT, the relaxant responses evoked by ATP were not significantly modified (Figure 4b). That ATP and adenosine induce independent relaxation is confirmed by data shown in Figure 5a: ATP-induced relaxation was additive with the relaxation induced by the hydrolysis-resistant adenosine analogue, 5'-N-ethylcarboxamido-

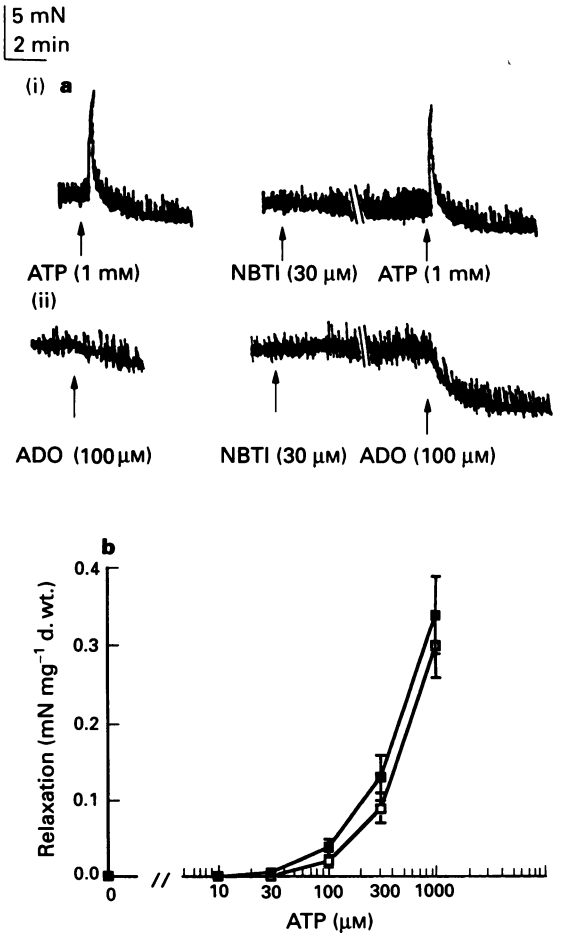

Figure 4 Adenosine does not contribute to the effects induced by ATP in rat urinary bladder. (a) Typical tracing showing the effect of nitro-benzyl-thioinosine (NBTI) on responses to ATP (i) and adenosine (ADO) (ii) in bladder preparations at resting tone. NBTI was added 1 h after the initial challenge with agonists. The second challenge with agonists was performed 15 min afterwards. (b) Concentration-dependent relaxation of rat urinary bladder induced by ATP in absence (□) or presence (■) of 100 μM 8-phenyltheophylline (8-PT). Relaxation was evaluated in preparations precontracted with 1 μM carbachol. 8-PT was added 20 min before starting the second concentration-response curve. Values are the mean ± s.e.mean of 8 separate experiments.

adenosine (NECA), suggesting the involvement of different receptors. In these experiments, NECA was tested at 10 μM, which induced a maximal relaxation as illustrated in Figure 5b.

We also tested the effects of the P_2-purinoceptor antagonist, suramin. Suramin (50 μM) did not modify significantly either ATP-induced contraction or ATP-induced relaxation ($n = 4$, Figure 6a and 6b). Notably, α,β-meATP concentration-response curve was shifted to the right by suramin in the same system ($n = 4$, Figure 7).

Figure 8 shows the effect of uridine-5'-triphosphate (UTP) on resting tone. No effect was detected at concentrations lower than 1 mM, at which UTP induced a potent monophasic contraction (0.67 ± 0.09 mN mg^{-1} d.wt., $n = 6$, Figure 8a), which was not statistically different from the contraction induced by ATP. Unlike the contractile response to ATP (Figure 2), the contractile response to UTP was not desensitized by pretreatment with α,β-meATP (Figure 8b).

In order to clarify the localization of the two different purinoceptor subtypes involved in the ATP-mediated responses, we evaluated the response to ATP in urinary bladder strips devoid of epithelium. The relaxant response evoked by 1 mM ATP at resting tone was significantly enhanced (0.10 ± 0.02 vs 0.29 ± 0.03 mN mg^{-1} d.wt., $n = 36$), whereas the contractile response was unaffected (0.76 ± 0.06 vs 0.76 ± 0.05 mN mg^{-1} d.wt., $n = 36$) by removal of epithelium. The integrity of the smooth muscle was evaluated with 1 μM ACh: no difference in response to ACh was detected in the presence or absence of epithelium (0.92 ± 0.08 vs 1.1 ± 0.08 mN mg^{-1} d.wt.).

Discussion

The existence of a purinergic innervation in bladder was initially proposed by Brown *et al.* (1979), who demonstrated that high concentrations of ATP caused contraction and that adenosine produced relaxation of the rat urinary bladder. Subsequent studies have confirmed the contractile action of ATP in guinea-pig (Cusack *et al.*, 1987; Hoyle *et al.*, 1990), in rabbit (Creed *et al.*, 1991) and in rat (Bo & Burnstock., 1992; Nicholls *et al.*, 1990) urinary bladder.

The pharmacological characterization performed in these studies suggested that the contraction evoked by ATP was mediated by the P_{2X} subtype of the P_2-purinoceptor (Burn-

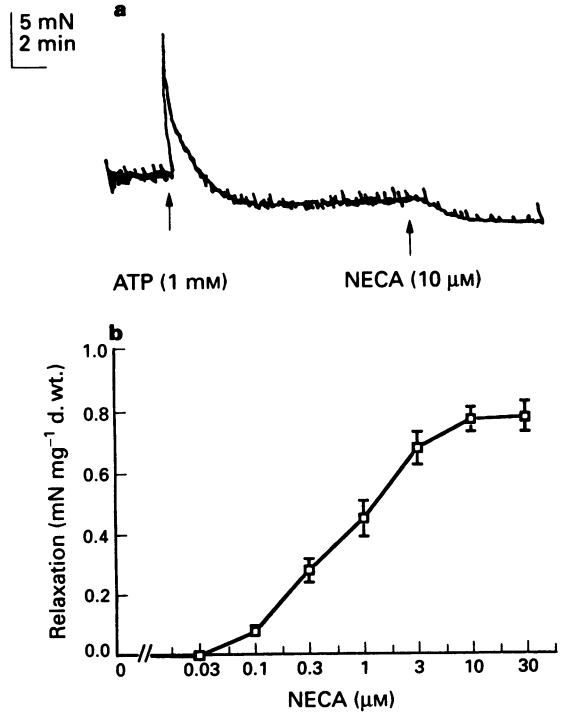

Figure 5 5'-N-ethylcarboxamidoadenosine (NECA) and ATP induce independent relaxation of rat bladder. (a) Effect of NECA on ATP-induced relaxation in rat urinary bladder at resting tone. (b) Concentration-response curve to NECA. Relaxation was assayed in preparations precontracted with 1 μM carbachol. Values represent the mean ± s.e.mean of 10 experiments.

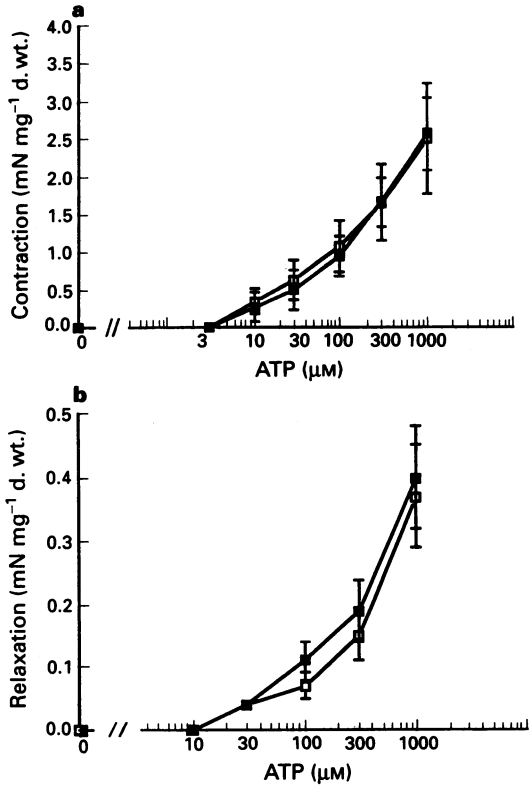

Figure 6 Effect of suramin on ATP-induced responses in rat urinary bladder. (a) ATP-induced contraction in the absence (□) or presence (■) or 50 μM suramin. (b) ATP-induced relaxation in the absence (□) or presence (■) of 50 μM suramin. Relaxation was assayed on rat bladder strips precontracted with 1 μM carbachol. Rat bladder preparations were exposed to suramin for 90 min before starting the second concentration-response curve for ATP. Values are the mean ± s.e.mean of 4 experiments.

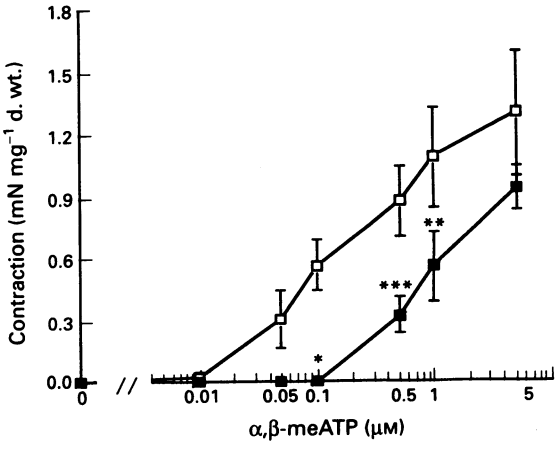

Figure 7 Effect of suramin on α,β-methylene ATP (α,β-meATP)-induced responses in rat urinary bladder. Concentration-response curves for α,β-meATP in the absence (□) and presence (■) of 50 μM suramin. The rat urinary bladder strips were precontracted with carbachol (1 μM) and suramin was added by perfusion. Values are the mean ± s.e.mean of 4 experiments.

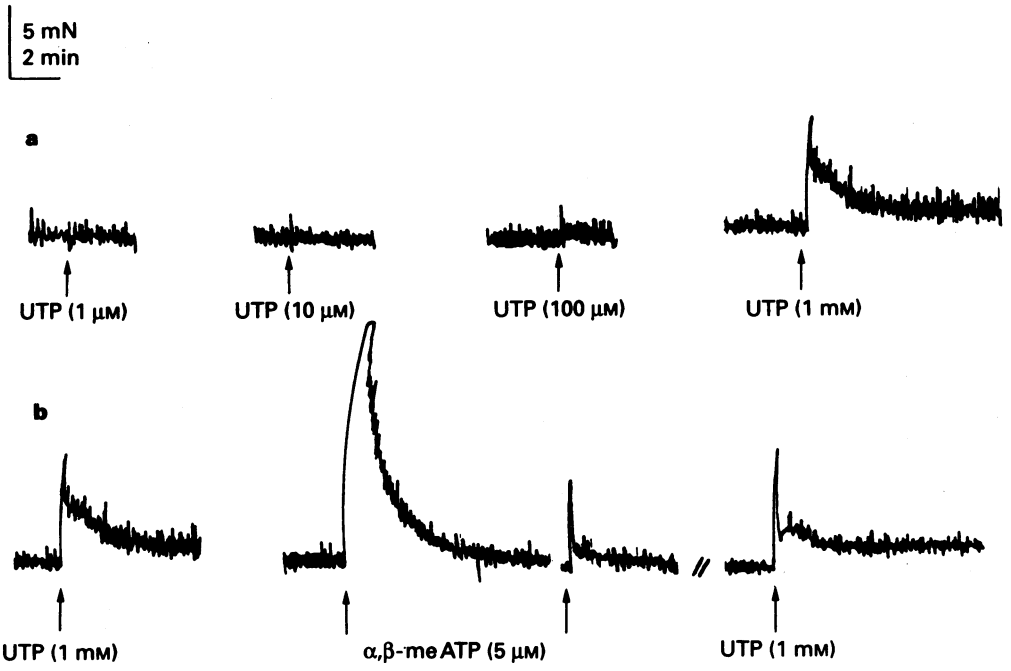

Figure 8 Typical tracings showing UTP-induced responses on urinary bladder strips at resting tone. (a) Concentration-related responses to UTP. (b) Effect of desensitizing α,β-methyleneATP (α,β-me ATP) concentrations on UTP-induced contraction. The first challenge with α,β-meATP was performed 1 h after the UTP application. After 30 min the tissue was washed and a second application of α,β-meATP was made, followed by the second UTP challenge.

stock & Kennedy, 1985). Dahlen & Hedqvist (1980) also reported an inhibitory action of ATP on transmural nerve stimulated contraction of rat urinary bladder preparations, implying the existence of multiple ATP receptors in this tissue. Furthermore, non-adrenergic, non-cholinergic nerve-mediated relaxation was discovered in pig and human detrusor (Klarskov, 1987a). More recently, Boland *et al.* (1993) have demonstrated for the first time that, besides its contractile action, ATP could also relax mouse urinary smooth muscle in carbachol-stimulated preparations, suggesting the involvement of P_{2Y}-purinoceptors.

In our study, we have investigated the action of ATP on resting tone and in carbachol precontracted strips in rat urinary bladder. The results show that ATP induces a biphasic response, characterized by an initial fast and transient contraction and by a subsequent slower long-lasting relaxation. To our knowledge, this is the first time that ATP (albeit at high concentration) has been reported to induce a direct relaxation of rat urinary bladder. Furthermore, in carbachol-prestimulated tissues, a concentration-dependent relaxation has been obtained. Under these experimental conditions, a relaxant response was detectable at 30 μM ATP and was maximal at 1 mM.

Formation of adenosine from ATP has been reported in guinea-pig urinary bladder preparations (Cusack & Hourani, 1984). In particular, 5 min after ATP addition, adenosine amounted to 20% of the active compounds in the incubation medium. With rabbit urinary bladder, on the other hand, no significant decrease in the ATP concentration present in organ bath was detected after 48 min (Levin *et al.*, 1981). Nicholls *et al.* (1992) demonstrated that in the rat urinary bladder preparations, about 25% of the ATP was degraded after 5 min but little adenosine was formed.

To rule out the possibility that adenosine could in any way contribute to the detected responses, we have performed experiments with modulators of adenosine effects. Results show that ATP-induced responses were not affected by either NBTI or 8-PT, ruling out the involvement of adenosine; this conclusion was also confirmed by the observation that ATP and NECA-induced relaxant effects were additive.

Experiments performed with the P_{2X}-selective agonist, α,β-meATP confirmed that the contractile phase could indeed be due to the activation of P_{2X}-purinoceptors.

The concentration-dependent relaxant responses obtained with the P_{2Y} agonist, 2-meSATP, suggest that ATP could indeed activate P_{2Y}-like receptors in rat urinary bladder. However, recent studies suggest that responses to this analogue cannot be taken as unequivocal proof for P_{2Y}-purinoceptor involvement. 2-meSATP can undergo enzymatic degradation *in vitro* similarly to ATP. In recent studies (Evans & Kennedy, 1994), in which ecto-ATPase activity was absent or blocked, 2-meSATP showed equivalent potency to α,β-meATP at P_{2X}-purinoceptors, suggesting caution in the interpretation of results obtained with this analogue.

However, the experiments performed with GTPγS and GDPβS, demonstrating amplification and inhibition, respectively, of ATP-induced relaxation, allow us to conclude that the purinoceptor mediating bladder relaxation belongs to the P_{2Y}-purinoceptor family (Abbracchio & Burnstock, 1994). On the other hand, these experiments also indicated that receptors involved in the initial transient contraction do not belong to the G-protein-linked purinoceptor superfamily, confirming that this response may be subserved by a receptor-regulated ion channel (Bean, 1990; Abbracchio & Burnstock, 1994).

Experiments with the P_2-purinoceptor antagonist, suramin, demonstrated that, unlike results reported for P_{2X}-purinoceptors in other tissues (Burnstock, 1993) and other species (Hoyle *et al.*, 1990), ATP-evoked responses were not affected by suramin, which is consistent with previous observations in mouse vas deferens (Von Kugelgen *et al.*, 1990). However, at least for the contractile effects induced by ATP, we were able to demonstrate that suramin can indeed cause a rightward shift of the concentration-response curve to the hydrolysis-resistant ATP analogue, α,β-meATP. This apparent discrepancy can now be interpreted in the light of the recently reported ability of suramin to block ecto-ATPase in the same concentration-range over which it exerts P_{2X}-purinoceptor antagonism (Crack *et al.*, 1994). The absence of any effect on the ATP concentration-response curve may therefore be attri-

buted to the ability of suramin to inhibit the degradation of ATP, consequently opposing the rightward shift of the curve, rather than to suramin-insensitivity of P_{2X}-purinoceptors. On the basis of the results, we can conclude that the P_{2X}-purinoceptor-mediating contraction of rat bladder is indeed suramin-sensitive.

Suramin did not significantly affect ATP-evoked relaxation. Whether this is due to a real receptor insensitivity to suramin or to effects similar to those above described for P_{2X}-purinoceptors still remains to be clarified. The utilization of new hydrolysis-resistant ATP derivatives endowed with P_{2Y}-purinoceptor selectivity (Abbracchio & Burnstock, 1994) will help in elucidating this point.

Since it has been reported that purinoceptors involved in the ATP responses could also respond to UTP (Abbracchio & Burnstock, 1994), we have also tested the action of UTP in our preparations. UTP induced only a rapid and concentration-dependent contraction of rat bladder preparations, which was not desensitized by α,β-meATP, suggesting that ATP and UTP might utilize different receptors. Although further experiments are needed before any conclusion can be drawn on this particular aspect, recent evidence suggests that an ATP/UTP receptor with similar characteristics is also present in the pulmonary vasculature (Rubino & Burnstock, 1994).

The experiments carried out in tissues devoid of epithelial cells indicated a possible localization in smooth muscle for both the P_{2X} and P_{2Y}-purinoceptors. In fact, the contractile phase was not modified by removal of the epithelium, whereas the relaxant phase was significantly increased. The latter result also suggested a modulation of relaxation by excitatory factor(s) released from the epithelium.

In conclusion, in rat urinary bladder, ATP coreleased with acetylcholine activates two subtypes of purinoceptors mediating different and opposite functional effects. In particular, the inhibitory action evoked by P_{2Y}-purinoceptors might counteract P_{2X}-purinoceptor-mediated contraction, therefore suggesting that ATP might play an important functional role in the physiological regulation of both micturition and bladder filling. This would also suggest a role for P_{2Y}-purinoceptors in the high compliance of urinary bladder and will be important in future studies aimed at assessing a possible defect of purinoceptors in pathological conditions characterized by bladder malfunctions.

The authors are grateful to Bayer Italia for kindly supplying suramin.

References

ABBRACCHIO, M.P. & BURNSTOCK, G. (1994). Purinoceptors: are there superfamilies of P2X and P2Y purinoceptors? *Pharmacol. Ther.*, **64**, 445–475.

BARNARD, E.A., BURNSTOCK, G. & WEBB, T.E. (1994). G-protein coupled receptors for ATP and others nucleotides: a new receptor family. *Trends Pharmacol. Sci.*, **15**, 67–70.

BEAN, B.P. (1990). ATP-activated channels in rat and bullfrog sensory neurons: concentration dependence and kinetics. *J. Neurosci.*, **10**, 1–10.

BO, X. & BURNSTOCK, G. (1992). Species differences in characteristics and distribution of (^{3}H) α,β-methylene ATP binding sites in urinary bladder and urethra of rat, guinea-pig and rabbit. *Eur. J. Pharmacol.*, **216**, 59–66.

BOLAND, B., HIMPENS, B., PAQUES, C., CASTEELS, R. & GILLIS, J.M. (1993). ATP induced-relaxation in the mouse bladder smooth muscle. *Br. J. Pharmacol.*, **108**, 749–753.

BROWN, C., BURNSTOCK, G. & COCKS, T. (1979). Effects of adenosine-5′-triphosphate (ATP) and β,γ-methylene ATP on the rat urinary bladder. *Br. J. Pharmacol.*, **65**, 97–102.

BURNSTOCK, G. (1978). A basis for distinguishing two types of purinergic receptor. In *Cell Membrane Receptors for Drugs and Hormones: A Multidisciplinary Approach.* ed. Straub, R.W. & Bolis, L. pp. 107–118, New York: Raven Press.

BURNSTOCK, G. (1993). Physiological and pathological roles of purines: an update. *Drug Dev. Res.*, **28**, 195–206.

BURNSTOCK, G. & KENNEDY, C. (1985). Is there a basis for distinguishing two types of P2-purinoceptor? *Gen. Pharmacol.*, **16**, 433–440.

CRACK, B.E., BEUKERS, M.W., MCKECHNIE, K.C.W., IJZERMAN, A.P. & LEFF, P. (1994). Pharmacological analysis of ecto-ATPase inhibition: evidence for combined enzyme inhibition and receptor antagonism in P_{2X}-purinoceptor ligands. *Br. J. Pharmacol.*, **113**, 1432–1438.

CREED, K.E., ITO, Y. & KATSUYAMA, H. (1991). Neurotransmission in the urinary bladder of rabbit and guinea pigs. *Am. J. Physiol.*, **261**, (*Cell Physiol.*, **30**), C271–C277.

CUSACK, N.J. & HOURANI, S.M.O. (1984). Some pharmacological and biochemical interactions of the enantiomers of adenylyl-5′-(β,γ-methylene)-diphosphonate with the guinea-pig urinary bladder. *Br. J. Pharmacol.*, **82**, 155–159.

CUSACK, N.J., HOURANI, S.M.O., LOIZOU, G.D. & WELFORD, L.A. (1987). Pharmacological effects of isopolar phosphonate analogues of ATP on P_2-purinoceptors in guinea-pig taenia coli and urinary bladder. *Br. J. Pharmacol.*, **90**, 791–795.

DAHLEN, S.E. & HEDQVIST, P. (1980). ATP, β,γ-methylene ATP and adenosine inhibit non-cholinergic, non-adrenergic transmission in the rat urinary bladder. *Acta Physiol. Scand.*, **109**, 137–142.

EVANS, R.J. & KENNEDY, C. (1994). Phamacological characterization of P2-purinoceptors in single acutely dissociated smooth muscle cells of the rat tail artery. *Drug Dev. Res.*, **31**, 285.

FREDHOLM, B.B., ABBRACCHIO, M.P., BURNSTOCK, G., DALY, J.W., HARDEN, T.K., JACOBSON, K.A., LEFF, P. & WILLIAMS, M. (1994). Nomenclature and classification of purinoceptors. *Pharmacol. Rev.*, **46**, 143–156.

HOYLE, C.H.V., KNIGHT, G.E. & BURNSTOCK, G. (1990). Suramin antagonizes responses to P_2-purinoceptor agonists and purinergic nerve stimulation in the guinea-pig urinary bladder and taenia coli. *Br. J. Pharmacol.*, **99**, 617–621.

KENNEDY, C. (1990). P1- and P2-purinoceptor subtypes-An update. *Arch. Int. Pharmacodyn.*, **303**, 30–50.

KLARSKOV, P. (1987a). Non-cholinergic, non-adrenergic nerve-mediated relaxation of pig and human detrusor muscle *in vitro*. *Br. J. Urol.*, **59**, 414–419.

KLARSKOV, P. (1987b). Non-cholinergic, non-adrenergic inhibitory nerve responses of bladder outlet smooth muscle *in vitro*. *Br. J. Urol.*, **60**, 337–342.

LANGLEY, J.N. & ANDERSON, H.K. (1985). The innervation of the pelvic and adjoining viscera. *The Bladder J. Physiol.* Part. 11, **19**, 71–139.

LEVIN, R.R., JACOBY, R. & WEIN, A.J. (1981). Effect of adenosine triphosphate on contractility and adenosine triphosphate activity of the rat urinary bladder. *Mol. Pharmacol.*, **19**, 525–528.

NICHOLLS, J., HOURANI, S.M.O. & KITCHEN, I. (1990). The ontogeny of purinoceptors in rat urinary bladder and duodenum. *Br. J. Pharmacol.*, **100**, 874–878.

NICHOLLS, J., HOURANI, S.M.O. & KITCHEN, I. (1992). Degradation of extracellular adenosine and ATP by adult and neonatal rat duodenum and urinary bladder. *Pharmacol. Commun.*, **2**, 203–210.

PINNA, C., CARATOZZOLO, O. & PUGLISI, L. (1992). A possible role for urinary bladder epithelium in bradykinin-induced contraction in diabetic rats. *Eur. J. Pharmacol.*, **214**, 114–117.

RUBINO, A. & BURNSTOCK, G. (1994). A new purinergic receptor may contribute to the control of pulmonary circulation of the heart. *Drug. Dev. Res.*, **31**, 315.

VON KUGELGEN, I., BULTMANN, R. & STARKE, K. (1990). Interaction of adenine nucleotides, UTP and suramin in mouse vas deferens: suramin-sensitive and suramin-insensitive components in the contractile effect of ATP. *Naunyn Schmied. Arch. Pharmacol.*, **342**, 198–205.

(Received June 27, 1994
Revised November 21, 1994
Accepted January 4, 1995)

British Journal of Pharmacology (1995) 114, 1563-1570 © 1995 Stockton Press All rights reserved 0007-1188/95 $12.00

Functional interaction between losartan and central tachykinin NK_3 receptors in the conscious rat

Pierre Picard, *Louise Chrétien & [1]Réjean Couture

Department of Physiology, Faculty of Medicine, Université de Montréal, C.P. 6128, Succursale Centre-Ville, Montréal, Québec, Canada H3C 3J7 and *Department of Pharmacology, Faculty of Medicine, Université de Sherbrooke, Sherbrooke, Québec, Canada J1H 5N4

1 The cardiovascular and behavioural effects elicted by the intracerebroventricular (i.c.v.) injection of substance P (SP), neurokinin A (NKA), [MePhe^7]neurokinin B ([MePhe^7]NKB) or angiotensin II (AII) in the conscious rat were assessed before and 5 min after i.c.v. pretreatment with antagonists selective for angiotensin AT_1 (losartan and its active metabolite EXP 3174), angiotensin AT_2 (PD 123,319) or tachykinin NK_3 (R 486) receptors.

2 I.c.v. administration of 25 pmol AII evoked an increase in mean arterial blood pressure (MAP) and water intake behaviour, accompanied by a transient bradycardia, whereas 25 pmol [MePhe^7]NKB caused a transient increase in MAP and heart rate (HR) concurrently with marked wet dog shake behaviour. At the same dose, SP and NKA were more potent than [MePhe^7]NKB in increasing MAP and HR, but did not produce water intake or wet dog shake behaviours.

3 Losartan (650 pmol, i.c.v.) reduced significantly the cardiovascular and behavioural responses to AII or [MePhe^7]NKB, but not to SP or NKA. While 65 pmol losartan was inactive, 260 pmol inhibited selectively the central effects of AII. Whereas EXP 3174 (6.5 nmol) blocked both AII and [MePhe^7]NKB-mediated responses, the dose of 650 pmol blocked only the responses to AII.

4 The central responses to AII and [MePhe^7]NKB were not affected by PD 123,319 (650 pmol). On the other hand, the [MePhe^7]NKB-induced central effects were significantly reduced by R 486 (650 pmol). The NK_3-selective antagonist had no effect against AII.

5 This study provides functional evidence, to support earlier binding data, that losartan (and to some extent its active metabolite EXP 3174) interact with the tachykinin NK_3 receptor in rat brain. However, the cardiovascular and behavioural responses induced by central tachykinin agonists (SP, NKA and [MePhe^7]NKB) and AII are mediated by unrelated mechanisms.

Keywords: Losartan; angiotensin II; NK_3 receptor; tachykinin; central cardiovascular regulation; behaviour

Introduction

The natural mammalian tachykinins, substance P (SP), neurokinin A (NKA) and neurokinin B (NKB) are the preferential agonists for the tachykinin NK_1, NK_2 and NK_3 receptors, respectively (Helke *et al.*, 1990; Maggi *et al.*, 1993). To date, several non-peptide NK_1 and NK_2 receptor antagonists have been described (Garret *et al.*, 1991; Snider *et al.*, 1991; Advenier *et al.*, 1992; Watling, 1992; McLean *et al.*, 1993). However, the search for non-peptide NK_3 receptor antagonists is still in its infancy. Although some NK_3 receptor antagonists exist, they are unstable peptide analogues (Drapeau *et al.*, 1990). Most recently, a stable, non-peptide NK_3 receptor antagonist named SR 142801 has been described (Emonds-Alt *et al.*, 1995). This compound is a potent antagonist of the human and guinea-pig NK_3 receptor while being almost inactive versus the rat NK_3 receptor. Recent binding studies have shown that losartan (DuP 753), a non-peptide angiotensin II (AII) antagonist at the AT_1 receptor, exhibits moderate affinities for the NK_3 receptor present in rat ($pK_i = 4.8$) and guinea-pig ($pK_i = 5.0$) brain membranes (Chrétien *et al.*, 1994).

Tachykinins and AII are known to participate in central cardiovascular, water and electrolyte balance regulation as well as in behavioural activity (Otsuka & Yoshioka, 1993; Bunnemann *et al.*, 1993). I.c.v. administration of senktide, an NK_3 receptor-selective agonist, leads to increases in mean arterial blood pressure (MAP) and heart rate (HR) through vasopressin release (Nagashima *et al.*, 1989; Takano *et al.*, 1990), decreases in water, salt and alcohol intake (Massi *et al.*, 1991; Ciccocioppo *et al.*, 1994), inhibition of gastric acid secretion (Improta & Broccardo, 1991) and induction of wet dog shake behaviour (Itoi *et al.*, 1992). The NK_3 receptor antagonist, [Trp^7,β-Ala^8]NKA(4-10) (R 486), attenuates significantly and selectively the central cardiovascular and wet dog shake responses to [MePhe^7]NKB, a selective NK_3 agonist (Picard *et al.*, 1994). On the other hand, losartan blocks i.c.v. AII-mediated increases in blood pressure and water intake (Wong *et al.*, 1990a; Kirby *et al.*, 1992; Timmermans *et al.*, 1993; Grupp & Harding, 1994), as well as vasopressin and luteinizing hormone secretion (Stephenson & Steele, 1992; Toney & Porter, 1993a; Palmer *et al.*, 1994). The antihypertensive action of orally administered losartan on the AT_1 receptor has been largely attributed to its metabolic transformation into EXP 3174 (Wong *et al.*, 1990b; Duncia *et al.*, 1992). Systemic losartan crosses the blood brain barrier and blocks central AT_1 receptors (Fregly & Rowland, 1991; Song *et al.*, 1991; Li *et al.*, 1993).

The role of central AT_2 receptors remains controversial (Toney & Porter, 1993a,b; Cooney & Fitzsimons, 1993). Although the AT_2 receptor-selective antagonist, PD 123,319 had no effect on central AII-mediated responses, combined treatment with losartan and PD 123,319 was more effective in blocking AII-induced pressor effects than losartan alone (Toney & Porter, 1993a,b). Furthermore, pressor responses induced by microinjection of AII into the rat paraventricular nucleus were significantly attenuated following systemic administration of losartan, but were not affected by PD 123,319 (Bains *et al.*, 1992). Thus, the vasopressor effect induced by i.c.v. AII appears to be primarily mediated by the AT_1 receptor, which is supported by autoradiographic studies (Gehlert *et al.*, 1990; Tsutsumi & Saavedra, 1991), and the i.c.v. treatment with AT_1 receptor antisense oligonucleotides (Gyurko *et al.*, 1993; Sakai *et al.*, 1994).

[1] Author for correspondence.

The objective of this study was (a) to confirm *in vivo* that losartan and other antagonists of AII can block the central tachykinin NK_3 receptor, (b) to examine whether or not the central cardiovascular and behavioural effects of AII are mediated by tachykinin NK_3 receptors and (c) to determine the putative role of AII in the central cardiovascular and behavioural effects of SP, NKA and [MePhe^7]NKB in the conscious rat.

Methods

Animal preparation

Male Wistar rats (Charles River, St. Constant, Québec, Canada) weighing 300–350 g were used. The animals were allowed free access to food and water and maintained on a 12 h light/dark cycle (lights on 06 h 00 min–18 h 00 min).

Rats were anaesthetized with intraperitoneal (i.p.) sodium pentobarbitone (65 mg kg^{-1}) (Somnotol; M.T.C. Pharmaceuticals, Cambridge, Ont. Canada) before an i.c.v. polyethylene cannula (PE-20; Intramedic, Clay Adams, NJ, U.S.A.) was implanted with a guide into the right lateral brain ventricle by use of a Kopf stereotaxic apparatus (David Kopf Instruments, Tujunga, CA, U.S.A.), and permanently secured to the skull with dental cement (Reliance Dental MFG. Co., Worth, IL, U.S.A.). The stereotaxic coordinates were 1.3 mm lateral to the midline, 0.6 mm caudal to the bregma and 5.0 mm vertical from the skull surface.

The animals were then housed in individual plastic cages (40 cm × 23 cm × 20 cm) for a recovery period of 24 h, after which rats were anaesthetized again before a second cannula (PE-50) was inserted through the left femoral artery into the abdominal aorta for measurement of blood pressure and heart rate. The pre-siliconized intraarterial catheter was filled with physiological saline containing heparin sodium salt (100 iu ml^{-1}) and passed through a subcutaneous tunnel to emerge at the back of the neck. Experiments were conducted 48 h after the intravascular surgery on conscious, unrestrained rats kept in their resident cages.

Measurement of cardiovascular and behavioural responses

The arterial blood pressure was monitored through the intraarterial catheter with a Statham pressure transducer (P231D) while the HR was measured with a cardiac tachometer (model 7P4) and both variables were registered on a Grass polygraph model 79D (Grass Instruments Co., Quincy, MA, U.S.A.). Experiments started when the animal was in a resting state and basal MAP and HR were stable. Wet dog shake behaviour was measured according to the number of episodes (less than 1 s each) occuring during the 30 min period of recording. Rats had access to a tap water distributor which allowed the measurement of the total ingested volume (ml) of water for a period of 30 min after i.c.v. injection.

Rats were injected i.c.v. with 25 pmol AII to verify the potency of the i.c.v. cannula. Only those animals which responded with an immediate sharp rise in blood pressure, associated with an intense dipsogenic activity as reported earlier (Kirby *et al.*, 1992), were included in the study. The correct position of the i.c.v. cannula was also verified histologically by post-mortem dissection.

Experimental protocols

In the first series of experiments, the animals received randomly a single i.c.v. injection of either 25 pmol AII, SP, NKA or [MePhe^7]NKB (1 µl peptide solution flushed with 4 µl of cerebrospinal fluid (CSF; composition in mM: NaCl 128.6, KCl 2.6, $MgCl_2$ 2.0 and $CaCl_2$ 1.4; pH adjusted to 7.2)). The cardiovascular and behavioural responses were then measured over a period of 30 min. Control rats received 5 µl CSF only. On the second day, vehicle or one of the four antagonists, losartan (65 pmol, 260 pmol, 650 pmol or 6.5 nmol), EXP 3174 (65 pmol, 650 pmol or 6.5 nmol), PD 123,319 (650 pmol) or R 486 (650 pmol), were randomly administered i.c.v., 5 min prior to 25 pmol AII or [MePhe^7]NKB. In addition, losartan (650 pmol) was tested against SP (25 pmol) and NKA (25 pmol) to evaluate its selectivity for AT_1 and NK_3 receptors. Only one antagonist was administered to each animal. On the third day, the test agonist was injected alone again to evaluate the reversibility of any inhibition produced by the antagonist on day 2. No tachyphylaxis to SP, NKA or [MePhe^7]NKB was seen when each agonist (25 pmol) was injected i.c.v. on three consecutive days (Picard *et al.*, 1994). The intrinsic activity of the antagonists was tested in separate experiments. Baseline MAP and HR values were calculated 1 min before the injection of agonists.

Peptides and non-peptides

Losartan (DuP 753 or MK-954; 2-n-butyl-4-chloro-5-hydroxymethyl-1-[(2′-(1*H*-tetrazol-5-yl)biphenyl-4-yl)methyl]imidazole potassium salt) and EXP 3174 (2-n-butyl-4-chloro-1-[(2′-(1*H*-tetrazol-5-yl)biphenyl-4-yl)methyl]imidazole-5-carboxylic acid) were obtained from Dupont (Delaware, U.S.A.). PD 123,319 (1-[4-(dimethylamino)3-methylphenyl]-methyl-5-(diphenylacetyl)-4,5,6,7-tetrahydro-1*H*-imidazole [4,5-*c*]pyridine-6-carboxylic acid) was obtained from Parke-Davis (Cambridge, England). The compound R 486 (H-Asp-Ser-Phe-Trp-β-Ala-Leu-Met-NH_2) is a competitive and selec-

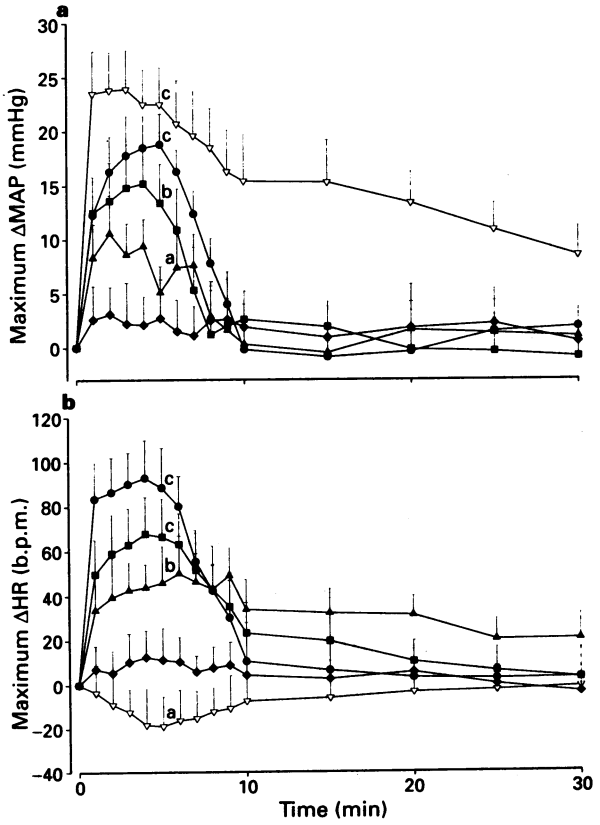

Figure 1 Time course of (a) mean arterial blood pressure (MAP) and (b) heart rate (HR) changes evoked by i.c.v. injections of 25 pmol substance P (SP, ●), neurokinin A (NKA, ■), [MePhe^7]neurokinin B (▲) and angiotensin II (AII, ▽) in conscious freely moving rats. Cardiovascular effects mediated by the vehicle (CSF) are also shown (◆). Each point represents the mean ± s.e. mean of results from 8 rats for each peptide. Statistical comparison to the vehicle for the period of 1–10 min following i.c.v. injection of peptides is indicated by $^aP<0.05$; $^bP<0.01$; $^cP<0.001$.

tive antagonist of the NK_3 receptor with a pA_2 of 7.5 on the rat portal vein (NK_3 receptor preparation; Drapeau *et al.*, 1990). R 486 and [MePhe^7]NKB (H-Asp-Met-His-Asp-Phe-Phe-MePhe-Gly-Leu-Met-NH_2) were provided by Dr D. Regoli of Sherbrooke University, Sherbrooke, Canada. SP, NKA and AII were purchased from Hükabel Scientific Ltd, Montréal, Canada. Heparin sodium salt Grade II from porcine intestinal mucosa was purchased from Sigma chemicals (St. Louis, MO, U.S.A.). The antagonists and [MePhe^7]NKB were dissolved in dimethylsulphoxide (DMSO; Fisher) and CSF was added to obtain the desired solution (the final solution contained a maximum of 20% of DMSO). SP, NKA and AII were dissolved directly in CSF. The stock solutions ($1-10$ mg ml^{-1}) of peptides and non-peptides were divided into 100 µl aliquots and stored at -20°C until used. Daily dilutions were made in CSF before each experiment.

Statistical analysis of data

The results are expressed as mean ± s.e.mean. Statistical differences were evaluated with Student's *t* test for paired samples or Wilcoxon-Mann-Whitney (U) test for unpaired samples on non parametric values (behaviour frequency). When more than one comparison was made, the significance of differences among groups was evaluated with a one-way analysis of variance (ANOVA) in conjunction with Bonferroni confidence intervals. Only probability values (P) smaller than 0.05 were considered to be statistically significant.

Results

Cardiovascular and behavioural effects induced by SP, NKA, [MePhe^7]NKB and AII

On the first experimental day, i.c.v. injections of equimolar doses (25 pmol) of SP, NKA, [MePhe^7]NKB or AII produced distinct cardiovascular and behavioural responses (Figures 1 and 2). AII was the most potent vasopressor agonist (peak ΔMAP = 23.6 ± 4.7 mmHg; $P<0.001$ with CSF peak value) the effect of which persisted over 45 min. On the other hand, tachykinins induced a transient (8–10 min) pressor response when injected i.c.v. with the rank order of potency: SP (peak ΔMAP = 17.6 ± 3.9 mmHg; $P<0.01$ with CSF peak value) > NKA (peak ΔMAP = 14.8 ± 4.2 mmHg; $P<0.01$ with CSF peak value) > [MePhe^7]NKB (peak ΔMAP = 10.4 ± 4.4 mmHg; $P<0.05$ with CSF peak value) (Figure 1). Whereas central tachykinins evoked transient increases in HR with the rank order of potency: SP (peak ΔHR = 92.3 ± 19.7 b.p.m.; $P<0.01$ with CSF peak value) > NKA (peak ΔHR = 69.8 ± 17.5 b.p.m.; $P<0.01$ with CSF peak value) > [MePhe^7]NKB (peak ΔHR = 50.1 ± 21.3 b.p.m.; $P<0.01$ with CSF peak value), AII caused a slight bradycardia (peak ΔHR = -18.7 ± 15.7 b.p.m.; $P<0.05$ with CSF peak value) which returned to baseline within 10 min. As expected, AII also evoked a marked dipsogenic response (15 ml × 30 min^{-1}) not shared by the tachykinins, which did not induce thirst when compared to CSF (Figure 2). Whereas NKA and SP did not induce wet dog shake, AII or [MePhe^7]NKB pro-

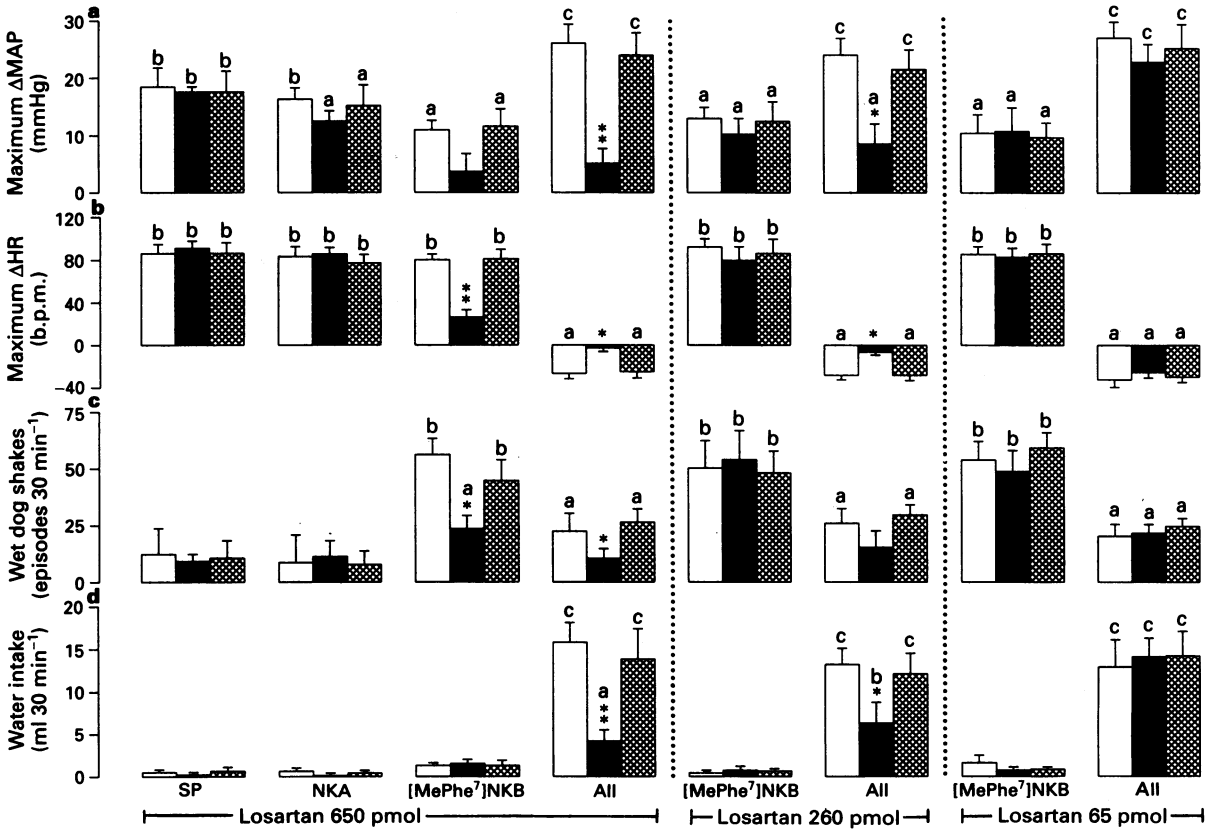

Figure 2 Cardiovascular and behavioural effects of 25 pmol substance P (SP), neurokinin A (NKA), [MePhe^7]neurokinin B ([MePhe^7]NKB) and angiotensin II (AII) were measured on three consecutive days in conscious rats. Agonists were injected i.c.v. alone on day 1 (open columns) or 5 min after the prior i.c.v. injection of losartan (65 pmol, 260 pmol or 650 pmol) on day 2 (solid columns). On day 3 (cross-hatched columns), agonists were readministered alone to assess the reversibility of the blockade. Shown are maximal increases in (a) mean arterial blood pressure (MAP) and (b) heart rate (HR) measured at 3–5 min post-injection. Total wet dog shake episodes (c) and water intake (d) were measured for a period of 30 min. Maximal CSF values are: ΔMAP = 4.0 ± 3.2 mmHg; ΔHR = 7.8 ± 5.0 b.p.m.; wet dog shake = 5.9 ± 4.5 episodes × 30 min^{-1}; water intake = 0.2 ± 0.1 ml × 30 min^{-1}; $n = 8$. Each value represents the mean ± s.e.mean of results from 8 rats for each agonist. Statistical comparison to the agonist alone on day 1 is indicated by $^*P<0.05$; $^{**}P<0.01$ and to the vehicle is indicated by $^aP<0.05$; $^bP<0.01$; $^cP<0.001$.

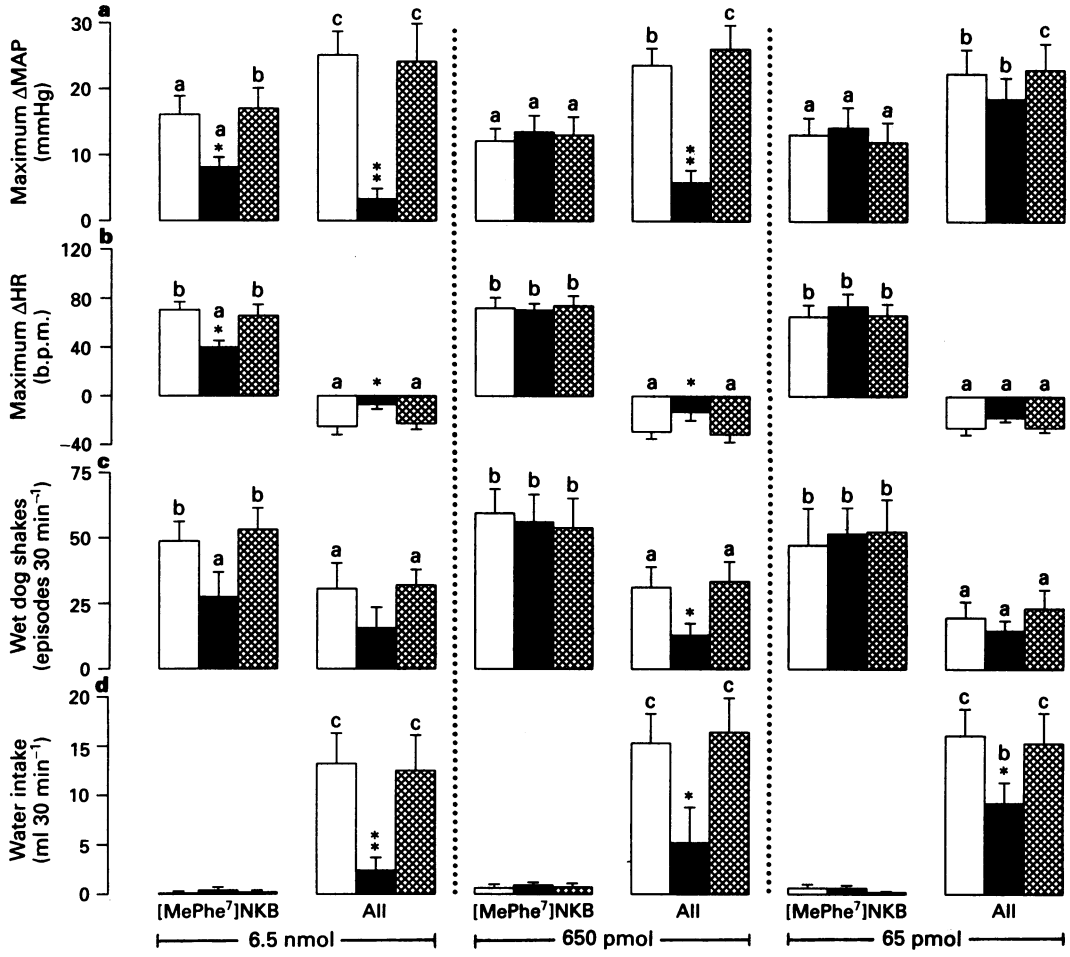

Figure 3 Cardiovascular and behavioural effects of 25 pmol [MePhe^7]neurokinin B ([MePhe^7]NKB) and angiotensin II (AII) were measured on three consecutive days in conscious rats. Agonists were injected i.c.v. alone on day 1 (open columns) or 5 min after the prior i.c.v. injection of EXP 3174 (65 pmol, 650 pmol or 6.5 nmol) on day 2 (solid columns). On day 3 (cross-hatched columns), agonists were readministered alone to assess the reversibility of the blockade. Shown are maximal increases in (a) mean arterial blood pressure (MAP) and (b) heart rate (HR) measured at 3–5 min post-injection. Total wet dog shake episodes (c) and water intake (d) were measured for a period of 30 min. Maximal CSF values are: ΔMAP = 5.9 ± 4.1 mmHg; ΔHR = 11.4 ± 8.3 b.p.m.; wet dog shake = 7.0 ± 4.8 episodes × 30 min^{-1}; water intake = 1.5 ± 1.3 ml × 30 min^{-1}; $n = 8$. Each value represents the mean ± s.e.mean of results from 8 rats for each agonist. Statistical comparison to the agonist alone on day 1 is indicated by $^*P<0.05$; $^{**}P<0.01$ and to the vehicle is indicated by $^aP<0.05$; $^bP<0.01$; $^cP<0.001$.

duced moderate and intense wet dog shakes, respectively (Figure 2).

Effects of antagonists on the responses to SP, NKA, [MePhe^7]NKB and AII

On the second day of experiments, 65 pmol of losartan had no effect on either [MePhe^7]NKB or AII-mediated responses while 260 pmol of losartan reduced significantly the cardiovascular and drinking responses to AII without affecting the responses to [MePhe^7]NKB (Figure 2). However, 650 pmol of losartan reduced significantly all responses induced by 25 pmol [MePhe^7]NKB or AII without affecting those mediated by SP or NKA (Figure 2). All inhibitions produced by losartan were reversible when agonists were tested alone 24 h later (Figure 2). Higher doses of losartan (6.5 nmol) induced intense episodes of convulsion-like behaviour lasting 1–5 min followed by short resting periods (1–2 min) for 15–30 min in four out of seven rats. At 650 pmol, losartan had no direct effect on any parameters (peak ΔMAP = 3.2 ± 2.8 mmHg; peak ΔHR = 10.3 ± 13.8 b.p.m.; wet dog shake for 30 min = 12.4 ± 16.3 episodes; water intake for 30 min = 1.1 ± 0.7 ml; $n = 8$).

Whereas the central effects of [MePhe^7]NKB remained unaffected with 65 and 650 pmol EXP 3174, the cardiovascular response was significantly reduced by 6.5 nmol (Figure 3). Pretreatment with 65 pmol EXP 3174 reduced the AII-induced water intake while 650 pmol or 6.5 nmol blocked significantly all the AII-induced effects (Figure 3). The inhibitions were no longer observed when AII or [MePhe^7]NKB was tested alone on day 3. When injected alone, EXP 3174 (650 pmol or 6.5 nmol) showed no intrinsic activity (6.5 nmol: peak ΔMAP = 2.9 ± 2.5 mmHg; peak ΔHR = 13.9 ± 12.8 b.p.m.; wet dog shake for 30 min = 9.7 ± 10.5 episodes; water intake for 30 min = 0.8 ± 0.4 ml; $n = 6$).

The cardiovascular and behavioural effects induced by [MePhe^7]NKB or AII were not affected by the AT_2 receptor antagonist, PD 123,319 (650 pmol) (Figure 4). On the third day, agonists were reinjected to verify whether PD 123,319 had a delayed action on either AII or [MePhe^7]NKB as reported earlier with AII (Widdop *et al.*, 1994). PD 123,319 (650 pmol) was still found inactive 24 h after injection (Figure 4). When injected alone, this antagonist (650 pmol) was without effect on any parameters (peak ΔMAP = 5.1 ± 3.8 mmHg; peak ΔHR = 16.8 ± 13.9 b.p.m.; wet dog shake for 30 min = 9.3 ± 5.8 episodes; water intake for 30 min = 2.0 ± 1.1 ml; $n = 8$).

The peptide NK_3 receptor antagonist, R 486 (650 pmol)

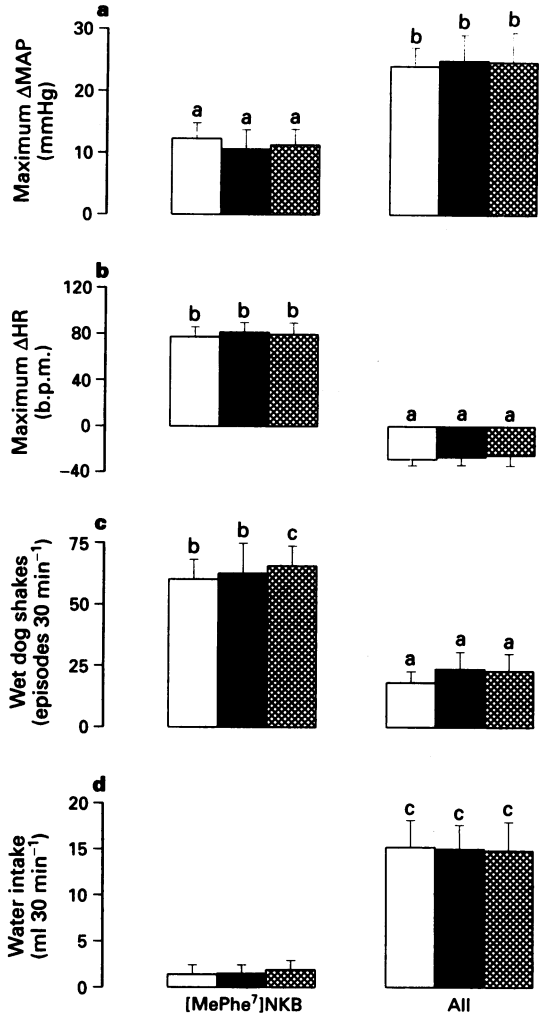

Figure 4 Cardiovascular and behavioural effects of 25 pmol [MePhe^7]neurokinin B ([MePhe^7]NKB) and angiotensin II (AII) were measured on three consecutive days in conscious rats. Agonists were injected i.c.v. alone on day 1 (open columns) or 5 min after the prior i.c.v. injection of PD 123,319 (650 pmol) on day 2 (solid columns). On day 3 (cross-hatched columns), agonists were readministered alone. Shown are maximal increases in (a) mean arterial blood pressure (MAP) and (b) heart rate (HR) measured at 3–5 min post-injection. Total wet dog shake episodes (c) and water intake (d) were measured for a period of 30 min. Maximal CSF values are: $\Delta MAP = 4.2 \pm 2.7$ mmHg; $\Delta HR = 13.2 \pm 9.0$ b.p.m.; wet dog shake $= 8.3 \pm 6.1$ episodes $\times$ 30 min^{-1}; water intake $= 1.2 \pm 0.5$ ml $\times$ 30 min^{-1}; $n = 8$. Each value represents the mean $\pm$ s.e.mean of results from 8 rats for each agonist. No statistical difference was observed in the presence of PD 123,319. Statistical comparison to the vehicle is indicated by $^aP<0.05$; $^bP<0.01$; $^cP<0.001$.

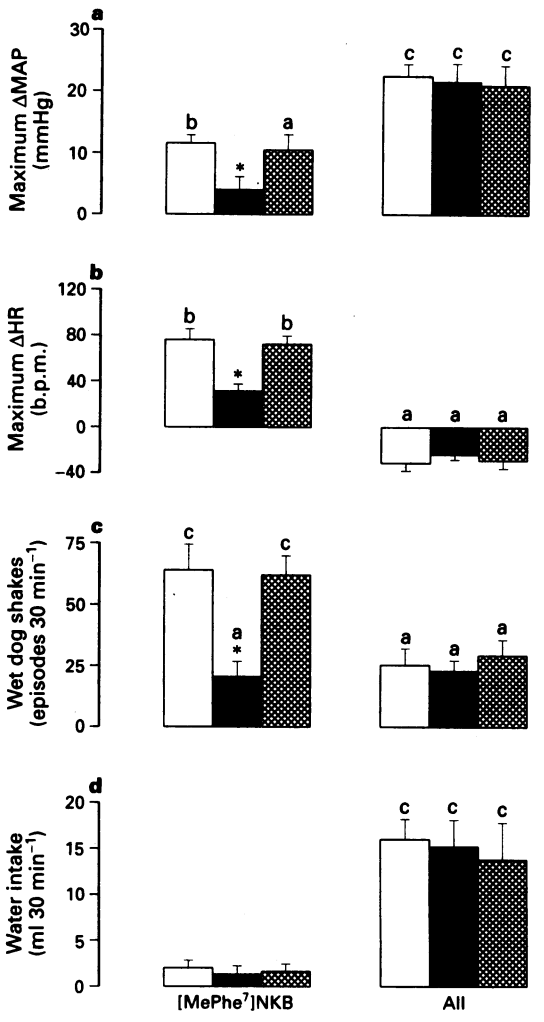

Figure 5 Cardiovascular and behavioural effects of 25 pmol [MePhe^7]neurokinin B ([MePhe^7]NKB) and angiotensin II (AII) were measured on three consecutive days in conscious rats. Agonists were injected i.c.v. alone on day 1 (open columns) or 5 min after the prior i.c.v. injection of R 486 (650 pmol) on day 2 (solid columns). On day 3 (cross-hatched columns), agonists were readministered alone. Shown are maximal increases in (a) mean arterial blood pressure (MAP) and (b) heart rate (HR) measured at 3–5 min post-injection. Total wet dog shake episodes (c) and water intake (d) were measured for a period of 30 min. Maximal CSF values are: $\Delta MAP = 1.3 \pm 1.4$ mmHg; $\Delta HR = 9.0 \pm 6.7$ b.p.m.; wet dog shake $= 7.1 \pm 6.2$ episodes $\times$ 30 min^{-1}; water intake $= 0.4 \pm 0.4$ ml $\times$ 30 min^{-1}; $n = 8$. Each value represents the mean $\pm$ s.e.mean of results from 8 rats for each agonist. Statistical comparison to the agonist alone on day 1 is indicated by $^*P<0.05$ and to the vehicle is indicated by $^aP<0.05$; $^bP<0.01$; $^cP<0.001$.

significantly reduced the effects of [MePhe^7]NKB without altering the AII-mediated effects (Figure 5). The inhibition was over when [MePhe^7]NKB was readministered alone on the third day. When injected alone, R 486 (650 pmol) showed no intrinsic activity (peak $\Delta MAP = 3.6 \pm 1.9$ mmHg; peak $\Delta HR = 17.8 \pm 14.0$ b.p.m.; wet dog shake for 30 min $= 12.4 \pm 7.6$ episodes; water intake for 30 min $= 0.3 \pm 0.1$ ml; $n = 8$).

Discussion

Losartan, a putative ligand for the NK$_3$ tachykinin receptor

Our results are in agreement with earlier binding studies showing an interaction between losartan and EXP 3174 and tachykinin NK$_3$ receptors (Chrétien *et al.*, 1994). Losartan blocks cardiovascular and behavioural responses mediated by central activation of AT$_1$ and NK$_3$ receptors in the conscious rat. However, losartan did not modify the central cardiovascular response to SP or NKA. The moderate affinity of losartan toward NK$_3$ receptors can be interpreted to some extent on the basis of amino acid sequence similarities between AT$_1$ and NK$_3$ mammalian receptors. In fact, Ji *et al.* (1994) have recently determined the structural requirement for the specific binding of losartan to the AT$_1$ receptor subtype. Using mutant receptors with point mutations of residues susceptible to influence the binding of losartan to AT$_1$ receptors, they showed that the two most important amino acids for the latter binding were a valine residue at the 6th position in transmembrane region III (TM-III^{-6}) and an alanine residue at the TM-IV^{-4} position of the AT$_1$ receptor. Interestingly, both these amino acids can be found on the

NK_3 receptor (valine[118] at the TM-III^{-12} position and alanine[153] at the TM-IV^{-4} position) and are absent at the same position in both NK_1 and NK_2 tachykinin receptors (Nakanishi, 1991). Moreover, in another study using AT_1 receptor chimeric constructs, the binding of eleven non-peptide AT_1 receptor antagonists was impaired by all of the chimeric exchanges involving the lower part of TM-VI and TM-VII, while these substitutions did not affect AII binding (Schambye *et al.*, 1994). However with NK_1 and NK_2 receptors, non-peptide antagonist binding is affected by mutations located spatially around the top of TM-VI. Substitutions in this area of the receptor, which severely impaired or eliminated the binding of non-peptide antagonists, had no effect on the binding of natural peptide ligands (Fong *et al.*, 1992; Zoffmann *et al.*, 1993; Gether *et al.*, 1993; Fong & Strader, 1994).

Another non-specific inhibitory effect of losartan has been reported on the bovine brain calcium/calmodulin-dependent 3':5'-cyclic nucleotide phosphodiesterase. In this model, losartan was found to be four times more potent than EXP 3174 in inhibiting the enzyme (Ishizaki & Ohtawa, 1994). Moreover, losartan was shown to possess high affinity for non-angiotensin binding sites in rat liver homogenates (Widdowson *et al.*, 1993) and in the rat central nervous system (Paré *et al.*, 1993). Even though losartan does not exhibit any intrinsic activity at 650 pmol, a higher dose (6.5 nmol) produced convulsion-like behaviours in 4 out of 7 rats. This behaviour is similar to what is observed with high doses of the NK_3 receptor agonist, [MePhe^7]NKB (6.5 nmol i.c.v.) (personal observation). It remains to be established whether high doses of losartan could exhibit a NK_3 agonistic-like activity. These side effects are not correlated with AT_1 or NK_3 receptor antagonism since the dose of EXP 3174 (6.5 nmol) which blocks both AT_1 and NK_3 receptors, or that of R 486 (6.5 nmol, in Picard *et al.*, 1994) which blocks NK_3 receptors exclusively, failed to cause convulsive effects. Since EXP 3174 (650 pmol) displays no antagonist activity at the NK_3 receptor, except at very high doses (6.5 nmol), this suggests that losartan has a greater affinity than its active metabolite at the NK_3 receptor site. Finally, central cardiovascular and behavioural effects of AII appear to be mediated solely by AT_1 receptors since losartan and EXP 3174, but not PD 123,319 block AII-mediated responses.

Although losartan is unstable *in vivo* and is largely converted to EXP 3174 when administered orally (Siegl, 1993), its potential interaction with central NK_3 receptors cannot be completely ruled out and further experiments are required to determine whether the antihypertensive effect of this compound can be partly related to its interaction with the NK_3 receptor. Nevertheless, the structure of losartan can provide useful information for the future development of a novel class of non-peptide NK_3 receptor antagonist. This would not be a precedent since losartan was synthesized using S 8307, S 8308 and other analogues of the benzylimidazoles as chemical leads (Duncia *et al.*, 1992). Indeed, the discovery of losartan followed the observation that several simple benzylimidazoles are weak AII receptor antagonists (Duncia *et al.*, 1992).

Lack of interaction between tachykinins and angiotensin in supraspinal cardiovascular regulation

As expected, the NK_3 peptide antagonist, R 486, is effective against [MePhe^7]NKB but not against AII-mediated responses. It is therefore unlikely that AII acts through the release of an NK_3 endogenous ligand. Likewise, central cardiovascular and wet dog shake effects of [MePhe^7]NKB are probably not due to the central release of AII since losartan and EXP 3174 blocked the effects of AII at doses that did not block [MePhe^7]NKB-mediated effects.

With the use of selective antagonists, we have previously reported that central SP-mediated responses in this paradigm are due primarily to NK_1 receptor activation and to some extent to NK_2 receptor activation (Picard *et al.*, 1994). Conversely, NKA activates mainly central NK_2 receptors, but under NK_2 receptor blockade a minor NK_1 receptor component is unmasked (Picard *et al.*, 1994). Furthermore, when injected i.c.v., neither SP nor NKA seem to release AII since losartan is unable to affect these tachykinin-induced responses. This is in agreement with earlier studies demonstrating fundamental differences in the mechanism by which SP and AII influence cardiovascular and autonomic functions (Unger *et al.*, 1981; 1985). It is conceivable that AII and SP are involved in haemodynamic adjustment to specific physiological states, such as dehydration inducing thirst and volume expansion, in the case of AII, or arousal following the central processing of pain (Foreman & Blair, 1988), stress (Herd, 1991) or fight or flight response (Unger *et al.*, 1981), in the case of SP.

NK_3 receptor activation exhibits strong similarities to AT_1 receptor activation in the induction of vasopressin release in the circulation (Unger *et al.*, 1981; Harland *et al.*, 1988; Nakayama *et al.*, 1992). Additionally, NK_3 receptor agonists are known to promote wet dog shake behaviour (Elliott & Iversen, 1986; Stoessl *et al.*, 1988; Itoi *et al.*, 1992) which may influence the drinking behaviour (Walsh *et al.*, 1992). However, these peptides seem to play parallel, but opposite roles in volume regulation. NK_1, NK_2 and NK_3 receptor activation has been associated with reduced salt and water intake (Fitzsimons & Evered, 1978; Massi *et al.*, 1988; 1991; Epstein, 1991; Walsh *et al.*, 1992) whereas central AII stimulates thirst and sodium appetite (Wright & Harding, 1992). It is therefore reasonable to suggest a common pathway of action by these peptides where AII is the main neurotransmitter in water balance regulation, whereas the endogenous NK_3 agonist (NKB) represents a negative modulator of this angiotensinergic pathway (Massi *et al.*, 1991; Epstein, 1991). Thus, one would expect that treatment with a NK_3 receptor antagonist has a facilitatory action on the angiotensergic pathway favouring volume expansion. However, R 486 had no effect on the cardiovascular changes or water intake induced by AII, suggesting that AII is not endogenously inhibited by the natural NK_3 agonist, NKB, under resting conditions. One can imagine a particular physiological state where endogenous NKB would be released to inhibit the body fluid volume expansion mediated by AII.

Supraspinal site of action of tachykinins and AII

Immunohistochemical studies have provided evidence for the presence of distinct populations of neurones expressing NKB and AII in various regions of the rat central autonomic network implicated in cardiovascular and water balance regulation (Marksteiner *et al.*, 1992; Bunnemann *et al.*, 1993). Moreover, the NK_3 receptor was found in moderate to high density in the paraventricular and supraoptic nuclei of the rat hypothalamus (Beaujouan *et al.*, 1986; Bergström *et al.*, 1987; Mantyh *et al.*, 1989; Mussap & Burcher, 1990). The forebrain cell bodies containing AT_1 receptors were distributed in the paraventricular, periventricular, suprachiasmatic and supraoptic nuclei, the organum vasculosum lamina terminalis, the median eminence, the median preoptic area and the subfornical organ (Wamsley *et al.*, 1990; Bunnemann *et al.*, 1993; Phillips *et al.*, 1993; Wright & Harding, 1994). These nuclei constitute the likely i.c.v. site of action of [MePhe^7]NKB and AII since they are circumventricular organs or closely apposed to the lateral ventricular walls in addition to being intimately associated with cardiovascular and body fluid regulation. On the other hand, although the central wet dog shake pathway is still poorly characterized, this behaviour could result from activation of functionally active NK_3 receptors in the medial habenula (Norris *et al.*, 1993) or in the striatum (Keegan *et al.*, 1992; Humpel & Saria, 1993) of the rat.

Conclusion

This study provides functional evidence that losartan and its active metabolite EXP 3174 interact with central NK_3 receptors in the rat. Losartan has a potency 10 fold greater than EXP 3174 in inhibiting NK_3 receptor-mediated effects and could represent a chemical lead toward the development of a new class of non-peptide NK_3 receptor antagonist.

Moreover, the cardiovascular and water intake responses induced by central injection of AII are probably mediated by AT_1 receptors and could be dissociated from the cardiovascular and behavioural responses produced by tachykinin agonists acting on NK_1, NK_2 and NK_3 receptors.

We are grateful to Dr Domenico Regoli, Sherbrooke University, Dept. of Pharmacology, who generously provided R 486 and [MePhe^7]NKB. This study was supported by the Kidney Foundation of Canada and a grant in aid (MT-8925) from the Medical Research Council of Canada to R.C. P.P. holds studentships from The Heart and Stroke Foundation of Canada and Fonds pour la Formation de Chercheurs et l'Aide à la Recherche.

References

ADVENIER, C., ROUISSI, N., NGUYEN, Q.T., EMONDS-ALT, X., BRELIERE, J-C., NELIAT, G., NALINE, E. & REGOLI, D. (1992). Neurokinin A (NK_2) receptor revisited with SR 48968, a potent non-peptide antagonist. *Biochem. Biophys. Res. Commun.*, **184**, 1418–1424.

BAINS, J.S., POTYOK, A. & FERGUSON, A.V. (1992). Angiotensin II actions in paraventricular nucleus: functional evidence for neurotransmitter role in efferents originating in subfornical organ. *Brain Res.*, **599**, 223–229.

BEAUJOUAN, J.C., TORRENS, Y., SAFFROY, M. & GLOWINSKI, J. (1986). Quantitative autoradiographic analysis of the distribution of binding sites for [^{125}I]Bolton hunter derivatives of eledoisin and substance P in the rat brain. *Neurosci.*, **18**, 857–875.

BERGSTRÖM, L., TORRENS, Y., SAFFROY, M., BEAUJOUAN, J.C., LAVIELLE, S., CHASSAING, G., MORGAT, J.L., GLOWINSKI, J. & MARQUET, A. (1987). [^{3}H]Neurokinin B and [^{125}I]-Bolton Hunter eledoisin label identical tachykinin binding sites in the rat brain. *J. Neurochem.*, **48**, 125–133.

BUNNEMANN, B., FUXE, K. & GANTEN, D. (1993). The renin-angiotensin system in the brain: an update 1993. *Regul. Pept.*, **46**, 487–509.

CHRÉTIEN, L., GUILLEMETTE, G. & REGOLI, D. (1994). Non peptide angiotensin receptor antagonists bind to tachykinin NK_3 receptors of rat and guinea pig brain. *Eur. J. Pharmacol.*, **256**, 73–78.

CICCOCIOPPO, R., PANOCKA, I., POMPEI, P., DE CARO, G. & MASSI, M. (1994). Selective agonists at NK-3 tachykinin receptors inhibit alcohol intake in sardinian alcohol-preferring rats. *Brain Res. Bull.*, **33**, 71–77.

COONEY, A.S. & FITZSIMONS, J.T. (1993). The effect of the putative AT_2 agonist, *p*-aminophenylalanine^6 angiotensin II, on thirst and sodium appetite in rats. *Exp. Physiol.*, **78**, 767–774.

DRAPEAU, G., ROUISSI, N., NANTEL, F., RHALEB, N.-E., TOUSIGNANT, C. & REGOLI, D. (1990). Antagonists for the neurokinin NK-3 receptor evaluated in selective receptor systems. *Regul. Pept.*, **31**, 125–135.

DUNCIA, J.V., CARINI, D.J., CHIU, A.T., JOHNSON, A.L., PRICE, W.A., WONG, P.C., WEXLER, R.R. & TIMMERMANS, P.B.M.W.M. (1992). The discovery of DuP 753, a potent, orally active nonpeptide angiotensin II receptor antagonist. *Med. Res. Rev.*, **12**, 149–191.

ELLIOTT, P.J. & IVERSEN, S.D. (1986). Behavioural effects of tachykinins and related peptides. *Brain Res.*, **381**, 68–76.

EMONDS-ALT, X., BICHON, D., DUCOUX, J.P., HEAULME, M., MILOUX, B., PONCELET, M., PROIETTO, V., VAN BROECK, D., VILAIN, P., NELIAT, G., SOUBRIÉ, P., LE FUR, G. & BRELIÈRE, J.C. (1995). SR 142801, the first potent non-peptide antagonist of the tachykinin NK_3 receptor. *Life Sci.*, **56**, No. 1, PL 27–32.

EPSTEIN, A.N. (1991). Neurohormonal control of salt intake in the rat. *Brain Res. Bull.*, **27**, 315–320.

FITZSIMONS, J.T. & EVERED, M.D. (1978). Eledoisin, substance P and related peptides: intracranial dipsogens in the pigeon and antidipsogens in the rat. *Brain Res.*, **150**, 533–542.

FONG, T.M., HUANG, R.-R.C. & STRADER, C.D. (1992). Localization of agonist and antagonist binding domains of the human neurokinin-1 receptor. *J. Biol. Chem.*, **267**, 25664–25667.

FONG, T.M. & STRADER, C.D. (1994). Functional mapping of the ligand binding sites of G-protein coupled receptors. *Med. Res. Rev.*, **14**, 387–399.

FOREMAN, R.D. & BLAIR, R.W. (1988). Central organization of sympathetic cardiovascular response to pain. *Annu. Rev. Physiol.*, **50**, 607–622.

FREGLY, M.J. & ROWLAND, N.J. (1991). Effects of a non peptide angiotensin II receptor antagonist, DuP 753, on angiotensin-related water intake in rats. *Brain Res. Bull.*, **27**, 97–100.

GARRET, C., CARRUETTE, A., FARDIN, V., MOUSSAOUI, S., PEYRONEL, J.-F., BLANCHARD, J.-C. & LADURON, P.M. (1991). Pharmacological properties of a potent and selective nonpeptide substance P antagonist. *Proc. Natl. Acad. Sci. U.S.A.*, **88**, 10208–10212.

GEHLERT, D.R., GACKENHEIMER, S.L., REEL, J.K., LIN, H.-S. & STEINBERG, M.I. (1990). Non-peptide angiotensin II receptor antagonists discriminate subtypes of ^{125}I-angiotensin II binding sites in the rat brain. *Eur. J. Pharmacol.*, **187**, 123–126.

GETHER, U., YOKOTA, Y., EMONDS-ALT, X., BRELIERE, J.-C., LOWE III, J.A., SNIDER, R.M., NAKANISHI, S. & SCHWARTZ, T.W. (1993). Two nonpeptide tachykinin antagonists act through epitopes on corresponding segments of the NK_1 and NK_2 receptors. *Proc. Natl. Acad. Sci. U.S.A.*, **90**, 6194–6198.

GRUPP, L.A. & HARDING, S. (1994). The reduction in alcohol drinking by peripherally injected angiotensin II is selectively mediated by the AT_1 receptor subtype. *Pharmacol. Biochem. Behav.*, **47**, 385–392.

GYURKO, R., WIELBO, D. & PHILLIPS, M.I. (1993). Antisense inhibition of AT1 receptor mRNA and angiotensinogen mRNA in the brain of spontaneously hypertensive rats reduces hypertension of neurogenic origin. *Regul. Pept.*, **49**, 167–174.

HARLAND, D., GARDINER, S.M. & BENNETT, T. (1988). Cardiovascular and dipsogenic effects of angiotensin II administered i.c.v. in Long-Evans and Brattleboro rats. *Brain Res.*, **455**, 58–64.

HELKE, C.J., KRAUSE, J.E., MANTYH, P.W., COUTURE, R. & BANNON, M.J. (1990). Diversity in mammalian tachykinin peptidergic neurons: multiple peptides, receptors, and regulatory mechanisms. *FASEB J.*, **4**, 1606–1615.

HERD, J.A. (1991). Cardiovascular response to stress. *Physiol. Rev.*, **71**, 305–331.

HUMPEL, C. & SARIA, A. (1993). Intranigral injection of selective neurokinin-1 and neurokinin-3 but not neurokinin-2 receptor agonists biphasically modulate striatal dopamine metabolism but not striatal preprotachykinin-A mRNA in the rat. *Neurosci. Lett.*, **157**, 223–226.

IMPROTA, G. & BROCCARDO, M. (1991). Inhibitory role on gastric secretion of a central NK-3 tachykinin receptor agonist, senktide. *Peptides*, **12**, 1433–1434.

ISHIZAKI, H. & OHTAWA, M. (1994). Inhibitory effect of the nonpeptide angiotensin II receptor antagonist losartan and its active metabolite, E-3174, on cAMP phosphodiesterase: additional action of the antagonists. *Biochem. Pharmacol.*, **48**, 201–204.

ITOI, K., TSCHÖPE, C., JOST, N., CULMAN, J., LEBRUN, C., STAUSS, B. & UNGER, TH. (1992). Identification of the central tachykinin receptor subclass involved in substance P-induced cardiovascular and behavioural responses in conscious rats. *Eur. J. Pharmacol.*, **219**, 435–444.

JI, H., LEUNG, M., ZHANG, Y., CATT, K.J. & SANDBERG, K. (1994). Differential structural requirements for specific binding of nonpeptide and peptide antagonists to the AT_1 angiotensin receptor. *J. Biol. Chem.*, **269**, 16533–16536.

KEEGAN, K.D., WOODRUFF, G.N. & PINNOCK, R.D. (1992). The selective NK_3 receptor agonist senktide excites a subpopulation of dopamine-sensitive neurones in the rat substantia nigra pars compacta *in vitro*. *Br. J. Pharmacol.*, **105**, 3–5.

KIRBY, R.F., THUNHORST, R.L. & JOHNSON, A.K. (1992). Effects of a non-peptide angiotensin receptor antagonist on drinking and blood pressure responses to centrally administered angiotensins in the rat. *Brain Res.*, **576**, 348–350.

LI, Z., BAINS, J.S. & FERGUSON, A.V. (1993). Functional evidence that the angiotensin antagonist losartan crosses the blood-brain barrier in the rat. *Brain Res. Bull.*, **30**, 33–39.

MAGGI, C.A., PATACCHINI, R., ROVERO, P. & GIACHETTI, A. (1993). Tachykinin receptors and tachykinin receptor antagonists. *J. Auton. Pharmacol.*, **13**, 23–93.

MANTYH, P.W., GATES, T., MANTYH, C.R. & MAGGIO, J.E. (1989). Autoradiographic localization and characterization of tachykinin receptor binding sites in the rat brain and peripheral tissues. *J. Neurosci.*, **9**, 258–279.

MARKSTEINER, J., SPERK, G. & KRAUSE, J.E. (1992). Distribution of neurons expressing neurokinin B in the rat brain: Immunohistochemistry and in situ hybridization. *J. Comp. Neurol.*, **317**, 341–356.

MASSI, M., DE CARO, G., PERFUMI, M. & VENTURI, F. (1988). Mapping of brain sites sensitive to the antidipsogenic effect of tachykinins. *Pept.*, **9**, 347–356.

MASSI, M., POLIDORI, C., PERFUMI, M., GENTILI, L. & DE CARO, G. (1991). Tachykinin receptor subtypes involved in central effects of tachykinins on water and salt intake. *Brain Res. Bull.*, **26**, 155–160.

MCLEAN, S., GANONG, A., SEYMOUR, P.A., SNIDER, R.M., DESAI, M.C., ROSEN, T., BRYCE, D.K., LONGO, K.P., REYNOLDS, L.S., ROBINSON, G., SCHMIDT, A.W., SIOK, C. & HEYM, J. (1993). Pharmacology of CP-99,994; a nonpeptide antagonist of the tachykinin neurokinin-1 receptor. *J. Pharmacol. Exp. Ther.*, **267**, 472–479.

MUSSAP, C.J. & BURCHER, E. (1990). [^{125}I]-Bolton-Hunter Scyliorhinin II: a novel, selective radioligand for the tachykinin NK_3 receptor in rat brain. *Peptides*, **11**, 827–836.

NAGASHIMA, A., TAKANO, Y., TATEISHI, K., MATSUOKA, Y., HAMAOKA, T. & KAMIYA, H. (1989). Central pressor actions of neurokinin B: increases in neurokinin B contents in discrete nuclei in spontaneously hypertensive rats. *Brain Res.*, **499**, 198–203.

NAKANISHI, S. (1991). Mammalian tachykinin receptors. *Annu. Rev. Neurosci.*, **14**, 123–136.

NAKAYAMA, Y., TAKANO, Y., SAITO, R. & KAMIYA, H. (1992). Central pressor actions of tachykinin NK-3 receptor in the paraventricular nucleus of the rat hypothalamus. *Brain Res.*, **595**, 339–342.

NORRIS, S.K., BODEN, P.R. & WOODRUFF, G.N. (1993). Agonists selective for tachykinin NK_1 and NK_3 receptors excite subpopulations of neurons in the rat medial habenula nucleus in vitro. *Eur. J. Pharmacol.*, **234**, 223–228.

OTSUKA, M. & YOSHIOKA, K. (1993). Neurotransmitter functions of mammalian tachykinins. *Physiol. Rev.*, **73**, 229–308.

PALMER, A.A., STEELE, M.K., SHACKELFORD, R.L. & GANONG, W.F. (1994). Intravenous losartan inhibits the increase in plasma luteinizing hormone and water intake produced by intraventricular angiotensin II. *Proc. Soc. Exp. Biol. Med.*, **205**, 263–266.

PARÉ, M.-C., MALTAIS, S. & ESCHER, E. (1993). The neurogenic origin of hypertension in SHR may be mediated by angiotensin II through a receptor different from AT1 and AT2. *Regul. Pept.*, **47**, 81–86.

PHILLIPS, M.I., SHEN, L., RICHARDS, E.M. & RAIZADA, M.K. (1993). Immunohistochemical mapping of angiotensin AT_1 receptors in the brain. *Regul. Pept.*, **44**, 95–107.

PICARD, P., REGOLI, D. & COUTURE, R. (1994). Cardiovascular and behavioural effects of centrally administered tachykinins in the rat: characterization of receptors with selective antagonists. *Br. J. Pharmacol.*, **112**, 240–249.

SAKAI, R.R., HE, P.F., YANG, X.D., MA, L.Y., GUO, Y.F., REILLY, J.J., MOGA, C.N. & FLUHARTY, S.J. (1994). Intracerebroventricular administration of AT_1 receptor antisense oligonucleotides inhibits the behavioral actions of angiotensin II. *J. Neurochem.*, **62**, 2053–2056.

SCHAMBYE, H.T., HJORTH, S.A., BERGSMA, D.J., SATHE, G. & SCHWARTZ, T.W. (1994). Differentiation between binding sites for angiotensin II and nonpeptide antagonists on the angiotensin II type 1 receptors. *Proc. Natl. Acad. Sci. U.S.A.*, **91**, 7046–7050.

SIEGL, P.K.S. (1993). Discovery of losartan, the first specific nonpeptide angiotensin II receptor antagonist. *J. Hypertension*, **11**, Suppl. 3, S19–S22.

SNIDER, R.M., CONSTANTINE, J.W., LOWE III, J.A., LONGO, K.P., LEBEL, W.S., WOODY, H.A., DROZDA, S.E., DESAI, M.C., VINICK, F.J., SPENCER, R.W. & HESS, H.-J. (1991). A potent nonpeptide antagonist of the substance P (NK_1) receptor. *Science*, **251**, 435–437.

SONG, K., ZHUO, J. & MENDELSOHN, F.A.O. (1991). Access of peripherally administered DuP 753 to rat brain angiotensin II receptors. *Br. J. Pharmacol.*, **104**, 771–772.

STEPHENSON, K.N. & STEELE, K.M. (1992). Brain angiotensin II receptor subtypes and the control of luteinizing hormone and prolactin secretion in female rats. *J. Neuroendocrinol.*, **4**, 441–447.

STOESSL, A.J., DOURISH, C.T. & IVERSEN, S.D. (1988). The NK-3 tachykinin receptor agonist senktide elicits 5-HT-mediated behaviour following central or peripheral administration in mice and rats. *Br. J. Pharmacol.*, **94**, 285–287.

TAKANO, Y., NAGASHIMA, A., HAGIO, T., TATEISHI, K. & KAMIYA, H. (1990). Role of central tachykinin peptides in cardiovascular regulation in rats. *Brain Res.*, **528**, 231–237.

TIMMERMANS, P.B.M.W.M., WONG, P.C., CHIU, A.T., HERBLIN, W.F., BENFIELD, P., CARINI, D.J., LEE, R.J., WEXLER, R.R., SAYE, J.A.M. & SMITH, R.D. (1993). Angiotensin II receptors and angiotensin II receptor antagonists. *Pharmacol. Rev.*, **45**, 205–251.

TONEY, G.M. & PORTER, J.P. (1993a). Functional role of brain AT1 and AT2 receptors in the central angiotensin II pressor response. *Brain Res.*, **603**, 57–63.

TONEY, G.M. & PORTER, J.P. (1993b). Functional roles of brain AT1 and AT2 receptors in the central angiotensin II pressor response in conscious young spontaneously hypertensive rats. *Develop. Brain Res.*, **71**, 193–199.

TSUTSUMI, K. & SAAVEDRA, J.M. (1991). Quantitative autoradiography reveals different angiotensin II receptor subtypes in selected rat brain nuclei. *J. Neurochem.*, **56**, 348–351.

UNGER, TH., RASCHER, W., SCHUSTER, C., PAVLOVITCH, R., SCHÖMIG, A., DIETZ, R. & GANTEN, D. (1981). Central blood pressure effects of substance P and angiotensin II: role of the sympathetic nervous system and vasopressin. *Eur. J. Pharmacol.*, **71**, 33–42.

UNGER, TH., BECKER, H., PETTY, M., DEMMERT, G., SCHNEIDER, B., GANTEN, D. & LANG, R.E. (1985). Differential effects of central angiotensin II and substance P on sympathetic nerve activity in conscious rats, Implications for cardiovascular adaptation to behavioural responses. *Circ. Res.*, **56**, 563–575.

WALSH, D.M., ELLIOTT, P.J. & HAGAN, R.M. (1992). Role of NK-2 receptors in the antidipsogenic activity of neurokinins in the mouse. *Gen. Pharmacol.*, **23**, 231–233.

WAMSLEY, J.K., HERBLIN, W.F., ALBURGES, M.E. & HUNT, M. (1990). Evidence for the presence of angiotensin II-type 1 receptors in brain. *Brain Res. Bull.*, **25**, 397–400.

WATLING, K.J. (1992). Nonpeptide antagonists herald new era in tachykinin research. *Trends Pharmacol. Sci.*, **13**, 266–269.

WIDDOP, R.E., GARDINER, S.M. & BENNETT, T. (1994). Effects of angiotensin II AT1-or AT2-receptor antagonists on drinking evoked by angiotensin II or water deprivation in rats. *Brain Res.*, **648**, 46–52.

WIDDOWSON, P.S., RENOUARD, A. & VILAINE, J.-P. (1993). Binding of [^{3}H]angiotensin II and [^{3}H]DuP 753 (losartan) to rat liver homogenates reveals multiple sites. Relationship to AT_{1a}- and AT_{1b}-type angiotensin receptors and novel nonangiotensin binding sites. *Peptides*, **14**, 829–837.

WONG, P.C., PRICE, W.A., CHIU, A.T., DUNCIA, J.V., CARINI, D.J., WEXLER, R.R., JOHNSON, A.L. & TIMMERMANS, P.B.M.W.M. (1990a). Nonpeptide angiotensin II receptor antagonists. VIII. Characterization of functional antagonism displayed by DuP 753, an orally active antihypertensive agent. *J. Pharmacol. Exp. Ther.*, **252**, 719–725.

WONG, P.C., PRICE, W.A., CHIU, A.T., DUNCIA, J.V., CARINI, D.J., WEXLER, R.R., JOHNSON, A.L. & TIMMERMANS, P.B.M.W.M. (1990b). Nonpeptide angiotensin II receptor antagonists. XI. Pharmacology of EXP 3174: an active metabolite of DuP 753, an orally active antihypertensive agent. *J. Pharmacol. Exp. Ther.*, **255**, 211–217.

WRIGHT, J.W. & HARDING, J.W. (1992). Regulatory role of brain angiotensins in the control of physiological and behavioural responses. *Brain Res. Rev.*, **17**, 227–262.

WRIGHT, J.W. & HARDING, J.W. (1994). Brain angiotensin receptor subtypes in the control of physiological and behavioral responses. *Neurosci. Biobehavioural Rev.*, **18**, 21–53.

ZOFFMANN, S., GETHER, U. & SCHWARTZ, T.W. (1993). Conserved His^{V1-17} of the NK-1 receptor is involved in binding of nonpeptide antagonists but not substance P. *FEBS Lett.*, **336**, 506–510.

(Received October 27, 1994
Revised December 28, 1994
Accepted January 4, 1995)

British Journal of Pharmacology (1995) 114, 1571-1576 © 1995 Stockton Press All rights reserved 0007-1188/95 $12.00

The effects of calyculin A upon calcium-, guanine nucleotides- and phorbol 12-myristate 13-acetate-stimulated ACTH secretion from AtT-20 cells

B.W. McFerran & [1]S.B. Guild

Molecular Endocrinology Unit, Bute Medical Building, School of Biological and Medical Sciences, University of St Andrews, St Andrews KY16 9TS

1 The mouse AtT-20/D16-16 anterior pituitary tumour cell line was used as a model system for the study of protein phosphatase involvement in the late stages of the secretory pathway for adrenocorticotrophin (ACTH) secretion. The effects of the type 1 and 2 phosphatase inhibitor calyculin A upon calcium-, guanine nucleotide- and phorbol 12-myristate 13-acetate (PMA)-stimulated ACTH secretion from electrically-permeabilized AtT-20 cells were studied.

2 Calyculin A (1 nM–1 μM) inhibited both calcium (10 μM)- and guanosine 5'-O-(3-thiotriphosphate) (GTP-γ-S) (100 μM)-evoked ACTH secretion from permeabilized cells in a concentration-dependent manner. These effects were maximal with 100 nM calyculin A.

3 ACTH secretion was stimulated from electrically-permeabilized cells when the cytosolic free calcium ion concentration, controlled by calcium-EGTA buffers, was raised over the concentration range of 100 nM to 10 μM. This calcium-stimulated ACTH secretion was inhibited by co-incubation with calyculin A (100 nM).

4 GTP-γ-S (10 nM–100 μM) stimulated ACTH secretion from permeabilized cells at concentrations greater than 1 μM GTP-γ-S. Co-incubation with calyculin A (100 nM) inhibited this stimulation of ACTH secretion observed at these concentrations of GTP-γ-S.

5 PMA (100 nM) significantly stimulated ACTH secretion from permeabilized cells in the absence of either calcium and guanine nucleotides and this action was enhanced by calyculin A (100 nM). Furthermore, an inhibition of GTP-γ-S (100 μM)-stimulated ACTH secretion observed in the presence of calyculin A (100 nM) was not observed in the presence of PMA (100 nM).

6 The results of the present study indicate that dephosphorylation by phosphatases plays an important role in stimulus-secretion coupling in AtT-20 cells and is involved in mediating the effects of G_E upon the secretory apparatus in these cells. Furthermore, the point of regulation of the secretory response by PKC which underlies the ability of PKC to amplify the calcium/G_E system may lie distal to both G_E and these phosphatases.

Keywords: Calyculin A; G-protein; phosphatase; anterior pituitary; ACTH

Introduction

Adrenocorticotrophin (ACTH) secretion from anterior pituitary corticotrophs is stimulated by the hypothalamic neuropeptides corticotrophin-releasing hormone-41 (CRH-41) and arginine vasopressin (AVP) (Axelrod & Reisine, 1984; Antoni, 1986). The stimulus-secretion coupling mechanisms for these agents are known to involve both second messenger-regulated protein kinases and changes in the cytosolic free calcium ion concentration. CRH-41 acts via the adenosine 3':5'-cyclic monophosphate (cyclic AMP)-dependent protein kinase (PKA) pathway in both anterior pituitary corticotrophs (Aguilera *et al.*, 1983) and in a tumour cell line of the anterior pituitary, AtT-20, consisting of a homogeneous population of ACTH-secreting cells (Luini *et al.*, 1985; Guild *et al.*, 1986; Guild & Reisine, 1987). The signal-transduction pathway of AVP involves protein kinase C (PKC) in pituitary corticotrophs (Abou-Samra *et al.*, 1986) and stimulants of PKC have been shown to alter cytosolic calcium concentrations and stimulate ACTH release from AtT-20 cells (Reisine & Guild, 1987). The influences of these two protein kinases lies not only at a 'pre-calcium' site to regulate calcium influx but also at a 'post-calcium' site to regulate the effect of particular cytosolic calcium concentrations upon ACTH secretion (Reisine & Guild, 1987; Reisine, 1989; Guild, 1991; McFerran & Guild, 1994).

Calcium ions have been shown to stimulate secretion from a variety of permeabilized cell types (for review see Knight & Scrutton, 1986) including ACTH secretion from AtT-20 cells (Guild, 1991; Luini & De Matteis, 1988). Alteration of the cytosolic free calcium ion concentration stimulates hormone secretion via a GTP-binding protein in AtT-20 cells (Guild, 1991). This GTP-binding protein involved in the late stages of the secretory pathway, termed G_E, is present in a variety of secretory cells (for review see Gomperts, 1990). Such a GTP-binding protein may be a target for regulation by PKA (Guild, 1991) and PKC (McFerran & Guild, 1994) as both kinases have distinct 'post-calcium' sites of action to potentiate the effects of calcium and guanine nucleotides upon the secretory apparatus (Guild, 1991; McFerran & Guild, 1994).

A study of the phosphorylation states of proteins in AtT-20 cells in response to activators of PKA and PKC revealed an increased phosphorylation of some proteins but also a decreased phosphorylation of others. Furthermore, the decrease in phosphorylation state of proteins could be correlated with secretion from AtT-20 cells (Bishop *et al.*, 1987). The hypothesis that dephosphorylation of a phosphoprotein may drive exocytosis is supported by the observation that exocytosis in pancreatic acini is controlled partially through the phosphorylation/dephosphorylation of a protein on the zymogen granule membrane (MacLean *et al.*, 1993). In addition, inhibition of a serine/threonine phosphatase by calyculin A resulted in a strong inhibition of both calcium

[1] Author for correspondence.

ion- and guanine nucleotide-stimulated amylase release from permeabilized pancreatic acinar cells (Wagner *et al.*, 1992; Meyer-Alber *et al.*, 1994). It was the aim of this study to investigate the effects of calyculin A upon calcium ion-, guanine nucleotide- and phorbol 12-myristate 13-acetate (PMA)-stimulated ACTH secretion from permeabilized AtT-20 cells. Each of these three stimulants is capable of stimulating secretion but they act at different stages in the secretory pathway for ACTH secretion in AtT-20 cells (Guild, 1991; McFerran & Guild, 1994). Therefore, the role and position of serine/threonine phosphatase mediated dephosphorylation in stimulus-secretion coupling mechanisms for ACTH secretion by AtT-20 cells could be assessed.

The results of the present study indicate that calyculin A inhibits calcium- and guanine nucleotide-stimulated ACTH secretion from permeabilized AtT-20 cells. This indicates that dephosphorylation by phosphatases plays an important role in stimulus-secretion coupling in AtT-20 cells and is involved in regulating the effects of G_E upon the secretory apparatus in these cells. However, calyculin A enhances the PMA-evoked stimulation of ACTH secretion observed in the absence of calcium and guanine nucleotides. This suggests that the point of regulation of the secretory response by PKC, which underlies the ability of PKC to amplify the calcium/G_E system, may lie distal to both G_E and the serine/threonine phosphatase.

Methods

Culture of AtT-20 cells

Cells of the mouse AtT-20/D16-16 pituitary tumour were grown and subcultured in Dulbecco's Modified Eagle's Medium (DMEM) (glucose, 4500 mg l^{-1}) supplemented with 10% (w:v) foetal calf serum as previously described (Guild, 1991). Cells were plated in 75 cm^2 flasks (Nunc, Gibco, UK) at an initial density of 2×10^6 cells/flask and were used 7–9 days after subculturing (80–90% confluency).

Preparation of AtT-20 cells for ACTH release experiments

The culture medium was removed and the cells liberated from the substrate by trypsin (0.05% w:v)/EDTA (1 mM). The cells were washed twice by centrifugation (200 *g*, 5 min)/resuspension in a balanced salt solution of the following composition (mM): NaCl 145, KCl 5.6, $CaCl_2$ 2, $MgCl_2$ 0.5, glucose 5.6, HEPES 5, sodium ascorbate 0.5, BSA 0.1% (w:v), pH 7.4. After washing, the cells were suspended at a density of 10^6 cells ml^{-1} in this buffer and incubated for a further 30 min at 37°C. The cell suspension was then centrifuged (200 *g*, 5 min) and the cell pellet washed twice by resuspension/centrifugation (200 *g*, 5 min) in the standard permeabilization buffer of the following composition (mM): potassium glutamate 129, PIPES (potassium salt) 20, $MgCl_2$ 1, glucose 5, ATP 5, EGTA 5, BSA 0.1% (w:v), pH 6.6. The cells were finally resuspended in this buffer at a density of 10^7 ml^{-1} and electrically permeabilized by subjection to intense electric fields of brief duration (Knight & Baker, 1982). The optimum permeabilization parameters of 10 discharges of 3000 V cm^{-1}, previously determined (Guild, 1991), were adopted in these experiments.

Measurement of calcium-, guanine nucleotide- and phorbol 12-myristate 13-acetate-stimulated ACTH secretion from permeabilized AtT-20 cells

The standard protocol for the determination of ACTH secretion from permeabilized AtT-20 cells was as follows: permeabilized cells were suspended at a cell density of 10^5 cells ml^{-1} either (a) in a series of permeabilization buffers supplemented with calcium-EGTA buffers chosen to give a free calcium ion concentrations of 1 nM, 10 nM, 100 nM, 1 μM, 10 μM, 100 μM and 1 mM (for experiments investigating the effects of calcium ions) or (b) in the standard permeabilization buffer which had a free calcium ion concentration of 1 nM (for experiments investigating the effects of various concentrations of the non-hydrolysable GTP analogue, guanosine 5'-O-(3-thiotriphosphate) (GTP-γ-S), or PMA) and prepared as previously described (Guild, 1991; McFerran & Guild, 1994). At this point the zero time samples were centrifuged (200 *g*, 5 min) and the supernatants were stored for subsequent measurement of ACTH content. The cell suspensions were incubated at 37°C for 30 min at which point incubations were terminated by centrifugation (200 *g*, 5 min) and removal of the supernatant. The ACTH content of the supernatant was measured by radioimmunoassay. In each experiment, six samples were run for each condition.

The effect of calyculin A upon calcium ion-, guanine nucleotide- and PMA-stimulated ACTH secretion from permeabilized AtT-20 cells

Modifications to the standard protocols were made to permit the measurement of the effect of the serine/threonine phosphatase inhibitor, calyculin A, upon calcium ion-, guanine nucleotide- and PMA-stimulated ACTH secretion from permeabilized AtT-20 cells and are detailed in the legends to the figure. The concentration-dependency of the effects of calyculin A was investigated by measuring the effects of various concentrations (1 nM–1 μM) of this inhibitor upon a free calcium ion concentration of 10 μM- and GTP-γ-S (100 μM)-stimulated ACTH secretion. These concentrations of calcium ions and GTP-γ-S have previously been shown to evoke significant stimulation of ACTH secretion from permeabilized AtT-20 cells (Guild, 1991; McFerran & Guild, 1994). The concentration of calyculin A chosen for subsequent experiments was 100 nM. The effects of co-incubations with calyculin A (100 nM) upon various free calcium ion, GTP-γ-S and PMA concentration-response curves was investigated. All three of these stimulants have been shown to stimulate ACTH secretion from permeabilized cells when acting singly but act at different points in the late stages of the secretory pathway in AtT-20 cells (McFerran & Guild, 1994). The actions of PMA and hence PKC in permeabilized cells are partly exerted at a late stage of the secretory pathway, distal to the calcium/G_E system. Therefore, the effects of calyculin A (100 nM) upon GTP-γ-S (100 μM) acting alone and in combination with PMA (100 nM) were studied.

Radioimmunoassays

The radioimmunoassay for ACTH was performed as previously described (McFerran & Guild, 1994). [^{125}I]-ACTH for radioimmunoassay use was produced using the lodogen reagent (1,3,4,6-tetrachloro-3α,6α-diphenylglycoluril) which was first described as a reagent for iodination by Fraker & Speck (1978). The amount of ACTH released was expressed as the amount present at the end of the specified incubation period less the amount present at zero time.

Statistics

In each experiment six determinations for each experimental condition were made and each experiment was repeated three times, on different days. ACTH secretion is expressed as the means ± s.e.mean of the mean values from these 3 separate experiments. Statistical significance was tested by the use of ANOVA tests with Scheffe's *F*-test post hoc analysis. A P value < 0.05 was considered significant and is the definition of the term used here. Two-way ANOVA was used to test for a statistically significant interaction between two groups (i.e.

the concentration-response curves to calcium ions, GTP-γ-S or PMA in the presence and absence of calyculin A) and the significance of these interactions is specified.

Materials

The following substances (with their sources) were used: DMEM, foetal calf serum and trypsin/EDTA were purchased from GIBCO, UK; human ACTH antiserum and human ACTH for standards were the gift of the National Hormone and Pituitary program, Baltimore, MD, U.S.A.; phorbol 12-myristate 13-acetate was purchased from Sigma, UK; calyculin A was purchased from Calbiochem-NovaBiochem, UK; guanosine 5'-O-(3-thiotriphosphate) (GTP-γ-S) was obtained from Boehringer Mannheim, UK. All other chemicals used were of Analar grade and readily commercially available.

Results

The concentration-dependency of calyculin A-evoked inhibition of calcium- and guanine nucleotide-stimulated ACTH secretion from permeabilized AtT-20 cells

Calyculin A (1 nM–1 μM) inhibited in a concentration-dependent manner both calcium ion (10 μM)- and GTP-γ-S (100 μM)-evoked ACTH secretion (Figure 1a) but had no significant effect upon control ACTH secretion. Co-incubation of both calcium ions (1 μM) and GTP-γ-S (100 μM) with increasing concentrations of calyculin A resulted in an inhibition of the effects of these agents which became significant ($P<0.05$) at 10 nM calyculin A for the inhibition of GTP-γ-S (10^{-4} M)-evoked secretion and at a concentration of 100 nM calyculin A for the inhibition of calcium ion (10 μM)-evoked ACTH secretion. The inhibition of calyculin A was maximal with 100 nM at which point ACTH secretion

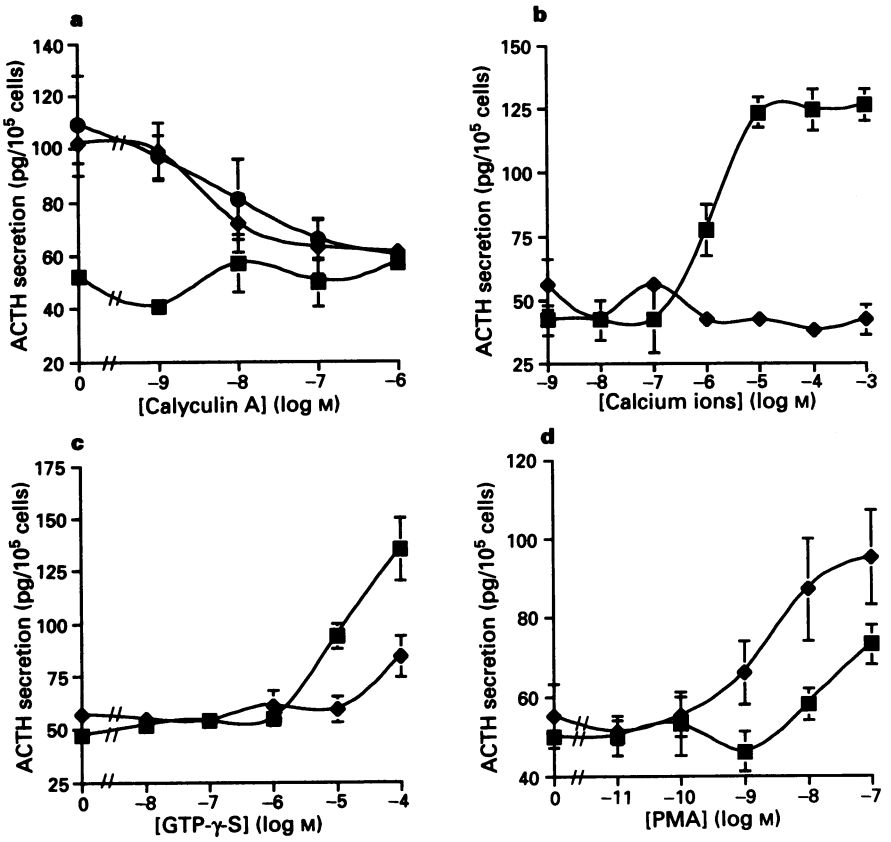

Figure 1 Permeabilized cells were incubated, as described in the Methods, in standard permeabilization medium supplemented with the indicated concentrations of substances as detailed below. ACTH release (pg/10^5 cells) is expressed as the mean ± s.e.mean from 3 separate experiments. (a) The effects of the indicated concentrations of calyculin A, either in the presence of calcium (10 μM) (●) or guanosine 5'-O-(3'-thiotriphosphate) (GTP-γ-S, 100 μM) (◆) or absence (■) of stimulants were investigated. Co-incubation of both calcium ions (10 μM) and GTP-γ-S (100 μM) with increasing concentrations of calyculin A resulted in an inhibition of their effects which became significant ($P<0.05$) at 10 nM calyculin A for the inhibition of GTP-γ-S (100 μM)-evoked secretion and at a concentration of 100 nM calyculin A for the inhibition of calcium ions (10 μM)-evoked ACTH secretion. (b) Standard permeabilization medium was supplemented with various quantities of calcium so that the indicated concentrations of free calcium ions resulted either in the presence (◆) or absence (■) of calyculin A (100 nM). ACTH secretion was significantly ($P<0.05$) stimulated above that obtained in the presence of 1 nM free calcium ions at concentrations of free calcium ions above 10 μM. In the presence of calyculin A (100 nM) there was no significant difference between ACTH secretion obtained at any of the free calcium ion concentrations. A comparison of the calcium ion concentration-response curves in the presence and absence of calyculin A (100 nM) revealed a significant ($P<0.001$) effect of the inhibitor on the calcium ion-evoked responses. (c) Permeabilization medium was supplemented with the indicated concentrations of GTP-γ-S either in the presence (◆) or absence (■) of calyculin A (100 nM). ACTH secretion was significantly ($P<0.05$) stimulated above the control value of concentrations of GTP-γ-S of 10 μM and above. In the presence of calyculin A there was no significant difference between the ACTH secretion obtained at any concentration of GTP-γ-S investigated. A comparison of the GTP-γ-S concentration-response curves in the presence and absence of calyculin A (100 nM) revealed a significant ($P<0.001$) effect of the inhibitor on the GTP-γ-S-evoked responses. (d) Permeabilization medium was supplemented with the indicated concentration of PMA either in the presence (◆) or absence (■) of calyculin A (100 nM). ACTH secretion was significantly ($P<0.05$) stimulated above control values only at a concentration of PMA of 100 nM both in the presence and absence of calyculin A.

evoked by calcium ions (10 μM) or GTP-γ-S (100 μM) was not different from control values. This concentration of calyculin A (i.e. 100 nM) was used in subsequent investigations of the effects of calyculin A.

The effect of calyculin A upon calcium-evoked ACTH secretion from permeabilized AtT-20 cells

ACTH secretion from permeabilized AtT-20 cells was dependent upon the concentration of free calcium ions in the permeabilization medium (Figure 1b). Calcium ions stimulated ACTH secretion in a concentration-dependent manner between 100 nM and 10 μM cytosolic free calcium ions (a significant ($P<0.05$) increase above that obtained at 1 nM was observed at 10 μM cytosolic free calcium ions and above). Co-incubation with calyculin A (100 nM) inhibited calcium-stimulated ACTH secretion (Figure 1b) resulting in no significant differences in ACTH secretion obtained at any concentration of calcium ions investigated. A comparison of the calcium ion concentration-response curves in the presence and absence of calyculin A (100 nM) by two-way ANOVA revealed a significant ($P<0.001$) effect of the inhibitor on the calcium ion-evoked responses.

The effect of calyculin A upon guanine nucleotide-evoked ACTH secretion from permeabilized AtT-20 cells

GTP-γ-S stimulated ACTH secretion, in the absence of calcium, in a concentration-dependent manner with a threshold of 1 μM (Figure 1c). Significant ($P<0.05$) increases above control ACTH secretion were observed at concentrations of GTP-γ-S of 10 μM and above. Calyculin A (100 nM) inhibited guanine nucleotide-stimulated ACTH secretion (Figure 1c) resulting in no significant differences in ACTH secretion obtained at any concentration of GTP-γ-S investigated. A comparison of the GTP-γ-S concentration-response curves in the presence and absence of calyculin A (100 nM) by two-way ANOVA revealed a significant ($P<0.001$) effect of the inhibitor on the GTP-γ-S-evoked responses.

The effect of calyculin A upon PMA-stimulated ACTH secretion from permeabilized AtT-20 cells

PMA (1 pM–100 nM) stimulated an increase in ACTH secretion from permeabilized AtT-20 cells, in the absence of calcium ions and guanine nucleotides, which was significant ($P<0.05$) at a concentration of 100 nM both in the presence and absence of calyculin A (100 nM) (Figure 1d). Co-incubation with calyculin A (100 nM) enhanced PMA-evoked ACTH secretion at this concentration of PMA (Figure 1d).

The effect of calyculin A upon guanine nucleotide-evoked ACTH secretion in the presence and absence of PMA

GTP-γ-S (100 μM) significantly ($P<0.05$) stimulated ACTH secretion from permeabilized AtT-20 cells (Table 1). This secretory response to the nucleotide was reduced by the presence of calyculin A (100 nM) so that the response was no longer significantly different from control (Table 1). Calyculin A (100 nM) did not significantly alter control ACTH secretion. PMA (100 nM) significantly ($P<0.05$) stimulated ACTH secretion (above the appropriate control value) in the presence and absence of calyculin A (100 nM) (Table 1). These results are consistent with the data presented in Figure 1c and d. In the presence of PMA (100 nM), however, the reduction of GTP-γ-S (100 μM)-stimulated ACTH, observed in the presence of calyculin A (100 nM), was no longer observed. A comparison of the effect of GTP-γ-S (100 μM), PMA (100 nM) and the combination of the two in the presence and absence of calyculin A (100 nM) by two-way ANOVA revealed a significant ($P<0.001$) effect of the inhibitor on the actions of these agents.

Table 1 The effect of calyculin A upon guanine nucleotide-evoked ACTH secretion in the presence and absence of phorbol 12-myristate 13-acetate (PMA)

	ACTH secretion (pg 10^5 cells)	
Treatment	*– Calyculin A* (100 nM)	*+ Calyculin A* (100 nM)
Control	29.3 ± 3.1	38.6 ± 7.3
PMA (100 nM)	46.3 ± 2.7	88.0 ± 16.1
GTP-γ-S (100 μM)	97.3 ± 5.4	60.3 ± 5.8
PMA (100 nM) +GTP-γ-S (100 μM)	121.7 ± 4.9	125.3 ± 7.6

Permeabilized cells were incubated in standard permeabilization medium supplemented with PMA (100 nM), guanosine 5'-O-(3'-thiotriphosphate) (GTP-γ-S, 100 μM) or GTP-γ-S (100 μM) plus PMA (100 nM) in the absence and presence of calyculin A (100 nM) and ACTH secretion measured as described in Methods. ACTH release is expressed as the mean ± s.e.mean from 3 separate experiments. In the absence of calyculin A PMA, GTP-γ-S and the combination of the two all significantly ($P<0.05$) stimulated ACTH secretion above the control value. In the presence of calyculin A, PMA and the combination of PMA and GTP-γ-S significantly ($P<0.05$) stimulated ACTH secretion above the control values. Control ACTH secretion was not significantly different in the presence and absence of calyculin A. ACTH secretion in response to GTP-γ-S (100 μM) was reduced in the presence of calyculin A so that the response was no longer significantly different from control. There was no significant difference between the ACTH secretion obtained in response to the com- bination of PMA and GTP-γ-S in the presence or absence of calyculin A. A comparison of the effect of GTP-γ-S (100 μM), PMA (100 nM) and the combination of the two in the presence and absence of calyculin A (100 nM) by two-way ANOVA revealed a significant ($P<0.001$) effect of the inhibitor on the actions of these agents.

Discussion

The results of the present study are consistent with previous reports supporting a late stage regulation of ACTH secretion by G_E in AtT-20 cells and that this GTP-binding protein mediates the effects of calcium upon the secretory apparatus (Guild, 1991; McFerran & Guild, 1994). In this study the effects of the phosphatase inhibitor, calyculin A upon calcium ion-, GTP-γ-S- and PMA-evoked secretion from permeabilized AtT-20 cells were investigated. This inhibitor is believed to be selective for serine/threonine phosphatases with no reported action upon tyrosine phosphatases or other kinases and phosphatases (Ishihara *et al.*, 1989; Wagner *et al.*, 1992; Meyer-Alber *et al.*, 1994). Calyculin A is a potent and effective inhibitor of type 1 and type 2 (both A and B) phosphatases (Ishihara *et al.*, 1989; Meyer-Alber *et al.*, 1994). The IC_{50} values for the inhibition of type 1 and 2-A phosphatases is in the nM range and full inhibition observed between 10–100 nM (Ishihara *et al.*, 1989). The inhibition of type 2-B phosphatase was reported to be maximal at 1 μM (Meyer-Alber *et al.*, 1994). The results of the present study indicate that calyculin A inhibits both calcium- and GTP-γ-S-evoked ACTH secretion from permeabilized cells in a concentration-dependent manner with a full effect seen at 100 nM. These data are consistent with the effects of calyculin A upon these two stimulants being due to its inhibition of type 1 and type 2 phosphatases.

Calyculin A inhibited both calcium ion- and GTP-γ-S-evoked ACTH secretion from permeabilized cells at every concentration of these stimulants investigated. This indicates that dephosphorylation by phosphatases plays an important role in stimulus-secretion coupling in AtT-20 cells and is involved in regulating the effects of G_E upon the secretory apparatus in these cells. AtT-20 cells join an ever increasing list of cell types including mast cells (Gomperts, 1990) and

pancreatic acinar cells (Ishihara *et al.*, 1989; Wagner *et al.*, 1992; Meyer-Alber *et al.*, 1994) in which the late stages of the secretory pathway involve a calcium/G_E mechanism and phosphatases. The observation that ATP retards the onset of secretion of permeabilized mast cells (Tatham & Gomperts, 1989) led to the suggestion that protein dephosphorylation as well as phosphorylation may be important in stimulus-secretion coupling and the hypothesis that dephosphorylation may be a step following G_E (for review see Gomperts, 1990).

The results of the present study indicate that calyculin A does not inhibit but rather enhances the stimulation of ACTH secretion obtained by PMA and hence PKC activation. The conditions under which this enhancement is observed involve an action of PMA in the absence of added calcium ions and guanine nucleotides so the physiological relevance of this is uncertain. However, it is known that PKC interacts with the ACTH secretory pathway at multiple points as shown by its 'pre-' and 'post-'calcium sites of action to regulate calcium influx and the effect of particular cytosolic calcium concentrations upon ACTH secretion (Reisine & Guild, 1987; Reisine, 1989; McFerran & Guild, 1994). Furthermore, the 'post'-calcium site of action of PKC is also 'post-'G_E (McFerran & Guild, 1994). Therefore, it is possible that there is a role for PKC modulation of the secretory response at a very late stage in the stimulus-secretion coupling pathway which entails a modulation of the actions of the calcium/G_E machinery. The action of calyculin A to inhibit the stimulation of exocytosis by G_E (as activated by calcium and GTP-γ-S in these studies) but not the late stage effect of PMA indicates that the important dephosphorylation mediated by the phosphatases of the type 1 and/or 2 (A and B) lies between G_E and the site of interaction between PKC and G_E-stimulated events.

The ability of PMA apparently to prevent the calyculin A-evoked inhibition of GTP-γ-S-stimulated ACTH secretion is difficult to interpret and great caution should be used in making any claims about physiological mechanisms revealed by these observations. It is clear that a G-protein does directly regulate exocytosis but its action is regulated by second messenger systems perhaps by increasing the readily releasable pool of stored hormone (Dannies, 1982). Calcium alone cannot stimulate the maximal possible hormone secretion and that co-operation with PKC and PKA increases the amount of hormone secreted in response to a particular concentration of calcium ions (Guild, 1991; McFerran & Guild, 1994). We have previously speculated that in AtT-20 cells, PKA and PKC modulate the secretory response by maintaining a 'primed' state and the size of the readily-releasable pool of hormone but that the exocytotic machinery is directly controlled by the calcium/G_E system (McFerran & Guild, 1994). Therefore, a possible explanation for the intriguing effect of PKC activation upon the actions of calyculin A in this study may lie in this regulation of the readily-releasable pool of ACTH by protein kinases. The inhibitory effects of calyculin A upon the calcium/G_E system could be attenuated by a PKC-evoked increase in the size of the readily releasable pool. Therefore, although one part of the exocytotic machinery is inhibited, an increase in the size of the pool of ACTH upon which this system acts results in the observed apparent lack of effect of calyculin A in the presence of PMA.

The authors would like to acknowledge gratefully the financial support of the Wellcome Trust, the Royal Society and the Nuffield Foundation. B.W.M. is supported by a Maitland-Ramsay scholarship.

References

ABOU-SAMRA, A., CATT, K.J. & AGUILERA, G. (1986). Involvement of protein kinase C in the regulation of adrenocorticotrophin release from rat anterior pituitary cells. *Endocrinology*, **118**, 212–217.

AGUILERA, G., HARWOOD, J., WILSON, J., BROWN, J. & CATT, K. (1983). Mechanism of action of corticotrophin-releasing factor and other regulators of corticotrophin release in rat pituitary cells. *J. Biol. Chem.*, **258**, 8039–8045.

ANTONI, F.A. (1986). Hypothalamic control of adrenocorticotrophin secretion – advances since the discovery of 41-residue corticotrophin-releasing factor. *Endocr. Rev.*, **7**, 351–361.

AXELROD, J. & REISINE, T. (1984). Stress hormones: their interaction and regulation. *Science*, **224**, 452–459.

BISHOP, J.F., FARAH, J.M., PATEL, J. & O'DONOHUE, T.L. (1987). Activation of distinct second messenger systems in anterior pituitary corticotrophic tumour cells alters the phosphorylation states of both shared and distinct cytosolic proteins. *Mol. Cell. Endocrinol.*, **52**, 17–26.

DANNIES, P.S. (1982). Prolactin: multiple intracellular processing routes plus several potential mechanisms for regulation. *Biochem. Pharmacol.*, **31**, 2845–2849.

FRAKER, P. & SPECK, J. (1978). Protein and cell membrane iodination's with a sparingly soluble chloramide, 1,3,4,6-tetrachloro-3α,6α-diphenylglycoluril. *Biochem. Biophys. Res. Commun.*, **80**, 849–857.

GUILD, S. (1991). Effects of adenosine 3':5'-cyclic monophosphate and guanine nucleotides on calcium-evoked ACTH release from electrically-permeabilised AtT-20 cells. *Br. J. Pharmacol.*, **104**, 117–122.

GUILD, S., ITOH, Y., KEBABIAN, J.W., LUINI, A. & REISINE, T. (1986). Forskolin enhances basal and potassium-evoked hormone release from normal and malignant pituitary tissue. The role of calcium. *Endocrinology*, **118**, 268–279.

GUILD, S. & REISINE, T. (1987). Molecular mechanisms of corticotrophin-releasing factor stimulation by calcium mobilization and adrenocorticotrophin release from anterior pituitary tumor cells. *J. Pharmacol. Exp. Ther.*, **241**, 125–130.

GOMPERTS, B.D. (1990). G_E: GTP-binding protein mediating exocytosis. *Ann. Rev. Physiol.*, **52**, 591–606.

ISHIHARA, H., MARTIN, B.L., BRAUTIGAN, D.L., KARAKI, H., OZAKI, H., KATO, Y., FUSETANI, N., WATABE, S., HASHIMOTO, K., UEMURA, D. & HARTSHORNE, D.J. (1989). Calyculin A and okadaic acid: inhibitors of protein phosphatase activity. *Biochem. Biophys. Res. Commun.*, **159**, 871–877.

KNIGHT, D.E. & BAKER, P.F. (1982). Calcium-dependence of catecholamine release from adrenal medulary cells after exposure to intense electric fields. *J. Memb. Biol.*, **68**, 107–140.

KNIGHT, D.E. & SCRUTTON, M.C. (1986). Gaining access to the cytosol: the technique and some applications of electropermeabilization. *Biochem. J.*, **234**, 497–450.

LUINI, A. & DE MATTEIS, M.A. (1988). Dual regulation of ACTH secretion by guanine nucleotides in permeabilized AtT-20 cells. *Cell. Mol. Biol.*, **8**, 129–138.

LUINI, A., LEWIS, D., GUILD, S., CORDA, D. & AXELROD, J. (1985). Hormone secretagogues elevate cytosolic calcium by increasing cAMP in corticotrophin-secreting cells. *Proc. Natl. Acad. Sci. U.S.A.*, **82**, 8034–8038.

MACLEAN, C.M., MARCINIAK, S.J., HALL, D.V. & EDWARDSON, J.M. (1993). Involvement of a phosphoprotein on the zymogen granule membrane in the control of regulated exocytosis in the exocrine pancreas. *J. Cell. Sci.*, **106**, 663–670.

MCFERRAN, B.W. & GUILD, S.B. (1994). Effects of protein kinase C activators upon the late stages of the ACTH secretory pathway of AtT-20 cells. *Br. J. Pharmacol.*, **113**, 171–178.

MEYER-ALBER, A., FETZ, I., WASCHULEWSKI, I.W., HOCKER, M., FOLSCH, U.R. & SCHMIDT, W.E. (1994). Calyculin A, okadaic acid and W-7 interfere with a distal step in pancreatic acinar signal transduction. *Biochem. Biophys. Res. Commun.*, **201**, 1470–1476.

REISINE, T. (1989). Phorbol esters and corticotrophin-releasing factor stimulate calcium influx in the anterior pituitary tumour cell line, AtT-20, through different intracellular sites of action. *Mol. Pharmacol.*, **248**, 984–990.

REISINE, T. & GUILD, S. (1987). Activators of protein kinase C and cyclic AMP-dependent protein kinase regulate intracellular calcium levels through distinct mechanisms in mouse anterior pituitary tumour cells. *Mol. Pharmacol.*, **32**, 488–496.

TATHAM, P.E.R. & GOMPERTS, B.D. (1989). ATP inhibits onset of exocytosis in permeabilised mast cells. *Biosci. Rep.*, **9**, 99–109.

WAGNER, A.C.C., SCHAFFER, C. & WILLIAMS, J.A. (1992). Effects of calyculin A on amylase release from streptolysin-O permeabilised acinar cells. *Biochem. Biophys. Res. Commun.*, **189**, 1606–1612.

(Received September 7, 1994
Revised December 23, 1994
Accepted January 6, 1995)

British Journal of Pharmacology (1995) 114, 1577-1586 © 1995 Stockton Press All rights reserved 0007-1188/95 $12.00

Stimulation of human umbilical vein endothelial cell proliferation by A_2-adenosine and β_2-adrenoceptors

[1]Veronika Sexl, Gudrun Mancusi, *Sabina Baumgartner-Parzer, Wolfgang Schütz & Michael Freissmuth

Institute of Pharmacology, University of Vienna, Währinger Str. 13a and *Clinic of Internal Medicine III, Vienna General Hospital, Währinger Gürtel 18-20; A-1090 Vienna, Austria

1 Adenosine is known to stimulate capillary outgrowth and endothelial cell proliferation, but the underlying mechanism has not been identified. In order to identify the receptor subtype involved, the effects of adenosine receptor agonists and antagonists on human umbilical vein endothelial cell (HUVEC) proliferation were investigated.

2 Raising intracellular adenosine levels by use of the adenosine transport inhibitor, 4-nitrobenzylthioinosine (NBMPR) did not affect cell growth. This observation suggests that stimulation of an extracellular adenosine receptor generates the mitogenic signal.

3 In the presence of adenosine deaminase (ADA), which was used to remove adenosine present in the culture medium, the adenosine receptor agonists N-ethylcarboxamidoadenosine (NECA, non-selective) and CGS21680 (A_{2A}-receptor-selective) stimulated [^{3}H]-thymidine incorporation with a half-maximum effect at about 10 nM, while N^6-cyclopentyladenosine (CPA, A_1-selective) was about 100 fold less potent. The adenosine receptor antagonist, xanthine amine congener (XAC) produced a concentration-dependent decrease in endothelial cell proliferation with a half-maximum effect at about 10 nM. Hence, stimulation of an endothelial A_{2A}-adenosine receptor seems responsible for the mitogenic signal.

4 In the presence of ADA, isoprenaline is also able to stimulate [^{3}H]-thymidine incorporation with a half maximal effect of about 3 nM, an effect, which is reversed by the highly β_2-selective antagonist, ICI 118,551. In the absence of ADA, isoprenaline exerts only a minor stimulatory effect. Combination of A_{2A} adenosine and β_2-adrenoceptor agonists did not further enhance [^{3}H]-thymidine incorporation when compared to the sole addition of each agonist. We therefore conclude that both receptors stimulate endothelial cell proliferation via a common signal transduction pathway.

5 Both receptors are coupled to stimulation of adenylyl cyclase via the stimulatory G protein G_s. However, *direct* activation of downstream effectors in the cyclic AMP-signalling cascade (G_s with cholera toxin, adenylyl cyclase with forskolin, protein kinase A with ^{8}Br-cyclic AMP) not only failed to mimic the action of receptor-activation, but even reduced cell proliferation.

6 Similarly, pertussis toxin-treatment which inactivated the G_{i2} protein present in HUVEC and thus inhibited cell proliferation *per se*, did not impair the ability of A_{2A}-receptor agonists to stimulate cell proliferation. This suggests that the A_{2A}-adenosine and β_2-adrenoceptor-mediated stimulation of endothelial cell proliferation occurs via a mechanism that is independent of G_s and G_i.

Keywords: Human umbilical vein endothelial cells (HUVEC); adenosine; β-adrenoceptor; cyclic AMP; proliferation

Introduction

Endothelial cell proliferation and angiogenesis occur in response to a variety of physiological and pathophysiological stimuli. As the initial response, the endothelial cells secrete proteolytic enzymes which results in fragmentation of the basal lamina; subsequently, the endothelial cells migrate through the fragmented lamina into the perivascular space where they proliferate and form new capillaries (Folkman & Shing, 1992). In the last decade, several mitogenic factors have been identified that stimulate endothelial cell proliferation and neo-vascularization; in particular, fibroblast growth factors, endothelial cell growth factor, transforming growth factors and angiogenin have been identified as important mitogens (Folkman & Shing, 1992; Bobik & Campbell, 1993). Hypoxia is also known to be a strong stimulus for angiogenesis, e.g. in processes like tumour growth, diabetic retinopathy, wound healing and collateralisation. Adenosine, which has long been known as a potent vasodilator (Berne, 1963), is released by hypoxic tissue in large amounts and findings on different animal models additionally suggest this nucleoside as an endothelial mitogen linking the altered metabolism in oxygen-deprived cells to the formation of new capillaries (Ziada *et al.*, 1984; Dusseau *et al.*, 1986). In the meantime, a mitogenic effect of adenosine in cultured endothelial cells has been verified by several authors (Meininger & Granger, 1990; Van Daele *et al.*, 1992; Ethier *et al.*, 1993), but the site as well as the mechanism of action of the nucleoside remain unclear at present (Folkman & Shing, 1992; Collis & Hourani, 1993). Van Daele *et al.* (1992) found only a mitogenic effect for adenosine itself and for ATP, but no effect for typical adenosine receptor ligands. Hence, they concluded that adenosine may act via an intracellular site and ATP via a P_2-purinoceptor on the plasma membrane. In contrast, other workers reported adenosine-induced endothelial cell proliferation which is mimicked by adenosine receptor agonists and blocked by antagonists, thus implying rather an extracellular adenosine receptor-mediated site of action (Meininger & Granger, 1990; Ethier *et al.*, 1993); however, there is still no information with respect to the responsible adenosine receptor subtype, the type of the G protein involved in signal transduction and the nature of the intracellular messenger.

In the present study, we have therefore determined *(i)* which adenosine receptor subtype (A_1, A_{2A}, A_{2B}, or A_3)

[1] Author for correspondence.

mediates the mitogenic action of adenosine on the endothelium and whether endothelial cell growth is also affected by changes in intracellular adenosine levels; *(ii)* which G protein (G_s, a subtype of G_i or neither) is involved in transduction of the mitogenic signal; and *(iii)* the role of adenosine 3':5'-cyclic monophosphate (cyclic AMP). The findings obtained with adenosine analogues were compared with those obtained for isoprenaline, since the β-adrenoceptor is also a prototypical G_s-coupled receptor known to reside on endothelial cells. All experiments were carried out on human umbilical vein endothelial cells (HUVEC).

Methods

Cell culture

HUVEC were isolated according to Jaffe *et al.* (1973). Cords were rinsed twice with phosphate-buffered-saline (PBS) and then incubated for 20 min with 0.2% collagenase in PBS. The cell suspension was collected, centrifuged and the cell pellet was resuspended in medium 199 enriched with endothelial cell growth supplement (ECGS), 100 μg ml^{-1} streptomycin, 100 u ml^{-1} penicillin, 0.25 μg ml^{-1} amphotericin and 20% foetal calf serum (FCS) and plated in 1% gelatine-coated culture dishes. The cells were grown at 37°C in a 5% CO_2 humidified incubator. The following day the medium was changed to remove erythrocytes and was renewed twice a week. After 4–6 days cells formed confluent monolayers and were further subcultured by trypsinisation (0.25%); cell plating efficiency after trypsinization was >98%. The cell population, thus obtained, consisted of >95% endothelial cells verified by their cobblestone morphology and immunofluorescence staining with antibody against von-Willebrand-factor antigen (Dako, Dakopatts, Denmark). Cells were used in the second and third passage.

Assessment of [^{3}H]-thymidine incorporation in cultured endothelial cells

HUVEC were allowed to grow until confluency. Cells were then washed twice with phosphate buffered saline (PBS) and synchronized by serum starvation for 48 h in medium 199 containing 0.2% bovine serum albumin. Subsequently, the cells were removed from their plastic support by brief trypsinisation, washed and seeded at 1–2 × 10^4 cells/well in flat bottomed 96-well tissue culture plates in medium 199 containing 5% FCS. After 2 h, which allowed the cells to adhere, the compounds indicated in the respective figures were added. [^{3}H]-thymidine (specific activity ~2 Ci mmol^{-1}) was added 24 h later to a final concentration of 1 μCi ml^{-1}. After an additional 24 h period, cells were lysed by a freeze-thaw cycle and the radioactivity incorporated into DNA was trapped onto glassfibre filters using a Skatron cell harvester. Determinations were carried out in quadruplicate. The amount of [^{3}H]-thymidine incorporated in the presence of 5% FCS (= control) varied between 2,000 and 10,000 c.p.m. in individual experiments with different cell batches. This interassay variance arises in part from modest differences in cell numbers and in the specific activity of [^{3}H]-thymidine; a further factor is the length of transition from G_0/G_1- to S-phase, which we found to vary between 24 h and 36 h under our assay conditions in individual cell batches. We stress that all effects of the compounds tested are not affected by these variations. In order to allow for interassay comparisons, the amount of [^{3}H]-thymidine incorporated in the presence of 5% FCS was set as 100% and the drug-induced changes were related to this value.

Short-pulse conditions

In experiments in which the time-dependent effect of ^{8}Br-cyclic AMP was determined (Figure 5b), [^{3}H]-thymidine (6–8 μCi ml^{-1}) was added after 48 h and the incubation was continued for an additional 3 h; thereafter the samples were processed as described above.

Determination of cell number

HUVEC were allowed to grow until confluency, washed twice with PBS and synchronized by serum starvation for 48 h. After trypsinisation cells were seeded at ~1.5 × 10^5 cells/well in flat bottomed 12-well tissue culture plates in medium 199 containing 5% FCS. After 2 h the compounds indicated in the legend to Figure 2 were added. Cells were dispersed 72 h thereafter with 0.25% trypsin and counted in a coulter counter (Coulter Electronics).

Determination of intracellular adenosine levels

The intracellular nucleoside- and nucleotide-pool was prelabelled by incubating HUVEC (~5 × 10^5/well) with [^{3}H]-adenine (10 μCi/well) for 24 h. The [^{3}H]-adenine containing medium was then replaced by medium containing the compounds indicated in Figure 2a. After 6, 12 and 24 h the medium was rapidly removed, the cells were washed in phosphate buffered saline and intracellular nucleosides and nucleotides were extracted with perchloric acid and analysed by h.p.l.c. on a Nucleosil-10-C_{18} reverse-phase column as described (Nees *et al.*, 1985). Chromatographic conditions were as follows: a flow rate of 100 ml h^{-1}, a linear elution gradient of 0.1 M potassium phosphate (pH 5.8) vs. 60% methanol in 0.1 M potassium phosphate (pH 5.8) over 60 min. The fractions corresponding to adenine nucleotides, adenosine, inosine and cyclic AMP were identified from the u.v. signal generated by the addition of unlabelled standards, collected and counted for radioactivity.

Adenylyl cyclase assay

HUVEC membranes were prepared in buffer containing 50 mM Tris HCl (pH 7.4), 1 mM EDTA, 1 mM EGTA and 20 μM aprotinin. After a rapid freeze-thaw cycle in liquid nitrogen, sucrose was added to a final concentration of 0.25 M; thereafter cells were homogenized by means of an Ultraturrax and centrifuged for 10 min at 20,000 *g*. The resulting membrane pellet was washed twice in sucrose-free buffer, resuspended at a protein concentration of ~5 mg ml^{-1}, frozen in liquid nitrogen and stored at −80°C. The protein concentration was determined by dye binding with the Bio-Rad Coomassie blue kit using bovine serum albumin as standard. Adenylyl cyclase activity was determined in a final volume of 0.1 ml containing (mM composition): HEPES NaOH 40, (pH 8), EDTA 1, $MgCl_2$ 2, [α-^{32}P]-ATP (specific activity ~200 cpm pmol^{-1}) 0.05, phosphocreatine 5, RO 20–1724 0.1, 5 units of creatinine kinase, 2 units of adenosine deaminase and 10 μg of membrane protein; activating ligands were present at the concentrations indicated in Figure 4. After 20 min at 25°C, the reaction was quenched and the [^{32}P]-cyclic AMP formed was separated from the substrate by sequential chromatography on Dowex 50W-X8 and neutral alumina (Salomon *et al.*, 1974) with [^{3}H]-cyclic AMP as an internal standard (recovery ~70%).

Detection of G-protein α-subunits by immunoblots and Pertussis toxin-catalyzed ADP-ribosylation

For immunoblot analysis, HUVEC membrane samples (75 μg of membrane protein) were resolved by SDS polyacrylamide gel electrophoresis (running gel: 10% acrylamide and 0.13% N,N'-methylene bisacrylamide) and proteins transferred to nitrocellulose. The following antisera were used at a 1 : 250 dilution: 84 (raised against the peptide KENLKDCGLF), which recognizes all three subtypes of G_i, and CS1 (raised against the peptide RMHLRQYELL), which is specific for $G_{s\alpha}$ (Selzer *et al.*, 1993). The antigen-antibody complexes

were visualized by a second antibody coupled to alkaline phosphatase using the ProtoBlot II kit (Promega). Recombinant G protein α-subunits (G_{sas}, $G_{sα\text{-}L}$, $G_{iα\text{-}1}$, $G_{iα\text{-}2}$) were purified from bacterial lysates as described (Freissmuth & Gilman, 1989; Linder *et al.*, 1990) and used as standards to verify comigration of the bands detected by the antisera. Labelling with pertussis toxin-catalyzed ADP-ribosylation was carried according to Bokoch *et al.* (1983): To reduce background labelling, G proteins were solubilized from the membranes prepared from HUVEC pretreated with increasing concentrations of pertussis toxin (as indicated in the legend to Figure 6). Incubation was 1 h on ice at a protein concentration of 4 mg ml^{-1} in the presence of 25 mM CHAPS; unsolubilized material was removed by centrifugation. The labelling reaction was carried out with an aliquot of the supernatant corresponding to 50 μg membrane protein for 40 min in the presence of [^{32}O]-NAD; subsequently, the reaction mixture was dissolved in Laemmli sample buffer containing 2% SDS and 40 mM dithiothreitol, and proteins were resolved on a SDS- polyacrylamide gel (running gel: 10% acrylamide and 0.13% N,N'-methylene bisacrylamide). A bovine brain G protein preparation containing a mixture of G_i and G_0 was purified according to Sternweis & Robishaw (1984) and used as a standard.

Data are reported as means ± s.d. from *n* independent experiments; intra-assay replicate variation was between 5–10% of the mean. All statistical comparisons were made with Student's *t* test for paired data.

Materials

Cell culture media were from GIBCO (Grand Island, NY), cell culture dishes from Greiner (Krems, Austria). [α-^{32}P]-ATP, [^{3}H]-thymidine, [^{3}H]-adenine were obtained from NEN. Cholera toxin and N^6-cyclopentyladenosine (CPA), 4-nitrobenzylthioinosine (NBMPR), (-)-isoprenaline, 8-bromo cyclic AMP (^{8}Br-cyclicAMP), collagenase (Type IV) and forskolin were from Sigma (St. Louis, MO, U.S.A.), pertussis toxin from Peninsula Laboratories (St. Helens, UK); GTPγS, R- and S-N^6(phenylisopropyl)adenosine (PIA), creatine kinase and adenosine deaminase were from Boehringer Mannheim (Germany); xanthine amine congener (XAC) was from Research Biochemicals (Natick, MA, U.S.A.), 5'-N-ethylcarboxamidoadenosine (NECA), 5'-N-ethylcarboxamido-2-[4-(2-carboxyethyl)phenethyl]adenosine (CGS 21680), DL-4-(3-butoxy-4-methoxylbenzyl)-2-imidazilidinone (Ro-20-1724), erythro-DL-1-(7-methylindan-4-yloxy)-3-isopropylaminobutane-2-ol (ICI 118,551) were generous gifts of Byk Gulden (Konstanz, Germany), Ciba-Geigy (Basel, CH), Hoffman-La Roche (Basel, Switzerland) and ICI (Cheshire, UK), respectively, Sodium-4-[2-(2-hydroxy-(3-chlorophenyl) ethylamino)-propyl] phenoxyacetate (BRL 37344) was kindly supplied by Dr A.D. Strosberg (ICGM, Paris).

Results

Determination of the adenosine receptor subtype

Incubation of HUVEC with adenosine deaminase in the presence of 5% FCS resulted in a significant ($P<0.001$; $n=14$) reduction of [^{3}H]-thymidine incorporation (Figure 1a), which varied between 20 and 30% (mean = 27 ± 2%) in different cell batches. This effect of adenosine deaminase was concentration-dependent and abolished by heat-inactivation of the enzyme (data not shown). Similarly, addition of the potent adenosine receptor antagonist, XAC resulted in a concentration-dependent inhibition of [^{3}H]-thymidine incorporation (Figure 1a); the maximal inhibition obtained with XAC was not statistically different from the effect of adenosine deaminase. The half-maximal effect was observed at ~10 nM, a concentration range at which this compound interacts with A_1 and A_2-adenosine receptors, but does not cause inhibition of cyclic nucleotide phosphodiesterases (Galen *et al.*, 1992). If the non-selective agonist NECA was added at a concentration of 10 μM, representing a 100 fold excess of NECA's maximally effective concentration the inhibitory effect of XAC was reversed (Figure 1a, insert; $P<0.01$, $n=4$). These findings indicate that endogenous adenosine present in the culture medium contributes to endothelial cell proliferation and imply a receptor-mediated mechanism of action. This assumption was verified by determining the effects of synthetic adenosine receptor agonists on DNA-synthesis in the presence of adenosine deaminase (Figure 1b); the efficacy and potency of CGS 21680 and N-ethylcarboxamidoadenosine (NECA) were found to be comparable with an EC_{50} of about 10 nM, and the effect of

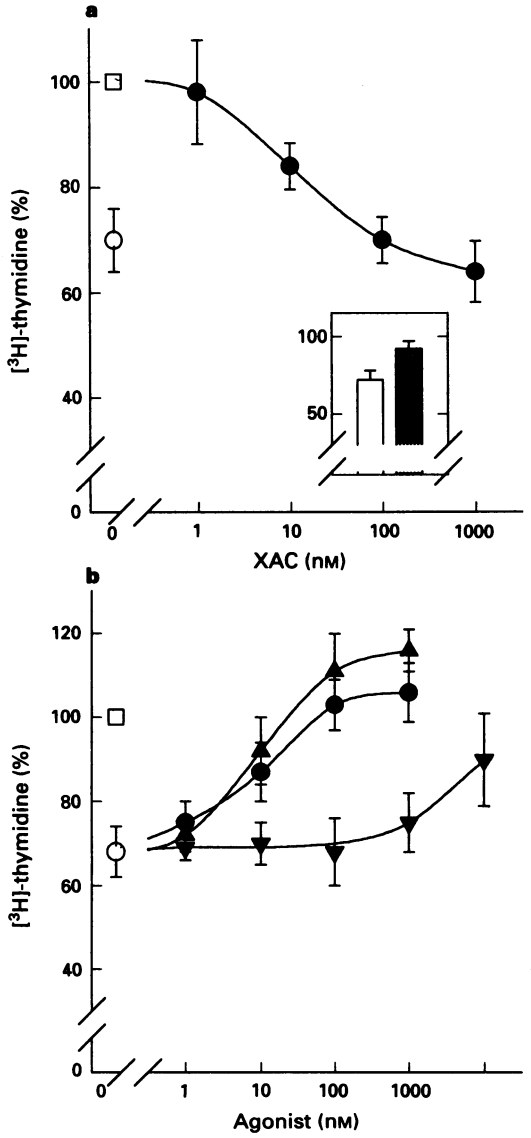

Figure 1 Effect of adenosine deaminase and adenosine receptor ligands on foetal calf serum (FCS)-induced [^{3}H]-thymidine incorporation. (a) Inhibition of [^{3}H]-thymidine incorporation in synchronized HUVEC (~1.1 × 10^4 cells/well) stimulated by 5% FCS (□), by 5% FCS + 2 u ml^{-1} adenosine deaminase (○), 5% FCS + QAC (●). Insert: The effect of XAC (100 nM, open column) is antagonized by addition of NECA (10 μM, cross hatched column, $P<0.01$, $n=4$). (b) Modulation of [^{3}H]-thymidine incorporation stimulated by 5% FCS (□), FCS in the presence of 2 u ml^{-1} adenosine deaminase alone (○), and combined with CGS 21680 (▲), NECA (●), or CPA (▼). Data represent means from three to four experiments carried out in quadruplicate under the conditions outlined under Methods; [^{3}H]-thymidine incorporation in the presence of 5% FCS was set as 100%.

these agonists was antagonized by XAC (data not shown). The concentration-response curves for cyclopentyl-adenosine (CPA, Figure 1a) and the R- and S-isomers of N^6-phenylisopropyladenosine (PIA, data not shown) were virtually identical; these compounds were found to be less potent than NECA and CGS 21680, a pharmacological profile consistent with the involvement of an A_{2A}-adenosine receptor. The observed changes in [^{3}H]-thymidine incorporation reflect an increased replication rate of HUVEC which was verified by carrying out a cell count assay over 72 h in the presence of FCS alone (Figure 2b, ▽), addition of adenosine deaminase (Figure 2b, □), and addition of adenosine deaminase + CGS 21680 (Figure 2b, ■). The results were in close agreement to the observations obtained by determining [^{3}H]-thymidine incorporation and also correspond to previously published results (Meininger & Granger, 1990; Ethier *et al.*, 1993).

Apart from interacting with cell-surface receptors, adenosine may exert some of its action via an intracellular site of action, e.g. via interaction with an A_2-like binding site for adenosine and adenosine analogues, in particular NECA (Hutchinson & Fox, 1989), or by binding to the inhibitory P-site of adenylyl cyclase (Olah & Stiles, 1992). Endothelial cells are known to have a very active adenosine metabolism characterized by a large capacity for uptake and release of the nucleoside (Nees *et al.*, 1985). We have tested whether increases in the intracellular level of adenosine were capable of altering the rate of endothelial cell proliferation by employing the adenosine transport inhibitor, NBMPR. Intracellular adenosine levels were determined after 6, 12 and 24 h, a time period relevant for triggering mitogenic activity. Addition of 1 μM NBMPR, a concentration leading to an almost complete inhibition of the nucleoside transporter (data not shown), resulted in a pronounced increase ($P<0.01$) of intracellular adenosine. The effect of NBMPR at the 12 h time point is shown in Figure 2a (bottom panel); in contrast, the presence of adenosine deaminase had no detectable effect on intracellular adenosine levels (Figure 2a, middle panel). Intracellular adenosine levels expressed as a percentage of the total incorporated radioactivity were 0.28 ± 0.09%, 0.26 ± 0.13, and 0.84 ± 0.04 for FCS, ADA, and NBMPR, respectively (mean ± s.d., $n=3$, $P<0.01$ for NBMPR vs FCS or ADA). The effect of NBMPR was comparable at the other two time points (i.e. 6 h and 24 h). Intracellular levels of cyclic AMP, which elutes immediately after adenosine, did not reveal any significant changes, irrespective of the time point and of whether NBMPR or adenosine deaminase were present (12 h-values 0.76 ± 0.10%, 0.83 ± 0.13%, and 0.73 ± 0.24% for FCS, ADA, and NBMPR, respectively, means ± s.d., $n=3$). Due to the affinity of NBMPR for the nucleoside transporter this compound also inhibits [^{3}H]-thymidine uptake; a cell count assay was therefore carried out to measure the effect of NBMPR treatment on HUVEC proliferation. As can be seen from Figure 2b, NBMPR did not produce any change in cell number. A cytotoxic effect was ruled out by trypan blue exclusion. Taken together, these findings rule out an intracellular site of action for adenosine and stress the importance of the A_{2A}-receptor as the site of action for the mitogenic activity of adenosine analogues.

Determination of the G protein involved

Since A_{2A}-adenosine receptors are coupled to activation of adenylyl cyclase via G_s, we investigated whether the β_2-adrenoceptor is also capable of mediating endothelial cell proliferation. The β_2-adrenoceptor is a G_s-coupled receptor expressed on endothelial cells (Steinberg *et al.*, 1984; Freissmuth *et al.*, 1986). At low concentrations, isoprenaline (EC_{50} ~3 nM) stimulates [^{3}H]-thymidine incorporation in the presence of adenosine deaminase (Figure 3a); in the absence of adenosine deaminase it exerts only a minor stimulatory effect. The requirement of adenosine deaminase for the observation of a stimulatory effect of isoprenaline suggested that the β-adrenoceptor and the A_{2A}-adenosine receptor shared a common signal transduction pathway. A further hint at a common mechanism is that combination of NECA and isoprenaline in maximally active concentrations did not enhance [^{3}H]-thymidine incorporation when compared to the sole addition of each agonist (Figure 3b). In order to define the

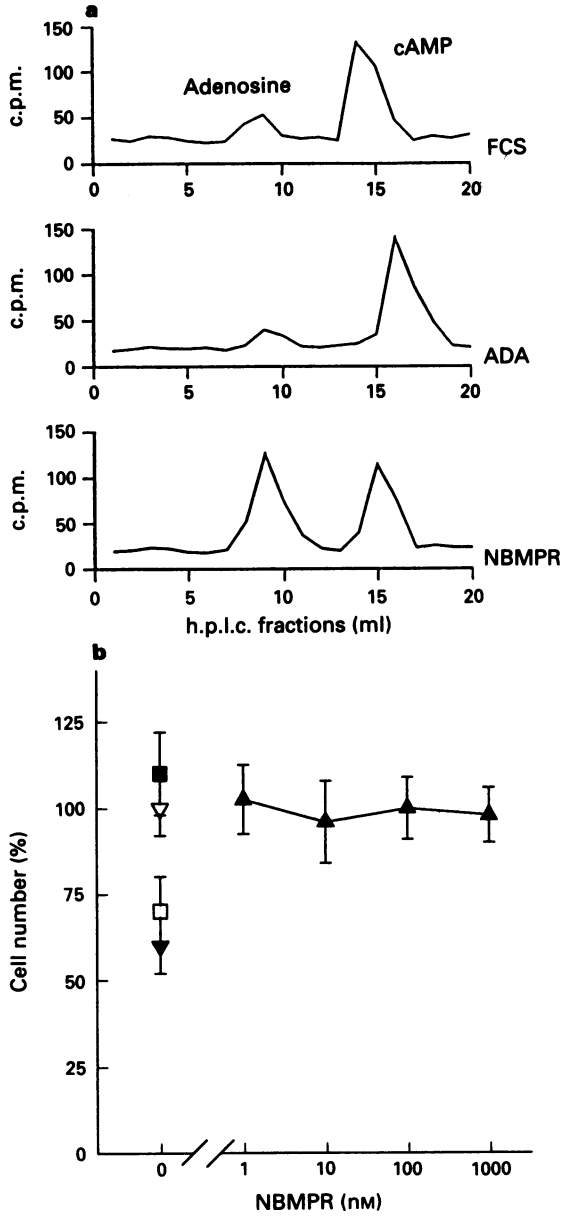

Figure 2 (a) H.p.l.c. analysis of the intracellular adenine nucleotide and nucleoside pool following treatment with adenosine deaminase (ADA, middle) and 4-nitrobenzylthioinosine (NBMPR, bottom): 5 × 10^5 cells/well were prelabelled with [^{3}H]-adenine for 24 h and subsequently incubated in the presence of FCS (top), 2 u ml^{-1} adenosine deaminase (ADA, middle) or 1 μM NBMPR (bottom) for 12 h. A neutralized perchloric acid extract was analysed by h.p.l.c. as described under Methods. The region of the chromatogram is shown, in which adenosine and cyclic AMP elute; no differences were noted for adenine nucleotides and the breakdown product inosine, which elute earlier. (b) Effect of NBMPR, CGS 21680 and pertussis toxin on cell number. For the determination of cell number, synchronized cells were plated at 1.5 × 10^5 cells/well in 5% FCS (FCS, ▽) and the combination of FCS and the following compounds: NBMPR (▲), 10 ng mg^{-1} pertussis toxin (PTX, ▼; $P<0.05$ vs. FCS), 2 u ml^{-1} adenosine deaminase (ADA, □; $P<0.05$ vs. FCS), and adenosine deaminase + 1 μM CGS 21680 (CGS, ■ $P<0.05$ vs. ADA). Cell number was determined 72 h after plating; the value determined in the presence of 5% FCS (2.2 ± 0.4 × 10^5 cells) was set as 100%.

pharmacological subtype of the β-adrenoceptor we used the β_3-selective agonist, BRL 37344 (Emorine *et al.*, 1989) and the highly β_2-selective antagonist ICI 118,551. BRL 37344 did not exert any effect ruling out the involvement of a β_3-adrenoceptor. On the other hand, the stimulatory effect of isoprenaline was competitively antagonized by ICI 118,551 (Figure 3a). A pA_2 of ~9 was estimated from the ICI 118,551-induced shift of the concentration-response curve for isoprenaline; this is in agreement with a K_D of ~1 nM determined for the interaction of ICI 118,551 with endothelial β_2-adrenoceptors (Freissmuth *et al.*, 1986). These findings establish that stimulation of the β_2-adrenoceptor generates a mitogenic signal in human endothelial cells.

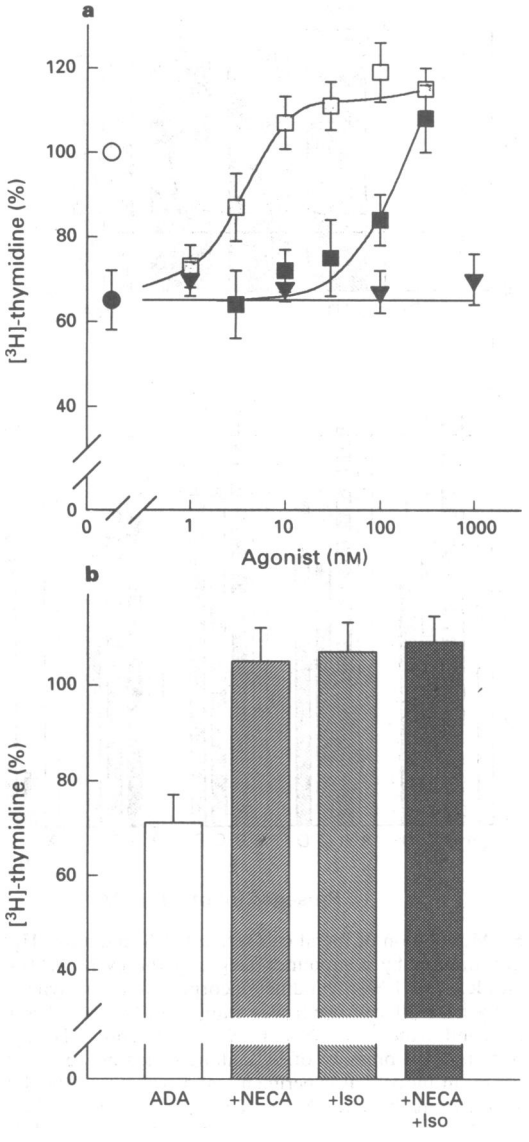

Figure 3 Effect of β-adrenoceptor ligands on foetal calf serum (FCS)-induced [^{3}H]-thymidine incorporation. (a) [^{3}H]-thymidine incorporation was determined in synchronized HUVEC (~1.2×10^4 cells/well) prestimulated by 5% FCS (○), by 5% FCS + 2 u ml^{-1} adenosine deaminase (●), 5% FCS + isoprenaline in the presence of 2 u ml^{-1} adenosine deaminase (□), isoprenaline in the presence of adenosine deaminase and 10 nM of the β_2-selective antagonist, ICI 118,551 (■), and 5% FCS + the β_3-selective agonist BRL 37,344 in the presence of adenosine deaminase (▼). (b) [^{3}H]-thymidine incorporation in synchronized HUVEC in the presence of 2 u ml^{-1} adenosine deaminase (ADA), the combination of adenosine deaminase and 1 μM NECA (+ NECA), adenosine deaminase and 100 nM isoprenaline (+ Iso), adenosine deaminase and 1 μM NECA and 100 nM isoprenaline (+ NECA + Iso). Data represent means from three to five experiments carried out in quadruplicate; [^{3}H]-thymidine incorporation in the presence of 5% FCS was set as 100%.

The coupling of A_2-adenosine receptors to activation of adenylyl cyclase has been described on microvascular and endothelial cell membrane preparations obtained from different species and vascular beds (Schütz *et al.*, 1982; Des Rosiers & Nees, 1987). Also in HUVEC, CGS 21680, NECA and isoprenaline were found to stimulate adenylyl cyclase activity with comparable efficacies (Figure 4); EC_{50}-values were 0.3 ± 0.2, 0.52 ± 0.08 and 0.09 ± 0.03 μM (mean ± s.d.; $n = 3$) for CGS 21680, NECA and isoprenaline, respectively. In contrast, the A_1-selective agonist, CPA (not shown) and the β_3-agonist BRL 37,344 (Figure 4b) failed to exert any effect up to concentrations of 10 μM.

Since the endothelial A_{2A}-adenosine receptor and the β_2-adrenoceptor were coupled to both adenylyl cyclase activation and stimulation of [^{3}H]-thymidine incorporation, we investigated whether a rise in intracellular cyclic AMP-levels

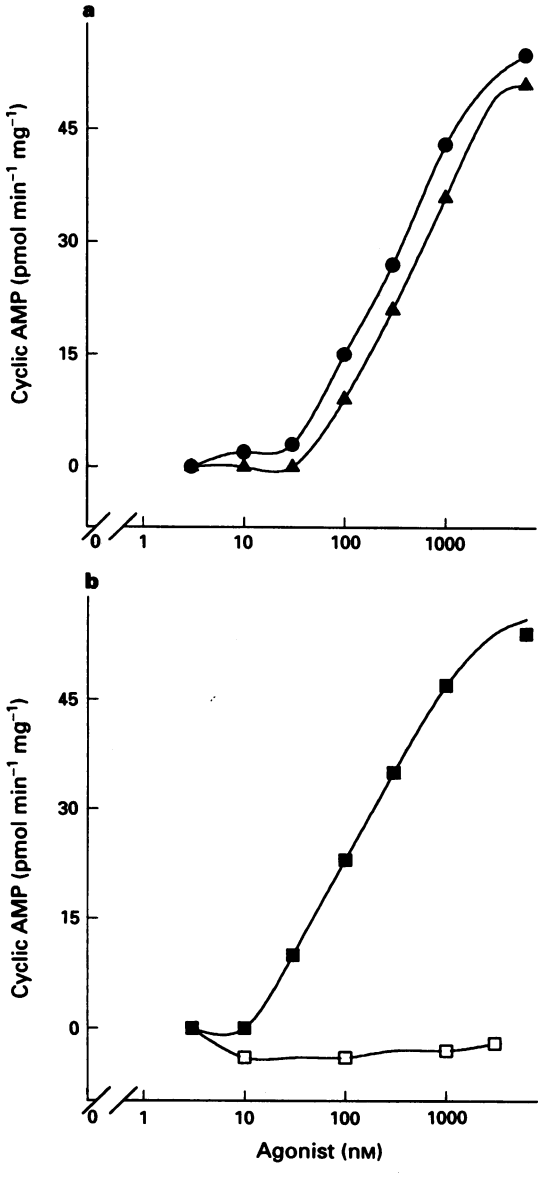

Figure 4 Effect of adenosine and β-adrenoceptor ligands on adenylyl cyclase activity in HUVEC membranes. (a) Membranes (10 μg of protein) prepared from HUVEC were incubated for 20 min in the presence of 10 nM GTPγS + CGS 21680 (●) and GTPγS + NECA (▲). (b) Membranes (10 μg of protein) prepared from HUVEC were incubated for 20 min in the presence of 10 nM GTPγS + isoprenaline (■), and GTPγS + BRL 37344 (□). Basal activity, i.e. activity in the presence of GTPγS alone was 30 ± 3 pmol cyclic AMP min^{-1} mg^{-1} and has been subtracted. Data are from a representative experiment carried out in triplicate; 2 additional experiments gave similar results.

directly mediates cell proliferation; agents known to raise intracellular cyclic AMP levels (i.e. forskolin) or to activate protein kinase A directly (i.e. ^{8}Br-cyclic AMP) were used. Rather surprisingly, both compounds exerted a concentration-dependent inhibition of [^{3}H]-thymidine incorporation (half-maximum inhibition occurring at 0.3 ± 0.1 and 14 ± 5 μM forskolin and ^{8}Br-cyclic AMP, $n = 3$, respectively), the maximum effect being comparable (Figure 5a). These effects were independent of the presence of adenosine deaminase (data not shown).

G proteins can control more than one effector system e.g. G_s is known to stimulate adenylyl cyclase as well as opening of voltage-sensitive calcium channels (Spiegel *et al.*, 1992). We therefore tested whether direct activation of G_s by cholera toxin, which constitutively activates G_s, can mimic the action of adenosine analogues. However, addition of cholera toxin (Figure 5a, hatched columns) decreased [^{3}H]-thymidine incorporation to a similar extent as forskolin and ^{8}Br-cyclic AMP. The concentration of cholera toxin employed (10 ng ml^{-1}) was maximally active; no additional inhibition was obtained, if the concentration of the toxin was raised to 100 ng ml^{-1}. These data obtained with cholera toxin argue against an involvement of G_s.

Due to desensitization, receptor-mediated increases of cyclic AMP are generally characterized by rapid fading in spite of continuous presence of agonists. We therefore designed an additional experiment to test the hypothesis that short-term increases in cyclic AMP are responsible for the A_{2A}-adenosine and β_2-adrenoceptor-induced increase in DNA-synthesis. ^{8}Br-cyclic AMP was added to the incubation medium for varying time periods in the presence and absence of adenosine deaminase (Figure 5b). Short-term incubation (1–5 h) failed to produce a stimulatory effect and to reverse the inhibitory action of adenosine deaminase; this effect would have been expected if the mitogenic effect of adenosine were mediated via a transient rise of cyclic AMP. Furthermore, at longer incubation times (>16 h), ^{8}Br-cyclic AMP causes a progressive inhibition of DNA-synthesis independent of whether adenosine deaminase is present or not in the culture medium. Both observations indicate distinct intracellular pathways for the inhibitory effect of cyclic AMP and the inhibitory effect of adenosine deaminase (and therefore the stimulatory effect exerted by the A_{2A}-adenosine and the β_2-adrenoceptor). The inhibitory effect of ^{8}Br-cyclic AMP after a 48 h incubation period in Figure 5b seems more pronounced than that given in Figure 5a; however, this discrepancy arises from the different assay conditions. Since in the experiments depicted in Figure 5b [^{3}H]-thymidine was present for the last 3 h of the incubation, only those cells that are in S-phase during this short period, incorporate the label. In all other experiments [^{3}H]-thymidine was present for 24 h, i.e. from the time point when cells enter S-phase, and thus an integrative response is obtained.

Under appropriate conditions, the mammalian β_2-adrenoceptor, albeit a prototypical G_s-coupled receptor, can be shown to interact with G_i (Abramson & Molinoff, 1985; Asano *et al.*, 1984; Freissmuth *et al.*, 1991); we therefore tested whether the mitogenic response promoted by activation of the A_{2A}-adenosine receptor was sensitive to pertussis toxin, which disrupts receptor-G protein coupling by ADP-ribosylating a cysteine-residue in the carboxy terminus of the α-subunits of the G_i- and G_0-group. Addition of pertussis toxin *per se* resulted in a concentration-dependent decrease of [^{3}H]-thymidine incorporation and cell number, respectively, with half-maximal effect of about 1 ng ml^{-1} (Figures 6a and 2b). The antiproliferative effect of pertussis toxin correlated with a loss of ADP-ribosylation substrate in membranes subsequently prepared from pertussis toxin-treated cells (Figure 6b). Under electrophoretic conditions, which allow resolution of several pertussis toxin-substrates in a bovine brain G protein preparation, a single labelled band is seen in membrane extracts from HUVEC. We identified this band by immunoblots as $G_{i\alpha\text{-}2}$ based on comigration with the $rG_{i\alpha\text{-}2}$-standard (Figure 6c); neither $G_{i\alpha\text{-}1}$ nor $G_{i\alpha\text{-}3}$, which comigrate under our electrophoretic conditions but can be resolved from $G_{i\alpha\text{-}2}$ (Selzer *et al.*, 1993), were detected in 3 different

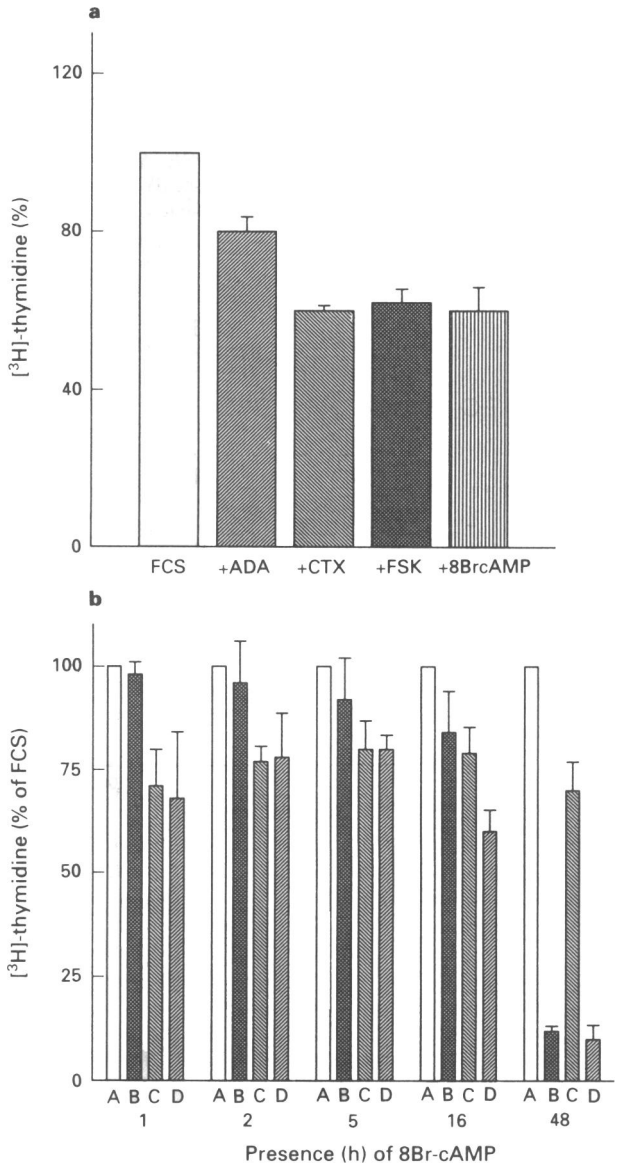

Figure 5 Modulation of foetal calf serum (FCS)-induced [^{3}H]-thymidine incorporation by compounds targeting the cyclic AMP-signalling cascade. (a) [^{3}H]-thymidine incorporation in synchronized HUVEC (~1.1×10^4 cells/well) was stimulated by 5% FCS and the indicated combinations of 5% FCS + compound; [^{3}H]-thymidine incorporation in the presence of FCS alone varied between 2,000 and 10,000 c.p.m. in individual experiments and was set at 100% for the purpose of normalisation. ADA: 2 u ml^{-1} adenosine deaminase; + CTX10: 10 ng ml^{-1} cholera toxin combined with 2 u ml^{-1} ADA; + FSK10: 10 μM forskolin combined with 2 u ml^{-1} ADA; + ^{8}Br-cyclic AMP: 1 mM ^{8}Br-cyclic AMP combined with 2 u ml^{-1} ADA. Data are means ± s.e.mean from 3 to 6 experiments carried out in quadruplicate under the conditions outlined under Methods. All reductions in [^{3}H]-thymidine incorporation are significant ($P < 0.01$) when compared to the paired FCS-control (*t*-test for paired data). (b) [^{3}H]-thymidine incorporation in synchronized HUVEC (~1.1×10^4 cells/well) was stimulated by 5% FCS (A) 5% FCS + 2 u ml^{-1} adenosine deaminase (C); 5% FCS + 1 mM ^{8}Br-cyclic AMP (B) and 5% FCS + 2 u ml^{-1} adenosine deaminase + 1 mM ^{8}Br-cyclic AMP (D) for 1, 2, 5, 16 and 48 h. After this time, medium was replaced by 5% FCS or 5% FCS + 2 u ml^{-1} adenosine deaminase. Using short-pulse conditions as outlined under Methods, [^{3}H]-thymidine was added for only 3 h. Statistical analysis revealed $P < 0.01$ for adenosine deaminase vs 5% FCS at all time points as well as $P < 0.01$ for ^{8}Br-cyclic AMP vs 5% FCS and ^{8}Br-cyclic AMP + ADA vs ADA after 16 and 48 h of incubation.

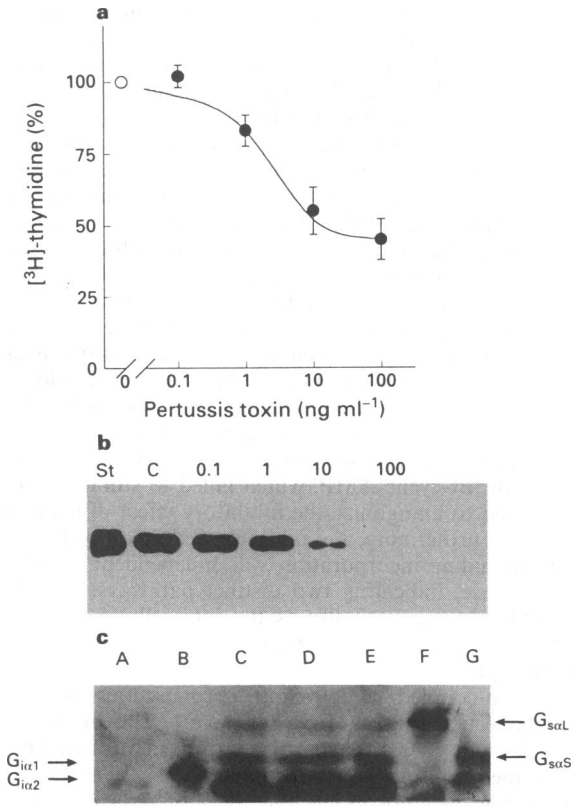

Figure 6 (a) Inhibition of serum-induced [^{3}H]-thymidine incorporation in HUVEC by pertussis toxin. About 10^6 cells were synchronized by serum starvation for 48 h and incubated with 5% FCS in the absence and presence of increasing concentrations of pertussis toxin; [^{3}H]-thymidine incorporation was assayed using 1×10^4 cells/well. Data represent means from four experiments carried out in quadruplicate; [^{3}H]-thymidine incorporation in the presence of 5% FCS was set as 100%. (b) Pertussis toxin-catalyzed ADP-ribosylation: the remainder of the cells were maintained in the absence of [^{3}H]-thymidine and harvested after 24 h. A membrane extract was prepared from these cells and subjected to pertussis-toxin catalyzed ADP-ribosylation by using [^{3}P]-NAD and resolved by SDS polyacrylamide gel electrophoresis. Lane St: purified bovine brain G_i/G_0; lane C: control cells maintained in the absence of pertussis toxin; lanes 0.1, 1, 10, 100, cells pretreated with the respective concentrations of pertussis toxin. (c) Immunoblot analysis of $G_{i\alpha}$ and $G_{s\alpha}$ in HUVEC membranes: membranes (75 μg) of 3 different batches of HUVEC (lanes CDE) were resolved on an SDS polyacrylamide gel and probed with antiserum 84 (specific for the three subtypes of $G_{i\alpha}$) and CS1 (specific for $G_{s\alpha}$); lane A: 10 ng $rG_{i\alpha 2}$, lane B: 100 ng $rG_{i\alpha 1}$, lane F: 50 ng $rG_{s\alpha\text{-}L}$, lane G: 50 ng $rG_{s\alpha\text{-}s}$. Only the 35 to 55 kDa region of the gel is shown.

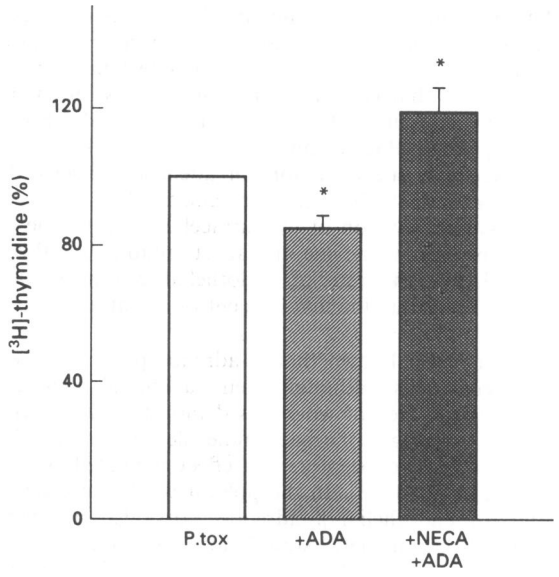

Figure 7 Influence of pretreatment of HUVEC with pertussis toxin on A_2-receptor mediated stimulation of [^{3}H]-thymidine incorporation. Synchronized HUVEC were plated at a density of 1×10^4 cells/well in 5% FCS followed by the addition of 10 ng ml^{-1} pertussis toxin (open column) or the combination of 10 ng ml^{-1} pertussis toxin + 2 u ml^{-1} adenosine deaminase (hatched and cross-hatched columns); after 6 h, 1 μM NECA (cross hatched column) or vehicle (open and hatched columns) was added. Data shown are means ± s.d. from 4 separate experiments, [^{3}H]-thymidine incorporation in the presence of 10 ng ml^{-1} PTX was set as 100%; $*P < 0.01$.

HUVEC preparations. Both the short and the long splice variant of $G_{s\alpha}$, $G_{s\alpha\text{-}s}$, $G_{s\alpha\text{-}L}$, were detected (Figure 6c). These experiments indicate an important role of G_{i2} in mediating serum-stimulated growth of HUVEC. However, pertussis toxin, which itself causes a profound inhibition of cell growth, abolished neither the stimulatory effect of CGS 21680 nor the inhibitory effect of adenosine deaminase (Figure 7).

Discussion

Four types of G protein-coupled adenosine receptors have been identified by molecular cloning, namely A_1, A_{2A} and A_{2B} and A_3-receptor (Maenhaut *et al.*,, 1990; Townsendnicholson & Shine, 1992; Pierce *et al.*, 1992; Zhou *et al.*, 1992), which can also be differentiated by their pharmacological profile. In the present paper, we show that the proliferation of HUVEC is stimulated by adenosine analogues via activation of a receptor that meets the criteria of the A_{2A}-subtype, namely high-affinity for NECA and CGS 21680, low affinity for N^6-substituted analogues such as CPA and potent antagonism by the methylxanthine XAC (Galen *et al.*, 1992). Mediation via an A_1-adenosine receptor, which displays stereoselectivity for the R-isomer of PIA and high affinity for CPA, is unequivocally ruled out (Galen *et al.*, 1992). Antagonism of the mitogenic activity by the methylxanthine XAC excludes an A_3-adenosine receptor. This subtype has recently been described and its prominent pharmacological feature is the lacking sensitivity to the antagonistic effect of methylxanthines; in addition, the affinity of CGS 21680 for the A_3-adenosine receptor is one order of magnitude lower than that of NECA (Zhou *et al.*, 1992). Similarly, CGS 21680 interacts only weakly with the A_{2B}-adenosine receptor (Pierce *et al.*, 1992).

Previous work has established that adenosine stimulates proliferation of endothelial cells, but did not provide information on the receptor-subtype involved. Our findings are in contrast to the conclusion reached by Van Daele *et al.* (1992), who reports that only the adenosine precursor ATP, ATP-analogues (P_2-receptor agonists) and adenosine itself initiate DNA-synthesis in bovine endothelial cells, whereas typical adenosine receptor agonists and antagonists were without effect. We do not believe that this discrepancy arises from the different origin of the endothelial cells, both with respect to species and to the vascular bed; instead, the differing results are most probably attributable to the variation in assay conditions, in particular the absence of foetal calf serum and therefore of serum-derived growth factors in the study of Van Daele *et al.*; in serum-free medium A_{2A}-adenosine as well as β_2-adrenoceptor agonists failed to stimulate [^{3}H]-thymidine incorporation, whereas the phorbol ester phorbol 12- myristate 13-acetate (TPA, an activator of the protein kinase C pathway) was still capable of inducing a profound increase in DNA synthesis (data not shown). This interpretation is also consistent with the concept that growth

stimulation via most G protein-coupled receptors requires the concomitant presence of an additional stimulus, typically activation of growth factor-sensitive tyrosine kinase-receptor linked pathways that generate obligatory signals for the progression through the cell cycle and entry into S-phase (Rozengurt, 1986; Pouyssegur & Seuwen, 1992). The tentative intracellular site of action for adenosine described by Van Daele *et al.* (1992) remains enigmatic, but our experiments, in which elevation of the intracellular adenosine concentration by the adenosine transport inhibitor, NBMPR, failed to change the rate of endothelial cell proliferation strongly argue against the involvement of an intracellular site of action.

It has long been known that β_2-adrenoceptors are present on endothelial cells, although their functional significance remained elusive. Recent work has demonstrated that transendothelial exchange of macromolecules is inhibited by activation of β_2-adrenoceptors, an effect mediated by cyclic AMP (Zink *et al.*, 1993). In the present work, we show that activation of endothelial β_2-adrenoceptors also produces a long-term effect, namely stimulation of endothelial cell growth, and that this effect is independent of increases in intracellular cyclic AMP (see below). Given the fact that endothelial cells can be exposed to high levels of catecholamines *in vivo*, one is led to suspect that circulating adrenaline and/or locally released noradrenaline act in concert with other angiogenetic factors to promote endothelial cell growth.

The effector system that is believed to mediate most if not all biological effects of the A_2-adenosine receptor (and of the β_2-adrenoceptor) is adenylyl cyclase (Galen *et al.*, 1992; Stiles, 1992; Collis & Hourani, 1993). Stimulation of adenylyl cyclase consistent with the pharmacological profile of an A_{2A}-receptor was also observed with the non-selective agonist NECA and the A_{2A}-selective agonist CGS 21680 in HUVEC membranes, but their potencies are clearly lower when compared to their potencies to enhance DNA- synthesis; a similar observation was also made for isoprenaline (EC_{50} 3 nM for proliferation, 90 nM for stimulation of adenylyl cyclase). This discrepancy between EC_{50}-values obtained in broken cell preparation and intact cells has been ascribed to the fragmentation of the membrane which results in limited receptor mobility, thereby reducing the signal amplification built into the catalytic nature of the receptor-G protein interaction (Stickle & Barber, 1989). Hence, we do not interpret the observed difference in potency for adenosine analogues and isoprenaline as an indication that different receptor subtypes mediate stimulation of endothelial adenylyl cyclase activity and of cell proliferation. However, this possibility cannot be ruled out.

Irrespective of whether the same A_{2A}-receptor or two different receptors with a related pharmacological profile are linked to an increase in intracellular cyclic AMP levels and to endothelial cell proliferation, this effector system is not responsible for the mitogenic effect of A_{2A}-adenosine and β-adrenoceptor agonists. All compounds that activate the cyclic AMP-cascade downstream of the receptor, i.e. at the level of G_s, adenylyl cyclase or protein kinase A, decreased DNA-synthesis. The role of cyclic AMP in promoting cell growth is cell type-dependent: in several specialized cells, such as brown fat, Schwann cells as well as endocrine cells elevated cyclic AMP levels exert a stimulatory effect (Dumont *et al.*, 1989; Morgan *et al.*, 1991; Bronnikov *et al.*, 1992). In others such as lymphocytes and smooth muscle cells, a sustained increase in cyclic AMP is associated with inhibition of proliferation (Souness *et al.*, 1992; Skalhegg *et al.*, 1992). Our observations in HUVEC are consistent with those obtained in endothelial cells derived from several species as well as from different vascular beds (Leitman *et al.*, 1986; Moodie *et al.*, 1991), where cyclic AMP-analogues, phosphodiesterase-inhibitors and forskolin reduced proliferation. All these manipulations are predicted to result in long-lasting increases in intracellular cyclic AMP. Based on brief incubations of bovine endothelial cells with cholera toxin, which caused a stimulation of cell growth, Meininger *et al.* (1990) proposed that the mitogenic effect of adenosine agonists is due to a *transient* rise of intracellular cyclic AMP. However, this argument appears weak, since (*i*) cholera toxin acts enzymatically once its A-subunit has penetrated the cell and should thus produce a long lasting rise in cyclic AMP; (*ii*) the B-subunit of cholera toxin *per se* can act as a mitogen (Spiegel, 1989). We have therefore analysed the effect of varying incubation periods with ^{8}Br-cyclic AMP, which failed to stimulate DNA synthesis and to antagonize the inhibitory effect of adenosine deaminase. Furthermore, the inhibitory effect of cyclic AMP on [^{3}H]-thymidine incorporation was independent of adenosine deaminase, indicating two distinct pathways. Therefore cyclic AMP does not qualify as the intracellular signal responsible for the mitogenic action of the A_{2A}-adenosine and β_2-adrenoceptor.

G protein-coupled receptors are promiscuous in that a defined molecular species of receptor can be shown to couple to several types of G proteins that do not necessarily belong to the same functional class (Milligan, 1993). The fact that cholera toxin does not mimic the effect of A_{2A}-adenosine or β_2-adrenoceptor activation implies a G_s-independent pathway. The involvement of pertussis toxin-sensitive G proteins, in particular the subtypes of G_i, in stimulating cell growth is well documented (Spiegel *et al.*, 1992; Seuwen & Pouyssegur, 1992). Our data suggest an important role of a G_{i2}-linked pathway for serum-induced growth of HUVEC and recent work on an endothelial-derived cell line (EA hy926) show that G_i also participates in later steps of angiogenesis (Bauer *et al.*, 1992). However, inactivation of G_{i2} by pertussis toxin does not abolish the effect of A_{2A}-adenosine receptor activation on DNA-synthesis.

Recently, a series of experiments had established that the β_2-adrenoceptor as well as other G_s protein coupled receptors stimulate the Na-H antiporter (Ganz *et al.*, 1990; Barber & Ganz, 1992). This stimulation occurs independent from G_s, but is mediated by a member of the pertussis and cholera toxin-insensitive G_{12} protein subgroup, i.e. G_{13} (Voyno-Yasenestkaya *et al.*, 1994). In addition constitutive activation of G_{12} promotes cellular growth and confers a transformed phenotype (Xu *et al.*, 1993). It is attractive to speculate that the interaction between a member of this G protein subgroup and the A_{2A} adenosine and the β_2-adrenoceptor is responsible for the proliferative response in HUVECs.

We are grateful to Dr L. Wagner for continuous support and advice, to Drs P. Gierschik and G. Milligan, and A.D. Strosberg for gifts of antiserum 84, antiserum CS1, and BRL 37344, respectively, and to Dr Diane Barber for communicating unpublished results. We thank the midwives and nurses and the new-born babies of the department of gynaecology and obstetrics, Wilhelminenspital der Stadt Wien, for providing us with umbilical cords. This work was supported by grants from the Austrian Science Foundation (FWF, P10672) and the Science Foundation of the Austrian National Bank (5095).

References

ABRAMSON, S.N. & MOLINOFF, P.B. (1985). Properties of β-adrenergic receptors of cultured mammalian cells. Interaction of receptors with a guanine nucleotide-binding protein in membranes prepared from L6 myoblasts and from wild type and cyc S49 lymphoma cells. *J. Biol. Chem.*, **260**, 14580–14588.

ASANO, T., KATADA, T., GILMAN, A.G. & ROSS, E.M. (1984). Activation of the inhibitory GTP-binding protein of adenylate cyclase, G_i, by the β-adrenergic receptors in reconstituted phospholipid vessels. *J. Biol. Chem.*, **259**, 9351–9354.

BARBER, D.L. & GANZ, M.B. (1992). Guanine nucleotides regulate β-adrenergic activation of NaH exchange independently of receptor coupling to G_s. *J. Biol. Chem.*, **267**, 20607–20612.

BAUER, J., MARGOLIS, M., SCHREINER, C., EDGELL, C.J., AZIZKHAN, J., LAZAROWSKI, E. & JULIANO, R.L. (1992). In vitro model for angiogenesis using a human endothelium-derived permanent cell line: contributions of induced gene expression, G proteins, and integrins. *J. Cell. Physiol.*, **153**, 437–449.

BOBIK, A. & CAMBELL, J.H. (1993). Vascular derived growth factors: cell biology, pathophysiology, and pharmacology. *Pharmacol. Rev.*, **45**, 1–42.

BERNE, R.M. (1963). Cardiac nucleotides in hypoxia: possible role in regulation of coronary blood flow. *Am. J. Physiol.*, **204**, 317–322.

BOKOCH, G.M., KATADA, T., NORTHUP, J.K., HEWLETT, E.L. & GILMAN, A.G. (1983). Identification of the pre-dominant substrate for ADP-ribosylation by islet activating protein. *J. Biol. Chem.*, **258**, 2072–2075.

BRONNIKOV, G., HOUSTEK, J. & NEDERGAARD, J. (1992). β-adrenergic, cAMP-mediated stimulation of proliferation of brown fat cells in primary culture. Mediation via β_1- but not via β_3-adrenoceptors. *J. Biol. Chem.*, **267**, 2006–2013.

COLLIS, M.G. & HOURANI, S.M.O. (1993). Adenosine receptor subtypes. *Trends Pharmacol. Sci.*, **14**, 360–366.

DES ROSIERS, C. & NEES, S. (1987). Functional evidence for the presence of adenosine A_2-receptors in cultured coronary endothelial cells. *Naunyn-Schmied. Arch. Pharmacol.*, **336**, 94–98.

DUMONT, J.E., JAUNIAUX, J.C. & ROGER, P.P. (1989). The cyclic AMP-mediated stimulation of cell proliferation. *Trends Biochem. Sci.*, **14**, 67–71.

DUSSEAU, J.W., HUTCHINS, PM. & MALBASA, D.S. (1986). Stimulation of angiogenesis by adenosine on the chick chorioallantoric membrane. *Circ. Res.*, **59**, 163–170.

EMORINE, L.J., MARULLO, S., BRIEND-SUTREN, M.M., PATEY, G., TATE, K., DELAVIER-KLUTCHKO, C. & STROSBERG, A.D. (1989). Molecular cloning of the human β_3-adrenergic receptor. *Science*, **245**, 1118–1121.

ETHIER, M.F., CHANDER, V. & DOBSON, J.G. (1993). Adenosine stimulates proliferation of human endothelial cells in culture. *Am. J. Physiol.*, **265**, H131–138.

FOLKMAN, J. & SHING, Y. (1992). Angiogenesis. *J. Biol. Chem.*, **267**, 10931–10934.

FREISSMUTH, M. & GILMAN, A.G. (1989). Mutations of $G_{s\alpha}$ designed to alter the reactivity of the protein with bacterial toxins: substitutions at arg^{187} result in loss of GTPase activity. *J. Biol. Chem.*, **264**, 21907–21914.

FREISSMUTH, M., HAUSLEITHNER, V., NEES, S., BÖCK, M. & SCHÜTZ, W. (1986). Cardiac β_2-adrenergic receptors in guinea pigs and rats are localized on the coronary endothelium: *Naunyn Schmieds. Arch. Pharmacol.*, **334**, 56–62.

FREISSMUTH, M., SELZER, E., MARULLO, S., SCHÜTZ, W. & STROSBERG, D. (1991). Expression of two human β-adrenergic receptors in Escherichia coli: Functional interaction with two forms of the stimulatory G protein. *Proc. Natl. Acad. Sci. U.S.A.*, **88**, 8548–8552.

GALEN, P.J.M., STILES, G.L., MICHAELS, G. & JACOBSON, K.A. (1992). Adenosine A_1- and A_2-receptors: structure-function relationships. *Med. Res. Rev.*, **12**, 423–471.

GANZ, M.B., PACHTER, J.A. & BARBER, D.L. (1990). Multiple receptors are coupled to adenylate cyclase regulate Na-H exchange independent of cAMP. *J. Biol. Chem.*, **265**, 8989–8992.

HUTCHINSON, K. & FOX, I.H. (1989). Purification and characterization of the adenosine A_2-like binding site from human placental membranes. *J. Biol. Chem.*, **264**, 19898–19903.

JAFFE, E.A., NACHMANN, R.L., BECKER, C.G. & MINICH, C.R. (1973). Culture of human endothelial cells derived from umbilical cord. *J. Clin. Invest.*, **52**, 2757–2764.

LEITMAN, D.C., FISCUS, R.R. & MURAD, R. (1986). Forskolin, Phosphodiesterase inhibitors, and cyclic AMP analogs inhibit proliferation of cultured bovine aortic endothelial cells. *J. Cell Physiol.*, **127**, 237–243.

LINDER, M.E., EWALD, D.A., MILLER, R.J. & GILMAN, A.G. (1990). Purification of $G_{0\alpha}$ and of three types of $G_{i\alpha}$ after expression in *Escherichia coli*. *J. Biol. Chem.*, **265**, 8243–8251.

MAENHAUT, C., VAN SANDE, J., LIBERT, F., ABRAMOWICZ, M., PARMENTIER, M., VANDERHAEGEN, J.J., DUMONT, J.E., VASSART, G. & SCHIFFMANN, S. (1990). RDC8 codes for an A_2-receptor with physiological constitutive activity. *Biochem. Biophys. Res. Commun.*, **173**, 1169–1178.

MEININGER, C.J. & GRANGER, H.J. (1990). Mechanism leading to adenosine-stimulated proliferation of microvascular endothelial cells. *Am. J. Physiol.*, **258**, H198–206.

MILLIGAN, G. (1993). Mechanisms of multifunctional signalling by G protein-linked receptors. *Trends Pharmacol. Sci.*, **14**, 239–244.

MOODIE, S.A. & MARTIN, W. (1991). Effects of cyclic nucleotides and phorbol myristate acetate on proliferation of pig aortic endothelial cells. *Br. J. Pharmacol.*, **102**, 101–106.

MORGAN, L., JESSEN, K.R. & MIRSKY, R. (1991). The effects of cAMP on cultured Schwann cells: progression from an early phenotype (04+) to a myelin phenotype (P_0+, GFAP-, N-CAM-, NGF- receptor-) depends on growth inhibition. *J. Cell. Biol.*, **112**, 457–467.

NEES, S., HERZOG, V., BECKER, F., BÖCK, M., DES ROSIERS, C. & GERLACH, E. (1985). The coronary endothelium is a highly active, metabolic barrier for adenosine. *Basic Res. Cardiol.*, **80**, 515–529.

OLAH, M.E., STILES, G.L. (1992). Adenosine receptors. *Annu. Rev. Physiol.*, **54**, 211–225.

PIERCE, K.D., FURLONG, T.J., SELBIE, L.A. & SHINE, J. (1992). Molecular cloning of an adenosine A2b-receptor from human brain. *Biochem. Biophys. Res. Commun.*, **187**, 86–93.

POUYSSEGUR, J. & SEUWEN, K. (1992). Transmembrane receptors and intracellular pathways that control cell proliferation. *Annu. Rev. Physiol.*, **54**, 195–210.

ROZENGURT, E. (1986). Early signals in the mitogenic response. *Science*, **234**, 161–166.

SALOMON, Y., LONDOS, C. & RODBELL, M. (1974). A highly sensitive adenylate cyclase assay. *Anal. Biochem.*, **58**, 41–548.

SCHÜTZ, W., STEURER, G. & TUISL, E. (1982). Functional identification of adenylate-cyclase coupled adenosine receptors in rat brain microvessels. *Eur. J. Pharmacol.*, **85**, 177–184.

SELZER, E., WILFING, A., SCHIFERER, A., HERMANN, M., GRUBECK-LOEBENSTEIN, B. & FREISSMUTH, M. (1993). Stimulation of human thyroid growth via the inhibitory guanine nucleotide binding G protein G_i: Constitutive expression of the G-protein subunit $G_{ia\text{-}1}$ in autonomous adenoma. *Proc. Natl. Acad. Sci. U.S.A.*, **90**, 1609–1613.

SEUWEN, K. & POUYESSEGUR, J. (1992). G Protein- controlled signal transduction pathways and the regulation of cell proliferation. *Adv. Cancer Res.*, **58**, 75–81.

SKALHEGG, B.S., LANDMARK, B.F., DOSKELAND, S.O., HANSSON, V., LEA, T. & JAHNESEN, T. (1992). Cyclic AMP-dependent protein kinase type I mediates the inhibitory effects of 3′,5′-cyclic AMP on cell replication in human T lymphocytes. *J. Biol. Chem.*, **267**, 15707–15714.

SOUNESS, J.E., HASSALL, G.A. & PARROTT, D.P. (1992). Inhibition of pig aortic smooth muscle cell DNA synthesis by selective type III and type IV cyclic AMP phospodiesterase inhibitors. *Biochem. Pharmacol.*, **44**, 857–866.

SPIEGEL, A.M., SHENKER, A. & WEINSTEIN, L.S. (1992). Receptor-effector coupling by G proteins: implications for normal and abnormal signal transduction. *Endocrine Rev.*, **13**, 536–565.

SPIEGEL, S. (1989). Possible involvement of a GTP-binding protein in a late event during endogenous ganglioside-modulated cellular proliferation. *J. Biol. Chem.*, **264**, 6766–6772.

STEINBERG, S.F., JAFFE, E.A. & BILEZIKIAN, J.P. (1984). Endothelial cells contain β-adrenoceptors. *Naunyn Schmied. Arch. Pharmacol.*, **325**, 310–313.

STERNWEIS, P.C. & ROBISHAW, J.D. (1984). Isolations of two proteins with high affinity for guanine nucelotides from membranes of bovine brain. *J. Biol. Chem.*, **256**, 11517–11526.

STICKLE, D. & BARBER, R. (1989). Evidence for the role of epinephrine binding frequency in activation of adenylate cyclase. *Mol. Pharmacol.*, **36**, 437–445.

STILES, G.L. (1992). Adenosine receptors. *J. Biol. Chem.*, **267**, 6451–6454.

TOWNSENDNICHOLSON, A. & SHINE, J. (1992). Molecular cloning and characterisation of a human brain A_1-adenosine receptor cDNA. *Mol. Brain Res.*, **16**, 365–370.

VAN DAELE, P., VAN COEVORDEN, P.P.R. & BOEYNAEMS, J.M. (1992). Effects of adenine nucleotides on the proliferation of aortic endothelial cells. *Circ. Res.*, **70**, 82–90.

VOYNO-YASENETSKAYA, T., CONKLIN, B., GILBERT, R., HOOLEY, R., BOURNE, H. & BARBER, D. (1994). G_{13} stimulates Na/H Exchange. *J. Biol. Chem.*, **269**, 4721–4724.

XU, N., BRADLEY, L., AMBDUKAR, I. & GUTKIND, S. (1993). A mutant subunit of G_{12} potentiates the eicosanoid pathway and is highly oncogenic in NIH 3T3 cells. *Proc. Natl. Acad. Sci. U.S.A.*, **90**, 6741–6745.

ZHOU, Q.Y., LI, C., OLAH, M.E., JOHNSON, R.A., STILES, G.A. & CIVELLI, O. (1992). Molecular cloning and characterization of an adenosine receptor: the A_3-adenosine receptor. *Proc. Natl. Acad. Sci. U.S.A.*, **89**, 7432–7436.

ZIADA, A.M.A.R., HUDLICKA, O., TYLER, K.R. & WRIGHT, A.J.A. (1984). The effect of long-term vasodilation on capillary growth and performance in rabbit heart and skeletal muscle. *Cardiovasc. Res.*, **18**, 724–732.

ZINK, S., RÖSEN, P., SACKMANN, B. & LEMOINE, H. (1993). Regulation of endothelial permeability by β-adrenoceptor agonists: contribution of β_1- and β_2-adrenoceptors. *Biochim. Biophys. Acta*, **1178**, 286–298.

(Received May 23, 1994
Revised October 18, 1994
Accepted January 6, 1995)

British Journal of Pharmacology (1995) 114, 1587–1594 © 1995 Stockton Press All rights reserved 0007–1188/95 $12.00

Vasorelaxant effect of isoliquiritigenin, a novel soluble guanylate cyclase activator, in rat aorta

[1]Sheu-Meei Yu & *Sheng-Chu Kuo

Department of Pharmacology, Chang Gung Medical College, Kwei-San, Tao-Yuan and *Institute of Pharmaceutical Chemistry, China Medical College, Taichung, Taiwan

1 The vasorelaxant activity of isoliquiritigenin, isolated from *Dalbergia odorifera T.*, was investigated in the phenylephrine-precontracted rat aorta by measuring tension, guanylate and adenylate cyclase activities, guanosine 3':5'-cyclic monophosphate (cyclic GMP) and adenosine 3':5'-cyclic monophosphate (cyclic AMP) levels.

2 Isoliquiritigenin concentration-dependently relaxed rat aorta contracted with phenylephrine, KCl, U-46619, endothelin and 5-hydroxytryptamine, with EC_{50}s of 7.4 ± 1.6, 10.5 ± 2.3, 14.3 ± 3.3, 11.8 ± 2.0 and 13.6 ± 3.7 μM, respectively.

3 Isoliquiritigenin caused endothelium-independent relaxation of phenylephrine-precontracted rat aortic rings. Neither N^G-monomethyl-L-arginine (L-NMMA) (an inhibitor of the L-arginine-NO pathway) nor oxyhaemoglobin (which binds NO) modified the relaxant effect of isoliquiritigenin. The relaxant action of isoliquiritigenin also persisted in intact aorta in the presence of indomethacin or glibenclamide. However, methylene blue, an inhibitor of soluble guanylate cyclase, abolished relaxation induced by isoliquiritigenin.

4 Incubation of rat aorta with isoliquiritigenin not only increased aortic cyclic GMP content but also caused small increases in aortic cyclic AMP content, and greatly potentiated the increases in cyclic AMP observed in the presence of forskolin. The maximum increase in cyclic GMP by isoliquiritigenin was reached earlier than the increase in cyclic AMP. This result suggests that the increases in cyclic GMP caused by isoliquiritigenin might stimulate the accumulation of cyclic AMP.

5 Concentration-dependent increases in soluble guanylate cyclase activity were observed in isoliquiritigenin (1–100 μM)- or sodium nitroprusside (SNP)-treated rat aortic smooth muscle cells, while adenylate cyclase activity was unchanged in isoliquiritigenin (100 μM)-treated cells.

6 Relaxation and cyclic AMP formation of rat aorta caused by isoliquiritigenin was potentiated in the presence of forskolin (10 nM), which had little effect when given alone. 2',5'-Dideoxyadenosine (DDA, 200 μM), an adenylate cyclase inhibitor, diminished the relaxation and cyclic AMP formation of rat aorta by isoliquiritigenin only in the presence of forskolin. DDA did not affect the increases in cyclic GMP formation induced by isoliquiritigenin. These results suggest that elevated levels of cyclic GMP may mediate the majority of the relaxation of the phenylephrine-precontracted aorta induced by isoliquiritigenin, while the synergistic interaction with a low concentration of forskolin depends on an enhanced accumulation of cyclic AMP.

7 Relaxation of phenylephrine-precontracted rat aorta and carbachol-precontracted guinea-pig trachea by rolipram (phosphodiesterase, PDE IV inhibitor) was markedly enhanced by isoliquiritigenin, while response to cilostamide (PDE III inhibitor) was not significantly changed by isoliquiritigenin.

8 It is concluded that isoliquiritigenin exerts a vasorelaxant effect by activating soluble guanylate cyclase and increasing cyclic GMP. Synergistic effects of isoliquiritigenin and forskolin on muscle relaxation and cyclic AMP accumulation indicate that inhibition of cyclic AMP breakdown by cyclic GMP via the inhibition of PDE III (cyclic GMP-inhibited PDE) is the dominant mechanism.

Keywords: Isoliquiritigenin; vasorelaxant; guanylate cyclase; cyclic GMP; cyclic AMP

Introduction

Relaxation of vascular smooth muscle, elicited by a number of agents, is well correlated with increases in intracellular guanosine 3':5'-cyclic monophosphate (cyclic GMP) concentration (Kukovetz *et al.*, 1981; Ignarro & Kadowitz, 1985). Cyclic GMP has been assumed to mediate vascular relaxation by stimulating the phosphorylation of critical protein substrates by cyclic GMP-dependent protein kinase (Waldman & Murad, 1987). In most tissues, the concentration and the action of cyclic GMP are regulated by guanylate cyclase and cyclic nucleotide phosphodiesterases (PDEs) (Schulz *et al.*, 1991). Guanylate cyclase, which catalyzes the formation of cyclic GMP from guanosine triphosphate (GTP), exists in both the soluble and particulate fractions of cells. The enzyme form found in the soluble fraction is a heterodimer that can be activated by free radicals and nitrovasodilators (Schulz *et al.*, 1989). Multiple PDE isoforms have been isolated from several tissues and they have been characterized by their substrate specificity, their modulation by Ca^{2+}/calmodulin or by cyclic GMP, their pharmacological responses to drugs and their primary sequence (Beavo & Reifsnyder, 1990).

Medicinal plants have been used as traditional remedies in oriental countries for hundreds of years. Especially in Chinese herbal medicines, many drugs have been claimed to improve the peripheral circulation. In recent decades, many active components have been isolated and proved to possess vasorelaxant effects (Ko *et al.*, 1993; Yu *et al.*, 1992; 1994). During random screening tests, we found that isoliquiritigenin (Figure 1), isolated from *Dalbergia odorifera T.*, inhibited vasoconstrictor-induced contraction of the rat thoracic aorta. Isoliquiritigenin is a chalcone derivative, com-

[1] Author for correspondence.

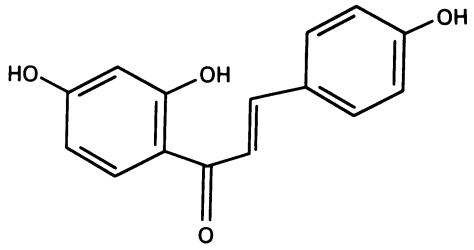

Figure 1 Chemical structure of isoliquiritigenin.

mercially available, which exerts anti-tumour promoting and anti-platelet activity (Yamamoto *et al.*, 1991). In the present study, the vasorelaxant activity of isoliquiritigenin was studied in the precontracted rat aorta.

Methods

Rat aortic contraction

Wistar rats of either sex (250–300 g) were killed by a blow to the head. The thoracic aorta was isolated and excess fat and connective tissue were removed. Vessels were cut into rings of about 5 mm in length and mounted in organ baths containing 5 ml Krebs solution of the following composition (mM): NaCl 118.4, KCl 4.7, $CaCl_2$ 1.9, $MgSO_4$ 1.2, KH_2PO_4 1.2, $NaHCO_3$ 25.0 and glucose 11.7. The tissue bath solution was maintained at 37°C and gassed with 95% O_2: 5% CO_2 mixture. Two stainless steel hooks were inserted into the aortic lumen, one was fixed while the other was connected to a transducer. Aortic segments were equilibrated in the medium for 90 min with three changes of Krebs solution and maintained under an optimal tension of 1 g before specific experimental protocols were initiated. Contractions were recorded isometrically via a force-displacement transducer connected to a Grass polygraph. The endothelium was removed from some aortic rings by gently rubbing the intimal surface with a wooden stick. Removal of functional endothelium was verified by the lack of any relaxation to acetylcholine (3 μM) in rings precontracted with phenylephrine (3 μM). Aortic rings with functional endothelium exhibited at least 75% relaxation under the same conditions. Aortic rings were precontracted with phenylephrine or other vasoconstrictors; when the contractile response reached a steady state (about 10 min after the addition of vasoconstrictor), isoliquiritigenin or other drugs were added cumulatively at 5 min intervals. Relaxation produced by each concentration of isoliquiritigenin was measured after 5 min incubation and the value was expressed as a percentage of the initial phenylephrine-induced tone. In interaction studies, aortic rings were preincubated with isoliquiritigenin or forskolin for 20 min prior to contraction of the aorta with phenylephrine and subsequent assessment of the relaxant activity of isoliquiritigenin or PDE inhibitors. Relaxant potency was expressed as EC_{50}, where EC_{50} is the concentration producing 50% relaxation of the contraction.

Cyclic AMP and cyclic GMP assay of rat aorta

The content of cyclic AMP or cyclic GMP was assayed on aortic rings as previously described (Itoh *et al.*, 1982; Kauffman *et al.*, 1987). After incubation of aortic rings with dimethylsulphoxide (DMSO, 0.1%), forskolin, sodium nitroprusside, cilostamide or isoliquiritigenin for 1 min (for cyclic GMP) or 2 min (for cyclic AMP), the aortic rings were rapidly frozen in liquid nitrogen and stored at −80°C until homogenized in 0.5 ml 10% trichloroacetic acid and 4 mM EDTA with a Potter glass/glass homogenizer. The homogenate was centrifuged at 10,000 *g* for 5 min and the supernatant was removed and extracted with 4 × 3 vol of ether, and the cyclic AMP or cyclic GMP content was then assayed with ELISA kits. The precipitate was used for protein assay (Lowry *et al.*, 1951). Cyclic AMP and cyclic GMP levels were expressed as pmol mg^{-1} protein.

Soluble guanylate cyclase and adenylate cyclase assay of rat aortic smooth muscle cells

For the soluble guanylate cyclase and adenylate cyclase assay, rat aortic smooth muscle cells (SMCs) were prepared by enzymatic dissociation techniques (Brock *et al.*, 1985; Yu *et al.*, 1990). In brief, aortae were removed aseptically from five Wistar rats, cleaned of adherent connective tissue and endothelium, and cut into small rings. These were incubated in 12 ml of Dulbecco's modified Eagle medium (DMEM) containing 0.2 mM $CaCl_2$, 1 mg ml^{-1} of collagenase (type I) and 0.125 mg ml^{-1} of elastase (type I) for 120 min at 37°C, and single cells were inoculated at equal density (2×10^5 cells ml^{-1}) on 35 mm^2 dishes containing DMEM supplemented with 10% foetal calf serum (FCS), 100 units ml^{-1} of penicillin G and 100 μg ml^{-1} streptomycin sulphate at 37°C in a humidified, 5% CO_2 in air atmosphere. At confluence, monolayer cells were washed with phosphate-buffered saline (PBS), treated with 0.1% trypsin/4 mM EDTA, and centrifuged at 600 *g* for 5 min. Cells were then resuspended in ice-cold 50 mM Tris-HCl buffer (pH 7.4) and sonicated at 4°C for 10 s bursts (Sonicator W-220F). Homogenates were used for adenylate cyclase determinations/or homogenates were centrifuged at 40,000 *g* for 10 min and the resulting supernatant fraction was used for soluble guanylate cyclase determinations. Guanylate cyclase activity was determined as previously described (White & Zenser, 1971; Gerzer *et al.*, 1983). Adenylate cyclase activity was determined as described by Insel *et al.* (1982). The incubation mixture for guanylate cyclase assay (100 μl total volume) contained 0.2 mM GTP, 1×10^6 c.p.m. of [α-^{32}P]-GTP, 5 mM $MgCl_2$, 2.5 mM cyclic GMP, 10 mM dithiothreitol, 15 mM creatine phosphate, 0.2 mg ml^{-1} of creatine phosphokinase, with or without isoliquiritigenin in a 50 mM Tris-HCl buffer, pH 7.4, The incubation mixture for adenylate cyclase assay (100 μl total volume) contained 0.5 mM ATP, 1×10^6 c.p.m. of [α-^{32}P]-ATP, 13 mM $MgCl_2$, 1.0 mM cyclic AMP, 10 mM dithiothreitol, 25 mM creatine phosphate, 1.0 mg ml^{-1} of creatine phosphokinase, with or without isoliquiritigenin in a 50 mM Tris-HCl buffer. Incubations were carried out at 37°C for 10 min with 50 μl (1 mg ml^{-1}) of enzyme preparation. Incubation was terminated by addition of 200 μl 0.5 N HCl and 200 μl 1 mM imidazole. The tubes were then heated to 100°C for 3 min in an electric heating block and cooled in an ice bath. To each tube was added 1 ml of 50 mM Tris-HCl buffer, pH 7.4. The contents were stirred and centrifuged at 1000 *g* for 10 min. The supernatant was applied to a neutral alumina column to isolate cyclic GMP (or cyclic AMP) for radioassay of ^{32}P and ^{3}H. Recovery of cyclic GMP (or cyclic AMP) was estimated by inclusion of [^{3}H]-GMP (or [^{3}H]-AMP) in the reaction mixture. Protein was determined by use of Bradford reagent (Bio-Rad, Germany) (Bradford, 1976), with BSA as standard.

Guinea-pig tracheal contraction

Tracheae from guinea-pigs were dissected out, transferred to a dish containing Krebs solution and cut transversely between the segments of cartilage. Several of these, usually about 5, were tied together to form a chain, which was then mounted in Krebs solution at 37°C, gassed with 95% O_2 plus 5% CO_2. One end of the chain was attached to a fixed pin in the bath and the other to a force-displacement transducer connected to a Grass polygraph. Resting tension on each tissue was set at 1 g. Tracheae were allowed to equilibrate for at least 1 h and washed periodically. Following a 60 min equilibration period, tissues were primed for contractile

activity by addition of 1 μM carbachol. This procedure was repeated 3 times after washing. Sustained contractions were elicited by addition of 1 μM carbachol. When the increase in tension had stabilized, the relaxant activity of isoliquiritigenin, rolipram (PDE IV inhibitor) or cilostamide (PDE III inhibitor) was investigated by their cumulative addition to the organ bath.

Data analysis

The experimental results are expressed as the mean ± s.e. mean and accompanied by the number of observations. A one-way analysis of variance (ANOVA) was performed for multiple comparison, and if there was a difference, then the mean values for an inhibitor were compared with those for control by Student's *t* test and *P* values of less than 0.05 were considered to be statistically significant.

Drugs

Isoliquiritigenin (Figure 1), was isolated from the plant *Dalbergia odorifera T.* (unpublished data), and its purity (>99%) were confirmed by n.m.r., mass, IR and proton spectrophotometer. The following drugs were used: phenylephrine HCl, acetylcholine HCl, collagenase (type I), elastase (type I), sodium nitroprusside, forskolin, glibenclamide, indomethacin, oxyhaemoglobin, endothelin-1, 5-hydroxytryptamine and methylene blue were obtained from Sigma Chemical Co.; rolipram and cilostamide and U-46619 (9,11-dideoxymethanoepoxy-9α-11α-$PGF_{2\alpha}$) were from Biomol Research Lab.; cyclic AMP and cyclic GMP ELISA kits were purchased from Amersham. Dulbecco's modified Eagle medium (DMEM), foetal calf serum (FCS), penicillin G, streptomycin sulphate and all other tissue culture reagents were obtained from Grand Island Biological Co. (GIBCO BRL, U.S.A.). Isoliquiritigenin was dissolved in dimethylsulphoxide (DMSO) and the final concentration of DMSO in the bathing solution did not exceed 0.1% and had no effect on the muscle contraction.

Results

Effects of isoliquiritigenin on relaxation of rat aorta

Rat aortic rings were precontracted with phenylephrine (3 μM), KCl (60 mM), U-46619 (1 μM), endothelin (1 nM) or 5-hydroxytryptamine (10 μM) to produce approximately 80–90% of maximum contraction. Isoliquiritigenin relaxed phenylephrine (3 μM)-, KCl (60 mM)-, U-46619 (1 μM)-, endothelin (1 nM)- and 5-hydroxytryptamine (10 μM)-precontracted rat aortic rings in a concentration-dependent manner, with EC_{50} of 7.4 ± 1.6, 10.5 ± 2.3, 14.3 ± 3.3, 11.8 ± 2.0 and 13.6 ± 3.7 μM, respectively. Relaxation of phenylephrine-precontracted rat aortic rings by isoliquiritigenin (0.1–100 μM) was endothelium-independent (Figure 2a). Relaxations to isoliquiritigenin were also endothelium-independent in KCl-, U-46619-, endothelin- or 5-hydroxytryptamine-precontracted aortae (data not shown). Relaxation of phenylephrine-precontracted rat aortic rings by isoliquiritigenin was abolished in the presence of methylene blue (50 μM) (Figure 2b), whereas the relaxation induced by isoliquiritigenin was unchanged in the presence of N^G-monomethyl-L-arginine (L-NMMA, 300 μM), oxyhaemoglobin (HbO, 10 μM), indomethacin (10 μM) or glibenclamide (10 μM) (Figure 2c).

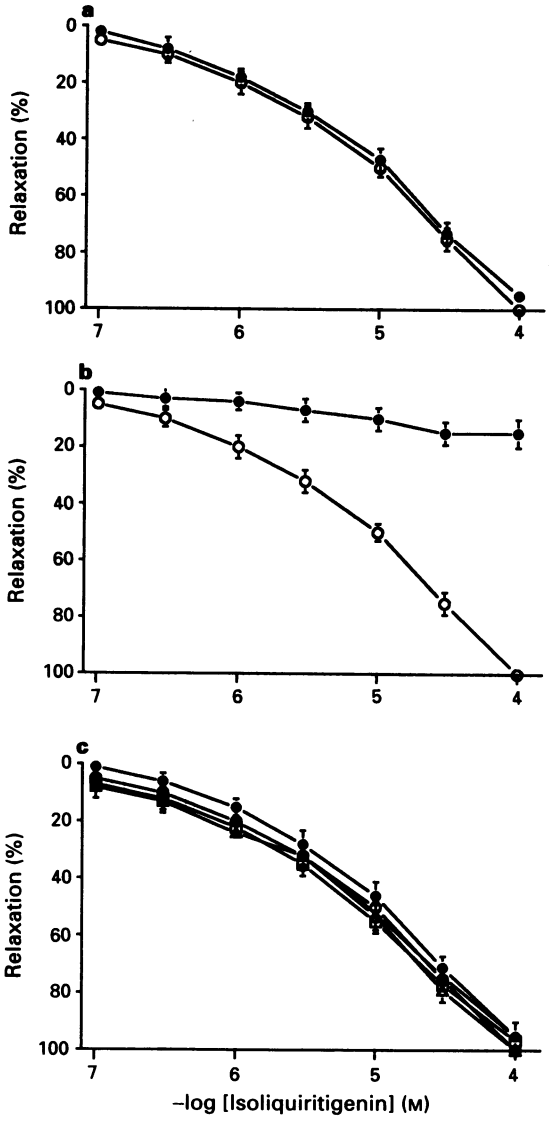

Figure 2 (a) Relaxation of phenylephrine-precontracted rat aortic rings by isoliquiritigenin in the presence (○) or absence (●) of endothelium. (b) Effects of methylene blue; (c) N^G-monomethyl-L-arginine, oxyhaemoglobin, indomethacin or glibenclamide on the vasorelaxant effect of isoliquiritigenin in endothelium-intact aorta. After pretreatment of rat aorta with (b) methylene blue (50 μM, ●); (c) N^G-monomethyl-L-arginine (300 μM, ●), oxyhaemoglobin (10 μM, △), indomethacin (10 μM, ▲), glibenclamide (10 μM, □) or dimethylsulphoxide (0.1%, ○) for 20 min, phenylephrine (3 μM) was used to induce muscle contraction for 10 min, then various concentrations of isoliquiritigenin were added. Each point represents the mean ± s.e.mean ($n = 6$).

Effects of isoliquiritigenin on the cyclic GMP and cyclic AMP content of rat aorta

Analysis of the time course of cyclic GMP and cyclic AMP formation caused by isoliquiritigenin (30 μM) showed that the maximum increase in cyclic GMP was reached earlier than that of cyclic AMP and declined rapidly after a 2 min incubation (Figure 3). The accumulation of cyclic AMP tended to lag behind that of cyclic GMP and continued to increase after cyclic GMP had begun to decline (Figure 3). These results suggested that the increase in cyclic GMP caused by isoliquiritigenin might stimulate the accumulation of cyclic AMP.

Incubation of rat aorta with isoliquiritigenin (10 and 30 μM) not only increased aorta cyclic GMP content (5.5 ± 0.3 fold and 6.8 ± 0.4 fold, respectively) but also caused small but significant increases in aortic cyclic AMP content (1.3 ± 0.1 fold and 1.6 ± 0.2 fold, respectively) and greatly potentiated the increases in cyclic AMP observed in the presence of 1 μM forskolin (12.1 ± 0.8 fold). Isoliquiritigenin at concentrations below 10 μM also increased cyclic GMP content (0.3 μM: 0.9 ± 0.2, 1 μM: 2.5 ± 0.4 and 3 μM: 3.3 ± 0.4 fold, respectively). However, the cyclic AMP

content was increased by isoliquiritigenin only at concentrations above 3 μM. Cilostamide, a selective phosphodiesterase III inhibitor, significantly increased rat aortic cyclic AMP at 1 μM. Moreover, isoliquiritigenin and cilostamide each greatly potentiated the increase in cyclic AMP caused by low concentrations of forskolin (Table 1). Finally, in the presence of cilostamide 1 μM, isoliquiritigenin had no additional effect on rat aortic cyclic AMP, whether forskolin was included in the incubation medium or not (Table 1). These results indicate that the increases in rat aortic cyclic AMP caused by isoliquiritigenin result from an inhibition of the cyclic AMP phosphodiesterase that is also the target of cilostamide. The presence of forskolin (1 μM) did not affect the increases in cyclic GMP caused by isoliquiritigenin (Table 1).

Effects of isoliquiritigenin on guanylate cyclase and adenylate cyclase activity

As shown in Table 2, concentration-dependent increases in soluble guanylate cyclase activity were observed in isoliquiritigenin or sodium nitroprusside (SNP)-treated rat aortic smooth muscle cells, while increases in adenylate cyclase activity were observed only in forskolin-treated cells.

Synergistic effects of isoliquiritigenin and forskolin on relaxation and formation of cyclic AMP in rat aorta

Although incubation of rat aorta with isoliquiritigenin (1–10 μM) alone caused a concentration-dependent relaxation of the phenylephrine-precontracted aorta, a much more potent relaxation was seen with isoliquiritigenin in the presence of a sub-threshold concentration of forskolin (10 nM) (Figure 4a). Thus, when isoliquiritigenin was added with forskolin (10 nM), the relaxation caused by isoliquiritigenin (1 μM) was increased from 20 ± 3% to 60 ± 4%. This synergism was less conspicuous with 10 μM isoliquiritigenin, which caused more potent relaxation of the aorta by itself (Figure 4a). When isoliquiritigenin was added with forskolin, the cyclic AMP formation caused by isoliquiritigenin (1 μM) was increased from 5.3 ± 0.3 to 27.0 ± 1.2 pmol mg^{-1} protein (Figure 4b); whereas cyclic GMP formation caused by isoliquiritigenin (1–10 μM) was unchanged (Figure 4c). The above results suggested that the synergistic relaxant effects of isoliquiritigenin and forskolin on phenylephrine-precontracted aorta were mediated by an increased accumulation of cyclic AMP. 2',5'-Dideoxyadenosine (DDA, 200 μM), an adenylate cyclase inhibitor, was able to reduce the relaxation caused by 1–10 μM isoliquiritigenin in the presence of forskolin (10 nM) (Figure 4a). This effect was associated with a marked decrease in cyclic AMP accumulation (Figure 4b). However, the relaxation of phenylephrine-precontracted rat aorta by isoliquiritigenin alone was not significantly decreased by DDA (Figure 4a). DDA did not affect the increases in cyclic GMP formation by isoliquiritigenin (Figure 4c).

Effects of isoliquiritigenin on PDE inhibitors-induced relaxation of rat aorta

Cilostamide (PDE III inhibitor), rolipram (PDE IV inhibitor) and isoliquiritigenin caused concentration-dependent relaxa-

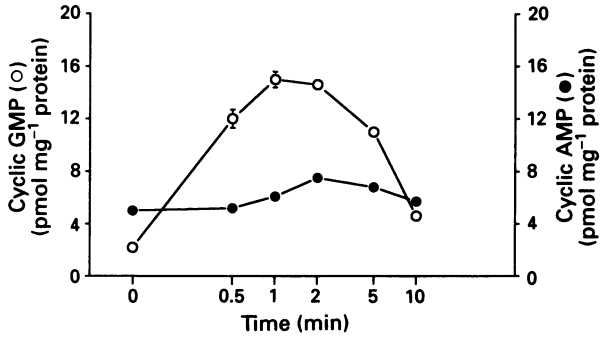

Figure 3 Time course of the isoliquiritigenin-induced accumulation of cyclic GMP and cyclic AMP in rat aorta. After preincubation of aortic rings in Krebs solution for 5 min, dimethylsulphoxide (0.1%, control) or isoliquiritigenin (30 μM) was added for the indicated time and the reaction was stopped by immersing the tissue in liquid nitrogen. Cyclic GMP (○) and cyclic AMP (●) content in rat aortae were measured. Basal values of cyclic GMP and cyclic AMP were 2.2 ± 0.2 and 4.8 ± 0.4 pmol mg^{-1} protein, respectively. Results are expressed as the mean ± s.e.mean ($n = 6$).

Table 2 Effects of isoliquiritigenin, sodium nitroprusside (SNP) and forskolin on soluble guanylate cyclase and adenylate cyclase activity in rat aortic smooth muscle cells

	Guanylate cyclase (pmol min^{-1} mg^{-1} protein)	*Adenylate cyclase* (pmol min^{-1} mg^{-1} protein)
None (basal)	26.5 ± 7.3	5.8 ± 1.9
SNP		
10 μM	50.5 ± 6.9*	–
100 μM	94.0 ± 7.6***	–
Forskolin		
10 μM	–	49.5 ± 4.9***
30 μM	–	83.5 ± 7.6***
Isoliquiritigenin		
1 μM	43.0 ± 3.0*	–
3 μM	57.6 ± 5.1**	–
10 μM	71.4 ± 7.6***	–
30 μM	87.3 ± 6.9***	5.7 ± 1.6
100 μM	96.9 ± 8.8***	6.0 ± 2.1

*$P<0.05$, **$P<0.01$, ***$P<0.001$ denote values significantly different from the respective basal values.

Table 1 Effects of isoliquiritigenin on the cyclic GMP and cyclic AMP formation of rat aorta

Treatment	*Cyclic GMP* (pmol mg^{-1} protein)	*Cyclic AMP* (pmol mg^{-1} protein)
Control	2.2 ± 0.2	4.8 ± 0.4
Isoliquiritigenin		
10 μM	12.0 ± 0.7***	6.5 ± 0.4**
30 μM	15.0 ± 0.6***	7.5 ± 0.5***
Forskolin	3.1 ± 0.5	21.7 ± 0.5***
Cilostamide	–	6.0 ± 0.3*
Isoliquiritigenin (30 μM) + forskolin	15.3 ± 0.8***	57.8 ± 1.6***
Cilostamide + forskolin	–	54.6 ± 2.3***
Isoliquiritigenin (30 μM) + cilostamide	–	7.0 ± 0.4*
Isoliquiritigenin (30 μM) + cilostamide + forskolin	–	56.4 ± 2.8***

*$P<0.05$, **$P<0.01$, ***$P<0.001$ as compared with the respective control.

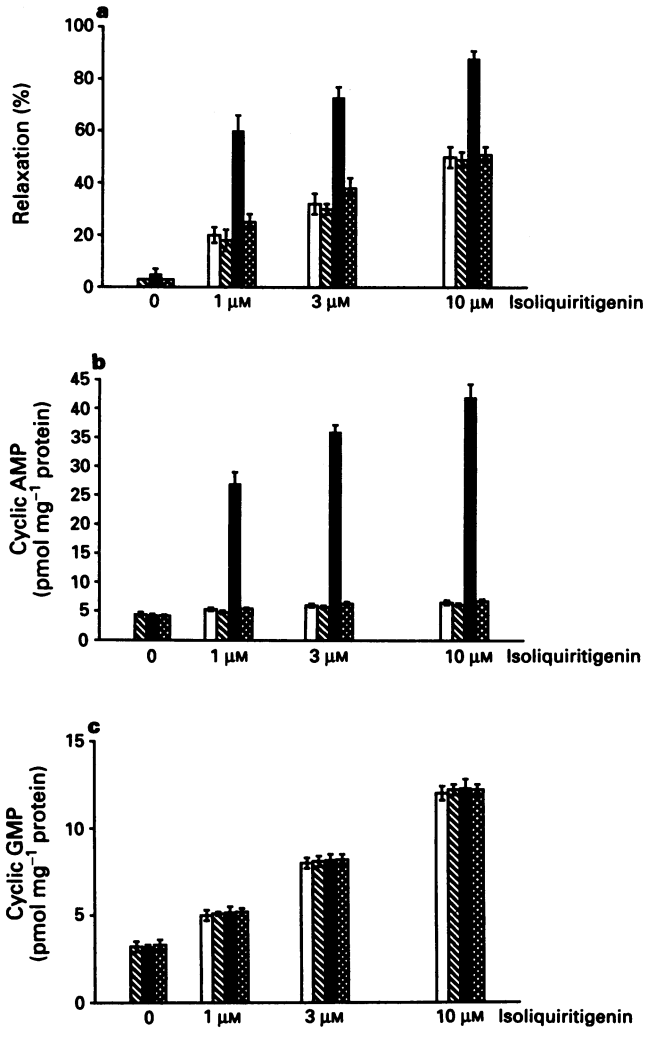

Figure 4 Effects of isoliquiritigenin on the phenylephrine-precontracted rat aorta, cyclic AMP and cyclic GMP formation in the absence or presence of forskolin and 2',5'-dideoxyadenosine. (a) After pretreatment of rat aorta with dimethylsulphoxide (open columns), 2',5'-dideoxyadenosine (DDA, 200 μM) (hatched columns), forskolin (10 nM) (solid columns), forskolin (10 nM) plus DDA (200 μM) (cross-hatched columns) for 20 min, phenylephrine (3 μM) was used to induce muscle contraction for 10 min, then various concentrations of isoliquiritigenin were added. (b), (c) After preincubation of aortic rings with dimethylsulphoxide (open columns), DDA (200 μM) (hatched columns), forskolin (10 nM) (solid columns), forskolin (10 nM) plus DDA (200 μM) (cross hatched columns) for 3 min, then isoliquiritigenin was added for another 2 min for cyclic AMP and 1 min for cyclic GMP and the reaction was stopped by immersing the tissue into liquid nitrogen. Cyclic AMP (b) and cyclic GMP (c) contents of rat aortae were measured. Results are expressed as mean ± s.e.mean ($n = 5-7$).

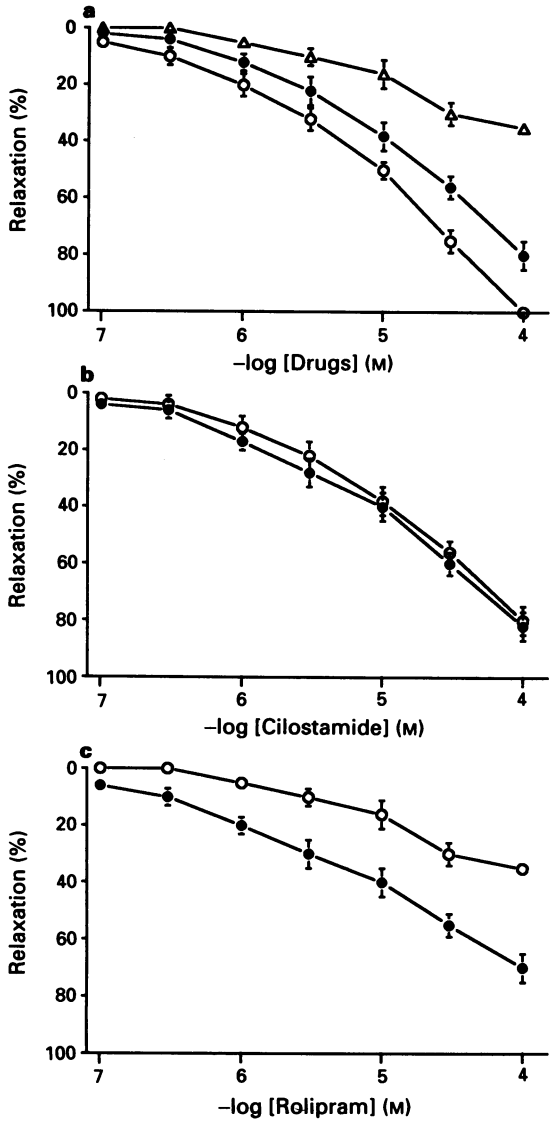

Figure 5 (a) Relaxant effects of isoliquiritigenin (○), cilostamide (●) and rolipram (△) in rat aortic rings precontracted with 3 μM phenylephrine. Rat aortic rings were preincubated with isoliquiritigenin (0.1 μM) (●) or dimethylsulphoxide (○) for 20 min, phenylephrine 3 μM was added for 10 min, then various concentrations of cilostamide (b) or rolipram (c) were added. Each point represents the mean ± s.e.mean ($n = 6$).

tion of rat aortic rings precontracted with phenylephrine (3 μM) (Figure 5a). However, rolipram did not produce complete relaxation, even at high concentrations, in rat aorta with endothelium. The relaxant activity of rolipram was markedly enhanced in the presence of isoliquiritigenin (0.1 μM) (Figure 5c), while the relaxant activity of cilostamide was unchanged in the presence of isoliquiritigenin (Figure 5b).

Effects of isoliquiritigenin on PDE inhibitors-induced relaxation of guinea-pig trachea

Cilostamide, rolipram and isoliquiritigenin caused concentration-dependent relaxation of carbachol (1 μM)-precontracted guinea-pig trachea (Figure 6a). However, cilostamide and isoliquiritigenin did not produce complete relaxation in guinea-pig trachea. The rolipram concentration-response curve was shifted to the left following preincubation of tissues with isoliquiritigenin (1 μM) (Figure 6b). The response to cilostamide was not significantly affected by isoliquiritigenin (Figure 6c).

Discussion

Isoliquiritigenin is a chalcone derivative which inhibits mouse epidermal 12-lipoxygenase activity and potently prevents skin tumour promotion caused by 12-O-tetradecanoylphorbol-13-acetate (TPA) (Yamamoto *et al.*, 1991). The present study has demonstrated that isoliquiritigenin, isolated from *Dalbergia odorifera T.*, relaxed phenylephrine-precontracted rat aorta by activating soluble guanylate cyclase and increasing cyclic GMP. Endothelial cells respond to a variety of neurohumoral and physical stimuli to release endothelium-

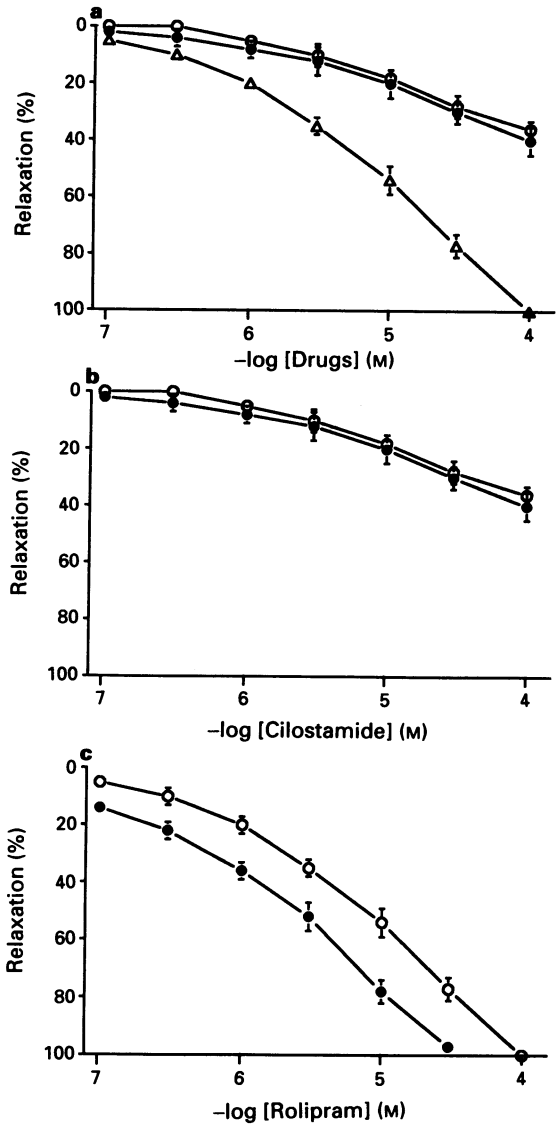

Figure 6 (a) Relaxant effects of isoliquiritigenin (○), cilostamide (●) and rolipram (△) in guinea-pig tracheal rings precontracted with 1 μM carbachol. (b) Tissues were preincubated with isoliquiritigenin (1 μM) (●) or dimethylsulphoxide (○) for 20 min, carbachol 1 μM was added for 10 min, then various concentrations of cilostamide (b) or rolipram (c) were added. Each point represents the mean ± s.e.mean ($n = 6$).

dependent vasodilators such as endothelium-derived relaxing factor (EDRF) (Furchgott & Zawadzki, 1980; Furchgott & Vanhoutte, 1989), prostacyclin (PGI_2) (Jaffe, 1985; Vanhoutte *et al.*, 1986) and endothelium-derived hyperpolarizing factor (EDHF) (Beny & Brunet, 1988; Feletou & Vanhoutte, 1988; Taylor & Weston, 1988). It is generally accepted that the release of EDRF, PGI_2 and EDHF may have important physiological roles as dilator mediators in certain vessels. The relaxant action of isoliquiritigenin persisted in endothelium-denuded aorta, or in intact aorta in the presence of N^G-monomethyl-L-arginine (L-NMMA) (an inhibitor of the L-arginine-NO pathway), oxyhaemoglobin (which binds nitric oxide), indomethacin (cyclo-oxygenase inhibitor) and glibenclamide (ATP-sensitive K^+ channel blocker). Thus, the vasorelaxation caused by isoliquiritigenin was independent of endothelium and not mediated by EDRF, PGI_2 and EDHF. However, methylene blue, a soluble guanylate cyclase inhibitor, was able to inhibit relaxation produced by isoliquiritigenin. This result implies that relaxation of the rat aorta caused by isoliquiritigenin, is mediated through activation of soluble guanylate cyclase and increased cyclic GMP content. Indeed, concentration-dependent increases in soluble guanylate cyclase activity and elevated cyclic GMP content were observed in isoliquiritigenin-treated rat aortae.

Other important mediators for relaxing the vascular smooth muscle are cyclic nucleotides (Murad, 1986). It is generally accepted that nitrovasodilators exert their effects on vascular smooth muscle by activating guanylate cyclase and increasing cyclic GMP, and that β-adrenoceptor agonists act by stimulating adenylate cyclase and increasing cyclic AMP. These mechanisms have generally been assumed to be parallel and independent. However, low concentrations of sodium nitroprusside act synergistically with isoprenaline to relax or inhibit the contraction of rat aortic smooth muscle (Maurice *et al.*, 1991). In addition to the large increases in cyclic GMP induced by isoliquiritigenin, we have found that isoliquiritigenin causes small, but significant increases in cyclic AMP in rat aorta. Analysis of the time course of cyclic nucleotide formation caused by isoliquiritigenin showed that the increase in cyclic GMP was reached earlier, the accumulation of cyclic AMP tended to lag behind that of cyclic GMP. These results suggested that the increases in cyclic GMP caused by isoliquiritigenin might stimulate the accumulation of cyclic AMP and that cyclic AMP might play a role in some of the inhibitory effects of isoliquiritigenin on muscle contraction. To test the latter possibility, we used DDA, an inhibitor of adenylate cyclase; however, the relaxation of phenylephrine-precontracted rat aorta by isoliquiritigenin was not significantly decreased by DDA. DDA also did not affect the increases in cyclic GMP induced by isoliquiritigenin. These results suggest that cyclic GMP is likely to mediate the majority of the relaxation of phenylephrine-precontracted aorta caused by isoliquiritigenin. In the presence of a low concentration of forskolin, the role of cyclic AMP was clearer; isoliquiritigenin then caused very large additional increases in rat aortic cyclic AMP, and much more marked relaxation of rat aorta. Because DDA reduced both the isoliquiritigenin-induced increases in aortic cyclic AMP and the associated relaxation of the phenylephrine-precontracted aorta only in the presence of forskolin, and DDA did not affect cyclic GMP levels, the synergistic effects of low concentrations of isoliquiritigenin and forskolin were mediated by cyclic AMP.

Four PDE isoenzymes are identified by DEAE-sephacel chromatography from rat aorta (Komas *et al.*, 1991). Of these, PDE I and III can utilize both cyclic AMP and cyclic GMP as substrate, PDE IV is a cyclic AMP-specific PDE and PDE V is a cyclic GMP-specific PDE (Beavo & Reifsnyder, 1990). Although non-selective PDE inhibitors, such as 3-isobutyl-1-methylxanthine (IBMX) have been known for some time, only recently have selective PDE inhibitors been identified. The selective inhibitors for individual PDE isozymes used in this study are: (1) cilostamide, a selective inhibitor of cyclic GMP-inhibited PDE (PDE III), IC_{50} for inhibition of platelet PDE III was 40 nM (Beavo & Reifsnyder, 1990; Tang *et al.*, 1994); (2) rolipram, a selective inhibitor of PDE IV (Grous & Barnette, 1994). In platelets, sodium nitroprusside causes small increases in cyclic AMP by itself, and potentiates the increases in cyclic AMP seen in the presence of activators of adenylate cyclase; this is due to inhibition of the major low K_m cyclic AMP phosphodiesterase of platelets by cyclic GMP (PDE III) (Maurice & Haslam, 1990a). In the present study, isoliquiritigenin greatly enhanced the accumulation of cyclic AMP that occurred in the presence of activators of adenylate cyclase, such as forskolin, but caused no further increase in the presence of cilostamide. The above findings raise the possibility that the increases in rat aortic cyclic AMP caused by isoliquiritigenin are secondary to increases in cyclic GMP, which acts by inhibiting the low K_m cyclic AMP-PDE. Recently, Lindgren *et al.* (1990) showed the existence of a cyclic GMP-inhibited low K_m cyclic AMP-PDE (CGI-PDE, PDE III) in rat aortic tissue. We therefore propose that inhibition of CGI-PDE by isoliquiritigenin mediates the synergistic effects of isoli-

quiritigenin and forskolin on cyclic AMP accumulation and on relaxation of rat aorta.

Although cilostamide (PDE III inhibitor), rolipram (PDE IV inhibitor) and isoliquiritigenin all relaxed phenylephrine-precontracted rat aorta or carbachol-precontracted guinea-pig trachea, there were marked differences in their potency. Cilostamide and isoliquiritigenin were more potent relaxants of the phenylephrine-precontracted rat aorta than carbachol-precontracted guinea-pig trachea, whereas rolipram more potently relaxed the carbachol-precontracted guinea-pig trachea. However, isoliquiritigenin potentiated both rolipram-induced relaxation of the phenylephrine-precontracted rat aorta or the carbachol-precontracted guinea-pig trachea. The results suggest that both isoliquiritigenin and cilostamide are involved in the inhibition of the same isoenzyme (PDE III). It is well established that PDE III inhibitors produce relaxation of vascular smooth muscle (Komas *et al.*, 1991), inhibition of platelet aggregation (Maurice & Haslam, 1990a,b) and positive inotropic effects (Muller *et al.*, 1990). Despite the fact that PDE IV is present in smooth muscle cells, selective inhibitors of PDE IV have not been shown to have marked vasodilator potential. Recently, it was suggested that PDE IV inhibitors are bronchodilators but PDE III inhibitors are only weakly active (Cortijo *et al.*, 1993; Turner *et al.*, 1994). In the present study, the marked enhancement of the relaxant activity of rolipram in carbachol-precontracted guinea-pig trachea by isoliquiritigenin, indicates that isoliquiritigenin combined with PDE IV inhibition (rolipram) might offer greater bronchodilator potential.

It is concluded that isoliquiritigenin exerts its vasorelaxant effect of activating soluble guanylate cyclase and increasing cyclic GMP. Synergistic effects of isoliquiritigenin and forskolin on muscle relaxation and cyclic AMP accumulation indicate that inhibition of cyclic AMP breakdown by the inhibition of cyclic GMP-inhibited PDE is the dominant mechanism.

This work was supported by research grants of CMRP 377 from Chang Gung Medical Research Foundation and the National Science Council of the Republic of China (NSC 84-2331-B-182-071).

References

BEAVO, J.A. & REIFSNYDER, D.H. (1990). Primary sequence of cyclic nucleotide phosphodiesterase isoenzymes and the design of selective inhibitors. *Trends Pharmacol. Sci.*, **11**, 150–155.

BENY, J.L. & BRUNET, P.C. (1988). Neither nitric oxide nor nitroglycerin accounts for all the characteristics of endothelially mediated vasodilation of pig coronary arteries. *Blood Vessels*, **25**, 308–311.

BRADFORD, M.M. (1976). A rapid and sensitive method for the quantitation of microgram quantities of protein utilizing the principle of protein-dye-binding. *Anal. Biochem.*, **72**, 248–254.

BROCK, T.A., ALEXANDER, R.W., EKSTEIN, L.S., ATKINSON, W.J. & GIMBRONE, M.A. (1985). Angiotensin increases cytosolic free calcium in cultured vascular smooth muscle cells. *Hypertension*, **7**, I-105–I-110.

CORTIJO, J., BELETA, B.J., LLENAS, I.C.J., MORCILLO, E. & GRISTWOOD, R.W. (1993). Investigation into the role of phosphodiesterase IV in bronchorelaxation, including studies in human bronchus. *Br. J. Pharmacol.*, **108**, 562–568.

FELETOU, M. & VANHOUTTE, P.M. (1988). Endothelium-dependent hyperpolarization of canine coronary smooth muscle. *Br. J. Pharmacol.*, **93**, 515–524.

FURCHGOTT, R.F. & VANHOUTTE, P.M. (1989). Endothelium-derived relaxing and contracting factors. *FASEB J.*, **3**, 2007–2018.

FURCHGOTT, R.F. & ZAWADZKI, J.V. (1980). The obligatory role of endothelial cells in the relaxation of arterial smooth muscle of acetylcholine. *Nature*, **288**, 373–376.

GERZER, R., HAMET, P., ROSS, A.H., LAWSON, J.A. & HARDMAN, J.G. (1983). Calcium-induced release from platelet membranes of fatty acids that modulate soluble guanylate cyclase. *J. Pharmacol. Exp. Ther.*, **226**, 180–186.

GROUS, M. & BARNETTE, M. (1994). Prevention by phosphodiesterase inhibitors of antigen-induced contraction of guinea-pig colonic smooth muscle. *Br. J. Pharmacol.*, **111**, 259–263.

IGNARRO, L.J. & KADOWITZ, P.J. (1985). The pharmacological and physiological role of cyclic GMP in vascular smooth muscle relaxation. *Annu. Rev. Pharmacol. Toxicol.*, **25**, 171–191.

INSEL, P.A., STENGEL, D., FERRY, N. & HANOUNE, J. (1982). Regulation of adenylate cyclase of human platelet membranes by forskolin. *J. Biol. Chem.*, **257**, 7485–7490.

ITOH, T., IZUMI, H. & KURIYAMA, H. (1982). Mechanisms of relaxation induced by activation of β-adrenoceptors in muscle cells of guinea-pig mesenteric artery. *J. Physiol.*, **326**, 475–493.

JAFFE, E.A. (1985). Physiological functions of normal endothelial cells. *Ann. N.Y. Acad. Sci.*, **454**, 279–291.

KAUFFMAN, R.F., SCHENCK, K.W., UTTERBACK, B.G., CROWE, V.G. & COHEN, M.L. (1987). In vitro vascular relaxation by new inotropic agents: relationship to phosphodiesterase inhibition and cyclic nucleotides. *J. Pharmacol. Exp. Ther.*, **242**, 864–871.

KO, F.N., YU, S.M., SU, M.J., WU, Y.C. & TENG, C.M. (1993). Pharmacological activity of (-)-discretamine, a novel vascular α-adrenoceptor and 5-hydroxytryptamine receptor antagonist, isolated from *Fissistigma glaucescens*. *Br. J. Pharmacol.*, **110**, 882–888.

KOMAS, N., LUGNIER, C. & STOCLET, J.C. (1991). Endothelium-dependent and independent relaxation of the rat aorta by cyclic nucleotide phosphodiesterase inhibitors. *Br. J. Pharmacol.*, **104**, 495–503.

KUKOVETZ, W.R., POCH, G. & HOLZMANN, S. (1981). Cyclic nucleotides and relaxation of vascular smooth muscle. In *Vasodilatation*. ed. Vanhoutte, P.M. & Leusen, I. pp. 339–351. New York: Raven Press.

LINDGREN, S., RASCON, A., DEGERMAN, E., BELFRAGE, P., MANGANIELLO, V. & ANDERSSON, K.-E. (1990). Identification of the cGMP-inhibited low km cAMP phosphodiesterase in rat smooth muscle. *Eur. J. Pharmacol.*, **183**, 806.

LOWRY, D.H., ROSEBROUGH, N.J., FARR, A.L. & RANDALL, R.J. (1951). Protein measurement with the Folin phenol reagent. *J. Biol. Chem.*, **193**, 265–275.

MAURICE, D.H., CRANKSHAW, D. & HASLAM, R.J. (1991). Synergistic actions of nitrovasodilators and isoprenaline on rat aortic smooth muscle. *Eur. J. Pharmacol.*, **192**, 235–242.

MAURICE, D.H. & HASLAM, R.J. (1990a). Molecular basis of the synergistic inhibition of platelet function by nitrovasodilators and activators of adenylate cyclase: inhibition of cyclic AMP breakdown by cyclic GMP. *Mol. Pharmacol.*, **37**, 671–681.

MAURICE, D.H. & HASLAM, R.J. (1990b). Nitroprusside enhances isoprenaline-induced increases in cAMP in rat aortic smooth muscle. *Eur. J. Pharmacol.*, **191**, 471–475.

MULLER, B., LUGNIER, C. & STOCLET, J.C. (1990). Implication of cyclic AMP in the positive inotropic effects of cyclic GMP-inhibited cyclic AMP phosphodiesterase inhibitors on guinea-pig isolated left atria. *J. Cardiovasc. Pharmacol.*, **15**, 444–451.

MURAD, F. (1986). Cyclic guanosine monophosphate as a mediator of vasodilation. *J. Clin. Invest.*, **78**, 1–5.

SCHULZ, S., CHINKERS, M. & GARBERS, D.L. (1989). The guanylate cyclase/receptor family of proteins. *FASEB J.*, **3**, 2026–2035.

SCHULZ, S., YUEN, P.S.T. & GARBERS, D.L. (1991). The expanding family of guanylyl cyclases. *Trends Pharmacol. Sci.*, **12**, 116–119.

TANG, K.M., JANG, E.K. & HASLAM, R.J. (1994). Photoaffinity labelling of cyclic GMP-inhibited phosphodiesterase (PDE III) in human and rat platelets and rat tissues: effects of phosphodiesterase inhibitors. *Eur. J. Pharmacol.*, **268**, 105–114.

TAYLOR, S.G. & WESTON, A.H. (1988). Endothelium-derived hyperpolarizing factor: a new endogenous inhibitor from the vascular endothelium. *Trends Pharmacol. Sci.*, **9**, 272–274.

TURNER, N.C., LAMB, J., WORBY, A. & MURRAY, K.J. (1994). Relaxation of guinea-pig trachea by cyclic AMP phosphodiesterase inhibitors and their enhancement by sodium nitroprusside. *Br. J. Pharmacol.*, **111**, 1047–1052.

VANHOUTTE, P.M., RUBANYI, G.M., MILLER, V.M. & HOUSTON, D.S. (1986). Modulation of vascular smooth muscle contraction by endothelium. *Annu. Rev. Physiol.*, **48**, 307–330.

WALDMAN, S.A. & MURAD, F. (1987). Cyclic GMP synthesis and function. *Pharmacol. Rev.*, **39**, 163–196.

WHITE, A.A. & ZENSER, T.V. (1971). Separation of cyclic 3',5'-nucleoside monophosphates from other nucleotides on aluminum oxide columns: Application to the assay of adenyl cyclase and guanylate cyclase. *Anal. Biochem.*, **14**, 372–396.

YAMAMOTO, S., AIZU, E., JIANG, H., NAKADATE, T., KIYOTO, I., WANG, J.C. & KATO, R. (1991). The potent anti-tumor-promoting agent isoliquiritigenin. *Carcinogenesis*, **12**, 317–323.

YU, S.M., CHEN, C.C., HUANG, Y.L., TSAI, C.W., LIN, C.H., HUANG, T.F. & TENG, C.M. (1990). Vasorelaxing effect in rat thoracic aorta caused by denudatin B, isolated from the Chinese herb, *Magnolia fargesii*. *Eur. J. Pharmacol.*, **187**, 39–47.

YU, S.M., HUS, S.Y., KO, F.N., CHEN, C.C., HUANG, Y.L., HUANG, T.F. & TENG, C.M. (1992). Haemodynamic effect of dicentrine, a novel α_1-adrenoceptor antagonist: comparison with prazosin in spontaneously hypertensive and normotensive Wistar-Kyoto rats. *Br. J. Pharmacol.*, **106**, 797–801.

YU, S.M., WU, T.S. & TENG, C.M. (1994). Pharmacological characterization of cinnamophilin, a novel dual inhibitor of thromboxane synthase and thromboxane A_2 receptor. *Br. J. Pharmacol.*, **111**, 906–912.

(Received September 2, 1994
Revised December 9, 1994
Accepted January 6, 1995)

British Journal of Pharmacology (1995) 114, 1595–1598 © 1995 Stockton Press All rights reserved 0007–1188/95 $12.00

Hypertension and enhanced β-adrenoceptor-mediated facilitation of noradrenaline release produced by chronic blockade of adenosine receptors

[1]S. Guimarães, A. Albino-Teixeira & M.Q. Paiva

Institute of Pharmacology and Therapeutics, Faculty of Medicine, 4200-Porto, Portugal

1 The study was undertaken to compare the β-adrenoceptor-mediated facilitation of noradrenaline release in the tail artery of vehicle-treated rats and of rats rendered hypertensive by chronic administration of 1,3-dipropyl-8-sulphophenylxanthine (DPSPX). Artery rings were loaded with [^{3}H]-noradrenaline, and five periods of electrical stimulation (1 Hz for 2 min) were applied. To eliminate the influence of prejunctional α_2-adrenoceptors, the tissues were pre-exposed to 1 μM phenoxybenzamine.

2 Isoprenaline caused a concentration-dependent increase of tritium overflow elicited by electrical stimulation. It was more effective in arteries from DPSPX-treated than in those from vehicle-treated rats; isoprenaline (27.8 nM) increased by 30% tritium overflow in vessels from vehicle-treated rats whereas isoprenaline (7.0 nM) produced a 30% increase in vessels from DPSPX-treated animals. Furthermore, the maximal effect of isoprenaline was a 32.6% increase in control rats but a 48.6% increase in DPSPX-treated rats.

3 These results show that the sympathetic nerve endings of the rat tail artery are endowed with prejunctional β-adrenoceptors which mediate facilitation of noradrenaline release elicited by electrical stimulation. They also suggest that adenosine receptors and β-adrenoceptors interact at the prejunctional level and that impairment of this 'talk' may lead to the development of a hypertensive state.

Keywords: Adenosine receptors; prejunctional β-adrenoceptors; hypertension; DPSPX; rat tail artery

Introduction

Many peripheral noradrenergic axons possess prejunctional β-adrenoceptors, activation of which increases the release of noradrenaline evoked by nerve stimulation (for reviews see Majewski, 1983; Misu & Kubo, 1986; Nedergaard & Abrahamsen, 1990; Floras, 1992). It is still uncertain if this β-adrenoceptor-mediated facilitation of transmitter release plays a physiological role. However, a substantial body of evidence supports the involvement of prejunctional β-adrenoceptors in the development and maintenance of some kinds of hypertension (Majewski *et al.*, 1981; Kubo *et al.*, 1984; Borkowski & Quinn, 1985; Misu *et al.*, 1987).

Recently, it was shown that chronic treatment of rats with the non-selective antagonist of adenosine receptors 1,3-dipropylsulphophenylxanthine (DPSPX) leads to a hypertensive state (Albino-Teixeira *et al.*, 1991; Matias *et al.*, 1991) and alters the prejunctional effects of the selective α_2-adrenoceptor agonist, UK-14,304 (Guimarães *et al.*, 1994). The present investigation was undertaken to compare the role of β-adrenoceptor-mediated facilitation of noradrenaline release in the tail artery of normotensive rats and of rats rendered hypertensive by long-term administration of DPSPX.

Methods

Male Wistar rats with an initial body weight of 200–250 g were used. Systolic and diastolic blood pressure were measured by the tail-cuff method (LE 500, Letica, Barcelona, Spain) in conscious animals. Blood pressure was measured on seven consecutive days before day 0 and every week thereafter for three weeks. Five determinations were made each time and the means used for further calculation. On day 0, an Alzet osmotic minipump (model 2ML1; Alza, Palo Alto, CA, U.S.A.) was implanted intraperitoneally under pentobarbitone sodium anaesthesia (30 mg kg^{-1}, i.p.) for continuous infusion for one week of DPSPX (90 μg kg^{-1} h^{-1}) or saline (vehicle of DPSPX). The infusion of DPSPX resulted in persistent hypertension that reached a maximum within two weeks (Albino-Teixeira *et al.*, 1991). The present experiments were carried out just at this time, i.e., two weeks after the end of the infusion.

Transmitter overflow

Vehicle- or DPSPX-treated animals were anaesthetized (see above). A segment of the proximal portion of the ventral tail artery, about 6 cm long, was dissected free and placed in aerated (95% O_2; 5% CO_2) modified Krebs-Henseleit medium (Guimarães & Osswald, 1969) of the following composition (mM): NaCl, 118.6, KCl, 4.70, $CaCl_2$ 2.52, KH_2PO_4 1.18, $MgSO_4$ 1.23, $NaHCO_3$ 25.0, glucose 10.0. To avoid autoxidation of [^{3}H]-noradrenaline, EDTA 0.027 mM and ascorbic acid 0.57 mM were added to the medium. The segment of the vessel was cut into four small rings which were preincubated for 30 min in medium containing 1 mM pargyline (to inhibit monoamine oxidase), 40 μM hydrocortisone and 40 μM U-0521 (3,4-dihydroxy-2-methylpropiophenone) (to inhibit extraneuronal removal of noradrenaline) (Guimarães *et al.*, 1978). Hydrocortisone and U-0521 were also kept in the medium for the remainder of the experiment. After preincubation, the vessel segments were exposed for 60 min to [^{3}H]-noradrenaline (0.2 μM). Thereafter they were mounted in 2 ml glass chambers between two platinum electrodes and perifused with amine-free medium (aerated and at 37°C). From $t = 110$ min ($t = 0$ min being the onset of the perifusion) the perifusion fluid was collected continuously as 5 min samples. Transmural electrical stimulation (1 Hz, 2 ms, 100 V, for 2 min; Stimulator II X, Hugo Sachs Elektronik, March-Hugstetten, Germany) was applied at min 120 (S_1), 160 (S_2), 200 (S_3), 240 (S_4) and 280 (S_5).

In most experiments, the vessel rings were exposed to 1 μM phenoxybenzamine, which was present in the fluid during a 45 min period starting at the beginning of the perifusion.

[1] Author for correspondence.

Isoprenaline was added to the perifusion fluid 15 min before S_3, S_4 and S_5 in concentrations increasing by half-log increments. In the experiments in which antagonism against isoprenaline was studied, the antagonist (atenolol or the compound ICI-118,551) was added to the perifusion fluid 30 min before S_1 and kept for the remainder of the experiment; pA_2 values were calculated according to the method of Van Rossum (1963) from the equation: $pA_2 = pA_x + \log (x - 1)$ in which x represents the factor or the shift of the concentration-response curve to the right and pA_x the negative logarithm of the molar concentration of the antagonist which caused this shift.

For the calculation of the overflow induced by electrical stimulation, those 5 min samples were taken into account in which the outflow of tritium exceeded that in the last pre-stimulation control sample; usually this applied to the 3 or 4 samples collected during and after stimulation. The spontaneous outflow measured in the last pre-stimulation sample was assumed to represent the spontaneous outflow in subsequent samples; it was subtracted from the outflow determined in stimulation and post-stimulation samples.

Fractional ^{3}H-efflux min^{-1} was calculated by dividing ^{3}H-efflux in each 5 min sample by tritium present in the tissue at the onset of the respective collection period and by 5. The fractional release per shock (FR) was calculated by dividing evoked tritium overflow by tritium present in the tissue at the beginning of the stimulation period and by the number of shocks. Drug effects are expressed as percentage of the FR of tritium evoked by S_3 (or S_4 or S_5) over that evoked by S_2. Each result was corrected for time-dependent changes as determined in parallel drug-free control experiments.

Radioactivity was measured by liquid scintillation counting (liquid scintillation counter 1209 Rackbeta, LKB Wallac, Turku, Finland) in 2 ml aliquots of perifusate or 0.5 ml of tissue extract + 1.5 ml of Krebs-Henseleit solution. The extraction was made in 3 ml of 0.1 M perchloric acid during 18 h.

Statistics

Results are expressed as arithmetic means ± s.e. mean. One-way analysis of variance was used to test differences between unpaired results. A probability level of 0.05 or less was considered statistically significant.

Drugs

The following were used: (±)-atenolol hydrochloride (ICI, Macclesfield, UK); cocaine hydrochloride (Uquipa, Lisboa, Portugal); DPSPX(1,3-dipropyl-8-sulphophenylxanthine; Research Biochemicals, Natick, U.S.A.); hydrocortisone 21-hemisuccinate sodium (Sigma, St Louis, MO, U.S.A.); (±)-ICI-118,551 hydrochloride (erythro-DL 1 (7-methylindan-4-yloxy)-isopropylaminobutan-2-ol); (−)-isoprenaline bitartrate (Sigma); [^{3}H-7]-(−)-noradrenaline(18.2-21.1 Ci $mmol^{-1}$, New England Nuclear, Dreieich, Germany); pargyline hydrochloride (Sigma); U-0521 (3,4-dihydroxy-2-methylpropiophenone; Upjohn Kalamazoo, MI, U.S.A.).

Results

The mean weight of vehicle-treated rats and DPSPX-treated rats was not significantly different: 312 ± 18 and 298 ± 20 g, ($n = 7$), respectively. The systolic and diastolic blood pressures of vehicle-treated rats were 138 ± 4 and 104 ± 3 mmHg ($n = 7$), respectively, while those of DPSPX-treated rats were 164 ± 5 and 130 ± 4 mmHg($n = 6$), respectively ($P < 0.05$).

Some experiments were carried out on tail arteries from either vehicle-treated or DPSPX-treated rats in the absence of phenoxybenzamine. In these experiments, in which the fractional release of tritium evoked by S_2 was $7.1 \pm 1.1 \times 10^{-5}$ ($n = 5$), isoprenaline (3.3–100 nM) caused concentration-dependent increases of tritium overflow, the maximal increase reaching 33.9 ± 3.2%.

To eliminate the influence of prejunctional α_2-autoreceptors, the tissues were pre-exposed to phenoxybenzamine (1 μM) in those experiments designed to compare the effect of the β-adrenoceptor agonist, isoprenaline, in the tail arteries from vehicle-treated and DPSPX-treated rats. In arteries from vehicle-treated rats exposed to phenoxybenzamine, the fractional release of tritium at S_2 was $43.3 \pm 2.7 \times 10^{-5}$ ($n = 5$; compare with smaller release above). In arteries from DPSPX-treated rats exposed to phenoxybenzamine the fractional release of tritium evoked by S_2 was $40.6 \pm 3.1 \times 10^{-5}$ ($n = 6$), not significantly different from vehicle-treated rats.

In the tissues pre-exposed to phenoxybenzamine, both from vehicle-treated (Figure 1) and from DPSPX-treated rats, isoprenaline caused a concentration-dependent enhancement of tritium overflow evoked by electrical stimulation. However, as shown in Figure 2, the concentration of isoprenaline required to increase tritium overflow by 30% was lower in the arteries from DPSPX-treated than in those from vehicle-treated rats: 7.0 nM isoprenaline in the arteries from DPSPX-treated rats were equieffective with 27.8 nM in the arteries from vehicle-treated animals. Furthermore, the maximal enhancement of tritium overflow evoked by electrical stimulation caused by isoprenaline was larger in the tissues from DPSPX-treated than in tissues from vehicle-treated rats: 48.6 ± 5.3% and 32.6 ± 2.7% ($n = 6$), respectively ($P < 0.05$).

In some experiments on arteries from vehicle-treated rats, the acute influence of DPSPX on the effect of isoprenaline was tested. DPSPX, 30 min before S_1, did not change the effect of isoprenaline (not shown).

The antagonist action of atenolol and ICI-118,551 against isoprenaline-induced facilitation was studied on rings obtained from vehicle-treated rats pre-exposed to phenoxybenzamine. Atenolol and ICI-118,551 did not change the overflow of tritium elicited by S_2. ICI-118,551 (1–10 nM) was a potent antagonist against isoprenaline. Atenolol (0.01–0.3 μM) did not shift the concentration-response curve of isoprenaline ($n = 4$).

Discussion

The results show that the sympathetic nerve endings of the rat tail artery are endowed with prejunctional β-adreno-

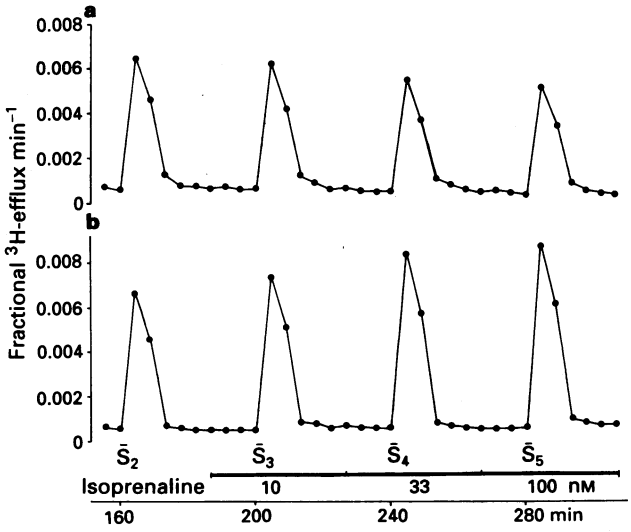

Figure 1 Tritium overflow evoked by electrical stimulation (1 Hz, for 2 min) from rat tail arteries, pre-exposed to phenoxybenzamine (1 μM), from vehicle-treated rats. (a) Control experiment; (b) in the presence of increasing concentrations of isoprenaline, from min 185 onwards. The Figure shows a typical experiment in which 10, 33 and 100 nM isoprenaline were used. In other experiments, isoprenaline was used in concentrations of 3.3, 10 and 33 nM.

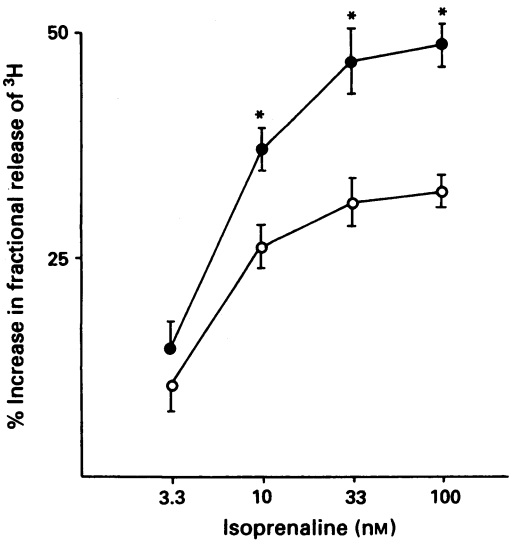

Figure 2 Effect of isoprenaline on tritium overflow evoked by electrical stimulation (1 Hz, for 2 min) from rat tail arteries, pre-exposed to phenoxybenzamine (1 μM), from vehicle-treated (○) and DPSPX-treated (●) rats. In some experiments S_3, S_4 and S_5 were applied in the presence of 3.3, 10 and 33 nM isoprenaline, respectively, while in other experiments S_3, S_4 and S_5 were applied in the presence of 10, 33 and 100 nM isoprenaline, respectively. Shown is the percentage increase in fractional release of tritium as compared to S_2, corrected for any change occurring in experiments without isoprenaline. *Significantly different from vehicle-treated rats ($n = 6$; $P < 0.05$).

ceptors which mediate facilitation of the noradrenaline release evoked by electrical stimulation. The maximal enhancement of noradrenaline release caused by isoprenaline was about 33%. The effect of isoprenaline was not changed by pretreatment with phenoxybenzamine, which *per se* increased noradrenaline release by 6.1 times. This indicates that the noradrenaline reaching the biophase does not stimulate prejunctional β-adrenoceptors in this tissue. That noradrenaline released from sympathetic nerve varicosities activates prejunctional β-adrenoceptors to facilitate the subsequent release of noradrenaline is a very unlikely possibility because in the vast majority of the tissues, prejunctional β-adrenoceptors belong to the β_2-subtype for which the affinity of noradrenaline is low (Lands *et al.*, 1967; Guimarães *et al.*, 1978; Guimarães & Paiva, 1981a,b; Dahlöf, 1981). The results obtained in the present study indicate that in the rat tail artery, the prejunctional β-adenoceptors are also β_2 since ICI-118,551 was a very potent antagonist against isoprenaline, while atenolol had no effect in concentrations up to 0.3 μM.

Long-term pretreatment of the rats with DPSPX enhanced the facilitatory effect of isoprenaline. There was not only a shift of the concentration-response curve of isoprenaline to the left, but also an increase in its maximal effect. These changes are compatible with an upregulation of the prejunctional β-adrenoceptors or some change at the level of G proteins. Long-term blockade of adenosine receptors in the rat by DPSPX also leads to an increase in the sensitivity of the sympathetic axons of the tail artery to the selective α_2-adrenoceptor agonist UK-14,304 (Guimarães *et al.*, 1994). Those experiments had suggested a 'crosstalk' between adenosine and α_2-adrenoceptors at the prejunctional level, an interaction already observed in different tissues, both peripherally and centrally (see Enero & Saidman, 1977; Allgaier *et al.*, 1987; Limberger *et al.*, 1988). The present data indicate an analogous 'crosstalk' in which β-adrenoceptors participate since the blockade of adenosine receptors *in vivo* enhanced β-adrenoceptor-mediated responses to isoprenaline *in vitro*.

In recent experiments carried out on rat hearts, Eikenburg & Apparsundaram (1992) showed that the facilitatory influence of salbutamol on tritium overflow elicited by electrical stimulation was increased in the presence of adenosine antagonists, suggesting that endogenous adenosine inhibits β-adrenoceptor-mediated facilitation of noradrenaline release. As the present results show, in the rat tail artery *in vitro* addition of DPSPX did not change the β-adrenoceptor-mediated facilitation of noradrenaline release indicating that no 'crosstalk' between adenosine receptors and β-adrenoceptors occurs *in vitro*.

The existence of a link between prejunctional β-adrenoceptor-mediated facilitation of noradrenaline release and the development of some hypertensive states is widely accepted. For example, infusion or depot implantation of adrenaline can cause facilitation of noradrenaline release and long-lasting hypertensive states at a time at which adrenaline plasma levels had returned to pre-infusion (or depot implantation) levels (Majewski *et al.*, 1981; Johnson *et al.*, 1983; Coppes *et al.*, 1994). In spontaneously hypertensive rats (SHR), Kubo *et al.* (1984) showed that facilitation of neurotransmission mediated by prejunctional β-adrenoceptors is enhanced in prehypertensive states. Furthermore, when SHR were adrenodemedullated at a pre-hypertensive age, the development of hypertension was attenuated but could be restored by adrenaline depot implants; this pro-hypertensive effect of adrenaline was abolished by β_2-adrenoceptor blockade (Borkowski & Quinn, 1985; Borkowski, 1991).

The present results show a new example for this relationship between prejunctional β-adrenoceptors and hypertension: chronic blockade of adenosine receptors (1) leads to a hypertensive state and (2) enhances prejunctional β-adrenoceptor-mediated facilitation of noradrenaline release, suggesting that both adenosine and β-adrenoceptors may be involved in the development of the hypertensive state.

References

ALBINO-TEIXEIRA, A., MATIAS, A., POLÓNIA, J. & AZEVEDO, I. (1991). Blockade of adenosine receptors causes hypertension and cardiovascular structural changes in the rat. *J. Hypertens.*, **9**, (Suppl.6), S196–S197.

ALLGAIER, C., HERTTING, G. & KUGELGEN, O. (1987). The adenosine receptor-mediated inhibition of noradrenaline release possibly involves a N-protein and is increased by α_2-autoreceptor blockade. *Br. J. Pharmacol.*, **90**, 403–412.

BORKOWSKI, K.R. (1991). Effects of adrenal demedullation and adrenaline on hypertension development and vascular reactivity in young spontaneously hypertensive rats. *J. Auton. Pharmacol.*, **11**, 1–14.

BORKOWSKI, K.R. & QUINN, P. (1985). Adrenaline and the development of spontaneous hypertension in rats. *J. Auton. Pharmacol.*, **5**, 89–100.

COPPES, R.P., BROUWER, F., FREIE, I., SMIT, J. & ZAAGSMA, J. (1994). Sustained prejunctional facilitation of noradrenergic neurotransmission by adrenaline as a co-transmitter in the portal vein of freely moving rats. *Br. J. Pharmacol.*, **113**, 342–344.

DAHLÖF, C. (1981). Studies on β-adrenoceptor mediated facilitation of sympathetic neurotransmission. *Acta Physiol. Scand.*, (Suppl.), **500**, 1–147.

EIKENBURG, D.C. & APPARSUNDARAM, S. (1992). Endogenous adenosine inhibits β-adrenoceptor facilitation of norepinephrine release in the heart nerve preparation. *Abstracts. Stichting 7th Int. Catecholamine Symposium* (Amsterdam), p.81.

ENERO, M.A. & SAIDMAN, B.Q. (1977). Possible feed-back inhibition of noradrenaline release by purine compounds. *Naunyn-Schmied Arch. Pharmacol.*, **297**, 39–46.

FLORAS, J.S. (1992). Epinephrine and the genesis of hypertension. *Hypertension*, **19**, 1–18.

GUIMARÃES, S., BRANDÃO, F. & PAIVA, M.Q. (1978). A study of the adrenoceptor-mediated feedback mechanisms by using adrenaline as a false transmitter. *Naunyn-Schmied Arch. Pharmacol.*, **305**, 185–188.

GUIMARÃES, S. & OSSWALD, W. (1969). Adrenergic receptors in the veins of the dog. *Eur. J. Pharmacol.*, **5**, 133–140.

GUIMARÃES, S. & PAIVA, M.Q. (1981a). Two distinct adrenoceptor-biophases in the vasculature: one for α- and the other for β-agonists. *Naunyn-Schmied. Arch. Pharmacol.*, **316**, 195–199.

GUIMARÃES, S. & PAIVA, M.Q. (1981b). Two different biophases for adrenaline released by electrical stimulation or tyramine from the sympathetic nerve endings of the dog saphenous vein. *Naunyn-Schmied. Arch. Pharmacol.*, **316**, 200–204.

GUIMARÃES, S., PAIVA, M.Q., MOURA, D., VAZ-DA-SILVA, M.J. & ALBINO-TEIXEIRA, A. (1994). Long-term administration of 1,3-dipropyl-8-sulfophenylxanthine (DPSPX) alters α_2-adrenoceptor-mediated effects at the pre- but not at the postjunctional level. *Naunyn-Schmied. Arch. Pharmacol.*, **350**, 692–695.

JOHNSON, M.D., GRIGNOLO, A., KUHN, C.M. & SCHANDBERG, S.M. (1983). Hypertension and cardiovascular hypertrophy during chronic catecholamine infusion in rats. *Life Sci.*, **33**, 169–180.

KUBO, T., KUWAHARA, M. & MISU, Y. (1984). Effect of isoproterenol on vascular adrenergic neurotransmission in prehypertensive and hypertensive spontaneously hypertensive rats. *Jpn. J. Pharmacol.*, **36**, 419–421.

LANDS, A.M., ARNOLD, A., MCAULIFF, J.P., LUDUENA, F.P. & BROWN, T.G. (1967). Differentiation of receptor systems activated by sympathomimetic amines. *Nature*, **214**, 597–598.

LIMBERGER, N., SPÄTH, L. & STARKE, K. (1988). Presynaptic α_2-adrenoceptor, opioid κ-receptor and adenosine A_1-receptor interaction on noradrenaline release in rabbit brain cortex. *Naunyn-Schmied. Arch. Pharmacol.*, **338**, 53–61.

MAJEWSKI, H. (1983). Modulation of norepinephrine release by activation of presynaptic β-adrenoceptors. *J. Auton. Pharmacol.*, **3**, 47–60.

MAJEWSKI, H., TUNG, L-H. & RAND, M.J. (1981). Adrenaline induced hypertension in rats. *J. Cardiovasc. Pharmacol.*, **3**, 179–185.

MATIAS, A., ALBINO-TEIXEIRA, A., POLÓNIA, J. & AZEVEDO, I. (1991). Long-term administration of 1,3-dipropyl-8-sulfophenylxanthine causes arterial hypertension. *Eur. J. Pharmacol.*, **193**, 101–104.

MISU, Y.M. & KUBO, T. (1986). Presynaptic β-adrenoceptors. *Med. Res. Rev.*, **612**, 197–225.

MISU, Y., KUWAHARA, M. & KUBO, T. (1987). Some relevance of presynaptic β-adrenoceptors to development of hypertension in spontaneously hypertensive rats. *Arch. Int. Pharmacodyn.*, **287**, 299–308.

NEDERGAARD, O.A. & ABRAHAMSEN, J. (1990). Modulation of noradrenaline release by activation of presynaptic β-adrenoceptors in the cardiovascular system. *Ann. N.Y. Acad. Sci.*, **604**, 508–544.

VAN ROSSUM, J.M. (1963). Cumulative dose-response curves. Technique for the making of dose-response curves in isolated organs and the evaluation of drug parameters. *Arch. Int. Pharmacodyn.*, **143**, 299–330.

(Received November 30, 1994
Revised January 9, 1995
Accepted January 12, 1995)

British Journal of Pharmacology (1995) 114, 1599–1604 © 1995 Stockton Press All rights reserved 0007–1188/95 $12.00

Differential effects of phosphoramidon on contractile responses to angiotensin II in rat blood vessels

Lihua Chen, J. Robert McNeill, Thomas W. Wilson & [1]Venkat Gopalakrishnan

Cardiovascular Risk Factor Reduction Unit (CRFRU), Department of Pharmacology, College of Medicine, University of Saskatchewan, Saskatoon, SK, S7N 0W0, Canada

1 Cumulative concentration-tension response (C-R) curves to angiotensin II (AII), big endothelin-1 (big ET-1), ET-1 and arginine vasopressin (AVP) were determined in endothelium intact-ring preparations of aorta, mesenteric artery and tail artery isolated from adult male Sprague-Dawley rats in the presence or absence of the neutral metalloprotease inhibitor, phosphoramidon.

2 The order of sensitivity of the three rat vascular smooth muscle preparations to AII, big ET-1 and ET-1 was aorta > mesenteric artery > tail artery whereas that for AVP was reversed, namely, tail artery > mesenteric artery > aorta.

3 Phosphoramidon blocked the responses to AII in a concentration-dependent manner, whereas even very high concentrations of phosphoramidon (100 μM) failed to affect the tension responses evoked by ET-1 and AVP in all three preparations. Low concentrations of phosphoramidon (10 μM) produced significant increases in EC_{50} values for AII in tail artery ($P<0.01$) and mesenteric artery ($P<0.05$) but not in aorta. The rank order of sensitivity to the inhibition by phosphoramidon was tail artery > mesenteric artery > aorta. Phosphoramidon-evoked rightward shifts in the C-R curves to AII were much higher than those to big ET-1 in both mesenteric artery and tail artery.

4 In endothelium-denuded preparations, AII failed to evoke any increases in tension in tail artery while the responsiveness of the mesenteric artery to AII was reduced significantly relative to endothelium-intact tissues with a rightward shift in the C-R curve and a decrease in the maximal response. On the other hand, the C-R curve to AII was shifted to the left in aorta following removal of the endothelium. Importantly, ET-1 and AVP evoked vasoconstrictor responses were unaffected by the inclusion of a high concentration of phosphoramidon (100 μM) in endothelium-denuded aorta and mesenteric artery.

5 The results suggest that AII-evoked tension responses of blood vessels such as tail artery are completely endothelium-dependent; in relatively larger blood vessels such as mesenteric artery they are partially endothelium-dependent while in much bigger conduit type blood vessel such as aorta, they are endothelium-independent. It is concluded that the vasoconstrictor responses to AII in mesenteric artery and tail artery may be mediated by the release of endothelins from the endothelium by increased formation from big ET, an effect that is blocked by phosphoramidon.

Keywords: Angiotensin II: endothelins; vasopressin; phosphoramidon; endothelium; endothelin converting enzyme; vascular smooth muscle; aorta; mesenteric artery; tail artery

Introduction

Recent studies have shown that prolonged incubation with angiotensin II (AII) promotes the release of endothelin-1 (ET-1) from endothelial cells and rat mesangial cells in culture (Emori *et al.*, 1991; Kohno *et al.*, 1992). Perfusion of the mesenteric arterial bed with AII (100 nM) for 5 h potentiated the vascular responses to noradrenaline via release of ET-1 in the spontaneously hypertensive rat (SHR) but not in the normotensive Wistar-Kyoto (WKY) rat (Dohi *et al.*, 1992). Despite these observations with either cultured endothelial cells or perfusion model systems, there is no direct evidence implicating a role for ETs in AII-mediated changes in vascular smooth muscle tone of normotensive rats. Although heterogeneity in the vascular responsiveness to AII has been shown (Toda *et al.*, 1990), the possibility that altered production of ETs could contribute to the differences in sensitivity has not been investigated in the same species with vascular smooth muscle tissues from different vascular beds.

It is now well-established that the 21 amino acid vasoconstrictor peptide, ET-1, is not stored in endothelial cells but that it is generated by cleaving a 39-(porcine) or 38-(human) amino acid intermediate, termed big ET-1. This unusual proteolytic processing is achieved by a putative ET peptide converting enzyme, a neutral metallopeptidase present in both vascular smooth muscle cells and endothelial cells. This enzyme is sensitive to blockade by phosphoramidon (Ikegawa *et al.*, 1991). Phosphoramidon has been shown to inhibit both the *in vivo* pressor effect and the *in vitro* contractile actions of big ET-1 without affecting the vasoconstrictor properties of exogenous ET-1 (Kashiwabara *et al.*, 1989; Fukuroda *et al.*, 1990; Auguet *et al.*, 1992; Opgenorth *et al.*, 1992). Therefore, our major aim was to investigate whether tension responses to AII are attenuated when ET converting enzyme is inhibited by phosphoramidon. We have used ring preparations of rat arteries, of varying sizes, namely aorta, mesenteric artery and tail artery obtained from normotensive adult Sprague-Dawley rats. In order to elucidate whether the observed effects are unique to AII, comparative studies with other vasoconstrictor peptides such as ET-1, arginine vasopressin (AVP) and big ET-1 were performed.

Methods

Tension measurement

Ring preparations of the thoracic portion of the aorta (length 5 mm aorta), the superior mesenteric artery (3 mm, mesenteric artery), and the ventral caudal artery (2 mm, tail artery) isolated from adult Sprague Dawley rats (14–16 weeks) were set up for isometric tension measurements in 20 ml organ baths containing modified Krebs physiological salt solution

[1] Author for correspondence.

(PSS) oxygenated with 95% O_2/5% CO_2 at 37°C. The composition of the PSS (in mM) was: NaCl 118, KCl 4.7, KH_2PO_4 1.2, $MgCl_2.6H_2O$ 1.2, $CaCl_2.2H_2O$ 1.8, $NaHCO_3$ 25.0 and glucose 11.1 (Gopalakrishnan *et al.*, 1985). We confirmed that all three vascular smooth muscle preparations were optimally stretched for maximum force development. This was carried out by plotting maximum tension developed at a fixed concentration of ET-1 (100 nM) at various levels of preload tension. Aorta and mesenteric artery developed maximum force when resting tensions of 2 g and 1 g respectively were applied to these vessels. However, tail artery generated a maximal tension response at a preload level of 0.8 g. At a preload tension of 0.5 g, it developed 93% of its maximal tension. To avoid undue stretching of this minute blood vessel, we maintained 0.5 g of preload tension for this vessel. Several laboratories have used a similar preload tension for the tail artery (Kosaki *et al.*, 1993; Szocik *et al.*, 1993).

The increases in isometric tension under resting and agonist(s) stimulated conditions were recorded on a Grass 7E polygraph with FTO.3 force transducers. After an initial 1 h equilibration period with repeated washings every 20 min, the tissues were challenged with KCl (80 mM) with isotonicity being maintained by appropriate reduction in NaCl. The presence of a functional endothelium was confirmed by studying the relaxation responses to 1 μM acetylcholine (ACh) in all three vascular smooth muscle tissues pre-contracted with a standard 1 μM concentration of phenylephrine (PE). In these initial responses, peptide agonists were not used in order to avoid desensitization. In other experiments, endothelium was removed through chemical stripping by incubating the tissues for 3 s with Triton X-100 (0.5% in PSS) followed by several repeated washings with normal PSS. Previous studies have shown that brief exposure to this detergent selectively destroys the endothelial layer of both vascular and cardiac preparations (Brutsaert *et al.*, 1988). The absence of endothelium was confirmed by lack of relaxation responses to ACh in tissues pre-contracted with PE.

Aorta, mesenteric artery and tail artery rings obtained from the same animal were set up for measurements of tension with intact endothelium (on the same day) for comparison of differences in responsiveness to AII. Each tissue was exposed to only a single cumulative concentration-response (C-R) determination for AII (either in the presence or absence of endothelium) to avoid tachyphylaxis. Thus, all determinations were carried out only once and a single cumulative concentration-response curve was generated for each preparation. In order to determine if tachyphylaxis occurred during the cumulative addition of AII, preliminary experiments in parallel rings were conducted as follows. Each ring was exposed to one single maximal concentration of AII (10 μM) or a similar concentration achieved by a step wise addition in a cumulative fashion.

Whenever phosphoramidon (10–100 μM) was included, it was added 30 min before the addition of the agonist. Ring preparations that did not receive any phosphoramidon were set up in parallel and served as controls. At the end of the experiment, tissues were blotted dry, weighed, and the cross sectional areas were calculated as described earlier (Wyse, 1980). This was necessary in order to express the data for maximal tension (E_{max}) developed as g mm^{-2} after the addition of the agonist in each preparation taking into consideration the cross sectional area of the preparation.

Drugs used

Angiotensin II octapeptide (AII), endothelin-1 (ET-1), big ET-1 and arginine vasopressin (AVP) were obtained from either Peninsula Laboratories (Belmont, CA, U.S.A.) or Bachem Inc. (Torrance, CA, U.S.A.). Phenylephrine hydrochloride (PE) and acetylcholine chloride (ACh), Triton X-100 and phosphoramidon were purchased from Sigma (St. Louis, MO, U.S.A.). In order to ensure the reproducibility of the effects of phosphoramidon, it was also obtained from another source (Peninsula Laboratories, Belmont, CA, U.S.A.). Drugs were added to the organ baths in volumes between 40–100 μl to provide the required final bath concentrations.

Data analyses

Each cumulative C-R curve was analysed individually to estimate the concentration required to produce 50% of the maximal response (EC_{50}) and the maximal increase in tension (E_{max}) by using ALL FIT programme (De Lean *et al.*, 1978). The data were expressed as mean ± s.e.mean values. The comparison of mean values between various groups was performed by analysis of variance (Super ANOVA package Macintosh). Simultaneous multiple comparisons were examined by Scheffe's F test.

Results

Responses to AII in the presence of endothelium

AII evoked concentration-dependent increases in vascular smooth muscle tone. Similar levels of maximal tension were obtained either by stepwise cumulative addition of AII or by the addition of a single maximal concentration of AII (10 μM). These data suggest that there was no tachyphylaxis to AII responses during the first cumulative C-R curve in these tissues. Initial experiments performed with a fixed concentration of AII (1 μM) revealed that preincubation with increasing concentrations of phosphoramidon (10–50 μM) for a period of 30 min led to concentration-dependent diminution in the maximal tension responses to AII. However, the inhibitory effect of AII-evoked responses by phosphoramidon was relatively less in aorta whereas incubation with a high concentration of phosphoramidon (50 μM) led to partial and complete abolition of the tension responses to AII in the mesenteric artery and tail artery rings respectively. Increasing the duration of incubation with phosphoramidon to 1 h did not result in further inhibition of AII responses (data not shown). The rank order of sensitivity to AII amongst these three blood vessels was: aorta > mesenteric artery > tail artery (Table 1).

Pretreatment with phosphoramidon produced concentration-dependent, non-competitive blockade with rightward shifts in the C-R curves and reduction of maximal responses to AII (Figure 1a, b, c). While both maximal tension responses (E_{max} values) and potency (EC_{50} values) were significantly diminished in mesenteric artery ($P<0.05$) and tail artery ($P<0.01$) with the lowest concentration of phosphoramidon (10 μM), the responses of aorta to AII remained unaffected. Incubation with a higher concentration of phosphoramidon (50 μM) led to complete abolition of the AII responses in tail artery whereas the responses of aorta to AII was only slightly but significantly diminished by this concentration of phosphoramidon. The order of sensitivity for blockade of AII-evoked tension responses by phosphoramidon was: tail artery > mesenteric artery > aorta (Table 1).

Responses to other peptides in aorta, mesenteric artery and tail artery with intact endothelium

In order to elucidate whether the inhibitory effect of phosphoramidon was selective for AII-evoked responses, comparative studies with other peptides such as big ET-1, ET-1 and AVP were performed. The cumulative C-R curves to big ET-1, ET-1 and AVP obtained either in the presence or the absence of a very high concentration of phosphoramidon (100 μM) are shown in Figure 2a, b and c respectively. The pooled data of EC_{50} and E_{max} values obtained from these C-R curves ($n = 4$) is shown in Table 2. The rank order of sen-

sitivity of these blood vessels to ET-1 and big ET-1 were similar to AII (aorta> mesenteric artery> tail artery) whereas the responsiveness of these blood vessels to AVP showed a reverse rank order of tail artery> mesenteric artery> aorta. Aorta was the least sensitive of the three blood vessels to AVP.

The C-R curves to big ET-1 were shifted to the right by phosphoramidon (100 μM) in all three blood vessels (Figure 2a and Table 2). However, as for AII, the non-competitive nature of blockade by phosphoramidon was most clearly evident for big ET-1-evoked responses only for tail artery. The evoked tension responses were almost completely

Table 1 Analyses of the cumulative concentration-tension response curves to angiotensin II (AII) in the ring preparations of rat aorta, mesenteric artery and tail artery with intact endothelium in the presence and absence of various concentrations of phosphoramidon (Phos) maintained in the bathing medium for 30 min

	Aorta		*Mesenteric artery*		*Tail artery*	
Treatment	EC_{50} (nM)	E_{max} (g mm^{-2})	EC_{50} (nM)	E_{max} (g mm^{-2})	EC_{50} (nM)	E_{max} (g mm^{-2})
Control	13.2 ± 1.1	0.30 ± 0.01	92.5 ± 4.2†	0.72 ± 0.04†	167.7 ± 7.2†	0.70 ± 0.04†
Phos 10 μM	13.4 ± 1.5	0.29 ± 0.01	138 ± 6.2*	0.64 ± 0.04*	2001 ± 40.8**	0.32 ± 0.05**
20 μM	17.0 ± 1.1	0.29 ± 0.02	190.3 ± 4.1**	0.61 ± 0.03*	>2 μM**	0.12 ± 0.03**
50 μM	21.7 ± 1.7*	0.24 ± 0.03*	386.7 ± 31.8**	0.57 ± 0.04**	NR**	NR**

NR denotes – no response. Each value is mean ± s.e.mean of 6 separate tissues from different animals.
*$P<0.05$ and **$P<0.01$ compared to respective control group data; †$P<0.01$ compared to respective control data for rat aorta.

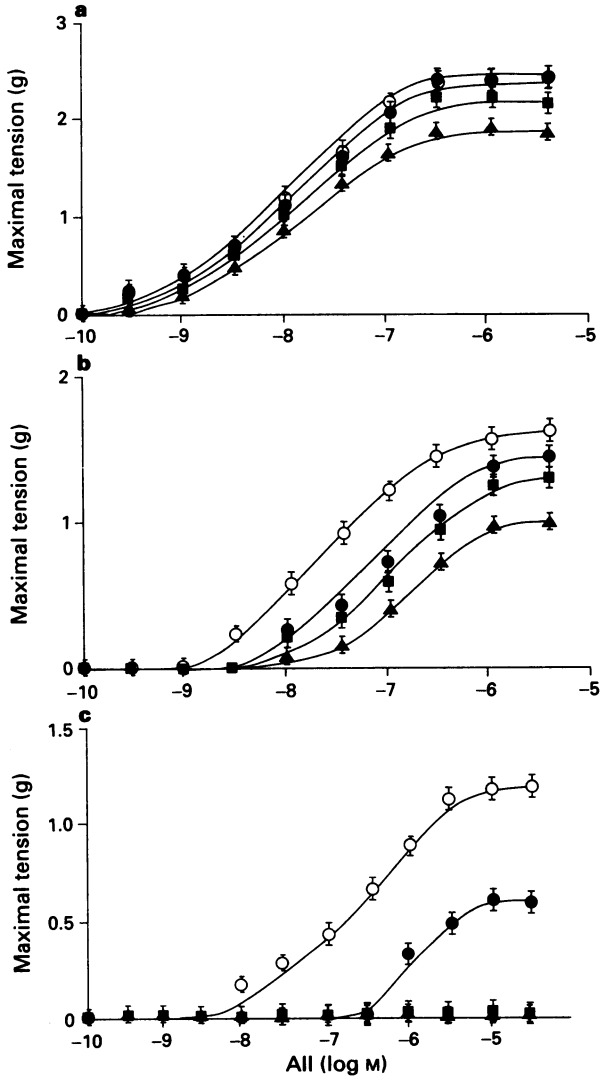

Figure 1 Cumulative concentration-tension response curves (C-R) to angiotensin II (AII) in ring preparations of rat aorta (a), rat mesenteric artery (b) and rat tail artery (c) with intact endothelium either in the presence or the absence (control group, O) of increasing concentrations of phosphoramidon (10 μM ●, 20 μM ■ and 50 μM ▲) maintained in the medium for a period of 30 min prior to the addition of AII. It was ascertained that there was no tachyphylaxis with the first C-R curve and each tissue was exposed to only one C-R curve. Each data point is the mean ± s.e.mean of 6 separate experiments.

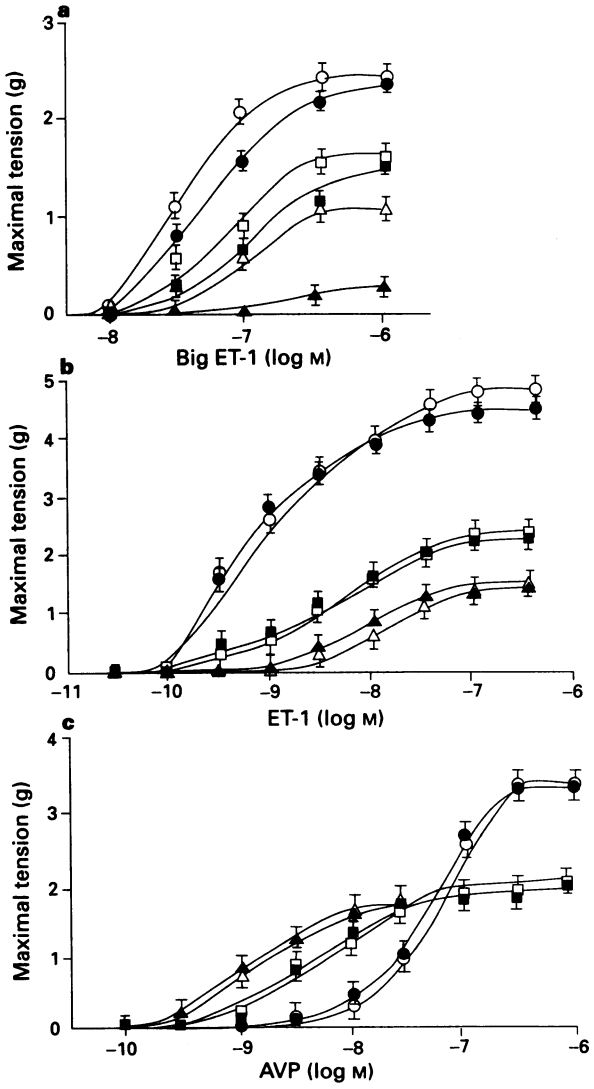

Figure 2 Cumulative concentration-response (C-R) curves to big endothelin-1 (big ET-1, a), endothelin-1 (ET-1, b) and arginine vasopressin (AVP, c) in the ring preparations of aorta (Control O, phosphoramidon ●), mesenteric artery (Control □, phosphoramidon ■) and tail artery (Control, Δ, phosphoramidon ▲) with intact endothelium either in the presence or the absence (control group) of a fixed concentration of phosphoramidon (100 μM). Each data point shown is the mean ± s.e.mean of 4 separate experiments using tissues obtained from different animals.

Table 2 Analyses of the cumulative concentration-tension response curves to big endothelin-1 (big ET-1), ET-1 and arginine vasopressin (AVP) in the ring preparations of rat aorta, mesenteric artery and tail artery with intact endothelium either in the presence or the absence of phosphoramidon (Phos) 100 μM for 30 min

		Big ET-1		*ET-1*		*AVP*	
Tissue	*Treatment*	EC_{50} (nM)	E_{max} (g mm^{-2})	EC_{50} (nM)	E_{max} (g mm^{-2})	EC_{50} (nM)	E_{max} (g mm^{-2})
Aorta	Control	46.3 ± 3.0	0.31 ± 0.01	1.1 ± 0.1	0.47 ± 0.02	44.2 ± 2.1	0.42 ± 0.03
	Phos	60.3 ± 2.3*	0.32 ± 0.01	1.3 ± 0.2	0.45 ± 0.02	44.1 ± 2.3	0.38 ± 0.03
Mesenteric artery	Control	62.6 ± 1.8	0.64 ± 0.04	2.7 ± 0.2	0.99 ± 0.03	18.5 ± 0.5	0.76 ± 0.03
	Phos	87.1 ± 3.7*	0.64 ± 0.02	2.8 ± 0.2	0.91 ± 0.03	18.2 ± 0.6	0.76 ± 0.04
Tail artery	Control	74.7 ± 2.9	0.56 ± 0.03	4.5 ± 0.3	0.84 ± 0.02	5.5 ± 0.2	0.77 ± 0.03
	Phos	NR**	0.22 ± 0.01**	4.6 ± 0.3	0.74 ± 0.04	5.4 ± 0.2	0.81 ± 0.03

*$P<0.05$; **$P<0.01$ compared to their respective control values in the same tissues. NR denotes – no response. Each value shown is mean ± s.e.mean of 4 separate experiments performed either in the presence or the absence (control group) of Phos using paired ring preparations set up on the same day.

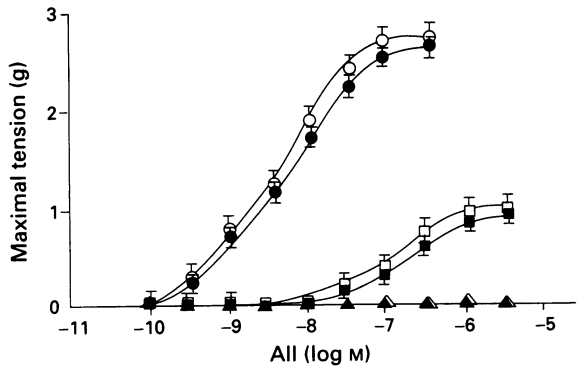

Figure 3 Cumulative concentration-response (C-R) curves to angiotensin II (AII) in endothelium-denuded ring preparations of aorta (Control ○, phosphoramidon, ●), mesenteric artery (Control, □, phosphoramidon, ■) and tail artery (Control △, phosphoramidon ▲) either in the presence or the absence (control group) of a fixed concentration of phosphoramidon (100 μM) maintained in the incubation medium for 30 min prior to the addition of AII. Endothelium was removed by a 3 s exposure of the tissues to Triton X-100 (0.5%) followed by repeated washings in PSS. The absence of a functional endothelium was confirmed by the attenuation of the relaxation response to 1 μM acetylcholine in phenylephrine precontracted tissues. Each data point shown is the mean ± s.e.mean of 4 separate experiments on tissues obtained from different animals. Note: Endothelium-denuded tail artery rings failed to elicit any tension responses to AII; however, the same tissues did respond to AVP and ET-1 with a closely similar response pattern to that in tail artery rings with intact endothelium.

abolished in tail artery rings exposed to phosphoramidon (100 μM). In the case of aorta and mesenteric artery, pretreatment with phosphoramidon (100 μM) led to a small but significant ($P<0.05$) increase in EC_{50} without significant change in the maximal response (Figure 2a and Table 2).

In contrast to AII and big ET-1, preincubation with a very high concentration of phosphoramidon (100 μM) failed to affect the C-R curves to ET-1 (Figure 2b) and AVP (Figure 2c) in all three arteries with intact endothelium. There were no significant differences in EC_{50} and E_{max} values between the control and phosphoramidon (100 μM) pretreated group (Table 2). Moreover, increasing the preincubation period to 1 h for phosphoramidon did not affect the responses to ET-1 and AVP (data not illustrated). PE-evoked tension responses were also unaffected by the inclusion of phosphoramidon (100 μM) in all three preparations (data not shown).

Responses to AII in endothelium-denuded aorta, mesenteric artery and tail artery

In endothelium-denuded tissues, incubation with very high concentrations of phosphoramidon (100 μM) failed to evoke significant alterations in the control C-R curves to AII in all the three preparations (Figure 3).

Discussion

This study demonstrates that there are regional variations in sensitivity to AII in rat arteries of varying sizes. To the best of our knowledge, this is the first paper which compares differences in sensitivity to AII in these three blood vessels. It provides a possible explanation that the release of ET evoked by AII could vary in different vascular beds and that this could be one amongst several factors that could contribute to the differences in sensitivity. The study also provides a comparison of differences in the rank order of sensitivity among these three blood vessels to AVP, AII and ET-1.

Previously, we have shown that AII evokes tension responses in conduit type blood vessels such as aorta by the direct stimulation of vascular AT_1 receptors, whereas in the case of blood vessels like the mesenteric artery and tail artery, the responses to AII are mediated by the activation of both vascular (direct) and endothelial (indirect) AT_1 receptors. Activation of endothelial AT_1 receptors are possibly linked to processes capable of endothelin release (Chen *et al.*, 1993; Gopalakrishnan *et al.*, 1994). In the present study, using the ET converting enzyme inhibitor, phosphoramidon, we provide further evidence for the probable participation of ET release from endothelium in AII-evoked tension responses in vascular smooth muscle preparations such as tail artery and mesenteric artery. The lack of responsiveness of these blood vessels to AII could not be due to tachyphylaxis or desensitization to AII because the inhibitory effects of phosphoramidon on AII responses were seen in tissues exposed to the first cumulative C-R curve to AII. Previously, desensitization/tachyphylaxis to AII has been characterized in aortic rings only for the second and third cumulative response determinations (Kuttan & Sim, 1993). The present data confirm that the level of dependence on indirect ET release may be much less in conduit type blood vessels such as aorta, whereas the responses of tail artery to AII are mediated mainly by the release of ETs. Increased expression of prepro ET mRNA by both AVP and AII has been demonstrated in cultured cells and isolated vascular beds subjected to perfusion for a prolonged time (Emori *et al.*, 1991; Kohno *et al.*, 1992; Dohi *et al.*, 1992; Tomobe *et al.*, 1993). However, these studies failed to examine whether acute addition of AII or AVP is linked to the immediate regulation of vascular smooth muscle tone via release of ETs. Earlier studies that attempted to examine the heterogeneity in vascular smooth muscle responsiveness to AII explained it on the basis of differences in the levels of eicosanoids (Toda *et al.*, 1990; Lin & Nasjletti, 1991) or the levels of sympathetic tone in different vascular beds (Malik & Nasjletti, 1976; Story & Ziogas, 1986). In the present study, we suggest that AII releases ET from endothelium, particularly in blood

vessels with smaller lumen such as tail artery and mesenteric artery and this could also contribute to the differences in sensitivity.

Since the discovery of ETs, the identification and characterization of endothelin converting enzyme has been the subject of intense investigation (Fukuroda *et al.*, 1990; Ikegawa *et al.*, 1991; Opgenorth *et al.*, 1992). Although earlier studies have demonstrated that AII and other peptides enhanced ET release via increased gene transcription, none of these studies has looked at the possibility that these effects could also take place at the posttranscription/posttranslational locus of increased conversion from big ET to ET. While it has been proposed that several different enzymes such as aspartic protease and cathespin E are involved in the formation of ET-1 from big ET-1, it is now recognized that the neutral endopeptidase that is susceptible to blockade by phosphoramidon, plays a crucial and perhaps a physiologically important role in the formation of ET-1 (Opgenorth *et al.*, 1992). Our observation that AII-evoked tension responses were abolished selectively by phosphoramidon in a concentration-dependent and non-competitive manner in the mesenteric artery and the tail artery preparations with intact endothelium suggests that AII could promote the formation of ET from big ET.

Three key observations made in this study strongly support the suggestion that ET release from endothelial cells could play a crucial role in the tension responses to AII in blood vessels such as tail artery and mesenteric artery. Firstly, in endothelium-denuded ring preparations, AII failed to evoke any increase in tension in tail artery and in the case of mesenteric artery, the responses were significantly attenuated. These data parallel those in the same preparations with intact endothelium preincubated with phosphoramidon suggesting that the endothelin converting enzyme inhibition by phosphoramidon occurs at the level of the endothelium. Secondly, there were no significant differences in the C-R curves between the control and phosphoramidon pretreated groups in endothelium-denuded preparations, confirming that phosphoramidon failed to evoke further inhibition after the removal of endothelium. The observations that the responses to AVP and ET-1 could be demonstrated in tail artery with either intact endothelium incubated with high concentration of phosphoramidon (100 μM) or endothelium-denuded tail artery preparations that failed to respond to AII confirmed that these tissues exhibited selective loss of responsiveness to AII. Thirdly, and most importantly, studies with big ET-1 revealed that the shifts in the C-R curves in phosphoramidon pretreated tissues were much higher in the case of mesenteric artery and that there was almost complete attenuation of responses to big ET-1 in the case of tail artery rings with intact endothelium. Thus, both AII and big ET-1 evoked responses were affected in a similar manner by phosphoramidon in mesenteric artery and tail artery. In support of our major observation, a recent report has also shown that AII potentiated the increased perfusion pressure induced by noradrenaline in tail artery *in vitro*, and that this effect of AII was abolished by removal of the endothelium. This report attributed this response to the existence of an endothelium-derived contracting factor (EDCF) whose release was stimulated by AII (Thorin & Atkinson, 1994). Previously, it was proposed that ET-1 could be the EDCF involved in potentiating noradrenaline-induced vasoconstriction in tail artery (Reid *et al.*, 1991).

Comparison of AII responses with other agonists

It is well known that phosphoramidon inhibits both *in vitro* and *in vivo* vasoconstrictor responses to big ET-1 and not those evoked by ET-1 (Fukuroda *et al.*, 1990). In the present study, although it was observed that higher concentration of phosphoramidon (100 μM) did produce rightward shifts in the C-R curves to big ET-1 in both aorta and mesenteric artery, the maximal responses could be restored. Moreover, the degrees of shift in the EC_{50} values attained for big ET-1 were much lower than those evoked by a low concentration of phosphoramidon (50 μM) for AII in both aorta and mesenteric artery. These data provide evidence that phosphoramidon produces more effective inhibition of AII-evoked vasoconstrictor responses than those caused by big ET-1 in these three blood vessels with intact endothelium. Although several studies have shown that phosphoramidon causes complete inhibition of the pressor response to big ET-1, it is known that *in vitro* vasoconstrictor effects of big ET-1 are not completely attenuated by phosphoramidon. For example, the C-R curve to big ET-1 was shifted to the right in rabbit saphenous artery but not in saphenous vein (Auguet *et al.*, 1992). These data suggest that big ET-1 can evoke vasoconstriction either by directly activating ET receptors on vascular smooth muscle cells or by being converted to ET-1 by processes independent of phosphoramidon-sensitive ET converting enzyme. Like AII, prolonged perfusion of the rat mesenteric artery bed with AVP was also shown to augment ET release (Tomobe *et al.*, 1993). However, in the present study, we failed to see any inhibition of AVP-evoked responses by the ET converting enzyme inhibitor. These data confirmed the selective inhibition of AII responses by phosphoramidon, a finding that has not been reported earlier.

In summary, the data obtained with phosphoramidon, suggest that AII can evoke ET release from endothelium and that this effect accounts for a major part of the evoked vasoconstrictor response to AII in small blood vessels such as tail artery and mesenteric artery than in the aorta. It is likely that locally generated AII could reach concentrations high enough to stimulate ET release in blood vessels with smaller lumens thereby contributing to the maintenance of enhanced peripheral vascular smooth muscle tone.

This work was supported by a grant in aid from the Heart & Stroke Foundation of Saskatchewan to V.G., a Scholar of the Heart & Stroke Foundation of Canada.

References

AUGUET, M., DELAFLOTTE, S., CHABRIER, P.-E. & BRAQUET, P. (1992). The vasoconstrictor action of big endothelin-1 is phosphoramidon sensitive in rabbit saphenous artery but not in saphenous vein. *Eur. J. Pharmacol.*, **224**, 101–102.

BRUTSAERT, D.L., MEULEMANS, A.L., SIPIDO, K.R. & SYS, S.U. (1988). Effects of damaging the endocardial surface on the mechanical performance of isolated cardiac muscle. *Circ. Res.*, **62**, 357–366.

CHEN, L., GOPALAKRISHNAN, V. & MCNEILL, J.R. (1993). Endothelin dependent increases in vascular smooth muscle tone to angiotensin II in three vascular smooth muscle preparations of normotensive rats. *FASEB J.*, **7**, A474.

DE LEAN, A., MUNSON, P.J. & RODBARD, D.L. (1978). Simultaneous analysis of families of sigmoidal curves: application to bioassay, radioligand assay, and physiological dose-response curves. *Am. J. Physiol.*, **235**, E97–E105.

DOHI, Y., HAHN, A.W.A., BOULANGER, C.M., BUHLER, F. & LUSCHER, T.F. (1992). Endothelin stimulated by angiotensin II augments contractility of hypertensive rat resistance arteries. *Hypertension*, **19**, 131–137.

EMORI, T., HIRATA, Y., OHTA, K., KANNO, K., EGUCHI, S., IMAI, T., SCHICHIRI, M. & MARUMO, F. (1991). Cellular mechanism of endothelin-1 release by angiotensin II and vasopressin. *Hypertension*, **18**, 165–170.

FUKURODA, T., NOGUCHI, S., TSUCHIDA, M., NISHIKIBE, F., IKEMOTO, K., OKADA, K. & YANO, M. (1990). Inhibition of biological actions of big endothelin-1 by phosphoramidon. *Biochem. Biophys. Res. Commun.*, **172**, 390–395.

GOPALAKRISHNAN, V., CHEN, L., WILSON, T.W. & MCNEILL, J.R. (1994). Tension responses of the rat tail artery to angiotensin II (AII) is predominantly mediated by endothelin (ET) release. *J. Hypertension*, **12** (Suppl. 3), S155.

GOPALAKRISHNAN, V., PARK, L.E. & TRIGGLE, C.R. (1985). The effect of calcium channel agonist, Bay K-8644 on human vascular smooth muscle. *Eur. J. Pharmacol.*, **113**, 447–451.

IKEGAWA, R., MATSUMARA, Y., TSUKAHARA, M., TAKAOKA, M. & MORIMOTO, S. (1991). Phosphoramidon inhibits the generation of endothelin-1 from exogenously applied big endothelin-1 in cultured vascular and endothelial cells and smooth muscle cells. *FEBS Lett.*, **293**, 45–48.

KASHIWABARA, T., INAGAKI, Y., OHTA, S., IWAMATSU, A., NOMIZU, M., MORITA, A. & NISHIKORI, K. (1989). Putative precursors of endothelin have less vasoconstrictor activity in vitro but a potent pressor effect in vivo. *FEBS Lett.*, **247**, 73–76.

KOHNO, M., HORIO, T., YOKOKAWA, K., FUKUI, T., YASUNARI, K., KURIHARA, N. & TAKEDA, T. (1992). Angiotensin II stimulates endothelin-1 secretion in cultured rat mesangial cells. *Kidney Int.*, **42**, 860–866.

KOSAKI, F., WAKABAYASHI, S., SATO, T., MOCHIZUKI, S., TOMIYAMA, A., ZHOU, Q., SATAKE, N. & SHIBATA, S. (1993). Pharmacologic properties of KT2-962 6-isopropyl-3-[4-(p-Chlorobenzenesulfonylamino-Butyl]-Azulene-1-sulfonic acid sodium salt); a new TXA_2/prostaglandin endoperoxide receptor antagonist. *J. Cardiovasc. Pharmacol.*, **21**, 441–447.

KUTTAN, S.C. & SIM, S.K. (1993). Angiotensin II-induced tachyphylaxis in aortas of normotensive and hypertensive rats: changes in receptor affinity. *Eur. J. Pharmacol.*, **232**, 173–180.

LIN, L. & NASJLETTI, A. (1991). Role of endothelium-derived prostanoid in angiotensin induced vasoconstriction. *Hypertension*, **18**, 158–164.

MALIK, K.U. & NASJLETTI, A. (1976). Facilitation of adrenergic transmission by locally generated angiotensin II in rat mesenteric arteries. *Circ. Res.*, **38**, 26–30.

OPGENORTH, T.J., WU-WONG, J.R. & SHIOSAKI, K. (1992). Endothelin converting enzymes. *FASEB J.*, **6**, 2653–2659.

REID, J.J., VO, P.P., LIEN, A.T., WONG-DUSTING, H.K. & RAND, M.J. (1991). Modulation of norepinephrine-induced vasoconstriction by endothelin-1 and nitric oxide in rat tail artery. *J. Cardiovasc. Pharmacol.*, **17**, S272–S275.

STORY, D.F. & ZIOGAS, J. (1986). Role of endothelium on the facilitatory effects of angiotensin I and angiotensin II on noradrenergic transmission in the caudal artery of the rat. *Br. J. Pharmacol.*, **87**, 249–255.

SZOCIK, J.F., GARDNER, C.A. & WEBB, R.C. (1993). Inhibitory effects of bupivacaine and lidocaine on adrenergic neuroeffector junctions in rat tail artery. *Anesthesiology*, **78**, 911–917.

THORIN, E. & ATKINSON, J. (1994). Modulation by the endothelium of sympathetic vasoconstriction in an in vitro preparation of the rat tail artery. *Br. J. Pharmacol.*, **111**, 351–357.

TODA, N., AYAZIKI, K. & OKAMU, T. (1990). Modifications by endogenous prostaglandins of angiotensin II induced contractions in dog and monkey cerebral and mesenteric arteries. *J. Pharmacol. Exp. Ther.*, **252**, 374–379.

TOMOBE, Y., YANAGISAWA, M., FUJIMORI, A., MASAKI, T. & GOTO, K. (1993). Arginine-vasopressin increases the release of ET-1 into perfusate of rat mesenteric artery. *Biochem. Biophys. Res. Commun.*, **191**, 654–661.

WYSE, D.G. (1980). On 'the normalization' of active developed force of isolated helical strips of muscular and elastic arteries for variation in wall thickness. *J. Pharmacol. Methods*, **4**, 313–326.

(Received October 10, 1994
Revised December 19, 1994
Accepted January 11, 1995)

British Journal of Pharmacology (1995) 114, 1605–1612 © 1995 Stockton Press All rights reserved 0007–1188/95 $12.00

Cardiovascular actions of the furoxan CAS 1609, a novel nitric oxide donor

[1]Helmut Bohn, Joachim Brendel, Piero A. Martorana & Karl Schönafinger

Departments of Pharmacology and Medicinal Chemistry, Cassella AG, Frankfurt/Main, Germany

1 This study examines the cardiovascular effects of CAS 1609 (4-hydroxymethyl-furoxan-3-carboxamide) *in vitro* as well as *in vivo* in various animal models.

2 CAS 1609 relaxed guinea-pig pulmonary artery strips without endothelium with IC_{50}-values of 0.9 μM (phenylephrine contracted) and 15 μM (KCl-depolarized). This effect was inhibited by oxyhaemoglobin. In these arteries CAS 1609 significantly increased (+ 192%) guanosine 3':5'-cyclic monophosphate levels, which indicates that the compound acts as a donor of nitric oxide (NO).

3 In the anaesthetized pig, CAS 1609 (0.3–1.0 mg kg^{-1}, i.d.) significantly lowered blood pressure and left ventricular end-diastolic pressure. Left ventricular contractility was slightly reduced and heart rate remained almost unchanged.

4 In anaesthetized dogs, i.v. or i.d. administration of CAS 1609 (0.3–3.0 mg kg^{-1}) decreased, in a dose-related fashion, preload and afterload of the heart, cardiac output, left ventricular work and myocardial oxygen consumption. This haemodynamic profile is similar to that of known NO-donors.

5 In anaesthetized dogs with acute heart failure due to intracoronary injection of microspheres, CAS 1609 (0.3 mg kg^{-1}, i.v.) improved the haemodynamic condition and reduced mortality by 80%.

6 In conscious dogs, oral treatment with a dose of 0.5 mg kg^{-1} given twice daily at 07 h 00 min and 19 h 00 min (each dose had a duration of action $\geqslant$ 12 h) for 5 days showed no signs of tolerance to the haemodynamic effects of the drug.

7 All these data indicate that CAS 1609 is a potent, long-lasting orally active donor of NO, devoid of tolerance development.

Keywords: NO donor; pulmonary artery; haemodynamics; cardiovascular effects in pig; cardiovascular effects in dog; heart failure; tolerance; furoxan; CAS 1609

Introduction

Endogenous formation of nitric oxide (NO) in various tissues plays an important role in cell function and cell communication both in health and disease (Moncada *et al.*, 1991; Moncada & Higgs, 1993). In the cardiovascular system, NO derived mainly from endothelial cells inhibits vascular tone, activation and adhesion of blood cells (platelets, neutrophils), and smooth muscle cell proliferation. Substitution therapy with exogenous NO released from organic nitrates has been used successfully for decades in the prophylaxis and termination of acute attacks of angina pectoris. However, recently clinical relevant attenuation or even loss of anti-anginal effects following long-term intravenous, oral or transdermal treatment with organic nitrates were also demonstrated (Silber, 1990). This stimulated the search for new NO donors devoid of the problem of tolerance development. Although, the mechanism of nitrate tolerance is not fully understood, a nitrate specific metabolism yielding NO is thought to be mainly responsible for tolerance development (Chung & Fung, 1990; Bennett *et al.*, 1992; Kojda *et al.*, 1993; Persson *et al.*, 1994). We therefore synthesized potential NO donors belonging to the class of furoxans which are chemically different from the organic nitrates. Derivatives of this new class of NO donors have recently been reported to have vasorelaxant activity *in vitro* and to inhibit platelet aggregation (Ghigo *et al.*, 1992; Calvino *et al.*, 1992; Gasco *et al.*, 1993; Ferioli *et al.*, 1993; Civelli *et al.*, 1994). The novel furoxan, CAS 1609 (4-hydroxymethyl-furoxan-3-carboxamide), was selected for further pharmacological characterization because of its high potency and long duration of action *in vivo* as revealed in preliminary studies. CAS 1609 is soluble in water and contains two NO moieties in its chemical structure (Figure 1). This strongly suggests NO donating properties as the probable mechanism of action.

The aim of this study was to present the first pharmacological results obtained with CAS 1609 *in vitro* in isolated vessels and *in vivo* in anaesthetized and conscious animals (pig, dog). In view of the problem of nitrate tolerance we also studied the effect of long-term administration of CAS 1609 in conscious dogs.

Methods

Relaxant activity in contracted vessel strips

Male guinea-pigs in the weight range of 350–400 g were killed by cervical dislocation. Helical strips of the pulmonary

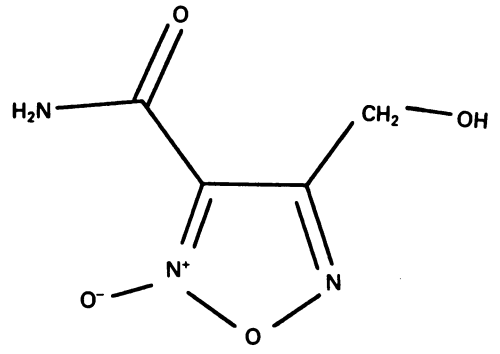

Figure 1 Chemical structure of CAS 1609 (4-hydroxymethyl-furoxan-3-carboxamide).

[1]Author for correspondence at: Cassella AG, Pharmaforschung, Hanauer Landstraße 526, D60386 Frankfurt/Main, Germany.

artery from which the endothelium had been mechanically removed were set up in an organ bath for recording isotonic changes in length. The composition of the oxygenated (95% O_2 and 5% CO_2 at 37°C) physiological salt solutions was as follows in mM: solution I: NaCl 112, KCl 5, $CaCl_2$ 1.2, $MgSO_4$ 0.56, KH_2PO_4 1.2, $NaHCO_3$ 25 and glucose 12; solution II: identical to solution I except for the omission of calcium and addition of EDTA 0.2; and solution III: NaCl 72, KCL 40, with no EDTA but otherwise identical to solution II. In the experiments with potassium depolarized artery strips, the protocol started with an equilibrium period of 30 min with solution I followed by solution II (three times 15 min to remove Ca^{2+}) and ended with the depolarizing solution. A sustained contraction of the depolarized artery was induced with Ca^{2+} (0.5 mM). In experiments with the α-adrenoceptor agonist, phenylephrine (1 μM) as contracting agent only solution I was used. When a stable plateau of the contraction was reached, the test compound was added. In order to obtain concentration-response curves, cumulative concentrations were given either at 1 h intervals or when the response of the previous dose had reached a steady level. In some experiments oxyhaemoglobin (10 μM, prepared according to Martin *et al.*, 1985) was added to the organ bath a few minutes before the first concentration of CAS 1609 was given. Oxyhaemoglobin was then present for the rest of the experiment. In another series of experiments, only one concentration of CAS 1609 was administered to record the time course of action.

Measurement of cyclic GMP

Guinea-pig pulmonary arteries, from which the endothelium had been removed, were placed into an oxygenated organ bath (37°C) containing 10 ml PSS, phenylephrine (1 μM) and 3-isobutyl 1-methylxanthine (IBMX) (1 mM). Five minutes later, vehicle or CAS 1609 (100 μM) was added. After another 30 min, the tissue was rapidly frozen in liquid-nitrogen, homogenized, and centrifuged in 0.05 M sodium acetate buffer at pH 4.0. Guanosine 3':5'-cyclic monophosphate (cyclic GMP) was quantified in the supernatant by a commercially available cyclic GMP enzyme-immunoassay. The protein content of each artery was quantified according to Lowry *et al.* (1951) and cyclic GMP levels were expressed as pmol cyclic GMP mg^{-1} protein.

Haemodynamic profile in anaesthetized pigs

Eleven male pigs of the German land race (20–26 kg) were anaesthetized with ketamine (20–25 mg kg^{-1}, i.m.), methomidate (8–10 mg kg^{-1}, i.p.), xylacine (2.5–3.0 mg kg^{-1}, i.m.) and pentobarbitone (25–30 mg kg^{-1}, i.v. as bolus followed by a continuous infusion at a rate of 0.16 mg kg^{-1} min^{-1}). After tracheal intubation, the animals were artificially ventilated with ambient air enriched with oxygen to maintain blood gas parameters within normal limits. A catheter was placed into the right femoral artery to measure blood pressure (BP) with a Statham 23Db pressure transducer. Left ventricular pressure, left ventricular end-diastolic pressure, contractility and heart rate (LVP, LVEDP, dP/dt, HR) were measured with a Millar PC 350 catheter-tipmanometer introduced into the left ventricle via the left carotid artery. When stable haemodynamic conditions were achieved for at least 30 min, CAS 1609 was administered through a catheter inserted into the duodenum. The haemodynamic effects were recorded continuously for 3 h.

Haemodynamic profile in anaesthetized dogs

Seventeen Labrador-Harrier dogs of either sex (17 to 25 kg), fasted overnight, were anaesthetized with pentobarbitone sodium (35 to 40 mg kg^{-1} as bolus i.v. plus 4 to 6 mg kg^{-1} h^{-1} as continuous i.v.-infusion). Artificial ventilation, surgical procedures and catheterization were similar to those described for the anaesthetized pig except for an additional catheter in the pulmonary artery to measure pulmonary artery pressures as well as cardiac output by the thermodilution method. The haemodynamic parameters determined included systolic blood pressure (BPs), diastolic blood pressure (BPd), left ventricular end-diastolic pressure (LVEDP), diastolic pulmonary artery pressure, heart rate (HR), maximal left ventricular contractility (dP/dt) and cardiac output (CO). Stroke volume was calculated as CO/HR, total peripheral resistance (TPR) as mean blood pressure (BPm/CO) × 79.9, left ventricular stroke work (LVSW) as (BPm – LVEDP) × SV × 0.000136, left ventricular minute work (LVMW) as LVSW × HR and myocardial oxygen consumption was calculated as pressure work index according to the formula $MVO_2 = 4.08 \times 10^{-4}(BPs \times HR) + 3.25 \times 10^{-4} \times ((0.8\ BPs + 0.2\ BPd) \times HR \times SV)/BW + 1.43$ where BW is body weight in kg (Rooke & Feigl, 1982). CAS 1609 was administered

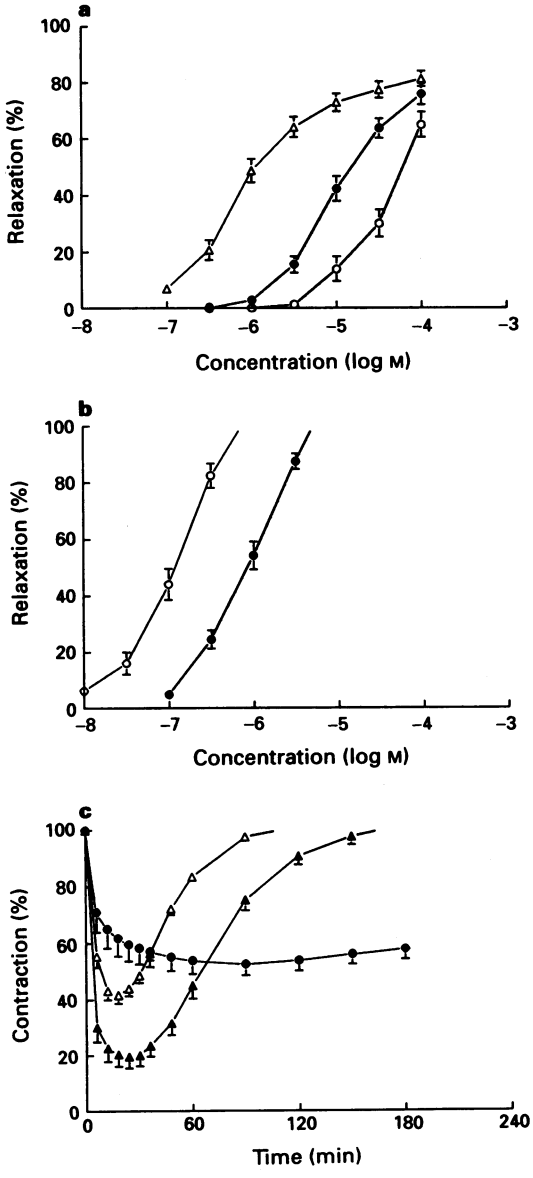

Figure 2 Relaxant activity of CAS 1609 and 3-morpholino sydnonimine (SIN-1) in strips of the guinea-pig pulmonary artery with the endothelium removed. (a) Concentration-response curves in potassium-depolarized strips (40 mM KCl): (Δ) SIN-1; (●) CAS 1609 and (○) CAS 1609 plus oxyhaemoglobin. The concentration of oxyhaemoglobin was 10 μM. (b) Concentration-response curves in phenylephrine (1 μM)-contracted strips. (○) SIN-1; (●) CAS 1609. (c) Time course of action of CAS 1609 (10 μM, ●) and SIN-1 (1 μM, Δ and 30 μM, ▲). Data are means ± s.e.mean, $n = 6–8$.

through a catheter either in the cephalic vein (i.v. administration) or in the duodenum (i.d. administration). Each dog received only one dose, except for the two lower doses which were tested in the same dogs. In that case, the interval between the administrations was 120 min.

Acute left ventricular failure in anaesthetized dogs

Twenty German shepherd dogs of either sex (21 to 34 kg) were anaesthetized with pentobarbitone sodium (35 mg kg^{-1}, i.v. as a bolus plus 4 mg kg^{-1} h^{-1} as continuous infusion) and artificially ventilated with ambient air enriched with oxygen such as to maintain blood gas parameters within normal limits. Surgical procedures included left thoracotomy at the fifth intercostal space and insertion of catheters in various veins and arteries similar to those mentioned above. Additionally, an electromagnetic flow probe was placed around the left circumflex coronary artery (LCX) and a cannula (Braunüle O-G 20 Braun, Melsungen, Germany) was retrogradely introduced into the left coronary artery. The position of the cannula was adjusted under X-ray control so that injected contrast medium (Conray 70, Byk Gulden, Konstanz, Germany) passed down both into the LCX and LAD. Acute ischaemic LV failure was induced by repeated intracoronary injections of plastic microspheres (3M Company, St. Paul, MN, U.S.A.) through this cannula. The microspheres (50 μm) were suspended in physiological saline with a drop of Tween-80 and sonified before use (approx. 12.000 microspheres ml^{-1}). Administration of the microspheres was performed every 5 min starting with a volume of 10 ml which was gradually reduced down to 1 ml. Each injection resulted in a stepwise increase in LVEDP. The embolization procedure was stopped when LVEDP increased by approximately 10 mmHg above baseline. Then the haemodynamic parameters were allowed to stabilize for 30 min. Animals were randomized in two experimental

Table 1 Haemodynamic effects of CAS 1609 in the anaesthetized pig: intraduodenal administration of 0.3 or 1.0 mg kg^{-1}

		Control values		*Effects*	
		0.3	1.0	0.3	1.0
BPs	(mmHg)	131 ± 6	133 ± 4	−26 ± 2*	−33 ± 3*
BPd	(mmHg)	91 ± 6	94 ± 3	−17 ± 3*	−23 ± 3*
LVEDP	(mmHg)	9.7 ± 1.4	8.4 ± 0.5	−1.4 ± 0.5	−3.1 ± 0.9*
LV dP/dt_{max}	(mmHg s^{-1})	2040 ± 117	1983 ± 149	−300 ± 45*	−350 ± 67*
HR	(beats min^{-1})	104 ± 8	102 ± 4	−4 ± 4*	−3 ± 5

BPs, systolic blood pressure; BPd, diastolic blood pressure; LVEDP, left ventricular end-diastolic pressure; LV dP/dt_{max}, left ventricular contractility; HR, heart rate. Data are means of the maximal effects ± s.e.mean, $n = 5$ with the low dose and 6 with the high dose. *Significant difference from control (Student's paired t test).

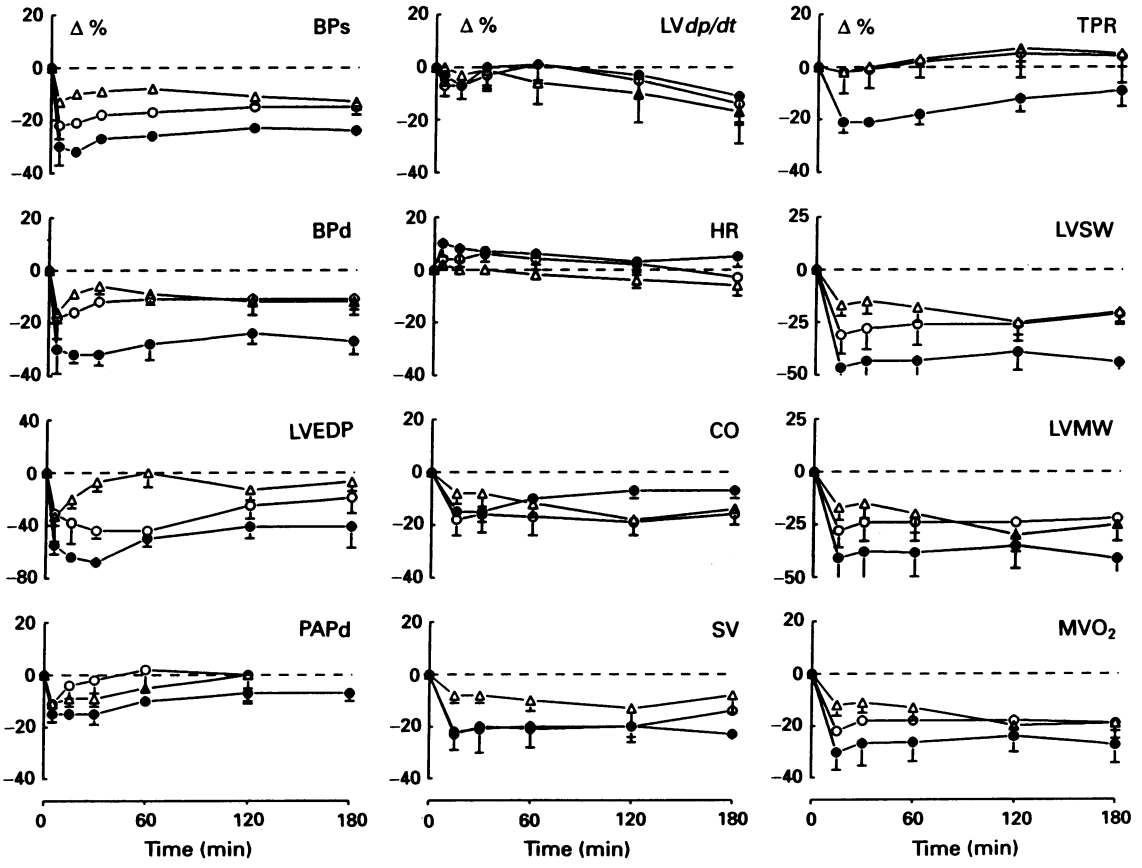

Figure 3 Haemodynamic effects of CAS 1609 in the anaesthetized dog. Intravenous administration of 0.3 mg kg^{-1} (Δ), 1.0 mg kg^{-1} (○), and 3 mg kg^{-1} (●). Changes in % of baseline values are shown for systolic blood pressure (BPs), diastolic blood pressure (BPd), left ventricular end-diastolic pressure (LVEDP), diastolic pulmonary artery pressure (PAPd), left ventricular contractility (LV$dp/dt$), heart rate (HR), cardiac output (CO), stroke volume (SV), total peripheral resistance (TPR), left ventricular stroke work (LVSW), left ventricular minute work (LVMW), and myocardial oxygen consumption (MVO_2). Notice the different scale of the Y-axis for LVEDP, LVSW, and LVMW. Data are means ± s.e.mean, $n = 4$.

groups. One group of ten dogs received saline (6 ml kg^{-1}, i.v.) and served as control. Ten other dogs received CAS 1609 (dissolved in water) at the dose of 0.3 mg kg^{-1}, i.v. as a bolus. Haemodynamic changes were then monitored for another 180 min.

Haemodynamic profile in conscious dogs

Six female Labrador-Harrier dogs (18 to 25 kg) were instrumented with catheters as described previously (Bohn & Rosenstein, 1986). Briefly the dogs were sedated with xylazine (2 mg kg^{-1}, i.m.) and anaesthetized with sodium pentobarbitone (20 mg kg^{-1}, i.v.). A fluid filled Micro-Renathane catheter (Braintree Scientific Inc., Braintree, Mass. 02184, U.S.A.) was inserted in the abdominal aorta for the recording of blood pressure and a second Tygon catheter (Norton Plastics and Synthetic Division, Akron, Ohio, U.S.A.) was implanted in the left ventricle through the apex of the heart to measure LVP. The catheters were tunnelled subcutaneously and exteriorized dorsally between the scapulae. The experiments started after a two-week recovery and conditioning period. In the conditioning period the dogs were trained to rest unrestrained and quietly on a laboratory table. For the haemodynamic measurement, the catheters were connected to Statham P23Db pressure transducers. The haemodynamic parameters recorded included BPs/d, LVP, LVEDP, HR and *dp/dt*. Recording was continuous for the first 2 h after i.v. or oral drug administration and later on at 1 h-intervals up to 6 h in order to give the dogs some periods of free movement between the recording sessions.

Tolerance study in conscious dogs

Surgical preparation of the dogs and recording methods were identical to those mentioned above. Each dog received 0.5 mg kg^{-1} p.o. of CAS 1609 twice daily, at 07 h 00 min and 19 h 00 min, for 5 days. Dose and treatment schedule were selected according to a pilot study which showed persistent effects throughout the whole day and no 'dose-free interval'. The haemodynamic effects of the 07 h 00 min treatment on day 1, day 3 and day 5 were recorded.

Materials

CAS 1609 (4-hydroxymethyl-furoxan-3-carboxamide, Mol. Wt. 159.1), 3-morpholino-sydnonimine (SIN-1), and molsidomine were synthesized in the Department of Medicinal Chemistry, Cassella AG (Frankfurt/M, Germany). The cyclic GMP enzyme-immunoassay was purchased from BIOTRAK, Amersham International plc, (Buckinghamshire, U.K.). Other reagents were from Sigma Chemical Co. (D-82039 Deisenhofen, Germany).

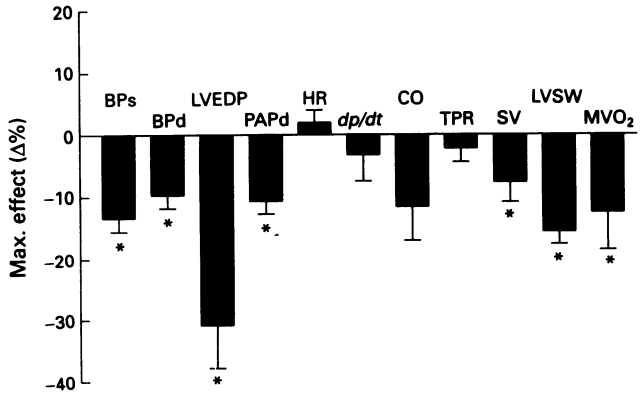

Figure 4 Haemodynamic profile of CAS 1609 in the anaesthetized dog given intravenously at a dose of 0.3 mg kg^{-1}. Systolic blood pressure (BPs), diastolic blood pressure (BPd), left ventricular end-diastolic pressure (LVEDP), diastolic pulmonary artery pressure (PAPd), heart rate (HR), left ventricular contractility (*dp/dt*), cardiac output (CO), total peripheral resistance (TPR), stroke volume (SV), left ventricular stroke work (LVSW), and myocardial oxygen consumption (MVO_2). Data are presented as means ± s.e.mean, $n = 4$. *Significant difference from control ($P < 0.05$).

Data analysis and presentation

In the *in vitro* study, relaxant effects of the compounds refer to the sustained contraction induced by potassium depolarization or by phenylephrine which was taken as 100%. IC_{50}-values were derived graphically from individual concentration-response curves (Langer & Trendelenburg, 1969). In the *in vivo* studies with anaesthetized animals, drug effects refer to control values obtained during the 20 to 30 min-control period before the administration of the test compound. In the tolerance study in conscious dogs, drug effects refer to control values obtained before the first administration of CAS 1609 on day 1 of the treatment. Results were expressed as means and standard error of the mean (s.e.mean). Differences between means were analysed either with Student's *t* test or chi-square test and considered to be significant at $P < 0.05$.

Results

Relaxant activity in the isolated pulmonary artery

CAS 1609 relaxed both potassium-depolarized and phenylephrine (PE)-contracted vessel strips in a concentration-dependent manner (Figure 2). The potency was approximately 15 times higher in PE-contracted strips than in strips depolarized by KCl – as indicated by the IC_{50} values (0.9 ± 2.5 μM vs. 15 ± 2.5 μM). While PE contractions were completely relaxed (Figure 2b), a 20% remainder of the KCl-contraction was left even at high concentrations of CAS 1609 (Figure 2a). CAS 1609 was approximately 7 to 14 times less potent than SIN-1.

Although, the onset of action of CAS 1609 was prompt, the maximum relaxation occurred only 60 to 90 min after administration, unlike SIN-1 with which the maximum occurred within 30 min (Figure 2c). While the relaxant effect of SIN-1 disappeared spontaneously within 90 to 120 min, relaxations due to CAS 1609 were only slightly reduced at 3 h. Oxyhaemoglobin attenuated the relaxant activity of CAS 1609 (IC_{50} 61 ± 9) and SIN-1 (IC_{50} 3.4 ± 0.4) significantly to a similar extent. The factor of attenuation was 3 to 4.

Effect on cyclic GMP levels and stimulation of the guanylate cyclase

Cyclic GMP levels in the pulmonary artery strips ($n = 7$) increased significantly during the 30 min incubation period with CAS 1609 (100 μM) from 1.7 ± 0.32 to 4.97 ± 0.76 pmol mg^{-1} protein.

Haemodynamic effects in the anaesthetized pig

After intraduodenal administration of CAS 1609 at doses 0.3 and 1.0 mg kg^{-1}, systolic and diastolic blood pressure (BP) and left ventricular end-diastolic pressure (LVEDP) decreased in a dose-related manner (Table 1). The onset of action was prompt and the maximal effects were obtained within 15 to 30 min. Left ventricular contractility was moderately reduced, whereas the heart rate remained almost unchanged. The duration of action on BP at both doses and on LVEDP at the higher dose was more than 3 h. At 0.3 mg kg^{-1}, LVEDP was reduced for 90 min.

Haemodynamic profile in the anaesthetized dog

The time course of action of CAS 1609 administered intravenously at the doses 0.3, 1.0 and 3.0 mg kg^{-1} is shown in Figure 3. The administration resulted in a marked dose-related decrease in blood pressure, left ventricular end-diastolic pressure, pulmonary artery pressure, cardiac output, stroke volume, left ventricular work and oxygen consumption. Left ventricular contractility showed a slight tendency to decrease whereas the heart rate increased slightly. Total peripheral resistance was reduced only at the highest dose. The haemodynamic profile of CAS 1609 is mainly characterized by a decrease in preload, left ventricular work, and myocardial oxygen consumption (Figure 4). Intraduodenal administration of CAS 1609 resulted in almost identical haemodynamic effects except for a slightly slower onset of action (data not shown).

Effect on acute left ventricular failure in the anaesthetized dog

Embolization by repeated injections of microspheres into the left coronary artery caused a marked increase in LVEDP which was accompanied by a decrease in cardiac output (CO) and left ventricular work (LVW) and an increase in total peripheral resistance (TPR) (Figure 5). Intravenous injection of a bolus of CAS 1609 (0.3 mg kg^{-1}, Figure 5, at time zero) lowered the elevated LVEDP promptly and significantly. The LVEDP reduction was accompanied by a moderate decrease

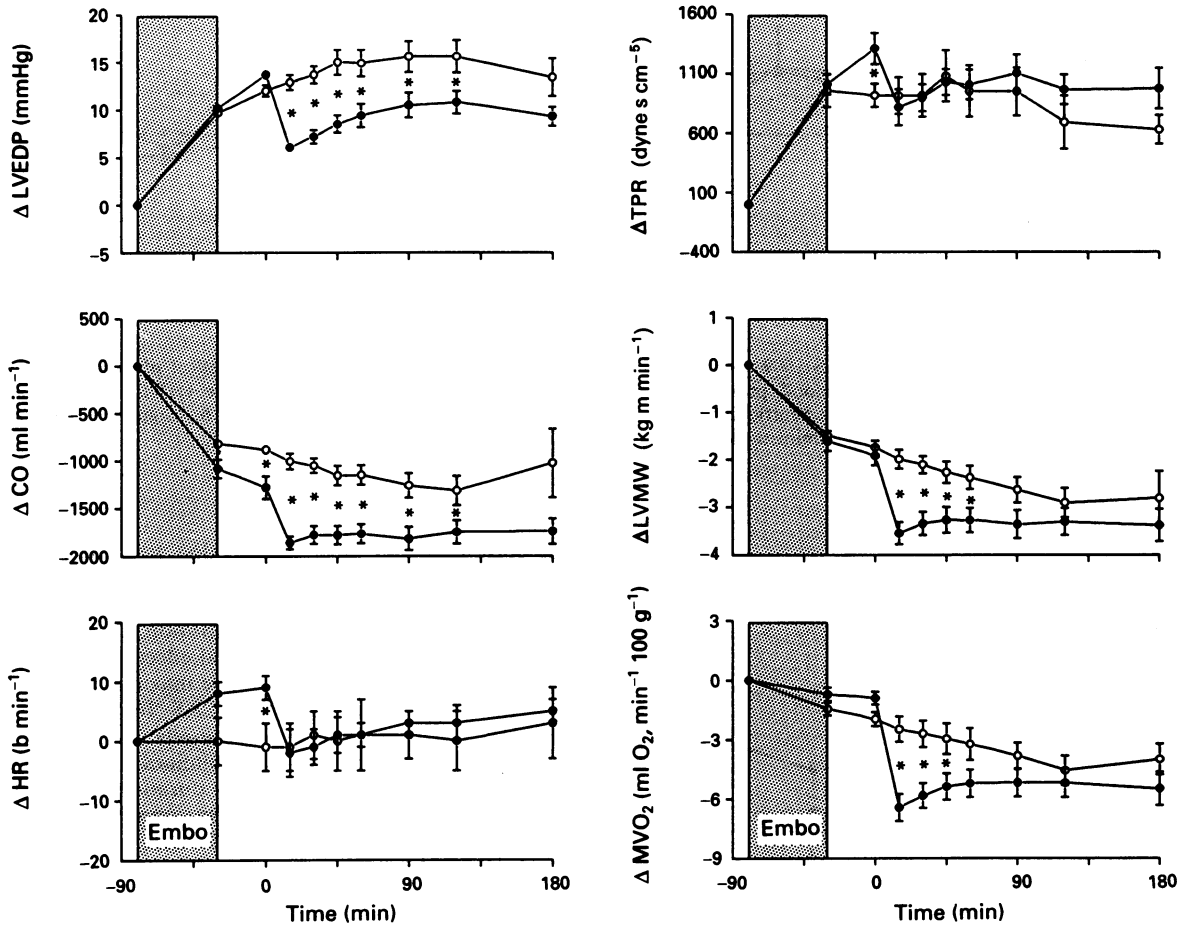

Figure 5 Induction of acute heart failure by repeated intracoronary injection of microspheres (Embo) in anaesthetized dogs and effect of CAS 1609. One group of dogs received CAS 1609 (0.3 mg kg^{-1}, i.v., ●) at time 0, the other group was treated with saline (○). Left ventricular end-diastolic pressure (LVEDP), cardiac output (CO), heart rate (HR), total peripheral resistance (TPR), left ventricular minute work (LVMW), and myocardial oxygen consumption (MVO_2). Data are means ± s.e.mean, $n = 10$. Significant differences between the two groups are indicated by asterisks (*$P < 0.05$).

Table 2 Haemodynamic effects of CAS 1609 in the conscious dog: intravenous or oral administration

	BPsyst (mmHg)		*BPdiast* (mmHg)		*LVEDP* (mmHg)		-- *LVdP/dt$_{max}$* (mmHg s^{-1})		*HR* (beats min^{-1})	
Dose (mg kg^{-1})	Control	Effect	Control	Effect	Control	Effect	Control	Effect	Control	Effect
0.05, i.v.	158 ± 5	−24 ± 3*	88 ± 2	−4 ± 3	14 ± 0.6	−3.8 ± 0.7*	3517 ± 183	50 ± 34	90 ± 5	9 ± 5
0.2, i.v.	158 ± 7	−37 ± 5*	89 ± 4	−10 ± 4*	14 ± 0.7	−5.5 ± 1.1*	3317 ± 327	−67 ± 95	89 ± 7	18 ± 4*
0.2, oral	167 ± 11	−30 ± 3*	98 ± 10	−6 ± 2	16 ± 0.4	−4.5 ± 0.6*	3300 ± 325	40 ± 76	86 ± 5	10 ± 8
1.0, oral	164 ± 8	−37 ± 2*	95 ± 7	−5 ± 2	16 ± 0.5	−6.7 ± 0.9*	3200 ± 214	317 ± 101	92 ± 3	20 ± 7*

BPs, systolic blood pressure; BPd, diastolic blood pressure; LVEDP, left ventricular end-diastolic pressure; LV dP/dt_{max}, left ventricular contractility; HR, heart rate. Data are mean maximal effects ± s.e.mean, $n = 6$. *Significant difference from control (Student's paired t test).

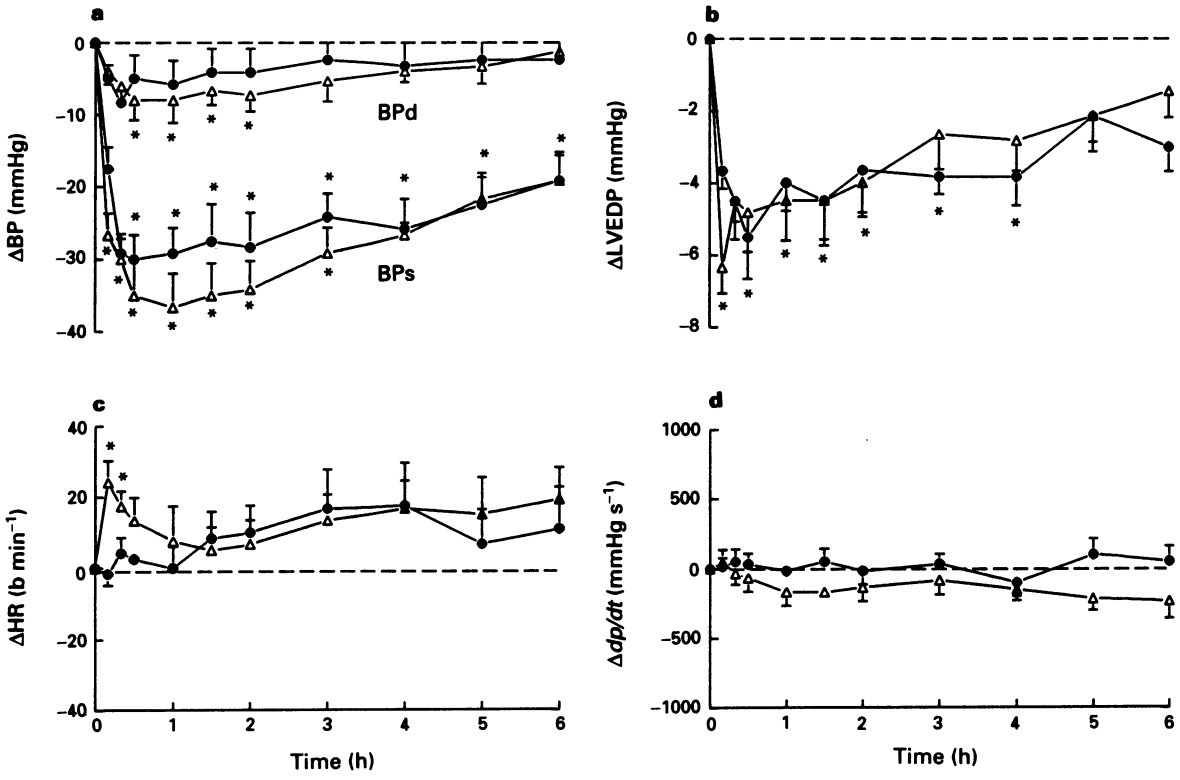

Figure 6 Time course of action of CAS 1609 given at the dose 0.2 mg kg^{-1} in the conscious dog: (Δ) effect of intravenous and (●) of oral administration. Systolic blood pressure (BPs), diastolic blood pressure (BPd), heart rate (HR), left ventricular end-diastolic pressure (LVEDP), and left ventricular contractility (dp/dt). Data are means ± s.e.mean, $n = 6$. *Significant difference ($P < 0.05$) from control before drug administration.

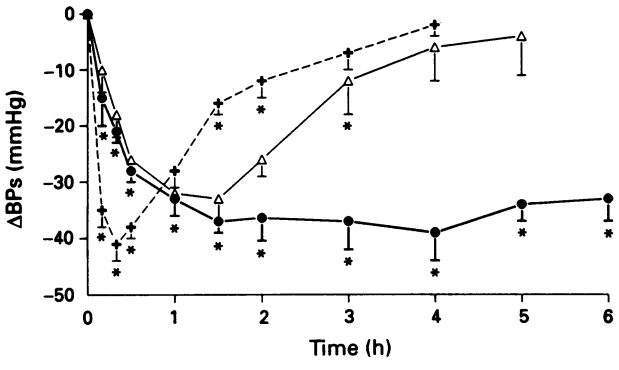

Figure 7 Effect of CAS 1609 on systolic blood pressure (BPs) as compared to 3-morpholino-sydnonimine (SIN-1) and molsidomine in the conscious dog. Oral administration of SIN-1 0.2 mg kg^{-1} (+), molsidomine 0.2 mg kg^{-1} (Δ), and CAS 1609 1 mg kg^{-1} (●). Data are means ± s.e.mean, $n = 6$. *Significant difference ($P < 0.05$) from control before drug administration.

in cardiac output and heart rate and a significant reduction in left ventricular work and oxygen consumption.

In the CAS 1609-group, only one animal out of ten died while in the control group, five animals out of ten died within 180 min.

Haemodynamic profile in conscious dog

CAS 1609 given at the dose 0.2 mg kg^{-1} intravenously or orally lowered systolic BP and LVEDP significantly (Figure 6). The heart rate showed a tendency to increase and left ventricular contractility was not significantly affected. Unlike the situation in the anaesthetized dog and anaesthetized pig, the diastolic BP of the conscious dog was much less reduced than the systolic BP (Figure 6a). The duration of action of BPs and LVEDP was more than 6 h both after i.v. and oral administration. After i.v. administration, the onset of action was slightly faster and the maximal effect was slightly greater than after oral administration. The maximal effects (Table 2) and the duration of action of CAS 1609 on systolic BP, LVEDP and heart rate were dose-related.

As compared to the sydnonimines, SIN-1 and molsidomine, CAS 1609 had a longer duration of action (Figure 7). The onset of action was also smoother than that of SIN-1. The haemodynamic profile of CAS 1609, of SIN-1 and of molsidomine in conscious dogs was almost identical consisting mainly of a decrease in BPs and LVEDP accompanied by a slight increase in heart rate.

Tolerance study in conscious dog

The haemodynamic effects of long-term administration of CAS 1609 at a dose of 0.5 mg kg^{-1} were studied in conscious dogs. The compound was given orally twice daily at 07 h 00 min and 19 h 00 min. The first administration on day 1 caused marked and long lasting haemodynamic effects (Figure 8). Two hours after the administration, the blood pressure decrease was on average 32 mmHg for BPs and 11 mmHg for BPd. LVEDP was also markedly reduced by 7.6 mmHg. The decrease in BP and LVEDP was accompanied by a moderate increase in heart rate (27 beats min^{-1}) whereas left ventricular contractility (data not shown) was not consistently affected. The duration of action on BP, LVEDP and heart rate was $\geq$ 12 h. The haemodynamic effects of the 07 h 00 min dose on day 3 and day 5 of the treatment were not significantly different from those on day 1. Thus no tolerance development occurred. On the contrary, there was a persistent reduction in the baseline values of LVEDP during the treatment (Figure 8).

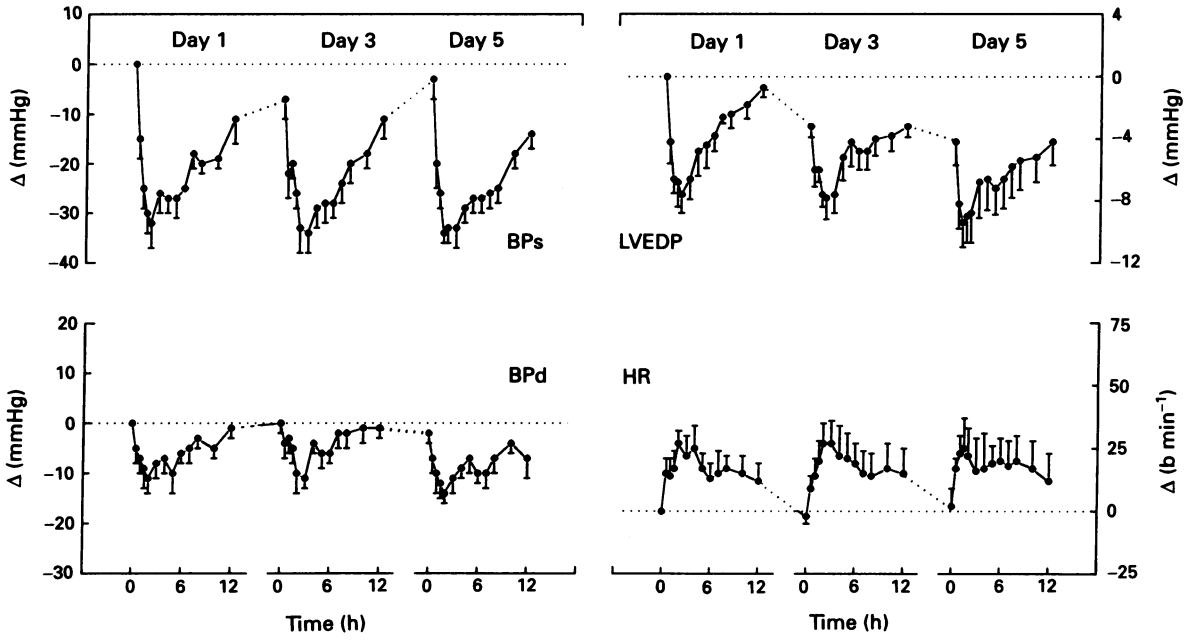

Figure 8 Haemodynamic effects of CAS 1609 in conscious dogs on day 1, day 3 and day 5 of long-term treatment. CAS 1609 was given orally at the dose 0.5 mg kg^{-1} twice daily at 07 h 00 min and 19 h 00 min. Systolic blood pressure (BPs), diastolic blood pressure (BPd), left ventricular end-diastolic pressure (LVEDP), and heart rate (HR). The response to the 07 h 00 min-dose is presented. Data are means ± s.e.mean, $n = 5$.

Discussion

The present study revealed a potent and long lasting vasodilator activity of the furoxan, CAS 1609. The compound relaxes *in vitro* isolated blood vessels and has *in vivo* a haemodynamic profile consisting mainly of a reduction of preload, systolic blood pressure, left ventricular work and myocardial oxygen consumption. This potential antianginal profile is similar to that of the NO donors, molsidomine and pirsidomine (Bohn *et al.*, 1992) and to that of the organic nitrates (Leitold *et al.*, 1986). Additionally, we also demonstrated a lack of tolerance development to the haemodynamic effects of CAS 1609 under our experimental conditions of long-term administration in conscious dogs.

Several lines of evidence indicate that CAS 1609 is a donor of NO. Consequently its biological activity should result from the stimulation of the soluble guanylate cyclase and intracellular accumulation of cyclic GMP. Arguments in favour of this hypothesis are as follows: the chemical structure of this furoxane contains two NO moieties, and several furoxans synthesized previously in our laboratories have already been shown to release NO *in vitro* in the presence of sulphydryl groups (Feelisch *et al.*, 1992). Additionally, CAS 1609 relaxes contractions of isolated vessels induced by phenylephrine with a higher potency than KCl-induced contractions. This phenomenon is known to be typical for cyclic GMP-mediated relaxations and has been described for NO donors such as SIN-1 (Bohn *et al.*, 1991) and sodium nitroprusside (Furchgott, 1983) and for acetylcholine-induced endothelium-dependent relaxations (Morrison & Pollock, 1988). The probable reason is an inhibition of cyclic GMP formation by high KCl concentrations (Rapoport *et al.*, 1985; Morrison & Pollock, 1988). Another argument that CAS 1609 acts as a donor of NO is the inhibitory effect of oxyhaemoglobin, a known scavenger of nitric oxide (Martin *et al.*, 1985; Gillespie & Sheng, 1988). More direct evidences for the NO donating properties of CAS 1609 are, the increase in cyclic GMP levels in the pulmonary artery strips exposed to CAS 1609; the *in vitro* formation of NO as measured by NO sensitive microelectrodes (T. Malinski, personal communication); and the increased levels of NO in vascular tissues of anaesthetized pigs after administration of CAS 1609 as demonstrated by electron spin resonance spectroscopy (A. Mülsch, personal communication).

The rate of NO release from CAS 1609 is lower than that of SIN-1 as indicated by the smoother onset and longer duration of action in the isolated pulmonary artery (Figure 2). This may also explain the longer duration of the *in vivo* effects observed after oral administration in conscious dogs (Figure 7).

The haemodynamic profile of CAS 1609 i.e. the unloading of the heart together with the antiaggregatory and antiadhesive properties (M. Just, personal communication) of the released NO is probably responsible for the marked reduction in the mortality and for the improvement of the haemodynamic situation in the model of acute heart failure in anaesthetized dogs. Long-term treatment in conscious dogs showed no attenuation of the haemodynamic responses to CAS 1609. In this model, tolerance development towards isosorbide-5-mononitrate has been demonstrated previously (Bohn *et al.*, 1992). Although, the mechanisms underlying nitrate tolerance are not fully understood, a nitrate-specific metabolism yielding NO is thought to be mainly responsible for tolerance development (see Kojda *et al.*, 1993). The absence of tolerance development with CAS 1609 suggests that its bioactivation is different from that of the nitrates. The knowledge regarding the transformation of CAS 1609 to NO is limited. Aqueous solutions of CAS 1609 are stable at physiological pH. Thus, spontaneous release of NO can be excluded as an explanation for its marked vasodilator activity. Therefore, bioactivation seems to be necessary. This is in sharp contrast to the situation with SIN-1 solutions of which are labile at physiological pH (Bohn & Schönafinger, 1989). The spontaneous decomposition of SIN-1 is accompanied by a rapid and marked release of NO which can explain the higher potency and the shorter duration of action of SIN-1 as compared to CAS 1609. Details of the bioactivation process of CAS 1609 are unknown. However, for other furoxans generation of NO has been demonstrated following chemical reaction with sulphydryl groups of low molecular weight thiols and proteins (Feelisch *et al.*, 1992). Since these are abundant in the membrane and the cytosolic fraction of

virtually every cell, no restriction in the bioactivation of furoxans to NO is expected. This could explain the lack of tolerance development observed with CAS 1609.

In conclusion, CAS 1609 is a potent, long-lasting orally active, vasodilator agent which belongs chemically to a new class of NO donors, the furoxans. These characteristics coupled with the lack of tolerance suggest the prevention and treatment of coronary heart disease as potential therapeutic indication.

We thank Mrs Sybille Buchheim, Birgit Göbel, Hanna Richter, Gabriele Schumacher-Voigt, Mr B. Rosenstein and Mr H. Weber for their expert technical assistance, and Mrs Hannelore Stockhausen for the determination of cyclic GMP.

References

BENNET, B.M., McDONALD, B.J. & ST JAMES, M.J. (1992). Hepatic cytochrome P-450-mediated activation of rat aortic guanylyl cyclase by glyceryl trinitrate. *J. Pharmacol. Exp. Ther.*, **261**, 716–723.

BOHN, H., BEYERLE, R., MARTORANA, P.A. & SCHÖNAFINGER, K. (1991). CAS 936, a novel sydnoninime with direct vasodilating and nitric oxide-donating properties, effects on isolated blood vessels. *J. Cardiovasc. Pharmacol.*, **18**, 522–527.

BOHN, H., MARTORANA, P.A. & SCHÖNAFINGER, K. (1992). Cardiovascular effects of the new nitric oxide donor, pirsidomine. Hemodynamic profile and tolerance studies in anesthetized and conscious dogs. *Eur. J. Pharmacol.*, **220**, 71–78.

BOHN, H. & ROSENSTEIN, B. (1986). Technical notes on fluid-filled catheters and renal artery constrictors for testing hemodynamic drug effects in conscious hypertensive dogs. *J. Pharmacol. Meth.*, **16**, 227–238.

BOHN, H. & SCHÖNAFINGER, K. (1989). Oxygen and oxidation promote the release of nitric oxide from sydnonimines. *J. Cardiovasc. Pharmacol.*, **14** (Suppl. 11), S6–S12.

CALVINO, R., FRUTTERO, R., GHIGO, D., BOSIA, A., PESCARMONA, G.P. & GASCO, A. (1992). 4-Methyl-3-(arylsulfonyl)furoxans: a new class of potent inhibitors of platelet aggregation. *J. Med. Chem.*, **35**, 3296–3300.

CHUNG, S.J. & FUNG, H.L. (1990). Identification of the subcellular site for nitroglycerin metabolism to nitric oxide in bovine coronary smooth muscle cells. *J. Pharmacol. Exp. Ther.*, **253**, 614–619.

CIVELLI, M., CARUSO, P., GIOSSI, M., BERGAMASCHI, M., RAZZETTI, R., BONGRANI, S. & GASCO, A. (1994). CHF 2206, a new potent vasodilating and antiaggregating drug as potential nitric oxide donor. *Eur. J. Pharmacol.*, **255**, 17–24.

FEELISCH, M., SCHÖNAFINGER, K. & NOACK, E. (1992). Thiol-mediated generation of nitric oxide accounts for the vasodilator action of furoxans. *Biochem. Pharmacol.*, **44**, 1149–1157.

FERIOLI, R., FAZZINI, A., FOLCO, G.C., FRUTTERO, R., CALVINO, R., GASCO, A., BONGRANI, S. & CIVELLI, M. (1993). NO-mimetic furoxans: arylsulphonylfuroxans and related compounds. *Pharmacol. Res.*, **28**, 203–212.

FURCHGOTT, R.F. (1983). Role of endothelium in responses of vascular smooth muscle. *Circ. Res.*, **53**, 557–573.

GASCO, A.M., DI SILVO, A., SORBA, G., FERIOLI, R., FOLCO, G., CIVELLI, M. & CARUSO, P. (1993). 1,1-Dinitroethyl substituted furoxans: a new class of vasodilators and inhibitors of platelet aggregation. *Eur. J. Med. Chem.*, **28**, 433–438.

GHIGO, D., HELLER, R., CALVINO, R., ALESSIO, P., FRUTTERO, R., GASCO, A., BOSIA, A. & PESCARMONA, G. (1992). Characterization of a new compound, S35b, as a guanylate cyclase activator in human platelets. *Biochem. Pharmacol.*, **43**, 1281–1288.

GILLESPIE, J.S. & SHENG, H. (1988). Influence of hemoglobin and erythrocytes on the effects of EDRF, a smooth muscle inhibitory factor, and nitric oxide on vascular and non-vascular smooth muscle. *Br. J. Pharmacol.*, **95**, 1151–1156.

KOJDA, G., MEYER, W. & NOACK, E. (1993). Influence of endothelium and nitrovasodilators on free thiols and disulfides in porcine coronary smooth muscle. *Eur. J. Pharmacol.*, **250**, 385–394.

LANGER, S.Z. & TRENDELENBURG, U. (1969). The effect of saturable uptake mechanism on the slopes of dose-response curves for sympathomimetic amines and on the shift of dose-response curves produced by competitive antagonists. *J. Pharmacol. Exp. Ther.*, **167**, 117–142.

LEITOLD, M., LAUFEN, H. & YEATES, R.A. (1986). Comparative pharmacology of glyceryl-1-nitrate and glyceryl trinitrate in various species. *Arzneim. Forsch./Drug Res.*, **36**, 814–821.

LOWRY, O.H., ROSEBROUGH, N.J., FARR, A.L. & RANDALL, R.J. (1951). Protein measurement with phenol reagent. *J. Biol. Chem.*, **193**, 265–275.

MARTIN, W., VILLANI, G.M., JOTHIANANDAN, D. & FURCHGOTT, R.F. (1985). Selective blockade of endothelium-dependent and glyceryl trinitrate-induced relaxation by hemoglobin and methylene blue in the rabbit aorta. *J. Pharmacol. Exp. Ther.*, **232**, 708–716.

MONCADA, S. & HIGGS, E.A. (1993). The L-arginine-nitric oxide pathway. *N. Engl. J. Med.*, **329**, 2002–2012.

MONCADA, S., PALMER, R.M.J. & HIGGS, E.A. (1991). Nitric oxide, physiology, pathophysiology, and pharmacology. *Pharmacol. Rev.*, **43**, 109–142.

MORRISON, K.J. & POLLOCK, D. (1988). Effects of vasodilators on tone, cyclic guanosine monophosphate levels and phosphatidylinositol hydrolysis in rat aortic rings. *Br. J. Pharmacol.*, **94**, 437P.

PERSSON, M.G., AGVALD, P. & GUSTAFSSON, L.E. (1994). Detection of nitric oxide in exhaled air during administration of nitroglycerin *in vivo*. *Br. J. Pharmacol.*, **111**, 825–828.

RAPOPORT, R.M., SCHWARTZ, K. & MURAD, F. (1985). Effect of sodium-potassium pump inhibitors and membrane-depolarizing agents on sodium nitroprusside-induced relaxations and cyclic guanosine monophosphate accumulation in rat aorta. *Circ. Res.*, **57**, 164–170.

ROOKE, G.Y. & FEIGL, E.O. (1982). Work as a correlate of canine left ventricular oxygen consumption and the problem of catecholamine oxygen wasting. *Circ. Res.*, **50**, 273–286.

SILBER, S. (1990). Nitrates, why and how should they be used today? Current status of the clinical usefulness of nitroglycerin, isosobide dinitrate and isosorbide-5-mononitrate. *Eur. J. Clin. Pharmacol.*, **38** (Suppl. 1), S35–S51.

(Received September 2, 1994
Revised December 22, 1994
Accepted January 12, 1995)

British Journal of Pharmacology (1995) 114, 1613-1620 © 1995 Stockton Press All rights reserved 0007-1188/95 $12.00

Heparin-insensitive calcium release from intracellular stores triggered by the recombinant human parathyroid hormone receptor

[1]Klaus Seuwen & Hendrikus G.W.M. Boddeke

Preclinical Research, Sandoz Pharma Ltd., CH-4002 Basel, Switzerland

1 In the present study we have characterized the parathyroid hormone (PTH)-induced calcium signalling in 293 cells stably transfected with the human PTH receptor cDNA. In these cells, human PTH-1(1-38) strongly stimulates adenosine 3':5'-cyclic monophosphate (cyclic AMP) formation ($EC_{50} = 0.39$ nM) but fails to activate phosphoinositide (PI) turnover. The latter pathway is strongly activated, however, by carbachol (CCh) acting through endogenous M_3-muscarinic receptors.

2 Despite the lack of detectable inositol phosphate (IP) formation, hPTH-(1-38) elicited calcium transients ($EC_{50} = 11.2$ nM) which were comparable to the signals evoked by CCh. These signals are independent of cyclic AMP generation as cyclic AMP elevating agents did not mimic or modify the PTH response.

3 The PTH-stimulated calcium signal still occurred in calcium-free medium but was absent in cells pretreated with thapsigargin, an inhibitor of the calcium pump of the endoplasmic reticulum (ER). hPTH-(1-38) did not accelerate Mn^{2+}-influx through the plasma membrane. These data indicate that PTH releases calcium from intracellular stores.

4 Using heparin, an inhibitor of the IP_3-activated calcium release channel of the ER, we tested whether the formation of a low amount of IP_3, escaping detection by our biochemical assay, might be the origin of the PTH-induced calcium response. However, intracellular infusion of heparin through patch pipettes in voltage clamp experiments failed to block hPTH-(1-38)-induced calcium signals, whereas it abolished the CCh response.

5 The PTH response, like the CCh response, was insensitive to micromolar concentrations of ryanodine and ruthenium red, eliminating the possibility that hPTH-(1-38) stimulates calcium-induced calcium release through ryanodine receptors.

6 We conclude that the recombinant human PTH receptor stimulates calcium release from intracellular stores through a novel pathway not involving IP_3- or ryanodine receptors.

Keywords: Parathyroid hormone; cyclic AMP; inositol trisphosphate; G protein; heparin; ruthenium red; ryanodine

Introduction

Parathyroid hormone (PTH) stimulates adenosine 3':5'-cyclic monophosphate (cyclic AMP) formation in target cells. In addition, the hormone has also been reported to increase intracellular free calcium ($[Ca^{2+}]_i$) in various cell types, as first demonstrated by Löwik *et al.* in 1985. Today, some controversy persists concerning the heterogeneity of responses and the origin of the calcium signal (Yamaguchi *et al.*, 1987; Reid *et al.*, 1987; Babich *et al.*, 1991; Civitelli *et al.*, 1992; Wiltink *et al.*, 1993). Data arguing both for PTH-stimulated calcium influx (Yamaguchi *et al.*, 1987) as well as release from intracellular stores (Babich *et al.*, 1991) have been reported. The fact that some groups found activation of protein kinase C and formation of IP_3 in response to PTH peptides provided support for the latter concept (Tamura *et al.*, 1989; Abou-Samra *et al.*, 1989; Fujimori *et al.*, 1992).

The molecular cloning of a PTH receptor from several species opened new opportunities to study PTH signal transduction. As there is no evidence for receptor subtypes, a single receptor seems to account for the different intracellular responses described for PTH (Schipani *et al.*, 1993; Kong *et al.*, 1994). Under conditions of transient expression in COS cells, the rat and human PTH receptor stimulate both cyclic AMP and inositol phosphate (IP) formation (Abou-Samra *et al.*, 1992; Schneider *et al.*, 1993). We were unable, however, to demonstrate coupling of the human receptor to the latter signalling system under the more physiological condition of stable receptor expression in 293 cells (Schneider *et al.*, 1994) or hamster fibroblasts (unpublished data). Likewise, we have observed previously that PTH failed to stimulate phosphoinositide (PI) turnover significantly in osteoblasts and various osteosarcoma cell lines, whereas other hormones like endothelin-1 were active in these cells (unpublished data). These results are in agreement with those of Babich and coworkers (1991), which suggested that thrombin and PTH elicit calcium transients through different pathways in rat osteosarcoma cells.

In the present study we have analysed the calcium signal triggered by the recombinant human PTH receptor stably expressed in 293 cells. We found that this receptor elicits calcium release from intracellular stores in the absence of detectable IP formation through a pathway which is insensitive to heparin, ryanodine, and ruthenium red.

Methods

Cells and culture conditions

293 p5 cells are human embryonic kidney 293 (HEK 293, American type culture collection) cells transfected with the human PTH receptor cDNA (Schneider *et al.*, 1994). They express approximately 1.5×10^5 receptors per cell. Cultures were grown in a 1:1 mixture of Dulbecco's modification of Eagles medium (DMEM) and Ham's F12 medium containing 10% foetal calf serum.

[1] Author for correspondence.

Measurements of $[Ca^{2+}]_i$ in cell suspensions

293 p5 cells were detached from culture plates by incubation for 10 min in calcium/magnesium-free phosphate buffered saline containing 50 μM EDTA. No trypsin was used in order to avoid a partial destruction of membrane receptors. Following centrifugation, cells were resuspended in serum-free DMEM medium and loaded with fura-2 acetoxymethylester (2.5 μM) for 45 min at 37°C. After loading, cells were washed three times with HEPES-buffered salt solution (HBS composition, mM: NaCl 130, KCl 5.4, NaH_2PO_4 0.8, $CaCl_2$ 1.8, $MgSO_4$ 0.9, glucose 10 and HEPES 20, pH 7.4) and cell density was adjusted to $\approx 5 \times 10^5$ cells ml^{-1}. Experiments were carried out in HBS using a Perkin Elmer LS 50B spectrofluorimeter equipped with a thermostated cuvette holder (37°C).

In the standard ratio mode, excitation wavelength was changed once per second between 340 and 380 nm, emission was recorded at 500 nm. Fluorescence ratios R = F340/F380 were recorded and the concentration of intracellular free calcium calculated from the equation

$$[Ca^{2+}]_i = K_d \times S_{f2}/S_{b2} \times ((R - R_{min})/(R_{max} - R))$$

as given by Grynkiewicz *et al.* (1985), using K_d = 135 nM and S_{f2}/S_{b2} = 5.6 (determined experimentally for our system). Values for R_{min} and R_{max} were determined after each experiment by successive addition of ionomycin (3 μM) and EGTA (10 mM), respectively.

Quenching of fura-2 fluorescence by Mn^{2+} was measured by exciting the dye at 360 nm, where emission measured at 500 nm is independent of ambient calcium concentration (isosbestic point). This technique detects agonist-stimulated opening of cation channels in different cell types (Merritt *et al.*, 1989; Fasolato *et al.*, 1993).

Combined patch-clamp and $[Ca^{2+}]_i$ measurements in single cells

Cells seeded on glass coverslips were loaded for 45 min with 5 μM fura-2 acetoxymethylester prior to experiments. Coverslips were mounted on a Zeiss Axiovert-M microscope and perfused with oxygenated buffer (composition, mM: NaCl 140, KCl 5, $CaCl_2$ 2, $MgCl_2$ 1, glucose 5.6, HEPES 5, pH 7.4).

Whole cell recordings were performed with a List LM-PC amplifier. Patch electrodes were prepared from thinwall capillary borosilicate glass. The intracellular pipette solution contained (mM): K-gluconate 150, $MgCl_2$ 2, $CaCl_2$ 0.1, EGTA 0.1, Mg-ATP 5, Li-GTP 0.1 and HEPES 5, adjusted to pH 7.2 with KOH. Where indicated, this solution was supplemented with 45 USP units ml^{-1} of heparin which corresponds to an approximate concentration of 10^{-4} M. Pipette resistances were 3–10 MΩ.

Calcium responses were recorded from cells, voltage-clamped at −50 mV (Boddeke *et al.*, 1993). hPTH-(1-38) or CCh were applied by low pressure (3–4 psi, 3 s) from a micropipette placed 5–10 μm from the cell. Changes in fura-2 fluorescence were determined with a photodiode array connected to a set of amplifiers. Excitation was alternated at 340 and 380 nm, emission was recorded at 509 nm. Fluorescence ratios $R = F_{340}/F_{380}$ were calculated on line. Calibration was performed with 5 μM ionomycin and EGTA at the end of each experiment as described above. The calcium responses were recorded and analysed using pClamp software (Axon Instruments).

Measurements of cyclic AMP and inositol phosphate formation

To measure cyclic AMP production, cells in 24 well plates were prelabelled with [2-^{3}H]-adenine at 2–4 μCi ml^{-1} for 2 h. Thereafter, cells were washed and incubated in HBS containing 1 mM isobutylmethylxanthine (IBMX) and the indicated agonists at 37°C for 15 min. The cells were then extracted with 5% ice-cold trichloroacetic acid (TCA). [^{3}H]-ATP and [^{3}H]-cyclic AMP were separated by sequential chromatography on Dowex and alumina columns as described by Salomon (1979).

IP formation was measured following prelabelling of cells with *myo*-[2-^{3}H]-inositol for 24 h at 2–4 μCi ml^{-1}. Cells were then washed and incubated in HBS containing 20 mM Li^+ and the indicated agonists at 37°C for 20 min. The cells were then extracted with ice-cold 10 mM formic acid and samples were processed by anion exchange chromatography as described by Seuwen *et al.* (1988). IP_1, IP_2, and IP_3 were eluted successively from the columns with 300, 800, and 2000 mM formate, respectively. Total inositol phosphates were collected by adding 2 M formate buffer immediately.

Chemicals

[2-^{3}H]-adenine and *myo*-[2-^{3}H]-inositol were purchased from Amersham, Dübendorf, Switzerland. Human PTH-(1-38) and rolipram were synthesized at Sandoz, Basel, Switzerland. Carbachol (CCh), isoprenaline, forskolin, fura-2 acetoxymethylester, heparin (low molecular weight, sodium salt), IBMX, ruthenium red (oxychloride), ryanodine, and thapsigargin were obtained from Sigma, Buchs, Switzerland. Ionomycin (calcium salt) was from Serva, Heidelberg, Germany. Cell culture media were obtained from Bioconcept, Basel. Foetal calf serum was from Gibco, Basel.

Results

Effects of hPTH-(1-38) and carbachol on cyclic AMP and inositol phosphate (IP) formation in 293 p5 cells

hPTH-(1-38) strongly stimulated adenylyl cyclase in 293 p5 cells but failed to activate PI turnover (Figure 1; Schneider *et al.*, 1994). CCh, on the other hand, was a potent inducer of IP formation and stimulated cyclic AMP production only very weakly. Combining data from 8 independent experiments we could not detect a statistically significant increase of IP production relative to control in hPTH-(1-38)-treated cells whereas the CCh response was clearly significant ($P < 0.01$ at 10^{-4} and 10^{-5} M; two-tailed t test). In order to detect possible transient effects of hPTH-(1-38) on IP production, we carried out time course experiments with high concentrations of hPTH-(1-38) (100 nM) and CCh (100 μM), and we collected individual IPs separately. The results of one of three experiments, all of which produced similar results, are shown in Figure 2. There was no significant increase of IP_1, IP_2, or IP_3 detectable with hPTH-(1-38), whereas CCh strongly stimulated the accumulation of all three IP species.

hPTH-(1-38) stimulates calcium transients which are not due to increases in cyclic AMP

Despite undetectable changes in PI turnover, hPTH-(1-38) stimulated calcium transients in 293 p5 cells. We quantified the responses to hPTH-(1-38) and CCh using fura-2-loaded cells in suspension. Figure 3 shows typical traces obtained with different concentrations of both agonists. High concentrations of CCh produced signals which were higher in amplitude and of longer duration than those elicited by maximal concentrations of hPTH-(1-38). The maximal amplitude of the PTH-response corresponded roughly to that obtained with 1 μM CCh, which stimulates a weak but detectable formation of IPs (Figure 1). Figure 4 compares dose-response data for the two agonists as obtained by averaging peak changes in $[Ca^{2+}]_i$ from several recordings. The EC_{50} for hPTH-(1-38)-induced calcium signalling was 11.2 nM, which is considerably higher than the EC_{50} for cyclic AMP formation in the same cells (0.39 nM; Schneider *et al.*, 1994; Figure 1).

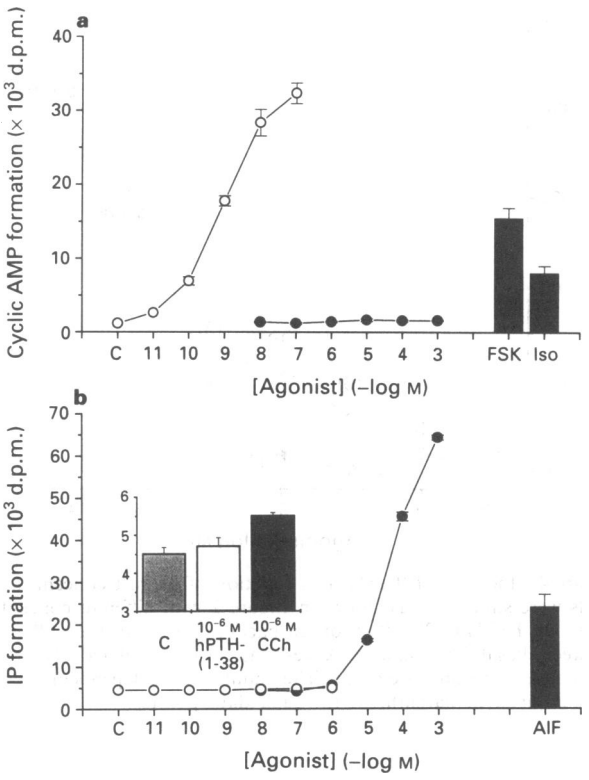

Figure 1 Stimulation of cyclic AMP (a) and inositol phosphate (IP) formation (b) by hPTH-(1-38) (○) and carbachol (CCh, ●) and other agents in 293 p5 cells. Forskolin (FSK) and isoprenaline (Iso) were used at 3 and 10 μM, respectively. To stimulate cells with the AlF_4^- complex (AIF), 10 μM $AlCl_3$ and 5 mM NaF were added. Control values (C) refer to the signal measured in the presence of isobutyl methylxanthine (a) or lithium (b) alone, respectively. The inset in (b) shows the responses to 1 μM of the agonists in greater detail. S.e.mean of triplicate determinations are shown except where exceeded by the symbol size.

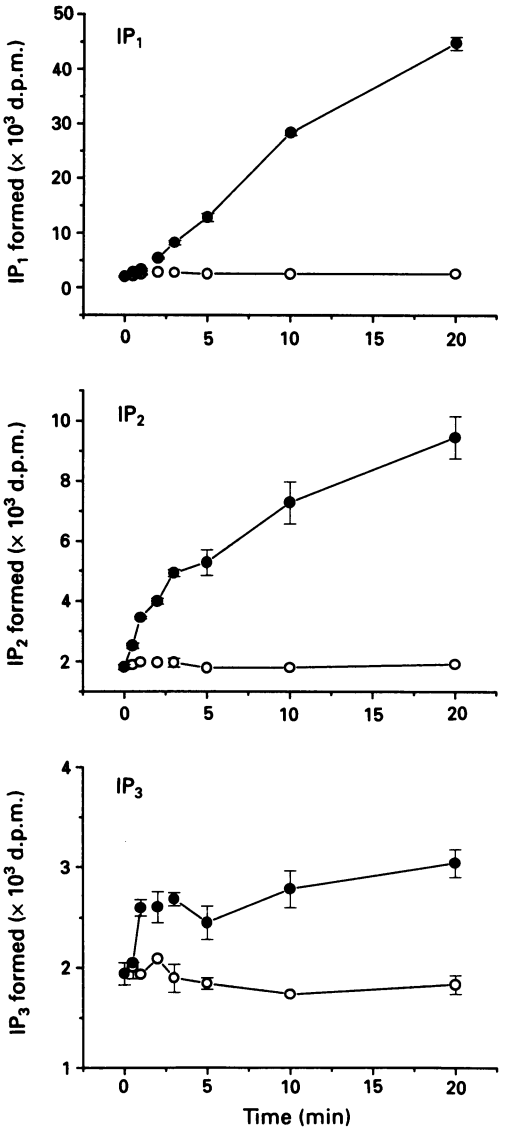

Figure 2 Time course of formation of IP_1, IP_2, and IP_3 following stimulation of cells with 100 nM hPTH-(1-38) (○) or 100 μM carbachol (●). S.e.mean of triplicate determinations are shown except where exceeded by the symbol size.

We next tested whether the PTH-induced calcium signal could be a consequence of cyclic AMP formation, as described for instance for thymocytes (Stojceva-Taneva *et al.*, 1993) and pancreatic islet cells (Fadda *et al.*, 1993). 293 p5 cells were therefore stimulated with the cyclic AMP-elevating agent, forskolin, in the presence or absence of the phosphodiesterase inhibitor, rolipram. Rolipram is equally active as IBMX as an inhibitor of phosphodiesterase activities in 293 cells (unpublished results). As is shown in Figure 5, forskolin with or without rolipram did not evoke a rapid calcium transient in 293 p5 cells and did not abrogate the subsequent responses to hPTH-(1-38) and to CCh. Thus, the calcium transients stimulated by hPTH-(1-38) seem not to be triggered by an elevation of intracellular cyclic AMP. In some experiments, however, a slow increase of intracellular free calcium was observed following forskolin (FSK) administration (Figure 5a), which may reflect sensitization of IP_3 receptors by PKA (Bird *et al.*, 1993).

Calcium transients induced by hPTH-(1-38) or CCh were not sensitive to a 4 h pretreatment of cells with 100 ng ml^{-1} of pertussis toxin (data not shown).

hPTH-(1-38) stimulates release of calcium from intracellular stores

To determine whether the PTH-induced calcium transient was caused by release from intracellular stores and/or due to stimulated influx across the plasma membrane, three different types of experiments were carried out. First, we tested whether the calcium signal persisted in calcium-free medium. To this end, an excess of the calcium chelator EGTA (3 mM vs. 1.8 mM Ca^{2+} in HBS) was added to the cell suspension shortly before the addition of hPTH-(1-38). As is shown in Figure 6a, hPTH-(1-38) still produced a calcium transient. It should be noted that longer preincubations with EGTA (>10 min) tend to deplete exchangeable intracellular calcium stores. Neither hPTH-(1-38) nor CCh were able to increase $[Ca^{2+}]_i$ following prolonged (>10 min) incubation of cells in calcium-free medium.

In a second set of experiments, the calcium pump inhibitor, thapsigargin (Lytton *et al.*, 1991) was used to empty the rapidly exchangeable calcium pool of the endoplasmic reticulum. As is shown in Figure 6b, thapsigargin led to a transient increase of $[Ca^{2+}]_i$ by itself, as expected. Subsequent addition of hPTH-(1-38) or CCh remained without effect.

A third series of experiments was carried out to test whether hPTH-(1-38) accelerated the influx of Mn^{2+} across the plasma membrane, which would indicate an opening of calcium-permeable cation channels (Merritt *et al.*, 1989; Fasolato *et al.*, 1993). The influx of Mn^{2+} into fura-2-loaded cells can be monitored conveniently due to the Mn^{2+}-induced quenching of fura-2 fluorescence. In these experiments,

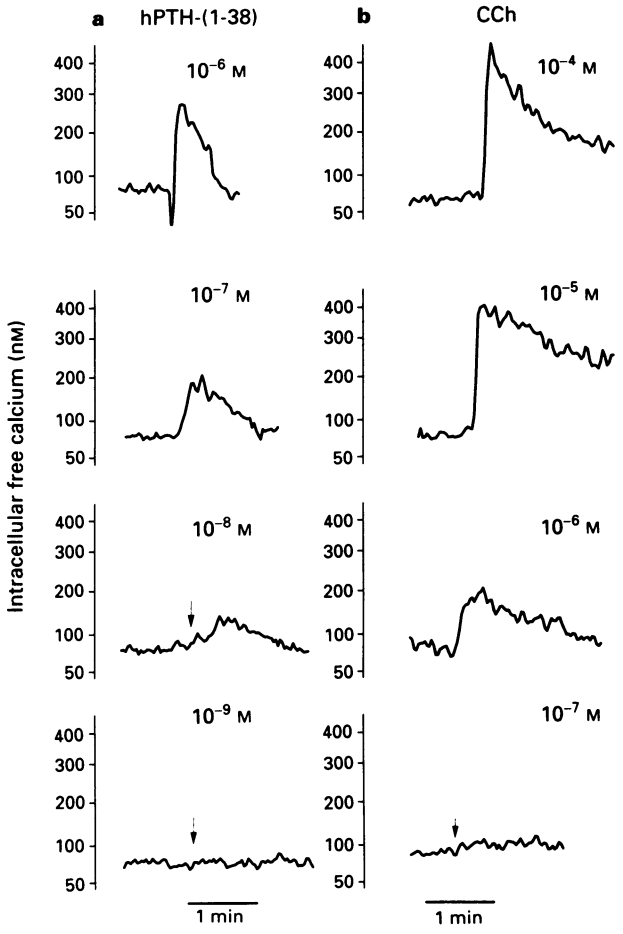

Figure 3 Changes of $[Ca^{2+}]_i$ observed following addition of the indicated concentrations of hPTH-(1-38) (column a) or carbachol (CCh, column b) to 293 p5 cells. The traces shown are representative of 4–20 independent recordings.

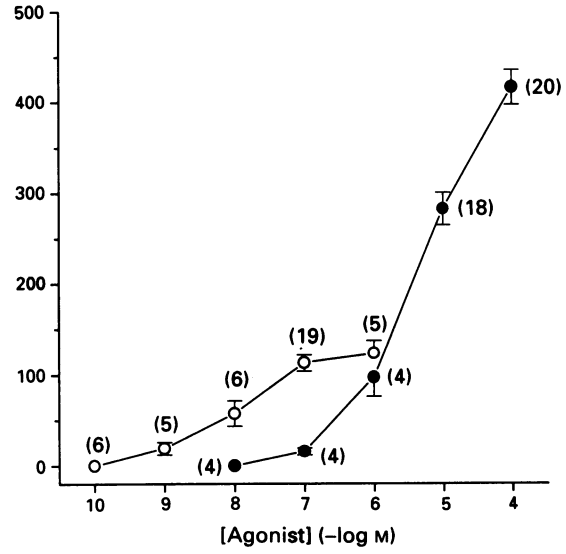

Figure 4 Increase of $[Ca^{2+}]_i$ as a function of agonist concentration. Cells were stimulated as shown in Figure 2 with different concentrations of hPTH-(1-38) (○) or carbachol (●) and the difference between basal level and peak response was calculated. Data are presented as mean ± s.e.mean. The number of independent recordings is given in parentheses for each data point.

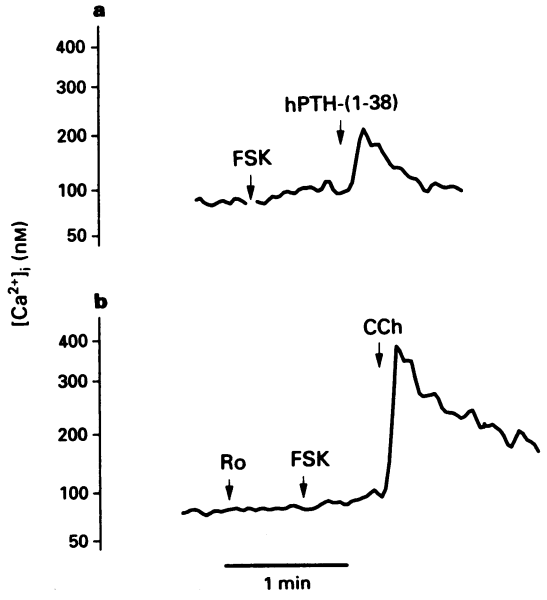

Figure 5 Effects of forskolin (FSK, 3 μM) added alone or in the presence of rolipram (Ro, 3 μM) on $[Ca^{2+}]_i$. After the addition of the cyclic AMP-elevating agents, cells were stimulated with hPTH-(1-38) (100 nM) or carbachol (CCh, 100 μM). The traces shown are representative of 4 independent experiments.

fluorescence is measured at the isosbestic point of the excitation spectrum as opposed to the ratio technique used for the determination of free intracellular calcium. The results of a typical experiment are shown in Figure 6c. hPTH-(1-38) did not accelerate Mn^{2+}-induced quenching of fura-2 fluorescence.

Using conventional voltage clamp experiments (Boddeke *et al.*, 1994) we found no evidence of an activation of voltage-gated calcium channels in 293 p5 cells in response to CCh or hPTH-(1-38) (data not shown).

Taken together, the data presented in this section show that hPTH-(1-38) can mobilize calcium from a thapsigargin-sensitive intracellular store. There is no evidence for PTH-stimulated calcium influx in 293 p5 cells.

Calcium signalling by hPTH-(1-38) is not affected by intracellular application of heparin

Heparin is an inhibitor of the IP_3-triggered calcium release channel of the endoplasmic reticulum (Gosh *et al.*, 1988; Bird *et al.*, 1993). In order to check the possibility that the hPTH-(1-38)-induced calcium signal was due to the formation of a small quantity of IP_3 which was not detected by our biochemical assay, we set out to test whether the polyanion interfered with calcium signalling. As the cell membrane is impermeable to heparin, these experiments were carried out with single cells in whole cell patch clamp mode. Heparin was included in the patch pipette solution. Figure 7a,b shows the result of these experiments. Infusion of heparin blocked calcium transients stimulated by CCh, as expected, but left the response to hPTH-(1-38) intact. Interestingly, in single cell recordings 100 nM hPTH-(1-38) produced signals which were of equal amplitude as those evoked by 100 μM CCh. The reasons for the discrepancies between experiments with cell suspensions and single cells are not yet clear.

At first glance, the data obtained with heparin seemed to rule out a participation of IP_3 receptors in PTH-induced calcium signalling. However, although unlikely, one possible explanation for this observation could be the sensitization of IP_3 receptors to low concentrations of the second messenger due to activation of protein kinase A, as has been demonstrated in hepatocytes (Bird *et al.*, 1993). hPTH-(1-38), but not CCh, strongly stimulates cyclic AMP formation in 293

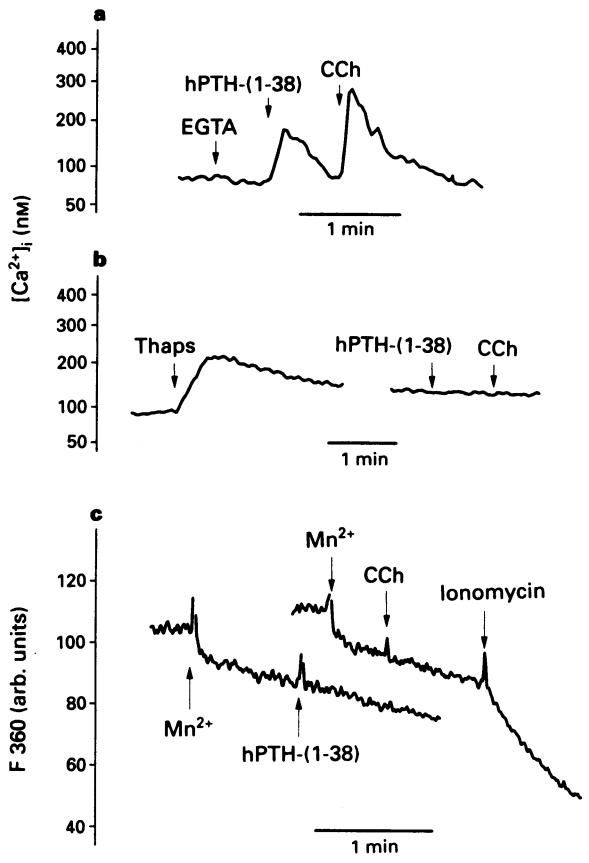

Figure 6 Effects of pretreatment of cells with EGTA (3 mM) (a) or thapsigargin (Thaps, 1 μM) (b) on the $[Ca^{2+}]_i$-response to hPTH-(1-38) and carbachol (CCh). (c) Effects of hPTH-(1-38) and CCh on Mn^{2+} (100 μM)-induced quenching of Fura-2 fluorescence. hPTH-(1-38) and CCh were used at 100 nM and 100 μM, respectively. Mn^{2+} was added as $MnCl_2$ from a 100 mM stock solution. The traces shown are representative of 4–6 independent experiments.

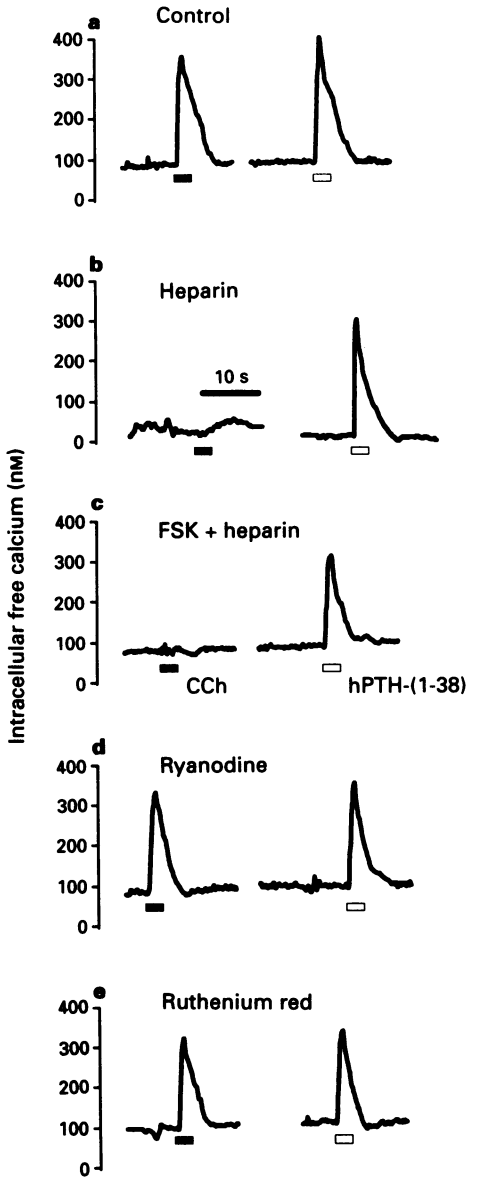

Figure 7 Single cell recordings of $[Ca^{2+}]_i$. Cells were patch clamped (a,b,c) and dialyzed with electrode buffer either with or without heparin (≈100 μM) as indicated. In (c), forskolin (FSK, 3 μM) was added to the bath solution 15 min before recording of a hPTH-(1-38) (100 nM; open bars) and carbachol (CCh, 100 μM; black bars) response. (d,e) Single cell recording without patch clamp. Ryanodine (10 μM) and ruthenium red (10 μM) were added to the bath solution 15 min before recording of a hPTH-(1-38) and CCh response. The traces shown are representative of 5–22 independent recordings.

p5 cells, and we hypothesized that such a sensitization mechanism might render the response heparin-insensitive, if the local heparin concentration near the IP_3 receptors was in a critical range. If this was the case we would expect that cyclic AMP elevating agents should render the CCh response heparin-insensitive. However, as is shown in Figure 7c, this is clearly not observed. Forskolin was unable to induce a heparin-resistant CCh signal. As CCh at 100 μM leads to the production of readily detectable amounts of IP_3 (Figure 2), it seems extremely unlikely that the lack of heparin sensitivity of the hPTH-(1-38) response can be attributed to a PKA-mediated sensitization of the IP_3-receptor.

Calcium signalling by hPTH-(1-38) is not affected by treatment of cells with ruthenium red and ryanodine

In several cell systems, cyclic adenosine diphosphate ribose (cADP-R) is a second messenger stimulating calcium release from intracellular stores in an IP_3-independent manner (Galione, 1994). This response seems to be mediated by a calcium-induced calcium release mechanism involving non-skeletal type ryanodine receptors (McPherson & Campbell, 1993). Calcium release through these receptors can be blocked by ruthenium red and by high concentrations of ryanodine. In order to verify whether this mechanism was involved in PTH-induced calcium signalling, cells were incubated in the presence of 10 μM ruthenium red or 10 μM ryanodine and the responses to hPTH-(1-38) and CCh were measured. As shown in Figure 7c and d, treatment with these two inhibitors interfered neither with the hPTH-(1-38)- nor with the CCh-response.

Heparin-insensitive calcium transients observed in UMR 106-06 rat osteosarcoma cells

In this study we have used a cell line expressing the recombinant human PTH receptor. In order to rule out that the heparin-insensitive calcium signals stimulated by hPTH-(1-38) observed were due to a peculiarity of this cell system, we tested whether the same results could be obtained in UMR 106-06 rat osteosarcoma cells, which express high numbers of PTH receptors and are widely used to study PTH signal transduction (Babich *et al.*, 1991; Wiltink *et al.*, 1993). As in 293 p5 cells, 100 nM hPTH-(1-38) also stimulated heparin-insensitive calcium transients in UMR 106-06 cells (Figure 8). These signals were of longer duration than in 293 p5 cells.

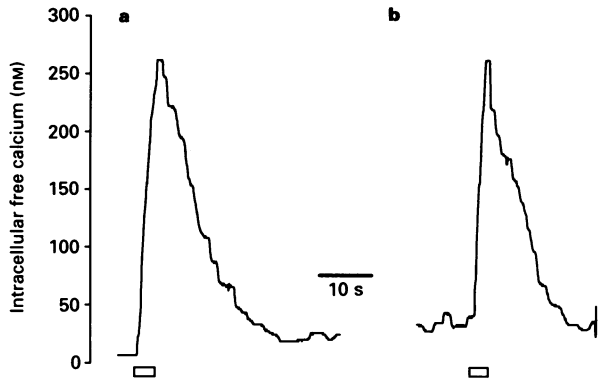

Figure 8 Single cell recordings of $[Ca^{2+}]_i$ in UMR 106-06 rat osteosarcoma cells. Cells were patch clamped and dialyzed with electrode buffer with (b) or without (a) heparin (≈100 μM). hPTH-(1-38) (100 nM, open bars) was applied and calcium responses were recorded. The traces shown are representative of 11 independent recordings, respectively.

Discussion

PTH, PTHrP and peptide analogues have been reported to increase intracellular free calcium rapidly in various cell types by different mechanisms. In osteoblasts and osteosarcoma cell lines, release from intracellular stores (Babich *et al.*, 1991; Civitelli *et al.*, 1992) as well as stimulated influx of calcium across the plasma membrane (Yamaguchi *et al.*, 1987; Bizzarri *et al.*, 1994) have been described. In kidney proximal tubule cells, PTH induces slow changes in $[Ca^{2+}]_i$ which reflect recruitment and activation of specific plasma membrane channels (Bacskai & Friedman, 1990; Friedman & Gesek, 1994).

The physiological relevance of the rapid PTH-induced calcium signals remains uncertain. Normal plasma levels of PTH are in the low picomolar range. At these concentrations, small effects on cyclic AMP formation become apparent, but effects on intracellular calcium are clearly not measurable *in vitro*. In most studies, the EC_{50} for PTH-induced calcium signalling was reported to be considerably higher than the EC_{50} for cyclic AMP formation (Babich *et al.*, 1991; Bringhurst *et al.*, 1993). With our recombinant 293 cells expressing the human receptor we obtained half maximal activation of the two signals at 11.2 and 0.39 nM, respectively. Interestingly, whereas constant infusion of low doses of PTH or analogues strongly activates bone resorption in rats *in vivo*, short intermittent application of high doses, where plasma levels in the nanomolar range are reached, produce anabolic effects (Tam *et al.*, 1982; Mosekilde *et al.*, 1994; Dempster *et al.*, 1994). It is possible that the PTH-induced calcium signals play an important role in this bone forming process.

According to current knowledge the various responses to PTH and analogues are triggered by only one type of PTH/PTHrP receptor (Schipani *et al.*, 1993; Kong *et al.*, 1994), although the existence of functionally different splice variants cannot be excluded at present (Urena *et al.*, 1993; Schneider *et al.*, 1994). A clear picture seemed to emerge when both the recombinant rat and human receptor were found to stimulate cyclic AMP as well as IP formation following transient expression in COS cells (Abou-Samra *et al.*, 1992; Schneider *et al.*, 1993). This dual coupling to second messenger systems was in keeping with results obtained with other receptors of this family, notably the calcitonin receptor (Chabre *et al.*, 1992). It therefore seemed legitimate to speculate that IP_3 generated in response to a PTH challenge was responsible for calcium release from intracellular stores and that the parallel activation of protein kinases A and C could lead, in certain cell types, to an opening of plasma membrane channels.

However, we have been unable to detect a significant formation of inositol phosphates in response to PTH in osteoblasts and osteosarcoma cell lines (unpublished results) as well as in cells stably transfected with the recombinant human PTH receptor cDNA (Schneider *et al.*, 1994; this paper). On the other hand, we could clearly demonstrate activation of this signalling pathway by other stimuli like CCh or AlF_4^- in the transfected 293 cells used in this study. It is possible, therefore, that the IP formation detected in transiently transfected COS cells is an artefact due to severe receptor overexpression. To our knowledge, activation of phosphoinositide turnover has so far not been demonstrated in cells stably expressing one of the cloned PTH receptors.

Despite undetectable IP formation, however, we observed a robust calcium signal in response to hPTH-(1-38) in our transfected 293 cells. This signal occurs independently of the cyclic AMP response and is largely due to release from intracellular stores, as it resists quenching of calcium in the extracellular buffer and is abolished by pretreatment of cells with thapsigargin. Also, hPTH-(1-38) did not stimulate the influx of Mn^{2+}, which can enter cells through certain types of agonist-regulated cation channels.

As the amplitudes of the PTH-induced calcium responses were relatively small, it seemed possible that they were due to the formation of a low amount of IP_3, escaping biochemical detection. We could rule this out using intracellular application of heparin, a strong inhibitor of the IP_3-triggered calcium release channel of the ER. The polyanion completely blocked the calcium responses to high doses of CCh, which elicit strong IP formation, but left the PTH signal intact. Heparin-independent calcium transients stimulated by hPTH-(1-38) were also observed in UMR 106-06 osteosarcoma cells, demonstrating that they are not a peculiarity of the recombinant 293 cells.

Our data provide strong evidence for a PTH-stimulated calcium release mechanism independent of IP_3 and thus confirm a conclusion drawn before by Babich *et al.* (1991). They had compared the calcium signalling mechanism stimulated by bovine PTH-(1-34) and thrombin in rat osteosarcoma cells. Thrombin, but not the PTH peptide, strongly stimulated IP formation. Nevertheless, both agents elicited similar and additive calcium signals.

What could be the nature of the PTH signal? One obvious candidate mechanism was calcium-induced calcium release involving non skeletal type ryanodine receptors. This mechanism was first demonstrated in sea urchin eggs and is now known to exist also in several mammalian cell types (Lee, 1993; Meszaros *et al.*, 1993; Galione, 1994; McPherson & Campbell, 1994). It is strongly inhibited by micromolar concentrations of ruthenium red and ryanodine. However, like heparin, these compounds had no effect on the PTH-induced calcium transients in our cells.

Other potential pathways will now have to be investigated. Whereas a few years ago IP_3 seemed to account for most, if not all cases of calcium release from intracellular stores in non-muscle cells, it is becoming increasingly clear today that several independent pathways seem to exist in different cell types (Mattie *et al.*, 1994; Rosales *et al.*, 1994).

To our knowledge, the present study is the first to demonstrate heparin-insensitive calcium signals triggered by a G protein coupled receptor. However, there is evidence that other receptors of this superfamily also elicit calcium responses in the absence of detectable IP formation (Michel *et al.*, 1992; Vassaux *et al.*, 1992; Frelin *et al.*, 1993). It is important to determine whether our observation can be generalized to a subclass of G protein coupled receptors.

We thank Barbara Wilmering and Viviane Boulay for expert technical assistance and Rainer Gamse and Urs Rüegg for discussions and critical reading of the manuscript.

References

ABOU SAMRA, A.B., JUEPPNER, H., WESTERBERG, D., POTTS, J.T., Jr. & SEGRE, G.V. (1989). Parathyroid hormone causes translocation of protein kinase-C from cytosol to membranes in rat osteosarcoma cells. *Endocrinology*, **124**, 1107–1113.

ABOU SAMRA, A.B., JUPPNER, H., FORCE, T., FREEMAN, M.W., KONG, X.F., SCHIPANI, E., URENA, P., RICHARDS, J., BONVENTRE, J.V., POTTS, J.T., Jr., KRONENBERG, H.M. & SEGRE, G.V. (1992). Expression cloning of a common receptor for parathyroid hormone and parathyroid hormone-related peptide from rat osteoblast-like cells: a single receptor stimulates intracellular accumulation of both cAMP and inositol trisphosphates and increases intracellular free calcium. *Proc. Natl. Acad. Sci. U.S.A.*, **89**, 2732–2736.

BABICH, M., CHOI, H., JOHNSON, R.M., KING, K.L., ALFORD, G.E. & NISSENSON, R.A. (1991). Thrombin and parathyroid hormone mobilize intracellular calcium in rat osteosarcoma cells by distinct pathways. *Endocrinology*, **129**, 1463–1470.

BACSKAI, B.J. & FRIEDMAN, P.A. (1990). Activation of latent Ca2+ channels in renal epithelial cells by parathyroid hormone. *Nature*, **347**, 388–391.

BIRD, G.S., BURGESS, G.M. & PUTNEY, J.W.J. (1993). Sulfhydryl reagents and cAMP-dependent kinase increase the sensitivity of the inositol 1,4,5-trisphosphate receptor in hepatocytes. *J. Biol. Chem.*, **268**, 17917–17923.

BIZZARRI, C. & CIVITELLI, R. (1994). Activation of the Ca2+ message system by parathyroid hormone is dependent on the cell cycle. *Endocrinology*, **134**, 133–140.

BODDEKE, H.W., HOFFMAN, B.J., PALACIOS, J.M., KNOT, H. & HOYER, D. (1993). Characterization of functional responses in A9 cells transfected with cloned rat 5-HT1C receptors. *Naunyn-Schmied. Arch. Pharmacol.*, **347**, 119–124.

BODDEKE, H.W., MEIGEL, I., SWOBODA, R. & BOEIJINGA, P.H. (1994). The amyloid precursor protein fragment His 657-Lys 676 inhibits noradrenaline- and enkephaline-induced suppression of voltage sensitive calcium currents in NG108-15 hybrid cells. *Neuroscience*, **62**, 631–634.

BRINGHURST, F.R., JUPPNER, H., GUO, J., URENA, P., POTTS, J.T., Jr., KRONENBERG, H.M., ABOU SAMRA, A.B. & SEGRE, G.V. (1993). Cloned, stably expressed parathyroid hormone (PTH)/PTH-related peptide receptors activate multiple messenger signals and biological responses in LLC-PK1 kidney cells. *Endocrinology*, **132**, 2090–2098.

CHABRE, O., CONKLIN, B.R., LIN, H.Y., LODISH, H.F., WILSON, E., IVES, H.E., CATANZARITI, L., HEMMINGS, B.A. & BOURNE, H.R. (1992). A recombinant calcitonin receptor independently stimulates 3',5'-cyclic adenosine monophosphate and Ca2+/inositol phosphate signaling pathways. *Mol. Endocrinol.*, **6**, 551–556.

CIVITELLI, R., FUJIMORI, A., BERNIER, S.M., WARLOW, P.M., GOLTZMAN, D., HRUSKA, K.A. & AVIOLI, L.V. (1992). Heterogeneous intracellular free calcium responses to parathyroid hormone correlate with morphology and receptor distribution in osteogenic sarcoma cells. *Endocrinology*, **130**, 2392–2400.

DEMPSTER, D.W., COSMAN, F., PARISIEN, M., SHEN, V. & LINDSAY, R. (1993). Anabolic actions of parathyroid hormone on bone. *Endocr. Rev.*, **14**, 690–709.

FADDA, G.Z., THANAKITCHARU, P., SMOGORZEWSKI, M. & MASSRY, S.G. (1993). Parathyroid hormone raises cytosolic calcium in pancreatic islets: study on mechanisms. *Kidney Int.*, **43**, 554–560.

FASOLATO, C., HOTH, M., MATTHEWS, G. & PENNER, R. (1993). Ca^{2+} and Mn^{2+} influx through receptor-mediated activation of nonspecific cation channels in mast cells. *Proc. Natl. Acad. Sci. U.S.A.*, **90**, 3068–3072.

FRELIN, C., BREITTMEYER, J.P. & VIGNE, P. (1993). ADP induces inositol phosphate-independent intracellular Ca2+ mobilization in brain capillary endothelial cells. *J. Biol. Chem.*, **268**, 8787–8792.

FRIEDMAN, P.A. & GESEK, F.A. (1993). Calcium transport in renal epithelial cells. *Am. J. Physiol.*, **264**, F181–F198.

FUJIMORI, A., CHENG, S.L., AVIOLI, L.V. & CIVITELLI, R. (1992). Structure-function relationship of parathyroid hormone: activation of phospholipase-C, protein kinase-A and -C in osteosarcoma cells. *Endocrinology*, **130**, 29–36.

GALIONE, A. (1994). Cyclic ADP-ribose, the ADP-ribosyl cyclase pathway and calcium signalling. *Mol. Cell. Endocrinol.*, **98**, 125–131.

GOSH, T.K., EIS, P.S., MULLANEY, J.M., EBERT, C.L. & GILL, D.L. (1988). Competitive, reversible, and potent antagonism of inositol 1,4,5-trisphosphate-activated calcium release by heparin. *J. Biol. Chem.*, **263**, 11075–11079.

GRYNKIEWICZ, G., POENIE, M. & TSIEN, R.Y. (1985). A new generation of Ca2+ indicators with greatly improved fluorescence properties. *J. Biol. Chem.*, **260**, 3440–3450.

KONG, X.-F., SCHIPANI, E., LANSKE, B., JOUN, H., KARPERIEN, M., DEFIZE, L.H.K., JÜPPNER, H., POTTS, J.T., Jr., SEGRE, G.V., KRONENBERG, H.M. & ABOU-SAMRA, A.B. (1994). The rat, mouse and human genes encoding the receptor for parathyroid hormone and parathyroid hormone-related peptide are highly homologous. *Biochem. Biophys. Res. Commun.*, **200**, 1290–1299.

LEE, H.C. (1993). Potentiation of calcium- and caffeine-induced calcium release by cyclic ADP-ribose. *J. Biol. Chem.*, **268**, 293–299.

LÖWIK, C.W.G.M., VAN LEEUWEN, J.P.T.M., VAN DER MEER, J.M., VAN ZEELAND, J.K., SCHEVEN, B.A.A. & HERRMANN-ERLEE, M.P.M. (1985). A two-receptor model for the action of parathyroid hormone on osteoblasts: a role for intracellular free calcium and cAMP. *Cell Calcium*, **6**, 311–326.

LYTTON, J., WESTLIN, M. & HANLEY, M.R. (1991). Thapsigargin inhibits the sarcoplasmic or endoplasmic reticulum Ca-ATPase family of calcium pumps. *J. Biol. Chem.*, **266**, 17067–17071.

MATTIE, M., BROOKER, G. & SPIEGEL, S. (1994). Sphingosine-1-phosphate, a putative second messenger, mobilizes calcium from internal stores via an inositol trisphosphate-independent pathway. *J. Biol. Chem.*, **269**, 3181–3188.

MCPHERSON, P.S. & CAMPBELL, K.P. (1993). The ryanodine receptor/Ca2+ release channel. *J. Biol. Chem.*, **268**, 13765–13768.

MERRITT, J.E., JACOB, R. & HALLAM, T.J. (1989). Use of manganese to discriminate between calcium influx and mobilization from internal stores in stimulated human neutrophils. *J. Biol. Chem.*, **264**, 1522–1527.

MESZAROS, L.G., BAK, J. & CHU, A. (1993). Cyclic ADP-ribose as an endogenous regulator of the non-skeletal type ryanodine receptor Ca^{2+} channel. *Nature*, **364**, 76–79.

MICHEL, M.C., FETH, F. & RASCHER, W. (1992). NPY-stimulated Ca^{2+} mobilization in SK-N-MC cells is enhanced after isoproterenol treatment [published erratum appears in *Am. J. Physiol.*, 1992 Dec; **263** (6 Pt 1): section E following table of contents]. *Am. J. Physiol.*, **262**, E383–E388.

MOSEKILDE, L., DANIELSEN, C.C. & GASSER, J. (1994). The effect on vertebral bone mass and strength of long term treatment with antiresorptive agents (estrogen and calcitonin), human parathyroid hormone-(1-38), and combination therapy, assessed in aged ovariectomized rats. *Endocrinology*, **134**, 2126–2134.

REID, I.R., CIVITELLI, R., HALSTEAD, L.R., AVIOLI, L.V. & HRUSKA, K.A. (1987). Parathyroid hormone acutely elevates intracellular calcium in osteoblastic cells. *Am. J. Physiol.*, **252**, E45–E51.

ROSALES, C., JONES, S.L., MCCOURT, D. & BROWN, E.J. (1994). Bromophenacyl bromide binding to the actin-binding protein I-plastin inhibits inositol trisphosphate-independent increase in Ca2+ in human neutrophils. *Proc. Natl. Acad. Sci. U.S.A.*, **91**, 3534–3538.

SALOMON, Y. (1979). Adenylate cyclase assay. *Adv. Cyclic Nucl. Res.*, **10**, 35–55.

SCHIPANI, E., KARGA, H., KARAPLIS, A.C., POTTS, J.T., Jr., KRONENBERG, H.M., SEGRE, G.V., ABOU SAMRA, A.B. & JUPPNER, H. (1993). Identical complementary deoxyribonucleic acids encode a human renal and bone parathyroid hormone (PTH)/PTH-related peptide receptor. *Endocrinology*, **132**, 2157–2165.

SCHNEIDER, H., FEYEN, J.H., SEUWEN, K. & MOVVA, N.R. (1993). Cloning and functional expression of a human parathyroid hormone receptor. *Eur. J. Pharmacol.*, **246**, 149–155.

SCHNEIDER, H., FEYEN, J.H. & SEUWEN, K. (1994). A C-terminally truncated human parathyroid hormone receptor is functional and activates multiple G proteins [published erratum appears in *FEBS Lett.*, **355**, p. 210]. *FEBS Lett.*, **351**, 281–285.

SEUWEN, K., LAGARDE, A. & POUYSSEGUR, J. (1988). Deregulation of hamster fibroblast proliferation by mutated ras oncogenes is not mediated by constitutive activation of phosphoinositide-specific phospholipase C. *EMBO J.*, **7**, 161–168.

STOJCEVA TANEVA, O., FADDA, G.Z., SMOGORZEWSKI, M. & MASSRY, S.G. (1993). Parathyroid hormone increases cytosolic calcium of thymocytes. *Nephron*, **64**, 592–599.

TAM, C.S., HEERSCHE, J.N., MURRAY, T.M. & PARSONS, J.A. (1982). Parathyroid hormome stimulates the bone apposition rate independently of its resorptive action: differential effects of intermittent and continuous administration. *Endocrinology*, **110**, 506–512.

TAMURA, T., SAKAMOTO, H. & FILBURN, C.R. (1989). Parathyroid hormone 1-34, but not 3-34 or 7-34, transiently translocates protein kinase C in cultured renal (OK) cells. *Biochem. Biophys. Res. Commun.*, **159**, 1352–1358.

URENA, P., KONG, X.F., ABOU SAMRA, A.B., JUPPNER, H., KRONENBERG, H.M., POTTS, J.T., Jr. & SEGRE, G.V. (1993). Parathyroid hormone (PTH)/PTH-related peptide receptor messenger ribonucleic acids are widely distributed in rat tissues. *Endocrinology*, **133**, 617–623.

VASSAUX, G., GAILLARD, D., AILHAUD, G. & NEGREL, D. (1992). Prostacyclin is a specific effector of adipose cell differentiation. Its dual role as a cAMP- and Ca(2+)-elevating agent. *J. Biol. Chem.*, **267**, 11092–11097.

WILTINK, A., VAN DEN BRINK, A.M., HERRMANN ERLEE, M.P., VAN DER MEER, J.M., VAN DER PLAS, A., WILLEMS, P.H., VAN DUIJN, B., NIJWEIDE, P.J. & YPEY, D.L. (1993). Heterogeneity of intracellular calcium responses to parathyroid hormone and thrombin in primary osteoblast-like cells and UMR106-01 cells: correlations with culture conditions, intracellular calcium concentration and differentiation state. *Cell Calcium*, **14**, 591–600.

YAMAGUCHI, D.T., HAHN, T.J., IIDA-KLEIN, A., KLEEMAN, C.R. & MUALLEM, S. (1987). Parathyroid hormone-activated calcium channels in an osteoblast-like clonal osteosarcoma cell line. *J. Biol. Chem.*, **262**, 7711–7718.

(Received October 3, 1994
Revised January 3, 1995
Accepted January 17, 1995)

British Journal of Pharmacology (1995) 114, 1621-1624 © 1995 Stockton Press All rights reserved 0007-1188/95 $12.00

Conversion of inhaled nitric oxide to nitrate in man

Ulla Nathorst Westfelt, *Günther Benthin, Stefan Lundin, Ola Stenqvist & [1,*]Åke Wennmalm

Department of Anaesthesiology and *Division of Clinical Physiology, Göteborg University, Göteborg, Sweden

1 Nitric oxide (NO) is potentially useful as a selective vasodilator drug in infants and adults with pulmonary hypertension. *In vitro* and *in vivo* observations demonstrate that NO may be converted to nitrate in the blood, to be further excreted into the urine. The aim of the present study was to assess quantitatively the importance of this pathway for inhaled NO in human subjects.

2 Healthy subjects inhaled ^{15}NO (25 p.p.m.) for 1 h. The plasma and urine levels of $^{15}NO_3^-$ were followed for 2 and 48 h, respectively.

3 The measured retention of ^{15}NO in the lungs was 224 ± 13 μmol, corresponding to $90 \pm 2\%$ of the inhaled amount. Plasma $^{15}NO_3^-$ increased during the inhalation of ^{15}NO, to about 15 μmol l^{-1}, and fell when inhalation of ^{15}NO was terminated.

4 Urinary excretion of $^{15}NO_3^-$ during the first 24 h after inhalation was 154 ± 12 μmol. During the following 24 h another 8 ± 2 μmol of $^{15}NO_3^-$ appeared in the urine.

5 We conclude that conversion of inhaled NO to nitrate is a major metabolic pathway in man, covering more than 70% of its inactivation. The metabolic fate of the remaining NO inhaled requires further study.

Keywords: Blood; endothelium-derived relaxing factor; lungs; nitrate; urine

Introduction

Nitric oxide (NO) is a biomediator with significant physiological actions in vascular endothelium (Furchgott & Zawadzki, 1980), nervous tissue (Garthwaite *et al.*, 1988) and macrophages (Iyengar *et al.*, 1987). Recent reports indicate that inhalation of low concentrations of NO elicits selective pulmonary vasodilatation in infants and adults with pulmonary hypertension, without any tendency to systemic hypotension (Pepke-Zaba *et al.*, 1991; Roberts *et al.*, 1992). Hence, NO may be a useful drug in certain clinical settings.

The application of NO as a drug calls for methods to assess circulating metabolites of NO and their excretion in the body. A suitable plasma or urine marker might be a tool to follow metabolite accumulation during NO inhalation therapy. Such methods may also possibly be useful in the evaluation of the endogenous formation of NO.

We earlier reported that NO was converted to nitrate in arterialized whole blood *in vitro* (Wennmalm *et al.*, 1992). It was later demonstrated that, during inhalation of NO, nitrate formation was parallelled by the appearance of significant amounts of methaemoglobin in the blood, suggesting that the conversion might involve oxygenated haemoglobin (Wennmalm *et al.*, 1993). Nitrate in plasma was excreted into the urine (Wennmalm *et al.*, 1993).

The technique utilized in these studies did not allow quantitative evaluation of the NO/nitrate pathway. The present study specifically addressed this issue by assessing the size of the fraction of inhaled ^{15}NO that was converted to ^{15}N-labelled nitrate.

Methods

Inhalation of ^{15}NO in healthy human subjects

Eight healthy female volunteers, aged 37 ± 3 (range 25-48) years, were recruited among the hospital staff. Their height was 166 ± 2 (range 162-172) cm, and their body weight was 62 ± 3 (range 53-74) kg. Three of them were smokers. The participants were instructed to refrain from intake of nitrate-rich food from two days before and to the end of the study. The provisions to be excluded were: alcoholic beverages, caviar, charcuteries, cheese, herbs, pickled fish, roots, and vegetables.

The subjects reported at the laboratory in the morning. Compliance concerning diet was assessed by asking the participants to review their diet during the preceding 48 h. After emptying the bladder for collection of basal urine, a short catheter was inserted into a medial cubital vein. Subsequently the subjects were allowed to rest comfortably in an arm chair for 10-15 min. The experimental procedure started with a 10 min control period of spontaneous respiration via a tight-fitting face mask in a non-rebreathing system.

The system for NO delivery to the breathing gas consisted of two mask flow regulators, one of them controlling the flow of ^{15}NO mixed in N_2 (1000 p.p.m., AGA Gas AB, Lidingö, Sweden), and the other controlling an O_2/air mixture (Stenqvist *et al.*, 1993). A final concentration of 25 p.p.m. of ^{15}NO was given at an adjustable flow rate. Gas flow and the concentration of ^{15}NO were continuously recorded during the inhalation period by fuel cell technique (City Technology, London, UK), which was calibrated with a test gas of 35 p.p.m. NO in N_2 (AGA Gas AB, Lidingö, Sweden). The expired air was likewise analyzed, recording the concentration of ^{15}NO in the mixed expired air throughout the inhalation period. To obtain the volume of alveolar ventilation, mixed and end-tidal expired CO_2 concentrations were measured with an infrared absorbtion CO_2 analyzer (Normocap, Datex, Helsinki, Finland), which was calibrated with a test gas with 3.0% CO_2 in air.

The subjects inhaled ^{15}NO for 1 h. Blood samples (5 ml) were drawn via a short catheter in an arm vein in the basal state, i.e. prior to inhalation of ^{15}NO, and 20, 40, 60, 80, 100 and 120 min after onset of inhalation. After separation, plasma was kept at -20°C until analysis.

Urine was collected in two 24 h portions following the start of the inhalation. The urine collection flasks were kept frozen during the collection periods. After volume recording, samples of the collected 24 h portions of urine were frozen and kept at -20°C until analysis.

The studies were approved by the local human investigations committee.

[1] Author for correspondence at: Division of Clinical Physiology, Sahlgrenska University Hospital, S-413 45 Göteborg, Sweden.

Analyses

The thawed plasma samples were diluted with 9 vol of water. Proteins were separated by centrifugation at 7500 *g* for 60 min through an ultrafilter with cut-off at 10 K. Following separation of proteins the following analyses were performed. The basal plasma samples, i.e. the samples taken prior to inhalation of ^{15}NO, were determined for mass concentration of nitrate with stable isotope dilution technique (addition of 1 μg of $K^{15}NO_3$ per 100 μl of undiluted plasma prior to separation of proteins), utilizing GC/MS for determination of the ratio between labelled and endogenous nitrate. The plasma samples taken during inhalation of ^{15}NO were also analyzed for the ratio between labelled and unlabelled nitrate with GC/MS; however, $K^{15}NO_3$ was not added to these samples.

Since the basal samples did not contain any $^{15}NO_3$- their mass concentration of nitrate could be determined with stable isotope dilution technique. The known concentration of added $^{15}NO_3$- was used as reference in the calculation of the concentration of endogenous NO_3-. The mass concentration of endogenous (unlabelled) nitrate was assumed not to vary during the 60 min period of inhalation. This assumption appeared justified since the volunteers had been subjected to nitrate-restricted diet for 48 h prior to the study occasion. In line with this, the subsequent plasma samples (taken during inhalation of ^{15}NO) were quantified with respect to mass concentration of $^{15}NO_3$- by determining the ratio between labelled and unlabelled nitrate in the samples with GC/MS, followed by calculating the mass concentration of $^{15}NO_3$- with the previous GC/MS-determined mass concentration of unlabelled (endogenous) nitrate in the basal plasma samples as reference.

In addition to these GC/MS analyses, all plasma samples were analyzed for total (labelled plus unlabelled) nitrite with liquid chromatography, to disclose any significant formation of ^{15}N-labelled nitrite during the inhalation period. The LC analyses were conducted on samples that had been diluted and separated for proteins in the same way as the samples subjected to GC/MS analysis.

Urine samples were centrifuged at 7500 *g* for 20 min without filter, for separation of precipitates. The supernatant was diluted with 199 vol of water before injection into the liquid chromatography system. The urine levels of total (labelled plus unlabelled) nitrite and nitrate were determined by use of internal standards (see below). The ratio between labelled and unlabelled nitrate in the urine samples collected following inhalation of ^{15}NO was determined with GC/MS, and the mass concentration of labelled nitrate in the urine samples was calculated from the ratio obtained and the corresponding mass concentration.

GC/MS analysis was performed as follows. Endogenous and ^{15}N-labelled nitrate in the plasma and urine samples was converted to nitrotoluene by shaking a 10 or 50 μl portion, respectively, for 20 min with 500 μl of toluene and 200 μl of conc. H_2SO_4. The organic phase was then separated and 10 vol of acetonitrile added.

A 1–2 μl portion of the derivatized samples was injected into a Varian 3400 gas chromatograph (Varian, Walnut Creek, CA) equipped with a 25 m SPB 5 capillary column operated isothermally at 85°C. It was connected to a Finnigan Incos 50 mass spectrometer (Finnigan, San Jose, CA, U.S.A.) operated in the negative ion-chemical ionization mode using methane as the reagent gas and selective monitoring of m/e 137 for unlabelled nitrate, and m/e 138 for ^{15}N-labelled nitrate. The detection limit for nitrate using GC/MS was 0.5 μmol l^{-1}.

Analysis of urine levels of total nitrite and nitrate, and plasma levels of total nitrite, was performed with liquid chromatography: 20 μl portions of diluted and centrifuged urine or plasma samples were injected into a chromatography system using a 50 mm column of IC-Pak A (Waters, Milford, MA, U.S.A.) as solid phase, and 1 mM phosphate buffer pH 8 as mobile phase. Quantitative analysis was performed against internal standards with u.v. absorbance at 214 nm. The retention time for external nitrite standard was about 6.5 min and that for external nitrate standard about 13 min. The retention time for nitrite and nitrate added to urine or plasma samples did not differ from the respective retention times of these compounds in buffer solution (external standard). The recovery of standards added to urine samples (internal standards) was 85–88% of the corresponding external standard. The calculations of mass concentrations were always made from the internal standards. The detection limit for nitrate using liquid chromatography was 0.5 μmol l^{-1}. The detection limit for nitrite using liquid chromatography was <0.1 μmol l^{-1}.

Calculations

The total volume of ^{15}NO inhaled was calculated as total ventilation volume × inhaled conc. of ^{15}NO. The uptake of ^{15}NO was calculated as total ventilation volume × (inhaled conc. of ^{15}NO – expired conc. of ^{15}NO). Conversion of gas volume to molar quantity was calculated using the constant 24.2 μl μmol^{-1}. CO_2 production was calculated as mixed expired CO_2 concentration × minute ventilation volume and corrected to standard pressure and temperature, dry (STPD). Alveolar ventilation was calculated from Bohr's formula (alveolar ventilation = CO_2 production/end-tidal CO_2 concentration).

Statistical analysis

Data are presented as mean ± s.e.

Results

The plasma level of nitrate in the participants prior to inhalation of ^{15}NO was 31.6 ± 2.7 μmol l^{-1}. The plasma level of nitrite prior to inhalation was consistently <1 μmol l^{-1}. The urine level of nitrate in the participants prior to inhalation of ^{15}NO was 925 ± 217 μmol l^{-1}. No nitrite was detectable in the basal urine samples.

Inhalation of ^{15}NO in healthy human subjects

The pulmonary ventilation during the 60 min period of inhalation of ^{15}NO was 6.7 ± 0.3 l min^{-1}. The total amount of ^{15}NO inhaled was 399 ± 15 μmol. The measured uptake of ^{15}NO was 224 ± 13 μmol. The alveolar ventilation averaged

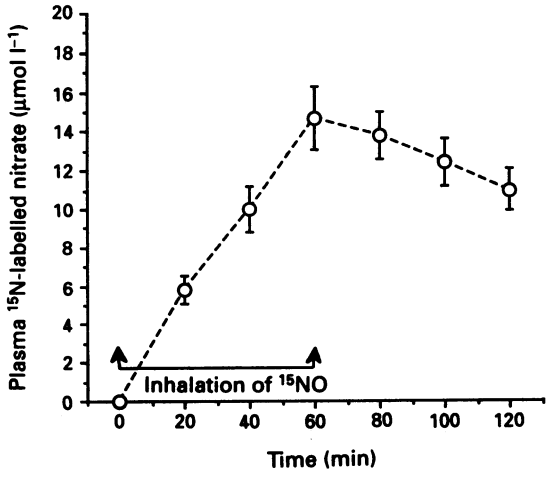

Figure 1 Plasma levels of $^{15}NO_3$- during the following inhalation of ^{15}NO as indicated by bar in eight healthy females. Symbols indicate mean ± s.e.

Table 1 Retained total amount of ^{15}N-labelled nitric oxide (^{15}NO), maximal plasma concentration of $^{15}NO_3^-$, amount of $^{15}NO_3^-$ in urine collected on days 1 and 2 after inhalation of ^{15}NO, and total recovery of inhaled ^{15}NO as $^{15}NO_3^-$ in urine (sum of days 1 and 2)

Subject	*Total amount of ^{15}NO retained* (μmol)	*Max. $^{15}NO_3^-$ in plasma* (μmol l^{-1})	*$^{15}NO_3^-$ in urine day 1* (μmol)	*day 2* (μmol)	*Total recovery of $^{15}NO_3^-$* (% of inhaled ^{15}NO)
1 (S)	206	14.2	189	9	96
2 (NS)	168	8.6	114	8	73
3 (NS)	230	20.7	142	2	63
4 (S)	264	14.8	169	8	67
5 (NS)	242	16.5	135	10	60
6 (NS)	193	19.1	107	5	58
7 (NS)	272	11.9	195	3	73
8 (S)	214	16.5	177	20	92
Mean ± s.e.	224 ± 13	15.3 ± 1.4	154 ± 12	8 ± 2	73 ± 5

(S) and (NS) after subject number indicates smoker and non-smoker, respectively.

62 ± 1% (4.2 ± 0.2 l min^{-1}) of the pulmonary ventilation. The calculated amount of ^{15}NO reaching the alveoli was 247 ± 12 μmol, implying that 90 ± 2% of the ^{15}NO reaching the alveoli was retained.

Inhalation of ^{15}NO elicited a rapid linear increase in the plasma concentration of $^{15}NO_3$-, as demonstrated in Figure 1. The maximal average plasma concentration of $^{15}NO_3$- was reached at the end of the inhalation. Subsequently the plasma concentration of $^{15}NO_3$- declined. The plasma concentrations of total nitrite in samples taken during inhalation of ^{15}NO were consistently <1 μmol l^{-1}.

The urinary excretions of $^{15}NO_3$- during days 1 and 2 after inhalation are shown in Table 1. About 154 μmol of $^{15}NO_3$- were excreted during the first 24 h after onset of inhalation. Another 8 μmol was excreted during the following 24 h (day 2). The percentage of ^{15}NO excreted as $^{15}NO_3$- during the 48 h following the start of inhalation was 73 ± 5% (Table 1). No nitrite was detectable in urine samples taken during the 48 h following inhalation of ^{15}NO.

Discussion

Healthy subjects inhaling ^{15}NO displayed increasing plasma levels of $^{15}NO_3$- during the inhalation. Upon cessation of inhalation of ^{15}NO, the levels of labelled nitrate dropped. $^{15}NO_3$- appeared in the urine following inhalation of ^{15}NO; the molar excretion during the 48 h following inhalation corresponded to more than 70% of the ^{15}NO uptake. No signs of nitrite formation during or following inhalation of ^{15}NO were obtained, either in plasma or urine.

NO and L-citrulline are formed when nitric oxide synthase acts on L-arginine and molecular oxygen in the vascular endothelium (Leone *et al.*, 1991). Administration of ^{15}N-labelled L-arginine has been shown to yield minute amounts of $^{15}NO_3$- in the urine, indicating that at least some fraction of the NO formed is converted to nitrate (Green *et al.*, 1982). Previous data from our laboratory demonstrated that nitrate may be a major metabolite of NO in the blood, and that this nitrate is excreted into the urine (Wennmalm *et al.*, 1992; 1993).

In the present experiments the plasma level of (unlabelled) nitrate in the participants prior to inhalation of ^{15}NO was 31.6 ± 2.7 μmol l^{-1}, i.e. roughly the same as that previously reported by us (Wennmalm *et al.*, 1993). The urine level of (unlabelled) nitrate in the participants prior to inhalation of ^{15}NO was 925 ± 217 μmol l^{-1}. This level is also in agreement with earlier observations in our laboratory (Wennmalm *et al.*, 1993).

Inhalation of ^{15}N-labelled nitric oxide yielded about 90% uptake of the isotope in the alveoli. In parallel, $^{15}NO_3$- appeared in the plasma of the inhaling subjects. The concentrations of labelled nitrate increased almost linearly throughout the inhalation, without any tendency to levelling off, and dropped upon cessation of inhalation of labelled NO. The appearance of $^{15}NO_3$- indicates that the inhaled ^{15}NO was rapidly converted to nitrate in the blood. The maximal plasma concentration of $^{15}NO_3$- was about 15 μmol l^{-1}. We have recently demonstrated that the distribution volume for nitrate in the body is about 30% of the body weight (Jungersten *et al.*, 1993). Assuming rapid conversion of NO to nitrate in the blood and immediately completed distribution of this ion, a plasma concentration of about 11 μmol l^{-1} would have been achieved at the end of the inhalation (224 μmol retained/0.30 × body wt.). The observed average plasma concentration of nitrate at the end of the inhalation was higher than that figure, indicating that distribution was not complete.

About 69% of the inhaled ^{15}NO was excreted into the urine as $^{15}NO_3$- within 24 h after the start of inhalation, and another 4% was excreted from 24 to 48 h after the start of inhalation. Hence, it is evident that a major part of the inhaled ^{15}NO was excreted as labelled nitrate in the urine. We recently estimated the half-life of endogenous nitrate in plasma to be about 6–7 h (Jungersten *et al.*, 1993); the current excretion of ^{15}N-labelled nitrate supports this notion.

In conclusion, the present experiments demonstrate that more than 70% of inhaled NO is inactivated and excreted as nitrate. However, further studies are required to evaluate whether conversion to nitrate is also a major metabolic pathway for endogenously formed NO.

This study was supported by the Swedish Medical Research Council, project 4341.

References

FURCHGOTT, R.F. & ZAWADZKI, J.F. (1980). The obligatory role of endothelial cells in the relaxation of arterial smooth muscle by acetylcholine. *Nature*, **288**, 373–376.

GARTHWAITE, J., CHARLES, S.J. & CHESS-WILLIAMS, R. (1988). Endothelium-derived relaxing factor release on activation of NMDA receptors suggests role as intercellular messenger in the brain. *Nature*, **336**, 385–388.

GREEN, L.C., WAGNER, D.A., GLOGOWSKI, J., SKIPPER, P.L., WISHNOK, J.S. & TANNENBAUM, S.R. (1982). Analysis of nitrate, nitrite, and [^{15}N]nitrate in biological fluids. *Anal. Biochem.*, **126**, 131–138.

IYENGAR, R., STUEHR, D.J. & MARLETTA, M.A. (1987). Macrophage synthesis of nitrite, nitrate, and N-nitrosamines: precursors and role of the respiratory burst. *Proc. Natl. Acad. Sci. U.S.A.*, **84**, 6369–6373.

JUNGERSTEN, L., EDLUND, A., PETERSSON, A.-S. & WENNMALM, Å. (1993). Plasma nitrate as an index of endogenous nitric oxide formation in man. Analysis of kinetics, confounding factors, and response to immunological challenge. *Circulation*, **88**, I–369.

LEONE, A.M., PALMER, R.M.J., KNOWLES, R.G., FRANCIS, P.L., ASHTON, D.S. & MONCADA, S. (1991). Constitutive and inducible nitric oxide synthases incorporate molecular oxygen into both nitric oxide and citrulline. *J. Biol. Chem.*, **66**, 23790–23795.

PEPKE-ZABA, J., HIGENBOTTAM, T.W., DINH-XUAN, A.T., STONE, D. & WALLWORK, J. (1991). Inhaled nitric oxide as a cause of selective pulmonary vasodilation in pulmonary hypertension. *Lancet*, **388**, 1173–1174.

ROBERTS, J.D., POLANER, D.M., LANG, P. & ZAPOL, W.M. (1992). Inhaled nitric oxide in persistent pulmonary hypertension of the newborn. *Lancet*, **340**, 818–819.

STENQVIST, O., KJELLTOFT, B. & LUNDIN, S. (1993). Evaluation of a new system for ventilatory administration of nitric oxide. *Acta Anaesth. Scand.*, **37**, 687–691.

WENNMALM, Å., BENTHIN, G. & PETERSSON, A.-S. (1992). Dependence of the metabolism of nitric oxide (NO) in healthy human whole blood on the oxygenation of its red cell haemoglobin. *Br. J. Pharmacol.*, **106**, 507–509.

WENNMALM, Å., BENTHIN, G., EDLUND, A., JUNGERSTEN, L., KIELER-JENSEN, N., LUNDIN, S., NATHORST WESTFELT, U., PETERSSON, A.-S. & WAAGSTEIN, F. (1993). Metabolism and excretion of nitric oxide in man. An experimental and clinical study. *Circ. Res.*, **73**, 1121–1127.

(Received January 3, 1995
Accepted January 17, 1995)

British Journal of Pharmacology (1995) 114, 1625–1630 © 1995 Stockton Press All rights reserved 0007–1188/95 $12.00

The protective action of chlormethiazole against ischaemia-induced neurodegeneration in gerbils when infused at doses having little sedative or anticonvulsant activity

[1]A.J. Cross, J.A. Jones, M. Snares, *K.-G. Jostell, *U. Bredberg & A.R. Green

Astra Neuroscience Research Unit, 1 Wakefield Street, London WC1N 1PJ & *Astra Arcus, Södertälje S-151 85, Sweden

1 The effect of chlormethiazole administration on delayed neuronal death in gerbil hippocampus following transient global ischaemia has been examined. Chlormethiazole was administered either intraperitoneally or by intravenous infusion with either the dose or the time of infusion varied.

2 Chlormethiazole (600 μmol kg^{-1}, i.p.) given 60 min after ischaemia produced substantial (>60%) neuroprotection when damage was assessed 5, 14 or 21 days later, indicating the drug does not merely delay cell death.

3 Infusion protocols were developed which would result in sustained and defined plasma concentrations. Chlormethiazole (930 μmol kg^{-1}) was then infused intravenously for 30 min, 76.5 min or 110 min in ways resulting in sustained plasma concentrations of 200, 100 and 50 nmol ml^{-1} respectively. When treatment was initiated 30 min after the ischaemic episode all protocols provided effective neuroprotection. There was a dose-dependent decline in protection when plasma chlormethiazole concentrations of 50, 30 and 10 nmol ml^{-1} were sustained for 110 min with no protection observed at 10 nmol ml^{-1}.

4 In contrast, when a plasma concentration of 10 nmol ml^{-1} was sustained by infusion for 24 h, almost total neuroprotection against the ischaemic damage was achieved. This plasma concentration produced no sedative or anticonvulsant activity.

5 These data suggest that neuroprotection depends on both dose and duration of chlormethiazole administration and that excellent neuroprotection is possible in the absence of the sedative and anticonvulsant effects of the drug.

Keywords: Neuroprotection; neurodegeneration; ischaemia; chlormethiazole; sedation; hippocampus; anticonvulsant activity

Introduction

Chlormethiazole (INN: clomethiazole) has previously been shown to prevent the delayed neuronal degeneration that occurs in the gerbil hippocampus 4 days following transient forebrain ischaemia (Cross *et al.*, 1991). This protection was first demonstrated histologically (Cross *et al.*, 1991) and subsequently also biochemically and behaviourally (Baldwin *et al.*, 1993).

Neuroprotection was observed when a single dose of chlormethiazole (622 μmol kg^{-1} = 100 mg kg^{-1}) was injected intra-peritoneally (i.p.) between 1 and 3 h after the ischaemic insult. A lower dose (300 μmol kg^{-1}) given 1 h post-ischaemia also provided some degree of neuroprotection (Cross *et al.*, 1991).

Since other pharmacological studies in this laboratory on the effects of chlormethiazole in rodents suggested that the drug had a short half-life (unpublished observations) it seemed possible that protection might be possible at lower doses if it were administered continuously over a period of time. Because intravenous administration would be the preferred route if the compound were to be given clinically to treat patients with acute ischaemic stroke, a study has now been undertaken on the dose-response characteristics of intravenously administered chlormethiazole. In addition, since chlormethiazole has sedative, hypnotic and anticonvulsant properties (see for example Evans *et al.*, 1986; Green & Murray, 1989), measures of sedative and anticonvulsant activity have also been made to examine whether these properties are present at the same plasma concentrations as those required for neuroprotective activity. Results indicate that neuroprotection is possible when chlormethiazole is given by intravenous infusion and at plasma levels that are well tolerated in human subjects. Some of these results have been communicated in preliminary form to the British Pharmacological Society (Baldwin *et al.*, 1991).

[1] Author for correspondence.

Methods

Animals

Male Mongolian gerbils (Bantin and Kingman, Hull, U.K.) weighing 60–80 g were used. They were housed singly in a room with controlled environment and lighting (lights on: 0.7 h 00 min-19 h 0 0min) and with free access to food and tap water.

Induction of ischaemia

Transient forebrain ischaemia was induced by bilateral carotid artery occlusion described in detail elsewhere (Cross *et al.*, 1991; Baldwin *et al.*, 1993). Briefly, gerbils were anaesthetized with Saffan (alphaxalone, 166 μmol kg^{-1} plus alphadalone 47 μmol kg^{-1}, i.p.) and placed on a heating mat and under heating lamps to maintain body temperature (monitored by rectal probe) at 37.5 ± 1.0°C for at least 2 h post ischaemia. Carotid arteries were exposed and occluded with aneurysm clips for 5 min, followed by a reperfusion period of 4 days (unless otherwise stated).

Measurement of hippocampal damage

Gerbils were anaesthetized, perfused with formaldehyde, the brains removed and brain sections prepared and stained with Cresyl Violet as described by Cross *et al.* (1991) and Baldwin *et al.* (1993). The extent of neurodegeneration was measured by a method similar to that described by Gill *et al.* (1987) and detailed by Cross *et al.* (1991). The length of degenerated CA1/CA2 region was expressed as a percentage of the entire CA1/CA2 region. All assessments of histological sections were made by an observer unaware of drug treatment of the animals.

Measurement of chlormethiazole in plasma and brain

Series of gerbils were infused with chlormethiazole as described below. At various times following the start of infusion the animals were either killed and trunk blood collected or, in the case of the 24 h infusion, blood samples collected from the uncatheterized jugular vein following brief anaesthesia with halothane in a N_2O/O_2 mixture.

Plasma was obtained and chlormethiazole extracted by solid phase extraction using a C8 sorbant and vacuum manifold. The eluate was used for analysis of chlormethiazole by high performance liquid chromatography as described by Kim & Khanna (1983).

For analysis of the chlormethiazole concentration in brain tissue, the brain was homogenized in H_2O with an Ultra Turrax homogenizer. The homogenate was centrifuged at 13,000 r.p.m. for 15 min and the supernatant treated in the same way as plasma for chlormethiazole analysis.

Measurement of the anticonvulsant action of chlormethiazole

The anticonvulsant activity was examined in groups of gerbils 90 min after the start of continuous infusion of chlormethiazole to conscious animals at doses designed to achieve plasma levels of chlormethiazole of 10 nmol ml^{-1}, 30 nmol ml^{-1} or 50 nmol ml^{-1}. The gerbils were injected with N-methyl-DL-aspartate (NMDLA) at a dose of 6.8 nmol kg^{-1}, i.p. and the latency to seizure recorded compared to saline-injected control animals.

Measurement of sedative activity following chlormethiazole administration

Locomotor activity of individual gerbils was measured in perspex boxes (40 × 40 × 35 cm) mounted with infrared photocell beams and linked to a computer (PMS Instruments, Maidenhead). The number of beam breaks made by the animal in a test period was used as a measure of locomotor activity.

Activity was measured for a 5 min period both 45 min and 90 min following the start of the chlormethiazole infusions (to achieve a plasma concentration of 10, 30, 50 or 100 nmol ml^{-1}). Activity values were summed to give an index of inhibition of locomotor activity compared to saline-infused control animals.

Catheterization of jugular vein for infusion studies in freely moving animals

Gerbils were anaesthetized with Saffan and the jugular vein exposed. The scalp was incised and skull exposed. Plastic tubing (i.d. = 0.28 mm; o.d. = 0.64 mm) was passed under the skin to emerge close to the scalp; the other end emerged at the jugular and was used for catheterizing the vessel. The tubing emerging from the scalp was held to the skull with dental cement, 10 cm being left for subsequent manipulation, the free end being sealed with hot plastic. The animals were placed in perspex boxes with free access to food and water.

On alternate days, 200 µl heparinised saline (100 u ml^{-1}) was flushed through the tubing. After 7 days recovery the animals were used for further investigation.

Protocol for 24 h infusion study

Gerbils were divided into 4 treatment groups following induction of ischaemia (as detailed above). One group received a single i.p. injection of chlormethiazole (600 µmol kg^{-1}) 60 min post-ischaemia while a second group received saline i.p. at the same time. A third group received an intravenous infusion of chlormethiazole (62.1 µmol kg^{-1} in saline) at the following rates; 6.3 ml kg^{-1} h^{-1} for the first 10 min; 2.32 ml mg^{-1} h^{-1} for 10 min–120 min and 1.74 ml kg^{-1} h^{-1} for 120 min until 24 h. The infusion was started 30 min post-ischaemia and the total chlormethiazole dose over this time was 2702 µmol kg^{-1}. The fourth group of gerbils received saline infused at the same rate.

Protocol for infusion of chlormethiazole up to 120 min duration

Thirty min after the carotid artery occlusion chlormethiazole or saline was infused for various periods of time by exposing the left jugular vein and inserting a 27 gauge needle, the needle being attached by plastic tubing to a Hamilton syringe in an infusion pump. The needle was held in the jugular vein with adhesive tape. At the end of the infusion gerbils were sutured and left to recover for various times before killing and removal of brains for histological evaluation or killing and removal of trunk blood for measurement of plasma chlormethiazole levels.

The infusion protocols used to achieve the desired plasma levels are detailed in Table 1. The pharmacokinetic assumptions and calculations used to construct these infusion protocols were based on the method of Wagner (1974).

Drugs

Dichlormethiazole edisylate ('chlormethiazole') was obtained from Astra Arcus, Södertälje, Sweden and Saffan (alphaxalone plus alphadalone) from Veterinary Drug Company, U.K. Doses of chlormethiazole refer to the free base.

Statistics

Data were evaluated by Student's *t* test or one way ANOVA as appropriate. In the latter case, individual group differences were determined by adjusted *t* tests with significance levels corrected by the Bonferroni method.

Results

Effect of a single injection of chlormethiazole (600 µmol kg^{-1}, i.p.) on hippocampal neurodegeneration

Initial experiments were undertaken to confirm the neuroprotective effect of a single i.p. dose of chlormethiazole of 600 µmol kg^{-1}. Gerbils were subjected to a 5 min bilateral carotid artery occlusion and chlormethiazole injected 60 min later.

A marked reduction (control 76 ± 8%, treated 30 ± 7%) in hippocampal damage was observed 5 days later (Figure 1). Similar protection was observed in other groups of animals when damage was assessed 14 (31 ± 9% damage) or 21 days (28 ± 12% damage) after the ischaemic insult (Figure 1).

Plasma chlormethiazole concentrations following intraperitoneal and intravenous administration

Following an intraperitoneal injection of chlormethiazole (600 µmol kg^{-1}) plasma chlormethiazole concentrations peaked within 2 min with no drug being detectable by 240 min

Table 1 Infusion protocols to achieve various plasma chlormethiazole (CMZ) concentrations in gerbils

Total dose of CMZ administered (μmol kg^{-1})	*Duration of infusion* (min)	*Plasma concentration required* (nmol ml^{-1})	*Infusion protocol details*
930	30	200	CMZ (62.1 μmol ml^{-1}) infused at 0.86 ml kg^{-1} min for 10 min and 0.323 ml kg^{-1}min for 20 min
930	76.5	100	CMZ (62.1 μmol ml^{-1}) infused at 0.43 ml kg^{-1} min for 10 min and 0.16 ml kg^{-1}min for 66.5 min
930	110	50	CMZ (45.7 μmol ml^{-1}) infused at 0.427 ml kg^{-1} min for 10 min and 0.161 ml kg^{-1}min for 100 min
630	110	30	CMZ (31.1 μmol ml^{-1}) infused at 0.427 ml kg^{-1} min for 10 min and 0.161 ml kg^{-1}min for 100 min
330	110	10	CMZ (15.2 μmol ml^{-1}) infused at 0.427 ml kg^{-1} min for 10 min and 0.161 ml kg^{-1}min for 100 min

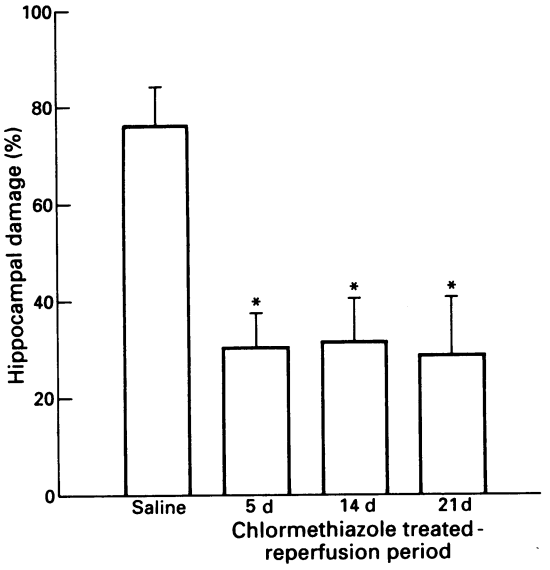

Figure 1 The effect of chlormethiazole (600 μmol kg^{-1}, i.p.) injected 60 min following 5 min transient ischaemia on hippocampal CA1/CA2 degeneration, measured 5, 14 or 21 days later. Columns represent mean % damage with s.e.mean; $n = 7-9$. ANOVA $F = 7.34$, d.f. 3,28, $P < 0.001$. All treatment groups are significantly different from control ($^*P < 0.05$) but not different from each other.

(Figure 2a). The peak plasma concentration was 200 nmol ml^{-1} and $t_{\frac{1}{2}} = 25$ min.

To generate kinetic data in order to be able to calculate infusion protocols, a study was also performed on the rate of disappearance of a dose of chlormethiazole (370 μmol kg^{-1}) infused intravenously over 5 min (Figure 2b). These data were fitted to a two compartment model which generated the following parameters; $t_{\frac{1}{2}}$: 15 min; Clearance: 102.6 ml min^{-1} kg^{-1}. Volume of distribution (Vd): 2.2 l kg^{-1}; area under curve (AUC): 60.1 μmol h l^{-1}.

Neuroprotection following an intravenous dose of chlormethiazole of 930 μmol kg^{-1}, infused for varying periods of time

The peak plasma concentration of chlormethiazole following an i.p. injection was approximately 200 nmol ml^{-1} (Figure 2a). An experiment was therefore designed to produce this concentration in plasma for a 30 min period. Subsequent experiments investigated the effects of administering the same total dose but infused at concentrations which resulted in a sustained plasma concentration of 100 nmol ml^{-1} (infusion period: 76.5 min) or 50 nmol ml^{-1} (infusion period: 110 min). The protocols used (see Methods) resulted in the required plasma levels being achieved, although some accumulation occurred at the end of each infusion period (Figure 3). All 3 infusion protocols resulted in a similar degree of neuroprotection (Table 2).

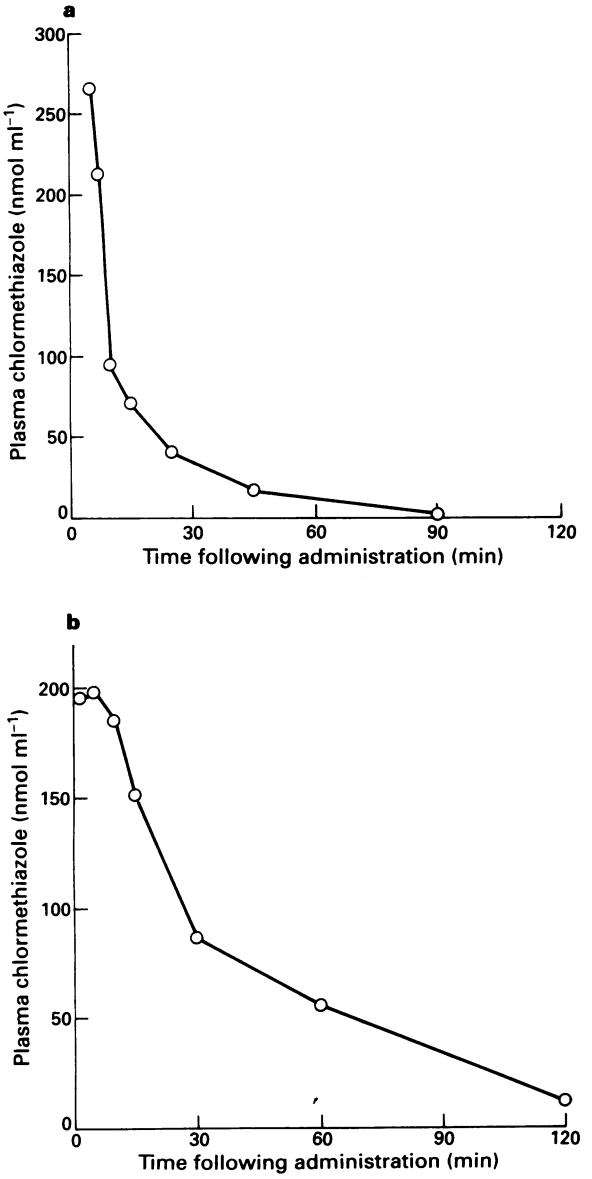

Figure 2 Plasma chlormethiazole concentration in the 120 min following injection of (a) chlormethiazole, 600 μmol kg^{-1}, i.p. or (b) chlormethiazole 370 μmol kg^{-1} infused intravenously over 5 min. Results shown as mean ± s.e.mean ($n = 4-5$). Kinetic parameters calculated from these data are given in the text.

Neuroprotection following a 2 h infusion period of chlormethiazole designed to produce different plasma levels

In the next experiments chlormethiazole was infused at doses which produced sustained plasma levels of drug of 30 and

10 nmol ml^{-1} over a 120 min period (Figure 3). Compared with a 50 nmol ml^{-1} plasma concentration, less neuroprotection was achieved by a 30 nmol ml^{-1} plasma level and no protection when the plasma concentration of chlormethiazole was kept at 10 nmol ml^{-1} (Table 3).

Measurement of sedative and anticonvulsant activity following chlormethiazole infusion for 90 min at varying plasma drug levels

By use of indwelling catheters in the jugular vein, studies could be performed on conscious freely moving gerbils. Infusions were performed to achieve sustained plasma chlormethiazole levels of 50, 30 and 10 nmol ml^{-1}. In some animals locomotor activity was measured both 45 min and 90 min after the start of the infusion, while others were injected with NMDLA (6.8 nmol kg^{-1}) immediately after the 90 min infusion in order to determine the anticonvulsant effect of the chlormethiazole.

The modest increase in mean time to convulsion seen in gerbils with plasma chlormethiazole concentrations of 10 and 30 nmol ml^{-1} was not statistically significant (Table 4). There was a significant increase in threshold in the group with plasma concentration of 50 nmol ml^{-1}, no seizures being observed in the 15 min period of observation (Table 4).

With regard to locomotor activity, animals with a plasma chlormethiazole level of 10 nmol ml^{-1} showed normal locomotor activity (Figure 4). However, gerbils with plasma levels above 30 nmol ml^{-1} had reduced locomotor activity and were clearly sedated (Figure 4).

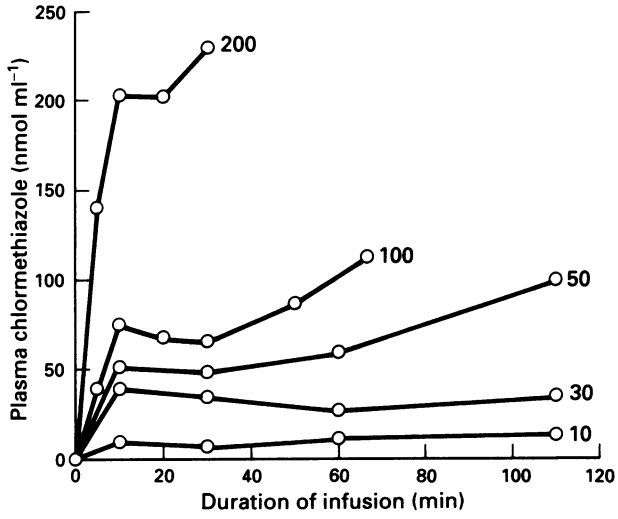

Figure 3 Plasma chlormethiazole concentrations achieved by infusion of chlormethiazole at various doses and times detailed in Table 1. Values show a mean for groups of animals ($n = 4-5$).

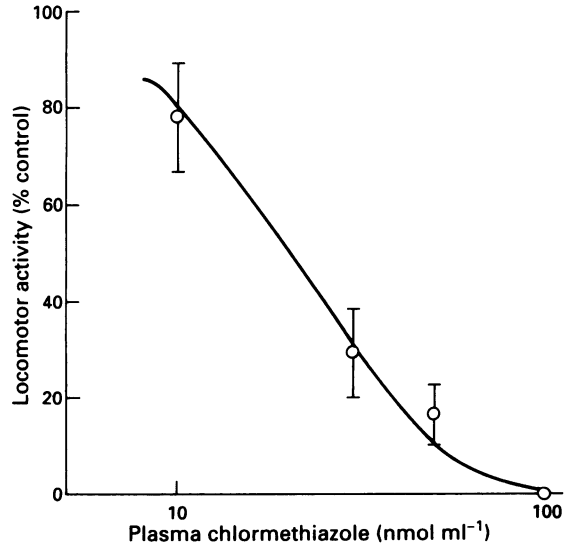

Figure 4 The degree of sedation in gerbils at defined plasma chlormethiazole concentrations. Activity is shown as the sum of a 5 min measure both 45 min and 90 min after the infusion as a % inhibition compared to saline-injected controls.

Effect of a sustained plasma concentration of chlormethiazole of 10 nmol ml^{-1} for 24 h

We next investigated whether a sustained low plasma concentration of chlormethiazole of 10 nmol ml^{-1} would be protective if the infusion were continued for 24 h rather than 2 h. Details for the infusion protocol are given in the Methods, but briefly the infusion was initiated 30 min after the removal of the carotid artery occlusion clips. The design of the experiment allowed chlormethiazole to be infused into awake freely moving animals. A 'positive' control study was also undertaken with a group of gerbils receiving either an i.p. injection of saline ($n = 10$) or chlormethiazole (600 μmol kg^{-1}, $n = 10$) 60 min after the 5 min bilateral carotid occlusion.

The sustained chlormethiazole infusion resulted in plasma chlormethiazole concentrations just below 10 nmol ml^{-1} for the duration of the infusion (Figure 5a). Rectal temperature

Table 2 Effect of varying the duration of intravenous infusion of chlormethiazole (CMZ) on the neuroprotective activity of the drug when given at a fixed dose of 930 μmol kg^{-1} to achieve defined plasma concentrations

Duration of infusion (min)	*Approx. plasma CMZ concn. during infusion* (nmol ml^{-1})	*% neuronal damage*
30	0 (Saline)	82 ± 8 (6)
30	200	16 ± 5 (6)**
76.5	100	36 ± 9 (8)**
110	50	9 ± 4 (11)**

Hippocampal damage is the mean ± s.e.mean, number of observations in parentheses. ANOVA, $F = 22.6$, d.f., 3,27, $P < 0.01$. **$P < 0.01$ vs saline.

Table 3 Effect of an infusion of chlormethiazole (CMZ) for 110 min at various doses to achieve defined plasma concentrations on the neuroprotective activity of the drug

Total dose of CMZ (μmol kg^{-1})	*Approx. plasma CMZ concn. during infusion* (nmol ml^{-1})	*% hippocampal neuronal damage*
–	0 (Saline)	70 ± 5 (12)
930	50	9 ± 4 (11)**
630	30	44 ± 10 (9)*
330	10	68 ± 21 (6)

Hippocampal damage is the mean ± s.e.mean, number of observations in parentheses. ANOVA, $F = 11.1$, d.f., 3,34, $P < 0.01$. **$P < 0.01$;*$P < 0.05$ vs saline.

Table 4 Effect of chlormethiazole (CMZ) on convulsant action of N-methyl-DL-aspartate (6.8 nmol kg^{-1})

Plasma CMZ concentration (nmol ml^{-1})	*Time* (min) *to tonic convulsion*
0	7.25 ± 0.63 (6)
10	10.67 ± 1.23 (6)
30	11.50 ± 1.64 (6)
50	>15* (6)

*Different from control group $P < 0.05$. No significant difference in threshold at either of the other two plasma concentrations. 'Cut off' time of 15 min used.

was also maintained at normal values during the first 6.5 h following the occlusion (Figure 5b) and was similar in control (average temperature 38.1 ± 0.21°C) and chlormethiazole-treated (average temperature 38.1 ± 0.17°C) groups throughout the study period.

Intravenous drug administration provided essentially total protection from the ischaemia-induced degenerative changes in the hippocampus (Figure 5c). The protection observed was greater than that achieved by a single intraperitoneal dose of chlormethiazole of 600 μmol kg^{-1} (Figure 5c).

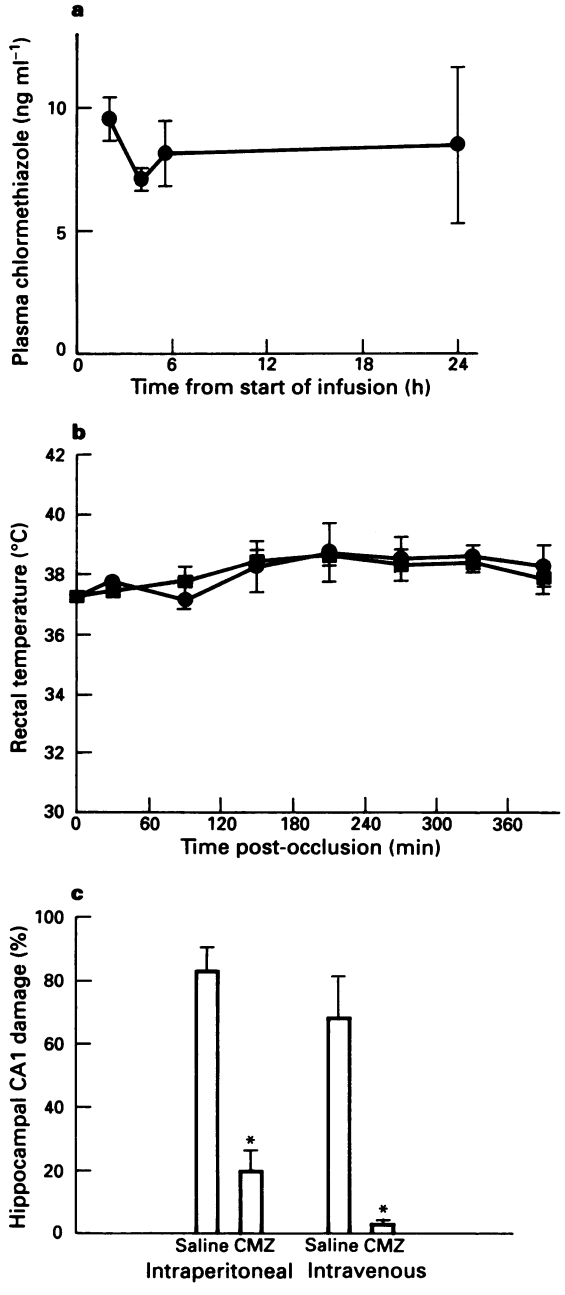

Figure 5 The effect of infusion of chlormethiazole (CMZ) for 24 h on (a) plasma chlormethiazole concentration, (b) rectal temperature and (c) neurodegeneration of hippocampal CA1/CA2 regions. Chlormethiazole was infused for 24 h as described in the Methods starting 30 min after a 5 min bilateral carotid occlusion. Results show (a) the plasma chlormethiazole concentration throughout the infusion period with mean ± s.e.mean values ($n = 4$), (b) the rectal temperature of control and experimental groups for the first 6 h following occlusion and (c) the % hippocampal neurodegeneration in the control (ischaemia + saline infusion, $n = 10$) and experimental (ischaemia + chlormethiazole, $n = 7$) groups. Also shown is a parallel 'positive control' study with the % neurodegeneration in a saline (i.p.) injected group ($n = 10$) and a chlormethiazole (600 μmol kg^{-1}, i.p.) injected group ($n = 10$). Results shown as mean ± s.e.mean. ANOVA $F = 18.0$, d.f. 3.33, $P < 0.001$. *$P < 0.001$ versus saline control (Bonferroni corrected t test).

Brain chlormethiazole concentration at the end of the infusion period

The brain chlormethiazole concentration at the end of the infusion period (24 h) was 16.0 ± 3.8 nmol g^{-1} (mean ± s.e.mean, $n = 3$).

Discussion

In gerbils, chlormethiazole was observed to have a short plasma half life ($t_{\frac{1}{2}} = 15$ min) and rapid clearance (102.6 ml min^{-1} kg) in comparison with human volunteers ($t_{\frac{1}{2}} = 6.6$ h; clearance = 15.1 ml min^{-1} kg; Pentikäinen *et al.*, 1980). Despite these possible pharmacokinetic limitations to therapeutic efficacy in the gerbil, a single intraperitoneal dose of the drug of 600 μmol kg^{-1} given 60 min after an ischaemic insult resulted in substantial neuroprotection to the hippocampus when measured 5 days after the insult, thereby confirming previous observations (Cross *et al.*, 1991; Baldwin *et al.*, 1993). Protection has now also been observed when hippocampal tissue was examined 14 and 21 days later, thereby showing that the drug is preventing cell death, not merely retarding it. When the drug was infused at a fixed dose, but over varying periods of time, similar neuroprotection was achieved, even when the mean plasma concentration was only 25% the peak concentration achieved after an i.p. injection (Table 2). This suggests that the neuroprotective effect of the drug is related not only to drug concentration but also duration of administration.

In the next experiments, when the time of administration was kept constant but the dose was lowered, protection was found to be dose-dependent. Only the lowest dose (plasma concentration 10 nmol ml^{-1} over 120 min) failed to provide some protection. Nevertheless, in support of the contention that both duration of drug administration and dose are important, maintaining the plasma concentration of chlormethiazole at 10 nmol ml^{-1} for 24 h resulted in almost total neuroprotection. The fact that the brain chlormethiazole concentration at the end of the infusion was only slightly higher than the plasma levels suggests that there was no significant accumulation of the drug in the brain during the period of administration which would account for this result.

Significant sedation was observed in gerbils with plasma chlormethiazole concentrations of 50 or 30 nmol ml^{-1}. A steady plasma concentration of 10 nmol ml^{-1}, in contrast, produced no inhibition of locomotor activity. Chlormethiazole can therefore be given by infusion and provide protection against ischaemic cell death at plasma concentrations at which there is no significant sedation. Our results also suggest that the neuroprotection is unrelated to the anticonvulsant activity of the drug. It is also important to note, given the evidence that hypothermia can be neuroprotective (Busto *et al.*, 1987), that there was no indication of any reduction in body temperature during the infusion.

We have shown previously that a single intraperitoneal administration of chlormethiazole is effective when given up to 3 h post-ischaemia (Cross *et al.*, 1991). The present experiments demonstrate that plasma chlormethiazole concentrations need to be maintained above 30 nmol ml^{-1} during this period to obtain a significant neuroprotective effect. Following transient forebrain ischaemia in the gerbil, hippocampal CA1 neurones do not show degenerative changes until 2 days post-ischaemia (Kirino, 1982). It would seem likely that the administration of chlormethiazole up to 3 h post-ischaemia interferes with the sequence of events leading to delayed neuronal death. The observation that prolonged infusion of chlormethiazole at low (10 nmol ml^{-1}) plasma concentrations is also neuroprotective suggests that in the

gerbil the period during which intervention with chlormethiazole is effective may be longer than 3 h. In this regard it is interesting to note that the N-channel calcium antagonist, SNX-111, may also exert a neuroprotective effect when given several hours after transient forebrain ischaemia in the gerbil (Valentino *et al.*, 1993).

Chlormethiazole has been shown to be neuroprotective in several animal models of cerebral ischaemia, namely transient global ischaemia in the gerbil (Cross *et al.*, 1991; Baldwin *et al.*, 1993), transient focal ischaemia following middle cerebral artery occlusion (Sydserff *et al.*, 1995) and permanent focal ischaemia in the rat following a photochemically induced thromboembolism (Snape *et al.*, 1993; Baldwin *et al.*, 1994). These data have been reviewed elsewhere (Green & Cross, 1994) and support our contention that chlormethiazole may be useful in the treatment of acute stroke (Cross *et al.*, 1991; Snape *et al.*, 1993). The current data strengthen this contention since the plasma drug levels necessary for neuroprotection in the gerbil are well below levels reported to be safely tolerated in clinical studies. For example, plasma chlormethiazole concentrations as high as 120 nmol ml^{-1} for more than 24 h have been used safely (Scott *et al.*, 1980). It should therefore be possible to test the efficacy of chlormethiazole in acute ischaemic stroke using a treatment regimen known to be effective in experimental models.

We thank Helen Baldwin and Irene Eromor for their assistance in these studies.

References

BALDWIN, H.A., JONES, J.A., CROSS, A.J. & GREEN, A.R. (1993). Histological, biochemial and behavioural evidence for the neuroprotective action of chlormethiazole following prolonged carotid artery occlusion. *Neurodegeneration*, **2**, 139–146.

BALDWIN, H.A., JONES, J.A., SNARES, M., DE SOUZA, R.J., CROSS, A.J., GREEN, A.R. & JOSTELL, K.-G. (1991). Chlormethiazole is neuroprotective when given as an intravenous infusion to the gerbil. *Br. J. Pharmacol.*, **104**, 279P.

BALDWIN, H.A., WILLIAMS, J.L., SNARES, M., FERREIRA, T., CROSS, A.J. & GREEN, A.R. (1994). Attenuation by chlormethiazole administration of the rise in extracellular amino acids following focal ischaemia in the cerebral cortex of the rat. *Br. J. Pharmacol.*, **112**, 188–194.

BUSTO, R., DIETRICH, W.D., GLOBUS, M.Y.-T., VALDES, T., SCHEINBERG, P. & GINSBERG, M.D. (1987). Small differences in intraischaemic brain temperature critically determine the extent of ischaemic neuronal injury. *J. Cereb. Blood Flow Metab.*, **7**, 729–738.

CROSS, A.J., JONES, J.A., BALDWIN, H.A. & GREEN, A.R. (1991). Neuroprotective activity of chlormethiazole following transient forebrain ischaemia in the gerbil. *Br. J. Pharmacol.*, **104**, 406–411.

EVANS, J.G., FEUERLEIN, W., GLATT, M.M., KANOWSKI, S. & SCOTT, D.B. (1986). Chlormethiazole 25 years: recent developments and historical perspectives. *Acta Psychiat. Scand.*, **73** (Suppl 327) pp. 198.

GILL, R., FOSTER, A.C. & WOODRUFF, G.N. (1987). Systemic administration of MK-801 protects against ischaemia-induced hippocampal neurodegeneration in the gerbil. *J. Neurosci.*, **7**, 3343–3349.

GREEN, A.R. & CROSS, A.J. (1994b). The neuroprotective actions of chlormethiazole. *Progr. Neurobiol.*, **44**, 463–484.

GREEN, A.R. & MURRAY, T.K. (1989). A simple intravenous method in rodents for determining the potency of anticonvulsants acting through GABAergic mechanisms. *J. Pharm. Pharmacol.*, **41**, 879–880.

KIM, C. & KHANNA, J.M. (1983). Determination of chlormethiazole in blood by high performance liquid chromatography. *J. Liquid Chromatogr.*, **6**, 907–916.

KIRINO, T. (1982). Delayed neuronal death in the gerbil hippocampus following ischaemia. *Brain Res.*, **239**, 57–69.

PENTIKÄINEN, P.J., NEUVONEN, P.J. & JOSTELL, K.-G. (1980). Pharmacokinetics of chlormethiazole in healthy volunteers and patients with cirrhosis of the liver. *Eur. J. Pharmacol.*, **17**, 275–284.

SCOTT, D.B., BEAMISH, D., HUDSON, I.N. & JOSTELL, K.-G. (1980). Prolonged infusion of chlormethiazole in intensive care. *Br. J. Anaesth.*, **52**, 541–545.

SNAPE, M.F., BALDWIN, H.A., CROSS, A.J. & GREEN, A.R. (1993). The effects of chlormethiazole and nimodipine on cortical infarct area after focal ischaemia in the rat. *Neuroscience*, **53**, 837–844.

SYDSERFF, S.G., CROSS, A.J., WEST, K.J. & GREEN, A.R. (1995). The effect of chlormethiazole on neuronal damage in a model of transient focal ischaemia. *Br. J. Pharmacol.*, **114**, 1631–1635.

VALENTINO, K., NEWCOMB, R., GADBOIS, T., SINGH, T., BOWERSON, S., BITNER, S., JUSTICE, A., YAMASHIRO, D., HOFFMAN, B.B., CIARANELLO, R., MILJANICH, G. & RAMACHANDRAN, J. (1993). A selective N-type calcium channel antagonist protects against neuronal loss after global cerebral ischaemia. *Proc. Natl. Acad. Sci. U.S.A.*, **90**, 7894–7897.

WAGNER, J.G. (1974). A safe method for rapidly achieving plasma concentration plateaus. *Clin. Pharmacol. Ther.*, **16**, 691–699.

(Received August 16, 1994
Revised January 11, 1995
Accepted January 13, 1995)

British Journal of Pharmacology (1995) 114, 1631-1635 © 1995 Stockton Press All rights reserved 0007-1188/95 $12.00

The effect of chlormethiazole on neuronal damage in a model of transient focal ischaemia

S.G. Sydserff, [1]A.J. Cross, K.J. West & A.R. Green

Astra Neuroscience Research Unit, 1 Wakefield Street, London WC1N 1PJ

1 The effect of chlormethiazole has been studied in a transient middle cerebral artery (MCA) occlusion model of cerebral ischaemia in the rat. The MCA was occluded for 1 h by use of an intraluminal suture technique, with reperfusion for 24 h following removal of the occluding filament. Neuronal damage was determined by measurement of the area of necrosis following Cresyl Violet staining of sections taken through the ischaemic region.

2 In the initial experiment, occlusion of the MCA produced a large volume of ischaemic damage in both cortex and striatum, characterized by necrosis and pyknosis (total volume of damage, 287 ± 13 mm^3; $n = 9$). Rats injected with chlormethiazole (1000 μmol kg^{-1}, i.p.) 60 min before occlusion had a reduced volume of damage in both regions (104 ± 11 mm^3; $n = 9$; $P < 0.001$).

3 In a subsequent study systemic physiological parameters (heart rate, blood pressure, blood pH, blood gases and rectal temperature) were measured throughout the ischaemic period.

4 Chlormethiazole (1000 μmol kg^{-1}) pretreatment produced little change in systemic physiology and the neuroprotective effect of the drug when given 60 min prior to the MCA occlusion was confirmed. Chlormethiazole was also neuroprotective when given 10 min following the start of reperfusion (control group: 244 ± 52 mm^3, $n = 10$; chlormethiazole pretreatment group: 102 ± 23 mm^3, $n = 10$; $P < 0.001$; chlormethiazole post-ischaemia group: 122 ± 16 mm^3; $P < 0.001$, $n = 10$).

5 It is concluded that chlormethiazole is an effective neuroprotective agent in this model of transient focal ischaemia. The observation that chlormethiazole is protective when given after reperfusion indicates that the effect of the drug is unlikely to be due to an alteration of intra-ischaemic cerebral blood flow, but is more probably a direct effect on the development of ischaemic damage.

Keywords: Cerebral ischaemia; middle cerebral artery occlusion; chlormethiazole; neurodegeneration; neuroprotection; model of stroke

Introduction

Chlormethiazole (INN: clomethiazole) is a sedative, anticonvulsant and hypnotic drug which has been shown to protect against hippocampal neuronal loss following ischaemia induced by carotid artery occlusion in the gerbil (Cross *et al.*, 1991; Baldwin *et al.*, 1993a). Chlormethiazole also reduced the size of infarction (Snape *et al.*, 1993; Baldwin *et al.*, 1994) and oedema (Green & Cross, 1994a) in a model of focal ischaemia in the rat involving photochemically induced thromboembolism (Watson *et al.*, 1985).

Whilst both of these models are useful in studying aspects of cerebral ischaemia experimentally, other models may be more clinically relevant. One of the more commonly observed forms of stroke results from embolic occlusion of the proximal middle cerebral artery (Mohr *et al.*, 1986; Karpiak *et al.*, 1989). This can be mimicked experimentally either by surgical occlusion or transection of the MCA resulting in permanent ischaemia, or by transient occlusion and subsequent reperfusion. The models combining occlusion and reperfusion resemble more closely clinical stroke than the permanent models since repeated angiography has demonstrated reperfusion in up to 50% of patients (Saito *et al.*, 1987). In the present study we adapted an intraluminal suture technique of transient MCA occlusion (Longa *et al.*, 1989) which allows the addition of a reperfusion phase and is minimally invasive in terms of disruption to the cranial environment.

The effect of chlormethiazole pretreatment on neuronal damage following transient focal ischaemia has been investigated together with a study of the physiological responses to chlormethiazole treatment in ischaemic animals. To rule out any interaction between chlormethiazole and either the ischaemic process or operative procedure, the effect of chlormethiazole was also examined when the drug was given after the ischaemic period.

[1] Author for correspondence.

Methods

Animals and drug administration

Adult (300-400 g) male Lister Hooded rats (Harlan Olac, Bicester) were used. They were housed in groups, in conditions of constant temperature (21°C) with 12 h light/dark cycle (lights on: 07 h 00 min) and given free access to food and water.

Chlormethiazole (dichlormethiazole ethanedisulphonate; Astra Arcus, Södertälje, Sweden) dissolved in 0.9% w/v NaCl (saline) was injected i.p. at a dose of 1000 μmol kg^{-1} either 60 min prior to MCA occlusion or 10 min after removal of the occluding filament. Control animals were injected with saline. Animals were given buprenorphine (Temgesic, Reckitt & Colman, Hull: 0.3 mg kg^{-1}, s.c.) 5 min after recovery. The animals were re-anaesthetized with pentobarbitone (Sagatal, Rhone Merieux, Harlow: 40 mg kg^{-1}, i.p.) before they were killed. All doses refer to the free base.

Middle cerebral artery occlusion method

Anaesthesia was induced with a halothane (6%), nitrous oxide (2 l min^{-1})/oxygen (0.7 l min^{-1}) mixture, and maintained with a halothane (2%), nitrous oxide/oxygen mix. A rectal probe was inserted and core temperature maintained by the use of a heating blanket at 37 ± 0.5°C intraoperatively and 37 ± 1.0°C post-operatively. The left femoral artery was exposed and cannulated with a 3FG paediatric

intravenous infusion cannula and connected via a three way tap to a Kontron Minimon 7136B cardiac monitor. Heart rate and blood pressure were monitored throughout the experiment and blood samples were taken at regular intervals for pH and blood gas analysis on a Corning M238 analyser. The femoral vein was cannulated with 0.96:0.58 mm tubing and connected to a syringe pump infusing saline (10 ml kg^{-1} h^{-1}).

The left carotid arteries were exposed through a midline cervical incision and silk sutures were looped around the common carotid, external carotid and internal carotid arteries. The arterial branches of the external carotid artery were all exposed and divided using diathermy forceps leaving a stump about 2–3 mm in length, and a microvascular clip was placed on the end of the stump to assist haemostasis. The pterygopalatine artery was exposed by developing a plane alongside the internal carotid artery, and was ligated at its origin with fine silk leaving the extracranial carotid circulation contiguous.

Occlusion of the MCA was achieved as follows; aneurysm clips were placed across the common carotid and internal carotid arteries and an arteriotomy was made in the external carotid artery stump allowing the introduction of a blunted, rounded length of monofilament nylon suture (3/O gauge). This was secured in place and the aneurysm clip on the internal carotid artery was removed. The suture was advanced into the internal carotid artery and passed into the intracranial circulation to lodge in the narrower lumen of the proximal anterior cerebral artery (20–22 mm distal to the carotid bifurcation) thereby occluding the origin of the MCA. The aneurysm clip on the common carotid artery was removed and haemostasis checked. After 60 min the suture was carefully removed, the arteriotomy closed, haemostasis re-checked and the cervical wound closed. Anaesthesia was terminated and the animals breathed oxygen-enriched air for a few minutes before being placed in clean, lined cages in an appropriate recovery environment (25–28°C).

Histology and measurement of neuronal damage

Twenty-four hours after reperfusion, the rats were anaesthetized with pentobarbitone (40 mg kg^{-1}, i.p.). Saline (50 ml) was perfused through the ascending aorta at normal pressure to exsanguinate the animal, followed by 100 ml of sucrose (5% w/v) in a formaldehyde (4% w/v) solution. Following fixation the brains were removed, and sections (20 μm) were cut on a cryostat at 0.25 mm intervals throughout and stained with Cresyl Fast Violet. The areas of ischaemic damage (defined by pyknotic-necrotic cells) were delineated onto corresponding stereotactic section maps and the areas calculated with a digitizer. The volume of damage was calculated by integrating the areas of damage against interaural position.

The plasma concentration of chlormethiazole was measured in arterial blood samples taken 60 and 120 min after administration. Chlormethiazole was extracted by solid phase extraction using a C8 sorbant and vacuum manifold. The eluate was analysed by high performance liquid chromatography (Kim & Khanna, 1983).

Statistics

Two-way analysis of variance (ANOVA) with repeated measures was used to determine group differences between physiological parameters. Student's *t* tests were used to examine the effects of treatment on ischaemic damage.

Results

The effect of chlormethiazole pretreatment on neuronal damage induced by MCA occlusion

An initial experiment was conducted to determine whether chlormethiazole was neuroprotective. Rectal temperature was maintained at normal values in both control and chlormethiazole-treated animals both during the ischaemic episode and for 3 h afterwards but no other physiological parameters were assessed.

The ischaemic episode resulted in degeneration of neurones in both cortex and striatum. Characteristically, the damaged neurones exhibited a shrunken densely stained appearance and were pyknotic (loss of nucleus). In the most severely affected tissue the lesion was characterized by a sharply defined border (Figure 1).

Rats injected with saline 60 min prior to the MCA occlusion showed substantial damage to the cortex and striatum 24 h after occlusion (Figure 2). Pretreatment with chlormethiazole (1000 μmol kg^{-1}, i.p., 60 min prior to MCA

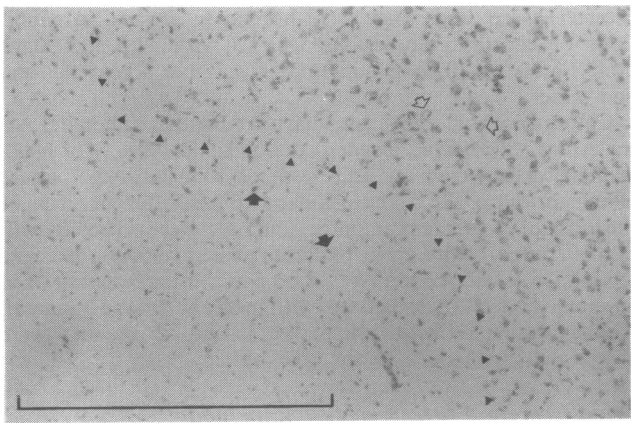

Figure 1 An example of an ischaemic margin in the rat brain. In the upper and right portions of the micrograph the intact neuronal cells appear large, and are slightly less densely stained, however the pyknotic cells in the lower left portion are shrunken, more densely stained and at high power the nuclei appear to be absent. The bar represents 1 mm (scale 1:75), the filled triangles represent the ischaemic boundary while healthy cells are highlighted by open arrows and ischaemic cells by filled arrows.

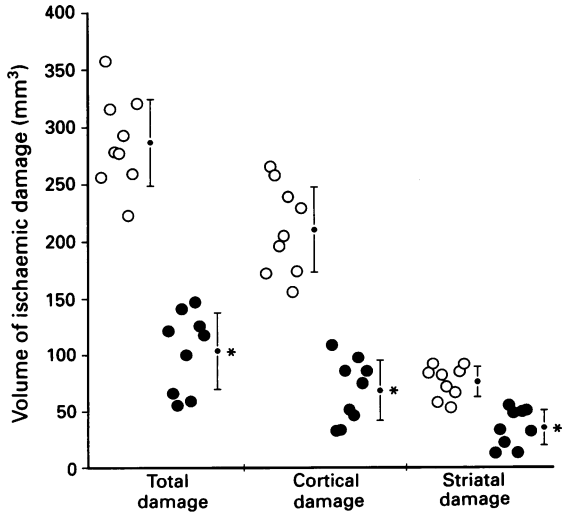

Figure 2 The effect of chlormethiazole (1000 μmol kg^{-1}, i.p., 60 min prior to middle cerebral artery occlusion) on total volume of damage, and damage in cortex and striatum. Vehicle-treated (○, $n = 9$); chlormethiazole-treated (●, $n = 9$). Results shown as individual animals with mean value ± s.d. *Different from vehicle-treatment group, $P < 0.001$ (Student's *t* test).

occlusion) resulted in an approximate 60% decrease in the volume of damage (Figure 2). The reduction of damage in the cortex (57 ± 4%) was similar to that in the striatum (62 ± 3%).

The effect of chlormethiazole when given 60 min prior to MCA occlusion on physiological parameters and neuronal damage

In the next experiment the first study was repeated but physiological measurements were made both in the 30 min period prior to the occlusion and for the duration of the ischaemic episode.

Following chlormethiazole (1000 μmol kg^{-1}, i.p.) no statistically significant changes in measures of general physiological state were seen prior to the onset of ischaemia. The first measurements were taken 30 min following chlormethiazole treatment; it is possible that some transient changes in vascular physiology occurred which normalised within 30 min. Rectal temperature was unchanged (Figure 3a) and no change was seen in heart rate (Figure 3b), mean arterial blood pressure (Figure 3c), pH (Figure 3d) or blood P_{O_2} (Figure 3e). Blood P_{CO_2} was decreased modestly but remained within normal limits (Figure 3f). There were no differences in these parameters between the saline and chlormethiazole-injected groups during the ischaemic period (Figure 3) with the exception of mean arterial blood pressure (Figure 3c) which was observed to be slightly elevated in the chlormethiazole-treated group. However, in this group, the halothane content of the anaesthetic mixture had been reduced to 1% to compensate for the sedative effect of the chlormethiazole.

Pretreatment with chlormethiazole (1000 μmol kg^{-1}, i.p.) resulted in a significant decrease in the volume of damage (Figure 4), confirming the first study. The plasma concentration of chlormethiazole was 52.1 ± 5.9 nmol ml^{-1} at the onset of ischaemic ($n = 6$) and 34.2 ± 2.9 nmol ml^{-1} ($n = 5$) at the time of reperfusion, 60 min later.

The effect of chlormethiazole when given 10 min following the start of reperfusion on physiological parameters and neuronal damage

There were no differences in the physiological parameters in the control group or treatment group either before or during the ischaemic episode (Figure 3). Rectal temperature in both groups was also similar in the post-ischaemic period (Figure 3a). Chlormethiazole (1000 μmol kg^{-1}, i.p.) injected 10 min following the start of reperfusion produced a similar degree of protection to that seen when the drug was given before the ischaemic episode (Figure 4).

Discussion

It has been suggested that one of the most clinically relevant animal models of stroke is that of middle cerebral artery occlusion (Macrae, 1992), since the MCA is the vessel most commonly affected in stroke (Mohr *et al.*, 1986; Berkow & Fletcher, 1981; Karpiak *et al.*, 1989). In addition because repeated angiography suggests that reperfusion occurs in up to 50% of stroke patients (Saito *et al.*, 1987), a reversible intraluminal MCA occlusion may represent most closely the situation that occurs in the majority of strokes due to emboli from cardiac or other sources. Reversible MCA occlusion should therefore be a valid model for examining possible therapeutic approaches to stroke since the damage produced may be the result of either the ischaemic period or the reperfusion phase and both are areas which might benefit from pharmacological intervention.

An initial experiment demonstrated that chlormethiazole produced substantial neuroprotection when given prior to the

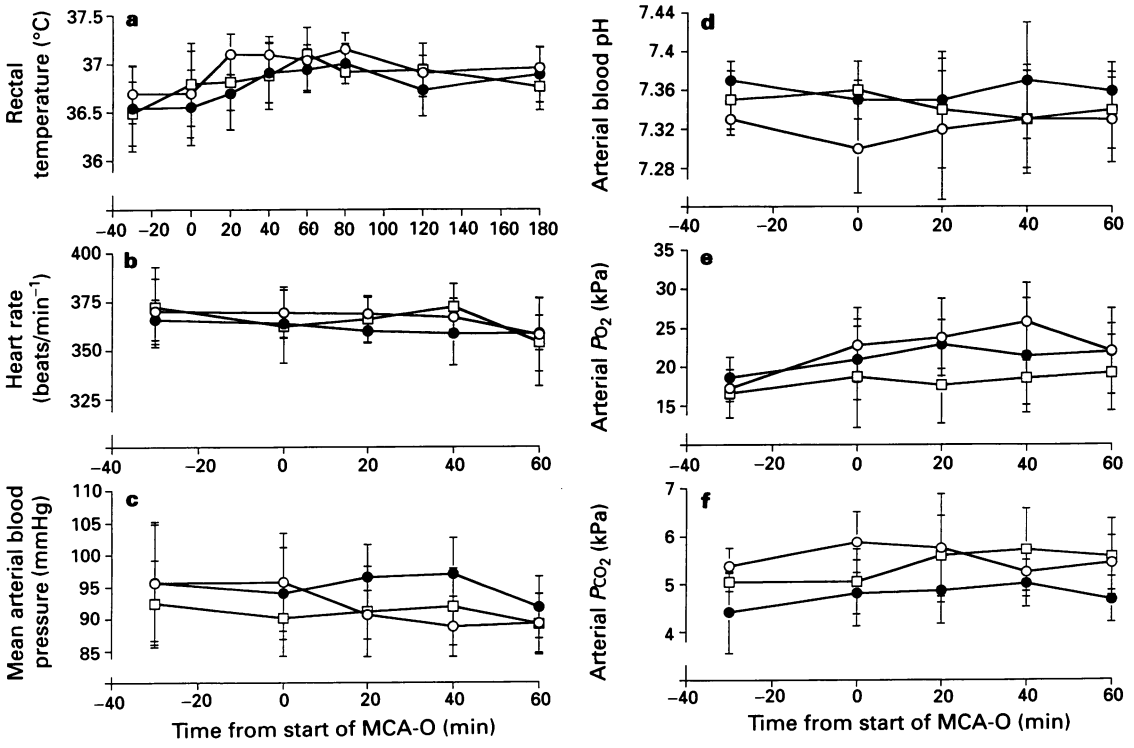

Figure 3 The effect of chlormethiazole (1000 μmol kg^{-1}, i.p., 60 min prior to middle cerebral artery (MCA) occlusion or 10 min after reperfusion) or vehicle on systemic physiological parameters. (a) Rectal temperature (°C); (b) heart rate (bts min^{-1}); (c) mean arterial blood pressure (mmHg); (d) blood pH; (e) arterial P_{O_2} (kPa); (f) arterial P_{CO_2} (kPa). Vehicle-treated group (○, $n = 10$); pre-MCA occlusion chlormethiazole-treated group (●, $n = 10$); post MCA occlusion chlormethiazole-treated group (□, $n = 10$). Results shown as individual animals with mean value ± s.d. Note different time scale in figure (a). There were no significant differences between treatments for any measure (ANOVA).

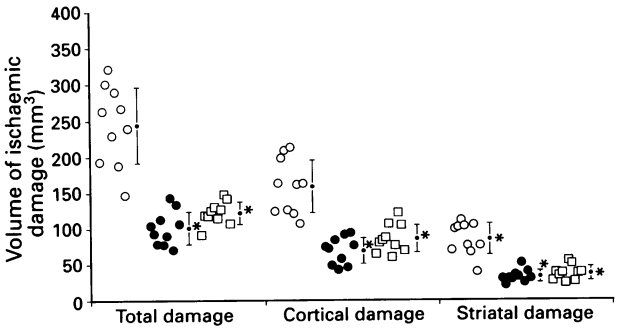

Figure 4 The effect of chlormethiazole (1000 μmol kg^{-1}, i.p., 60 min prior to middle cerebral artery (MCA) occlusion or 10 min after reperfusion) on total volume of damage, and damage in cortex and striatum. Vehicle-treated (○, $n = 10$); pre-MCA occlusion, chlormethiazole-treated (●, $n = 10$); post MCA occlusion, chlormethiazole-treated (□, $n = 10$). Results shown as individual animals with mean value ± s.d. *Different from vehicle treatment group, $P < 0.001$ (Student's t test).

ischaemic insult. However, it could have been argued that the drug was altering physiological parameters such as cerebral blood flow, thereby achieving protection by a vascular rather than a cellular mechanism. A second study was therefore undertaken which confirmed the neuroprotective activity of the drug and also indicated that there were no significant changes in heart rate, blood pressure or blood gas tensions which might complicate interpretation. Most importantly, chlormethiazole was also found to be effective when given 10 min after the start of reperfusion. In this case the drug cannot be providing protection by interacting in some way with the ischaemic episode.

There are many agents reported to be neuroprotective when treatment is initiated prior to permanent focal ischaemia including N-methyl-D-aspartate (NMDA) antagonists such as dizocilpine (MK-801) (Bielenberg & Beck, 1991; Buchan *et al.*, 1992) and CPPene (Park *et al.*, 1992) and Ca^{2+} channel antagonists including, for example, nimodipine (Jacewicz *et al.*, 1990). Similar treatment strategies also produced neuroprotection in transient focal ischaemia when given either before or during the ischaemic episode. Drugs shown to produce protection in this model include dizocilpine (Park *et al.*, 1988; Gill *et al.*, 1991; Buchan *et al.*, 1992) the AMPA antagonist NBQX (2,3-dihydroxy-6-nitro-7-sulphamoylbenzol [F]quinoxaline) (Xue *et al.*, 1994) and nilvadipine (Kawamura *et al.*, 1991). However, to our knowledge chlormethiazole is the first compound to be shown to be effective when given *after* the start of reperfusion.

The protection afforded by chlormethiazole given post-ischaemia was considerable and comparable with dizocilpine (Buchan *et al.*, 1992), nilvadipine (Kawamura *et al.*, 1991) and the nitric oxide synthase inhibitor N^G-nitro-L-arginine methyl ester (L-NAME) (Buisson *et al.*, 1992) when the latter were given before or during the ischaemic period. It has been suggested that dizocilpine may have attenuated ischaemic damage by increasing cerebral blood flow (Buchan *et al.*, 1992) and certainly Ca^{2+} channel antagonists such as nimodipine and nilvadipine may markedly alter cerebral blood flow. However, the similarity in the degree of protection produced by pre and post-occlusion treatment strongly suggests that chlormethiazole is not achieving neuroprotection by increasing the cerebral perfusion pressure to the ischaemic focus.

While dizocilpine, nimodipine and nilvadipine have been shown to be effective at reducing cortical ischaemic damage, a neuroprotective effect in the striatum has not always been reported (Park *et al.*, 1988; Gill *et al.*, 1991; Kawamura *et al.*, 1991; Bielenberg & Beck, 1991). In contrast an unequivocal protective effect of chlormethiazole was seen in both brain regions. It is possible that striatal tissue areas supplied by parenchymal end arteries (terminating branches) are particularly susceptible to ischaemic damage, in which case intervention with drugs which increase blood flow is likely to be less effective since collateral hyperperfusion is not possible. True neuroprotective agents will be beneficial in these regions provided the drugs can be transported to the threatened cells.

Chlormethiazole is known to interact with the $GABA_A$ receptor to potentiate the effects of GABA and it has been suggested that a GABA-mimetic effect could provide neuroprotection following ischaemia (Sternau *et al.*, 1989; Shuaib *et al.*, 1993; Baldwin *et al.*, 1993b). The plasma concentrations of chlormethiazole following pretreatment (30–50 nmol ml^{-1}) are quite consistent with the affinity of the drug for the $GABA_A$ receptor (Cross *et al.*, 1989). It is not known whether other GABA-mimetic compounds produce an equivalent neuroprotective effect in this model of ischaemia. Thus, whilst a mechanism of neuroprotection involving GABA potentiation remains a possibility, understanding of the precise mechanism of action awaits further experimentation.

The present study has demonstrated a neuroprotective effect of chlormethiazole in transient focal ischaemia which is independent of changes in vascular physiology and which is similar when the drug is given prior to or following transient cerebral ischaemia. The protection afforded by the drug to both cortical and striatal tissue regions is further evidence for its unique profile of action (see also Green & Cross, 1994b). The effectiveness of chlormethiazole as a neuroprotective agent in both the gerbil model of transient global ischaemia (Cross *et al.*, 1991; Baldwin *et al.*, 1993a), and the rat photochemical model of permanent focal ischaemia (Snape *et al.*, 1993; Baldwin *et al.*, 1994) has already been established and as a result it has been suggested that chlormethiazole might be of use in the treatment of acute ischaemic stroke (Cross *et al.*, 1991; Snape *et al.*, 1993). The current study, showing that chlormethiazole has considerable efficacy in the reversible MCA occlusion model, supports this proposal. However, at the present time no neuroprotective compounds have been shown to be effective in the treatment of ischaemic stroke in man and therefore the predictive value of these models is unknown. Whilst the present study demonstrates the reliability of the transient MCA occlusion model for pharmacological investigation, its predictive value can only be fully assessed following clinical studies.

References

BALDWIN, H.A., JONES, J.A., CROSS, A.J. & GREEN, A.R. (1993a). Histological, biochemical and behavioural evidence for the neuroprotective action of chlormethiazole following prolonged carotid artery occlusion. *Neurodegeneration*, **2**, 139–146.

BALDWIN, H.A., SNAPE, M.F., WILLIAMS, J.L., MISRA, A., JONES, J.A., SNARES, M., GREEN, A.R. & CROSS, A.J. (1993b). The role of glutamate and GABA in a rat model of focal cerebral ischaemia: biochemical and pharmacological investigations. *Neurodegeneration*, **2**, 129–138.

BALDWIN, H.A., WILLIAMS, J.L., SNARES, M., FERREIRA, T., CROSS, A.J. & GREEN, A.R. (1994). Attenuation by chlormethiazole administration of the rise in extracellular amino acids following focal ischaemia in the cerebral cortex of the rat. *Br. J. Pharmacol.*, **112**, 188–194.

BERKOW, R. & FLETCHER, A.J. (1981). Neurological disorders. In the *Merck Manual of Diagnosis and Therapy*. ed. Berkow, R. & Fletcher, A.J., pp. 1381–1386. Germany: Merck.

BIELENBERG, G.W. & BECK, T. (1991). The effects of dizocilpine (MK-801), phencyclidine, and nimodipine on infarct size 48 h after middle cerebral artery occlusion in the rat. *Brain Res.*, **552**, 338–342.

BUCHAN, A.M., SLIVKA, A. & XUE, D. (1992). The effect of the NMDA receptor antagonist MK-801 on cerebral blood flow and infarct volume in experimental focal stroke. *Brain Res.*, **574**, 171–177.

BUISSON, A., PLOTKINE, M. & BOULU, R.G. (1992). The neuroprotective effect of a nitric oxide inhibitor in a rat model of focal cerebral ischaemia. *Br. J. Pharmacol.*, **106**, 766–767.

CROSS, A.J., JONES, J.A., BALDWIN, H.A. & GREEN, A.R. (1991). Neuroprotective activity of chlormethiazole following transient forebrain ischaemia in the gerbil. *Br. J. Pharmacol.*, **104**, 406–411.

CROSS, A.J., STIRLING, J.M., ROBINSON, T.N., BOWEN, D.M., FRANCIS, P.T. & GREEN, A.R. (1989). The modulation by chlormethiazole of the $GABA_A$-receptor complex in rat brain. *Br. J. Pharmacol.*, **98**, 284–290.

GILL, R., BRAZELL, C., WOODRUFF, G.N. & KEMP, J.A. (1991). The neuroprotective action of dizocilpine (MK-801) in the rat middle cerebral artery occlusion model of focal ischaemia. *Br. J. Pharmacol.*, **103**, 2030–2036.

GREEN, A.R. & CROSS, A.J. (1994a). Attenuation by chlormethiazole of oedema following focal ischaemia in the cerebral cortex of the rat. *Neurosci. Lett.*, **173**, 27–30.

GREEN, A.R. & CROSS, A.J. (1994b). The neuroprotective actions of chlormethiazole. *Progr. Neurobiol.*, **44**, 463–484.

JACEWICZ, M., BRINT, S., TANABE, J., WANG, X.-J. & PULSINELLI, W. (1990). Nimodipine pretreatment improves cerebral blood flow and reduces brain edema in conscious rats subjected to focal cerebral ischaemia. *J. Cerebr. Blood Flow Metab.*, **10**, 903–913.

KARPIAK, S.E., TAGLIAVIA, A. & WAKADE, C.G. (1989). Animal models for the study of drugs in ischaemic stroke. *Annu. Rev. Pharmacol. Toxicol.*, **29**, 403–414.

KAWAMURA, S., YASUI, N., SHIRASAWA, M. & FUKASAWA, H. (1991). Effects of a Ca^{2+} entry blocker (nilvadipine) on acute focal cerebral ischaemia in rats. *Exp. Brain Res.*, **83**, 434–438.

KIM, C. & KHANNA, J.M. (1983). Determination of chlormethiazole in blood by high performance liquid chromatography. *J. Liquid Chromatogr.*, **6**, 907–916.

LONGA, E.Z., WEINSTEIN, P.R., CARLSON, S. & CUMMINS, R. (1989). Reversible middle cerebral artery occlusion without craniectomy in rats. *Stroke*, **20**, 84–91.

MACRAE, I.M. (1992). New models of focal cerebral ischaemia. *Br. J. Clin. Pharmacol.*, **34**, 302–308.

MOHR, J.P., GAUTIER, J.C., HIER, D. & STEIN, R.W. (1986). Middle cerebral artery. In *Stroke*, Vol. 1: *Pathophysiology, Diagnosis and Management*, ed. Barnett, H.J.M., Stein, B.M., Mohr, J.P. & Yatsu, F.M. pp. 377–450. New York: Churchill Livingstone.

PARK, C.K., MCCULLOCH, J., KANG, J.K. & CHOI, C.R. (1992). Efficacy of D-CPPene, a competitive N-methyl-D-aspartate antagonist in focal cerebral ischaemia in the rat. *Neurosci. Lett.*, **147**, 41–44.

PARK, C.K., NEHLS, D.G., GRAHAM, D.I., TEASDALE, G.M. & MCCULLOCH, J. (1988). The glutamate antagonist MK-801 reduces focal ischaemic brain damage in the rat. *Ann. Neurol.*, **24**, 543–551.

SAITO, I., SEGAWA, H., SHIOKAWA, Y., TANIGUCHI, M. & TSUTSUMI, K. (1987). Middle cerebral artery occlusion: correlation of computed tomography and angiography with clinical outcome. *Stroke*, **18**, 863–868.

SHUAIB, A., MAZAGRI, R. & IJAZ, S. (1993). GABA agonist 'muscimol' is neuroprotective in repetitive transient forebrain ischaemia in gerbils. *Exp. Neurol.*, **123**, 284–288.

SNAPE, M.F., BALDWIN, H.A., CROSS, A.J. & GREEN, A.R. (1993). The effects of chlormethiazole and nimodipine on cortical infarct area after focal ischaemia in the rat. *Neuroscience*, **53**, 837–844.

STERNAU, L.L., LUST, W.D., RICCI, A.J. & RATCHESON, R. (1989). Role for γ-aminobutyric acid in selective vulnerability in gerbils. *Stroke*, **20**, 281–287.

WATSON, B.D., DIETRICH, W.D., BUSTO, R., WACHTEL, M.S. & GINSBERG, M.D. (1985). Induction of reproducible brain infarction by photochemically initiated thrombosis. *Ann. Neurol.*, **17**, 497–504.

XUE, D., HUANG, Z.-G., BARNES, K., LESIUK, H.J., SMITH, K.E. & BUCHAN, A.M. (1994). Delayed treatment with AMPA, but not NMDA, antagonists reduces neocortical infarction. *J. Cerebr. Blood Flow Metab.*, **14**, 251–261.

(Received August 16, 1994
Revised January 11, 1995
Accepted January 13, 1995)

British Journal of Pharmacology (1995) 114, 1636-1640 © 1995 Stockton Press All rights reserved 0007-1188/95 $12.00

Enhancement by 5-hydroxytryptamine and analogues of desensitization of neuronal and muscle nicotinic receptors expressed in *Xenopus* oocytes

K.M.L. Cross, R.C. Foreman & J.E. Chad

Department of Physiology and Pharmacology, University of Southampton SO9 3TU

1 The action of 5-hydroxytryptamine (5-HT) on neuronal and muscle nicotinic acetylcholine receptors (nicotinic AChR) expressed in *Xenopus* oocytes was studied.

2 5-HT enhanced the rate of desensitization of the acetylcholine (ACh) current response in all receptor subtypes investigated (muscle, $\alpha\beta_2\gamma\delta$ and $\alpha_4\beta_2$), acting in a dose-dependent manner.

3 5-HT also reduced the peak current elicited by ACh in a dose-dependent manner. The IC_{50} value for the muscle type receptor was $227 \pm 0.44\,\mu M$, and $166 \pm 0.47\,\mu M$ and $283 \pm 0.28\,\mu M$ for the combinations $\alpha\beta_2\gamma\delta$ and $\alpha_4\beta_2$ respectively.

4 The effect of 5-HT on the responses to ACh ($10\,\mu M$) was found to be independent of membrane voltage over the range tested (-80 to -10 mV), and to be readily reversed by washout.

5 The action of 5-HT could be mimicked by structurally similar molecules. The homologue tryptamine was less potent than 5-HT in blocking the ACh current, with an IC_{50} of 1.0 ± 0.02 mM. Ketanserin, a 5-HT_2 receptor antagonist, was more potent than 5-HT, the IC_{50} being $49.0 \pm 1.4\,\mu M$.

6 We postulate that a highly conserved portion of the tertiary structure of nicotinic AChRs, which includes some part of the ACh binding site, has affinity for 5-HT and structural analogues.

Keywords: Desensitization; nicotinic acetylcholine receptors; ketanserin; 5-hydroxytryptamine; *Xenopus* oocytes

Introduction

There are a wide variety of neurotransmitters in the nervous system, each of which acts at its own specific receptors to exert its effects. When a neurotransmitter acts on its target cells it often modulates the action of another neurotransmitter, for example, there is evidence that both histamine and 5-hydroxytryptamine (5-HT) can act to modulate the release of acetylcholine (ACh) from presynaptic nerve terminals in sympathetic ganglia (Hirai & Koketsu, 1980; Yamada *et al.*, 1982). There is also evidence that these compounds can directly modulate the effect of ACh postsynaptically by action on the nicotinic receptor itself. In 1985, Ariyoshi *et al.* showed that histamine depressed the peak current elicited by ACh at the frog endplate, shifting the dose-response curve to the right, suggesting a competitive antagonism. In addition, histamine reduced the block of the nicotinic receptor by erabutoxin when applied to the preparation beforehand (Koketsu *et al.*, 1982). Erabutoxin is a sea snake toxin which is known to bind irreversibly to the specific ACh binding site (Kato *et al.*, 1978). A similar reduction in the blocking action of erabutoxin at frog endplates was shown in the presence of 5-HT (Koketsu *et al.*, 1982). In addition Akasu & Koketsu (1986) showed in bullfrog sympathetic ganglion cells that 5-HT appeared to act as a competitive antagonist. They found that 5-HT decreased the amplitude of the ACh elicited current in a dose-dependent manner, with a dose of $100\,\mu M$ 5-HT depressing the peak current by around half, but that the time course of the ACh response was not altered. The effect of 5-HT was rapidly reversed by washout. The presence of 5-HT caused a parallel shift of the ACh dose-response curve to the right and increased the apparent dissociation constant without altering the maximum ACh current, implying a competitive antagonism. Grassi *et al.* (1993) extended these observations to nicotinic receptors in mouse myotubes, human cloned TE671/RD cells and *Xenopus laevis* oocytes injected with mRNA extracted from C2 myotubes, *Torpedo* electroplaques, or cloned mouse muscle AChR subunit mRNAs. They found that 5-HT reduced the size and accelerated the decay of ACh elicited currents in a dose-dependent manner. The effect was reversible by washout or depolarizing the oocyte beyond -10 mV, and appeared to be by direct action of 5-HT on the nicotinic receptor. The effect of 5-HT on both muscle and neuronal type mammalian nicotinic receptors expressed in *Xenopus laevis* oocytes was investigated here by use of voltage-clamp techniques. The voltage-dependence of the effect was examined, and also whether structurally similar molecules could mimic the effect of 5-HT, by use of the homologue tryptamine, which is less active than 5-HT at 5-HT receptors, and the 5-HT_2 receptor competitive antagonist ketanserin, in order to try to interpret the mechanism of modulation of the acetylcholine response by 5-HT.

Methods

Synthesis of nicotinic AChR mRNA in vitro

The muscle subunits were mouse cDNAs, whilst the neuronal subunits were from rat. All were kindly provided by Dr S. Heinemann (Salk Institute, San Diego, CA, U.S.A.). The cDNA clones of each subunit were linearised using the appropriate restriction enzymes, and the DNA then purified by phenolic extraction. mRNAs were then transcribed *in vitro* from these templates using the Promega RiboMAX TM system (Promega, Southampton, Hants) for the muscle subunits, and the Boehringer Mannheim SP6/T7 Transcription Kit (Boehringer Mannheim, Lewes, Sussex) in the case of the neuronal subunits, following the manufacturers instructions. After transcription the mRNAs were kept stored as an ethanolic precipitates at -70°C.

[1] Author for correspondence.

Experimental procedure

Mature adult female *Xenopus laevis* (African Xenopus Facility, Noordhoek, RSA) were anaesthetized by immersion in 0.15% 3-aminobenzoic acid ethyl ester (Tricaine, Sigma, Poole, Dorset). Oocytes were removed by biopsy, and the follicular cell layer removed by digestion with collagenase (Sigma, Poole, Dorset, 2 mg ml^{-1} in Ca^{2+}-free SOS, composition (mM): NaCl 82, KCl 2.7, $MgCl_2$ 1, HEPES 5, pH 7.6) at 18°C with rotation at 10 rev min^{-1} for 28 min, followed by manual dissection.

Stage V and VI oocytes were selected and injected with 5–10 ng of each nicotinic AChR subunit, dissolved in diethylpyrocarbonate-treated autoclaved water. The cells were then incubated at 18°C in full SOS (composition (mM): NaCl 100, Ca_2Cl 1.8, KCl 2, MgCl 1, HEPES 5, pH = 7.6) for 24–48 h.

Two electrode voltage clamp was used to record from the cells. The holding voltage was −80 mV unless otherwise stated. The oocytes were continually superfused at approximately 10 ml min^{-1} with SOS containing atropine (10^{-7} M) to block any endogenous muscarinic responses. Drugs were added via a gravity-driven perfusion system leading to some variation in the onset time as shown in the raw data traces. Care was taken to ensure that the pH of all solutions was kept at 7.6, and all drug solutions were made up freshly every day. Control experiments of vehicle addition alone produced no changes. Data were collected and analyzed using pClamp (Axon Instruments Inc.) version 5.5, sampling at 28.6 Hz. Results are expressed as mean ± s.e.mean, with P values from Student's t test for the difference of the means.

Results

The effect of 5-HT on muscle nicotinic AChR

ACh was applied to oocytes injected with the mouse muscle nicotinic receptor subunits $\alpha\beta\gamma\delta$. Administration of 10 μM ACh to oocytes clamped at −80 mV elicited a current of 2.9 ± 0.37 μA (n = 10 oocytes, from 2 batches). Figure 1a shows a sample trace. The peak current was transient, and decayed with a $t_{0.5}$ of 46.4 ± 10.5 s (n = 10, $t_{0.5}$ being the time for the peak current to decay by half). The peak current was found to be fairly constant between oocyte batches, whereas the $t_{0.5}$ values were much more variable.

The application of 100 μM 5-HT alone did not give rise to any current, but when co-perfused with 10 μM ACh the 5-HT decreased the size of the peak current (Figure 1a). 5-HT acted in a dose-dependent manner (Figure 1b), with an IC_{50} of 227 ± 0.44 μM. 5-HT also increased the rate of desensitization of the nicotinic AChR and at 100 μM was sufficient to reduce the rate of desensitization of the peak current to 17% of the control value, i.e. from 46.4 ± 10.5 s to 8.1 ± 1.7 s, $P < 0.005$, Figure 1c.

The effect of 5-HT was found to be independent of holding voltage over the range −80 to −10 mV. Figure 2a shows the raw data in response to application of 10 μM ACh at a range of holding potentials. The response at each holding potential was reduced in the presence of 100 μM 5-HT as shown by the data traces in Figure 2b. However, when the size of the currents were normalized it was found that 5-HT reduced the peak current by the same proportion in each case (Figure 2c; n = 6). This shows that the effect of 5-HT was voltage-independent over the range tested, implying that it does not act within the open channel as a charged species. The effect was readily reversed by washout (Figure 2c), even after being blocked totally by 10 mM 5-HT (Figure 2d).

The effect of 5-HT on neuronal nicotinic receptors

The agonist binding site is located on the α-subunit, but the pharmacology of the nicotinic AChR is affected by the

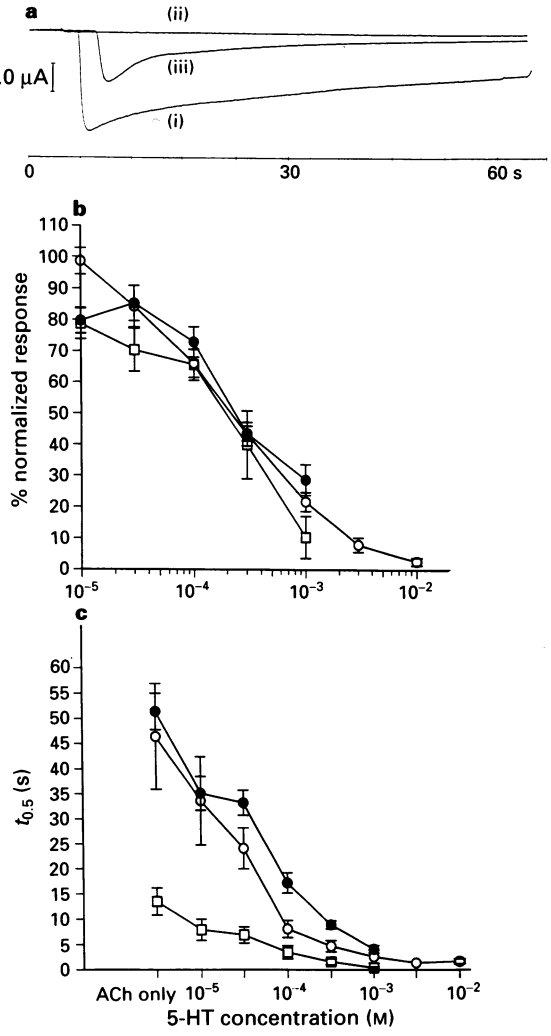

Figure 1 Inward current responses to acetylcholine (ACh) are reduced in the presence of 5-hydroxytryptamine (5-HT). (a) Trace (i): the application of 10 μM ACh to oocytes expressing muscle type nicotinic receptors caused a current which rose rapidly to a peak, and then desensitized with time. The mean peak value was 2.9 ± 0.37 μA, and the current decayed with a $t_{0.5}$ of 46.4 ± 10.5 s (n = 10). Trace (ii): The application of 100 μM 5-HT did not elicit any current (n = 5). Trace (iii): application of ACh in the presence of 100 μM 5-HT produced a reduced peak current and accelerated desensitization. The mean peak was reduced to 66.0 ± 4.5% of control value and the $t_{0.5}$ value was reduced to 8.1 ± 1.7 s (n = 10). (b) The effect of 5-HT on nicotinic AChRs is dose-dependent, with IC_{50} values for muscle(○), $\alpha\beta_2\gamma\delta$ (□), and $\alpha_4\beta_2$(●) being 227 ± 0.44 μM, 166 ± 0.47 μM, and 283 ± 0.28 μM respectively (n = 5–10). (c) 5-HT also increased the rate of desensitization of the current in all receptor subtypes. A dose of 100 μM 5-HT was able to reduce the $t_{0.5}$, to 17% of the control value in the case of the muscle receptor (○), 26% in the $\alpha\beta_2\gamma\delta$ subtype (□), and to 33% for the $\alpha_4\beta_2$ neuronal subtype (●).

nature of the β-subunit (Luetje & Patrick, 1989; 1991; Luetje *et al.*, 1990; Duvoisin *et al.*, 1990), thus the effect of the β-subunit on the action of 5-HT was investigated by substituting the neuronal β_2 subunit for the normal muscle β_1 subunit, and the neuronal combination $\alpha_4\beta_2$. The size of the current elicited by 10 μM ACh was smaller in these combinations than in the normal muscle combination, with a peak current of 237 ± 44 nA (n = 10) and 580 ± 122 nA (n = 7) respectively (sample traces shown in Figure 3a). Once again 5-HT modulated the response of the receptor complexes to ACh (Figure 3b) in a dose-dependent manner, (Figure 1b) with the IC_{50} being 166 ± 0.47 μM for the $\alpha\beta_2\gamma\delta$ combination, and 283 ± 0.28 μM for $\alpha_4\beta_2$. Neither value was significantly

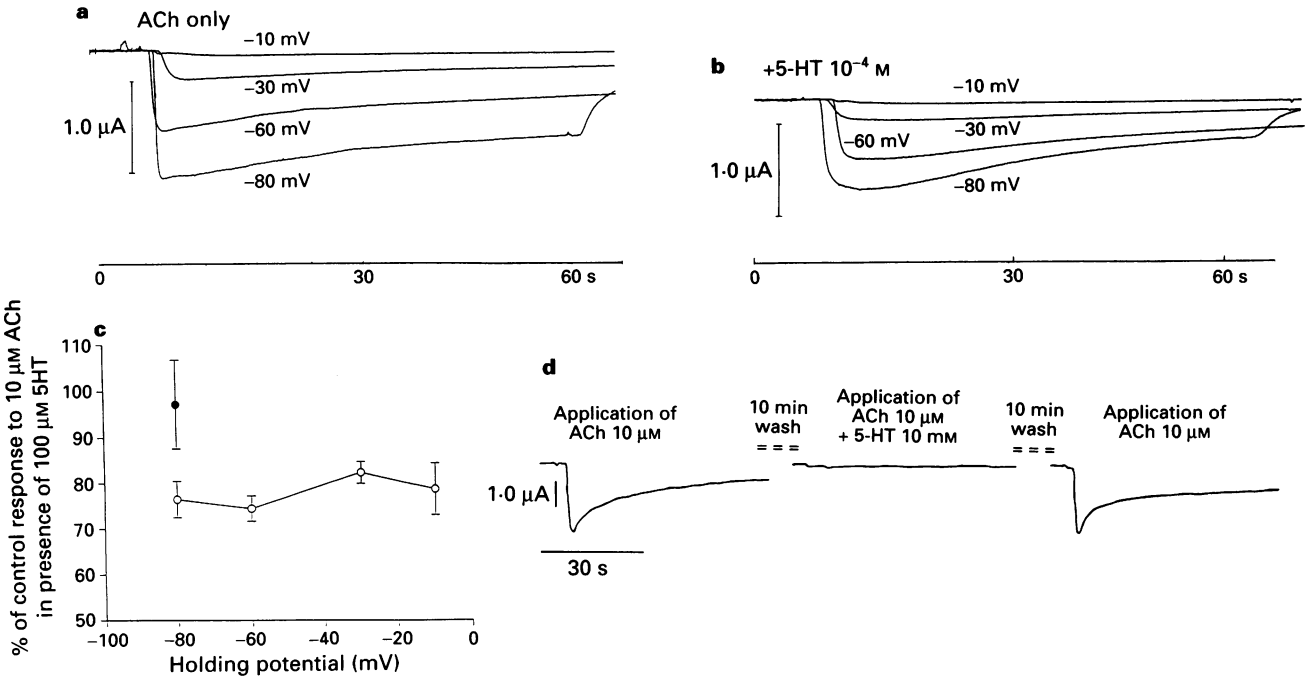

Figure 2 Dependence of the 5-hydroxytryptamine (5-HT) effect on membrane potential. (a) Superimposed traces showing that the current elicited by a given dose of acetylcholine (ACh) is dependent on the holding potential. (b) The ACh current is reduced in the presence of 5-HT at all holding potentials. (c) When the size of the responses in the absence and presence of 5-HT were normalized to the control response to ACh it was found that the reduction in the peak current in response to 10 μM ACh caused by 100 μM 5-HT was independent of the holding voltage (○) ($n = 6$). It was also readily reversible by washout (●), ($n = 5$). (d) The ACh current was almost completely abolished by the presence of 10 mM 5-HT, but this effect could be reversed by washing for 10 min.

different from the muscle receptor IC_{50} value ($P = 0.40$ and 0.35 respectively). Although both neuronal subunit containing receptors showed different desensitization kinetics to the normal muscle combination, the rate of decay was increased by similar proportions. In the $\alpha\beta_2\gamma\delta$ combination the $t_{0.5}$ was reduced to 26% of the control value, from 13.5 ± 2.7 s in the presence of 10 μM ACh, to 3.5 ± 1.3 s ($P < 0.02$) in the presence of 100 μM 5-HT, and in the $\alpha_4\beta_2$ subtype $t_{0.5}$ was reduced to 33% of the control value with 100 μM 5-HT from 51.4 ± 3.6 s to 17.2 ± 2.0 s ($P < 0.001$) Figure 1c.

The effect of structurally similar molecules

Tryptamine, a structural analogue of 5-HT, which is less active than 5-HT at 5-HT receptors, and ketanserin, a competitive antagonist of 5-HT at 5-HT_2 receptors, were tested. Perfusion of either tryptamine or ketanserin alone did not give rise to a current in oocytes expressing muscle type nicotinic receptors, but when co-perfused with ACh both compounds reduced the peak current. Figure 4a shows the effect of a 100 μM dose of each compound on the current elicited by 10 μM ACh in one oocyte. 5-HT (100 μM) reduced the peak current elicited by 10 μM ACh by 66.0 ± 4.5%. Tryptamine was less active than 5-HT, and ketanserin more potent, with 100 μM doses reducing the peak ACh current by 75.0 ± 3.3% and 42.9 ± 4.7% respectively. Both drugs acted in a dose-dependent manner, with the IC_{50} value for tryptamine being 1.0 ± 0.02 mM, which is significantly different from the muscle IC_{50} ($P < 0.0001$), and that for ketanserin being 49.0 ± 1.3 μM ($P < 0.01$ compared to the muscle value). Both compounds also increased the rate of desensitization, 100 μM tryptamine reduced the $t_{0.5}$ to 20% of the control value, that is from 43.0 ± 6.3 s to 8.5 ± 2.2 s ($P < 0.001$), (Figure 4c).

These results suggest that a specific binding site for 5-HT might be responsible for the effect on currents elicited by ACh as structurally similar molecules can mimic the effect.

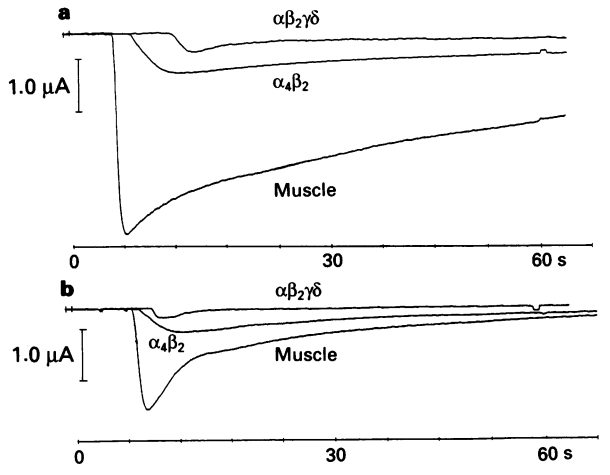

Figure 3 5-Hydroxytryptamine (5-HT) reduces the peak current and enhances the rate of desensitization in all receptor subtypes. (a) The neuronal subtypes gave smaller responses than the muscle receptors to a given dose of acetycholine (ACh). ACh (10 μM) gave rise to a current of 2.9 ± 0.37 μA ($n = 10$) in the muscle type receptor, whilst the $\alpha\beta_2\gamma\delta$ combination had a peak current of 237 ± 44 nA ($n = 5$), and the $\alpha_4\beta_2$ type had a peak current of 580 ± 122 nA ($n = 7$). (b) When 100 μM 5-HT was co-perfused with 10 μM ACh, it caused a reduction in the peak current in all nicotinic AChR subtypes studied.

Discussion

We have demonstrated here that the presence of 5-HT affects the response of the nicotinic AChR to acetylcholine. It alters the kinetics of desensitization of the receptor, and reduces the peak current elicited by a given dose of ACh in a dose-

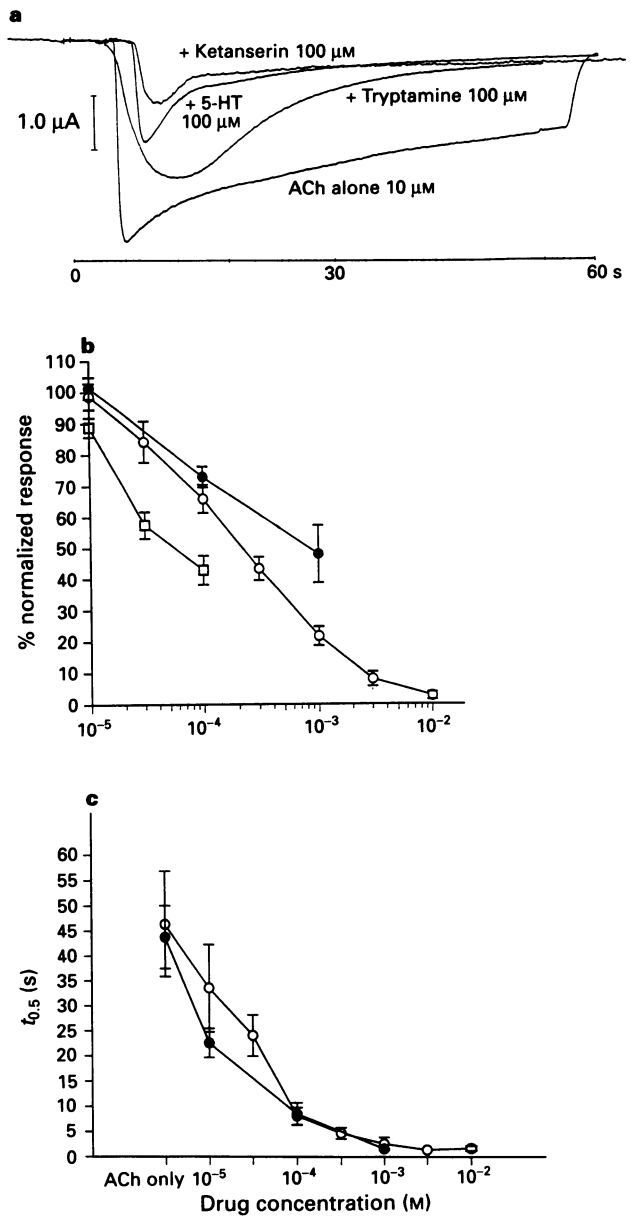

Figure 4 Structural analogues of 5-hydroxytryptamine (5-HT) also affect the acetylcholine (ACh) response in a dose-dependent manner. (a) Both tryptamine and ketanserin reduced the ACh current. 5-HT (100 μM) reduced the peak current to 66.0 ± 4.5% of control, whereas tryptamine was less effective than 5-HT, a 100 μM dose reducing the peak to 75.0 ± 3.3%. Ketanserin was more potent, 100 μM reduced the peak current to 42.9 ± 4.7%. (b) Both drugs worked in a dose-dependent manner. Tryptamine had an IC_{50} of 1.0 ± 0.02 mM (●, $P<0.0001$ compared to the IC_{50} for 5-HT, shown by ○), and ketanserin had an IC_{50} value of 49 ± 1.3 μM (□, $P<0.01$). (c) Tryptamine (100 μM) reduced the $t_{0.5}$ from 43.0 ± 6.3 s to 8.5 ± 2.2 s, 20% of the control value.

dependent manner. The effect seems to be via a direct action on the nicotinic AChR itself, as 5-HT application alone does not give rise to any current. Grassi *et al.* (1993) provide further evidence for 5-HT acting directly on the nicotinic AChR. They showed that 5-HT alone did not give rise to a current in any of the preparations they studied, neither did it give rise to membrane oscillations in *Xenopus* oocytes, which would be indicative of the presence of G-protein linked 5-HT receptors (Gundersen *et al.*, 1983; 1984). Additionally, Grassi *et al.* (1993) found that 5-HT modified the action of ACh on its receptors only when added within the patch pipette solution, and not when added externally, suggesting that the modulation is via a direct action on the nicotinic AChR as opposed to a second messenger pathway. This may have physiological relevance in two ways; in inflammation processes, the level of 5-HT in the blood may be enough to alter nicotinic AChR function; in addition, local concentrations at synapses may be high enough to have functional effects (Grassi *et al.*, 1993).

We have found the effect of 5-HT to be similar on both neuronal and muscle types of nicotinic AChR with the IC_{50} values for all the subunit combinations studied being comparable. This generality of 5-HT action was also seen by Grassi *et al.* (1993) who found that 5-HT had an effect in all the cell types they studied, mouse myotubes, human TE671/RD cells, and *Xenopus* oocytes injected with muscle or *Torpedo* nicotinic AChR mRNA, and Akasu & Koketsu (1986) who demonstrated 5-HT inhibited ACh responses in bull-frog sympathetic ganglia. This suggests that the 5-HT is acting at a highly conserved common site, which may be at, or overlapping, the ACh binding site. Evidence for 5-HT acting at the ACh binding site itself comes from the fact 5-HT can protect the nicotinic AChR from the blocking action of the sea snake toxin erabutoxin (Koketsu *et al.*, 1982), which is known to bind specifically to the ACh binding site of the muscle receptor (Kato *et al.*, 1978). However, the similarity of effect on the different receptor combinations studied is somewhat unexpected in that the pharmacologies are distinct, with agonists having different potencies at receptor subtypes (Luetje & Patrick, 1989; 1991; Luetje *et al.*, 1990; Duvoisin *et al.*, 1990). This would imply that the ACh binding site is not identical between subtypes, yet 5-HT has a similar degree of effect in each case. We also found that the effect of 5-HT could be mimicked by application of structurally similar molecules, including a 5-HT_2 receptor competitive antagonist. This implies that the action of 5-HT is at a specific site, presumably on the nicotinic AChR.

We found the effect of 5-HT on the ACh response (10 μM) to be readily reversible by washout, and voltage-independent over the range tested (−80 to −10 mV), indicating that 5-HT is not acting within the open channel as a charged species. However, Grassi *et al.* (1993) observed a reduction of the 5-HT block of nicotinic AChR peak responses (1 μM) in oocytes at potentials above 0 mV, possibly reflecting a degree of open channel block at these higher membrane potentials.

Our data show that 5-HT modulates the action of ACh at its receptor, by decreasing the peak current elicited, and increasing the rate of desensitization. The effect is dose-dependent, readily reversed by washout, and is independent of the holding voltage. There is some evidence to suggest that 5-HT exerts these effects by acting as a competitive antagonist; Akasu & Koketsu (1986) found that 5-HT gave rise to a shift in the ACh dose-response curve to the right without altering the maximum ACh current in neurones of bull-frog sympathetic ganglia. We postulate that a highly conserved portion of the tertiary structure of nicotinic AChRs, which includes some part of the ACh binding site, has affinity for 5-HT and structural analogues. Interestingly, the extended polycyclic antagonist ketanserin has a significantly lower IC_{50} (49.0 ± 1.3 μM) than 5-HT itself (227 ± 0.44 μM: $P<0.01$) possibly due to an increase in steric occlusion at the agonist binding site. The observation that the shape of the current response to ACh changes in the presence of 5-HT as opposed to a simple scaling, suggests that rather than a pure competitive antagonism, 5-HT modifies the kinetics of channel opening during ACh binding.

We would like to thank Dr L. Holden-Dye for her helpful comments, and the Wessex Medical Trust for financial support. K.M.L.C. is a Wellcome Prize Student.

References

AKASU, T. & KOKETSU, K. (1986). 5-Hydroxytryptamine decreases the sensitivity of nicotinic acetylcholine receptor in bull-frog sympathetic ganglion cells. *J. Physiol.*, **380**, 93–109.

ARIYOSHI, M., HASUO, H., KOKETSU, K., OHTA, Y. & TOKIMASA, T. (1985). Histamine is an antagonist of the acetylcholine receptor at the frog endplate. *Br. J. Pharmacol.*, **85**, 65–73.

DUVOISIN, R.M., DENERIS, E.S., PATRICK, J. & HEINEMANN, S. (1989). The functional diversity of the neuronal nicotinic acetylcholine receptors is increased by a novel subunit: beta 4. *Neuron*, **3**, 487–496.

GRASSI, F., POLENZANI, A.M., MILEO, C.G., CARATSCH, F., EUSEBI, F. & MILEDI, R. (1993). Blockage of nicotinic acetylcholine receptors by 5-hydroxytryptamine. *J. Neurosci. Res.*, **34**, 562–570.

GUNDERSEN, C.B., MILEDI, R. & PARKER, I. (1983). Serotonin receptors induced by exogenous messenger RNA in *Xenopus* oocytes. *Proc. R. Soc.*, **B219**, 103–109.

GUNDERSEN, C.B., MILEDI, R. & PARKER, I. (1984). Messenger RNA from human brain induces drug- and voltage-operated channels in *Xenopus* oocytes. *Nature*, **308**, 421–424.

HIRAI, K. & KOKETSU, K. (1980). Presynaptic regulation of the release of acetylcholine by 5-hydroxytryptamine. *Br. J. Pharmacol.*, **70**, 499–500.

KATO, E., KUBA, K. & KOKETSU, K. (1978). Effects of erabutoxins on neuromuscular transmission in frog skeletal muscles. *J. Pharmacol. Exp. Ther.*, **204**, 446–453.

KOKETSU, K., AKASU, T., MIYAGAWA, M. & HIRAI, K. (1982). Biogenic antagonists of the nicotinic receptor: their interactions with erabutoxin. *Brain Res.*, **250**, 391–393.

LUETJE, C.W. & PATRICK, J. (1991). Both α and β subunits contribute to the agonist sensitivity of neuronal nicotinic acetylcholine receptors. *J. Neurosci.*, **11**, 837–845.

LUETJE, C.W. & PATRICK, J. (1989). Members of the neuronal nicotinic acetylcholine receptor family display distinct pharmacological and toxicological properties. *Soc. Neurosci. Abstr.*, **15**, 275–312.

LUETJE, C.W., PATRICK, J. & SEGUELA, P. (1990). Nicotine receptors in the mammalian brain. *FASEB J.*, **4**, 2753–2760.

YAMADA, M., TOKIMASA, T. & KOKETSU, K. (1982). Effects of histamine on acetylcholine release in bullfrog sympathetic ganglia. *Eur. J. Pharmacol.*, **82**, 15–20.

(Received September 6, 1994
Revised December 22, 1994
Accepted December 23, 1994)

British Journal of Pharmacology (1995) 114, 1641-1651 © 1995 Stockton Press All rights reserved 0007-1188/95 $12.00

The interaction of trichloroethanol with murine recombinant 5-HT_3 receptors

[2]David L. Downie, Anthony G. Hope, Delia Belelli, Jeremy J. Lambert, [1]John A. Peters, *Kim R. Bentley, *Lucinda J. Steward, *[3]Chong-Yang Chen & *Nicholas M. Barnes

Neuroscience Research Group, Department of Pharmacology and Clinical Pharmacology, Ninewells Hospital and Medical School, The University of Dundee, Dundee, DD1 9SY and *Department of Pharmacology, The Medical School, University of Birmingham, Edgbaston, Birmingham B15 2TT

1 The effects of ethanol, chloral hydrate and trichloroethanol upon the 5-HT_3 receptor have been investigated by use of electrophysiological techniques applied to recombinant 5-HT_3 receptor subunits (5-HT_3R-A or 5-HT_3R-A_S) expressed in *Xenopus laevis* oocytes. Additionally, the influence of trichloroethanol upon the specific binding of [^{3}H]-granisetron to membrane preparations of HEK 293 cells stably transfected with the murine 5-HT_3R-A_S subunit and 5-HT_3 receptors endogenous to NG 108-15 cell membranes was assessed.

2 Ethanol (30–300 mM), chloral hydrate (1–30 mM) and trichloroethanol (0.3–10 mM), produced a reversible, concentration-dependent, enhancement of 5-HT-mediated currents recorded from oocytes expressing either the 5-HT_3R-A, or the 5-HT_3R-A_S subunit.

3 Trichloroethanol (5 mM) produced a parallel leftward shift of the 5-HT concentration-response curve, reducing the EC_{50} for 5-HT from $1 \pm 0.04\,\mu M$ ($n = 4$) to $0.5 \pm 0.01\,\mu M$ ($n = 4$) for oocytes expressing the 5-HT_3R-A. A similar shift, from $2.1 \pm 0.05\,\mu M$ ($n = 11$) to $1.3 \pm 0.1\,\mu M$ ($n = 4$), was observed in oocytes expressing the 5-HT_3R-A_S subunit. Trichloroethanol (5 mM) had little or no effect upon the maximum current produced by 5-HT for either recombinant receptor.

4 Trichloroethanol (5 mM) similarly reduced the EC_{50} for 2-methyl-5-HT from $13 \pm 0.4\,\mu M$ ($n = 4$) to $4.6 \pm 0.2\,\mu M$ ($n = 4$) and from $15 \pm 2\,\mu M$ ($n = 4$) to $5 \pm 0.4\,\mu M$ ($n = 4$) for oocytes expressing the 5-HT_3R-A and 5-HT_3R-A_s subunit respectively. Additionally, trichloroethanol (5 mM) produced a clear enhancement of the maximal current to 2-methyl-5-HT (expressed as a percentage of the maximal current to 5-HT) from $63 \pm 0.7\%$ ($n = 4$) to $101 \pm 1.6\%$ ($n = 4$) and from $9 \pm 0.2\%$ ($n = 4$) to $74 \pm 2\%$ ($n = 4$) for oocytes expressing the 5-HT_3R-A and 5-HT_3R-A_S subunit respectively.

5 Trichloroethanol (2.5 mM) had no effect upon the K_d, or B_{max}, of specific [^{3}H]-granisetron binding to membrane homogenates of NG 108-15 cells or HEK 293 cells. Similarly, competition for [^{3}H]-granisetron binding by the 5-HT_3 receptor antagonists ondansetron and tropisetron was unaffected. However, competition for [^{3}H]-granisetron binding by the 5-HT_3 receptor agonists, 5-HT, 2-methyl-5-HT and phenylbiguanide was enhanced by trichloroethanol (2.5 mM).

6 Unexpectedly, the competition for [^{3}H]-granisetron binding by the 5-HT_3 receptor antagonist, quipazine, was enhanced by 2.5 mM trichloroethanol. Quipazine (1 nM–0.3 μM) antagonized 5-HT-evoked currents recorded from oocytes expressing the 5-HT_3R-A subunit with an IC_{50} of 18 ± 3 nM ($n = 4$). Additionally, quipazine (30 nM–0.3 μM) produced a small inward current which was greatly enhanced by 5 mM trichloroethanol and antagonized by 100 nM ondansetron. Collectively, these observations suggest that quipazine may act as a partial agonist.

7 The demonstration that a recombinant homo-oligomeric receptor, expressed in a foreign membrane, retains a sensitivity to alcohols, together with the sequencing of alcohol-insensitive 5-HT_3 receptor subunits, may lead to a better definition of the alcohol binding site(s).

Keywords: 5-HT_3 receptor; recombinant 5-HT_3 receptor; splice variants; *Xenopus laevis* oocytes; trichloroethanol; ethanol; chloral hydrate; ligand-gated ion channel

Introduction

The 5-HT_3 receptor is a ligand-gated ion channel that demonstrates functional properties similar to those of nicotinic acetylcholine receptors, including cation selectivity, cooperativity in agonist binding and rapid activation and desensitization kinetics (Lambert *et al.*, 1994; Peters *et al.*, 1994; Boess & Martin, 1994). The nucleotide sequence of a cDNA encoding a 5-HT_3 receptor subunit (5-HT_3R-A), cloned from the NCB-20 hybridoma cell line, predicts a protein which exhibits considerable structural commonality with nicotinic receptor subunits (Maricq *et al.*, 1991). Each subunit is thought to consist of a large extracellular amino terminal domain which contains the agonist binding site, four putative transmembrane regions (M_1–M_4), with M_2 probably forming the lining of the ion channel, and a large intracellular loop between M_3 and M_4. This model is supported by recent experiments investigating the properties of a chimaeric receptor. The chimaera which consisted of the amino terminal extracellular domain of the chick α_7 nicotinic receptor and the M_1 to carboxyl terminus of the 5-HT_3R-A subunit formed functional receptors gated by acetylcholine, but with the ion channel properties characteristic of the recombinant 5-HT_3R-A (Eiselé *et al.*, 1993).

Recently, a splice variant of the 5-HT_3R-A subunit, which lacks 6 consecutive amino acid residues within the large

[1] Author for correspondence.
[2] Present address: The Biophysics Section, The Blackett Laboratory, Imperial College, Prince Consort Road, London, SW7 2BZ.
[3] Present address: Department of Pharmacology, Guilin Medical College, Guilin, Guangxi 541001, China.

intracellular loop between M_3 and M_4 (the 5-HT$_3$R-A$_s$, s = short form) has been obtained from N1E-115 cells (Hope *et al.*, 1993). Both forms have been detected in N1E-115, NCB-20 and NG 108-15 cells, and the cerebral cortex, hippocampus and superior cervical ganglion of the mouse (Hope *et al.*, 1993; Werner *et al.*, 1993). A species homologue of the short form has additionally been found in rat superior cervical ganglion (Isenberg *et al.*, 1993). Either subunit forms functional, presumably homo-oligomeric, receptors when expressed in *Xenopus laevis* oocytes, or mammalian cell lines which reproduce many of the pharmacological and biophysical properties of the receptor native to the murine neuroblastoma cell lines (Maricq *et al.*, 1991; Gill *et al.*, 1993; Hope *et al.*, 1993; Yakel *et al.*, 1993; Downie *et al.*, 1994; Sepúlveda & Lummis, 1994; Uetz *et al.*, 1994). A detailed comparison of the agonist and antagonist pharmacology of the two subunits expressed in *Xenopus* oocytes revealed little difference between them, with the exception that the maximal effect of the agonist, 2-methyl-5-HT, was reduced for the 5-HT$_3$R-A$_S$ subunit (Downie *et al.*, 1994; see also Sepúlveda & Lummis, 1994).

Little information exists concerning the influence of potential allosteric regulators upon recombinant 5-HT$_3$ receptors. For receptors endogenous to peripheral neurones and neuronal cell lines, such agents may include the dissociative anaesthetic ketamine (Peters *et al.*, 1991), indole derivatives (Kooyman *et al.*, 1994) and certain alcohols (e.g. Lovinger, 1991). Reports describing the potentiation of 5-HT$_3$ receptor-mediated currents recorded from NCB-20 cells and rat nodose ganglion neurones by ethanol (Lovinger, 1991; Lovinger & White, 1991) and trichloroethanol (Lovinger & Zhou, 1993) prompted the present investigation of the effects of these agents upon recombinant 5-HT$_3$ receptors. Primarily, it was of interest to determine whether the heterologously expressed subunits were susceptible to modulation by ethanol and trichloroethanol and if so, whether the splice variants of the 5-HT$_3$R-A would respond differentially to these agents. The latter consideration arose from work indicating the alternatively spliced forms of the GABA$_A$ receptor γ_2 subunit (γ_{2S} and γ_{2L}) to be an important determinant of the ethanol sensitivity of hetero-oligomeric GABA$_A$ receptor complexes expressed in *Xenopus* oocytes (Wafford *et al.*, 1991). Notably, the γ_{2S} subunit, which lacks a consensus sequence for phosphorylation by protein kinase C due to the deletion of 8 consecutive amino acids located within the large intracellular loop between M_3 and M_4, does not support the enhancement by ethanol of GABA-evoked currents observed with receptors containing the γ_{2L} subunit. In this regard, it is interesting that the 6 amino acids absent from the intracellular loop of the 5-HT$_3$R-A$_S$ have been suggested to form a site for phosphorylation by casein kinase II (Werner *et al.*, 1993).

Species differences in the agonist and antagonist pharmacology of the 5-HT$_3$ receptor are well known (e.g. Butler *et al.*, 1990; Newberry *et al.*, 1991; Peters *et al.*, 1992) and it would appear that such differences extend to allosteric modulators. For example, trichloroethanol blocks, rather than potentiates, 5-HT$_3$ receptor-mediated currents recorded from nodose ganglion neurones of the guinea-pig (Gill *et al.*, 1994). Comparisons of the primary amino acid sequence of 5-HT$_3$ receptor subunits displaying differential responses to alcohol may lead to the definition of sites involved in allosteric regulation. In the present study, electrophysiological techniques were employed to investigate the interaction of ethanol, trichloroethanol and chloral hydrate (which is reduced to trichloroethanol *in vivo*; Garrett & Lambert, 1973) with the alternatively spliced variants of the 5-HT$_3$R-A expressed in *Xenopus* oocytes. In addition, the interaction of trichloroethanol with recombinant 5-HT$_3$ receptors in stably transfected HEK 293 cells (Hope, 1993) and 5-HT$_3$ receptors native to NG 108-15 cells (Neijt *et al.*, 1988) was examined in ligand binding assays employing the antagonist [^{3}H]-granisetron. A preliminary account of a part of this work has appeared in abstract form (Downie *et al.*, 1993).

Methods

Preparation of in vitro *transcripts*

The 5-HT$_3$R-A cDNA (Maricq *et al.*, 1991) and the 5-HT$_3$R-A$_S$ cDNA (Hope *et al.*, 1993) were linearised by use of the restriction enzymes *Not I* and *Bam HI* respectively. A Riboprobe System II transcription kit (Promega Limited, U.K.) was employed to synthesize capped *in vitro* transcripts from individual template cDNA using either an SP6 (5-HT$_3$R-A) or T$_3$ (5-HT$_3$R-A$_S$) RNA polymerase. The integrity of the RNA transcripts was determined by electrophoresis through a denaturing 1% agarose formaldehyde gel (Sambrook *et al.*, 1989), alongside standard RNA size markers (Gibco BRL, U.K.).

Expression and electrical recordings

Xenopus laevis oocytes were isolated as described by Hope *et al.* (1993) and incubated in Barth's saline comprising in (mM): NaCl 88, KCl 1, $NaHCO_3$ 2.4, $MgSO_4$ 1, $CaCl_2$ 0.5, $Ca(NO_3)_2$ 0.5; HEPES 15 (pH 7.5). Stage VI oocytes were identified and injected with 20–100 nl of nuclease free water containing 10–40 ng of the appropriate cRNA, using a Drummond Digital Microdispenser 510 (Drummond Scientific Co., Broomhall, PA, U.S.A.). Injected oocytes were individually stored in wells of 96 well microtitre plates containing 200 µl of Barth's saline supplemented with penicillin (50 iu ml^{-1}), streptomycin (50 µg ml^{-1}) and gentamycin (100 µg ml^{-1}). Oocytes were maintained at 19–20°C for 2 to 10 days prior to use.

Electrical recordings were made in modified Barth's solution containing (in mM): NaCl 88, KCl 1, $NaHCO_3$ 2.4, $MgCl_2$ 1, $CaCl_2$ 1 and HEPES 15 (pH 7.5; adjusted with NaOH). Agonist-induced currents were recorded at a holding potential of −30 mV with an Axoclamp 2A (Axon Instruments, Foster City, CA, U.S.A.) voltage-clamp amplifier in the twin electrode voltage-clamp mode. The voltage-sensing and current-passing microelectrodes were filled with 3 M KCl and 3 M CsCl respectively and had resistances of 0.4–1.5 MΩ when determined in the standard extracellular saline. Oocytes were continuously superfused at a rate of 5–6 ml min^{-1}. Antagonist, agonist and modulatory compounds were applied via the superfusion system. In the case of modulatory and antagonist compounds, the substances were preapplied for 1 min prior to their simultaneous application with the appropriate agonist for a further 20–60 s. Membrane currents were low-pass filtered at 100 Hz (8-pole Bessel filter; Fylde Instruments U.K.), recorded onto video tape via a PCM 2 VCR adapter (Medical Systems Corporation, Greenvale, N.Y., U.S.A.) or onto magnetic tape using a Racal Store 4 DS F.M. tape recorder and simultaneously displayed on a chart recorder (Multitrace 2, Lectromed, Jersey, C.I.). All recordings were performed at ambient temperature (18–23°C).

Cell culture

The neuroblastoma-glioma hybrid cell line NG 108-15 (N18TG2 mouse neuroblastoma × rat glioma C6BY-1; Klee & Nirenberg, 1974) was grown in Dulbecco's modified Eagle's medium containing 10% (v/v) foetal calf serum supplemented with hypoxanthine (100 µM), aminopterin (1.0 µM) and thymidine (16 µM) (i.e. HAT supplement). HEK 293 cells stably transfected with the 5-HT$_3$R-A$_S$ subunit (Hope, 1993) were grown under similar conditions although the growth medium additionally contained geneticin (200 µg ml^{-1}) and lacked the HAT supplement. NG 108-15 and HEK 293 cells were harvested by agitation in Ca^{2+}- and Mg^{2+}-free Dulbecco's phosphate buffered saline (between passage 30 and 40 for NG 108-15 and 4 and 45 for HEK 293 cells) and pelleted by centrifugation (900 *g*, 10 min, 4°C). Pelleted cells were

immediately frozen at −80°C and stored for periods of up to 2 months with no loss of binding activity.

Preparation of cell homogenate for radioligand binding

To prepare membranes for radioligand binding assays, cells were thawed and then homogenized in 20 ml of ice-cold Tris/PMSF/EGTA buffer (in mM: Tris 50, phenylmethyl sulphonyl fluoride (PMSF) 0.1, ethylene glycol-*bis*(β-aminoethyl ether) N,N,N′,N′-tetraacetic acid (EGTA) 5.0, final pH 7.4) using a Polytron blender (full power, 10 s) and centrifuged (48000 *g*, 10 min, 4°C). The resultant pellet was gently resuspended in 20 ml of Tris-Krebs buffer (in mM: Tris 50, NaCl 118, KCl 4.75, KH_2PO_4 1.2, $MgSO_4$ 1.2; $CaCl_2$ 2.5; $NaHCO_3$ 25 and glucose 11; final pH 7.4) and recentrifuged. The final pellet was gently resuspended in Tris-Krebs buffer to form the radioligand binding homogenate at a concentration of approximately 0.2 mg protein ml^{-1}. Protein content was assayed by the Bio-Rad Coomassie Brilliant Blue method (Bradford, 1976) with bovine serum albumin used as standard.

[^{3}H]-granisetron binding assay

For [^{3}H]-granisetron binding, assay tubes (in triplicate) contained 500 µl of competing drug, or vehicle (Tris-Krebs buffer), 150 µl trichloroethanol, or vehicle (Tris-Krebs buffer) and 100 µl [^{3}H]-granisetron (final concentration 0.9–1.1 nM for competition studies, or at a range of concentrations between 0.1–12.6 nM for saturation studies; radioligand concentrations calculated by assay of the incubation solutions). The assay tubes were preincubated for 2 min at 37°C before the addition of 250 µl cell homogenate to initiate binding, which was allowed to proceed at 37°C for 60 min before termination by rapid filtration under vacuum through pre-wet (0.1% v/v polyethyleneimine in Tris-Krebs buffer) Whatman GF/B filters followed by washing with ice-cold Tris-Krebs buffer (wash time 8 s). Bound radioactivity remaining on the filters was assayed in 10 ml of Ecoscint A (National Diagnostics) by liquid scintillation spectroscopy at an efficiency of approximately 47%.

Data analysis

For radioligand binding experiments, saturation and competition data were analysed by computer assisted iterative curve fitting according to the equation:

$$\frac{B}{B_{max}} = \frac{[L]^n}{[L]^n + [K]^n}$$

where B = bound radioligand; B_{max} = maximum binding at equilibrium; for saturation studies K = molar equilibrium dissociation constant, or for competition studies K = molar concentration of competing compound to reduce the specific binding by 50%; for saturation studies L = free molar concentration of radioligand, or for competition studies L = molar concentration of competing compound, n = Hill coefficient.

For electrophysiological studies, the peak amplitudes of agonist-evoked currents were measured manually from chart recorder traces. EC_{50} values of agonists, together with the Hill coefficient or slope factor, were derived from full log concentration-effect relationships. Each of these was fitted iteratively with a sigmoidal function equivalent to that given above by use of Fig P version 6.0c (Biosoft, U.K.) to estimate the appropriate parameters. Data are reported as the arithmetic mean ± the standard error of the mean (s.e.mean).

Drugs

Reagents were obtained from the following sources: 5-HT maleate, 5-HT creatinine sulphate, metoclopramide hydrochloride, cocaine hydrochloride, (+)-tubocurarine chloride, trichloroethanol, chloral hydrate (Sigma Chemical Co.), ethanol (BDH-Analar grade), 2-methyl-5-HT maleate, quipazine maleate (Research Biochemicals Inc.), phenylbiguanide (Aldrich Chemical Co.), ondansetron hydrochloride (Glaxo), granisetron hydrochloride and BRL 46470 (endo-*N*-(8-methyl-8-azabicyclo-[3,2,1] oct-3-yl)-2,3-dihydro-3,3-dimethyl-indol-1-carboxamide hydrochloride; SmithKline Beecham); tropisetron hydrochloride (Sandoz). [^{3}H]-granisetron (84.5 Ci mmol^{-1} New England Nuclear) was supplied in ethanol and diluted into Tris-Krebs buffer solution. With the exception of the latter, all drugs were freshly prepared and dissolved as concentrated stock solutions in either twice distilled water or the appropriate buffer solution.

Results

Previous studies have demonstrated that the potentiation of 5-HT$_3$ receptor-mediated currents by ethanol and trichloroethanol is most pronounced at low agonist concentrations (Lovinger & White, 1991; Lovinger & Zhou, 1993). In the present study, concentration effect relationships for ethanol, chloral hydrate and trichloroethanol were constructed using 5-HT concentrations of 0.5 µM and 1.0 µM in recordings performed on oocytes expressing the 5-HT$_3$R-A and 5-HT$_3$R-A$_S$ subunits respectively. On average, these concentrations of agonist correspond to the EC_{20} of the relevant 5-HT concentration response curve (Downie *et al.*, 1994).

Ethanol

Relatively high concentrations of ethanol enhance the 5-HT$_3$ receptor-mediated current recorded from murine NCB-20 hybridoma cells (Lovinger, 1991) and rat nodose ganglion neurones (Lovinger & White, 1991). In the present study, very high concentrations of ethanol (100 mM–300 mM) clearly potentiated inward current responses to 5-HT recorded from all oocytes expressing either the 5-HT$_3$R-A, or the 5-HT$_3$R-A$_S$ subunit (Figure 1). For example, at the highest concentration of ethanol tested (300 mM), responses elicited by 5-HT (1 µM) acting at the 5-HT$_3$R-A$_S$ were increased to 186 ± 6% (n = 4) of control. Similarly, currents evoked by 0.5 µM 5-HT at the 5-HT$_3$R-A were increased to

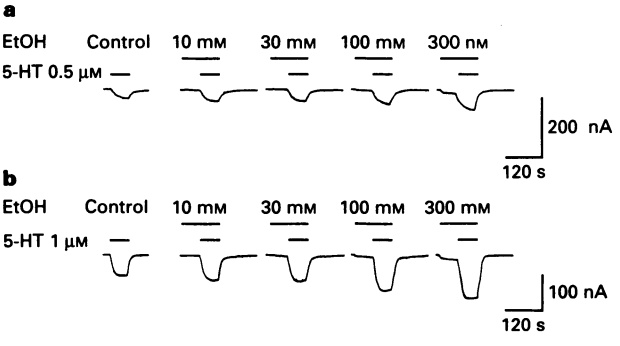

Figure 1 Ethanol (EtOH) potentiates 5-HT$_3$ receptor-mediated currents. All records illustrated are from *Xenopus laevis* oocytes voltage-clamped at −30 mV and expressing the 5-HT$_3$R-A (a) or the 5-HT$_3$ R-A$_S$ (b) subunit. Inward currents elicited by bath-applied 5-HT (0.5 µM for 5-HT$_3$R-A; 1 µM for 5-HT$_3$R-A$_S$) are enhanced in a concentration-dependent manner by ethanol (30 mM–300 nM). The concentration of 5-HT used approximates to the EC_{20} of the relevant concentration-effect relationship for 5-HT. In this and all subsequent figures, the periods of drug application are indicated by the horizontal bars above each current record. In all illustrations currents were low pass filtered at 100 Hz.

176 ± 8% (n = 4) of control. A modest potentiation of 5-HT-induced responses, to 119 ± 3% (n = 4) and 115 ± 5% (n = 5) of control, was observed with 30 mM ethanol acting at the 5-HT$_3$R-A$_S$ and 5-HT$_3$-R-A respectively. At concentrations between 1 and 10 mM, ethanol had little or no effect upon currents elicited by 5-HT acting at either subunit (n = 3–4; Figure 1). At concentrations > 100 mM, ethanol induced a direct inward current. Such currents were not blocked by the 5-HT$_3$ receptor antagonist, ondansetron (10 nM), and were also observed on non-injected oocytes. Therefore, this direct current is unlikely to involve 5-HT$_3$ receptor activation.

Chloral hydrate

Trichloroethanol has been shown to enhance the 5-HT$_3$ receptor-mediated current of rat nodose ganglion neurones (Lovinger & Zhou, 1993). Trichloroethanol is an active metabolite of the sedative and anaesthetic chloral hydrate (Garrett & Lambert, 1973). The effect of chloral hydrate (0.1–30 mM) was studied using the experimental conditions employed for ethanol. For either subunit, clear concentration-dependent enhancement of 5-HT-induced currents was observed with concentrations of chloral hydrate ≥ 3 mM

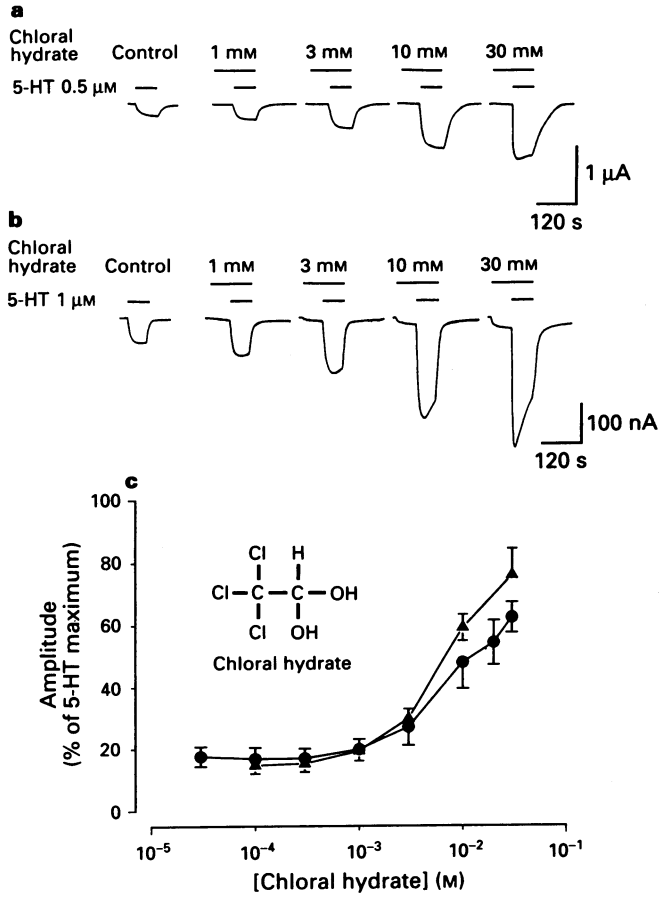

Figure 2 Chloral hydrate potentiates 5-HT$_3$ receptor-mediated currents. All records illustrated are from *Xenopus laevis* oocytes voltage-clamped at −30 mV and expressing the 5-HT$_3$R-A (a) or the 5-HT$_3$ R-A$_S$ (b) subunit. The inward current produced by bath application of 5-HT (0.5 μM for 5-HT$_3$R-A; 1 μM for 5-HT$_3$R-A$_S$) is enhanced in a concentration-dependent manner by chloral hydrate (1 mM–30 mM). The concentrations of 5-HT used produce a response approximating to 20% of maximum attainable with a saturating concentration of 5-HT (i.e. EC_{20} values). (c) The relationship between the concentration of bath-applied chloral hydrate (log scale; x-axis) and the magnitude of the potentiation of the 5-HT-induced current (expressed as a percentage of the maximum response to a saturating concentration of 5-HT, y-axis) for the 5-HT$_3$R-A (●) and 5-HT$_3$ R-A$_S$ (▲) subunit. Each point represents the mean ± s.e.mean of data obtained from 4 oocytes.

(Figure 2). The maximal effect of chloral hydrate could not be determined because at concentrations > 30 mM the compound proved toxic to both injected and non-injected oocytes. Clearly, chloral hydrate is more potent than ethanol and is effective upon both splice variants of the 5-HT$_3$R-A. On some oocytes chloral hydrate (> 3 mM) alone induced an inward current. Such currents were not antagonized by ondansetron (10 nM) and were also observed on uninjected oocytes. Therefore, this direct effect of chloral hydrate is not mediated through 5-HT$_3$ receptor activation.

Trichloroethanol

Trichloroethanol (0.3–10 mM) produced a concentration-dependent enhancement of the 5-HT-induced current recorded from oocytes expressing either splice variant of the 5-HT$_3$R-A (Figures 3 and 4). In both cases, enhancement was evident at 0.3 mM, and the maximal effect of trichloroethanol occurred at 10 mM. At higher concentrations of trichloroethanol, the magnitude of the potentiation was reduced and currents evoked by low concentrations of 5-HT (i.e. 1 μM) demonstrated a rapid decay from their peak value in the continued presence of the agonist (Figure 3). This phenomenon, which was not apparent in control responses elicited by 1 μM 5-HT, or those recorded in the presence of lower concentrations of trichloroethanol, might reflect either enhancement of desensitization, or a channel blocking action, that becomes evident at high concentrations of the compound. Concentrations of trichloroethanol > 0.3 mM induced a direct current which was not blocked by ondansetron (10–100 nM; see Figure 7c for example) and was observed on uninjected oocytes. Thus this direct action is unrelated to 5-HT$_3$ receptor activation and was not studied further.

Previous work has established that the potentiation of the 5-HT$_3$ receptor-mediated current of rat nodose ganglion neurones by trichloroethanol is associated with an increase in the apparent affinity of the receptor for 5-HT (Lovinger & Zhou, 1993). Consistent with this observation, experiments performed on oocytes expressing the 5-HT$_3$R-A subunit demonstrated 5 mM trichloroethanol to produce a parallel leftward shift of the 5-HT concentration-response curve with no change of the maximal current produced (Figure 3). Analysis of these concentration-response curves revealed the 5-HT EC_{50} to be reduced from 1 ± 0.04 μM (n = 4) to 0.5 ± 0.01 μM (n = 4) in the presence of 5 mM trichloroethanol (Figure 3). Similarly, for oocytes expressing the 5-HT$_3$R-A$_S$ subunit, trichloroethanol (5 mM) reduced the 5-HT EC_{50} from 2.1 ± 0.05 μM (n = 11) to 1.3 ± 0.1 μM (n = 4) although additionally a small increase of the 5-HT maximum response was evident (Figure 4).

Radioligand binding studies

To investigate further the interaction of trichloroethanol with the 5-HT$_3$ receptor, its influence upon the specific binding of the radiolabelled antagonist [^{3}H]-granisetron to membrane preparations made from NG 108-15 cells and HEK 293 cells (stably transfected with the 5-HT$_3$R-A$_S$ subunit; Hope, 1993) was determined. [^{3}H]-granisetron (0.1–12.6 nM) bound to a saturable population of binding sites (non-specific binding being defined by the presence of 10 μM tropisetron) in HEK 293 and NG 108-15 cell homogenates (Table 1). Trichloroethanol, at a concentration (2.5 mM) producing a substantial enhancement of the 5-HT$_3$ receptor-mediated current (Figures 3 and 4), had little or no effect upon the K_d, B_{max}, or the Hill coefficient of [^{3}H]-granisetron binding to homogenates of either cell line (Table 1).

The 5-HT$_3$ receptor agonists, 5-HT, 2-methyl-5-HT and phenylbiguanide and the 5-HT$_3$ receptor antagonist tropisetron competed for a similar proportion of [^{3}H]-granisetron (0.9–1.1 nM) binding in both the HEK 293 and NG 108-15 cell preparations (approximately 90–95%). In both prepara-

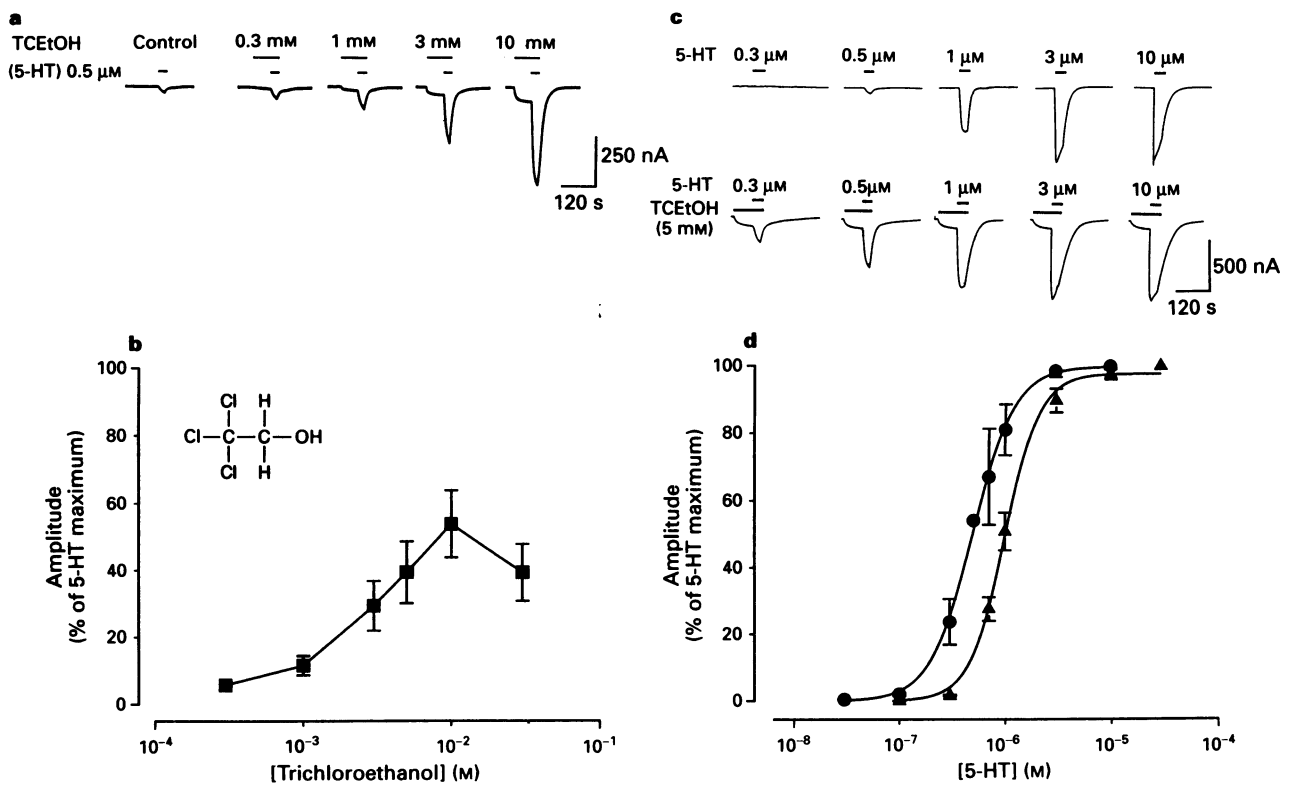

Figure 3 Trichloroethanol (TCEtOH) potentiates currents mediated by the 5-HT$_3$R-A subunit. All records illustrated are from *Xenopus laevis* oocytes voltage-clamped at a holding potential of −30 mV. (a) Inward currents evoked by a bath applied 5-HT (0.5 μM) are enhanced in a concentration-dependent manner by trichloroethanol. Note that the inward current elicited by trichloroethanol (⩾1.0 mM) alone was resistant to antagonism by 10 nM ondansetron and was evident on control (non-injected) oocytes (not illustrated). (b) The relationship between the concentration of bath-applied trichloroethanol (log scale, x-axis) and the potentiation of the 5-HT-induced current (expressed as a percentage of the maximum response to 5-HT, y-axis). (c) The traces illustrate the concentration-dependent inward current response to bath applied 5-HT (0.3–10 μM) in the presence and absence of 5 mM trichloroethanol. (d) The relationship between the concentration of bath applied 5-HT (log scale; x-axis) and peak current amplitude (expressed as a percentage of the current produced by a saturating concentration (30 μM) of 5-HT, y-axis) in the presence (●) and absence (▲) of 5 mM trichloroethanol. The curves were fitted to the data points as described in the Methods. In control, the EC_{50} and Hill slope were found to be 1.0 ± 0.04 μM and 2.6 ± 0.3 (n = 4) respectively. In the presence of 5 mM trichloroethanol, an EC_{50} of 0.5 ± 0.01 μM and a Hill slope of 2.2 ± 0.1 (n = 4) were estimated. In both (b) and (d), each point represents the mean ± s.e.mean of data obtained from 4 oocytes.

tions, the agonists were effective in the micromolar range, whereas the potent 5-HT$_3$ receptor antagonist, tropisetron, was active at nanomolar concentrations. Analysis of the competition curves indicated that generally the agonists competed for [^{3}H]-granisetron binding with Hill coefficients greater than unity, although the Hill coefficients were higher with the NG 108-15 than the HEK 293 cell preparation (Figure 5, Table 2). Competition with the antagonist tropisetron generated Hill coefficients of approximately unity in both preparations (Figure 5, Table 2).

The presence of trichloroethanol (2.5 mM) enhanced the affinity with which 5-HT, 2-methyl-5-HT and phenylbiguanide competed for the [^{3}H]-granisetron-labelled 5-HT$_3$ receptor in both the HEK 293 and NG 108-15 cell preparations (increases in affinity were between 2–4 fold, Figure 5, Table 2). However, the presence of trichloroethanol (2.5 mM) did not change the affinity with which tropisetron or ondansetron competed for the radiolabelled receptor in both preparations (Figure 5, Table 2). In addition, trichloroethanol (2.5 mM) modified the nature of the agonist competition curves for the [^{3}H]-granisetron-labelled receptor in the NG 108-15 cell preparation (Figure 5, Table 2). Thus, the presence of trichloroethanol (2.5 mM) reduced the Hill coefficients with which each of the agonists competed such that they approached unity (Figure 5, Table 2). This phenomenon was not apparent with the HEK 293 cell preparation (Figure 5, Table 2). In both the HEK 293 and NG 108-15 cell preparation, the presence of trichloroethanol (2.5 mM) did not change the nature in which tropisetron competed for the [^{3}H]-granisetron-labelled receptor (Figure 5, Table 2).

2-Methyl-5-HT and trichloroethanol

As discussed above, trichloroethanol enhanced the displacement of [^{3}H]-granisetron binding by 2-methyl-5-HT (Table 2). We have previously demonstrated that 2-methyl-5-HT acts as a partial agonist on the 5-HT$_3$R-A and 5-HT$_3$R-A$_S$ subunits (Hope *et al.*, 1993; Downie *et al.*, 1994). Hence, it was of interest to determine the influence of trichloroethanol on currents induced by 2-methyl-5-HT. For oocytes expressing the 5-HT$_3$R-A subunit, 2-methyl-5-HT (1 μM–0.3 mM) induced a concentration-dependent inward current with an estimated EC_{50} of 13 ± 0.4 μM (n = 4) and a maximal effect amounting to 63 ± 0.7% (n = 4) of the maximal current produced by a saturating concentration of 5-HT. Trichloroethanol (5 mM) reduced the 2-methyl-5-HT EC_{50} to 4.6 ± 0.2 μM (n = 4), but additionally increased the maximum to 101 ± 1.6% (n = 4) of that produced by 5-HT (Figure 6). Similarly, for oocytes expressing the 5-HT$_3$R-A$_S$ subunit, 2-methyl-5-HT (1 μM–0.3 mM) evoked a concentration-dependent inward current with an estimated EC_{50} of 15 ± 2 μM (n = 4), but with a maximal effect that was only 9 ± 0.2% (n = 4) of that elicited by a maximally effective concentration of 5-HT. Trichloroethanol (5 mM) reduced the EC_{50} for 2-methyl-5-HT to 5 ± 0.4 μM (n = 4) and greatly increased the

maximal response to 74 ± 2% ($n = 4$) of that produced by 5-HT (Figure 6).

Quipazine and trichloroethanol

Unusually, the competition for [^{3}H]-granisetron binding by the antagonist quipazine was enhanced by trichloroethanol, whereas the competition by the antagonists ondansetron and tropisetron was unaffected (Figure 5; Table 2). In this respect, the influence of trichloroethanol on quipazine is similar to its effect on the 5-HT$_3$ receptor agonists. Therefore, the interaction of quipazine and trichloroethanol was investigated further on *Xenopus* oocytes expressing the 5-HT$_3$R-A subunit. Quipazine (1–300 nM) produced a concentration-dependent inhibition of the current elicited by a submaximal concentration of 5-HT (1.5 μM) giving an IC_{50} value of 18 ± 3 nM ($n = 4$; Figure 7). In the absence of 5-HT, quipazine (10 nM–0.3 μM) induced a small inward current, amounting to 0.7–1.6% of the maximal current that could be elicited with a saturating concentration of 5-HT (see Figure 7). However, in the presence of 5 mM trichloroethanol, the quipazine-induced current response was increased substantially, such that 0.3 μM quipazine now induced a response approximately 40% of that produced by a maximal concentration of 5-HT (Figure 7). The current elicited by quipazine in the presence of trichloroethanol was

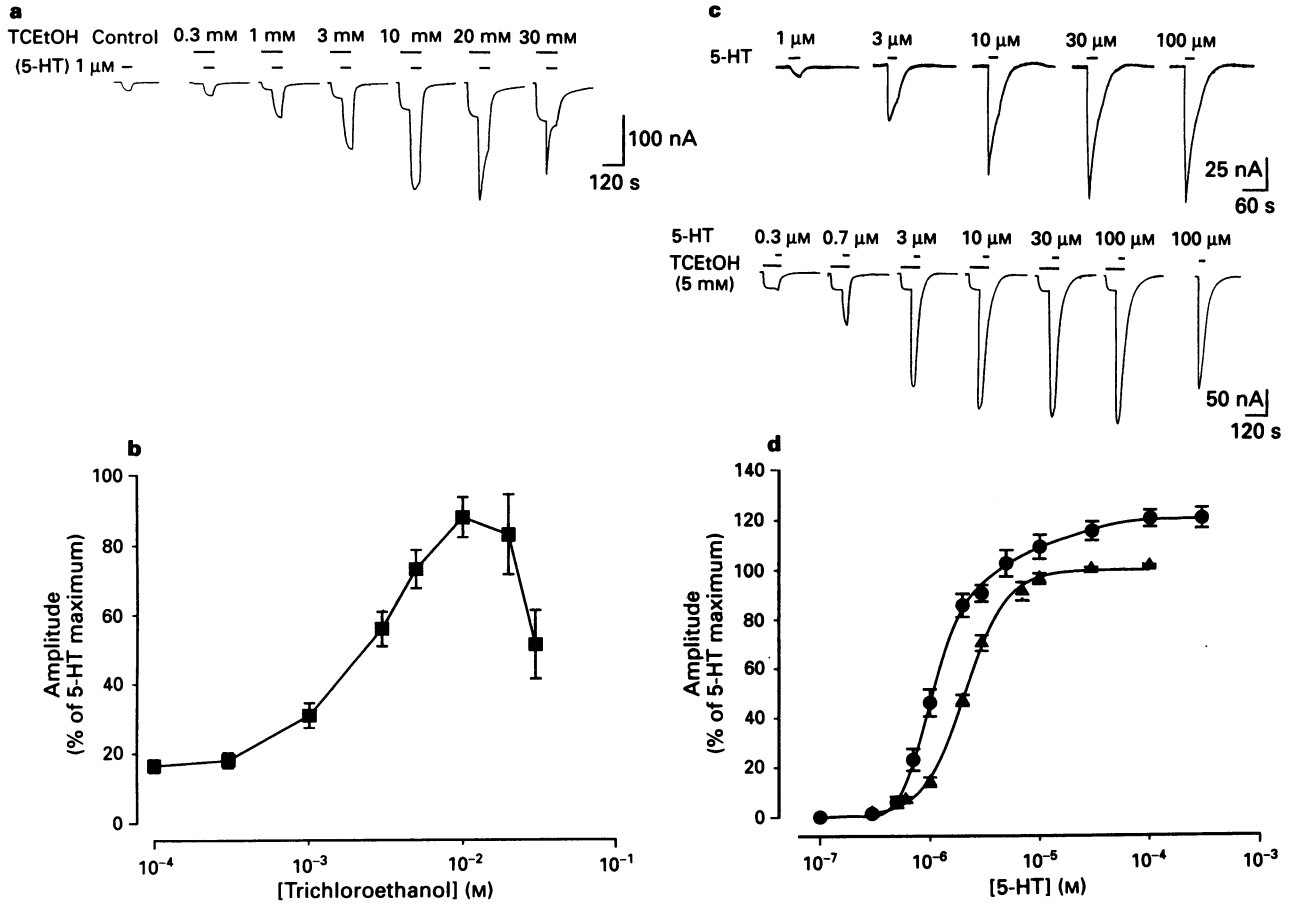

Figure 4 Trichloroethanol (TCEtOH) potentiates currents mediated by the 5-HT$_3$R-A$_S$ subunit. All records illustrated are from *Xenopus laevis* oocytes voltage-clamped at −30 mV. (a) The inward current produced by bath applied 5-HT (1 μM) is enhanced in a concentration-dependent manner by trichloroethanol (0.3–30.0 mM). The inward current produced by trichloroethanol alone was not blocked by 10 nM ondansetron and was evident on control (non-injected) oocytes. (b) The relationship between the concentration of bath-applied trichloroethanol (log scale, x-axis) and the potentiation of the 5-HT-induced current (expressed as a percentage of the maximum response to 5-HT, y-axis). (c) Records illustrating the concentration-dependent inward current response to bath applied 5-HT (0.3–100 μM) in the presence and absence of 5 mM trichloroethanol. (d) The relationship between the concentration of bath-applied 5-HT (log scale; x-axis) is plotted against the current amplitude (expressed as a percentage of the current produced by a saturating concentration (100 μM) of 5-HT) in the presence (●) and absence (▲) of 5 mM trichloroethanol. The curves were fitted to the data points as described in the Methods and gave a control EC_{50} of 2.1 ± 0.0.5 μM and a Hill slope of 2.2 ± 0.1 ($n = 4$). In the presence of 5 mM trichloroethanol an EC_{50} of 1.3 ± 0.1 μM and a Hill slope of 1.9 ± 0.2 ($n = 4$) were estimated. For both (b) and (d), each point represents the mean ± s.e.mean of data obtained from 4 oocytes.

Table 1 Trichloroethanol (2.5 mM) has no effect upon the K_d, B_{max} or Hill coefficient (n_H) of [^{3}H]-granisetron binding to membrane homogenates prepared from either NG 108-15 cells or HEK 293 cells expressing the 5-HT$_3$R-A$_S$

	Without trichloroethanol			*With 2.5 mM trichloroethanol*		
Tissue	K_d (nM)	B_{max} (fmol mg^{-1})	n_H	K_d (nM)	B_{max} (fmol mg^{-1})	n_H
HEK 293 cells	2.01 ± 0.39	913 ± 163	1.06 ± 0.11	1.86 ± 0.46	912 ± 99	1.13 ± 0.05
NG 108-15 cells	2.43 ± 0.68	786 ± 133	1.11 ± 0.06	1.67 ± 0.27	728 ± 80	1.18 ± 0.04

Binding data were obtained with concentrations of [^{3}H]-granisetron in the range 0.1–12.6 nM. Non-specific binding was defined by the inclusion of tropisetron (10 μM). Data represent the mean ± s.e.mean from three independent experiments.

Table 2 The influence of trichloroethanol (2.5 mM) upon the affinity of agonist and antagonist ligands for the [^{3}H]-granisetron-labelled 5-HT$_3$ receptor endogenous to NG 108-15 cells and the 5-HT$_3$R-A$_S$ expressed in HEK 293 cells

NG 108-15 cells ([^{3}H]-granisetron concentration = 0.98–1.51 nM)				
	Without trichloroethanol		*With trichloroethanol* (2.5 mM)	
Drug	IC_{50} (nM)	n_H	IC_{50} (nM)	n_H
5-HT	752 ± 140	1.67 ± 0.08	170 ± 24	0.99 ± 0.03
2-Me-5-HT	2113 ± 195	2.10 ± 0.16	907 ± 122	1.29 ± 0.13
PBG	1790 ± 283	2.47 ± 0.90	620 ± 89	1.32 ± 0.13
Quipazine	4.88 ± 0.94	1.62 ± 0.13	2.32 ± 0.49	1.25 ± 0.22
Tropisetron	3.85 ± 0.83	0.98 ± 0.05	5.23 ± 1.04	0.99 ± 0.07
Ondansetron	34.3 ± 6.8	1.10 ± 0.17	35.3 ± 4.2	0.90 ± 0.06
HEK 293 cells ([^{3}H]-granisetron concentration = 0.90–1.10 nM)				
Drug	IC_{50} (nM)	n_H	IC_{50} (nM)	n_H
5-HT	548 ± 21	1.35 ± 0.11	229 ± 35	1.17 ± 0.05
2-Me-5-HT	2847 ± 590	1.30 ± 0.03	1097 ± 114	1.36 ± 0.12
PBG	2907 ± 753	1.10 ± 0.08	837 ± 73	1.34 ± 0.13
Tropisetron	3.80 ± 1.13	0.88 ± 0.03	4.03 ± 1.25	0.97 ± 0.05

Data are the mean ± s.e.mean of 3–6 independent experiments.
Abbreviations: 2-Me-5-HT, 2-methyl-5-HT; PBG, 1-phenylbiguanide.

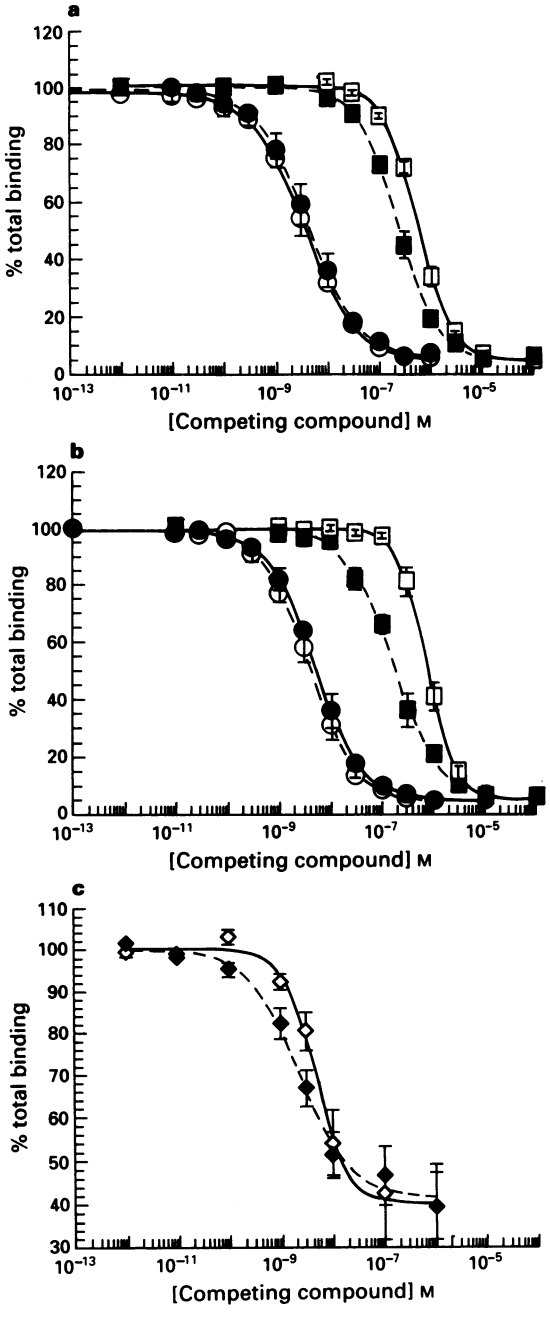

abolished by ondansetron (100 nM) indicating that it was due to 5-HT$_3$ receptor activation (Figure 7). Under identical recording conditions, no such current was observed with the 5-HT$_3$ receptor antagonists, granisetron (1 nM), BRL 46470 (1 nM), ondansetron (10 nM), (+)-tubocurarine (30 nM), metoclopramide (1 μM) or cocaine (1 μM) applied alone, or in the presence of 5 mM trichloroethanol (results not shown).

Discussion

Many of the properties of 5-HT$_3$ receptors endogenous to neurones and neuronal cell lines are faithfully represented by the recombinant 5-HT$_3$R-A subunit, or its splice variant, 5-HT$_3$R-A$_S$ (Maricq *et al.*, 1991; Hope *et al.*, 1993; Yakel *et al.*, 1993; Downie *et al.*, 1994). However, the actions of putative positive allosteric modulators of the 5-HT$_3$ receptor (Peters *et al.*, 1992) on these recombinant subunits have not been determined. Previous electrophysiological studies have demonstrated that ethanol and trichloroethanol enhance 5-HT$_3$ receptor-mediated currents recorded from NCB-20 cells and rat nodose ganglion neurones (Lovinger, 1991; Lovinger & White, 1991; Lovinger & Zhou, 1993). By contrast, the 5-HT$_3$ receptor-mediated uptake of [^{14}C]-guanidinium into NG 108-15 cells is markedly suppressed by 100 mM ethanol (Emerit *et al.*, 1993). The present study demonstrates that ethanol, trichloroethanol and chloral hydrate potentiate 5-HT-induced currents recorded from *Xenopus laevis* oocytes expressing either the 5-HT$_3$R-A, or the 5-HT$_3$R-A$_S$ splice variants. Splice variants of the γ_2 GABA$_A$ receptor subunit (γ_{2S} and γ_{2L}) have been identified, which in some studies appear to impart a differential sensitivity to ethanol upon the receptor complex (Wafford *et al.*, 1991 cf. Sigel *et al.*, 1993). Here, homo-oligomeric receptors formed from either splice variant of the 5-HT$_3$R-A subunit were enhanced by ethanol and more potently by chloral hydrate and trichloroethanol.

Figure 5 Competition for [^{3}H]-granisetron binding by 5-HT (□, ■), tropisetron (○, ●) and quipazine (◇, ◆) in the absence (open symbols) or presence (closed symbols) of trichloroethanol (2.5 mM). Experiments were performed with homogenates prepared from NG 108-15 cells (a,c) or HEK 293 cells (b) expressing the 5-HT$_3$R-A$_S$ receptor subunit. Data represent the mean ± s.e.mean (in some cases, s.e.mean smaller than the size of the symbol) from at least three independent experiments.

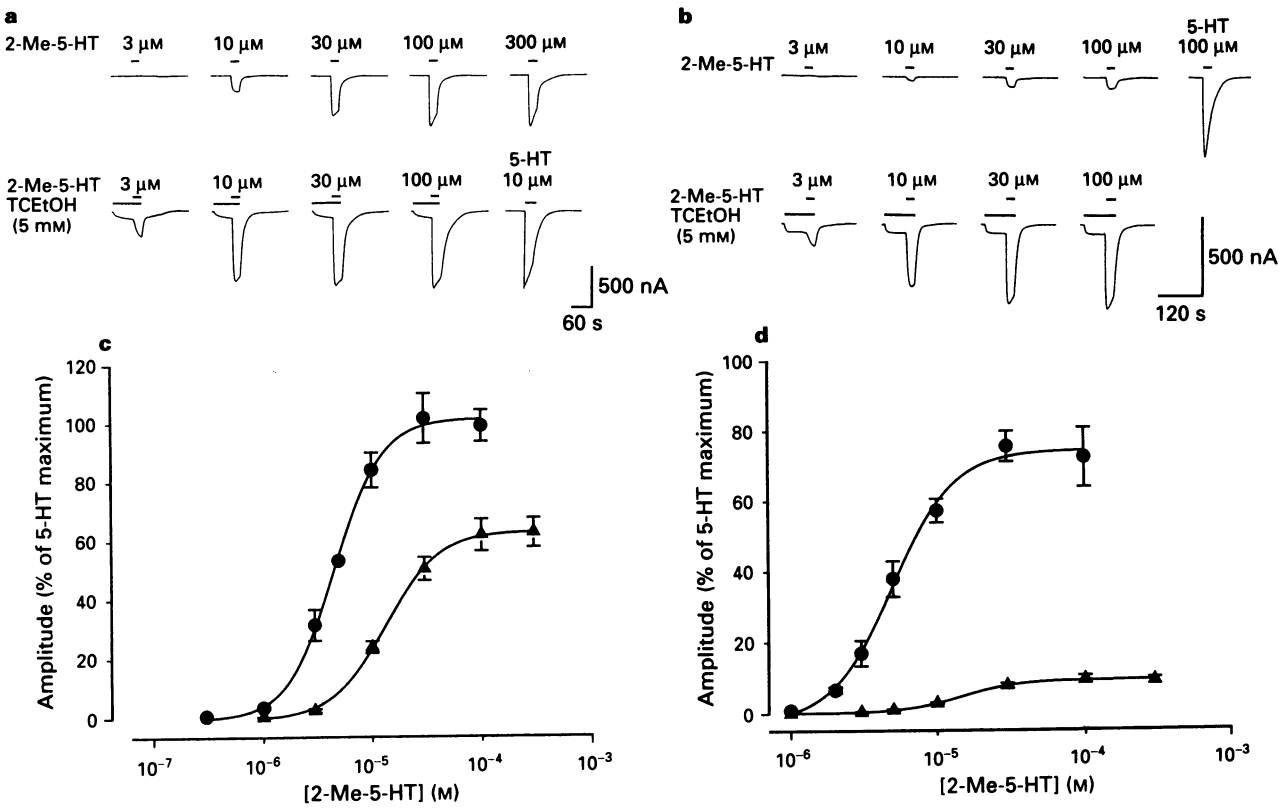

Figure 6 The interaction of trichloroethanol (TCEtOH) with 2-methyl-5-HT (2-Me-5-HT). All records illustrated are from *Xenopus laevis* oocytes voltage-clamped at −30 mV and expressing the 5-HT$_3$R-A (a) or the 5-HT$_3$R-A$_S$ subunit (b). The traces illustrate the concentration-dependent inward current response to bath applied 2-methyl-5-HT (3–300 μM) in the presence and absence of 5 mM trichloroethanol. In each set of traces, the current response evoked by a maximal concentration of 5-HT is illustrated for comparison. Note that in both cases, the maximal current produced by 2-methyl-5-HT is less than that elicited by 5-HT and that the maximal effect for the 5-HT$_3$R-A$_S$ is much less than for the 5-HT$_3$R-A subunit. For both subunits, trichloroethanol clearly increases the amplitude of the maximum response to 2-methyl-5-HT. (c and d) The concentration of bath-applied 2-methyl-5-HT (log scale, x-axis) is plotted against the current amplitude (expressed as a percentage of the current produced by a maximum concentration of 5-HT) in the presence (●) and absence (▲) of 5 mM trichloroethanol for the 5-HT$_3$R-A (c) and the 5-HT$_3$R-A$_S$ (d) subunit. The curves were fitted to the data points as described in the Methods. For the 5-HT$_3$R-A (c), the control 2-methyl-5-HT EC_{50} is 13 ± 0.4 μM with a calculated maximum amounting to 63 ± 0.7% of that produced by 5-HT ($n = 4$). In the presence of 5 mM trichloroethanol, the 2-methyl-5-HT EC_{50} is reduced to 4.6 ± 0.2 μM and the calculated maximum is increased to 101 ± 1.6% of that produced by 5-HT ($n = 4$). For the 5-HT$_3$R-A$_S$ (d), the control 2-methyl-5-HT EC_{50} is 15 ± 1 μM and the caclulated maximum is only 9 ± 0.2% of that produced by 5-HT ($n = 4$). In the presence of 5 mM trichloroethanol, the 2-methyl-5-HT EC_{50} is reduced to 5 ± 0.4 μM and the maximum is augmented to 74 ± 2% of that produced by 5-HT ($n = 4$). In both (c) and (d), each point represents the mean ± s.e.mean of data obtained from 4 oocytes.

A number of studies have reported 5-HT$_3$ receptor antagonists to reduce ethanol intake in animals and man (see Sellers *et al.*, 1992). The concentrations of ethanol necessary to produce clear potentiation of 5-HT-induced currents recorded from oocytes expressing either splice variant are broadly consistent with previous results obtained with NCB-20 cells (Lovinger, 1991) and rat nodose ganglion neurones (Lovinger & White, 1991). However, such concentrations are relatively high in relation to the behavioural effects of ethanol. Here, threshold effects were observed with 30 mM ethanol, which corresponds to a plasma concentration in man that is associated with gross intoxication. A robust potentiation of 5-HT-induced currents occurred only at concentrations (100–300 mM) of ethanol known to produce marked neurological impairment, coma and death due to respiratory depression. Furthermore, a variety of ligand-gated ion channels are influenced by similar concentrations of ethanol including the NMDA (Lovinger *et al.*, 1989), AMPA (Lovinger, 1993), $GABA_A$ (Aguayo, 1990; Nakahiro *et al.*, 1991; Wafford *et al.*, 1991; Kurata *et al.*, 1993 cf. Sigel *et al.*, 1993) and nicotinic (Dilger & Brett, 1991) receptor channel complexes. Hence, the behavioural actions of ethanol probably involve multiple molecular targets.

The actions of trichloroethanol were investigated in detail. In rat nodose ganglion neurones, 5 mM trichloroethanol has been shown to shift the 5-HT-concentration-response curve to the left, but to have little effect on the maximum current produced by 5-HT (Lovinger & Zhou, 1993). In the present study, 5 mM trichloroethanol, acting at either the 5-HT$_3$R-A or 5-HT$_3$R-A$_S$ subunits, produced an approximately 2 fold sinistral shift in the concentration-response curve to 5-HT, indicating an increase in the apparent affinity of the receptor for the agonist. Consistent with this observation, the agonists 5-HT, phenylbiguanide and 2-methyl-5-HT displaced [^{3}H]-granisetron binding from NG 108-15 and HEK 293 cell homogenates with enhanced potency in the presence of trichloroethanol (2.5 mM). This effect is unlikely to involve an alteration in the affinity of the receptor for the radiolabelled antagonist, since trichloroethanol (2.5 mM) had no effect on the binding of [^{3}H]-granisetron *per se*, nor the displacement of this binding by the 5-HT$_3$ receptor antagonists, tropisetron and ondansetron. Collectively, these observations suggest a selective influence of trichloroethanol upon agonist binding and subsequent receptor activation.

The effect of trichloroethanol upon the agonist action of 2-methyl-5-HT was of particular interest. In voltage-clamp studies made on NG 108-15, N1E-115 and PC12 cell lines, frog dorsal root ganglion neurones and *Xenopus* oocytes

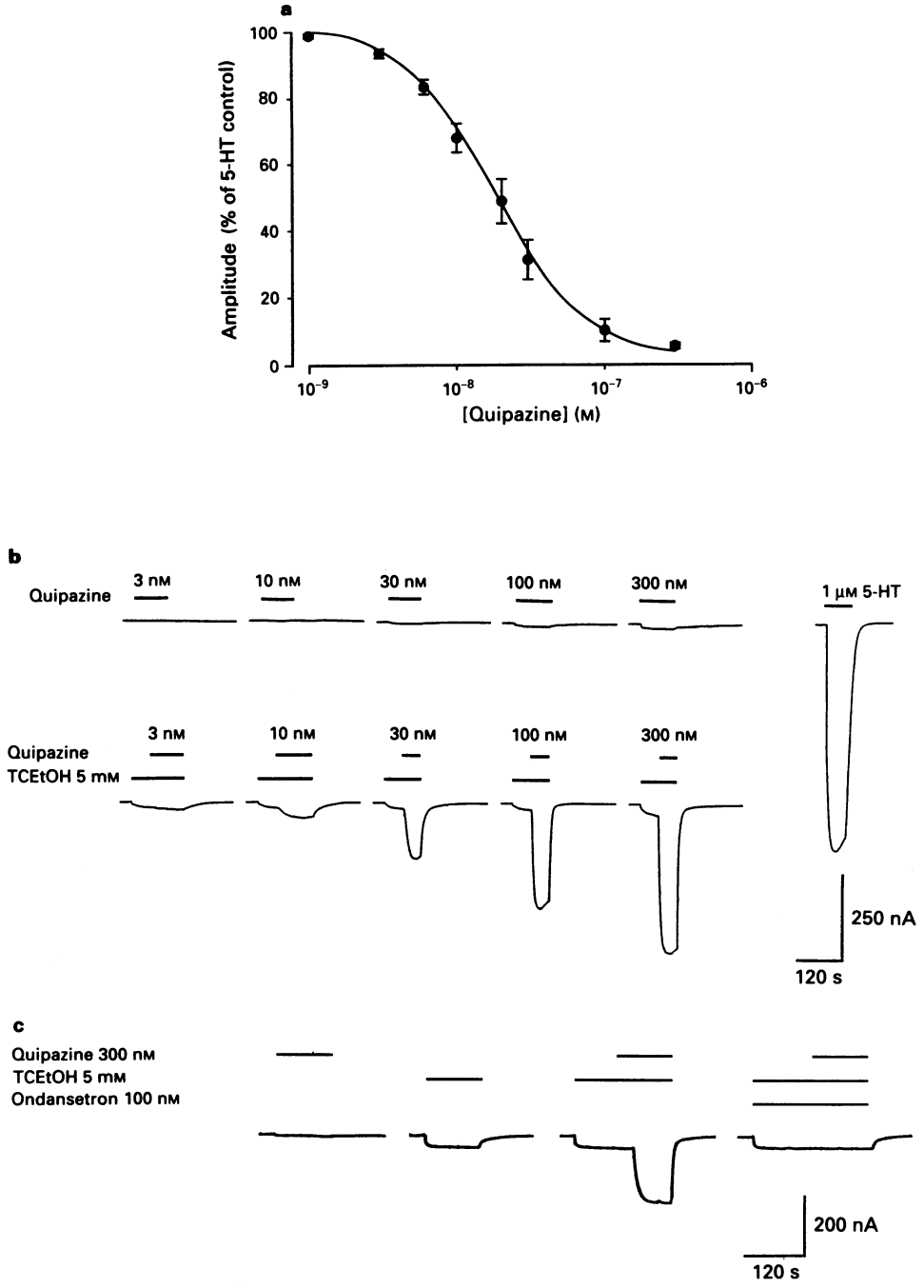

Figure 7 The interaction of trichloroethanol (TCEtOH) with quipazine. (a) Concentration-inhibition curve for bath applied quipazine (log scale, x-axis) as an antagonist of inward current responses evoked by bath applied 5-HT (1.5 μM, y-axis) on *Xenopus* oocytes expressing the 5-HT$_3$R-A subunit. The fitted curve (see Methods) yields an IC_{50} for quipazine of 18 ± 3 nM. Data points are the mean ± s.e.mean of 4 observations made on different oocytes. (b, upper row of traces) Bath applied quipazine (3 nM–300 nM) elicits concentration-dependent inward current responses in a *Xenopus* oocyte expressing the 5-HT$_3$R-A subunit. To emphasize the low amplitude of the quipazine-induced response, a current evoked by 5-HT (1 μM) is illustrated for comparison. In the same oocyte (lower row of traces), responses to quipazine are greatly potentiated in amplitude by trichloroethanol (5 mM). (c) Quipazine-induced currents recorded in the presence of trichloroethanol (5 mM) are abolished by ondansetron (100 nM). Note that the direct effect of trichloroethanol is resistant to antagonism by ondansetron. All recordings were performed at a holding potential of −30 mV.

expressing the 5-HT$_3$R-A or 5-HT$_3$R-A$_S$ subunit, the maximal current response to 2-methyl-5-HT is less than that produced by saturating concentrations of 5-HT (Sepúlveda *et al.*, 1991; Boess *et al.*, 1992; Yakushiji & Akaike, 1992; Furukawa *et al.*, 1992; Hope *et al.*, 1993; Downie *et al.*, 1994). This effect is subunit-dependent, with 2-methyl-5-HT being far less effective at the 5-HT$_3$R-A$_S$ than the 5-HT$_3$R-A subunit (Hope *et al.*, 1993; Downie *et al.*, 1994; Sepúlveda & Lummis, 1994). One interpretation of these data is that 2-methyl-5-HT acts as a partial agonist, but with greater efficacy at the 5-HT$_3$R-A splice variant, a notion supported by experiments investigating the interaction of 2-methyl-5-HT and 5-HT (Downie *et al.*, 1994). For both 5-HT$_3$R-A and 5-HT$_3$R-A$_S$ subunits, trichloroethanol (5 mM) produced an approximately 3 fold sinistral shift of the concentration-response curve to 2-methyl-5-HT. Moreover, in contrast to the results obtained with 5-HT, the maxima of the 2-methyl-5-HT concentration-response curves were greatly enhanced.

In preliminary studies (D.L.D., J.A.P. & J.J.L., unpublished observations), the 5-HT$_3$ receptor agonist, SR5722A (Bachy *et al.*, 1993) was found to act as a partial agonist at the 5-HT$_3$R-A expressed in oocytes. Interestingly, the maximal effect of this compound, like that of 2-methyl-5-HT, was greatly enhanced by trichloroethanol. Hence, trichloroethanol may selectively enhance the maximal effect of at least some partial agonists (see below also). Single channel studies are required to determine the molecular mechanism of this intriguing interaction. Unfortunately, this approach is hampered by the extremely low single channel conductance (< 1pS) of the murine recombinant 5-HT$_3$ subunits (Gill *et al.*, 1995) and the 5-HT$_3$ receptors of the cell lines from which these cDNAs were derived (see Peters *et al.*, 1992; 1994). Future experiments utilizing solutions designed to increase the single channel conductance (van Hooft *et al.*, 1994), or employing preparations with larger single channel conductances (Peters *et al.*, 1992; 1994) may be instructive.

In contrast to the other antagonists tested, the competition for [^{3}H]-granisetron by quipazine was enhanced by trichloroethanol. In this respect, the actions of quipazine resembled those of an agonist. The majority of functional studies indicate that quipazine behaves as a 5-HT$_3$ receptor antagonist (e.g Lansdown *et al.*, 1980; Ireland & Tyers, 1987; Round & Wallis, 1987). However, in ligand binding studies, quipazine competes for [^{3}H]-GR65630 (Kilpatrick *et al.*, 1987), [^{3}H]-granisetron, [^{3}H]-LY 274,584 and [^{3}H]-GR 67330 (Barnes *et al.*, 1992) binding in rat cortical membranes with Hill coefficient greater than unity, an effect that is shared with 5-HT$_3$ receptor agonists, but not commonly with other antagonists. More directly, it has recently been reported that quipazine causes the uptake of [^{14}C]-guanidinium into NG 108-15 cells via 5-HT$_3$ receptor activation (Emerit *et al.*, 1993).

In the present study, quipazine produced a concentration-dependent antagonism of the 5-HT-induced current recorded from *Xenopus* oocytes expressing the 5-HT$_3$R-A subunit. During these experiments, quipazine (10–300 nM) was noted to induce a small inward current, the magnitude of which was greatly enhanced by trichloroethanol (5 mM). Such potentiated currents were abolished by ondansetron (100 nM) indicating them to be 5-HT$_3$ receptor-mediated. The most parsimonious interpretation of these data is that quipazine is a partial agonist with very low efficacy and that the weak agonist effect, like that of 2-methyl-5-HT, is amplified in the presence of trichloroethanol. This interaction may be relevant to *in vivo* studies. For example, quipazine has been reported to evoke a 5-HT$_3$-receptor-mediated bradycardia and hypotension in ritanserin pretreated rats anaesthetized with chloral hydrate (which is reduced to trichloroethanol *in vivo*; Garrett & Lambert, 1973) (Vayssettes-Courchay *et al.*, 1990).

Whether the effects of alcohols on ligand gated ion channels represent a specific interaction with the receptor-channel protein, or are secondary to a perturbation of the surrounding membrane is not known. The present demonstration that a recombinant homo-oligomeric receptor expressed in a foreign membrane (HEK 293 cells or oocytes) retains the sensitivity to alcohols exhibited by native receptors is, therefore, of interest. The pharmacological properties of the 5-HT$_3$ receptor are highly species-dependent (Peters *et al.*, 1992). Although trichloroethanol enhances 5-HT$_3$ receptor-mediated currents recorded from murine neuroblastoma cells (Lovinger & White, 1991), HEK 293 cells stably transfected with the murine 5-HT$_3$R-A subunit (Gill *et al.*, 1994) and rat (Lovinger & Zhou, 1993) and rabbit nodose ganglion neurones (Gill *et al.*, 1994), we have recently demonstrated that it inhibits those of guinea-pig nodose ganglion neurones (Gill *et al.*, 1994). Hence, the sequencing of 5-HT$_3$ cDNAs encoding 5-HT$_3$ receptors exhibiting such differential effects (Lambert *et al.*, 1994) may lead to a better definition of the alcohol binding site(s).

We thank the Wellcome Trust, the M.R.C. and SmithKline Beecham for financial support. Dr David Julius for the generous gift of the 5-HT$_3$R-A cDNA, Drs Tom Blackburn and Brian Jones for helpful discussion and Gillian Thomson for typing the manuscript. We are grateful to Mrs Margaret West and Mr Phillip McWilliams for help with the cell culture.

References

AGUAYO, L.G. (1990). Ethanol potentiates the GABA$_A$-activated Cl$^-$ current in mouse hippocampal and cortical neurones. *Eur. J. Pharmacol.*, **187**, 127–130.

BACHY, A., HÉAULME, M., GUIDICE, A., MICHAUD, J.-C., LEFEVRE, I.A., SOUILHAC, J., MANARA, L., EMERIT, M.B., GOZLAN, H., HAMON, M., KEANE, P.E., SOUBRIÉ, P. & LE FUR, G. (1993). SR 5722A: a potent and selective agonist at central and peripheral 5-HT$_3$ receptors *in vitro* and *in vivo*. *Eur. J. Pharmacol.*, **237**, 299–309.

BARNES, J.M., BARNES, N.M., COSTALL, B., JAGGER, S.M., NAYLOR, R.J., ROBERTSON, D.W. & ROE, S.Y. (1992). Agonist interactions with 5-HT$_3$ receptor recognition sites in the rat entorhinal cortex labelled by structurally diverse ligands. *Br. J. Pharmacol.*, **105**, 500–504.

BOESS, F.G. & MARTIN, I.L. (1994). Molecular biology of 5-HT receptors. *Neuropharmacology*, **33**, 275–317.

BOESS, F.G., SEPÚLVEDA, M.-I., LUMMIS, S.C.R. & MARTIN, I.L. (1992). 5-HT$_3$ receptors in NG 108-15 neuroblastoma × glioma cells: effect of the novel agonist 1-(m-chlorophenyl)-biguanide. *Neuropharmacology*, **31**, 561–564.

BRADFORD, M.M. (1976). A rapid and sensitive method for the quantification of microgram quantities of protein utilizing the principle of protein-dye binding. *Anal. Biochem.*, **72**, 248–254.

BUTLER, A., ELSWOOD, C.J., BURRIDGE, J., IRELAND, S.J., BUNCE, K.T., KILPATRICK, G.J. & TYERS, M.B. (1990). The pharmacological characterization of 5-HT$_3$ receptors in three isolated preparations derived from guinea-pig tissues. *Br. J. Pharmacol.*, **94**, 591–598.

DILGER, J.P. & BRETT, R.S. (1991). Actions of volatile anaesthetics and alcohols on cholinergic receptors channels. In *Molecular and Cellular Mechanisms of Alcohol and Anaesthetics*, ed. Rubin, E., Miller, K.W. & Roth, S.H. *Ann. N.Y. Acad. Sci.*, **625**, 616–627.

DOWNIE, D.L., HOPE, A.G., LAMBERT, J.J., PETERS, J.A., BLACKBURN, T.P. & JONES, B.J. (1994). Pharmacological characterization of the apparent splice variants of the murine 5-HT$_3$ R-A subunit expressed in *Xenopus laevis* oocytes. *Neuropharmacology*, **33**, 473–482.

DOWNIE, D.L., HOPE, A.G., LAMBERT, J.J., PETERS, J.A., BURCHELL, B. & JULIUS, D. (1993). Enhancement by trichloroethanol of agonist-induced currents mediated by a cloned murine 5-HT$_3$ receptor subunit (5-HT$_3$R-A) expressed in *Xenopus* oocytes. *Br. J. Pharmacol.*, **109**, 53P.

EISELÉ, J.-L., BERTRAND, S., GALZI, J.-L., DEVILLERS-THIÉRY, A., CHANGEUX, J.-P. & BERTRAND, D. (1993). Chimaeric nicotinic-serotonergic receptor combines distinct ligand binding and channel specificities. *Nature*, **366**, 479–483.

EMERIT, M.B., RIAD, M., FATTACINI, C.M. & HAMON, M. (1993). Characteristics of [^{14}C] guanidinium accumulation in NG 108-15 cells exposed to serotonin 5-HT$_3$ receptor ligands and substance P. *J. Neurochem.*, **60**, 2059–2067.

FURUKAWA, K., AKAIKE, N., ONODERA, H. & KOGURE, K. (1992). Expression of 5-HT$_3$ receptors in PC12 cells treated with NGF and 8-Br-cAMP. *J. Neurophysiol.*, **67**, 812–819.

GARRETT, E.R. & LAMBERT, H.J. (1973). Pharmacokinetics of trichloroethanol and metabolites and interconversions among variously referenced pharmacokinetic parameters. *J. Pharmaceut. Sci.*, **62**, 550–572.

GILL, C.H., LAMBERT, J.J. & PETERS, J.A. (1994). The actions of ketamine and trichloroethanol on 5-HT$_3$ receptors are species dependent. *Can. J. Physiol. Pharmacol.*, **72**, Suppl. 1, p 18.4.24.

GILL, C.H., PETERS, J.A. & LAMBERT, J.J. (1995). An electrophysiological investigation of the properties of a murine recombinant 5-HT$_3$ receptor stably expressed in HEK 293 cells. *Br. J. Pharmacol.* (in press).

GILL, C.H., PETERS, J.A., LAMBERT, J.J., HOPE, A.G. & JULIUS, D. (1993). Modulation by divalent cations of current responses mediated by a cloned murine 5-HT receptor (5-HT$_3$ R-A) expressed in HEK 293 cells. *Br. J. Pharmacol.*, **109**, 98P.

HOPE, A.G. (1993). The molecular cloning and functional expression of a murine 5-HT$_3$ receptor. *Ph.D. Thesis, The University of Dundee, Scotland.*

HOPE, A.G., DOWNIE, D.L., SUTHERLAND, L., LAMBERT, J.J., PETERS, J.A. & BURCHELL, B. (1993). Cloning and functional expression of an apparent splice variant of the murine 5-HT$_3$ receptor A subunit. *Eur. J. Pharmacol. (Mol. Pharmacol. Sect.)*, **245**, 187–192.

IRELAND, S.J. & TYERS, M.B. (1987). Pharmacological characterization of 5-hydroxytryptamine-induced depolarization of the rat isolated vagus nerve. *Br. J. Pharmacol.*, **90**, 229–238.

ISENBERG, K.E., UKHUN, I.A., HOLSTAD, S.G., JAFRI, S., UCHIDA, U., ZORUMSKI, C.F. & YANG, J. (1993). Partial cDNA cloning and NGF regulation of a rat 5-HT$_3$ receptor subunit. *NeuroReport*, **5**, 121–124.

KILPATRICK, G.J., JONES, B.J. & TYERS, M.B. (1987). Identification and distribution of 5-HT$_3$ receptors in rat brain using radioligand binding. *Nature*, **330**, 746–748.

KLEE, W.B. & NIRENBERG, M. (1974). A neuroblasoma × glioma hybrid cell line with morphine receptors. *Proc. Natl. Acad. Sci. U.S.A.*, **71**, 3474–3477.

KOOYMAN, A.R., VAN HOOFT, J.A., VANDERHEIJDEN, P.M.L. & VIJVERBERG, H.P.M. (1994). Competitive and non-competitive effects of 5-hydroxyindole on 5-HT$_3$ receptors in N1E-115 neuroblastoma cells. *Br. J. Pharmacol.*, **112**, 541–546.

KURATA, K., MARSZALEC, W., HAMILTON, B.J., CARTER, D.B. & NARAHASHI, T. (1993). Alcohol modulation of cloned GABA$_A$ receptor-channel complex expressed in human kidney cell lines. *Brain Res.*, **631**, 143–146.

LAMBERT, J.J., PETERS, J.A. & HOPE, A.G. (1995). 5-HT$_3$ receptors. In *CRC Handbook of Ion Channels*, ed. North, R.A. pp. 177–211. Boca Raton: CRC Press.

LANSDOWN, M.J.R., NASH, H.L., PRESTON, P.R., WALLIS, D.I. & WILLIAMS, R.G. (1980). Antagonism of 5-hydroxytryptamine receptors by quipazine. *Br. J. Pharmacol.*, **68**, 525–532.

LOVINGER, D.M. (1991). Ethanol potentiation of 5-HT$_3$ receptor-mediated ion current in NCB-20 neuroblastoma cells. *Neurosci. Lett.*, **122**, 57–60.

LOVINGER, D.M. (1993). High ethanol sensitivity of recombinant AMPA-type glutamate receptors expressed in mammalian cells. *Neurosci. Lett.*, **159**, 83–87.

LOVINGER, D.M. & WHITE, G. (1991). Ethanol potentiation of 5-hydroxytryptamine$_3$ receptor-mediated ion current in neuroblastoma cells and isolated adult mammalian neurons. *Mol. Pharmacol.*, **40**, 263–270.

LOVINGER, D.M., WHITE, G. & WEIGHT, F.F. (1989). Ethanol inhibits NMDA-activated ion current in hippocampal neurons. *Science*, **243**, 1721–1724.

LOVINGER, D.M. & ZHOU, Q. (1993). Trichloroethanol potentiation of 5-hydroxytryptamine$_3$ receptor-mediated ion current in nodose ganglion neurons from the adult rat. *J. Pharmacol. Exp. Ther.*, **265**, 771–776.

MARICQ, A.V., PETERSON, A.S., BRAKE, A.J., MYERS, R.M. & JULIUS, D. (1991). Primary structure and functional expression of the 5-HT$_3$ receptor, a serotonin gated ion channel. *Science*, **254**, 432–437.

NAKAHIRO, M., ARAKAWA, O. & NARAHASHI, T. (1991). Modulation of γ-aminobutyric acid receptor-channel complex by alcohols. *J. Pharmacol. Exp. Ther.*, **259**, 235–240.

NEIJT, H.C,, KARPF, A., SCHOEFFTER, P., ENGEL, G. & HOYER, D. (1988). Characterisation of 5-HT$_3$ recognition sites in membranes of NG 108-15 neuroblastoma-glioma cells with [^{3}H]ICS 205-930. *Naunyn-Schmied. Arch. Pharmacol.*, **337**, 493–499.

NEWBERRY, N.R., CHESHIRE, S.H. & GILBERT, M.J. (1991). Evidence that the 5-HT$_3$ receptors of the rat, mouse and guinea-pig superior cervical ganglion may be different. *Br. J. Pharmacol.*, **102**, 615–620.

PETERS, J.A., LAMBERT, J.J. & MALONE, H.M. (1994). Electrophysiological studies of 5-HT$_3$ receptors. In *5-HT$_3$ Receptor Antagonists*, ed. Jones, B.J., King, F.D. & Sanger, G.J. pp. 115–153. Boca Raton: CRC Press.

PETERS, J.A., MALONE, H.M. & LAMBERT, J.J. (1991). Ketamine potentiates 5-HT$_3$ receptor mediated currents in rabbit nodose ganglion neurones. *Br. J. Pharmacol.*, **103**, 1623–1625.

PETERS, J.A., MALONE, H.M. & LAMBERT, J.J. (1992). Recent advances in the electrophysiological characterization of 5-HT$_3$ receptors. *Trends Pharmacol. Sci.*, **13**, 391–397.

ROUND, A. & WALLIS, D.I. (1987). Further studies on the blockade of 5-HT depolarizations of rabbit vagal afferent and sympathetic ganglion cells by MDL 72222 and other antagonists. *Neuropharmacology*, **26**, 39–48.

SAMBROOK, J., FRITSCH, E.F. & MANIATIS, T. (1989). *Molecular Cloning: A Laboratory Manual* (2nd Ed.). ed. Nolan, C., pp. 7.43–7.45. New York: Cold Spring Harbor Press.

SELLERS, E.M., HIGGINS, G.A. & SOBELL, M.B. (1992). 5-HT and alcohol abuse. *Trends Pharmacol. Sci.*, **13**, 69–75.

SEPÚLVEDA, M.-I. & LUMMIS, S.C.R. (1994). 5-HT$_3$ agonists can distinguish cloned 5-HT$_3$ receptors from NCB-20 and NG108-15 cell lines. *Br. J. Pharmacol.*, **112**, 316P.

SEPÚLVEDA, M.-I., LUMMIS, S.C.R. & MARTIN, I.L. (1991). The agonist properties of m-chlorophenylbiguanide and 2-methyl-5-hydroxytryptamine on 5-HT$_3$ receptors in N1E-115 neuroblastoma cells. *Br. J. Pharmacol.*, **104**, 536–540.

SIGEL, E., BAUR, R. & MALHERBE, P. (1993). Recombinant GABA$_A$ receptor function and ethanol. *FEBS Lett.*, **234**, 140–142.

UETZ, P., ABDELATTY, F., VILLAROEL, A., RAPPOLD, G., WEISS, B. & KOENEN, M. (1994). Organisation of the 5-HT$_3$ receptor gene and assignment to human chromosome 11. *FEBS Lett.*, **339**, 302–306.

VAN HOOFT, J.A., KOOYMAN, A.R., VERKERK, A., VAN KLEEF, R.G.D.M. & VIJVERBERG, H.P.M. (1994). Single 5-HT$_3$ receptor-gated ion channel events resolved in N1E-115 mouse neuroblastoma cells. *Biochem. Biophys. Res. Commun.*, **199**, 227–233.

VAYSSETTES-COURCHAY, C., BOUYSSET, F., VERBEUREN, T.J., LAUBIE, M. & SCHMITT, H. (1990). The cardiovascular effects of quipazine are mediated by peripheral 5-HT$_2$ and 5-HT$_3$ receptors in anaesthetised rats. *Eur. J. Pharmacol.*, **184**, 75–85.

WAFFORD, K.A., BURNETT, D.M., LEIDENHEIMER, N.J., BURT, D.R., WANG, J.B., KOJUJI, P., DUNWIDDIE, T.V., HARRIS, R.A. & SIKELA, J.M. (1991). Ethanol sensitivity of the GABA$_A$ receptor expressed in *Xenopus* oocytes requires 8 amino acids contained in the gamma-2L subunit. *Neuron*, **7**, 27–33.

WERNER, P., HUMBERT, Y., BOESS, F.G., REID, J., JONES, K. & KAWASHIMA, E. (1993). Organisation of the murine 5-HT$_3$ receptor gene and investigation of its splice variants. *Soc. Neurosci. Abs.*, **19**, 1164.

YAKEL, J.L., LAGRUTTA, A., ADELMAN, J.P. & NORTH, R.A. (1993). Single amino acid substitution affects desensitization of the 5-hydroxytryptamine type 3 receptor expressed in *Xenopus* oocytes. *Proc. Natl. Acad. Sci. U.S.A.*, **90**, 5030–5033.

YAKUSHIJI, T. & AKAIKE, N. (1992). Blockade of 5-HT$_3$ receptor-mediated currents in dissociated frog sensory neurones by benzoxazine derivative, Y-25130. *Br. J. Pharmacol.*, **107**, 853–857.

(Received September 19, 1994
Revised November 21, 1994
Accepted December 21, 1994)

British Journal of Pharmacology (1995) 114, 1652–1656 © 1995 Stockton Press All rights reserved 0007–1188/95 $12.00

Inhibition of rabbit aortic smooth muscle cell proliferation by selective inhibitors of protein kinase C

[1]Andrew C. Newby, Karene Lim, Marilyn A. Evans, Nicholas P.J. Brindle & *Robert F.G. Booth

Department of Cardiology, Welsh Heart Research Institute, University of Wales College of Medicine, Heath Park, Cardiff CF4 4XN and *Roche Research Centre, Roche Products Ltd., Welwyn Garden City, Herts AL7 3AY

1 We studied the effect of two structurally-related, selective inhibitors of protein kinase C, Ro 31-8220 and Ro 31-7549, on the reinitiation of proliferation in quiescent first passage rabbit aortic smooth muscle cells in response to (a) the direct activator of protein kinase C, phorbol dibutyrate (PDBu), (b) platelet-derived growth factor (PDGF), (c) a combination of PDGF and 5-hydroxytryptamine (5-HT) or (d) serum.

2 Ro 31-8220 and Ro 31-7549 concentration-dependently inhibited proliferation in response to each mitogen. The inhibitory potency (IC_{50}) of Ro 31-8220 and Ro 31-7549, respectively, was similar against proliferation induced by PDBu (0.55 and 1.1 μM), PDGF (0.6 and 0.9 μM), PDGF and 5-HT (0.68 and 1.1 μM), although slightly less against serum (1.7 and 5 μM). The effects of the protein kinase C inhibitors on proliferation could not be ascribed to cytotoxicity. Neither Ro 31-8220 nor Ro 31-7549 (0.3–3 μM) inhibited PDGF receptor tyrosine phosphorylation.

3 The results show that Ro 31-8220 and Ro 31-7549 are potent inhibitors of smooth muscle cell proliferation in response to a direct activator of protein kinase C, the defined growth factors, PDGF and 5-HT, and the complex mixture of mitogens in serum. Protein kinase C activation thus appears to be an important growth transducing mechanism for each of these agents.

Keywords: Arteriosclerosis; vascular smooth muscle, rabbit aorta; protein kinase C; cell proliferation

Introduction

Vascular smooth muscle proliferation is a key process underlying the formation of atherosclerotic plaques (Ross, 1993). It is also the primary factor in reocclusion of arteries after angioplasty or atherectomy (Waller *et al.*, 1991), in the transplanted heart (Rose & Uyr, 1984), and in saphenous vein coronary artery bypass grafts (Angelini & Newby, 1989). There is therefore considerable interest in inhibitors of smooth muscle proliferation. One approach is to develop agents that interfere with growth factor transduction pathways, particularly if they inhibit elements common to diverse agents. Responses to classic growth factors such as platelet-derived growth factor (PDGF) and basic fibroblast growth factor are thought to be mediated by stimulation of receptor tyrosine kinases followed by activation of phospholipase C-γ (PLC-γ), triggering of calcium mobilization and activation of protein kinase C (PKC) (Meldrum *et al.*, 1991; Rhee, 1991). Vasoconstrictor agents, including 5-hydroxytryptamine (5-HT) and endothelin that act as co-mitogens with PDGF also cause calcium mobilization via PLC-β (Meldrum *et al.*, 1991) and activate PKC (Nishizuka, 1986; 1988). Activation of PKC may therefore contribute to mitogenic responses to both growth factors and vasoconstrictor agents. Phorbol esters that are direct activators of PKC, stimulate vascular smooth muscle proliferation, although to a lesser degree than serum (Kariya *et al.*, 1987a). PKC activating phorbol esters inhibit maximal responses to serum (Kariya *et al.*, 1987a), so that they may be regarded as 'partial agonists' of proliferation. Prolonged exposure to phorbol esters down-regulates PKC α isoforms and abolishes both the stimulatory and inhibitory effects of phorbol esters on proliferation (Kariya *et al.*, 1987a; 1989). Thus, while the effects of phorbol esters on proliferation are clearly mediated by PKC, activation of PKC alone is insufficient to account for the mitogenic responses to serum. Tyrosine phosphorylation of growth factor receptors also leads to activation of the MAP kinase cascade (Egan & Weinberg, 1994) providing an alternative pathway for mitogenic signalling in many cells including vascular smooth muscle (Graves *et al.*, 1993).

This calls into question whether PKC activation is essential at all for mitogenic responses to growth factors and vasoconstrictor agents. In favour of this proposal, inhibitors of PKC including staurosporine and K525a have been found to inhibit smooth muscle proliferation (Kariya *et al.*, 1987b; Tagaki *et al.*, 1988; Matsumoto & Sasaki, 1989; Ohmi *et al.*, 1990), although these agents are poorly-selective and potently inhibit other kinases that may be important for proliferation. For example, K252a and staurosporine are more potent inhibitors of phosphorylase kinase than PKC and both are also potent inhibitors of adenosine 3′:5′-cyclic monophosphate (cyclic AMP) dependent and Ca^{2+}/calmodulin-dependent kinases (Davis *et al.*, 1989; Elliot *et al.*, 1990). To clarify further the role of PKC in proliferation in response to PDGF, 5-HT and the complex mitogen, serum, the effects of two highly selective PKC inhibitors, Ro 31-8220 and Ro 31-7549 (Davis *et al.*, 1989), have been investigated.

Methods

Culture of rabbit aortic explants

This was conducted by a slight modification of the method described previously (Southgate & Newby, 1990; Assender *et al.*, 1992). Briefly, healthy New Zealand White Rabbits (age 9 weeks) were killed by a blow on the neck, the thorax was opened and 1000 units of heparin were injected into the left ventricle of the beating heart. The thoracic aorta was removed and immersed in sterile Dulbecco's modified Eagle's medium (DMEM) containing 20 mM HEPES buffer, pH 7.4, 100 iu ml^{-1} of penicillin and 100 μg ml^{-1} of streptomycin. The aorta was opened, the endothelium was removed from

[1] Author for correspondence.

the intimal surface by abrasion, and segments of tunica media were peeled off from the adventitia. The segments of tunica media were then cut up into 1 mm^2 explants with a McIlwain tissue chopper. The explants (approximately 100 per 75 cm^2 flask) were cultured in medium lacking HEPES but containing 25 mM sodium bicarbonate, 8 mM L-glutamine, 1 mM sodium pyruvate and 15% foetal bovine serum for 10 days at 37°C under an atmosphere of air: CO_2 (95:5 v/v). The outgrown cells were then dispersed by incubation for 5 min at 37°C with a 0.05% solution of trypsin, 0.02% EGTA and 154 mM NaCl. The cells were counted in a haemocytometer and replated at a density of 2.5×10^4 cells per 2 cm^2 well of 24 well culture plates. After 24 h, when the cells had attached and spread out, proliferation was arrested by changing to a quiescing medium, which consisted of DMEM and Hams F12 media in a 1:1 (v/v) ratio supplemented with ovalbumin (1 mg ml^{-1}), L-ascorbic acid (25 $\mu g\ ml^{-1}$), sodium selenate (25 ng mg^{-1}) Cohn factor IV (10 $\mu g\ ml^{-1}$), epidermal growth factor (10 ng ml^{-1}), transferrin (10 $\mu g\ ml^{-1}$), hydrocortisone (50 μM), L-glutamine (6 mM), penicillin (1000 units ml^{-1}) and streptomycin (1000 $\mu g\ ml^{-1}$) (Nemecek *et al.*, 1986). The cells were maintained in this medium for 96 hours before growth was re-initiated by adding the same medium containing mitogens, inhibitors (see below) and 1 $\mu Ci\ ml^{-1}$ of [6-^{3}H]-thymidine. Cultures were terminated 24 h later.

Termination of cultures and measurements of ATP, DNA and thymidine incorporation

Cultures were terminated by removing the medium and adding 1 ml of ice cold 10% w/v trichloroacetic acid, scraping off the cells and centrifuging the mixture at 1500 *g* for 5 min at 4°C. The supernatants were neutralised with a solution of 0.5 M tri-n-octylamine in 1,1,2, trichlorotrifluoroethane (Khym, 1975) and the aqueous phase was then separated and retained for measurement of ATP concentration by the firefly luciferase method (Spielmann *et al.*, 1981). The pellet was used for the measurement of DNA concentration (Kissane & Robins, 1958) and thymidine incorporation by liquid scintillation spectrometry as described previously (Southgate & Newby, 1990).

Measurement of tyrosine phosphorylation

Primary rabbit aortic smooth muscle cells were grown from explants and dispersed in trypsin/EDTA as described above. After counting in a haemocytometer, 2.5×10^5 cells were plated out in 29 cm^2 sterile plastic Petri dishes, left to adhere and rendered quiescent for 96 h as described above. The medium was then replaced with 2 ml of HEPES buffered DMEM (see above) supplemented as indicated in the text with 0.1% of dimethylsulphoxide with or without Ro 31-8220 or Ro 31-7549. Cultures were preincubated at 37°C in air for 10 min before the addition of 20 ng ml^{-1} final concentration of PDGFBB. After a further 10 min at 37°C, the medium was removed and replaced with 100 μl of a boiling hot SDS sample buffer (Laemmli, 1970) supplemented with 100 mM dithiothreitol, 10 mM sodium orthovanadate, 10 mM sodium fluoride, 30 mM sodium pyrophosphate and 10 mM EDTA, pH 6.7. The cells were removed with a cell scraper and the solution was boiled for 10 min. After centrifuging for 8 min at 10,000 *g* at room temperature, 100 μl of supernatants were subjected to SDS polyacrylamide gel electrophoresis using 7.5% (w/v) gels (Laemmli, 1970). After electroblotting onto nitrocellulose membranes, the presence of tyrosine phosphorylated proteins was detected as described previously (Brindle *et al.*, 1990). Briefly, membranes were incubated with blocking buffer (25 mM Tris/HCl, pH 7.4, 137 mM NaCl and 5% w/v bovine serum albumin) followed by a 0.5 $\mu g\ ml^{-1}$ solution of anti-phosphotyrosine monoclonal antibody in blocking buffer for 1 h at 25°C. Bound antibodies were detected by with peroxidase-labelled sheep anti-(mouse IgG) (0.2 $\mu g\ ml^{-1}$ in blocking buffer) and the ECL Western blotting detection system as described in the manufacturers instructions. X-ray film (Kodak XAR 5) was exposed for between 1 to 30 s to optimise contrast. The developed film was subjected to densitometric analysis using a UVP (Cambridge, U.K.) GDS 2000 gel documentation and analysis system. The area under the curve for designated peaks was computed above the grey level set from the minimum in each individual track.

Drugs and chemicals

Ro 31-8220 (3-[1-[3-(amidinothio)propyl]-3-indolyl]-4-(1-methyl-3-indolyl)-1*H*-pyrrole-2,5-dione methylsulfonate) and Ro 31-7549 (3-[1-(3-hydroxypropyl)-3-indolyl]-4-(1-methyl-3-indolyl)-1*H*-pyrrole-2,5-dione acetate) were synthesized as described previously (Davis *et al.*, 1992) and were obtained from Roche Products Ltd, Welwyn Garden City, Herts. The agents were dissolved in dimethylsulphoxide (DMSO) to concentrations ranging from 0.2 to 20 mM and were then diluted into tissue culture media to maintain a constant final concentration of 0.1% DMSO, which was used as control vehicle. [6-^{3}H]-thymidine (20–30 Ci $mmol^{-1}$) was obtained from New England Nuclear, Du Pont (U.K.) Ltd, Stevenage, Herts, or Amersham International, Aylesbury, Bucks. Foetal calf serum (FCS) was obtained from Imperial Laboratories Ltd, Andover, Hants. Recombinant platelet derived growth factor BB homodimer (PDGFBB) was obtained from Boehringer Mannheim, Lewes, Sussex. 5-Hydroxytryptamine (5-HT), phorbol 12,13-dibutyrate (PDBu), anti-phosphotyrosine monoclonal antibodies (clone PT 66) and prestained molecular weight markers were obtained from Sigma Chemical Company, Poole, Dorset. Nitrocellulose membranes (Hybond N), peroxidase-labelled sheep anti-(mouse IgG) and the ECL Wester blotting detection system were supplied by Amersham International, Amersham, Bucks. All tissue culture reagents were obtained from ICN Flow, High Wycombe, Bucks. All other chemicals were obtained from Fisons Scientific Ltd, Loughborough, Leics.

Statistical methods

Values are expressed throughout as mean ± s.e.mean and were compared by Student's *t* test using paired values. For IC_{50} values, the logarithms were subjected to significance testing.

Results

Mitogenic responses

Proliferation of quiescent first passage rabbit aortic smooth muscle cells was stimulated in a concentration-dependent way by PDBu, PDGF and serum (Figure 1a-c). The proliferation response to 0.1 μM PDBu measured in 8 paired experiments, including those shown in Figure 1c amounted to 10 ± 4% of the corresponding response to serum. This partial response agreed with previous work in rabbit aortic smooth muscle cells (Kariya *et al.*, 1987a). We also confirmed in 3 experiments the previous report (Kariya *et al.*, 1987a) that 0.1 μM PDBu inhibited the response to 5% serum by 76 ± 1%. The response to PDGF was potentiated by 5-HT (Figure 1b), being half maximal at 12 ± 1 ng ml^{-1} in the absence and 7 ± 2 ng ml^{-1} in the presence of 5-HT ($P < 0.05$, $n = 4$). The maximal response to 20 ng ml^{-1} of PDGF was not significantly increased, however, by 5-HT (Figure 1b). The maximal responses to 20 ng ml^{-1} PDGF measured in 7 paired experiments, including those in Figure 1b was 52 ± 17% of the response to 5% serum. The response to 20 ng ml^{-1} PDGF and 10 μM 5-HT measured in 9 paired experiments including those in Figure 1b was 61 ± 12% of the response to 5% serum.

Effects of protein kinase C inhibitors

The PKC inhibitors, Ro 31-8220 and Ro 31-7549, concentration-dependently inhibited cell proliferation in response to PDBu, PDGF alone, PDGF plus 5-HT or serum (Figure 2a). This inhibition was almost complete for each mitogen with 3 μM Ro 31-8220 or 10 μM Ro 31-7549 (Figure 2a, Table 1). Ro 31-7549 was consistently slightly less potent than Ro 31-8220, although the difference was statistically significant only for the data with serum (Table 2). The inhibitory potency of Ro 31-8220 or Ro 31-7549 was similar against phorbol dibutyrate, PDGF alone or PDGF plus 5-HT; however, the inhibitors exhibited a 3 or 5 fold reduced potency, respectively, against serum (Figure 2a, Table 2). The effects of Ro 31-8220 (or Ro 31-7549, results not shown) on proliferation were not accompanied by a decrease in cell viability as measured by ATP concentration (Figure 2b).

Neither Ro 31-8220 nor Ro 31-7549 (0.3–3 μM) inhibited the PDGF induced tyrosine phosphorylation of a 180 kDa band, presumed to be PDGF receptor subunits (Figure 3).

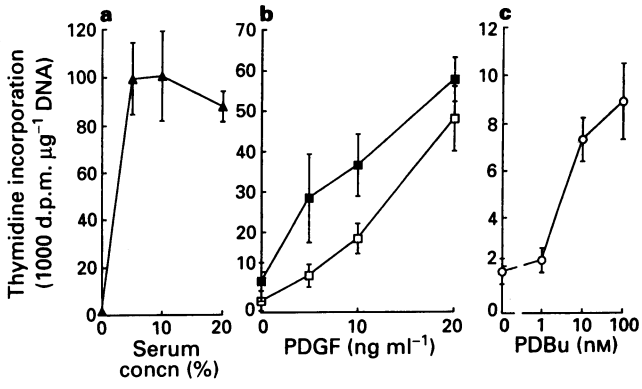

Figure 1 Proliferation responses: incorporation of [^{3}H]-thymidine into the DNA of quiescent rabbit aortic vascular smooth muscle cells was measured in response to stimulation for 24 h with serum (▲, $n = 3$), platelet-derived growth factor (PDGF) (□, $n = 4$), PDGF plus 10 μM 5-hydroxytryptamine (■, $n = 4$) or phorbol dibutyrate (PDBu, ○, $n = 4$). Responses were measured in quadruplicate for the number of aortae (n) shown. Values shown are means ± s.e.mean.

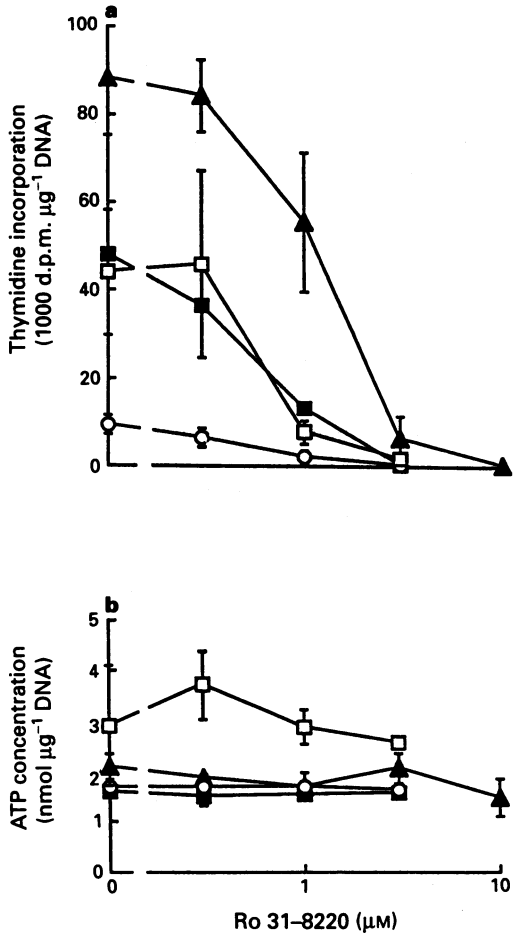

Figure 2 Effect of protein kinase C (PKC) inhibitors on proliferation: (a) The effects of 0.1–3 μM Ro 31-8220 or 0.1–10 μM Ro 31-7459 on incorporation of [^{3}H]-thymidine into DNA were measured in quadruplicate cultures of quiescent rabbit aortic smooth muscle cells restimulated for 24 h with 0.1 μM phorbol dibutyrate (○, $n = 6$), 20 ng ml^{-1} of platelet-derived growth factor (PDGF) alone (□, $n = 3$), PDGF with 10 μM 5-hydroxytryptamine (■, $n = 6$) or 5% (v/v) foetal calf serum (▲, $n = 3$). All cultures also contained vehicle (0.1% DMSO). (b) The concentrations of ATP (a marker of cell viability) were measured in the same cultures as panel (a). Values are means for the number of aortae shown for (a).

Table 1 Effectiveness (% residual proliferation) of protein kinase C (PKC) inhibitors against various mitogens

Mitogen	*PDBu*	*PDGF*	*PDGF + 5-HT*	*FCS*
Ro 31-8220 3 μM	3.7 ± 0.7% (6)	6.7 ± 3.0% (3)	2.2 ± 1.3% (6)	6.8 ± 4.8% (3)
Ro 31-7549 10 μM	1.2 ± 0.5% (3)	5.9 ± 3.0% (3)	4.5 ± 2.5% (4)	0.6 ± 0.3% (5)

The effects of Ro 31-8220 or RO 31-7459 were measured in quadruplicate cultures of quiescent rabbit aortic smooth muscle cells restimulated for 24 h with 0.1 μM phorbol dibutyrate (PDBu), 20 ng ml^{-1} of platelet derived growth factor (PDGF) with or without 10 μM 5-hydroxytryptamine (5-HT) or 5% (v/v) foetal calf serum (FCS). The residual rate of proliferation was then calculated for each experiment as a percentage of the rate in the presence of vehicle (0.1% DMSO) alone. The values shown are the means ± s.e.mean for the number of aortae shown in parentheses.

Table 2 Potency (IC_{50} values) of protein kinase C (PKC) inhibitors against various mitogens

Mitogen	*PDBu*	*PDGF*	*PDGF + 5-HT*	*FCS*
Ro 31-8220 μM	0.55 ± 0.13 (6)	0.6 ± 0.2 (3)	0.68 ± 0.22 (6)	1.7 ± 0.7 (3)
Ro 31-7549 μM	1.1 ± 0.7 (3)	0.91 ± 0.12 (3)	1.1 ± 0.5 (3)	5 ± 1(3)

The effects of 0.1–3 μM Ro 31-8220 or 0.1–10 μM RO 31-7459 were measured in quadruplicate cultures of quiescent rabbit aortic smooth muscle cells restimulated for 24 h with 0.1 μM phorbol dibutyrate (PDBu), 20 ng ml^{-1} of platelet derived growth factor (PDGF) with or without 10 μM 5-hydroxytryptamine (5-HT) or 5% (v/v) foetal calf serum (FCS). The concentrations giving 50% inhibition were then calculated for each experiment. The values shown are the means ± s.e.mean for the number of aortae shown in parentheses.

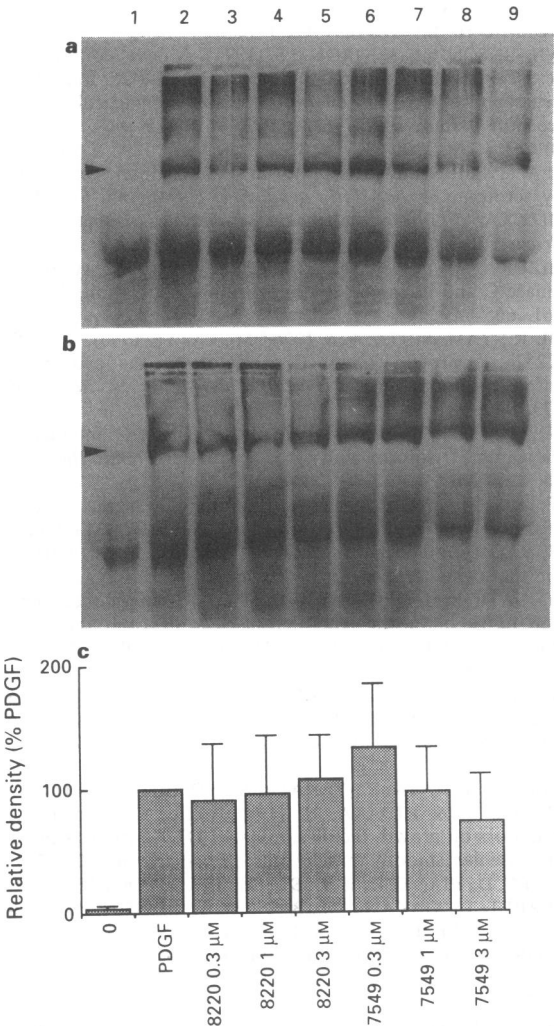

Figure 3 Effect of protein kinase C (PKC) inhibitors on tyrosine phosphorylation: (a) and (b) show 2 representatives of 4 similar experiments conducted on different preparations of rabbit aortic smooth muscle cells. Lane 1 has no additions, lanes 2–9 have 20 ng ml^{-1} of platelet-derived growth factor (PDGF) and lanes 3–9 have 0.1% of dimethylsulphoxide. Ro 31-8220 (lanes 4–6) or Ro 31-7549 (lanes 7–9) were also present at the μM concentrations shown. The arrows show the positions of the 180 kDa molecular weight markers in the two separate blots. Panel (c) shows the results of densitometric analysis of all 4 blots. The value (mean ± s.e.mean) for the other conditions was expressed relative to the optical density of the 180 kDa band in the PDGF alone lane, which was taken as 100%.

Discussion

Ro 31-8220 and Ro 31-7549 are conformationally restricted, substituted bisindolylmaleimides, which possess at least 100 fold greater potency against PKC than against cyclic AMP- or Ca^{2+}/calmodulin-dependent protein kinases (Davis *et al.*, 1989; 1992; Muid *et al.*, 1991). Both compounds act competitively with ATP, exhibiting IC_{50} values of approximately 10 and 80 nM, respectively, in *in vitro* assays using 10 μM ATP as substrate, but much higher values in intact cells, where ATP concentrations are millimolar. For example, both compounds inhibited PKC-induced phosphorylation in intact platelets and PKC-mediated responses in T-lymphocytes with IC_{50} values in the low micromolar range; Ro 31-8220 was approximately 6 fold more potent than Ro 31-7549 (Davis *et al.*, 1989; Muid *et al.*, 1991). We observed similar potencies here (0.5–1 μM) for inhibition of smooth muscle proliferation in response to the direct activator of PKC, PDBu. The mitogenic response to PDBu was small compared to that produced by serum, in agreement with previous studies of PDBu and other PKC activators in rabbit aortic smooth muscle cells, owing to 'partial agonist' behaviour (Kariya *et al.*, 1987a). Nevertheless, the stimulatory effect of PDBu is mediated by PKC, because it is abolished after down-regulation of PKC (Kariya *et al.*, 1987a; 1989). The proliferation response to PDBu is therefore an adequate positive control for the effects of Ro 31-8220 and Ro 31-7549, which takes into account penetration of the agents into smooth muscle cells and competition with intracellular ATP. Ro 31-8220 and Ro 31-7549 completely inhibited proliferation responses to PDBu.

A relatively greater proliferation response was obtained to PDGF than PDBu. The effect of PDGF was potentiated by 5-HT, in agreement with other published work (Araki *et al.*, 1990). Ro 31-8220 and Ro 31-7549 completely inhibited proliferation responses to PDGF alone or PDGF plus 5-HT. The similar inhibitory potencies against responses to PDBu, PDGF and PDGF plus 5-HT imply that inhibition of PKC accounts for the observed effects on proliferation. PKC activation therefore appears essential for responses to all these agents, consistent with previous studies of less specific PKC inhibitors (Kariya *et al.*, 1987b; Tagaki *et al.*, 1988; Ohmi *et al.*, 1990). The reduced inhibitory potency of Ro 31-8220 and Ro 31-7549 against serum, may imply that in this complex mixture there are mitogens that act independently of PKC but other explanations, such as protein-binding of the inhibitors or the need to overcome the larger response to serum, cannot be ruled out.

Based on previous data, it was unlikely that inhibition of a receptor tyrosine kinase rather than PKC accounted for the antiproliferative effects of Ro 31-8220 and Ro 31-7549. These agents exhibit only weak inhibitory activity against $p56^{lck}$, a lymphocyte specific tyrosine kinase or the insulin receptor tyrosine kinase (Welsh & Proud, 1993). Related bisindolylmaleimides also show only weak effects against PDGF, EGF or insulin receptor tyrosine kinases (Toullec *et al.*, 1991). To rule out an effect on the PDGF-receptor tyrosine kinase directly in our cells, we measured tyrosine phosphorylation in response to PDGF and found it to be unaffected by Ro 31-8220 and Ro 31-7549 at antiproliferative concentrations. We cannot, of course, rule out the possibility that Ro 31-8220 and Ro 31-7549 also inhibit one of the many other kinases known to be involved in cell proliferation.

Ro 31-8220 and Ro 31-7549 are potent inhibitors of smooth muscle cell proliferation irrespective of the nature of the mitogenic stimulus. They therefore fulfil one important criterion for use as treatment for vascular pathologies, including angioplasty restenosis. Inhibition by Ro 31-8220 and Ro 31-7459 implies an essential role for PKC in vascular smooth muscle cell proliferation, which needs to be further established by molecular biology methods.

This work was supported by grants from the British Heart Foundation.

References

ANGELINI, G.D. & NEWBY, A.C. (1989). The future of saphenous vein as a coronary artery bypass conduit. *Eur. Heart J.*, **10**, 273–280.

ARAKI, S.-I., KAWAHARA, Y., FUKUZAKI, H. & TAKAI, Y. (1990). Serotonin plays a major role in serum-induced phospholipase C-mediated hydrolysis of phosphoinositides and DNA synthesis in vascular smooth muscle cells. *Atherosclerosis*, **83**, 29–34.

ASSENDER, J.W.A., SOUTHGATE, K.M., HALLETT, M.B. & NEWBY, A.C. (1992). Inhibition of proliferation but not Ca^{2+} mobilization by cAMP and cGMP in rabbit aortic smooth muscle cells. *Biochem J.*, **288**, 527–532.

BRINDLE, N.P.J., TAVARE, J.M., DICKENS, M., WHITTAKER, J. & SIDDLE, K. (1990). Anti- (insulin receptor) monoclonal antibodies-stimulated tyrosine phosphorylation in cells transfected with human insulin receptor cDNA. *Biochem J.*, **268**, 615–620.

DAVIS, P.D., ELLIOT, L., HARRIS, W., HILL, C.H., HURST, S.A., KEECH, E., KUMAR, M.K.H., LAUGHTON, G., NIXON, J.S. & WILKINSON, S.E. (1992). Inhibitors of protein kinase C. 2. Substituted Bisinolylmaleimides with improved potency and selectivity. *J. Med. Chem.*, **35**, 994–1001.

DAVIS, P.D., HILL, C.H., KEECH, E., LAWTON, G., NIXON, J.S., SEDGWICK, A.D., WADSWORTH, J., WESTMACOTT, D. & WILKINSON, S.E. (1989). Potent selective inhibitors of protein kinase C. *FEBS Lett.*, **259**, 61–63.

EGAN, S.E. & WEINBERG, R.A. (1994). The pathway to signal achievement. *Nature*, **365**, 781–783.

ELLIOT, L., WILKINSON, S.E., SEDGWICK, A.D., HILL, C.H., LAUGHTON, G., DAVIS, P.D. & NIXON, J.S. (1990). K252a is a potent inhibitor of phosphorylase kinase. *Biochem. Biophys. Res. Commun.*, **171**, 148–154.

GRAVES, L.M., BORNFELDT, K.E., RAINES, E.W., POTTS, B.C., MACDONALD, S.G., ROSS, R. & KREBS, E.G. (1993). Protein kinase A antagonizes platelet-derived growth factor signaling by mitogen-activated protein kinase in human arterial smooth muscle cells. *Proc. Natl. Acad. Sci. U.S.A.*, **90**, 10300–10304.

KARIYA, K., FUKUMOTO, Y., TSUDA, T., KAWAHARA, Y., FUKUZAKI, H., YAMAMOTO, T. & TAKAI, Y. (1987a). Inhibition of DNA synthesis by phorbol esters through protein kinase C in cultured rabbit aortic smooth muscle cells. *FEBS Lett.*, **217**, 69–73.

KARIYA, K., KAWAHARA, Y., FUKUZAKI, H., HAGIWARA, M., HIDAKA, H., FUKUMOTO, Y. & TAKAI, Y. (1989). Two types of protein kinase C with different functions in cultured rabbit aortic smooth muscle cells. *Biochem. Biophys. Res. Commun.*, **161**, 1020–1027.

KARIYA, K., KAWAHARA, Y., TSUDA, T., FUKUZAKI, H. & TAKAI, Y. (1987b). Possible involvement of protein kinase C in platelet-derived growth factor-stimulated DNA synthesis in vascular smooth muscle cells. *Atherosclerosis*, **63**, 251–255.

KHYM, J.X. (1975). An analytical system for rapid separation of tissue nucleotides at low pressures on conventional anion exchangers. *Clin. Chem.*, **21**, 1245–1252.

KISSANE, J.M. & ROBINS, E. (1958). The fluorimetric measurement of deoxyribonucleic acid in animal tissues with special reference to the central nervous system. *J. Biol. Chem.*, **233**, 184–188.

LAEMMLI, U.K. (1970). Cleavage of structural proteins during assembly of the head of bacteriophage T4. *Nature*, **227**, 680–685.

MATSUMOTO, H. & SASAKI, Y. (1989). Staurosporine, a protein kinase C inhibitor, interferes with proliferation of arterial smooth muscle cells. *Biochem. Biophys. Res. Commun.*, **158**, 105–109.

MELDRUM, E., PARKER, P.J. & CAROZZI, A. (1991). The PtdIns-PLC superfamily and signal transduction. *Biochim. Biophys. Acta*, **1092**, 49–71.

MUID, R.E., DALE, M.M., DAVIS, P.D., ELLIOT, L.H., HILL, C.H., KUMAR, H., LAUGHTON, G., TWOMEY, B.M., WADSWORTH, J., WILKINSON, S.E. & NIXON, J.S. (1991). A novel conformationally restricted protein kinase C inhibitor, Ro 31-8425, inhibits human neutrophil superoxide generation by soluble, particulate and post-receptor stimuli. *FEBS Lett.*, **293**, 169–172.

NEMECEK, G.M., COUGHLIN, S.R., HANDLEY, D.A. & MOSKOWITZ, M.A. (1986). Stimulation of aortic smooth muscle cell mitogenesis by serotonin. *Proc. Natl. Acad. Sci. U.S.A.*, **83**, 674–678.

NISHIZUKA, Y. (1986). Studies and perspectives of protein kinase C. *Science*, **233**, 305–312.

NISHIZUKA, Y. (1988). The molecular heterogeneity of protein kinase C and its implications for cellular regulation. *Nature*, **334**, 661–665.

OHMI, K., YAMASHITA, S. & NONOMURA, Y. (1990). The effect of K252a, a protein kinase C inhibitor on the proliferation of vascular smooth muscle cells. *Biochem. Biophys. Res. Commun.*, **173**, 976–981.

RHEE, S.G. (1991). Inositol-specific phospholipase C: interaction with the gamma1 isoform with tyrosine kinase. *Trends Biochem. Sci.*, **16**, 297–301.

ROSE, A.G. & UYR, C.J. (1984). Pathology of acute rejection. In *Heart Transplantation*. pp. 157–176. Lancaster: MTP Press.

ROSS, R. (1993). The pathogenesis of atherosclerosis: a perspective for the 1990s. *Nature*, **362**, 801–809.

SOUTHGATE, K.M. & NEWBY, A.C. (1990). Serum-induced proliferation of rabbit aortic smooth muscle cells from the contractile state is inhibited by 8-Br-cAMP but not 8-Br-cGMP. *Atherosclerosis*, **82**, 113–123.

SPIELMANN, H., JACOB-MULLER, U. & SCHULZ, P. (1981). Simple assay of 0.1–1.0 pmol of ATP, ADP and AMP in single somatic cells using purified luciferin luciferase. *Anal Biochem.*, **113**, 172–178.

TAGAKI, Y., HIRATA, Y., TAKATA, S., YOSHIMI, H., FUKUDA, Y., FUJITA, T. & HIDAKA, H. (1988). Effects of protein kinase inhibitors on growth factor-stimulated DNA synthesis in cultured rat vascular smooth muscle cells. *Atherosclerosis*, **74**, 227–230.

TOULLEC, D., PIANETTI, P., COSTE, H., BELLEVERGUE, P., GRAND-PERRET, T., AJAKANE, M., BAUDET, V., BOISSIN, P., BOURSIER, E., LORIOLLE, F., DUHAMEL, L., CHARON, D. & KYRILOVSKY, J. (1991). The bisindolylmaleimide GF109203X is a potent and selective inhibitor of protein kinase C. *J. Biol. Chem.*, **266**, 15771–15781.

WALLER, B.F., PINKERTON, C.A., ORR, C.M., SLACK, J.D., VAN-TASSEL, J.W. & PETERS, T. (1991). Restenosis 1 to 24 months after clinically successful coronary balloon angioplasty: a necropsy study of 20 patients. *J. Am. Coll. Cardiol.*, **17**, (Suppl. B.), 58B–70B.

WELSH, G.I. & PROUD, C.G. (1993). Evidence for a role for protein kinase C in the stimulation of protein synthesis by insulin in Swiss 3T3 fibroblasts. *FEBS Lett.*, **316**, 241–246.

(Received May 13, 1994
Revised October 6, 1994
Accepted January 6, 1995)

British Journal of Pharmacology (1995) 114, 1657–1665 © 1995 Stockton Press All rights reserved 0007–1188/95 $12.00

Effect of UK-84149 on voltage-activated calcium currents of single smooth muscle cells from guinea-pig and rabbit jejunum and rabbit coronary artery

[1]H. Zhang & T.B. Bolton

Department of Pharmacology & Clinical Pharmacology, St. George's Hospital Medical School, Cranmer Terrace, London SW17 0RE

1 Smooth muscle cells of the longitudinal muscle of the guinea-pig and the rabbit jejunum and rabbit coronary artery were dispersed by enzyme treatment and recordings of membrane current were made in the standard whole cell voltage-clamp mode and by perforated patch technique. The effect of UK-84149 on the voltage-dependent calcium inward current of single isolated smooth muscle was studied at room temperature.

2 When inward and outward currents were evoked by stepping to 0 mV or + 10 mV from − 80 mV every 20 s, UK-84149 reduced the voltage-dependent inward current in guinea-pig jejunum smooth muscle cells with a ID_{50} of 2.3 μM, and also reduced voltage-dependent outward current with a ID_{50} of 7.2 μM. The effect of UK-84149 was difficult to wash out.

3 The inactivation of the inward current was studied by holding at various potentials for 10 s before evoking inward current at a test potential of 0 mV. The voltage-inactivation curve was shifted to the left by 3 μM UK-84149. The voltage at which current was 50% available (V_h) was changed from − 37 ± 2 mV to − 50 mV ± 2.2 ($n = 6$, means ± s.e.mean).

4 When inward current was evoked by stepping to 0 mV from − 80 mV for 50 ms, every 20 s, nicardipine immediately, and verapamil and UK-84149 slowly, reduced the peak amplitude. Inhibition by the latter two drugs depended on the number of stimulations applied. So, like verapamil, UK-84149 had a use-dependent action.

5 The effect of UK-84149 on inward current from rabbit jejunum and coronary artery smooth muscle cells was compared with the effect of nicardipine and D600. When inward current was evoked by stepping to 0 mV from − 80 mV every 20 s, UK-84149 inhibited inward currents from both types of smooth cell with an ID_{50} of 1.7 μM for jejunum and an ID_{50} of 3.2 μM for coronary artery. ID_{50} values of D600 were 8.1 μM for jejunum and 3.9 μM for coronary artery. ID_{50} values of nicardipine were 24 nM for jejunum and 12 nM for coronary artery.

6 The results of the present studies indicate that UK-84149 has a calcium-antagonist action that can explain its inhibitory action on bowel motility. Its bowel selectivity may arise due to its use-dependent, and persistent, action.

Keywords: UK-84149; nicardipine; D600; calcium channel; smooth muscle

Introduction

UK-84149 (S-5,11-dihydro-5-[1-(4 methoxyphenethyl)2-pyrrolidinylmethyl]-dibenzo [b.e] [1,4] thiazepinemaleate]), a newly developed calcium antagonist drug, showed a significant tissue selectivity for intestine smooth muscle in preliminary experiments (Quinn & Wallis, 1994; Wallis *et al.*, 1994). UK-84149 potently inhibited small and large bowel motility stimulated by cholesytokinin octapeptide, with cardiovascular effects being evident only at doses 10 times higher. This contrasted with calcium channel blockers such as nifedipine and diltiazem which produced dose-related cardiovascular effects over the same dose-range as those required to inhibit motility (Quinn & Wallis 1994). UK-84149 was able to inhibit calcium-induced contracture of depolarized guinea-pig ileum which could be reversed by the addition of excess calcium, indicating that a calcium antagonist effect might be involved in the effects of UK-84149 (Wallis *et al.*, 1994). The purpose of the present experiments was to investigate the action of UK-84149 on calcium currents from the guinea-pig jejunum, rabbit jejunum, and coronary artery smooth muscle cells, and to compare it with verapamil, nicardipine and D600 by using the whole-cell voltage clamp recording technique.

[1] Author for correspondence.

Methods

Single cell dispersion

Rabbits were killed by overdose of pentobarbitone and guinea-pigs by cervical dislocation and exsanguination. Strips of the longitudinal smooth muscle layer of the guinea-pig or rabbit jejunum were cut into small pieces (3–4 mm) and incubated for 10 min in low Ca (10 μM) physiological salt solution (PSS) and then transferred to a low-Ca medium containing 0.4 mg ml^{-1} collagenase (Sigma, type XI) and 0.4 mg ml^{-1} protease (Sigma, type E) for 20 min at 37°C. At the end of digestion, the tissue was washed with low-Ca PSS without enzyme and agitated mildly by sucking in and out of a wide-bore pipette. The suspension of cells was then centrifuged and the pellet re-suspended in PSS containing about 0.4 mM Ca. Cells were maintained at 4°C and used within 6 h. All experiments were at room temperature (20–26°C). The left descending coronary artery of rabbit was identified under the binocular microscope and was isolated carefully. The connective tissue was removed and the artery was cut into small pieces (2–3 mm). The procedure for dispersion

was similar to that for jejunum except higher levels of enzymes (collagenase 0.6 mg ml^{-1}, protease 0.6 mg ml^{-1}) and longer incubation time (30 min) were used.

Electrical recordings

Cells were voltage-clamped by use of the whole-cell configuration of the patch-clamp technique (Hamill *et al.*, 1981) or perforated patch recording technique in which nystatin (100 $\mu g\ ml^{-1}$) was added to the pipette solution (Horn & Marty, 1988). The current-voltage converter was a patch-clamp amplifier (Biologic). Analogue signals were recorded on FM-tape (Racal) at a tape speed of 3.75 in s^{-1}. Fire-polished pipettes were prepared from borosilicate glass using a patch electrode puller (Narishige Sci. Inst. Lab.). The resistances of the pipettes were 2–4 MΩ for jejunum smooth muscle cell recordings and 3–5 MΩ for rabbit coronary artery smooth muscle cell recordings. Cells were placed in the chamber (0.3 ml) on the stage of an inverted microscope, which was perfused continuously with solution at a rate of about 2 ml min^{-1}. Command pulses were applied and signals were digitized at 2 kHz using a CED 1401 interface in conjunction with a 386 PC or a BBC microcomputer.

Solutions

The normal PSS (physiological salt solution) in the bath had the following ionic composition (mM): NaCl 130, KCl 5, $MgCl_2$ 1.2, $CaCl_2$ 1.7 or 2.5, glucose 10, HEPES 10, and was titrated to pH 7.4 with NaOH. The pipette solutions had the following ionic composition (mM): (1) Cs solution; CsCl 135, $MgCl_2$ 5, EGTA 5, HEPES 5. To make an ATP-generating solution ATP (3 mM), GTP (0.1 mM), creatine phosphate (15 mM), and creatine phosphokinase (50 u ml^{-1}) were added or nystatin (100 $\mu g\ ml^{-1}$) was added for perforated patch recording. (2) K solution: KCl 130, $MgCl_2$ 2, EGTA 5, HEPES 20. The solutions were titrated to pH 7.4 with CsOH or KOH. In some cases, 20 mM TEA chloride was included in the pipette and bath solution.

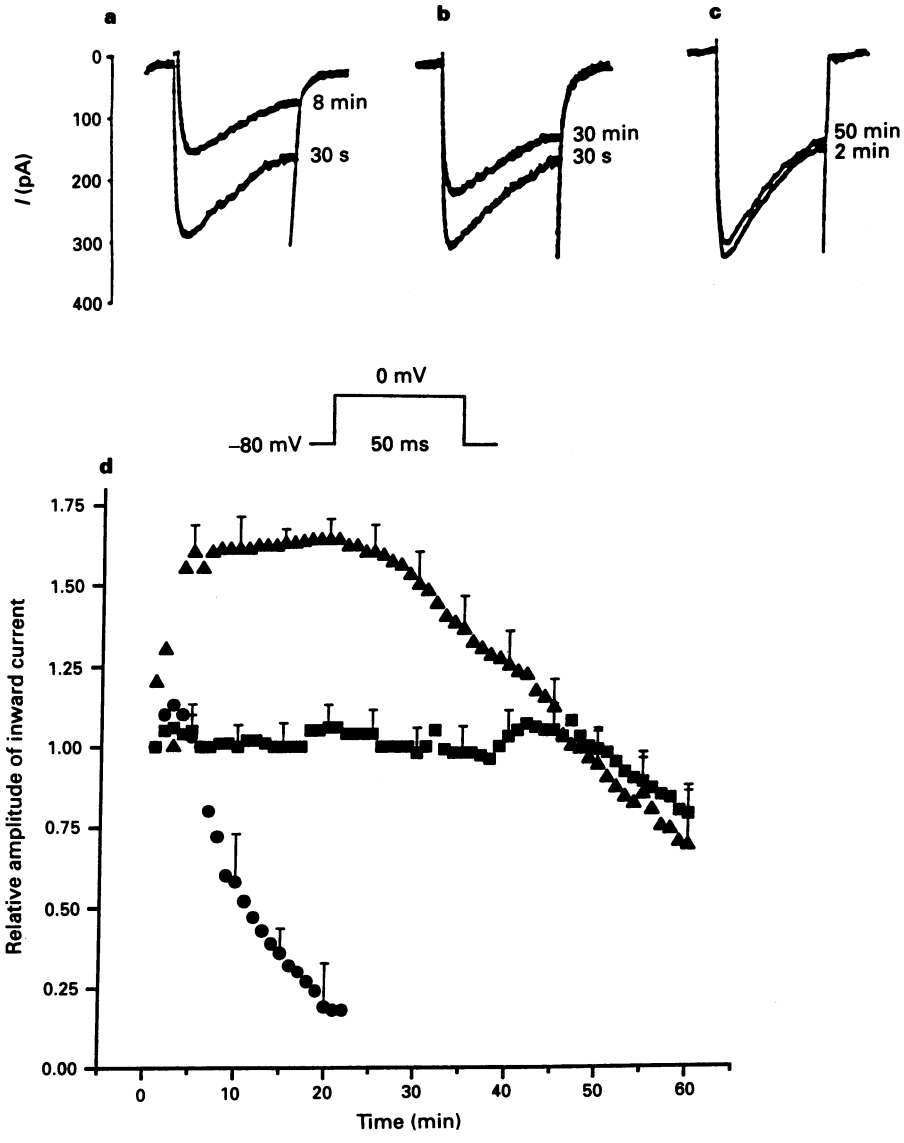

Figure 1 Time course of changes in size of peak inward current in guinea-pig jejunum smooth muscle cell recorded using three types of Cs-containing pipette solution. (a) Conventional whole cell recording with ATP-free pipette solution; (b) conventional whole cell recording with 3 mM ATP, 15 mM creatine phosphate and 50 u ml^{-1} creatine phosphokinase in the peptide solution; (c) 'perforated patch' whole cell recording with 100 $\mu g\ ml^{-1}$ nystatin in the pipette solution. The times after the cell membrane was ruptured are indicated. Cells were held at −80 mV and stepped to 0 mV for 50 ms every 20 s as shown below. (d) Relative amplitude of peak inward current recorded with the three types of solution. The inward current amplitude evoked by the first pulse after rupture of the cell membrane was normalized as 1.0. ATP-generating pipette solution (▲), nystatin pipette solution (■), and ATP-free pipette solution (●). Means and 1 s.e.mean from 4–5 cells.

Drugs

UK-84149 as its maleate salt UK-84149-11 (S-5,11-dihydro-5-[1-(4 methoxyphenethyl)2-pyrrolidinylmethyl] -dibenzo [b.e] [1,4]thiazepinemaleate]) was obtained from Pflizer Central Research, Sandwich, Kent and was dissolved first in dimethylsulphoxide (DMSO) and diluted with PSS to the final concentration given in the text. The final concentration of DMSO was less than 0.3%. Nicardipine, verapamil and methoxyverapamil (D600) were all from Sigma, and were dissolved directly in water to make stock solutions. Collagenase (type XI), protease (type E), EGTA, Na_2ATP, creatine phosphate, creatine phosphokinase, and GTP were from Sigma.

All results are expressed as mean ± s.e.mean. Statistical significance was evaluated by analysis of variance with repeated measurements or Student's bilateral unpaired *t* tests, when appropriate. Differences with values of $P<0.05$ were considered to be significant.

Results

Ca current rundown

Figure 1 shows inward Ca current from rabbit jejunum smooth muscle cell evoked by stepping from a holding potential of − 80 mV to 0 mV. With caesium chloride in the pipette, outward K current was apparently abolished because no difference was observed when 20 mM TEA was included in the pipette and bath solution (data not shown). In standard whole cell recording mode when no ATP was included in the pipette solution, the peak amplitude of the voltage-activated Ca current gradually decreased with time after a transient increase; the peak inward current decreased to 19 ± 14% ($n = 5$) of its initial value 20 min after rupture of the membrane patch. ATP (5 mM) markedly delayed the rundown of inward current (data not shown). When the ATP-generating pipette solution (see Methods) was used, the

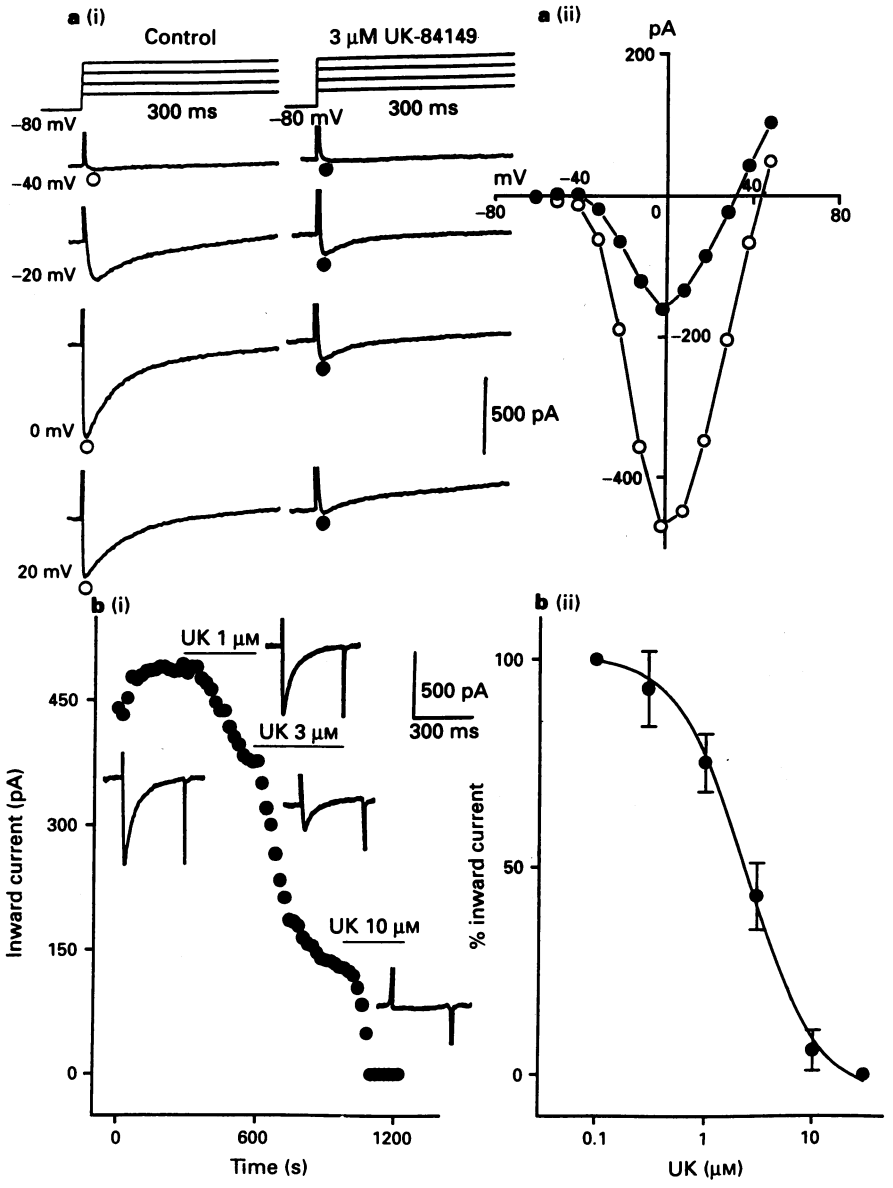

Figure 2 Effect of UK-84149 on inward currents in guinea-pig jejunal single smooth muscle cells. The cells were bathed in PSS containing 1.7 mM Ca^{2+} and perfused continuously at the rate of 2 ml min^{-1}. (a)(i) Cells were held at − 80 mV and stepped to various potentials for 300 ms, every 20 s. Open (○) and closed (●) circles indicated the peak inward currents in the control and with UK-84149 (3 μM), respectively. (a)(ii) Current-voltage curves in the absence (○) and presence (●) of UK-81149 (3 μM). Open and closed circles indicated peak inward current. (b)(i) Peak inward currents in the absence and presence of UK-84149 (1–10 μM) plotted against time. Cells were held at − 80 mV and stepped to 0 mV for 300 ms, every 20 s. (b)(ii) The relative amplitude of inward current against various concentrations of UK-84149. The peak inward current amplitude in the absence of the drug was normalised as 100%. The ID_{50} was about 2.3 μM. Mean ± s.e.mean ($n = 6$).

rundown was delayed further and the initial increase of the peak inward current persisted even as long as 20 min; thereafter the Ca current eventually declined to 58 ± 17% ($n = 3$) of its initial peak amplitude at 60 min. With 100 μg ml^{-1} nystatin in the pipette solution ('perforated patch' recording mode), run down of inward current was usually negligible for 30 min or longer but by 60 min run down was apparent. Thus, run down was very slow compared with standard whole cell recordings. The peak inward current 50 min after gaining electrical access to cell (series resistance 10–30 MΩ) was still 96 ± 16% of its initial value ($n = 3$). Rundown of inward current is a problem when constructing concentration-response relationships for calcium antagonists, because the block often took a long time to reach steady-state. Thus, nystatin pipette solution was used for constructing concentration-response relationship for the effects of UK-84149, D600 and nicardipine on inward calcium current from rabbit jejunum and coronary artery cells and ATP-generating pipette solution was used for the rest of the experiments which involved observations on inward calcium current.

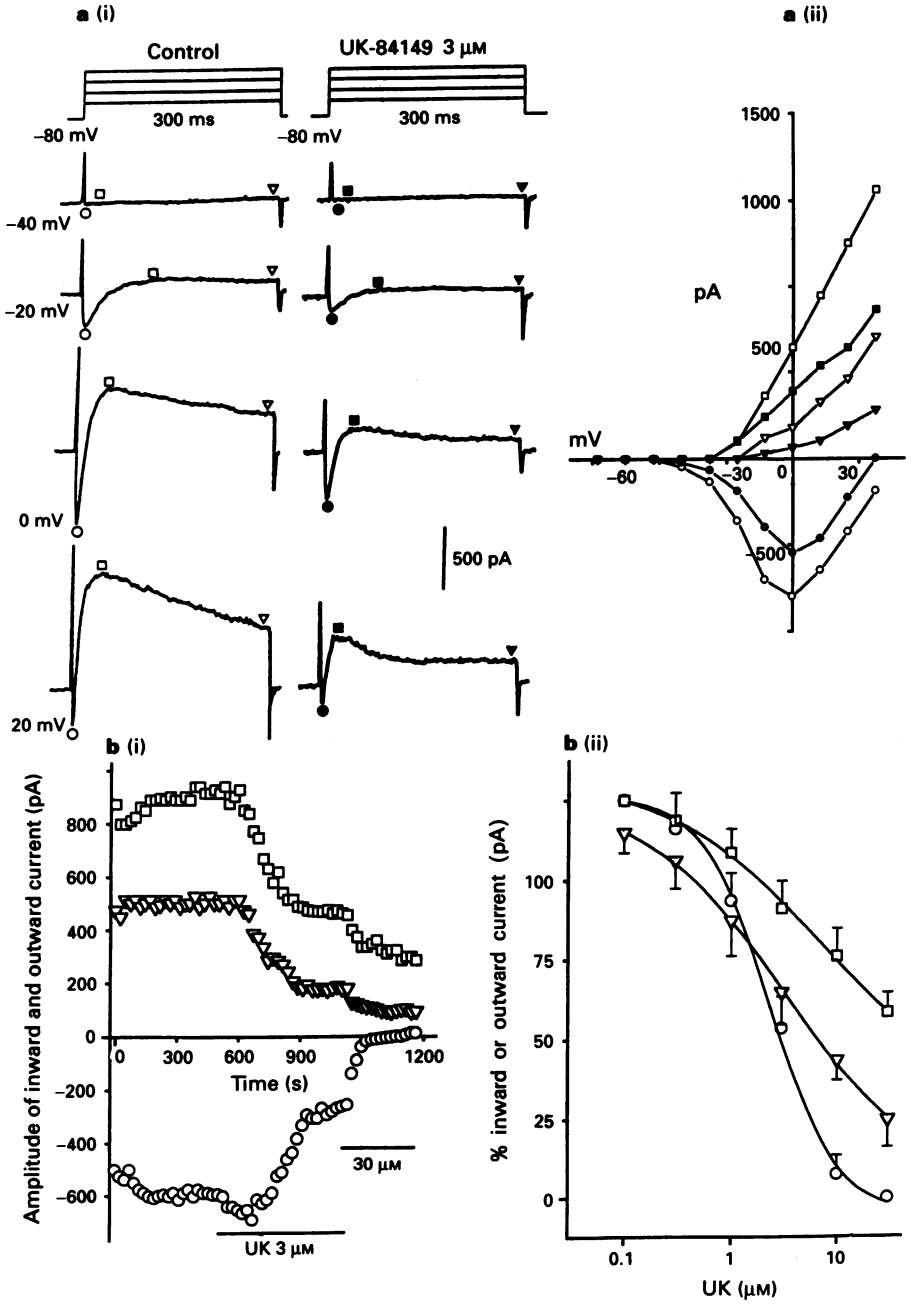

Figure 3 Effect of UK-84149 on inward and outward currents in guinea-pig jejunum smooth muscle cells. (a)(i) Cells were held at − 80 mV and stepped to various potentials for 300 ms, every 20 s. Peak inward current (circles), peak (squares) and end of pulse (triangles) outward current in the absence (open symbols) and presence (closed symbols) of 3 μM UK-84149 were measured. (a)(ii) Current-voltage curve obtained in the absence and presence of 3 μM UK-84149. Symbols are as in (a)(i). (b)(i) Inward and outward current in one cell, plotted against time. Cells were held at − 80 mV and stepped to + 10 mV for 300 ms, every 20 s. (b)(ii) The relative amplitude of inward and outward current (evoked by a step to + 10 mV) against various concentrations of UK-84149 (means ± s.e.mean, $n = 4$). The amplitude of inward and outward current in the absence of the drug were normalized as 100%. the ID_{50}s were 2.3 μM for peak inward (○), 7.2 μM and 3.3 μM for peak (□) and end (▽) of pulse outward current, respectively.

Effects of UK-84149 on inward and outward current from guinea-pig jejunum smooth muscle cells

Figure 2(a)(i) and (a)(ii) show the effect of UK-84149 on the current-voltage relationships of the inward Ca current. Cells were held at − 80 mV and stepped to various potentials. The inward current was evoked by stepping more positive than − 30 mV from − 80 mV. Outward current was inhibited by including Cs instead of K in the pipette solution. Figure 2 (a) (i) shows inward current before and 10 min after application of UK-84149 (3 μM). UK-84149 consistently inhibited the peak inward current amplitude observed at any given potential (from − 30 to + 40 mV) (Figure 2(a)(i) and (ii)). Figure 2(b)(i) and (ii) show the relationship between the amplitude of inward current and concentrations of UK-84149. In these experiments, the inward current was evoked by stepping to 0 mV for 300 ms from a holding potential of − 80 mV, every 20 s. Figure 2(b) (i) shows the effect in a cell of different concentrations of UK-84149 on peak inward current. About 5 min or longer was needed for the drug to reach its steady-state effect at the lower concentrations. Figure 2(b)(ii) shows data from 6 cells. The peak inward current before application of UK-84149 was normalized at 100%. The ID_{50} value for the effect of UK-84149 on peak inward current was 2.3 μM.

Figure 3 shows the effects of UK-84149 on inward and outward currents from guinea-pig jejunum smooth muscle cells. In these experiments, high K solution was used in the pipette solution. When the cell was stepped more positive than − 20 mV from − 80 mV, both inward and outward currents were observed (Figure 3(a)(i) and (ii)). Figure 3(a)(i) and (a)(ii) shows the effect of UK-84148 on the current-voltage relationship of inward and outward currents which were inhibited at all potentials (− 20 to + 30 mV) after application for 10 min. Figure 3(b)(i) and (ii) shows the relationship between the amplitude of inward and outward currents and concentrations of UK-84149. Inward and outward currents were evoked by stepping to + 10 mV for 300 ms from − 80 mV, every 20 s. Figure 3(b)(i) shows the effect of UK-84149 on peak inward, peak and end of pulse outward current from one cell. It seems that UK-84149 was much slower to take effect on inward current than on outward currents, with a delayed start and a delayed steady-state (Figure 3(b)(i)). Figure 3(b)(ii) shows the data from 4 cells. UK-84149 was a more potent inhibitor of the end of pulse outward current than the peak outward current and accelerated the decay of the outward current. The ID_{50}s for the effects of UK-84149 on peak inward, peak outward and end of pulse outward current were 2.3, 7.2 and 3.3 μM, respectively.

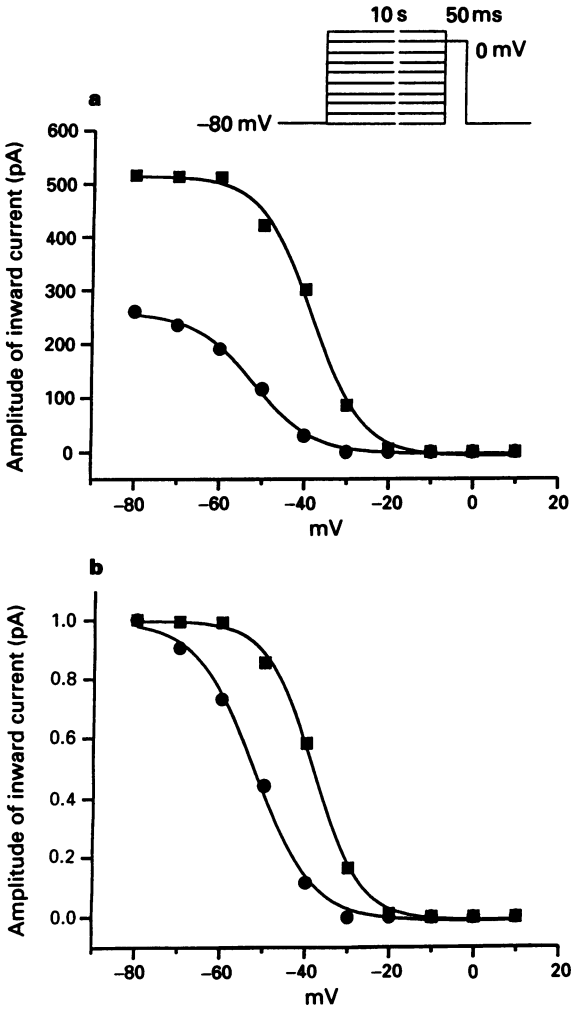

Figure 4 Effect of UK-84149 on voltage-dependent inactivation of the inward current in a guinea-pig jejunal smooth muscle cell. The duration of the conditioning pulse (pre-pulse) was 10 s. (a) Absolute amplitude of inward current evoked by the test pulse (50 ms in duration, stepped to 0 mV from the appropriate membrane potential set by the conditioning pulse). The interval between conditioning pulses was 20 s. (b) Relative amplitude of inward current. The inward current amplitude evoked by the test pulse, without conditioning (the holding potential was − 80 mV) was normalized as 1.0. (■) Control; (●) 3 μM UK. Solid lines were drawn from Boltzmann's equation (see text). The value of V_h in this cell was − 39 mV for control and − 52 mV in 3 μM UK-84149. The slope was 5.5 for control, and 7 in 3 μM UK-84149. Average V_h values from another 5 cells were − 37 ± 2 mV (mean ± s.e.mean) for control and − 50 ± 2.2 mV in 3 μM UK-84148, and for the slope, 6.2 ± 0.4 for control and 7.3 ± 0.1 in 3 μM UK-84149.

The effect of UK-84149 on the availability of the inward current

The availability of the inward current was tested by means of a double pulse protocol. The peak inward current was evoked by a test potential of 0 mV after holding for 10 s at various conditioning potentials. The holding potential was − 80 mV. Double pulses were applied at 20 s intervals. In the control, the inward current amplitude evoked by a test pulse was reduced when conditioning potentials were more positive than − 60 mV. Figure 4a shows that the current was half available at $V_h = -30$ mV, and the slope, V_s, was 5.5, when a Boltzmann equation of the form $I/I_{max} = (1 + \exp((V\text{-}V_h)/V_s))^{-1}$ was fitted to the inactivating component of the current. V is the conditioning potential and I/I_{max} the fraction of the current available relative to that available from − 80 mV. UK-84149 (3 μM) reduced the inward current amplitude from all potentials and shifted the steady state inactivation curve to the left (Figure 4b). V_h was shifted to − 58 mV, and the slope value to 7 in this cell. Similar changes were observed in another 5 cells, with a mean value of V_h shifted from − 37 ± 2 mV (control, $n = 5$) to − 50 ± 2.2 mV ($n = 5$), and of V_s from 6.2 ± 0.4 (control, $n = 5$) to 7.3 ± 0.1 ($n = 5$).

Use-dependent actions of UK-84149

Inward current block by verapamil and D600 is known to be use-dependent; UK-84149 seemed to have a similar property. As shown in Figures 2 and 3, it took a long time for UK-84149 to reach its steady-state effect. Figure 5 shows the results of an investigation of the use-dependence of UK-84149, verapamil and nicardipine on inward current in guinea-pig jejunum smooth muscle cells. Inward current was evoked by stepping from − 80 mV to 0 mV for 50 ms, every 20 s. The amplitude of the peak inward current was plotted against time. After rupture of the cell membrane the drugs were not applied until the inward current became stable. Figure 5a shows the effect of control PSS and verapamil (3 μM) on inward current. The cell had an inward current size

of about 600 pA. When the command pulse was stopped for 3 min in control PSS, which is indicated by the first interruption between the open circles, the peak inward current amplitude was temporarily very slightly increased. When the command pulse was stopped for another 3 min in verapamil (3 μM), the inward current amplitude evoked by the first command pulse after rest was not changed, compared with that before rest. Thereafter the current gradually decreased in the continuous presence of 3 μM verapamil and reached a steady state after about 3 min. When pulses were again stopped in the presence of verapamil (3 μM), inward current evoked by the first pulse after stopping had recovered to about 80% of the control size. Figure 5b shows that a high concentration of verapamil (10 μM) also had a use-dependent action. Both cells showed good recovery of inward current after washout of verapamil. Figure 5c shows the effect of nicardipine on inward current. In contrast to verapamil, nicardipine had little use-dependent action on the inward current. Upon resting in the presence of nicardipine (0.1 μM) for 3 min, the inward current evoked by the first pulse was 33% of current size before rest, which was almost the same value as that after 5 min stimulation. UK-84149, more like verapamil, showed similar use-dependent action on inward current (Figure 5d). After resting in the presence of 3 μM UK-84149 for 3 min, the amplitude of the inward current evoked by the first pulse did not change, compared with that before rest. Thereafter it decreased gradually and reached a steady state about 10 min later. However unlike verapamil, resting in the continuous presence of UK-84148 (3 μM) did not improve inward current, and also it took a long time to

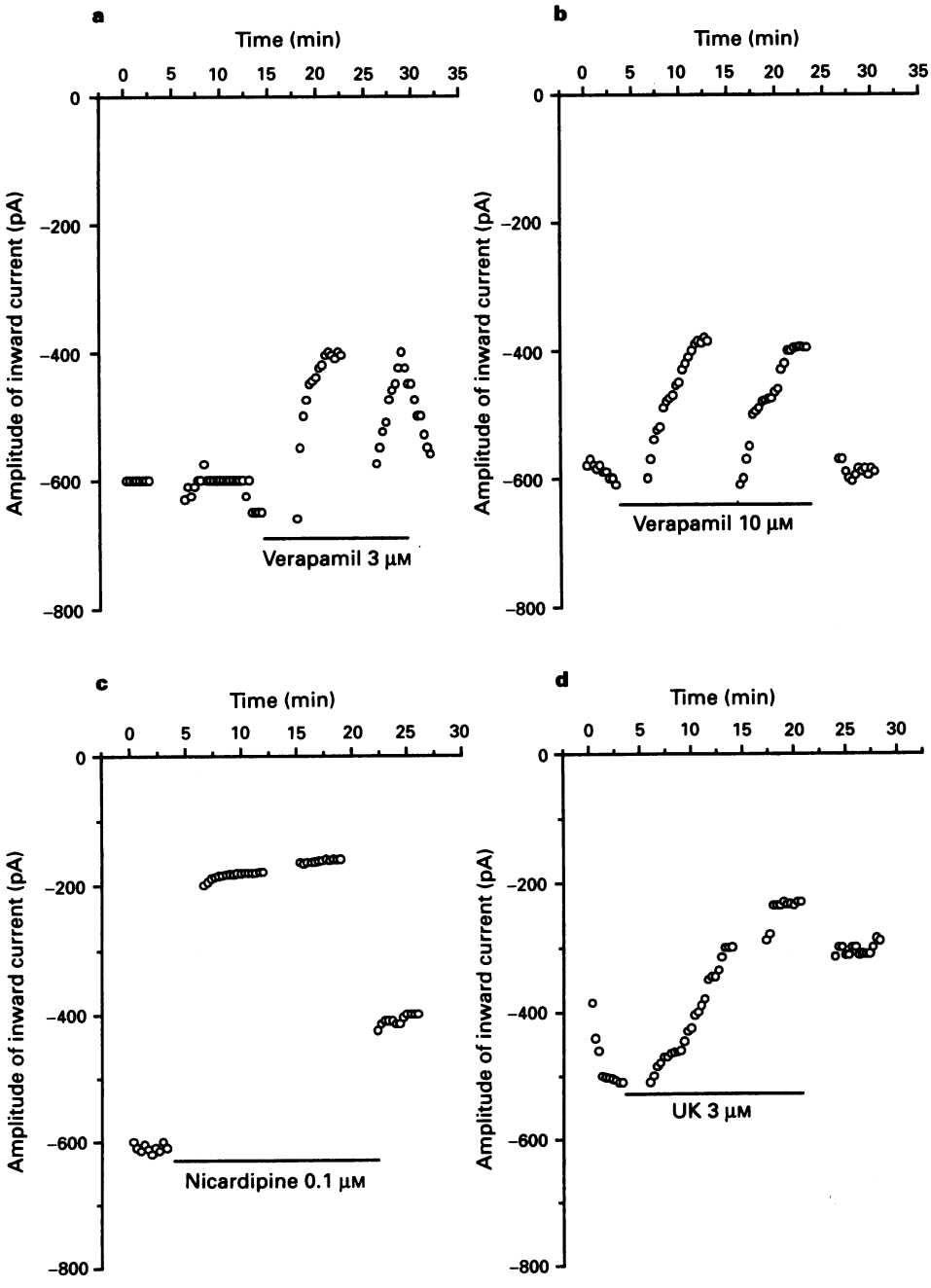

Figure 5 Time courses of inhibition by verapamil (a,b), nicardipine (c) and UK-84149 (d) of inward current in guinea-pig jejunum smooth muscle cells. Inward current was evoked by stepping from − 80 mV to 0 mV for 50 ms every 20 s. Peak inward current before and after application of 3 μM (a) and 10 μM (b) verapamil, 0.1 μM nicardipine (c) and 3 μM UK-84149 (d) were plotted against time. The interruption between the circles indicates that command pulses were stopped for 3 min. Some recovery of inward current occurred after rest periods in the cases of verapamil (3 and 10 μM) but not nicardipine or UK-84149.

wash out the effect of UK-84149 on inward current. The poor recovery of the inward current after stopping stimulation in the continuous presence of UK-84148 (3 μM) was probably due to the strong binding of UK-84148 to the receptor. To clarify the use-dependent effect of UK-84148, cells from guinea-pig jejunum were exposed to UK-84148 (3 μM) for 10 min before stimulating, and the block of the inward current was compared with that achieved with continuous repetitive simulation for 10 min in the presence of UK-84148 (3 μM). Figure 6 shows the results of these experiments. When cells were exposed to UK-84148 (3 μM) for 10 min before stimulating, the inward current was only slightly inhibited, although the inward current gradually decreased after the stimulation was reapplied to the cell in the continuous presence of UK-84148 (Figure 6a). However, when the cell was exposed to UK-84148 (3 μM) for 10 min and was repetitively simulated without any rest period the inward current was greatly inhibited (Figure 6b). Figure 6c shows the summarized data. In 4 cells, the inhibition of the inward current by UK-84148 (3 μM) without stimulation was 5.3 ± 3.6% (from 486 ± 60 pA to 470 ± 51 pA) which was significantly ($P < 0.01$) less than that with repetitive stimulation (52 ± 8%; from 455 ± 59 pA to 219 ± 50 pA, $n = 4$).

Effects of UK-84149, D600 and nicardipine on inward currents from rabbit jejunum and coronary artery smooth muscle cell

Figure 7 shows the effect of UK-84149 on inward current from rabbit jejunum and coronary artery smooth muscle cells, compared with the effects of D600 and nicardipine. The nystatin recording method was used in these experiments. The cell was held at − 80 mV and stepped to 0 mV for 50 ms, every 20 s. A 10 ms 10 mV depolarizing pulse was used to monitor the series resistance. The drugs were bath applied and perfusion was continuous at a rate of 2 ml min^{-1}. Cadmium (100 μM) was used to abolish inward current completely at the end of the experiments and create a base line for measurement. Figure 7(a)(i) shows the effect of UK-84149 (3 μM) on inward current in jejunum (left) and coronary artery (right) smooth muscle cells. UK-84149 (3 μM) inhibited inward current from both types of smooth muscle cells and with a similar potency. At this concentration, the effect could be reversed by washing, although it took a long time (about 15 min). Figure 7(a)(ii) shows the concentration-effect relationship for the effect of UK-84149 on inward current from the two types of smooth muscle cells. The amplitude of inward current before application was normalised as 100%. The ID_{50} values were not significantly different (analysis of variance, $P > 0.05$) (1.7 μM for jejunum (squares) and 3.2 μM for coronary artery (circles) smooth muscle cells). Figure 7(b)(i) shows the effect of D600, and Figure 7(c)(i) shows the effect of nicardipine on the two types of smooth muscle cell. Again, no significant differences were found. The ID_{50} values for the effect of D600 on inward current were 8.1 μM for jejunum and 3.9 μM for coronary artery smooth muscle cells (Figure 7(b)(ii)). The ID_{50} values for the effect of nicardipine on inward current were 24 nM for jejunum and 12 nM for coronary artery smooth muscle cells. Among the three Ca antagonists, nicardipine was most potent in both jejunum and coronary artery cells. UK-84149 was 2–5 times more potent than D600 but 200–300 times less potent than nicardipine.

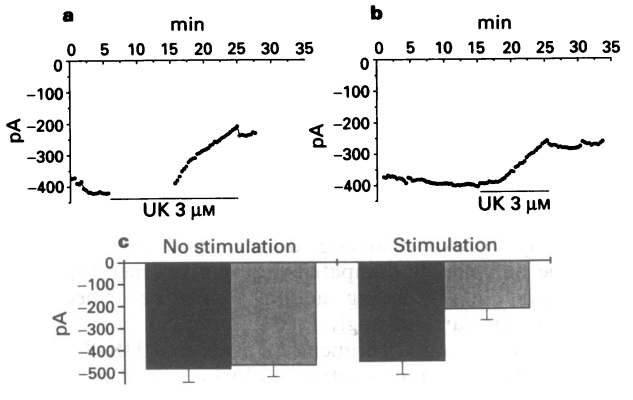

Figure 6 Use-dependency of inhibition of UK-84149 of inward current in guinea-pig jejunum smooth muscle cells. Inward current was evoked by stepping from − 80 mV to 0 mV for 50 ms every 20 s. (a) Stimulation was stopped (as indicated by interruption between the circle symbols) for 10 min in the presence of UK-84149 (3 μM). (b) UK-84149 (3 μM) was applied to a repetitively stimulated cell for 10 min. (c) The peak inward current amplitude is shown (mean ± s.e.mean) in the absence (solid columns) and presence (stippled columns) of 3 μM UK-84149 with and without stimulation.

Discussion

The main finding of the present experiments was that UK-84149 inhibited the Ca inward current evoked in smooth muscle cells from the guinea-pig and rabbit jejunum and rabbit coronary artery cell with a potency similar to that of D600 although it was less potent than nicardipine. The effect of UK-84149 was long-lasting and voltage-dependent. Like verapamil, UK-84149 showed use-dependent block. UK-84149 inhibited voltage-dependent outward current as well as inward current. This was not surprising because many Ca antagonists, including nicardipine, verapamil and diltiazem have been shown to be blockers of voltage-dependent outward currents in smooth muscle cells (Terada *et al.*, 1987a). Since 5 mM EGTA was included in the pipette in the present experiments and the outward current was evoked by stepping only to + 10 mV, there should be little activation of large-conductance, Ca-activated potassium channels. Therefore the effect of UK-84149 on outward current is unlikely to be due to the inhibition of Ca^{2+} influx via voltage-dependent Ca channels. The ratio of ID_{50} values for the inhibition of UK-84149 of peak outward and inward current was about 3 (7.2 μM/2.3 μM) which was much lower than that of nicardipine on rabbit jejunum cell which and had a similar ratio to D600 (ratio of ID_{50} values was 11, Terada *et al.*, 1987a). Like the effect of verapamil and nicardipine on rabbit ileum smooth muscle cells (Terada *et al.*, 1987a), UK-84149 accelerated the outward current decay. In general, the selectivity of the Ca antagonists for the Ca inward current in smooth muscle cells was low in comparison with that seen in cardiac cells (Hume, 1985). However, the ID_{50} values for the inhibition of outward current by different Ca antagonists in different tissues (smooth muscle, cardiac and neurone) were quite similar, ranging from 1–16 μM (Nishi *et al.*, 1983; Hume, 1985; Terada *et al.*, 1987a; Figure 3), but the ID_{50} values for the inhibition of inward current by different Ca antagonists in different tissues were dramatically different, ranging from 16 nM to 9 μM (Nishi *et al.*, 1983; Hume, 1985; Terada *et al.*, 1987b,c; Figure 6). Hence, inhibition of voltage-dependent outward currents by Ca antagonists seems to be due to a non-specific blocking action of higher concentrations.

UK-84149 shifted the voltage-dependent inactivation curve to the left. Nicardipine and other dihydropyridines have been shown to shift the voltage-dependent inactivation curve to the left when the conditioning pulses were 10 s (the same condition as used in the present experiment) (Terada *et al.*, 1987b,c). Therefore, shifting the voltage-dependent inactivation curve to the left seems to be one of the common features of calcium channel blockers.

In most smooth muscles the Ca current can be dissected into components on the basis of its voltage- and time-dependent properties (Aaronson *et al.*, 1986; Caffrey *et al.*,

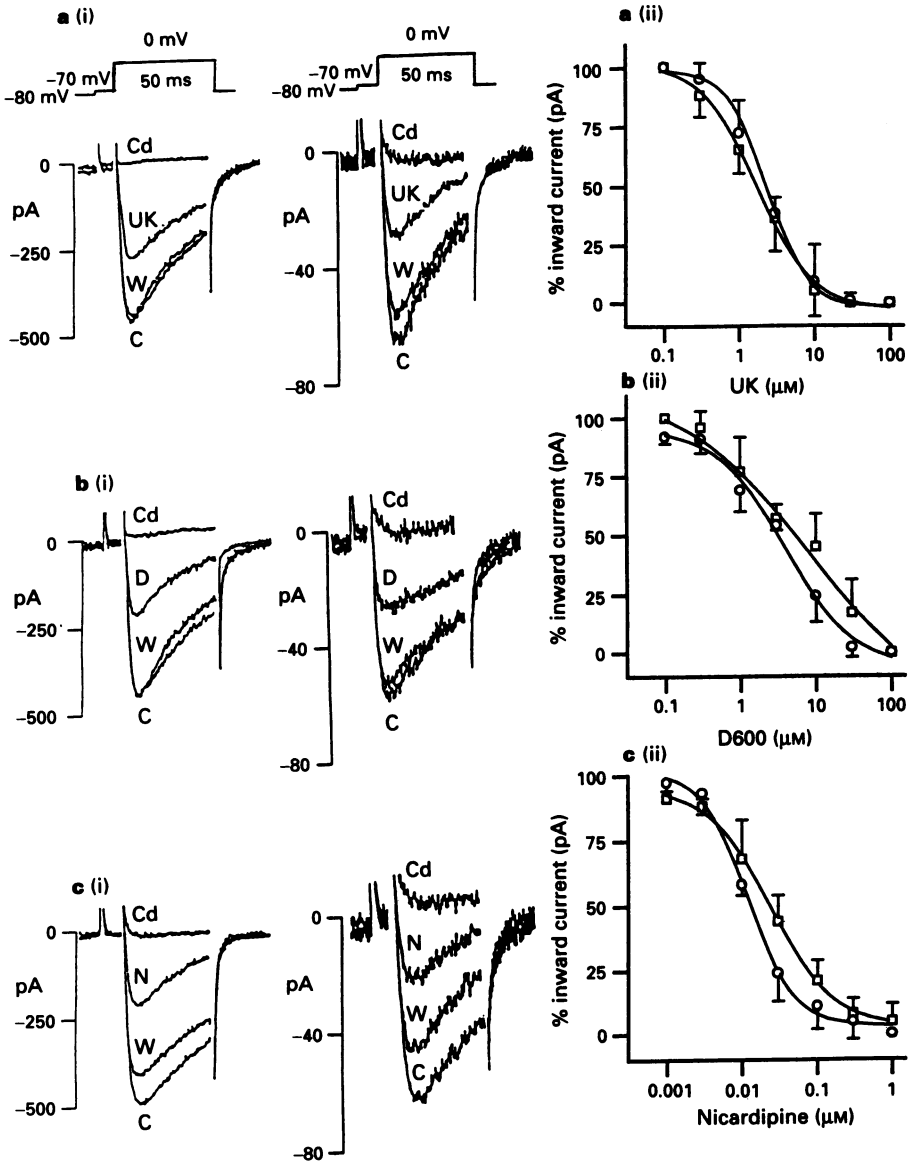

Figure 7 Effect of UK-84149, D600 and nicardipine on inward current of rabbit coronary artery and jejunum smooth muscle cells. Cell was held at − 80 mV and stepped to 0 mV for 50 ms, every 20 s. Nystatin (100 μg ml^{-1}) was included in $CsCl_2$ pipette solution to make perforated patch whole cell recordings. (a)(i), (b)(i), (c)(i): Effect of 3 μM UK-84149 (UK), 3 μM D600 (D) and 0.03 μM nicardipine (N) on inward current from jejunum (left panel) and coronary artery (right panel) smooth muscle cells. Cadmium (Cd) 100 μM was applied at the end of the experiments. C control, W after washout. (a)(ii), (b)(ii), (c)(ii): Concentration-effect relationship for the effect of UK-84149, D600 and nicardipine on inward current from jejunum (□) and coronary artery (○) smooth muscle cell. No significant differences were found for all three drugs among jejunum and coronary artery smooth muscle cells. The ID_{50}s: UK-84149, 1.7 μM for jejunum cells, and 3.2 μM for coronary artery cells (analysis of variance, $P > 0.05$, 3–8 cells); D600, 8.1 μM for jejunum cells, and 3.9 μM for coronary artery cells ($P > 0.05$, 3–6 cells); nicardipine, 0.024 μM for jejunal cell, and 0.012 μM for coronary artery cells ($P > 0.05$, 2–7 cells).

1986). The diversity of Ca channels might contribute to the diversity of responses of Ca current to Ca antagonists. The effect of calcium antagonists on Ca current may be tissue-dependent, voltage-dependent and use or frequency-dependent. Nicardipine and other dihydropyridines are the most potent calcium antagonists and their effects are voltage-dependent. Verapamil and D600 have a use-dependent action (Terada *et al.*, 1987b; present data). In the present experiments, UK-84149 showed a use-dependent block which may explain, at least partially, why UK-84149 was more potent on the bowel than on blood vessel (Quinn & Wallis, 1994; Wallis *et al.*, 1994), since bowel has a high rate of spontaneous activity and artery is quiescent under normal conditions. Any blockade arising during spontaneous activity would be only slowly dissipated during a rest period; during hypermotility its blocking action would be expected to develop particularly strongly.

In conclusion, our experiments indicate that UK-84149 is a calcium antagonist and is active in blocking voltage-activated calcium current. UK-84149 might be expected to be useful in conditions such as irritable bowel syndrome which are characterized by hypermotility of the smooth muscle.

This work was supported by Pfizer Ltd. We are grateful to Dr R.M. Wallis for advice.

References

AARONSON, P.I., BENHAM, C.D., BOLTON, T.B., HESS, P., LANG, T.J. & TSIEN, R.W. (1986). Two types of single-channel and whole-cell calcium or barium currents in single smooth muscle cells of rabbit ear artery. *J. Physiol.*, **377**, 36P.

CAFFREY, J.M., JOSEPHSON, I.R. & BROWN, A.M. (1986). Calcium channels of amphibian stomach and mammalian aorta smooth muscle cells. *Biophys. J.*, **49**, 1237–1242.

HAMILL, O.P., MARTY, A., NEHER, E., SAKMANN, B. & SIGWORTH, F.J. (1981). Improved patch clamp techniques for high resolution current recordings from cells and cell-free membrane patches. *Pflügers Arch.*, **391**, 85–100.

HORN, R. & MARTY, A. (1988). Muscarinic activation of ionic currents measured by a new whole-cell recording method. *J. Gen. Physiol.*, **92**, 145–149.

HUME, J.R. (1985). Comparative interaction of organic Ca^{2+} channel antagonists with myocardial Ca^{2+} and K^+ channel. *J. Pharmacol. Exp. Ther.*, **234**, 134–140.

NISHI, K., AKAKE, N., OYAMA, Y. & ITO, H. (1983). Actions of calcium antagonists on calcium currents in helix neurones: specificity and potency. *Circ. Res.*, **52** (suppl I), 53–59.

QUINN, P. & WALLIS, R.M. (1994). UK-84,149: a potent and gut-selective spasmolytic in the anaesthetised dog. *Br. J. Pharmacol.*, **112**, 573P.

TERADA, K., KITAMURA, K. & KURIYAMA, H. (1987a). Different inhibition of the voltage-dependent K^+ current by Ca^{2+} antagonists in the smooth muscle cell membrane of rabbit small intestine. *Pflügers Arch.*, **408**, 558–564.

TERADA, K., KITAMURA, K. & KURIYAMA, H. (1987b). Blocking actions of Ca antagonists on the Ca channels in the smooth muscle cell membrane of rabbit small intestine. *Pflügers Arch.*, **408**, 552–557.

TERADA, K., NAKAO, K., OKABE, K., KITAMURA, K. & KURIYAMA, H. (1987c). Action of 1,4-dihydropyridine derivative, KW-3049, on the smooth muscle membrane of the rabbit mesenteric artery. *Br. J. Pharmacol.*, **92**, 615–625.

WALLIS, R.M., ALKER, D., BURGES, R.A., CROSS, P.E., GREENGRASS, P.M., MCINTYRE, P. & QUINN, P. (1994). UK-84,149: A novel gut-selective spasmolytic with calcium antagonist activity. *Br. J. Pharmacol.*, **112**, 574P.

(Received November 24, 1994
Revised December 28, 1994
Accepted January 6, 1995)

British Journal of Pharmacology (1995) 114, 1666-1672 © 1995 Stockton Press All rights reserved 0007-1188/95 $12.00

Aminoguanidine attenuates the delayed circulatory failure and improves survival in rodent models of endotoxic shock

Chin-Chen Wu, Shiu-Jen Chen, Csaba Szabó, [1]Christoph Thiemermann & John R. Vane

The William Harvey Research Institute, St. Bartholomew's Hospital Medical College, Charterhouse Square, London EC1M 6BQ

1 We have investigated the effects of aminoguanidine, a relatively selective inhibitor of the cytokine-inducible isoform of nitric oxide synthase (iNOS), on the delayed circulatory failure, vascular hyporeactivity to vasoconstrictor agents, and iNOS activity in a rat model of circulatory shock induced by bacterial endotoxin (*E. coli* lipopolysaccharide; LPS). In addition, we have evaluated the effect of aminoguanidine on the 24 h survival rate in a murine model of endotoxaemia.

2 Male Wistar rats were anaesthetized and instrumented for the measurement of mean arterial blood pressure (MAP) and heart rate (HR). Injection of LPS (10 mg kg^{-1}, i.v.) resulted in a fall in MAP from 115 ± 4 mmHg (time 0, control) to 79 ± 9 mmHg at 180 min ($P<0.05$, $n=10$). The pressor effect of noradrenaline (NA, 1 μg kg^{-1}, i.v.) was also significantly reduced at 60, 120 and 180 min after LPS injection. In contrast, animals pretreated with aminoguanidine (15 mg kg^{-1}, i.v., 20 min prior to LPS injection) maintained a significantly higher MAP (at 180 min, 102 ± 3 mmHg, $n=10$, $P<0.05$) when compared to rats given only LPS (LPS-rats). Cumulative administration of aminoguanidine (15 mg kg^{-1} and 45 mg kg^{-1}) given 180 min after LPS caused a dose-related increase in MAP and reversed the hypotension. Aminoguanidine also significantly alleviated the reduction of the pressor response to NA: indeed, at 180 min, the pressor response returned to normal in aminoguanidine pretreated LPS-rats.

3 Thoracic aortae obtained from rats at 180 min after LPS showed a significant reduction in the contractile responses elicited by NA (10^{-9}-10^{-6} M). Pretreatment with aminoguanidine (15 mg kg^{-1}, i.v., at 20 min prior to LPS) significantly prevented this LPS-induced hyporeactivity to NA *ex vivo*.

4 Endotoxaemia for 180 min resulted in a significant increase in iNOS activity in the lung from 0.6 ± 0.2 pmol mg^{-1} min^{-1} (control, $n=4$) to 4.8 ± 0.3 pmol mg^{-1} min^{-1} ($P<0.05$, $n=6$). In LPS-rats treated with aminoguanidine, iNOS activity in the lung was attenuated by 44 ± 5% ($n=6$, $P<0.05$). Moreover, when added *in vitro* to lung homogenates obtained from LPS-rats, aminoguanidine and N^{ω}-nitro-L-arginine methyl ester (L-NAME; 10^{-8} to 10^{-3} M) caused a concentration-dependent inhibition of iNOS activity ($n=3$-6, IC_{50}: 30 ± 12 and 11 ± 6 μM, respectively $P>0.05$). In contrast, aminoguanidine was a less potent inhibitor than L-NAME of the constitutive nitric oxide synthase in rat brain homogenates ($n=3$-6, IC_{50} is 140 ± 10 and 0.6 ± 0.1 μM, respectively, $P<0.05$). In addition, the inhibitory effect of aminoguanidine on iNOS activity showed a slower onset than that of L-NAME (maximal inhibition at 90 min and 30 min, respectively).

5 Treatment of conscious Swiss albino (T/O) mice with a high dose of endotoxin (60 mg kg^{-1}, i.p.) resulted in a survival rate of only 8% at 24 h ($n=12$). However, therapeutic application of aminoguanidine (15 mg kg^{-1}, i.p. at 2 h and 6 h after LPS) increased the 24 h survival rate to 75% ($n=8$), whereas L-NAME (3 mg kg^{-1}, i.p. at 2 h and 6 h after LPS) did not affect the survival rate (11%, $n=9$).

6 Thus, aminoguanidine inhibits iNOS activity and attenuates the delayed circulatory failure caused by endotoxic shock in the rat and improves survival in a murine model of endotoxaemia. Aminoguanidine, or novel, more potent selective inhibitors of iNOS may be useful in the therapy of septic shock.

Keywords: Aminoguanidine; nitric oxide; endotoxic shock; nitric oxide synthase; vascular hyporeactivity; survival rate

Introduction

The formation of nitric oxide (NO) from one of the terminal guanidino nitrogen atoms of L-arginine is catalysed by NO synthase (NOS). Three distinct isoforms of NOS have recently been cloned, sequenced and expressed (see Dinerman *et al.*, 1993; Moncada & Higgs, 1993). The NOS in endothelial cells (eNOS; M_r 130 kD) and neuronal cells (nNOS; M_r 150 kD) are expressed constitutively and their activity is regulated by changes in intracellular calcium. Under physiological conditions, the release of NO by the eNOS in endothelial cells causes vasodilatation and in concert with the sympathetic nerves, regulates blood vessel diameter, organ blood flow and blood pressure (see Moncada *et al.*, 1991). Activation of macrophages with endotoxin and/or cytokines results in the *de novo* biosynthesis of a calcium-independent (inducible) isoform of NOS (iNOS; M_r 130 kD), which produces large amounts of NO (see Moncada & Higgs, 1993). The induction of iNOS by endotoxin or cytokines greatly contributes to the bactericidal and tumouricidal effects of these cells (Stuehr & Nathan, 1989; see Nathan, 1992). However, endotoxin also induces iNOS in vascular smooth muscle cells, fibroblasts, hepatocytes, Kupffer cells, keratinocytes and megakaryocytes *in vitro*, which is reflected by induction in tissues *in vivo* such as lung, spleen, liver, heart, kidney and blood vessels (see Nathan, 1992; Moncada & Higgs, 1993; Thiemermann, 1994).

The circulatory failure in shock of various aetiologies is characterized by systemic vasodilatation, hyporeactivity to vasoconstrictor agents and organ ischaemia leading to multiple organ failure and death. An enhanced formation of NO importantly contributes to the acute (eNOS) and delayed (iNOS) hypotension and vascular hyporeactivity to

[1] Author for correspondence.

noradrenaline in endotoxic shock (Thiemermann & Vane, 1990; Julou-Schaeffer *et al.*, 1990; Kilbourn *et al.*, 1990; Meyer *et al.*, 1992; Suba *et al.*, 1992; Wright *et al.*, 1992; Szabo *et al.*, 1993a). An enhanced formation of NO by iNOS also accounts for the hypotension associated with cytokine-chemotherapy (Kilbourn & Griffith, 1992). Thus, there is strong experimental evidence that the overproduction of NO, particularly by iNOS, is a key factor in the development of circulatory failure in shock of various aetiologies (see Thiemermann, 1994).

With non-selective inhibitors of iNOS, the concomitant inhibition of eNOS in the endothelium may increase the incidence of organ ischaemia, microvascular thrombosis and mortality (Hutcheson *et al.*, 1990; Harbrecht *et al.*, 1992; Shultz & Raij, 1992; Wright *et al.*, 1992). Thus, the beneficial haemodynamic effects of non-selective NOS inhibitors may well be due to iNOS inhibition, while the reported adverse effects may be due to inhibition of eNOS.

Aminoguanidine is a more potent inhibitor of iNOS than N^{ω}-substituted arginine analogues. In addition, aminoguanidine is less potent as an inhibitor of the constitutive NOS activity in cultured cells, isolated blood vessels and enzyme preparations *in vitro* (Corbett *et al.*, 1992; Griffiths *et al.*, 1992; Misko *et al.*, 1993; Tilton *et al.*, 1993). Here, we investigate the effects of aminoguanidine on the delayed circulatory failure (vasodilatation, hyporeactivity to vasoconstrictor agents) and induction of iNOS in endotoxic shock in the anaesthetized rat. In addition, we have evaluated the effects of aminoguanidine and N^{ω}-nitro-L-arginine methyl ester (L-NAME), a non-isoenzyme selective NOS inhibitor, on survival rate in a murine model of endotoxaemia.

Methods

Endotoxic shock

Male Wistar rats (240–300 g; Glaxo Laboratories Ltd., Greenford, Middx.) were anaesthetized with thiopentone sodium (Trapanal; 120 mg kg^{-1}, i.p.). The trachea was cannulated to facilitate respiration and rectal temperature was maintained at 37°C with a homeothermic blanket (Bio-Sciences, Sheerness, Kent). The right carotid artery was cannulated and connected to a pressure transducer (P23XL, Spectramed, Statham, U.S.A.) for the measurement of phasic and mean arterial blood pressure (MAP) and heart rate (HR) which were displayed on a Grass model 7D polygraph recorder (Grass Instruments, Quincy, MA, U.S.A.). The left femoral vein was cannulated for the administration of drugs. Upon completion of the surgical procedure, cardiovascular parameters were allowed to stabilize for 20 min. After recording baseline haemodynamic parameters, animals were treated with vehicle (0.1 N HCl neutralized to pH 7.4 with 0.1 N NaOH, $n = 10$) or aminoguanidine (15 mg kg^{-1}, i.v., $n = 10$), and 10 min later the pressor response to noradrenaline (NA, 1 μg kg^{-1}, i.v.) was recorded. At 20 min after injection of vehicle or aminoguanidine, animals received *E. coli* lipopolysaccharide (LPS, 10 mg kg^{-1}, i.v.) as a slow injection over 10 min and pressor responses to NA were reassessed at 30, 60, 120, and 180 min after LPS injection.

In other experiments, the pressor effects elicited by aminoguanidine in sham-operated rats (control) were compared with those in rats treated with LPS for 180 min. The effects of aminoguanidine on the delayed hypotension caused by LPS were also studied. In these experiments, rats were anaesthetized and instrumented (as above) and treated with either vehicle (control, $n = 5$) or LPS (10 mg kg^{-1}, i.v., $n = 8$). At 180 min after injection of vehicle or LPS, two doses of aminoguanidine (15 and 45 mg kg^{-1}, i.v. bolus) were administered in a cumulative manner and the haemodynamic parameters were monitored for a period of 30 min.

Organ bath experiments

At 180 min after the injection of LPS, thoracic aortae were obtained from sham-operated controls as well as from rats pretreated either with vehicle or with aminoguanidine. The vessels were cleared of adhering periadventitial fat and the thoracic aortae were cut into rings of 3–4 mm width. The endothelium was removed by gently rubbing the intimal surface. The lack of a relaxation to acetylcholine (1 μM) following pre-contraction of rings with NA (1 μM) was considered as evidence that the endothelium had been removed. The rings were mounted in 10 ml organ baths filled with warmed (37°C), oxygenated (95% O_2/5% CO_2) Krebs solution (pH 7.4) consisting of (mM): NaCl 118, KCl 4.7, KH_2PO_4 1.2, $MgSO_4$ 1.17, $CaCl_2$ 2.5, $NaHCO_3$ 25 and glucose 5.6. Indomethacin (5.6 μM) was added to prevent the production of prostanoids. Isometric force was measured with Grass FT03 type transducers (Grass Instruments, Quincy, MA, U.S.A.) and recorded on a Grass model 7D polygraph recorder (Grass Instruments, Quincy, MA, U.S.A.). A tension of 2 g was applied and the rings were equilibrated for 60 min, changing the Krebs solution every 15 min (Thiemermann *et al.*, 1993). Dose-response curves to NA (10^{-9}–10^{-6} M) were obtained in all experimental groups.

Nitric oxide synthase assay

Lungs from LPS-rats pretreated with either vehicle (saline, control) or aminoguanidine were removed at 180 min and frozen in liquid nitrogen. Lungs from sham-operated rats were also prepared for determination of baseline NOS activity. Lungs were stored for no more than 2 weeks at −80°C before assay. Frozen lungs were homogenized on ice with an Ultra-Turrax T 25 homogenizer (Janke & Kunkel, IKA Labortechnik, Staufen i. Br., Germany) in a buffer composed of: Tris-HCl 50 mM, EDTA 0.1 mM EGTA 0.1 mM, 2-mercaptoethanol 12 mM and phenylmethylsulphonyl fluoride 1 mM (pH 7.4). Conversion of [^{3}H]-L-arginine to [^{3}H]-L-citrulline was measured in the homogenates as described by Szabo *et al.* (1993). Briefly, tissue homogenates (30 μl, approx. 60 μg protein) were incubated in the presence of [^{3}H]-L-arginine (10 μM, 5 kBq/tube), NADPH (1 mM), calmodulin (30 nM), tetrahydrobiopterin (5 μM) and calcium (2 mM) for 25 min at 25°C in HEPES buffer (pH 7.5). Reactions were stopped by dilution with 1 ml of ice cold HEPES buffer (pH 5.5) containing EGTA (2 mM) and EDTA (2 mM). Reaction mixtures were applied to Dowex 50W (Na^+ form) columns and the eluted [^{3}H]-L-citrulline activity was measured by scintillation counting (Beckman, LS3801; Fullerton, CA, U.S.A.). Experiments performed in the absence of NADPH determined the extent of [^{3}H]-L-citrulline formation independent of a specific NOS activity. Experiments in the presence of NADPH, without calcium and with EGTA (5 mM), determined the calcium-independent iNOS activity.

The effects of aminoguanidine and L-NAME on iNOS activity (lungs from LPS-rats) were compared with those on nNOS activity (brains from control rats). Homogenates of lungs obtained from rats treated with LPS for 180 min and brains obtained from control rats were prepared by the above method. Lung or brain homogenates (20 μl, approximately 40 μg protein) were incubated with either vehicle (control), aminoguanidine or L-NAME (10^{-8} to 10^{-3} M) and the conversion of [^{3}H]-L-arginine to [^{3}H]-L-citrulline was measured as described above.

Protein concentration was measured spectrophotometrically in 96-well plates with Bradford reagent (Bradford, 1976), with bovine serum albumin used as standard.

Survival studies

Survival studies were performed in Swiss albino mice (T/O mice; 28–30 g; Tuck Laboratories, U.K.). LPS (60 mg kg^{-1},

i.p.) was injected in the presence of vehicle or drugs and survival was monitored every 3 h for 24 h. Different groups of animals received vehicle (saline) together with LPS ($n = 12$), LPS plus L-NAME (3 mg kg^{-1} at 2 h and 6 h after LPS, $n = 9$), or LPS plus aminoguanidine (15 mg kg^{-1} at 2 h and 6 h after LPS, $n = 8$). Thus, we chose a dose of aminoguanidine for these survival studies, which did not cause a significant rise in blood pressure in normal rats in order to evaluate whether a dose which has only minor effects on eNOS is sufficient to improve survival. Similarly, a relatively low dose of L-NAME, which causes a moderate, but not dramatic increase in blood pressure in normal rats (Hecker *et al.* 1990), was chosen for comparison.

Materials

Calmodulin, bacterial lipopolysaccharide (*E. coli* serotype 0.127:B8), NADPH, aminoguanidine bicarbonate, acetylcholine chloride, noradrenaline bitartrate, N^{ω}-nitro-L-arginine methyl ester, and Dowex 50W anion exchange resin were obtained from Sigma Chemical Co. (Poole, Dorset). Aminoguanidine, like other guanidine derivatives (see Hasan *et al.* 1993 for chemical structures), contains the guanidino group that is found in the side chain of L-arginine and L-arginine based derivatives. Aminoguanidine was dissolved in 0.1 N HCl and subsequently neutralized (pH 7.4) in 0.1 N NaOH. All other solutions were made in saline or distilled water. L-[2,3,4,5-^{3}H]-arginine hydrochloride was obtained from Amersham (Buckinghamshire). Tetrahydrobiopterin (6R-L-erythro-5,6,7,8-tetrahydrobiopterin) was obtained from Dr B. Schircks Laboratories (Jona, Switzerland).

Statistical evaluation

All values in the figures and text are expressed as mean ± s.e. mean of n observations, where n represents the number of animals or blood vessels studied. A two way analysis of variance (ANOVA) followed by, if appropriate, a Bonferoni's test was used to compare means between groups. A P-value less than 0.05 was considered to be statistically significant.

Results

Aminoguanidine attenuates the cardiovascular changes caused by LPS in the anaesthetized rat

Baseline values for MAP and HR of the vehicle- and aminoguanidine-pretreated animal groups were 115 ± 4 and 112 ± 2 mmHg, and 400 ± 16 and 401 ± 17 beats min^{-1} respectively, and were not significantly different between these groups. Administration of LPS (10 mg kg^{-1}, i.v.) caused a fall in MAP from 115 ± 4 mmHg to 78 ± 6 mmHg ($n = 10$, $P < 0.05$) at 60 min. Thereafter, MAP remained significantly reduced (e.g. at 180 min, MAP was 79 ± 9 mmHg; $n = 10$; Figure 1a). Endotoxaemia for 180 min was not associated with a significant change in HR (Figure 1b). However, LPS-treatment significantly attenuated the pressor responses to NA (1 μg kg^{-1}, i.v.) at 30, 60, 120 and 180 min ($P < 0.05$, $n = 10$; Figure 1c). Administration of aminoguanidine (15 mg kg^{-1}, i.v., 20 min prior to LPS) had no significant effect on MAP or HR (Figure 1). However, LPS-rats that had been pretreated with aminoguanidine maintained significantly higher MAP values when compared with rats treated with LPS alone (Figure 1a). Pretreatment of rats with aminoguanidine did not affect the hyporeactivity to NA seen at 30 min after LPS (Figure 1c). However, at 60, 120 and 180 min after LPS, the pressor responses to NA in LPS-rats treated with aminoguanidine were significantly greater than in rats treated with LPS alone. Most notably, the pressor responses afforded by NA at 180 min in LPS-rats treated with aminoguanidine were not different from the

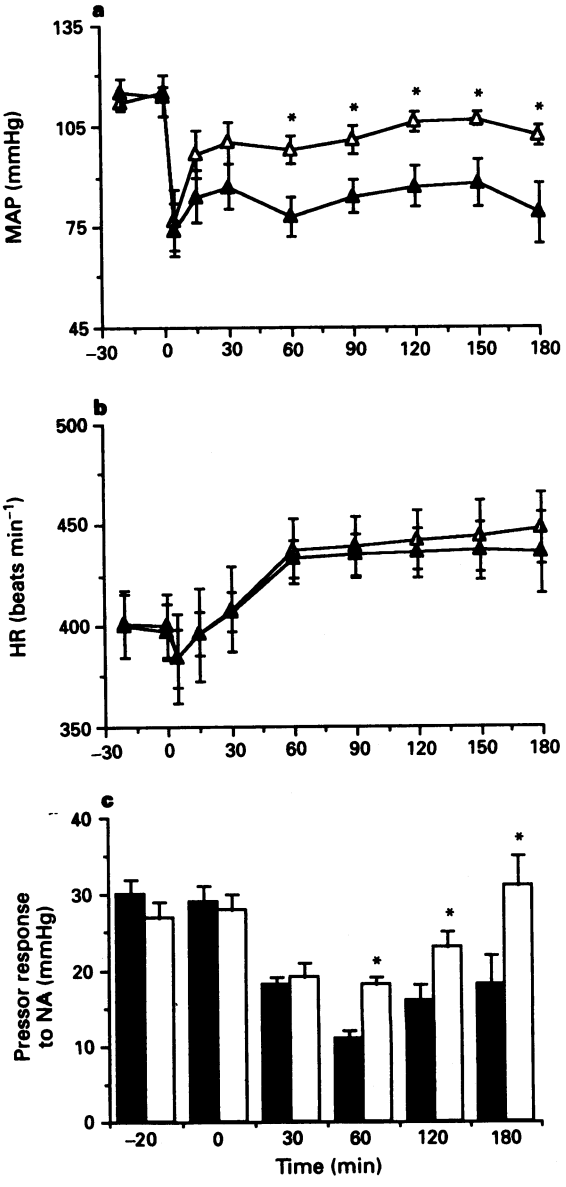

Figure 1 Aminoguanidine ameliorates the delayed hypotension and vascular hyporeactivity to noradrenaline (NA) in endotoxic shock in the anaesthetized rat. Depicted are the changes in (a) mean arterial blood pressure (MAP), (b) heart rate (HR) and (c) pressor responses to NA (1 μg kg^{-1}, i.v.) in rats treated with *E. coli* lipopolysaccharide (LPS, 10 mg kg^{-1}, i.v. at time 0). Different groups of animals were pretreated either with vehicle (saline, ▲ and solid column; $n = 10$) or aminoguanidine (15 mg kg^{-1}, i.v. for 20 min prior to LPS; △ and open column; $n = 10$). Data are expressed as means ± s.e.mean of n observations. *$P < 0.05$ represents significant differences when compared to control at the same time point.

pressor responses caused by NA prior to LPS administration, while they were markedly reduced (at 180 min) in LPS-treated rats (Figure 1c).

When injected at 180 min after LPS, aminoguanidine (15 and 45 mg kg^{-1}, i.v.) caused a dose-related rise in blood pressure and, hence, reversed the hypotension elicited by LPS in a dose-dependent manner (Figure 2). Interestingly, the rise in blood pressure caused by aminoguanidine in LPS-treated rats was significantly greater than the one produced in sham-operated controls (Figure 2).

Aminoguanidine attenuates the LPS-induced vascular hyporeactivity to noradrenaline ex vivo

In rat aortic rings obtained from sham-operated rats (control), NA (10^{-9} to 10^{-6} M) caused a dose-dependent increase

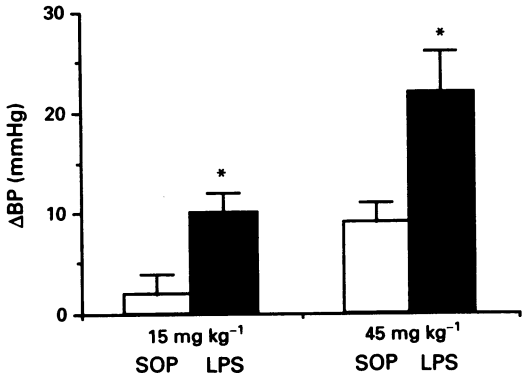

Figure 2 Comparison of the pressor responses elicited by aminoguanidine in sham-operated control rats (SOP) or rats subjected to endotoxic shock. Different groups of animals were subjected to vehicle (SOP, open column; $n = 5$) or *E. coli* lipopolysaccharide (LPS, 10 mg kg^{-1}; solid column; $n = 8$) for 180 min. Thereafter, two doses of aminoguanidine (15 and 45 mg kg^{-1}, i.v.) were administered in a cumulative manner. Aminoguanidine caused a slow rise in blood pressure (maximum approx. 30 min). Thus, the data are expressed as change in mean arterial blood pressure (MAP) observed within 30 min. Note that the higher (45 mg kg^{-1}), but not the lower dose of aminoguanidine (15 mg kg^{-1}) caused a significant rise in MAP in SOP rats. *$P<0.05$ represents significant differences when compared to SOP-control.

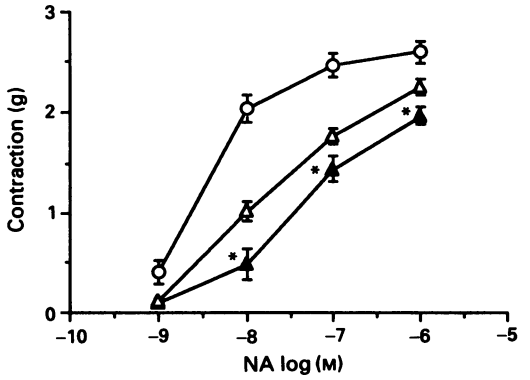

Figure 3 Aminoguanidine attenuates the endotoxin-induced vascular hyporeactivity to noradrenaline (NA) in rat aortic rings *ex vivo*. Depicted are concentration-response curves to NA (10^{-9}–10^{-6} M) in aortic rings without endothelium obtained from sham-operated control rats (○; $n = 6$), from rats treated with lipopolysaccharide (LPS, 10 mg kg^{-1}, i.v.) for 180 min (▲; $n = 10$) and from LPS-rats pretreated with aminoguanidine (15 mg kg^{-1}, i.v. at 20 min prior to LPS; △; $n = 10$). Data are expressed as means ± s.e.mean of n observations. Note that the contractions caused by NA after 180 min of LPS in rats pretreated with either vehicle (▲) or aminoguanidine (△) were significantly reduced when compared to control rats (○). *$P<0.05$ represents significant differences between LPS-rats pretreated with vehicle and those pretreated with aminoguanidine.

in vascular tone. The contractions caused by NA were significantly reduced in aortic rings obtained from rats after 180 min of endotoxaemia ($P<0.05$ at 10^{-9}–10^{-6} M; Figure 3). In contrast, pretreatment with aminoguanidine of LPS-rats significantly ameliorated the vascular hyporeactivity to NA of rat aortic rings *ex vivo* ($P<0.05$ at 10^{-8} to 10^{-6} M; Figure 3). However, the contractions produced by NA in aortic rings obtained from LPS-rats pretreated with aminoguanidine were still significantly reduced when compared to control responses ($P<0.05$ at 10^{-9}–10^{-6} M; Figure 3).

Aminoguanidine inhibits the activity of inducible nitric oxide synthase (iNOS) in endotoxic shock

A small, calcium-independent NOS activity was detectable in lung samples from sham-operated control animals. After 180 min of endotoxaemia, there was a substantial increase in iNOS activity in lung homogenates (Figure 4). However, iNOS activity was significantly reduced (by 44 ± 5%, $P<0.05$) in lung homogenates obtained from animals pretreated with aminoguanidine at 20 min prior to LPS administration.

To elucidate whether aminoguanidine directly inhibits iNOS activity *in vitro*, iNOS activity (in lung homogenates of rats treated with LPS for 180 min) and nNOS activity (in brain homogenates of control animals) were measured after incubation for 25 min with vehicle and increasing concentrations of aminoguanidine (10^{-8} to 10^{-3} M) or L-NAME (10^{-8} to 10^{-3} M). Clearly, aminoguanidine and L-NAME were equipotent and caused a dose-related inhibition of iNOS activity (IC_{50}: 30 ± 12 and 11 ± 6 μM, respectively; $n = 3$–6, $P>0.05$; Figure 5). Interestingly, the inhibition of iNOS activity seen with aminoguanidine was slow in onset and only reached a maximal effect after a lag period of more than 90 min. In contrast, the inhibition of iNOS activity by L-NAME was immediate and reached a maximum within 30 min (Figure 6). Aminoguanidine, however, was a less potent inhibitor than L-NAME of the activity of nNOS (IC_{50}: 140 ± 10 and 0.6 ± 0.1 μM, respectively; $n = 3$–6, $P<0.05$; Figure 5).

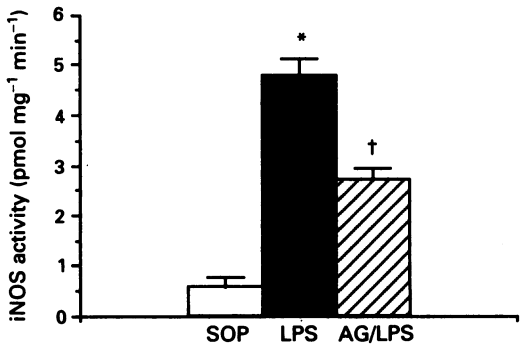

Figure 4 Pretreatment of rats with aminoguanidine inhibits the activity of a calcium-independent (inducible) isoform of nitric oxide synthase (iNOS) in lung homogenates obtained from animals subjected to 180 min of endotoxic shock. Calcium-independent iNOS activity was measured in lung homogenates obtained from sham-operated control rats (SOP, open column, $n = 4$) or rats treated with *E. coli* lipopolysaccharide (10 mg kg^{-1}, i.v.) for 180 min. Different groups of LPS-rats were pretreated with vehicle (LPS, solid column, $n = 6$) or aminoguanidine (AG/LPS, hatched column; 15 mg kg^{-1}, i.v., $n = 6$). Data are expressed as means ± s.e.mean of n observations. *$P<0.05$ represents a significant increase in iNOS activity when compared to control. †$P<0.05$ represents a significant reduction in iNOS activity when compared to LPS.

Aminoguanidine increases the survival rate of mice treated with LPS

The administration of a high dose (60 mg kg^{-1}, i.p.) of LPS to T/O mice was associated with a 24 h survival rate of only 8% of the animals. In contrast, LPS-mice treated with aminoguanidine (15 mg kg^{-1}, i.p. at 2 h and 6 h after LPS, $n = 8$) had a survival rate of 75% at 24 h. In contrast to aminoguanidine, treatment of LPS-mice with L-NAME (3 mg kg^{-1}, i.p. at 2 h and 6 h after LPS, $n = 9$) did not improve the survival rate (Figure 7).

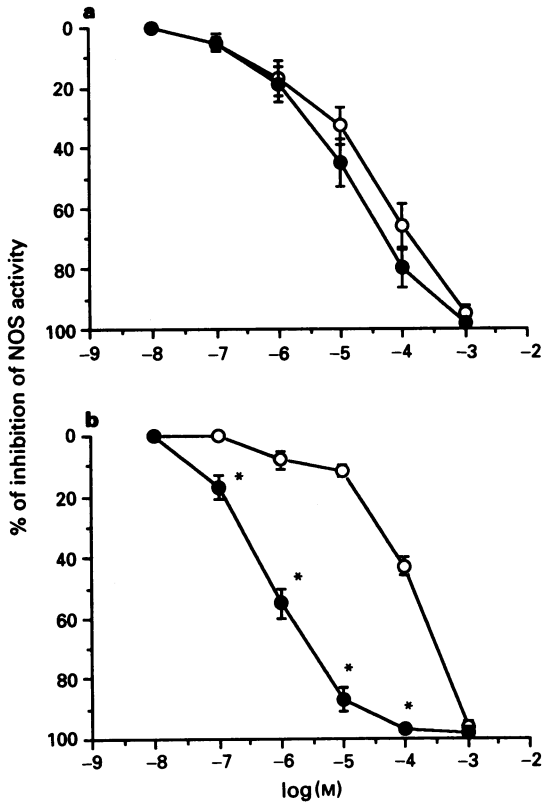

Figure 5 Aminoguanidine and N$^{\omega}$-nitro-L-arginine methyl ester (L-NAME) dose-dependently inhibit (a) the activity of the inducible nitric oxide synthase (iNOS) in lung homogenates from LPS-rats and (b) the activity of constitutive nitric oxide synthase (nNOS) in brain homogenates from normal control rats *in vitro*. Lung homogenates were prepared from rats at 180 min after injection of *E. coli* lipopolysaccharide (10 mg kg^{-1}, i.v.) and the inhibition of iNOS activity was measured in the absence and with increasing concentrations (10^{-7}–10^{-3} M) of aminoguanidine (○) or L-NAME (●). Brain homogenates were prepared from control animals and the inhibition of nNOS activity was measured in the absence and with the same increasing concentrations of aminoguanidine or L-NAME. Data are expressed as means ± s.e.mean of n observations and as percentage inhibition of control iNOS or nNOS activity. *$P<0.05$ represents significant differences between aminoguanidine and L-NAME.

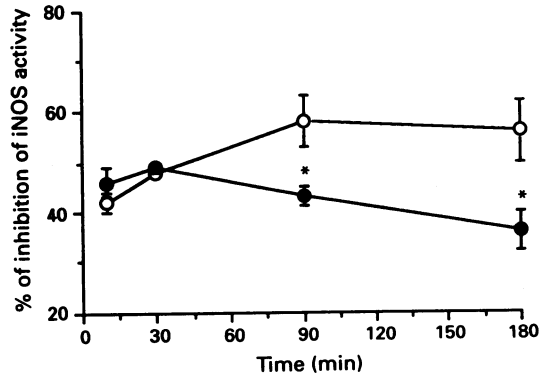

Figure 6 Time course study of inhibition of the activity of inducible nitric oxide synthase (iNOS) by aminoguanidine or N$^{\omega}$-nitro-L-arginine methyl ester (L-NAME) in lungs obtained from rats treated with LPS for 180 min. The IC_{50} of aminoguanidine (○, $n = 5$) and L-NAME (●, $n = 5$) on inhibiting iNOS activity were added to the lung homogenates then incubated for 10, 30, 90, and 180 min to measure the activity of iNOS. Data are expressed as percentage inhibition of iNOS activity by comparing iNOS activity measured in the different time points to those in the absence of these inhibitors (as control). Values are means ± s.e.mean of n observations. *$P<0.05$ represents significant differences between aminoguanidine and L-NAME at the same time point.

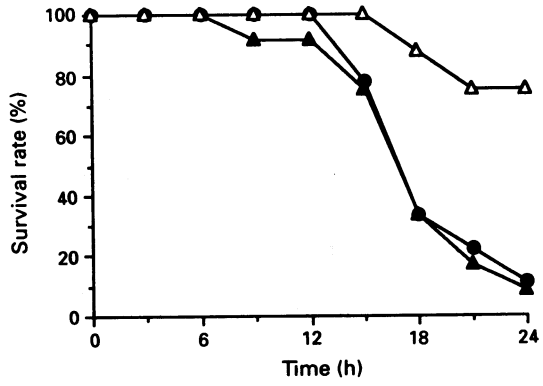

Figure 7 Aminoguanidine improves the survival rate of mice treated with *E. coli* lipopolysaccharide (LPS). T/O mice were injected with LPS (60 mg kg^{-1}, i.p.) then vehicle (saline, $n = 12$, ▲), aminoguanidine (15 mg kg^{-1}, i.p., $n = 8$, △), or N$^{\omega}$-nitro-L-arginine methyl ester (L-NAME, 3 mg kg^{-1}, i.p., $n = 9$, ●) were administered at 2 h and 6 h after LPS, and the survival rate was monitored every 3 h.

Discussion

This study demonstrates that aminoguanidine, a relatively selective inhibitor of the cytokine inducible isoform of nitric oxide synthase attenuates the delayed circulatory failure associated with endotoxic shock in the rat and improves survival in a murine model of endotoxaemia. In particular, we show that aminoguanidine attenuates the delayed fall in blood pressure and the vascular hyporeactivity to NA elicited by prolonged periods of endotoxaemia in the rat. In addition to causing beneficial haemodynamic effects in a rat model of endotoxic shock, aminoguanidine, but not the non-selective NOS inhibitor L-NAME, improves survival in a murine model of severe endotoxaemia.

What, then, is the mechanism by which aminoguanidine affords the beneficial effects on haemodynamics and survival in the animal models of endotoxic shock in this study? Clearly, aminoguanidine attenuates the activity of iNOS in the lung of rats subjected to prolonged periods of endotoxaemia. The observed reduction in iNOS activity is due to an inhibition by aminoguanidine of iNOS activity, since (i) aminoguanidine dose-dependently inhibited iNOS activity in lung homogenates obtained from rats treated with LPS for 180 min *ex vivo* (this study), (ii) aminoguanidine attenuated the reduction of the vasoconstrictor responses to NA (vascular hyporeactivity) in rat aortic rings from rats with endotoxic shock *ex vivo*, and (iii) aminoguanidine also attenuated the vascular hyporeactivity to phenylephrine in rat aortic rings *in vitro* (Joly *et al.*, 1994). When given at 180 min after endotoxin, aminoguanidine also reversed the severe delayed hypotension elicited by endotoxin, which is due to an enhanced formation of NO by iNOS (Wright *et al.*, 1992; Szabo *et al.*, 1993a). Several recent studies suggest that aminoguanidine is a less potent inhibitor of eNOS activity in cultured cells, isolated blood vessels and enzymes preparations *in vitro* (Corbett *et al.*, 1992; Griffiths *et al.*, 1993; Misko *et al.*, 1993; Tilton *et al.*, 1993). The hypothesis that aminoguanidine is a relatively selective inhibitor of iNOS is supported by this study. First, aminoguanidine is equipotent to L-NAME in inhibiting the iNOS activity in lung homogenates obtained from rats treated with endotoxin for 180 min, but is significantly weaker than L-NAME in inhibiting the nNOS activity in brain homogenates obtained from control rats. Second, aminoguanidine is a weaker inhibitor of eNOS than iNOS *in vivo*, for aminoguanidine did not cause an increase in blood pressure in control rats (at 15 mg kg^{-1}), at a dose which caused a significant inhibition of iNOS activity. Third, aminoguanidine did not affect the acute vas-

cular hyporeactivity to NA associated with endotoxic shock, which is due to an enhanced formation of NO by eNOS (Szabo *et al.*, 1993a). These results clearly demonstrate that low doses of aminoguanidine inhibit iNOS activity *in vivo* without causing a significant inhibition of eNOS activity. Interestingly, the inhibition of iNOS activity seen with aminoguanidine was slow in onset and reached a maximum effect only after a prolonged incubation period, while the inhibition of iNOS activity by L-NAME was immediate and reached a maximum within 30 min. Although we demonstrate that aminoguanidine is a less potent inhibitor than L-NAME of the activity of nNOS (brain homogenates; incubation period: 25 min), the time-dependency of this effect was not investigated. One could, therefore, argue that longer incubation periods of aminoguanidine with constitutive NOS preparations (nNOS or eNOS) would reveal a more potent inhibition of eNOS by aminoguanidine. This is, however, unlikely, since incubations of rat aortic rings with aminoguanidine (0.1 mM) for 1 h did not result in any inhibition of endothelium-dependent vasodilatations (to acetylcholine, calcium ionophore, or adenosine triphosphate) and hence, eNOS activity. In contrast, L-NAME (0.1 mM) caused a complete inhibition of endothelium-dependent vasodilatation under these experimental conditions (Joly *et al.*, 1994).

It has been suggested that some of the adverse effects of non-selective inhibitors of NOS observed in animal models of endotoxic shock (see introduction) are due to the inhibition of eNOS activity in the endothelium. Thus, it has been proposed that relatively selective inhibitors of iNOS activity should be superior to non-selective NOS inhibitors in improving survival in animal models of circulatory shock. We demonstrate here that aminoguanidine causes a substantial improvement in 24 h survival rate in mice treated with a high dose of endotoxin. In contrast, L-NAME, at a dose that is lower than that used for aminoguanidine but high enough to produce a rise in MAP in anaesthetized rats (Hecker *et al.*, 1990), did not improve survival in this murine model of severe endotoxaemia. It is tempting to speculate that the improvement in survival seen with aminoguanidine but not L-NAME, is due to the fact that aminoguanidine is a relatively selective inhibitor of iNOS. However, aminoguanidine has many pharmacological properties including inhibition of advanced glycosylation end products formation (Brownlee *et al.*, 1988; Edelstein & Brownlee, 1992); inhibition of histamine metabolism (Bieganski *et al.*, 1983), inhibition of polyamine catabolism (Seiler *et al.*, 1985) and inhibition of catalase (Ou & Wolff, 1993). Thus, it is difficult to conclude that the beneficial effect of aminoguanidine on survival in our murine model of endotoxaemia is solely due to inhibition of iNOS activity. Moreover, we have not investigated the dose-related effects of L-NAME in survival in our murine model of endotoxaemia and hence, cannot exclude that an improvement in survival could be achieved with either higher (more potent inhibition of iNOS activity) or lower doses (reduced side effects) of L-NAME.

Interestingly, aminoguanidine did not completely reverse the vascular hyporeactivity caused by LPS *ex vivo*. In addition, treatment of rat aortic rings with aminoguanidine *in vitro* does not completely restore the vascular hyporeactivity to phenylephrine (Joly *et al.*, 1994). We have recently demonstrated that another mediator, which is not blocked by inhibitors of NOS, may also be involved in the activation of soluble guanylyl cyclase occurring in vascular smooth muscle after LPS exposure and, hence, may also contribute to the vascular hyporeactivity (Wu *et al.*, 1994). It should be pointed out, however, that a partial inhibition of iNOS activity is sufficient to cause a substantial improvement of the haemodynamic alterations caused by endotoxin *in vivo* (Thiemermann *et al.*, 1993; Szabo *et al.*, 1993b,c).

In conclusion, this study demonstrates that aminoguanidine is a relatively selective inhibitor of iNOS *in vitro* and attenuates the delayed circulatory failure associated with endotixic shock in the rat. In addition, we demonstrate that aminoguanidine, when given therapeutically after the onset of endotoxaemia, improves survival in a murine model of severe septic shock. These results suggest that aminoguanidine may be useful in the therapy of patients with circulatory shock, and lends further support to the hypothesis that relatively selective inhibitors of iNOS activity may be superior to non-selective inhibitors of NOS activity, in the therapy of circulatory shock of various aetiologies.

This work was supported by a grant from Glaxo Group Research Ltd. The authors are grateful to Mrs J. Piper for technical assistance. The help of Dr M. Perreti with the survival studies is also gratefully acknowledged. C.C.W. is supported by the National Defense Medical Center of Taiwan. C.T. is supported by a grant from the Commission of the European Communities (Biomed I, BMHI, CT 92/1893). C.S. is a fellow of Lloyd's of London Tercentenary Foundation.

References

BIEGANSKI, T., KUSCHE, J., LORENZ, W., HEXTERBERG, R., STAHLKNECHT, C.D. & FEUSSNER, K.D. (1983). Distribution and properties of human intestinal diamine oxidase and its relevance for the histamine metabolism. *Biochim. Biophys. Acta*, **31**, 196–203.

BRADFORD, M.M. (1976). A rapid and sensitive method for the quantification of protein dye binding. *Anal. Biochem.*, **72**, 248–254.

BROWNLEE, M., CERAMI, A. & VLASSARA, H. (1988). Advanced glycosylation end products in tissue and the biochemical basis of diabetic complications. *N. Engl. J. Med.*, **318**, 1315–1321.

CORBETT, J.A., TILTON, R.G., CHANG, K., HASAN, K.S., IDO, Y., WANG, J.L., SWEETLAND, M.A., LANCASTER, J.R., WILLIAMSON, J.R. & MCDANIEL, M.L. (1992). Aminoguanidine, a novel inhibitor of nitric oxide formation, prevents diabetic vascular dysfunction. *Diabetes*, **41**, 552–556.

DINERMAN, J.L., LOWENSTEIN, C.J. & SNYDER, S.H. (1993). Molecular mechanisms of nitric oxide regulation: potential relevance to cardiovascular disease. *Circ. Res.*, **73**, 217–222.

EDELSTEIN, D. & BROWNLEE, M. (1992). Mechanistic studies of advanced glycosylation end product inhibition by aminoguanidine. *Diabetes*, **41**, 26–29.

GRIFFITHS, M.J.D., MESSENT, M., MACALLISTER, R.J. & EVANS, T.W. (1993). Aminoguanidine selectively inhibits inducible nitric oxide synthase. *Br. J. Pharmacol.*, **110**, 963–968.

HARBRECHT, B.G., BILLIAR, T.R., STADLER, J., DEMETRIS, A.J., OCHOA, J., CURRAN, R.O. & SIMMONS, R.L. (1992). Inhibition of nitric oxide synthesis during endotoxaemia promotes intrahepatic thrombosis and an oxygen radical-mediated hepatic injury. *J. Leukoc. Biol.*, **52**, 390–394.

HASAN, K., HEESEN, B.J., CORBETT, J.A., MCDANIEL, M.L., CHANG, K., ALLISON, W., WOLFFENBUTTEL, B.H.R., WILLIAMSON, J.R. & TILTON, R.G. (1993). Inhibition of nitric oxide formation by guanidines. *Eur. J. Pharmacol.*, **249**, 101–106.

HECKER, M., MITCHELL, J.A., HARRIS, H.J., KATSURA, M., THIEMERMANN, C. & VANE, J.R. (1990). Endothelial cells metabolize N^G-monomethyl-L-arginine to L-citrulline and subsequently to L-arginine. *Biochem. Biophys. Res. Commun.*, **167**, 1037–1043.

HUTCHESON, I.R., WHITTLE, B.J.R. & BOUGHTON-SMITH, N.K. (1990). Role of nitric oxide in maintaining vascular integrity in endotoxin-induced acute intestinal damage in the rat. *Br. J. Pharmacol.*, **101**, 815–820.

JOLY, G.A., AYRES, M., CHELLY, F. & KILBOURN, R.G. (1994). Effects of N^G-methyl-L-arginine, N^G-nitro-L-arginine, and aminoguanidine on constitutive and inducible nitric oxide synthase in rat aorta. *Biochem. Biophys. Res. Commun.*, **199,** 147–154.

JULOU-SCHAEFFER, G., GRAY, G.A., FLEMING, I., SCHOTT, C., PARRATT, J.R. & STOCLET, J.C. (1990). Loss of vascular responsiveness induced by endotoxin involves the L-arginine pathway. *Am. J. Physiol.*, **259,** H1038–H1043.

KILBOURN, R.G. & GRIFFITH, O.W. (1992). Overproduction of nitric oxide in cytokine-mediated and septic shock. *J. Natl. Cancer Inst.*, **84,** 827–877.

KILBOURN, R.G., GROSS, S.S., JUBRAN, A., ADAMS, J., GRIFFITH, O.W., LEVI, R. & LODATO, R.F. (1990). N^G-methyl-L-arginine inhibits tumor necrosis factor-induced hypotension: Implications for the involvement of nitric oxide. *Proc. Natl. Acad. Sci. U.S.A.*, **87,** 3629–3632.

MEYER, J., TRABER, L.D., NELSON, S., LENTZ, C.W., NAKAZAWA, H., HERNDON, D.N., NODA, H. & TRABER, D.L. (1992). Reversal of hyperdynamic response to continuous endotoxin administration by inhibition of NO synthesis. *J. Appl. Physiol.*, **73,** 324–328.

MISKO, T.P., MOORE, W.M., KASTEN, T.P., NICKOLS, G.A., CORBETT, J.A., TILTON, R.G., MCDANIEL, M.L., WILLIAMSON, J.R. & CURRIE, M.G. (1993). Selective inhibition of the inducible nitric oxide synthase by aminoguanidine. *Eur. J. Pharmacol.*, **233,** 119–125.

MONCADA, S. & HIGGS, A. (1993). The L-arginine-nitric oxide pathway. *N. Engl. J. Med.*, **329,** 2002–2012.

MONCADA, S., PALMER, R.M.J. & HIGGS, E.A. (1991). Nitric oxide: physiology, pathophysiology, and pharmacology. *Pharmacol. Rev.*, **43,** 109–141.

NATHAN, C. (1992). Nitric oxide as a secretory product of mammalian cells. *FASEB J.*, **6,** 3051–3064.

OU, P. & WOLFF, S.P. (1993). Aminoguadinine: a drug proposed for prophylaxis in diabetes inhibits catalase and generates hydrogen peroxide *in vitro*. *Biochem. Pharmacol.*, **46,** 1139–1144.

SEILER, N., BOLENIUS, F.N. & KNODGEN, B. (1985). The influence of catabolic reactions on polyamine excretion. *Biochem. J.*, **225,** 219–226.

SHULTZ, P.J. & RAIJ, L. (1992). Endogenously synthesized nitric oxide prevents endotoxin-induced glomerular thrombosis. *J. Clin. Invest.*, **90,** 1718–1725.

STUEHR, D.J. & NATHAN, C.F. (1989). Nitric oxide: a macrophage product responsible for cytostasis and respiratory inhibition in tumour target cells. *J. Exp. Med.*, **169,** 1543–1555.

SUBA, E.A., MCKEENNA, T.M. & WILLIAMS, T.J. (1992). *In vivo* and *in vitro* effects of endotoxin on vascular responsiveness to noradrenaline and signal transduction in the rat. *Circ. Shock*, **36,** 127–133.

SZABÓ, C., MITCHELL, J.A., THIEMERMANN, C. & VANE, J.R. (1993a). Nitric oxide-mediated hyporeactivity to noradrenaline precedes nitric oxide synthase induction in endotoxin shock. *Br. J. Pharmacol.*, **108,** 786–792.

SZABÓ, C., WU, C.C., GROSS, S.S., THIEMERMANN, C. & VANE, J.R. (1993b). Interleukin-1 contributes to the induction of nitric oxide synthase by endotoxin in vivo. *Eur. J. Pharmacol.*, **250,** 157–160.

SZABÓ, C., WU, C.C., MITCHELL, J.A., GROSS, S.S., THIEMERMANN, C. & VANE, J.R. (1993c). Platelet-activating factor contributes to the induction of nitric oxide synthase by bacterial lipopolysaccharide. *Circ. Res.*, **73,** 991–999.

THIEMERMANN, C. (1994). The role of the arginine: nitric oxide pathway in circulatory shock. *Adv. Pharmacol.*, **28,** 45–79.

THIEMERMANN, C. & VANE, J.R. (1990). Inhibition of nitric oxide synthesis reduces the hypotension induced by bacterial lipopolysaccharides in the rat *in vivo*. *Eur. J. Pharmacol.*, **182,** 591–595.

THIEMERMANN, C., WU, C.C., SZABÓ, C., PERRETTI, M. & VANE, J.R. (1993). Role of tumour necrosis factor in the induction of nitric oxide synthase in a rat model of endotoxin shock. *Br. J. Pharmacol.*, **110,** 177–182.

TILTON, R.G., CHANG, K., HASAN, K.S., SMITH, S.R., PETRASH, J.M., MISKO, T.P., MOORE, W.M., CURRIE, M.G., CORBETT, J.A., MCDANIEL, M.L. & WILLIAMSON, J.R. (1993). Prevention of diabetic vascular dysfunction by guanidines: inhibition of nitric oxide synthase versus advanced glycation end-product formation. *Diabetes*, **42,** 221–232.

WRIGHT, C.E., REES, D.D. & MONCADA, S. (1992). Protective and pathological roles of nitric oxide in endotoxin shock. *Cardiovasc. Res.*, **26,** 48–57.

WU, C.C., SZABÓ, C., CHEN, S.J., THIEMERMANN, C. & VANE, J.R. (1994). Activation of soluble guanylyl cyclase by a factor other than nitric oxide or carbon monoxide contributes to the vascular hyporeactivity to vasoconstrictor agents in the aorta of rats treated with endotoxin. *Biochem. Biophys. Res. Commun.*, **201,** 436–442.

(Received July 18, 1994
Revised September 26, 1994
Accepted September 28, 1994)

British Journal of Pharmacology (1995) 114, 1673–1679 © 1995 Stockton Press All rights reserved 0007–1188/95 $12.00

Comparison of effects of chronic and acute administration of N^G-nitro-L-arginine methyl ester to the rat on inhibition of nitric oxide-mediated responses

[1]Clare E. Bryant, Graham H. Allcock & Timothy D. Warner

The William Harvey Research Institute, The Medical College of Saint Bartholomews' Hospital, Charterhouse Square, London EC1M 6BQ

1 Vascular responses to acetylcholine and sodium nitroprusside *in vivo* and *in vitro*, in the isolated perfused kidney and in rings of rat thoracic aorta, were measured in rats treated chronically with N^G-nitro-L-arginine methyl ester (L-NAME; approx, 70 mg kg^{-1}) and compared to responses in age-matched control animals, and age-matched animals after the acute administration of L-NAME (3–100 μmol kg^{-1}). Parallel experiments examined alterations in responsiveness in rings of trachea and anococcygeus muscles taken from the same animals.

2 Chronic oral administration of L-NAME elevated the blood pressure in anaesthetized animals from 114 ± 5 mmHg to 153 ± 11 mmHg ($n = 5$). The hypotensive responses to both acetylcholine (1 nmol kg^{-1}) and sodium nitroprusside (10 nmol kg^{-1}) were enhanced by chronic L-NAME treatment ($n = 5–7$) whereas acute L-NAME administration enhanced only the response to sodium nitroprusside ($n = 5$).

3 After chronic treatment with L-NAME, the basal perfusion pressure in the isolated perfused kidney was elevated. However, vasodilator responses to either acetylcholine (1 nmol) or sodium nitroprusside (3 nmol) were unaltered ($n = 5–7$). The vasodilatation induced by acetylcholine was inhibited in a concentration-dependent manner by the administration of acute L-NAME (0.1–100 μM; $n = 5$), such that significant inhibition was seen at 10 μM L-NAME. The response to sodium nitroprusside was unaffected by L-NAME.

4 The relaxations of isolated rings of rat thoracic aorta induced by acetylcholine were inhibited in tissues prepared from rats treated chronically with L-NAME ($n = 5–7$). Acute administration of L-NAME (0.1–100 μM) concentration-dependently inhibited the relaxations induced by acetylcholine in this preparation, with significant inhibition occurring at 1 μM L-NAME ($n = 5$). Responses to sodium nitroprusside were unaffected by either chronic or acute exposure to L-NAME ($n = 5–7$).

5 Relaxations of precontracted anococcygeus muscles induced by electrical field stimulation, or contractions of rings of trachea induced by carbachol or endothelin-1, were unaffected by chronic oral administration of L-NAME ($n = 4–6$). Acute addition of L-NAME (0.1–100 μM) to the organ baths inhibited in a concentration-dependent manner the relaxations of anococcygeus muscles taken from control animals, with a significant effect being seen at a concentration of 10 μM ($n = 4–6$).

6 Our cardiovascular data are consistent with chronic oral administration of L-NAME inhibiting the production of nitric oxide (NO) within the vasculature, although the pattern of inhibition is not uniform between different tissues. Despite the inhibition of endothelial NO production, chronic L-NAME does not alter the vasodepressor activity of acetylcholine *in vivo* or in the isolated perfused kidney. This may be explained by an enhanced responsiveness of guanylyl cyclase pathways, the increased release of vasodilators other than nitric oxide or a decreased importance of nitric oxide in resistance vessels compared with conductance vessels. The resistance of peripheral neuronal NO responses to chronic treatment with L-NAME indicates that selective inhibition of different isoforms of NOS may be achieved *in vivo*.

Keywords: L-NAME; nitric oxide synthase; nitric oxide

Introduction

Nitric oxide (NO) is an intra- and extra-cellular signalling molecular, derived from L-arginine by the action of the enzyme NO synthase (NOS), that is formed and active throughout the body (Moncada *et al.*, 1991). In the vasculature, for instance, NO is released by the endothelium and passes to the underlying smooth muscle where it stimulates guanylyl cyclase and so promotes vasodilatation. Similarly, in non-vascular smooth muscle, NO may produce relaxation following its release from intrinsic nerve endings (Hobbs & Gibson, 1990; Moncada *et al.*, 1991; Barnes, 1993).

Arginine analogues such as N^G-monomethyl-L-arginine (L-NMMA) and N^G-nitro-L-arginine methyl ester (L-NAME) are potent inhibitors of NOS (Moore *et al.*, 1990; Rees *et al.*, 1990). Acute administration of L-NAME, *in vivo*, elevates mean arterial blood pressure, constricts the renal, mesenteric and hind-quarters vascular beds and depresses cardiac output (Gardiner *et al.*, 1990a; Baylis *et al.*, 1990). It also reduces the glomerular filtration rate, but in these short time course experiments the accompanying hypertension is not driven by changes in the renin-angiotensin system (Lehera *et al.*, 1991; Baylis *et al.*, 1993). As may be expected, the effects of acute L-NAME treatment are reversed by administration of L-arginine, to restore the production of NO, or by agents such as glyceryl trinitrate or cyclic GMP analogues, which mimic the effects of NO (Gardiner *et al.*, 1990a; Lehera *et al.*, 1992).

In contrast to the effects of acute administration, chronic

[1] Author for correspondence.

administration of L-NAME to rats produces a hypertension accompanied by profound changes in renal structure (Ribeiro *et al.*, 1992). This hypertension is associated with thickening of the resistance vessel media, depression of aortic cyclic GMP levels, alteration of plasma renin levels and sclerotic renal changes (Arnal *et al.*, 1992; Deng *et al.*, 1993; Pollock *et al.*, 1993; Baylis *et al.*, 1993). In this situation the hypertension produced is, at least partly, dependent upon the renin-angiotensin system (Ribeiro *et al.*, 1992; Morton *et al.*, 1993). It is therefore clear that acute and chronic administration of L-NAME produce different changes within the vasculature. To investigate these further we have compared the effects of long term (4–6 weeks) and acute administration of L-NAME on the cardiovascular responses of the rat, and on the responses of isolated vascular preparations. Furthermore, we have also investigated the activities of other tissues in which endogenously produced NO has been reported to have important regulatory functions.

Methods

Animal treatment

To examine the effects of chronic administration of L-NAME, male Wistar rats (220–250 g) were given L-NAME (approximately 70 mg kg^{-1} day^{-1}) in the drinking water, and compared with a group of rats with normal water, for a period of 4–6 weeks. Water intake, food intake and body weight were recorded and compared with the group of age matched controls. After use in the experiments the left kidney was removed from animals after chronic administration of L-NAME for gross examination. Untreated male Wistar rats (280–320 g) were used to compare the effects of acute L-NAME administration.

Blood pressure measurement

Rats were anaesthetized with sodium thiopentone (Intraval, 4 ml kg^{-1} i.p. of a 3% solution). The carotid artery was cannulated and mean arterial blood pressure recorded by a pressure transducer (Elcomatic 750) linked to a chart recorder (Graphtec Linearcorder WR3101). The jugular vein was also cannulated for drug administration. Blood pressure was then allowed to stabilize for 30 min before changes in mean arterial blood pressure caused by intravenous drug administration were recorded. The changes in blood pressure were allowed to return to basal levels before the next drug was given. Responses to the following agents, in the following order, were recorded; phenylephrine (10 nmol kg^{-1}), angiotensin II (50 pmol kg^{-1}), sodium nitroprusside (10 nmol kg^{-1}), acetylcholine (1 nmol kg^{-1}) and endothelin-1 (0.5 nmol kg^{-1}). Endothelin-1 was administered last because of its very long duration of action. To examine the effects of acute L-NAME, after an initial 30 min of stabilization L-NAME (3–100 μmol kg^{-1}) or vehicle was given intravenously and the blood pressure left to stabilise. Responses to acetylcholine (1 nmol kg^{-1}) or sodium nitroprusside (10 nmol kg^{-1}) were then recorded. When the blood pressure returned to a stable level the next dose of L-NAME or vehicle was administered and the cardiovascular responses to acetylcholine and sodium nitroprusside retested. Blood pressure responses were recorded, when the response to the drug reached the point of maximum change. The duration of vasodilatation was also recorded. Results are expressed as changes in mean arterial blood pressure (diastolic pressure plus one third of pulse pressure) ± standard error of the mean (s.e.mean).

Urinary bladder function

The abdomens of anaesthetized rats, prepared as above, were opened and the ureters isolated and cut. Cannulae were passed down the ureters into the bladder for the infusion of saline (left ureter) and the measurement of intrabladder pressure (right ureter). Following a 30 min equilibration period the bladder was emptied, via the saline infusion line, and saline infused (0.25 ml min^{-1}) until the intrabladder pressure reached a plateau and micturition began. The bladder was emptied and the procedure repeated twice more.

Isolated perfused kidney preparation

After completion of the *in vivo* cardiovascular study the rats were given heparin 200 i.u. intravenously. The superior mesenteric artery was cannulated retrogradely and the cannula passed into the right renal artery. The kidney was perfused (5 ml min^{-1}) with warmed (37°C) and gassed (95% O_2:5% CO_2) Krebs buffer (composition, mM: NaCl 118, KCl 4.7, KH_2PO_4 1.2, $MgSO_4.7H_2O$, 1.17, $CaCl_2.6H_2O$ 2.5, $NaHCO_3$ 25, glucose 5.6, dexamethasone 0.001; pH 7.4). The rat was killed by exsanguination and the kidney excised while being continuously perfused with Krebs buffer. The perfusion rate was then increased to 10 ml min^{-1} and changes in perfusion pressure measured by a pressure transducer (Elcomatic 750) linked to a chart recorder (Graphtec Linearcorder WR3101). The kidney was allowed to equilibrate for 30 min before drug administration. Vasoconstrictor responses to phenylephrine (1–3 nmol) or angiotensin II (1–5 pmol) were then recorded and the maximum responses measured. Vascular responses to acetylcholine (1 nmol) or sodium nitroprusside (3 nmol) were measured at the point of maximum change after preconstricting the renal vasculature with an infusion of phenylephrine (1–20 μM). The duration of vasodilatation was also recorded. The response induced by endothelin-1 (1–2.5 pmol) was measured after the responses to the other agents had been recorded. In experiments examining the acute effects of L-NAME, only the vasodilatation to acetylcholine (1 nmol) or sodium nitroprusside (3 nmol) were measured. After the equilibration period L-NAME (0.1 μM) or vehicle was infused with phenylephrine (10 μM) and the vasodilator responses to acetylcholine or sodium nitroprusside measured. The perfusion pressure was allowed to return to pre-vasodilator levels and further concentrations of L-NAME (0.3–100 μM) were infused to produce a cumulative increase in L-NAME concentration. After 20 min at the new concentration of L-NAME the effects of acetylcholine and sodium nitroprusside were retested.

Isolated tissue preparations

Immediately after removal of the kidney, the thoracic aorta and the trachea were dissected free and placed into Krebs buffer gassed with 95% O_2:5% CO_2. The aorta and trachea were then dissected free of connective tissue, and rings 2–3 mm wide, were prepared. The intimal surfaces of some rings were rubbed gently to remove the endothelium or epithelium, respectively. The rings were suspended in organ baths under a tension of 1 g for the aortic rings, and 2 g for the tracheal rings, and allowed to equilibrate for 60 min, with washing every 15 min. Changes in tension were recorded with an isometric transducer (Hugo Sachs Electronik, Germany) connected to a chart recorder (Graphtec Linearcorder WR 3101). In the rat aorta preparations, cumulative concentration-response curves to phenylephrine were then constructed in rings with and without endothelium. After washing to reverse the response to phenylephrine, the rings of thoracic aorta were preconstricted with phenylephrine (10–300 nM) to produce 70% of the maximum tone. Relaxations to cumulative concentrations of acetylcholine (0.01–3 μM) or sodium nitroprusside (0.1 nM–0.1 μM) were then recorded. To study its acute effect L-NAME (0.1–100 μM) was added to the organ bath after 30 min of the stabilization period and incubated for a further 30 min, before preconstricting the aorta rings with phenylephrine (0.1 μM). Responses were recorded once the constriction had

reached a plateau. In the tracheal preparations cumulative concentration-response curves were constructed to carbachol (0.1 nM–10 μM) after which the preparations were washed and left to re-equilibrate for 30 min. Cumulative concentration curves were then constructed to endothelin-1 (10 pM–0.1 μM).

The rat anococcygeus muscle (Gillespie, 1972) was also removed and placed in an organ bath in Krebs buffer gassed with 95% O_2:5% CO_2, under a resting tension of 0.5 g. Tissues were left to stabilise for 45 min with washing every 15 min. To inhibit the effects of sympathetic nerve stimulation, phentolamine (1 μM) was present in the Krebs buffer and guanethidine (30 μM) applied for 10 min during the incubation period. Tone was raised with carbachol (50 μM) and field stimulation (0.3 mA, 10 Hz, 0.1 ms, 10 s every 100 s) was applied (Grass S48 stimulator; Med Lab Stimu Splitter II) to produce stable relaxations. After a washout period of 15 min, the tissues were again pre-contracted with carbachol and stimulated. When stable relaxations were achieved L-arginine (1 mM) was added to the preparation and its effect noted. In experiments investigating its acute effects, L-NAME (0.1 μM) was added to the bath once a stable response to electrical stimulation was obtained and the tissue stimulated until the response reached a steady state, when the concentration of L-NAME was further increased (0.3–100 μM). After administration of 100 μM L-NAME to the anococcygeus preparation the effects of addition of L-arginine (1 mM) were recorded.

NOS activity assay

The cerebella from both control and chronic L-NAME-treated rats were removed and frozen in liquid nitrogen. Cerebella were thawed and homogenized (ratio of 1 g of tissue to 5 ml of buffer: Tris/HCl 50 mM; EDTA 0.1 mM; EGTA 0.1 mM; 2-mercaptoethanol 12 mM; leupeptin 2 μM; pepstatin 1 μM and phenylmethylsulphonyl fluoride 1 mM; pH 7.4) on ice. NOS activity was measured as the ability of tissue homogenates to convert [^{3}H]-L-arginine to [^{3}H]-L-citrulline. Samples were incubated at room temperature for 30 min in the presence of NADPH (1 mM), calmodulin (2 mM) and a mixture of unlabelled and [^{3}H]-L-arginine (10 μM). L-Valine (50 mM), which inhibits the conversion of L-arginine to L-citrulline by arginase and the transcarbamoylase cycle, was included in the reaction mixture to increase specificity of the assay. L-Citrulline formation was determined in the absence of NADPH as a measure of nonspecific conversion of L-arginine. Incubations were terminated by the addition of 1 ml of HEPES (20 mM, pH 5.5) containing 1 mM EGTA and EDTA. The newly formed L-citrulline was separated from L-arginine by passing the reaction mixture over Dowex columns (1 ml), and the eluted labelled material was measured with a Beckman scintillation counter. Activity is expressed as pmol citrulline mg^{-1} protein $30\ min^{-1}$. Protein content of the homogenates was measured by the Bradford (1976) assay. Activities were compared with the Mann-Whitney U test, significance being taken at $P<0.05$.

Materials

L-NAME hydrochloride, phenylephrine hydrochloride, angiotensin II, sodium nitroprusside, acetylcholine chloride, phentolamine, guanethidine, carbachol, Tris/HCl, EDTA, EGTA, 2-mercaptoethanol, leupeptin, pepstatin, phenylmethylsulphonyl fluoride, NADPH, calmodulin, HEPES, Dowex, L-valine and L-arginine were purchased from Sigma Chemical Co. (Poole, Dorset). [^{3}H]-L-arginine was purchased from Amersham International plc. Endothelin-1 was purchased from Peptide Institute (Osaka, Japan) and dissolved in 0.9% w.v saline containing 0.1% w/v bovine serum albumin (Sigma Chemical Co.) All other drugs were dissolved in saline. The salts for the Krebs solution were obtained from BDH (Lutterworth, U.K.). Intraval was bought from May & Baker (U.K.).

Statistical analysis

Statistical differences between data points were assessed by a paired or unpaired one- or two-tail Student's t test, as appropriate. Significance was taken at $P<0.05$.

Results

General effects of chronic and acute L-NAME

Chronic administration of L-NAME resulted in a decreased weight gain over 4 weeks (control, 120 ± 25 g; L-NAME, 80 ± 13 g, $n=12$) and an enhanced water intake (from 100 ± 10 to 150 ± 25 ml per box of 3 rats/day, $n=12$). Animals became susceptible to gastroenteritis and peritonitis after 4–5 weeks of a 6 week L-NAME administration period, so animals were subsequently used after 4 weeks treatment. Chronic administration of L-NAME also caused gross changes in the renal architecture characterised by the loss of renal cortical tissue ($n=7$). Basal heart rate was unchanged

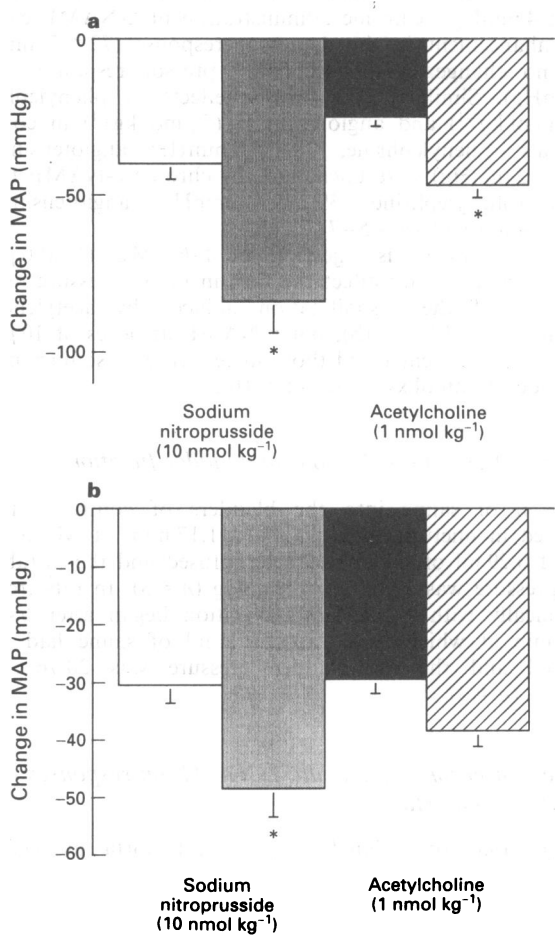

Figure 1 Changes in mean arterial blood pressure (mmHg) following i.v. bolus injections of sodium nitroprusside (SNP, 10 nmol kg^{-1}) or acetylcholine (ACh, 1 nmol kg^{-1}). N^G-nitro-L-arginine methyl ester (L-NAME) was administered orally (approx. 70 mg kg^{-1} day^{-1} for 4–5 weeks) and the responses to SNP or ACh compared to those in control age-matched rats ($n=5$–7, a). L-NAME (10 μmol kg^{-1}) or saline was administered acutely and the hypotensive responses to SNP or ACh (SNP: control, open column; L-NAME, stippled column; ACh: control, solid column; L-NAME, hatched column; $n=5$) recorded (b). Values are mean ± s.e.mean; *$P<0.05$ versus baseline (Student's unpaired t test). Basal blood pressure values are given in the results.

by chronic L-NAME treatment (control, 338 ± 25; L-NAME, 369 ± 41).

The mean arterial blood pressure of anaesthetized control rats was 114 ± 5 mmHg ($n = 5$). This was elevated in anaesthetized rats receiving L-NAME chronically to 153 ± 11 mmHg ($n = 5$, $P < 0.05$). Acute administration of L-NAME (3–100 μmol kg^{-1}) to anaesthetized control animals caused an initial increase in basal blood pressure after injection of 3 μmol kg^{-1} (21.3 ± 3.4 mmHg, $P < 0.05$, $n = 5$), but no increase with subsequent doses (data not shown, $n = 5$).

Effects of chronic and acute L-NAME on haemodynamic responses

Falls in blood pressure induced by acetylcholine (1 nmol kg^{-1}) were not inhibited by chronic treatment with L-NAME (pressure changes: control, 31.1 ± 2.3 mmHg; chronic L-NAME, 48.7 ± 4.4 mmHg, $P < 0.05$; duration changes: control, 5.4 ± 0.6 s, chronic L-NAME, 11.4 ± 3 s, $P < 0.05$; $n = 5–7$) whereas those induced by sodium nitroprusside (10 nmol kg^{-1}) were enhanced (control, 40 ± 4.9 mmHg; chronic L-NAME, 83.4 ± 10 mmHg, $P < 0.05$; Figure 1a). Intravenous injection of endothelin-1 produced a biphasic response in control animals with an initial depressor response (−41 ± 3.3 mmHg) followed by a sustained pressor response (34 ± 4 mmHg). Chronic administration of L-NAME caused an enhancement in the depressor response (72 ± 7 mmHg) but no change in the secondary pressor response (38 ± 4 mmHg). Similarly, the pressor effects of phenylephrine (10 nmol kg^{-1}) and angiotensin II (5 pmol kg^{-1}) in control animals (phenylephrine, 38 ± 3.5 mmHg; angiotensin II, 30 ± 3.5 mmHg) were unchanged by chronic L-NAME treatment (phenylephrine, 39 ± 5.7 mmHg; angiotensin II, 37 ± 2.4 mmHg) ($n = 5–7$).

Acute intravenous injection of L-NAME (1–100 μmol kg^{-1}; $n = 5$) did not affect the falls in blood pressure or the duration of the vasodilatation induced by acetylcholine (1 nmol kg^{-1}, Figure 1b), but L-NAME at doses of 10 μmol kg^{-1} or greater enhanced those in response to sodium nitroprusside (10 nmol kg^{-1}) (Figure 1b).

Effects of chronic L-NAME on bladder function

Infusion of saline into the bladders of control animals resulted in micturition after 3.49 ± 1.17 min, at which time 0.87 ± 0.29 ml of saline had been infused and the intrabladder pressure was 22.05 ± 0.59 mmHg ($n = 3$). In rats treated chronically with L-NAME, micturition began after 6.49 ± 1.23 min at which time 1.62 ± 0.31 ml of saline had been infused and the intrabladder pressure was 20.76 ± 1.58 mmHg ($n = 3$).

Effects of chronic and acute L-NAME on responses of the thoracic aorta

Contractions of isolated rings of rat aorta induced by phenylephrine were unaffected by chronic L-NAME treatment ($n = 5–7$, data not shown). Acetylcholine caused concentration-dependent relaxations of endothelium-intact preparations taken from control animals ($n = 7$) but was without effect on tissues taken from rats chronically treated with L-NAME ($n = 5$, Figure 2a). Sodium nitroprusside caused similar relaxations of rings taken from either group of animals (data not shown, $n = 5–7$).

Acute addition of L-NAME (0.1–100 μM) to the organ baths inhibited in a concentration-dependent manner relaxations of control rat aortic rings induced by acetylcholine, with a significant effect being seen at a concentration of 1 μM ($n = 5$, Figure 2b). Responses to sodium nitroprusside (0.1 nM–1 μM) were unaffected by acute L-NAME administration ($n = 4–5$, data not shown).

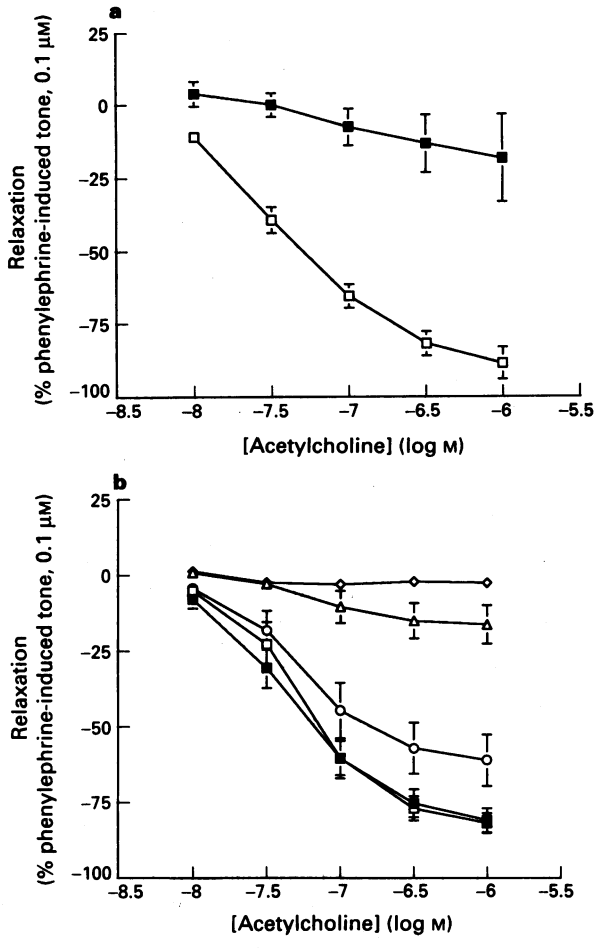

Figure 2 Percentage relaxation of the rat thoracic aorta after preconstriction with phenylephrine (0.1 μM) to increasing concentrations of acetylcholine (ACh). N^{G}-nitro-L-arginine methyl ester (L-NAME) was administered orally (approx. 70 mg kg^{-1} day^{-1} for 4–5 weeks) and the relaxations induced by ACh compared to responses in the aorta from control age-matched rats (ACh control with endothelium, □; ACh + L-NAME with endothelium, ■; $n = 5–7$, a). Increasing concentrations of L-NAME (0.1–100 μM) were administered acutely in tissues from animals not receiving chronic L-NAME and the vascular relaxations induced by increasing concentrations of ACh recorded (ACh control with endothelium, ■; ACh + L-NAME (0.1 μM) □; ACh + L-NAME (1 μM), ○; ACh + L-NAME (10 μM), △; ACh + L-NAME (100 μM), ◇; $n = 5$, b). Values are mean ± s.e. mean.

Effects of chronic and acute L-NAME on responses of the isolated perfused kidney

The basal perfusion pressure of the isolated kidney was 86 ± 6.7 mmHg which was increased to 112 ± 9.1 mmHg in organs taken from rats chronically treated with L-NAME ($P < 0.05$) ($n = 5–7$).

The falls in perfusion pressure induced by acetylcholine (1 nmol) or sodium nitroprusside (3 nmol) in kidneys from L-NAME-treated rats (acetylcholine, 79.6 ± 9.4 mmHg; sodium nitroprusside, 65.8 ± 16 mmHg) were not different from those recorded in control kidneys (acetylcholine, 74.4 ± 10.0 mmHg; sodium nitroprusside, 46.7 ± 10.3 mmHg) (Figure 3a). The duration of the vasodilatation induced by acetylcholine was also unchanged by chronic L-NAME (control, 48 ± 0; L-NAME, 50.4 ± 1.2 s, $P < 0.05$). Conversely, vasoconstriction induced by either phenylephrine (1–3 nmol) or angiotensin II (1–5 pmol) were significantly enhanced by chronic L-NAME treatment (Table 1) although the response

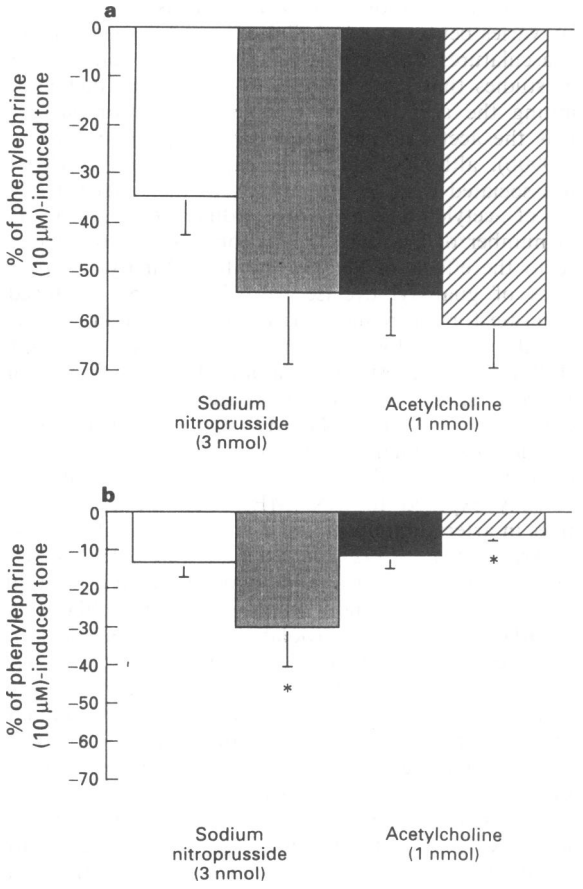

Figure 3 Changes in the perfusion pressure (mmHg) of the isolated perfused kidney following i.v. bolus injections of sodium nitroprusside (SNP, 3 nmol) or acetylcholine (ACh, 1 nmol). N^G-nitro-L-arginine methyl ester (L-NAME) was administered orally (approx. 70 mg kg^{-1} day^{-1} for 4–5 weeks) and the responses to SNP or ACh compared to those in control age-matched rats ($n = 5-7$, a). L-NAME (70 μM) or saline was administered acutely and the vasodilator responses to SNP or ACh recorded (SNP control, open column; SNP + L-NAME, stippled column; ACh control, solid column; ACh + L-NAME, hatched column; $n = 5$, b). Values are mean ± s.e.mean; $*P < 0.05$ versus baseline (Student's unpaired t test). Basal perfusion pressure values are given in the results.

Table 1 Changes in the perfusion pressure (mmHg) of the isolated perfused kidney caused by bolus injections of phenylephrine (1–3 nmol) or angiotensin II (1–5 pmol)

Drug	*Dose*	*Control*	*L-NAME*
Phenylephrine	1 nmol	10.63 ± 6.67	69.76 ± 16.85**
	3 nmol	51.98 ± 6.67	111.18 ± 17.67*
Angiotensin II	1 pmol	4.18 ± 2.01	52.21 ± 19.24*
	3 pmol	25.50 ± 9.51	99.88 ± 22.39**
	5 pmol	32.67 ± 10.84	99.04 ± 22.27*

The table shows the effect of chronic (4–6 weeks) oral administration of N^G-nitro-L-arginine methyl ester (L-NAME; approx. 70 mg kg^{-1} day^{-1}) on the responses to phenylephrine or angiotensin II ($n = 5-7$). Values are means ± s.e.mean ($*P < 0.05$; $**P < 0.01$ versus control; Student's unpaired t test).

to endothelin-1 (2.5 pmol) was unchanged (control, 58 ± 11.5 mmHg; chronic L-NAME, 51 ± 12.3 mmHg).

Acute administration of L-NAME (0.1–100 μM) inhibited in a concentration-dependent manner the falls in perfusion pressure, but did not affect the duration of vasodilatation, induced by acetylcholine (1 nmol) in the isolated perfused kidney. L-NAME did not affect the basal perfusion pressure (control, 12 ± 3; 10 μM L-NAME, 11 ± 3; 100 μM L-NAME, 6 ± 2% fall in perfusion pressure; duration: control, 48 ± 0, L-NAME, 48 ± 0 s, $n = 5$, Figure 3b). Conversely, vasodilatations induced by sodium nitroprusside (3 nmol) were unaffected by increasing concentrations of L-NAME compared to the vehicle time controls (Figure 3b).

Effects of chronic and acute L-NAME on responses of the anococcygeus and trachea

Anococcygeus muscles from control and chronically L-NAME-treated rats relaxed in a similar way in response to electrical field stimulation ($n = 5$, Figure 4a). However, acute addition of L-NAME (0.1–100 μM) to the organ baths inhibited in a concentration-dependent manner the relaxations, but not the duration of relaxation, of tissues taken from control animals, with a significant effect being seen at a concentration of 10 μM (Figure 4b) ($n = 4-6$).

Contractile responses to carbachol were largely unaffected by chronic treatment with L-NAME in rings of epithelium-intact or denuded trachea. For instance, in control preparations 0.3 μM carbachol caused a contraction of 1.0 ± 0.17 g ($n = 7$) in epithelium-intact rings and 0.92 ± 0.08 g ($n = 7$) in epithelium-denuded rings. In matched tissues taken from animals treated chronically with L-NAME the same concen-

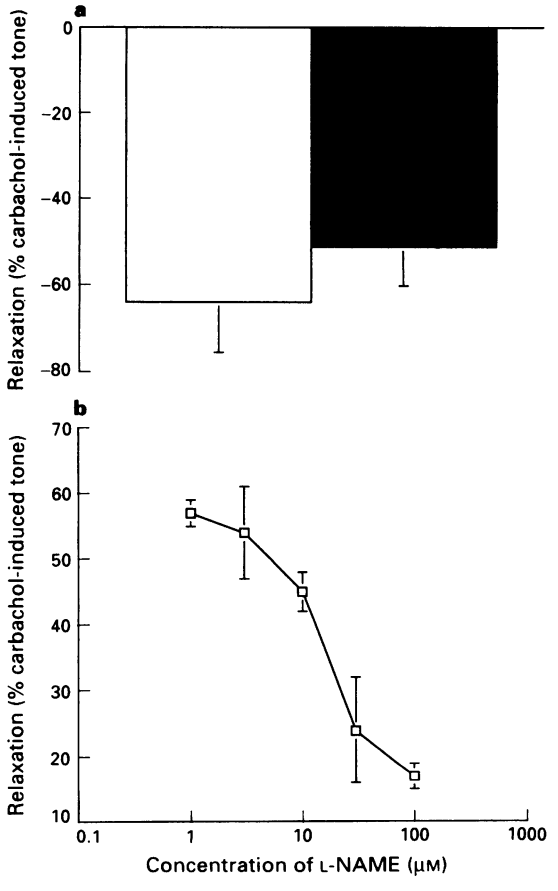

Figure 4 Relaxations of the rat anococcygeus muscle pre-contracted with carbachol (50 μM) induced by electrical field stimulation (0.3 mA, 10 Hz, 0.1 ms, 10 s every 100 s). (a) Shows the effect of chronic oral administration of N^G-nitro-L-arginine methyl ester (L-NAME; approx. 70 mg kg^{-1} day^{-1}) for 4–5 weeks on the electrically stimulated relaxations (control, open column; L-NAME, solid column; $n = 5$). (b) Shows the acute effects of increasing concentrations of L-NAME (0.1–100 μM) on the relaxations induced by electrical field stimulation (□; $n = 5$). Values are mean ± s.e.mean.

tration of carbachol induced contractions of 0.84 ± 0.18 (g) ($n = 4$) and 0.51 ± 0.12 (g) ($n = 5$), respectively. Similarly, endothelin-1 (30 nM) caused contractions of 0.82 ± 0.11 (g) ($n = 7$) and 0.9 ± 0.14 (g) ($n = 7$) in control preparations, respectively, with and without epithelium, and of 0.68 ± 0.17 (g) ($n = 4$) and 0.53 ± 0.1 (g) ($n = 5$) in the corresponding tissues prepared from rats chronically treated with L-NAME.

Effect of chronic L-NAME on nitric oxide synthase activity in the rat cerebellum

Cerebellar nitric oxide synthase activity was significantly reduced after treatment of rats with chronic L-NAME (control, 218.8 ± 18.8; L-NAME, 91.2 ± 18.0 pmol citrulline mg^{-1} protein $30\ min^{-1}$).

Discussion

Chronic administration of L-NAME to rats caused a marked increase in blood pressure and a complete loss of endothelial-dependent relaxations in isolated aortic rings. These data suggest that the increase in blood pressure observed was driven by a loss in NO-vasodilator tone. However, at the same time there was an enhancement in the hypotensive response to acetylcholine *in vivo*, and no reduction in the size of vasodilatations induced by acetylcholine in the isolated perfused kidney or in relaxations mediated by NO in the anococcygeus. These data suggest that chronically administered L-NAME does not produce a uniform inhibition of the activity of NO synthase. To investigate these differences further we examined the effects of the acute administration of L-NAME on the same preparations.

In isolated aortic rings, i.e. the simplest model of vascular activity used, endothelium-dependent relaxations induced by acetylcholine were significantly inhibited by L-NAME at a concentration of 1 μM. This result clearly suggests that the aortic rings taken from chronically treated animals had been exposed to a concentration of L-NAME of 1 μM or higher, as they did not relax in response to acetylcholine. In contrast to the aortic rings, relaxations of the anococcygeus induced by electrical field stimulation were inhibited by L-NAME only at concentrations greater than 10 μM, and tissues taken from chronically L-NAME-treated rats did not respond differently from controls. Similarly, tracheal rings, in which NO has been reported to be an inhibitory transmitter (Barnes, 1993), did not show an enhanced responsiveness to the spasmogens, carbachol and endothelin. Thus, it would appear that in animals chronically treated with L-NAME the anococcygeus had not been exposed to a high enough concentration of L-NAME, equivalent to less than 10 μM. The lack of inhibition in the anococcygeus from chronically treated animals cannot be explained by metabolism of the inhibitor as L-NAME and L-NOARG inhibit responses in this tissue similarly (Hobbs & Gibson, 1990). Together these *in vitro* organ bath data suggest that ingestion by rats of approximately $70\ mg\ kg^{-1}\ day^{-1}$ L-NAME produces an effect on individual tissues similar to the acute application of 1–10 μM of L-NAME.

Chronic treatment with L-NAME did not affect the vasodilatations of the isolated perfused kidney induced by acetylcholine or sodium nitroprusside. This may have been expected as vasodilatations induced by acetylcholine were only inhibited acutely by L-NAME administered at a concentration higher than 10 μM, i.e. more than the equivalent concentration achieved *in vivo* following chronic administration of L-NAME. It is interesting, however, that endothelium-dependent relaxation of the rat aorta were inhibited by 1 μM L-NAME whereas more than 10 times this concentration was required to inhibit vasodilatation in the isolated kidney. This suggests that within the kidney vasculature, vasodilatation induced by acetylcholine is mediated by mechanisms in addition to NO, as there is no evidence that eNOS varies between endothelial cells in different portions of the vasculature. This conclusion would be consistent with other studies that have found L-NAME to be ineffective at inhibiting the acetylcholine renal vasodilatation *in vivo* as well as the acetylcholine hypotensive response (Gardiner *et al.*, 1990b), although long term exposure to L-NAME has been associated with an attenuation of the renal vasodilator effects of acetylcholine *in vivo* (Gardiner *et al.*, 1993). There are a number of possible explanations for this relative resistance to the effects of eNOS inhibition. Firstly, the responsiveness of guanylyl cyclase to NO may be enhanced to compensate for the reduced basal activation that would follow a fall in the endogenous production of NO (Moncada *et al.*, 1991). This suggestion is supported by our finding of an enhanced response *in vivo* to sodium nitroprusside after chronic treatment with L-NAME. On the other hand, we found no such enhancement in the responses of isolated perfused kidneys or thoracic aortae prepared from animals chronically exposed to L-NAME, as is the case for both changes in arterial blood pressure and regional blood flows *in vivo* (Arnal *et al.*, 1992; Gardiner *et al.*, 1993). A second explanation may be that acetylcholine stimulates, in addition to NO, the release of endothelium-derived vasodilators such as endothelial-derived hyperpolarizing factor (Komori *et al.*, 1988). These could explain the relative resistance of acetylcholine *in vivo* and *in vitro* to the acute or chronic administration of L-NAME. Thirdly, it may be that the differences are due to variations in the tissue distribution of L-NAME, i.e. that the endothelial cells within the kidney are exposed to a lower concentration of L-NAME than the endothelium in the aorta. This appears unlikely, although it is known that while L-NAME is readily taken up into cells, it is also rapidly metabolised in blood and plasma into its active, stable metabolite, L-NOARG (Krejcy *et al.*, 1993). L-NOARG, for its part, is poorly taken up by cells, and differential cellular uptake can therefore occur (Krejcy *et al.*, 1993). However, the differences seen in experiments examining the acute effects of L-NAME cannot be explained in this way. Interestingly, the isolated perfused kidney demonstrated greatly exaggerated vasoconstrictions in response to both phenylephrine and angiotensin II, although not to endothelin-1. This marked increase may also explain the effectiveness of inhibitors of the renin-angiotensin system in reducing the hypertension caused by chronic administration of L-NAME (Riberio *et al.*, 1992; Pollock *et al.*, 1993), for an increased sensitivity of the renal vasculature to angiotensin II would lead to renal vasoconstriction which could further enhance the production of renin.

Our examination of the kidney showed gross changes similar to those noted before (Ribeiro *et al.*, 1992; Baylis *et al.*, 1993) and these appeared associated with increases in bladder content. To examine this further we investigated the differences in bladder capacity and intrabladder pressure at the time of micturition. There was a clear tendency to an increase in bladder capacity although this was not associated with an increase in intrabladder pressure. Possibly, this is an adaptive change due to the role of NO in regulating the activity of the lower urinary tract of the rat (Persson *et al.*, 1992; Parlani *et al.*, 1993). This result suggests that the changes in renal structure could in part be due to alterations in bladder emptying.

We conclude that chronic oral treatment of animals with L-NAME affects NO-dependent responses in a non-uniform manner. The possible mechanisms for these differences include alterations in the sensitivity of the guanylyl cyclase pathways or increased activity of other complementary mechanisms, such as other vasodilators. It is also interesting to note that peripheral neuronal NO responses were resistant to inhibition by chronic treatment with L-NAME, while endothelial NO responses were markedly affected, indicating that selective inhibition of different isoforms of NOS may be achieved *in vivo*.

This work was supported by a grant from Glaxo Group research. C.E.B. is a Wellcome Veterinary Research Fellow. We would like to thank Professor Sir John Vane for helpful discussions.

References

ARNAL, J.F., WARIN, L. & MICHEL, J.B. (1992). Determinants of aortic cyclic guanosine monophosphate in hypertension induced by chronic inhibition of nitric oxide synthase. *J. Clin. Invest.*, **90**, 647–652.

BARNES, P.J. (1993). Nitric oxide and airways. *Eur. Respir. J.*, **6**, 163–165.

BAYLIS, C., ENGELS, K., SAMSELL, L. & HARTON, P. (1993). Renal effects of acute endothelial-derived relaxing factor blockade are not mediated by angiotensin II. *Am. J. Physiol.*, **264**, F74–F78.

BAYLIS, C., HARTON, P. & ENGELS, K. (1990). Endothelial derived relaxing factor controls renal haemodynamics in the normal rat kidney. *J. Am. Soc. Nephrol.*, **1**, 875–881.

BAYLIS, C., MITRUKA, B. & DENG, A. (1992). Chronic blockade of nitric oxide synthesis in the rat produces systemic hypertension and glomerular damage. *J. Clin. Invest.*, **90**, 278–281.

BRADFORD, M.M. (1976). A rapid and sensitive method for the quantification of protein dye binding. *Anal. Biochem.*, **72**, 248–254.

DENG, L.Y., THIABAULT, G. & SCHIFFRIN, E.L. (1993). Effect of hypertension induced by nitric oxide synthase inhibition on structure and function of resistance arteries in the rat. *Clin. Exp. Hypertens.*, **15**, 527–537.

GARDINER, S.M., COMPTON, A.M., KEMP, P.A. & BENNETT, T. (1990a). Regional and cardiac haemodynamic effects of N^G-nitro-L-arginine methyl ester in conscious, Long Evans Rats. *Br. J. Pharmacol.*, **101**, 625–631.

GARDINER, S.M., COMPTON, A.M., & BENNETT, T. (1990b). Regional and cardiac haemodynamic responses to glyceryl trinitrate, acetylcholine, bradykinin and endothelin-1 in conscious rats: effects of N^G-nitro-L-arginine methyl ester. *Br. J. Pharmacol.*, **101**, 632–639.

GARDINER, S.M., KEMP, P.A. & BENNETT, T. (1993). Effects of chronic treatment with nitric oxide synthase inhibitors on regional haemodynamic responses to vasodilators in conscious Brattlebro rats. *Br. J. Pharmacol.*, **109**, 222–228.

GILLESPIE, J.S. (1972). The rat anococcygeus muscle and its response to nerve stimulation and to some drugs. *Br. J. Pharmacol.*, **45**, 404–416.

HOBBS, A.J. & GIBSON, A. (1990). L-N^G-nitro-arginine and its methyl ester are potent inhibitors of non-adrenergic, non-cholinergic transmission in the rat anococcygeus. *Br. J. Pharmacol.*, **100**, 749–752.

KOMORI, K., LORENZ, R.R. & VANHOUTTE, P.M. (1988). Nitric oxide, acetylcholine and electrical and mechanical properties of arterial smooth muscle. *Am. J. Physiol.*, **255**, H207–H212.

KREJCY, K., SCHWARZACHER, S. & RABERGER, G. (1993). Distribution and metabolism of N^G-nitro-L-arginine methyl ester in canine blood *in vitro*. *Naunyn-Schmied. Arch. Pharmacol.*, **347**, 342–345.

LEHERA, V., SALAZAR, J., SALOM, M.G. & ROMERO, J.C. (1992). Deficient production of nitric oxide induces volume-dependent hypertension. *J. Hypertens.* (suppl. 7), S173–S177.

LEHERA, V., SALOM, M.G., MIRANDA-GUARDIOLA, F., MONCADA, S. & ROMERO, J.C. (1991). Effects of N^G-nitro-L-arginine methyl-ester on renal function and blood pressure. *Am. J. Physiol.*, **261**, F1033–F1037.

MONCADA, S., PALMER, R.M.J. & HIGGS, E.A. (1991). Nitric oxide: physiology, pathophysiology and pharmacology. *Pharmacol. Rev.*, **43**, 109–142.

MOORE, P.K., AL-SWAYEH, O.A., CHONG, N.W.S., EVANS, R.A. & GIBSON, A. (1990). L-N^G-nitro-arginine (L-NOARG), a novel, L-arginine reversible inhibitor of endothelium-dependent vasodilation *in vitro*. *Br. J. Pharmacol.*, **99**, 408–412.

MORTON, J.J., BEATTIE, E.C., SPIERS, A. & GULLIVER, F. (1993). Persistent hypertension following inhibition of nitric oxide formation in the young Wistar rat: role of renin and vascular hypertrophy. *J. Hypertens.*, **11**, 1083–1088.

PARLANI, M., CONTE, B. & MANZINI, S. (1993). Nonadrenergic, noncholinergic inhibitory control of the rat external urethral sphincter: involvement of nitric oxide. *J. Pharmacol. Exp. Ther.*, **265**, 713–719.

PERSSON, K., IGAWA, Y., MATTIASSON, A. & ANDERSON, K.E. (1993). Effects of inhibition of the L-arginine/nitric oxide pathway in the rat lower urinary tract *in vivo* and *in vitro*. *Br. J. Pharmacol.*, **107**, 178–184.

POLLOCK, D.M., POLAKAWSKI, J.S., DIVISH, B.J. & OPGENORTH, T.J. (1993). Angiotensin blockade reverses hypertension during long-term nitric oxide synthase inhibition. *Hypertension*, **21**, 660–666.

REES, D.D., PALMER, R.M.J., SCHULZ, R., HODSON, H.F. & MONCADA, S. (1990). Characterisation of three inhibitors of endothelial nitric oxide synthase *in vitro* and *in vivo*. *Br. J. Pharmacol.*, **101**, 746–752.

RIBERIO, M.O., ANTUNES, E., DE NUCCI, G., LOVISOLO, S.M. & ZATZ, R. (1992). Chronic inhibition of nitric oxide synthesis: a new model of arterial hypertension. *Hypertension*, **20**, 298–303.

(Received October 10, 1994
Revised December 20, 1994
Accepted December 22, 1994)

British Journal of Pharmacology (1995) 114, 1680–1686 © 1995 Stockton Press All rights reserved 0007–1188/95 $12.00

Vascular actions of thrombin receptor-derived polypeptides: structure-activity profiles for contractile and relaxant effects in rat aorta

Adebayo A. Laniyonu & [1]Morely D. Hollenberg

Endocrine Research Group, Department of Pharmacology & Therapeutics and Department of Medicine, The University of Calgary, Faculty of Medicine, Calgary, AB Canada T2N 4N1

1 Using endothelium-denuded and intact rat aortic rings, we have determined the contractile and relaxant structure-activity profile for a series of thrombin receptor-derived polypeptides (TRPs) based on the human and rat receptor sequences: SFLLR (P5), SFLLR-NH_2 (P5-NH_2) SFFLR (Rat P5), SFFLR-NH_2 (Rat P5-NH_2), SFLLRNP (P7), SFLLRNP-NH_2 (P7-NH_2), SFFLRNP (Rat P7), SFFLRNP-NH_2 (Rat P7-NH_2), and SFLLRNPNDKYEPF (P14).

2 A contractile response to thrombin and the TRPs in the endothelium-denuded aortic tissue was minimal or absent in preparations obtained from animals weighing less than 180 g (<6 weeks of age), but increased with animal size, plateauing in tissues derived from animals weighing between 320 and 420 g (about 9 to 14 weeks of age). In contrast, the contractile responses to KCl and noradrenaline did not differ in the tissues and relaxant responses to the TRPs in endothelium-intact aortic preparations were comparable for tissues obtained from either young ($\leqslant$ 180 g) or older ($\geqslant$ 320 g) animals.

3 The contractile response of the endothelium-denuded preparation to thrombin and the TRPs showed marked cross-desensitization: the relaxation response of the intact rings did not desensitize to the TRPs.

4 The relative potencies for the TRPs in the aortic contraction assay were comparable to those for the relaxation assay, but were distinct from the relative potencies we measured previously in a rat gastric longitudinal muscle contraction assay. Further, P5 behaved as a partial agonist in the aortic contraction assay, whereas it had been observed to be a full agonist in the gastric contraction assay.

5 The contractile activity of P5-NH_2 in endothelium intact aortic rings was low or absent, but in the presence of the nitric oxide synthase inhibitor, N^{ω}-nitro-L-arginine-methyl ester (L-NAME), the contractions in the intact preparation were equivalent to the response of the endothelium-denuded preparation in the absence of L-NAME.

6 The contractile response of the endothelium-denuded aortic preparation to P5-NH_2 was inhibited by nifedipine and the kinase C antagonist, chelerythrine, but was resistant to the action of indomethacin, tetrodotoxin and the tyrosine kinase inhibitor, genistein.

7 We conclude that the receptor system for the TRPs in the aortic smooth muscle elements, responsible for the contractile response, is similar to the aortic endothelial cell receptor responsible for the relaxation response, but is distinct from the receptor that we have previously characterized in gastric longitudinal smooth muscle, results pointing to the presence of receptor subtypes in the vascular and gastric smooth muscle elements.

Keywords: Thrombin; thrombin receptor; thrombin receptor-derived peptides; rat aorta

Introduction

Thrombin, apart from its widely recognized role as a coagulation factor, *via* the proteolytic cleavage of fibrinogen and the activation of platelets, has also been known for some time to regulate vascular contractility (White *et al.*, 1980; DeMey *et al.*, 1982; Rapoport *et al.*, 1984; White *et al.*, 1984; Haver & Namm, 1984; Walz *et al.*, 1986). Depending on the vascular preparation, thrombin can cause either an endothelium-dependent relaxation (DeMey *et al.*, 1982; Rapoport *et al.*, 1984; White *et al.*, 1984; Walz *et al.*, 1985) or an endothelium-independent contraction (Haver & Namm, 1984; White *et al.*, 1984; Walz *et al.*, 1985). The proteolytic mechanism whereby thrombin activates target tissues such as the platelet has been elucidated by Coughlin and colleagues (Vu *et al.*, 1991; Coughlin *et al.*, 1992), who in parallel with others (Rasmussen *et al.*, 1991) cloned the G-protein-coupled receptor for thrombin and demonstrated that proteolytic activation of the receptor involves the exposure of an amino-terminal sequence (beginning with serine-42 in the human receptor), that acts as an 'anchored' or 'tethered' receptor-activating moiety. Remarkably, peptides derived from the thrombin-revealed amino-terminal sequence of the receptor (TRPs), beginning with serine and ranging from five (P5) to fourteen (P14) amino acids, have been found to mimic the actions of thrombin in a variety of target tissues ranging from platelets (Chao *et al.*, 1992; Hui *et al.*, 1992; Sabo *et al.*, 1992; Vassallo *et al.*, 1992) to vascular and gastric smooth muscle (Yang *et al.*, 1992; Muramatsu *et al.*, 1992; deBlois *et al.*, 1992).

In our own work studying the action of TRPs in rat aortic tissue derived from relatively young rats (<200 g; 6 weeks or younger), we observed that the principal response of the tissue to thrombin and to the TRPs was an endothelium-dependent relaxation (Muramatsu *et al.*, 1992; Yang *et al.*, 1992); we were unable to detect a thrombin-dependent contraction in endothelium-free rat aortic tissue, although guinea-pig aortic tissue contracted in response to thrombin and to the fourteen amino acid human TRP, P14 (Muramatsu *et al.*, 1992). In subsequent studies with rat vascular and gastric tissues, using a variety of TRPs ranging

[1] Author for correspondence.

in length from five (P5) to seven (P7) amino acids, both in their carboxylate (P5, P7) and amidated (P5-NH_2, P7-NH_2) forms (Hollenberg *et al.*, 1993), we observed distinct structure-activity profiles for the endothelium-dependent aortic relaxation response (potency order: P7-NH_2 $\geqslant$ P5-NH_2 > Rat P5-NH_2 > P5 $\simeq$ P7), compared with the gastric longitudinal muscle contractile response (potency order: Rat P5-NH_2 > P7-NH_2 > P5-NH_2 > P7 > P5), so as to suggest the existence of functional receptor subtypes. We were puzzled to learn from a study appearing after the completion of our structure-activity work, that the TRPs, P7 and P14, could elicit a contractile response in endothelium-denuded rat aortic rings (Antonaccio *et al.*, 1993), whereas our own work with rat aortic preparations failed to detect such a response; and we were intrigued to see that the human TRPs, P7 and P14, were apparently equipotent in terms of the rat aortic contraction assay (Antonaccio *et al.*, 1993), whereas our own work indicated that P7 and P14 exhibit distinct potencies in other bioassay systems (Hollenberg *et al.*, 1992; 1993). The study we describe here was done with two main aims: first, to determine conditions under which a reproducible contractile response to TRPs could be observed in the endothelium-free rat aortic ring preparation; and second, to determine the structure-activity relationships for a spectrum of TRPs in the rat aortic contraction assay. In addition to comparing the structure-activity relationships for the contraction assay, with results obtained in parallel in the endothelium-dependent aortic relaxation assay, we were especially interested to compare the results using the aortic contraction assay with data we obtained previously using a rat gastric contractile assay (Hollenberg *et al.*, 1993). Our data demonstrated that a contractile response to the TRPs was observed reliably in tissues derived from older animals (240 to 420 g; 7.5 to 14 weeks), but was barely detectable in young animals (< 180 g; < 6 weeks). Further, although there were only subtle differences between the TRP structure-activity profiles for the two vascular assays (contraction and relaxation), there was a clear difference between the structure-activity profile for the vascular contractile assay and the profile we observed in the previous study with the rat gastric longitudinal smooth muscle contractile assay.

Methods

Bioassay procedures

Procedures for the humane treatment of animals, according to the Declaration of Helsinki and as approved by an institutional committee on animal care were followed. Male Sprague-Dawley rats (140 to 430 g, as indicated) were killed by cervical dislocation, and the thoracic aorta was removed for the preparation of ring segments (2 mm × 3 mm) to be used for bioassay purposes. Rings were used either intact or after mechanical disruption of the endothelium by rolling the interior aspect of the ring gently over the inserted end of a fine forceps. Rings were mounted in a plastic organ bath (4 ml total capacity) and were bathed at 37°C in gassed (95% O_2/5% CO_2) Krebs-Henseleit buffer (pH 7.4) of the following composition (mM): NaCl 118, KCl 4.7, $CaCl_2$ 2.5, $MgCl_2$ 1.2, $NaHCO_3$ 25, KH_2PO_4 1.2 and glucose 10. Tissue was equilibrated for about 1 h before the start of an experiment and the tension (base line, 1.0 g) was monitored isometrically with Grass force-displacement transducers. The presence (or absence) of an intact endothelium was ascertained by monitoring the relaxation response to 1 μM acetylcholine in a preparation that was submaximally contracted with 0.1 μM noradrenaline in the presence of 0.1 mM ascorbic acid (to preserve the catecholamine). For intact preparations, only tissues yielding a relaxation concentration-response curve between 0.01 and 10 μM acetylcholine (maximal relaxation of 70–90%, relative to the tension developed with 0.1 μM noradrenaline) were used to evaluate the actions of the TRPs. The relaxation responses to the TRPs were measured (e.g. see Figure 2) in tissues that were pre-contracted with 0.1 μM noradrenaline at 30 min time intervals. Tissues were washed approximately 5 min after the application of TRPs. In previous work (Hollenberg *et al.*, 1993) it was observed that 215 μM (137 μg ml^{-1}) P5 caused a maximal relaxation of the pre-contracted endothelium-intact rat aortic preparation. Therefore, as in previous work (Hollenberg *et al.*, 1993), to normalize data between individual tissue preparations and to construct concentration-effect curves, the relaxation responses to P5 and to the other TRPs were expressed as a percentage (% $P5_{215}$) of the relaxation caused by 215 μM P5. Concentration-response curves for relaxation were carried out on tissues obtained from animals weighing from 320 to 420 g. As will be described in the results section, large animals (320 to 420 g) were required for monitoring a contractile response; and the contractile response exhibited desensitization towards repeated exposures to the TRPs. Therefore, in the endothelium-free ring preparations, the contractile response to the TRPs was monitored only once, after assessing the tissue response to 50 mM KCl (1.4 ± 0.4 g: mean ± standard error for $n = 195$). Thus, to construct concentration-response curves for the TRPs and to normalize data between different tissue preparations, the contractile responses to the TRPs were expressed as a percentage (% KCl) of the response elicited by 50 mM KCl, which concentration was at the plateau of the KCl concentration-response curve. For purposes of comparison, the same stock solutions of the individual TRPs were evaluated in both the contractile and relaxation assays.

Peptides and other reagents

The TRPs based on the human receptor sequence (P5, SFLLR; P5-NH_2, SFLLR-NH_2; P7, SFLLRNP; P7-NH_2, SFLLRNP-NH_2; P14, SFLLRNPNDKYEPF) and on the rat receptor sequence (Rat P5, SFFLR; Rat P5-NH_2, SFFLR-NH_2; Rat P7, SFFLRNP; Rat P7-NH_2, SFFLRNP-NH_2), prepared by standard solid phase synthesis procedures, were provided either by BioChem Therapeutic Inc., Laval PQ, Canada, with the assistance of Dr John DiMaio or by the Core Peptide Synthesis Laboratory at the Department of Biochemistry, Queens University, Kingston, ON, Canada. Peptides were > 95% pure by chromatographic criteria (h.p.l.c.). Weighed peptide samples were routinely dissolved in 50 mM phosphate buffer, pH 7.4 to yield stock solutions, from which volumes of up to 0.2 ml were added directly to the organ bath; the concentrations and amino acid compositions of all TRP stock solutions used were verified by quantitative amino acid analysis of aliquots. Acetylcholine, indomethacin, noradrenaline, nifedipine, N^{ω}-nitro-L-arginine methyl ester (L-NAME), chelerythrine and thrombin (1000 units mg^{-1}; catalogue No. T3010: 1 clotting unit of thrombin ml^{-1} is equivalent to approximately 10 nM pure enzyme) were from Sigma (St. Louis, MO, U.S.A.); genistein was from ICN Bio Chemicals (Costa Mesa, CA, U.S.A.) and tetrodotoxin was from Calbiochem (San Diego, CA, U.S.A.). Indomethacin was dissolved in ethanol, such that the final ethanol concentration in the organ bath was $\leqslant$ 0.01% (v/v); this concentration of ethanol alone did not affect the bioassay systems. Stock solutions of genistein were prepared with dimethylsulphoxide, which alone upon dilution in the organ bath to a concentration lower than 0.01% v/v did not affect the bioassay.

Results

Characteristics of the contractile response to TRPs: roles of animal size and desensitization

In keeping with our previous observations (Muramatsu *et al.*, 1992), we were not able to observe a reproducible contractile

response either to the TRPs or to thrombin in tissues obtained from rats weighing less than 180 g ($\leqslant$ 6 weeks old, data not shown). In view of the findings of Antonaccio *et al.* (1993), we decided to evaluate the responsiveness of tissues obtained from older animals, using body weight as an index of age, according to a chart provided by the animal supplier. When we examined tissues from animals more than 7 weeks old ($\geqslant$ 240 g), it proved possible to monitor a contractile response. Upon studying tissue responsiveness as a function of animal weight, we determined that there was a marked increase in contractile responsiveness to the TRPs between animals weighing from 180 to 240 g (6 to 8 weeks of age); a plateau in responsiveness was observed in tissues obtained from animals weighing between 320 and 420 g (9 to 14 weeks of age) (Figure 1). In contrast, there was no appreciable difference in the relaxation response to the TRPs of endothelium-intact preparations obtained from either young ($\leqslant$ 180 g) or older ($\geqslant$ 320 g) animals. Moreover, no such change in the contractile response with animal age of the gastric longitudinal muscle response to the TRPs had been noted in connection with our previous study. Further, in the aortic tissue, in contrast to the change in responsiveness to the TRPs, the magnitude of the contractile response to 50 mM KCl of tissues derived from the younger (1.4 ± 0.2 g, mean ± s.e. for $n = 8$) and older animals (1.4 ± 0.6 g, mean ± s.e. for $n = 15$) did not differ, nor did the response to 0.1 μM noradrenaline (Figure 1). In view of these observations, subsequent work was done only with tissues obtained from animals weighing 320 g or more ($\geqslant$ 9 weeks of age), in which both the contractile and relaxant responses were measured.

We had previously observed that the contractile response of guinea-pig aortic tissue desensitized both to thrombin and to the TRP, P14 (Muramatsu *et al.*, 1992). Since we wished to obtain concentration-effect curves for the contractile actions of the TRPs, we first wished to determine if desensitization would also occur for the contractile action of the TRPs in the rat aortic preparation. As illustrated in Figures 2 and 3, the contractile response did desensitize towards the repeated exposure of the tissue to the TRP, P5-NH_2, resulting in a greater than 60% desensitization after 3 exposures. In keeping with our previous observations (Hollenberg *et al.*, 1993), the relaxant response did not desensitize to P5-NH_2 (Figure 3) but did so to thrombin (not shown). Thrombin (3 u ml^{-1}; 30 nM) also caused a contractile response in the endothelium-free preparations from animals weighing from 320 to 420 g in contrast with the lack of response to thrombin of tissues derived from young animals ($\leqslant$ 180 g). However, once exposed to thrombin, the responsive tissue became completely refractory to subsequent exposures to the enzyme (data not shown). Although refractory to thrombin, a thrombin-treated tissue was still able to contract in response to P5-NH_2 (not shown). Nonetheless, prior treatment of a

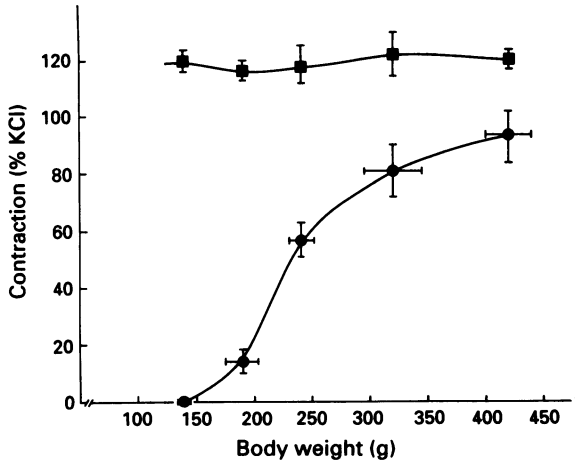

Figure 1 Contractile response of endothelium-denuded aorta rings as a function of animal age. The contractile responsiveness of 10 μM P5-NH_2 (●) and 0.1 μM noradrenaline (■) of preparations obtained from animals ranging in weight from 140 g (approximately 5 weeks old) to 420 g (about 12 to 14 weeks old) was measured (% KCl) relative to the contractile response of the same tissues to 50 mM KCl. Values for the contractile responses represent averages ± s.e. (vertical bars) for observations done with eight or more individual tissue strips obtained from each of 3 to 5 different animals, for which the average weights (± s.e.: horizontal bars) are shown on the abscissa scale.

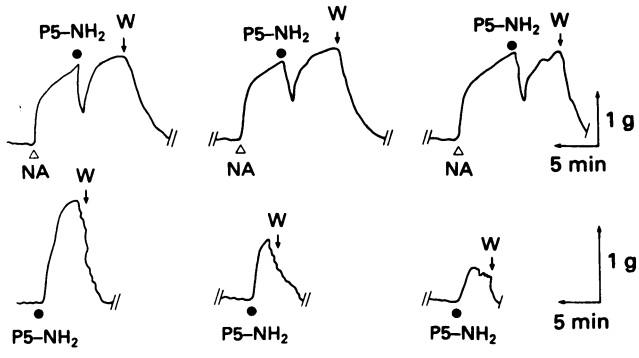

Figure 2 Relaxant and contractile responses of intact and endothelium-denuded aortic preparations. Representative relaxant (upper tracings) or contractile (lower tracings) responses to sequential replicate applications of 10 μM P5-NH_2 (●) are shown for individual tissue strips, exposed to P5-NH_2 at 30 min intervals for the relaxation assay and at 70 min intervals for the contraction assay, followed by washing (W, arrows) and re-equilibration in fresh buffer. The relaxant response was monitored in a tissue that was pre-contracted with 0.1 μM noradrenaline (NA, Δ). The scales for time and tension are shown to the right of the tracings.

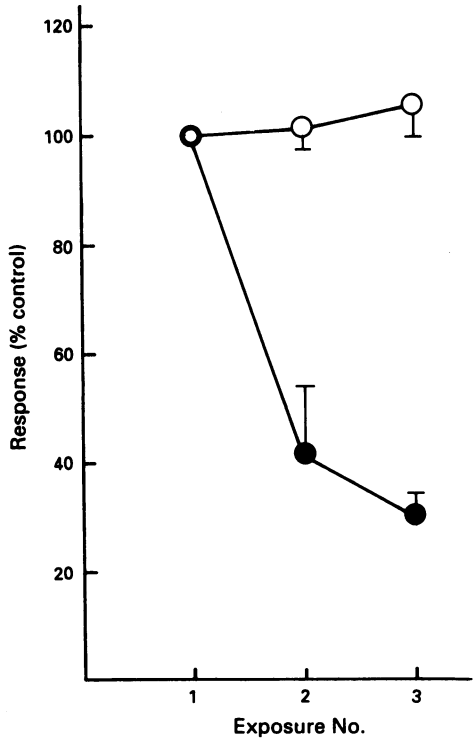

Figure 3 Desensitization of the contractile but not the relaxation response. The contractile (●) and relaxant (○) responses of intact (○) or endothelium-denuded (●) aortic preparations were measured in tissues exposed sequentially to P5-NH_2 (10 μM) as illustrated in Figure 2. The average responses (± s.e.) of 4 to 6 individual tissue preparations, relative to the first contractile or relaxant response (% control) are shown for three consecutive exposures to P5-NH_2.

tissue with thrombin (3 u ml^{-1}; 30 nM) reduced the contractile response of the tissue (% KCl) to P5-NH_2 (10 μM) from 98 ± 10% (mean ± s.e. for $n = 7$) in untreated tissues to 57 ± 8% (mean ± s.e. for $n = 6$) of the contractile response caused by 50 mM KCl. Similarly, in a tissue that was partially desensitized by multiple exposures to P5-NH_2 (see Figure 3), the contractile response (% KCl) to 3 u ml^{-1} (30 nM) thrombin was also reduced from 27 ± 7% (mean ± s.e. for $n = 4$) to 3 ± 1% (mean ± s.e. for $n = 5$) of the contractile response to 50 mM KCl. Thus, there was cross-desensitization of the contractile response caused by thrombin and P5-NH_2. In tissues that were desensitized either to thrombin or the TRPs, there was no desensitization of the response to either KCl (50 mM) or noradrenaline (0.1 μM) (not shown).

Concentration-effect curves

For the construction of concentration-effect curves, it was necessary to take into account desensitization properties described for the contractile assay in the previous section. Thus, the contractile responsiveness of an endothelium-denuded preparation was standardized using 50 mM KCl as a stimulus and the first response of the tissue either to the TRPs or thrombin was then measured, relative to the KCl-induced contraction. As shown in Figure 4, TRPs based both on the human and rat receptor sequences yielded concentration-effect curves over a concentration-range of 1 to 200 μM. In the contraction assay, the order of potencies of the peptides was: P7-NH_2 = P5-NH_2 > Rat P7-NH_2 ≥ P14 = Rat P5-NH_2 > P7 ≥ Rat P7 ≥ P5 > Rat P5. Although all of the peptides appeared to be full agonists in the relaxation assay (see below: Figure 4b), Rat P5 and human P5 behaved only as partial agonists in the contraction assay. The maximal contractile response to P5 was equivalent to the maximal contractile effect caused by thrombin. However, the maximal contractile effect of the other TRPs was 3 to 4 fold greater than that caused by either thrombin or P5 (Figure 4). The comparatively low response to thrombin, which would presumably be the physiological agonist, may have been due to its desensitizing properties, as described above.

It was necessary to repeat with tissues from the older animals (≥ 320 g), the relaxation assays done previously with tissues obtained from younger animals, to permit a direct comparison with the contractile assay done in the present study. For the relaxant concentration-effect curves, as in previous work (Hollenberg *et al.*, 1993), tissues were exposed to TRPs at 30 min intervals and the relaxation response was expressed as a percentage of the maximal relaxant effect in the same tissue of 215 μM P5(% P_{215}). In the relaxation assay done with tissues from the older animals, the relative order of potencies of the peptides examined was: P7-NH_2 ≥ P5-

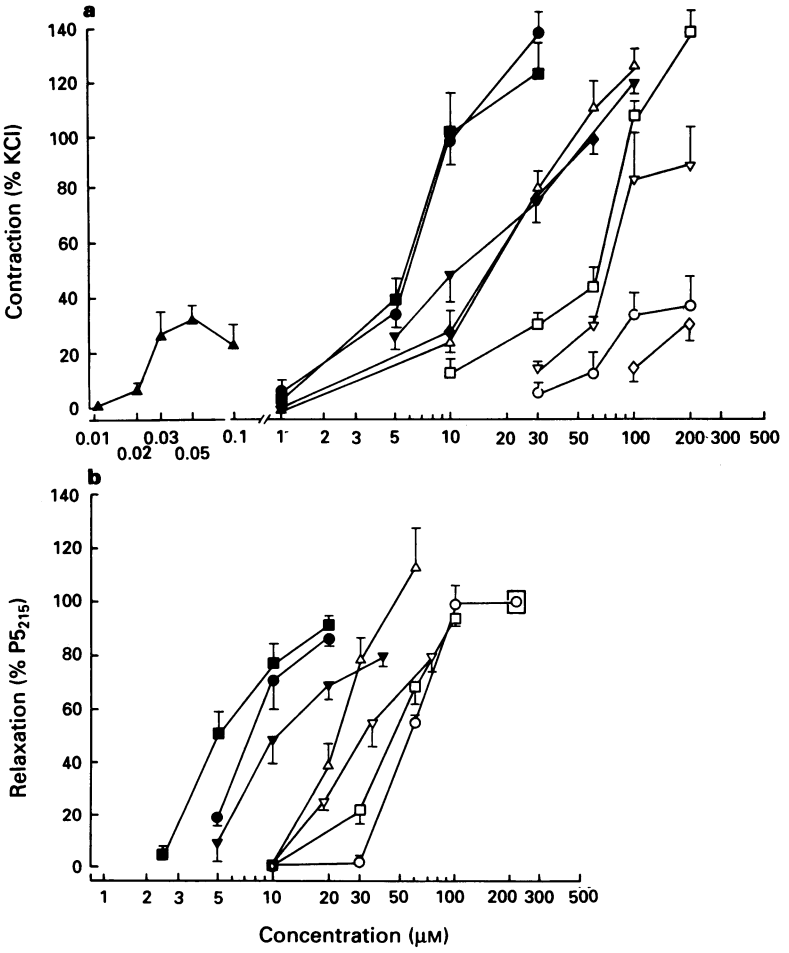

Figure 4 Concentration-effect curves for TRPs and thrombin in the contractile (a) and relaxant (b) assays. Tissues were exposed to increasing concentrations of the TRPs to obtain responses such as those shown in Figure 2. Contractile preparations were exposed only once to each TRP and the responses (% KCl) were measured relative to the contraction caused by 50 mM KCl in the same preparation. The relaxation responses in individual pre-contracted rings (0.1 μM noradrenaline) were quantitated as a percentage (% P_{215}) of the relaxation caused by 215 μM P5 (boxed open circle) (48 ± 3% relaxation, mean ± s.e. for $n = 20$). The concentration-response curves for each agonist represent data from assays done with tissue from three or more animals, using five or more independent tissues in each assay. The figure shows the average response at each concentration, with the s.e. ($n = 5-12$) represented at each point with a bar. The symbols used for thrombin and the various TRPs are: (○) P5; (◇) Rat P5; (●) P5-NH_2; (◆) Rat P5-NH_2; (□) P7; (▼) Rat P7-NH_2; (■) P7-NH_2 (▽) Rat P7; (△) P-14 and (▲) thrombin.

NH_2 > Rat P7-NH_2 > P14 ≥ Rat P7 > P7 ≃ P5, entirely in keeping with our previous work.

As we observed previously with a contractile assay using rat gastric tissue (Hollenberg *et al.*, 1993), establishing a single maximum response level in the aortic contractile assay was problematic because of differences in apparent agonist efficacies. Thus, the precise determinations of the EC_{50} values were not attempted. Rather, for comparative quantitative purposes for this study and for comparison with our previous work, the potencies of the TRPs were expressed relative to the activity of P5-NH_2. By use of at least three response levels on the linear portions of the concentration-effect curves, a potency ratio (R_{EC}) for each TRP was calculated, relative to the concentrations of P5-NH_2 causing an equivalent contractile or relaxant response (i.e. $R_{EC} = EC_{TRP} \div EC_{P5\text{-}NH_2}$). With this approach, it was possible to calculate the relative equi-effective concentration values (R_{EC} values, Table 1) for all agonists evaluated in the present study and to place in the table, calculated values obtained from our previous study of the aortic relaxation assay and the gastric longitudinal muscle contraction assay (Hollenberg *et al.*, 1993). A comparison of the values in the table revealed a pattern of concordance between potency profiles of the TRPs in the two vascular assays, but a clear distinction between the values for the aortic contraction assay and the gastric contractile assay.

Role of peptide proteolysis

Both in a human platelet aggregation assay and in a rabbit vascular contractile assay, the aminopeptidase inhibitor, amastatin, has been found to potentiate the actions of TRPs (Coller *et al.*, 1992; Godin *et al.*, 1994). In contrast, in our own work with the rat vascular assay system (Hollenberg *et al.*, 1993), we found by h.p.l.c. analysis that the TRPs were not subject to proteolysis in the organ bath during the course of an assay and we observed that, functionally, the addition of amastatin to the organ bath did not potentiate the action of P5 in the vascular relaxation assay. Nonetheless, we wished to rule out the possibility that the low intrinsic activity of P5 in the aorta contractile assay (Figure 4a) might be due to the presence of aminopeptidase activity. Therefore, the contractile activity of P5 (100 μM) was measured both in the absence and presence of 10 μM amastatin. Relative to the contractile response of preparations to 50 mM KCl, 100 μM P5 caused a 34 ± 3% (mean ± s.e. for $n = 7$) response in the absence of amastatin and a 38 ± 10% (mean ± s.e. for $n = 4$) response in the presence of the aminopeptidase inhibitor. Thus, aminopeptidase activity did not appear to be a factor in the rat aortic contractile assay and did not appear to account for the relatively low contractile response of the tissue to P5, compared with the other TRPs.

Signal transduction pathways

In our previous work comparing the aortic relaxation assay with the guinea-pig and rat gastric longitudinal smooth muscle assays (Hollenberg *et al.*, 1993), we established that both genistein and indomethacin could attenuate the contractile, but not the relaxant actions of P5-NH_2, thereby suggesting roles for tyrosine kinase and cyclo-oxygenase pathways in the gastric smooth muscle contractile response. Further, we observed that the calcium channel blocking reagent, verapamil could inhibit the contractile action of P14 in a guinea-pig aortic preparation (Muramatsu *et al.*, 1992). Accordingly, we evaluated the effects of genistein, indomethacin and the calcium channel blocker, nifedipine, on the contractile action of P5-NH_2 in rat aortic contraction assay. Further, we assessed the effects of the kinase C inhibitor, chelerythrine and the neuronal toxin, tetrodotoxin. As summarized in Table 2, indomethacin was without effect and genistein caused only a 25% inhibition in the rat aortic contractile assay, whereas we previously determined that these two reagents markedly affected the gastric contractile assays (Hollenberg *et al.*, 1993). Tetrodotoxin also had no effect. In contrast, nifedipine and chelerythrine caused a 60 to 70% inhibition of the contractile activity of P5-NH_2 in the endothelium-denuded aortic preparation.

Role of endothelial nitric oxide synthase

Although the predominant action of P5-NH_2 in the endothelium-intact aorta preparation was to cause a relaxation of pre-contracted tissue (see Figure 2), we also observed a small but consistent increase in tension in this preparation when a comparatively high concentration of P5-NH_2 alone (> 10 μM) was added to the organ bath (Figure 5 and data

Table 2 Effects of antagonists on P5-NH_2-induced contractions

Addition	*Contractile response (% KCl)*
None	98 ± 10 (7)
Genistein (15 μM)	74 ± 5 (4)
Indomethacin (3 μM)	94 ± 12 (4)
Nifedipine (1 μM)	38 ± 2 (4)
Tetrodotoxin (10 μM)	96 ± 11 (5)
Chelerythrine (5 μM)	30 ± 6 (4)

The contractile response to 10 μM P5-NH_2 was measured, relative to the action of 50 mM KCl (% KCl), either for untreated tissues (no addition) or for tissues treated with the indicated antagonist for 20 min prior to the addition of P5-NH_2. Values represent the means ± s.e. for the number of estimates shown in parentheses.

Table 1 Relative potencies of TRPs in the aortic and gastric bioassay systems

		R_{EC} value (relative to P5-NH_2)[a]		
Peptide	*Designation*	*Aortic relaxation*	*Aortic contraction*	*Gastric contraction*[b]
SFLLR	P5	7.5 ± 0.1	29 ± 3[c]	5.0
SFLLR-NH_2	P5-NH_2	1	1	1
SFFLR	Rat P5	44[b]	55 ± 2	5.0
SFFLR-NH_2	Rat P5-NH_2	2.0[b]	2.9 ± 0.04	0.35
SFLLRNP	P7	6.0 ± 0.02	11 ± 0.6	1.5
SFLLRNP-NH_2	P7-NH_2	0.69 ± 0.04	1.0 ± 0.01	0.5
SFFLRNP	Rat P7	4.0 ± 0.4	14 ± 1[c]	1.5
SFFLRNP-NH_2	Rat P7-NH_2	1.6 ± 0.3	2.3 ± 0.8	ND
SFLLRNPNDKYEPF	P14	2.7 ± 0.2	3.0 ± 0.3	ND

[a]The potencies of the TRPs, relative to P5-NH_2, as expressed by the R_{EC} values, were calculated from the concentration-effect curves shown in Figure 4, as outlined in the text, according to the formula: $R_{EC} = EC_{TRP} \div EC_{P5\text{-}NH_2}$. Values represent the means ± s.e.mean for R_{EC} values calculated from measurements at 3 to 4 levels of response along linear portions of the concentration-response curves for the various TRPs and P5-NH_2. An R_{EC} value > 1 denotes a TRP with a potency lower than that of P5-NH_2. [b]Values calculated from Table 1 of Hollenberg *et al.*, 1993. [c]Partial agonist. ND = not determined.

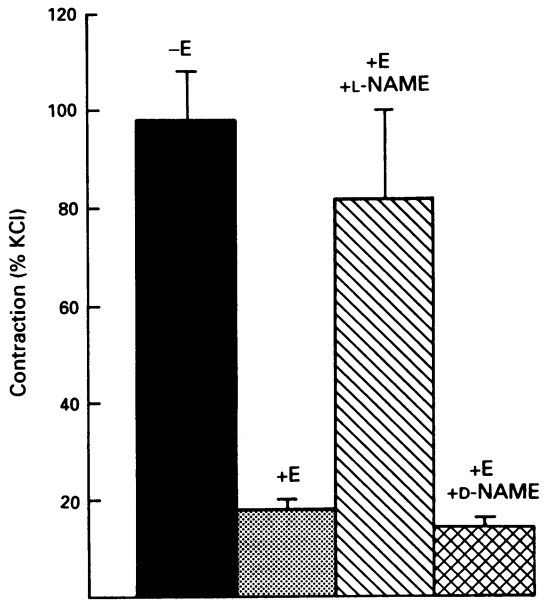

Figure 5 Effect of N$^{\omega}$-nitro-L-arginine methyl ester (L-NAME) on the contractile response of endothelium-intact aortic rings. The response of preparations with an intact endothelium (+ E) to 10 μM P5-NH_2 was measured in the absence (stippled column) or in the presence of either L-NAME (100 μM: hatched column) or D-NAME (100 μM: cross-hatched column). Responses of the intact preparations were compared with the response to 10 μM P5-NH_2 of endothelium-denuded preparations (− E) in the absence of L-NAME (solid column). Contractile responses, representing the average ± s.e. for 4 to 8 individual tissue strips, were measured as a percentage (% KCl) of the tissue response to 50 mM KCl.

not shown). Since the relaxant effect of the TRPs in the aortic preparation is due to the production of nitric oxide (Muramatsu *et al.*, 1992), we wished to determine the degree to which the inhibition of nitric oxide synthase by L-NAME in an endothelium-intact aorta preparation could unmask the contractile action of P5-NH_2. As illustrated in Figure 5, in the presence of 100 μM L-NAME, the contractile action of P5-NH_2 in the endothelium-intact preparation was equivalent to the contractile effect of P5-NH_2 in the absence of L-NAME in an endothelium-denuded preparation. In contrast, the D-isomer of the synthase inhibitor, D-NAME, was ineffective in unmasking a contractile effect of P5-NH_2 in the endothelium-intact preparation.

Discussion

Our work has revealed two significant factors that are relevant to a study of the contractile activity of thrombin and the receptor-derived TRPs in rat vascular tissues. First, it is evident that the vascular contractile response to the TRPs is dependent on animal age, as reflected by body weight. Second, it appears that both thrombin and the TRPs cause desensitization of the contractile response, whereas the relaxant response of the vascular preparation to the TRPs does not desensitize. The desensitizing property of thrombin, which may explain its action only as a partial agonist in the contractile assay, may be of physiological relevance because the thrombin-mediated signal at a site of injury would be short-lived. Since tetrodotoxin did not block the action of the TRPs in the aortic contractile assay, and since the aortic tissue is minimally innervated, the desensitization process would appear to occur at the level of the smooth muscle rather than nerve elements in the aortic tissue. The dependence of the contractile response on the age of the animal would explain the apparent discrepancies between our earlier work using vascular tissues from young rats (< 200 g), wherein thrombin failed to elicit a contractile response (Muramatsu *et al.*, 1992), and the more recent results of Antonaccio *et al.* (1993), who observed a contractile response to TRPs in endothelium-denuded vascular preparations obtained from older animals (14 weeks; > 420 g). The marked increase in contractile responsiveness to TRPs of the aortic tissue from rats between about 6 and 9 weeks of age points to interesting changes in the receptor system in the vascular smooth muscle elements that merit further study.

One main outcome of our work was that by using aortic preparations from older animals and by measuring the non-desensitized contractile responses to thrombin and the TRPs, it was possible to obtain a contractile structure-activity profile for comparison with the profile obtained using the endothelium-dependent relaxation assay and with the profile we determined previously for the gastric longitudinal muscle contraction assay (Hollenberg *et al.*, 1993). The main finding (Figure 4 and Table 1) was that the order of peptide potencies in the aortic contractile assay were in keeping with the potency order observed in the endothelium-dependent relaxation assay, but did not agree with the potency order we observed previously in the gastric longitudinal muscle contraction assay (see Figure 3 in Hollenberg *et al.*, 1993). For instance, for both the aortic contraction and relaxation assays, the order of potency of the TRPs, P5-NH_2, Rat P5-NH_2 and P7 was: P5-NH_2 > Rat P5-NH_2 >> P7 (R_{EC} values for contractile assay, 1:2.9:11; and for the relaxation assay, 1:2.0:6.0), whereas the order of potency of these three peptides measured previously in the gastric contractile assay was distinctly different: Rat P5-NH_2 > P5-NH_2 ≥ P7 (R_{EC} values, 0.35:1:1.5). Further similarities between the endothelial and smooth muscle receptor systems conferring relaxation and contraction in the aorta preparation can be seen in the comparable potencies, relative to P5-NH_2 (R_{EC} values, Table 1), of Rat P7-NH_2, P7-NH_2 and P14. In this context it can be pointed out that in both of the aortic tissue assays done according to our procedures, P7 and P14 had distinct relative potencies (P14 > P7 for both assays) as opposed to the equal potencies observed for P14 and P7 by Antonaccio *et al.* (1993), who used a cumulative concentration-effect procedure for the aortic contraction assay. We believe the potency differences between P14 and P7 observed by us in the aortic contractile assay are due to our conduct of the assay in a manner that took into consideration the ability of the TRPs to cause receptor desensitization.

In addition to the distinct structure-activity profiles for the TRPs, differences between the receptor system responsible for the contractile response of the aortic tissue and the contraction of the gastric longitudinal muscle preparation (Hollenberg *et al.*, 1993) can be seen in: (1) the desensitization of the contractile response to TRPs in the aortic tissue but not in the gastric preparation, (2) the inability of P5 to act as a full agonist in the contractile aorta preparation, compared with its high degree of intrinsic activity in the gastric contraction assay and (3) the differences in the signal transduction system used in the aortic contraction assay (see Table 2), which, as opposed to the gastric contractile assay, does not appear to involve either tyrosine kinase or cyclooxygenase pathways, but rather appears to depend on a kinase C-mediated pathway, linked to the influx of extracellular calcium. Given these differences between the contractile assays employing the aortic tissue on the one hand and the gastric tissue on the other, particularly in terms of the distinct TRP structure-activity profiles, it is possible to suggest, according to classical criteria (Ahlquist, 1948), that the vascular and gastric smooth muscle element possess distinct thrombin receptor subtypes, with the vascular smooth muscle receptor closely resembling the one present in vascular endothelial cells. Unfortunately, antagonists of the vascular and endothelial thrombin receptors are not yet available to evaluate this possibility by a bioassay procedure. As an alternative to rationalizing the different structure-activity

profiles in the gastric and vascular smooth muscle tissue in terms of distinct receptor subtypes, it could be suggested on the theoretical grounds (Kenakin *et al.*, 1989), that the coupling of the same thrombin receptor to distinct transducer proteins in the gastric and vascular tissue might alter the relative potencies of the agonists. Further work will thus be required to determine the molecular basis for the differences in the receptor systems present in vascular and gastric tissue. Nonetheless, from a practical point of view, the data we have obtained point to the possibility of synthesizing tissue-specific agonists or antagonists that may target selectively either the gastric or the vascular receptor for the TRPs.

These studies were supported primarily by funding provided by the Canadian Medical Research Council, partly in conjunction with BioChem Therapeutic Inc., Laval PQ Canada (University-Industry programme). We are grateful to Dr S. Ahmad for his critical reading of this manuscript.

References

ALQUIST, R.P. (1948). A study of the adrenotropic receptors. *Am. J. Physiol.*, **153**, 586–600.

ANTONACCIO, M.J., NORMANDIN, D., SERAFINO, R. & MORELAND, S. (1993). Effects of thrombin and thrombin receptor activating peptides on rat aortic vascular smooth muscle. *J. Pharmacol. Exp. Ther.*, **266**, 125–132.

CHAO, B.H., KALKUNTE, S., MARAGANORE, J.M. & STONE, S.R. (1992). Essential groups in synthetic agonist peptides for activation of the platelet thrombin receptor. *Biochemistry*, **31**, 6175–6178.

COLLER, B.S., WARD, P., CERUSO, M., SCUDDER, L.E., SPRINGER, K., KUTOK, J. & PRESTWICH, G.D. (1992). Thrombin receptor activating peptide: Importance of the N-terminal serine and its ionization state as judged by pH dependence, nuclear magnetic resonance spectroscopy, and cleavage by aminopeptidase M. *Biochem.*, **31**, 11713–11720.

COUGHLIN, S.R., VU, T.-K., HUNG, D.T. & WHEATON, V.I. (1992). Characterization of a functional thrombin receptor. *J. Clin. Invest.*, **89**, 351–355.

DEBLOIS, D., DRAPEAU, G., PETITCLERC, E. & MARCEAU, F. (1992). Synergism between the contractile effect of epidermal growth factor and that of des-Arg_9-bradykinin or of α-thrombin in rabbit aortic rings. *Br. J. Pharmacol.*, **105**, 959–967.

DE MEY, J.G., CLAEYS, M. & VANHOUTTE, P.M. (1982). Endothelium-dependent inhibitory effects of acetylcholine, adenosine triphosphate, thrombin and arachidonic acid in the canine femoral artery. *J. Pharmacol. Exp. Ther.*, **222**, 166–173.

GODIN, D., MARCEAU, F., BEAULÉ, C., RIOUX, F. & DRAPEAU, G. (1994). Aminopeptidase modulation of the pharmacological responses to synthetic thrombin receptor agonists. *Eur. J. Pharmacol.*, **253**, 225–230.

HAVER, V.M. & NAMM, D.H. (1984). Characterization of the thrombin-induced contraction of vascular smooth muscle. *Blood*, **21**, 53–63.

HOLLENBERG, M.D., LANIYONU, A.A., SAIFEDDINE, M. & MOORE, G.J. (1993). Role of the amino- and carboxyl-terminal domains of thrombin receptor-derived polypeptides in biological activity in vascular endothelium and gastric smooth muscle: evidence for receptor subtypes. *Mol. Pharmacol.*, **43**, 921–930.

HOLLENBERG, M.D., YANG, S.-G., LANIYONU, A.A., MOORE, G.J. & SAIFEDDINE, M. (1992). Action of thrombin receptor polypeptide in gastric smooth muscle: identification of a core pentapeptide retaining full thrombin-mimetic intrinsic activity. *Mol. Pharmacol.*, **42**, 186–191.

HUI, K.Y., JAKUBOWSKI, J.A., WYSS, V.L. & ANGLETON, E.L. (1992). Minimal sequence requirement of thrombin receptor agonist peptide. *Biochem. Biophys. Res. Commun.*, **184**, 790–796.

KENAKIN, T.P. & MORGAN, P.H. (1989). Theorectical effects of single and multiple transducer receptor coupling proteins on estimates of the relative potency of agonists. *Mol. Pharmacol.*, **35**, 214–222.

MURAMATSU, I., LANIYONU, A.A., MOORE, G.J. & HOLLENBERG, M.D. (1992). Vascular actions of thrombin receptor peptide. *Can. J. Physiol. Pharmacol.*, **70**, 996–1003.

RAPOPORT, R.M., DRAZNIN, M.B. & MURAD, F. (1984). Mechanisms of adenosine triphosphate-, thrombin-, and trypsin-induced relaxation of rat thoracic aorta. *Circ. Res.*, **55**, 468–479.

RASMUSSEN, U.G., VOURET-CRAVIARI, V., JALLAT, S., SCHLESINGER, Y., PAGÈS, G., PAVIRANI, A., LECOCQ, J.P., POUYSSÉGUR, J. & VAN OBBERGHEN-SCHILLING, E. (1991). cDNA cloning and expression of a hamster α-thrombin receptor coupled to Ca^{2+} mobilization. *FEBS Lett.*, **288**, 123–128.

SABO, T., GURWITZ, D., MOTOLA, L., BRODT, P., BARAK, R. & ELHANATY, E. (1992). Structure-activity studies of the thrombin receptor activating peptide. *Biochem. Biophys. Res. Commun.*, **188**, 604–610.

VASSALLO, JR, R.R., KIEBER-EMMONS, T., CICHOWSKI, K. & BRASS, L.F. (1992). Structure-function relationships in the activation of platelet thrombin receptors by receptor-derived peptides. *J. Biol. Chem.*, **267**, 6081–6085.

VU, T.-K.H., HUANG, D.T., WHEATON, V.I. & COUGHLIN, S.R. (1991). Molecular cloning of a functional thrombin receptor reveals a novel proteolytic mechanism of receptor activation. *Cell*, **64**, 1057–1068.

WALZ, D.A., ANDERSON, G.F., CIAGLOWSKI, R.E., AIKEN, M. & FENTON, J.W. (1985). Thrombin-elicited contractile responses of aortic smooth muscle. *Proc. Soc. Exp. Biol. Med.*, **180**, 518–526.

WALZ, D.A., ANDERSON, G.F., & FENTON, J.W. (1986). Responses of aortic smooth muscle to thrombin and thrombin analogues. *Annals New York Acad. Sci.*, **485**, 323–334.

WHITE, R.P., CHAPLEAU, C.E. DUGDALE, M. & ROBERTSON, J.T. (1980). Cerebral arterial contractions induced by human and bovin thrombin. *Stroke*, **11**, 363–368.

WHITE, R.P., SHIRASAWA, Y. & ROBERTSON, J.T. (1984). Comparison of responses elicited by alpha-thrombin in isolated canine basilar, coronary, mesenteric, and renal arteries. *Blood Vessels*, **21**, 12–22.

YANG, S.-G., LANIYONU, A.A., SAIFEDDINE, M., MOORE, G.J. & HOLLENBERG. M.D. (1992). Actions of thrombin and thrombin receptor peptide analogues in gastric and aortic smooth muscle: Development of bioassays for structure-activity studies. *Life Sci.*, **51**, 1325–1332.

(Received November 14, 1994
Revised December 5, 1994
Accepted December 23, 1994)

British Journal of Pharmacology (1995) 114, 1687-1693 © 1995 Stockton Press All rights reserved 0007-1188/95 $12.00

Protein kinase A and nicotinic activation of bovine adrenal tyrosine hydroxylase

[1]Philip D. Marley, Kerrie A. Thomson & Roger A. Bralow

Department of Pharmacology, University of Melbourne, Parkville, Victoria 3052, Australia

1 Stimulation of nicotinic cholinoceptors on bovine chromaffin cells increases phosphorylation of three serine residues in tyrosine hydroxylase (TOH) and activates TOH. One of the serines is a target for protein kinase A phosphorylation, and phosphorylation of this serine is adequate alone to cause TOH activation. The role of protein kinase A in nicotinic activation of TOH was therefore investigated.

2 TOH activity was studied *in situ* in intact, cultured, bovine adrenal chromaffin cells, by measuring $^{14}CO_2$ evolved following the hydroxylation and rapid decarboxylation of [^{14}C]-tyrosine offered to the cells.

3 Nicotine (5 μM), forskolin (1 μM) and 8-bromo-cyclic AMP (8-Br-cyclic AMP, 1 mM) each increased TOH activity by up to 200% over 10 min. The effect of nicotine was completely abolished by removal of extracellular Ca^{2+}.

4 TOH activation by all three drugs was blocked by H89 (3–20 μM), which inhibits protein kinase A by competing for the ATP binding site on the kinase. Adenosine 3':5'-cyclic monophosphorothioate Rp-diastereomer (Rp-cAMPS) (1 mM), an inhibitor of protein kinase A that competes with cyclic AMP for the regulatory subunit of the kinase, abolished the activation of TOH by nicotine, and reduced that by forskolin and 8-Br-cyclic AMP. Both H89 and Rp-cAMPS inhibited basal TOH activity by 50–80%.

5 A structural analogue of H89, H85 (3–20 μM), which lacks activity as a protein kinase A inhibitor, did not inhibit either the activation of TOH by nicotine (5 μM) or basal TOH activity. Neither sodium nitroprusside (0.3–10 μM) nor 8-Br-cyclic GMP (1 mM) increased TOH activity.

6 In digitonin-permeabilized chromaffin cells, forskolin (3 μM), cyclic AMP (10 μM) and Ca^{2+} (approx. 2 μM free Ca^{2+}) each increased TOH activity. The response to all three drugs was blocked by H89 (10 μM), which also reduced basal TOH activity in the permeabilized cells.

7 Maximal activation of TOH by forskolin was achieved with 10 μM forskolin. This concentration was less than the EC_{50} for forskolin-induced cyclic AMP accumulation in these cells. The activations of TOH by forskolin (10 μM) and nicotine (5 μM) were additive.

8 The results indicate that both basal TOH activity and nicotinic activation of TOH in bovine chromaffin cells require protein kinase A activity. However, it is unlikely that nicotinic activation of TOH is directly mediated by an activation of protein kinase A in response to elevated cyclic AMP levels. It is possible that protein kinase A plays a permissive role in allowing nicotinic cholinoceptors to activate TOH by another signalling pathway.

Keywords: Tyrosine hydroxylase; nicotinic cholinoceptors; chromaffin cells; protein kinase A; cyclic AMP; kinases

Introduction

Stimulation of the splanchnic nerves innervating the adrenal medulla not only causes catecholamine secretion but also a concomitant increase in catecholamine biosynthesis (Haycock & Wakade, 1992). This is the result of acute activation of tyrosine hydroxylase (TOH), the rate-limiting enzyme for adrenaline and noradrenaline synthesis (Zigmond *et al.*, 1989). Cholinergic activation of adrenal chromaffin cells mimics the effect of splanchnic nerve activation, in producing Ca^{2+}-dependent increases in catecholamine secretion, TOH phosphorylation and TOH activity (Haycock *et al.*, 1982b). Early studies demonstrated that stimulation also produced an increase in adrenal medullary adenosine 3':5'-cyclic monophosphate (cyclic AMP) levels (Guidotii & Costa, 1973; 1974). Since protein kinase A (PK-A) was shown to phosphorylate and activate TOH from bovine adrenal medulla (Yamauchi & Fujisawa, 1979; Meligeni *et al.*, 1982), it was suggested that cyclic AMP and protein kinase A may mediate the nicotinic activation of TOH in bovine chromaffin cells (see Meligeni *et al.*, 1982).

More recent work has demonstrated that both rat and bovine TOH are phosphorylated on four distinct serine residues (Ser^8, Ser^{19}, Ser^{31} and Ser^{40}) in the N-terminal regulatory domain of the enzyme (Haycock, 1990; 1993). The phosphorylation state of these residues has been reported to affect the pH optimum of TOH, the K_m for the substrate tyrosine, the K_m for the tetrahydrobiopterin cofactor and the K_i for feedback inhibition of TOH by dopamine and other catechols (Zigmond *et al.*, 1989). However, it is unclear which of these mechanisms is responsible for activating TOH under physiological conditions. In bovine chromaffin cells, PK-A increases the phosphorylation of only one of these sites, Ser^{40}, both *in situ* in intact cells, and *in vitro* in chromaffin cell supernatants using endogenous TOH and endogenous protein kinase A, and this phosphorylation is known to activate TOH (Meligeni *et al.*, 1982; George *et al.*, 1989; see Haycock, 1993). In contrast, nicotinic stimulation of bovine chromaffin cells causes increased phosphorylation on more than one serine, namely serines 19, 31 and 40 (Haycock *et al.*, 1982a,b; Pocotte *et al.*, 1986; Waymire *et al.*, 1988; Haycock, 1993). *In situ*, phosphorylation of Ser^{19} appears to be mediated by Ca^{2+}/calmodulin-dependent protein kinase II (CAM-K-II) and that of Ser^{31} by the ERKs (extracellular signal regulated kinases; MAP-kinases), which may in turn be activated by protein kinase C (PK-C: Haycock *et al.*, 1992, see Haycock, 1993). However, phos-

[1] Author for correspondence.

phorylation of TOH by CAM-K-II or by ERK *in vitro* do not on their own produce substantial activation of TOH (Yamauchi & Fujisawa, 1981; Haycock *et al.*, 1992).

The question arises, therefore, which of the phosphorylations produced by nicotinic stimulation causes the activation of TOH, and how is this phosphorylation mediated. Since nicotinic stimulation of chromaffin cells produces Ca^{2+}-dependent increase in cyclic AMP levels (Anderson *et al.*, 1992), and PK-A phosphorylates TOH on one of the serine residues affected by nicotine, and this phosphorylation is sufficient to activate TOH, we have investigated the role of PK-A in the nicotinic activation of TOH. Our approach has been to study TOH activity *in situ* in intact, cultured, bovine adrenal chromaffin cells, under normal prevailing cellular pH, subcellular compartmentation and aggregation state of TOH, and concentrations of tyrosine, biopterin cofactor and feedback inhibitors. The role of PK-A has been assessed by use of cell-permeant pharmacological inhibitors of protein kinases. Preliminary reports of this work have been published (Bralow *et al.*, 1992; Marley *et al.*, 1993; Thomson *et al.*, 1993).

Methods

Measurement of TOH activity in bovine chromaffin cells

Bovine adrenal chromaffin cells were isolated as described (Livett *et al.*, 1987b), and cultured for two or three days at a density of 55×10^6 cells per 35 ml in 650 ml culture flasks. Cells were then harvested by use of a disposable cell scraper. Quantitatively similar data were obtained with cells harvested by trypsinisation. Cells were washed three times by centrifugation (200 *g*, 10 min, room temperature) in a HEPES-buffered saline solution (HBS) prewarmed to 37°C of composition (mM): NaCl 150, HEPES 15, D-glucose 5.5, K_2HPO_4 3.8, $MgSO_4$ 1, $CaCl_2$ 1.5, and sodium ascorbate 0.5, supplemented with 0.5% BSA, pH 7.4. Cells were then equilibrated in HBS for 60 min at 37°C, before a final centrifugation and resuspension at a density of 6×10^6 cells ml^{-1}.

TOH activity was measured at 37°C *in situ* in the isolated chromaffin cells by the method of Meligeni *et al.* (1982). In brief, aliquots of the cell suspension (100 µl containing 0.6×10^6 cells) were added to prewarmed glass test tubes, followed by addition of 100 µl of HBS containing L-[carboxyl-^{14}C]-tyrosine to give a final concentration of 10 µM (specific activity 50–60 mCi $mmol^{-1}$), together with agonists at twice their final concentration. When kinase inhibitors were used, they were added to the 100 µl of cells in a volume of 50 µl for a 15 min preincubation period, before the addition of [^{14}C]-tyrosine and agonists together with inhibitors in a further 50 µl volume. Upon addition of [^{14}C]-tyrosine, each tube was immediately capped with a rubber stopper from which was suspended a filter paper wick (Whatmann 3MM) wetted with 100 µl of 1 M NaOH, to absorb the $^{14}CO_2$ emitted. Cells were incubated for 10 min, after which the reaction was terminated by transfering the tubes to ice and immediately injecting 200 µl of 10% trichloroacetic acid through the stopper to lyse the cells. The tubes were then placed in a shaking water bath for at least 50 min, to ensure efficient trapping of evolved $^{14}CO_2$. The filter paper wicks were subsequently removed for counting.

TOH activity in Ca^{2+}-free buffer and in digitonin-permeabilized cells

TOH activity was studied in Ca^{2+}-free buffer by twice washing the cells after the 60 min equilibration period in HBS solution from which the $CaCl_2$ was omitted (HBS-Ca^{2+}). All subsequent treatments were then performed with this buffer.

To study TOH activity after permeabilization with digitonin, cells were washed twice after the 60 min equilibration period in HBS solution from which both the $CaCl_2$ and BSA were omitted (HBS-BSA-Ca^{2+}). Aliquots of cells suspended in this buffer (100 µl containing 0.6×10^6 cells) were then added to glass tubes as above. Kinase inhibitors were added in 50 µl in HBS-BSA-Ca^{2+} solution, for a 15 min preincubation before the cells were permeabilized. Permeabilization and stimulation was then achieved by the addition of digitonin and [^{14}C]-tyrosine together with stimulators and kinase inhibitors in 50 µl of high potassium glutamate buffer (HKGB) of composition (mM): L-glutamic acid monopotassium salt 139, HEPES 20, $MgCl_2$ 5, ATP 5, D-glucose 5.1, EGTA (ethylene glycol-*bis*(β-aminoethylether)-N,N,N′,N′-tetraacetic acid) 5, pH 6.6. The final concentration of digitonin was 10 µM. When Ca^{2+} was used as the agonist, 2.5 mM $CaCl_2$ was added to the digitonin solution in HKGB, to give a [Ca^{2+}]/[EGTA] ratio of 0.5 (approximate free Ca^{2+} concentration, 2 µM).

Cyclic AMP responses and catecholamine secretion from bovine cultured chromaffin cells

Cellular cyclic AMP responses were measured by radioimmunoassay, as described in detail previously (Marley *et al.*, 1991). Catecholamine secretion was measured by h.p.l.c. with electrochemical detection essentially as described (Livett *et al.*, 1987a).

Data presentation and statistics

All results are presented as mean ± s.e. mean for the stated number of determinations from a single preparation of cells. The number of cell preparations on which similar observations were made is given in the figure legends. Statistical significance for multiple comparisons has been assessed by the modified *t*-statistic provided by Fisher's least significant difference (LSD) test, protected by a one-way analysis of variance (ANOVA). Interactions between combinations of drugs were assessed by two-way ANOVA or by determining whether the observed effect of combining the drugs lay outside the 95% confidence limits for the expected value had the drugs been simply additive (see Moeller *et al.*, 1989). In all cases, a P value of <0.05 was taken to indicate statistical significance.

Drugs

H89 (N-[2-(*p*-bromocinnamylamino)ethyl]-5-isoquinolinesulphonamide) and H85 (N-[2-(N-formyl-*p*-chlorocinnamylamino)ethyl]-5-isoquinolinesulphonamide) were from Seikagaku Co, Tokyo, Japan. Rp-cAMPS (adenosine-3′:5′-cyclic monophosphorothioate Rp-diastereomer, triethylamine salt) was from BioLog Life Science Institute, Bremen, Germany and from Research Biochemicals International, Natick, U.S.A. Nicotine, 8-bromo-adenosine-3′:5′-cyclic monophosphate sodium salt, and digitonin were from Sigma Chemical Co, St Louis, U.S.A. Forskolin was from Calbiochem-Novabiochem Pty Ltd, Australia. L-[carboxyl-^{14}C]-tyrosine, 50–60 mCi $mmol^{-1}$, was from Amersham International Plc, U.K.

Results

Effect of PK-A inhibitors on nicotinic activation of TOH

Nicotine produced a concentration-dependent activation of TOH that was completely dependent on extracellular Ca^{2+} (data not shown), as reported by others (Haycock *et al.*, 1982b; Pocotte *et al.*, 1986). The EC_{50} was approximately 5 µM. The rate of $^{14}CO_2$ production was linear for over 15 min. In the remaining experiments, all stimulations were for 10 min and with 5 µM nicotine.

The activation of TOH by nicotine was blocked by H89

(Figure 1a), a specific PK-A inhibitor that competes for the ATP binding site on PK-A (Hidaka *et al.*, 1991). H89 also inhibited the TOH activation produced by forskolin (1 μM, approximately the EC_{50} Figure 1b). It was noteworthy that H89 consistently reduced basal TOH activity by 50–80%.

Although H89 has been reported to be a very selective inhibitor of PK-A, its full pharmacological profile has not been well characterized. Consequently, its specificity has been assessed here by a number of approaches. Firstly, as an ATP binding site inhibitor, H89 might inhibit the responses to nicotine and forskolin by inhibiting adenylate cyclase. This was found not to be the case, since forskolin-stimulated cyclic AMP formation in cultured bovine chromaffin cells was *enhanced*, not inhibited, by H89. (Cellular cyclic AMP levels after a 5 min incubation were (fmol per 10^6 cells): basal 311 (±24), 1 μM forskolin *951 (±34), 20 μM H89 383 (±35), 1 μM forskolin plus 20 μM H89 *1305 (±44), $n = 4$ or 5; $^*P < 0.01$ compared to all other conditions, Fisher LSD test). Furthermore, H89 also inhibited the TOH activation produced by the membrane-permeant cyclic AMP analogue 8-bromo-adenosine-3':5'-cyclic monophosphate (8-Br-cyclic AMP; Figure 1c), which bypasses the adenylate cyclase and activates PK-A directly.

H89 might inhibit the nicotinic activation of TOH by blocking nicotine-induced Ca^{2+} entry through Ca^{2+} channels in the plasma membrane. However, H89 had only weak inhibitory effects on adrenaline and noradrenaline secretion induced by nicotine (adrenaline and noradenaline release respectively (% of cell content $10\ min^{-1}$): basal 0.57 (±0.07) and 0.74 (±0.07), 10 μM H89 0.73 (±0.08) and 0.92 (±0.12), 20 μM H89 0.77 (±0.08) and 0.89 (±0.06), 5 μM nicotine 11.9 (±0.02) and 20.7 (±0.64), 5 μM nicotine + 10 μM H89 11.9 (±0.13) and 19.8 (±0.01), 5 μM nicotine + 20 μM H89 *10.7 (±0.37) and *17.1 (±0.15); $^*P < 0.01$ compared with 5 μM nicotine alone). H89 might also inhibit the uptake of [^{14}C]-tyrosine by the cells. However, if chromaffin cells were permeabilized with digitonin, TOH could be activated by adding Ca^{2+} thus bypassing both the Ca^{2+} channels and the amino acid transporters in the plasma membrane (see Yanagihara *et al.*, 1987). Under these conditions using digitonin-permeabilised chromaffin cells, H89 inhibited TOH activation produced by adding Ca^{2+} or cyclic AMP (10 μM; Figure 2) or by adding forskolin (3 μM: data not shown). H89 also reduced basal TOH activity in permeabilized cells (Figure 2).

If H89 inhibited the nicotinic activation of TOH by inhibition of PK-A, its effects should be mimicked by other PK-A inhibitors. Rp-cAMPS is a PK-A inhibitor which is structurally unrelated to H89 and inhibits PK-A by competing for cyclic AMP binding to the regulatory subunits. Rp-cAMPS inhibited the activation of TOH produced by forskolin and 8-Br-cyclic AMP and almost abolished the response to nicotine (Figure 3). It also reduced basal TOH activity by 50–80%. In contrast, H85 is structurally very similar to H89

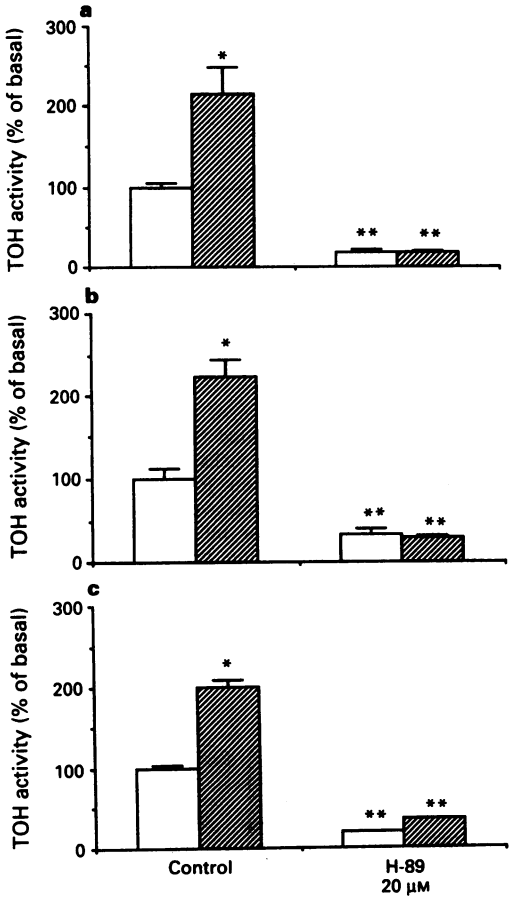

Figure 1 Effect of H89 (20 μM) on basal and stimulated tyrosine hydroxylase (TOH) activity in intact bovine chromaffin cells. Open columns, basal; hatched columns, stimulated with (a) 5 μM nicotine; (b) 1 μM forskolin; (c) 1 mM 8-Br-cyclic AMP. Results are mean ± s.e. mean for $n = 4–5$ from a single preparation of cells, and are representative of similar results on three cell preparations. $^*P < 0.01$ compared to all other conditions; $^{**}P < 0.01$ compared with all other conditions except each other, where $P > 0.1$ (Fisher LSD test). $P < 0.001$ for interaction between H89 and each of the three agonists (two-way ANOVA).

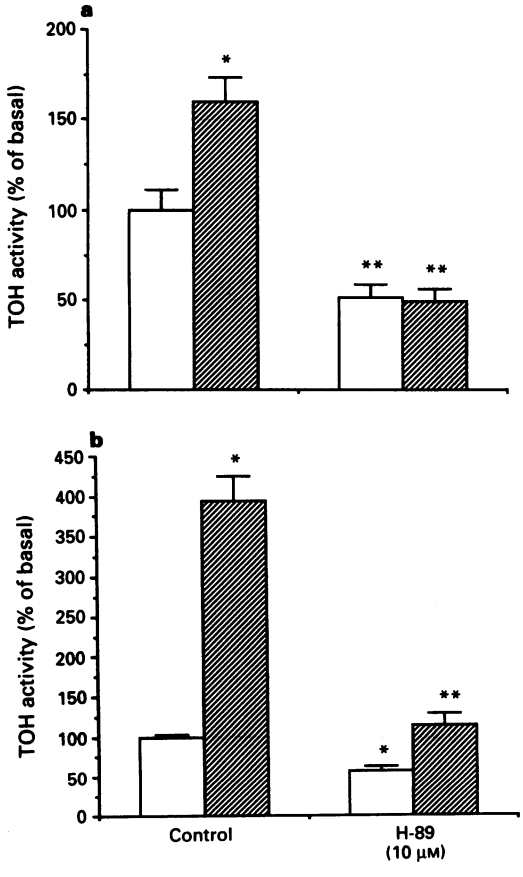

Figure 2 Effect of H89 (10 μM) on cyclic AMP- and Ca^{2+}-induced activation of tyrosine hydroxylase (TOH) in digitonin-permeabilised bovine chromaffin cells. Open columns, basal; hatched columns, stimulated with (a) cyclic AMP (10 μM); (b) Ca^{2+} (approximate free [Ca^{2+}] 2 μM). Results are mean ± s.e.mean for $n = 7$ from a single preparation of cells. Data in (b) are representative of similar results from three cell preparations. (a) $^*P < 0.01$ compared with all other conditions, $^{**}P < 0.01$ compared with all other conditions except each other, where $P > 0.1$. (b) $^*P < 0.01$ compared with all other conditions; $^{**}P < 0.01$ compared with all other conditions except control basal, where $P > 0.1$, (Fisher LSD test).

but has less than 0.05% of the activity of H89 as an inhibitor of PK-A (Chijiwa *et al.*, 1990). H85 had no effect on basal TOH activity or on forskolin activation of TOH (Figure 4).

Rp-cAMPS is weakly active as an inhibitor of the cyclic GMP-dependent protein kinase, PK-G (Butt *et al.*, 1990), and at high concentrations cyclic AMP can activate PK-G (Jiang *et al.*, 1992). Consequently, the ability of cyclic GMP to activate TOH was assessed. However, neither sodium nitroprusside nor 8-Br-cyclic GMP increased TOH activity (TOH activity (% of basal): sodium nitroprusside (10 μM) 93.2 (±9.5), $n=5$, $P>0.1$; 8-Br-cyclic GMP (1 mM) 97.7 (±10.7), $n=6$, $P>0.1$).

Interaction between nicotine and forskolin activation of TOH

Nicotine might activate TOH by producing a Ca^{2+}-dependent increase in cyclic AMP levels (Anderson *et al.*, 1992) and a subsequent activation of PK-A. If this is the case, then under conditions when cyclic AMP formation is already maximal for PK-A to activate TOH, nicotine should have no further effect on TOH activity. This was tested by using combinations of forskolin and nicotine to stimulate TOH activity.

Maximal activation of TOH by forskolin was achieved with 10 μM forskolin (Figure 5; compare 10 μM forskolin with 50 μM). This concentration was less than the EC_{50} for forskolin-induced cyclic AMP accumulation in these cells and was therefore clearly a submaximal concentration for cyclic AMP formation (cellular cyclic AMP levels (fmol/10^6 cells): basal 361 (±37), 10 μM forskolin 3670 (±170), 50 μM forskolin 21,770 (±1040), mean ± s.e.mean, $n=12$). Conse-

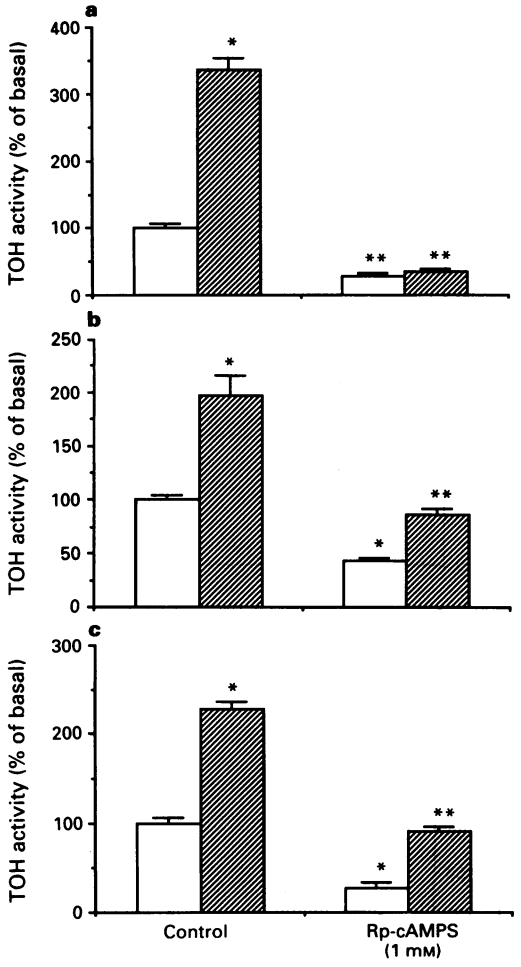

Figure 3 Effects of adenosine 3':5'-cyclic monophosphorothioate Rp-diastereomer (Rp-cAMPS, 1 mM) on basal and stimulated tyrosine hydroxylase (TOH) activity in intact bovine adrenal chromaffin cells. Open columns, basal: hatched columns, stimulated with (a) 5 μM nicotine; (b) 1 μM forskolin; (c) 1 mM 8-Br-cyclic AMP. Results are mean ± s.e.mean for $n=4-5$ from a single preparation of cells, and are representative of similar results from two (b,c) or three (a) cell preparations. (a) $*P<0.01$ compared with all other conditions, $**P<0.01$ compared with all other conditions except each other, where $P>0.1$. (b,c) $*P<0.01$ compared with all other conditions, $**P<0.01$ compared with all other conditions except control basal, where $P>0.1$ (Fisher LSD test). $P<0.005$ for interaction between Rp-cAMPS and each of the three agonists (two-way ANOVA).

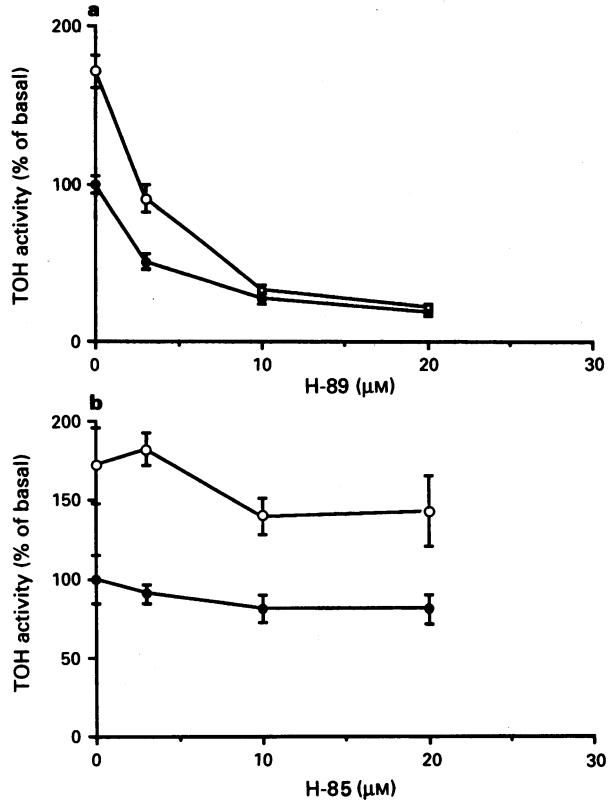

Figure 4 Concentration-dependence of effects of (a) H89 and (b) H85 on basal and forskolin-stimulated tyrosine hydroxylase (TOH) activity in intact bovine chromaffin cells: (●) basal; (○) 1 μM forskolin. Results are mean ± s.e.mean for $n=4-5$ from a single preparation of cells, and are representative of similar results on seven cell preparations. (a) $P<0.001$ for interaction between H89 and forskolin. (b) $P>0.1$ for interaction between H85 and forskolin (two-way ANOVA).

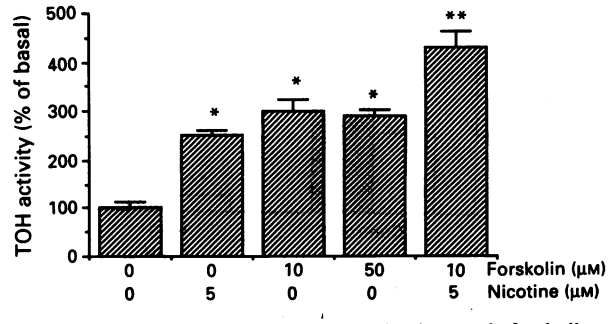

Figure 5 Effect of combinations of nicotine and forskolin on tyrosine hydroxylase (TOH) activity in intact bovine chromaffin cells. Results are mean ± s.e.mean for $n=4-5$ from a single preparation of cells, and are representative of similar results from three cell preparations. $*P<0.01$ compared to basal and to nicotine with forskolin. $**P<0.01$ compared with all other conditions. The effects of 10 μM forskolin and 5 μM nicotine were not significantly different from additive (see Methods, and Moeller *et al.*, 1989).

quently, at 10 μM forskolin, the formation of cyclic AMP is adequate to give the maximum possible activation of TOH through PK-A. However, in the presence of this concentration of forskolin (10 μM), nicotine still activated TOH. Indeed the effects of nicotine (5 μM) and forskolin (10 μM) were additive (Figure 5). As reported previously, the effects of nicotine on cellular cyclic AMP levels were small compared with those of forskolin (typically 2–3 fold over basal at 5 μM nicotine; see Anderson *et al.*, 1992).

Discussion

Actions of the PK-A inhibitors

Previous studies have shown that nicotinic activation of TOH requires extracellular Ca^{2+} and is accompanied by Ca^{2+}-dependent phosphorylation of TOH on three different serine residues (see Introduction and Haycock *et al.*, 1982b and Pocotte *et al.*, 1986). However the identity of the kinases that mediate these phosphorylations, and which phosphorylation or combination of phosphorylations causes activation of TOH following nicotinic stimulation are not known. The present study establishes that nicotinic activation of TOH in bovine chromaffin cells requires protein kinase A.

Inhibition of PK-A in intact chromaffin cells with H89 completely prevented nicotinic activation of TOH. Several lines of evidence suggest that this effect of H89 was due to its inhibition of PK-A. Firstly, H89 inhibited TOH activation by agents that selectively activate the adenylate cyclase/PK-A signalling pathway (forskolin and 8-Br-cyclic AMP). Secondly, H89 did not have a number of possible non-specific actions (Ca^{2+} channel blockade, adenylate cyclase inhibition, tyrosine transport inhibition) that could have blocked the nicotinic response. Thirdly, a related compound (H85) that is structurally very similar to H89 but lacks activity as a PK-A inhibitor, was inactive against PK-A activation of TOH. Finally, another PK-A inhibitor (Rp-cAMPS) that is structurally unrelated to H89 and inhibits PK-A by a distinct mechanism, also blocked the nicotinic activation of TOH. It is unlikely that H89 produced its effects by inhibiting the ATP binding site on kinases other than PK-A (e.g., Ca^{2+}-sensitive kinases), since its effects were mimicked by Rp-cAMPS but not by H85: the latter compound shares weak inhibitory actions with H89 on several other kinases. Taken together, these observations provide strong evidence that inhibition of PK-A blocks nicotinic activation of TOH.

H89 not only inhibited stimulation of TOH by nicotine, forskolin and 8-Br-cyclic AMP, it also reduced basal TOH activity, often by almost 80%. This appears to be a true effect of H89 inhibiting PK-A since it was seen in both intact and digitonin-permeabilized cells, was mimicked by the other PK-A inhibitor Rp-cAMPS and was not observed with the inactive analogue H85. This observation suggests that basal PK-A activity contributes to the maintenance of basal TOH activity. Under basal conditions there is a modest turnover of phosphate on all four phosphorylation sites in TOH (Haycock, 1990; 1993). This is particularly striking when cells are exposed to the phosphatase inhibitor, okadaic acid, which results in high levels of phosphate incorporation into all the serines and a substantial activation of TOH (Haavik *et al.*, 1989; Haycock, 1990; 1993). These data suggest that, under basal conditions, protein kinases and phosphatases are active in phosphorylating and dephosphorylating TOH, and that this basal turnover of phosphates contributes to basal TOH activity. Our data suggest that a major contributor to this basal TOH activity is phosphorylation due to resting PK-A activity. Site-directed mutagenesis studies on rat TOH support this conclusion (Wu *et al.*, 1992). Mutation of Ser^{40} to either Leu^{40} or Tyr^{40} had the same effect on the kinetic constants and pH profile of rat TOH as did phosphorylation of the native Ser^{40} enzyme, suggesting that a dephosphorylated state of Ser^{40} exerts an inhibitory influence on TOH activity (Wu *et al.*, 1992). The dephosphorylated-Ser^{40} form of TOH however still retains some activity.

H89 completely inhibited TOH activation due to nicotine, forskolin and 8-Br-cyclic AMP (Figure 1). In contrast, Rp-cAMPS was much more effective in inhibiting nicotinic activation of TOH than activation due to forskolin or 8-Br-cyclic AMP (Figure 3). This is likely to be due to the different mechanisms by which these two drugs inhibit PK-A. Since H89 is competitive with respect to ATP (Chijiwa *et al.*, 1990), its inhibition of PK-A should be independent of activation of PK-A by cyclic AMP. Rp-cAMPS on the other hand inhibits PK-A competitively with respect to cyclic AMP. Consequently, under conditions where cellular cyclic AMP concentrations are greatly increased (e.g., with forskolin) or when membrane-permeant cyclic AMP analogues are used to stimulate PK-A (e.g., 8-Br-cyclic AMP), Rp-cAMPS is a less effective inhibitor. Rp-cAMPS is particularly weak when cellular cyclic AMP levels are elevated, since Rp-cAMPS is also an inhibitor of phosphodiesterase (Erneux *et al.*, 1986). Since nicotine produces very minor increases in cyclic AMP levels compared with forskolin (see Anderson *et al.*, 1992; Marley & Thomson, 1992), the degree of PK-A inhibition produced by Rp-cAMPS is greater when nicotine is used to activate TOH.

Protein kinase G does not appear to be involved in the nicotinic activation of bovine adrenal TOH. This is in agreement with the lack of effect of cyclic GMP on bovine TOH phosphorylation or activity (Meligeni *et al.*, 1982; George *et al.*, 1989), but in contrast to rat TOH (Roskoski & Roskoski, 1987).

Mechanism of PK-A action in the nicotinic activation of TOH

The effects of H89 and Rp-cAMPS indicate that nicotine cannot activate TOH when PK-A is inhibited. This suggests that nicotinic activation of TOH *requires* PK-A. However, the additivity experiment with nicotine and forskolin (Figure 5) indicates that an increase in cyclic AMP levels and a subsequent activation of PK-A are not the sequence of events that bring about the nicotinic activation of TOH.

There are three possible explanations for this. Fistly, nicotine may activate a kinase or kinases other than PK-A but the actions of these kinases on TOH are dependent on resting PK-A activity. Such hierarchal inter-dependence of kinases is common (Roach, 1991). This dependence may be at the level of TOH phosphorylation: PK-A may have to phosphorylate TOH before the nicotine-activated kinase can phosphorylate it. However, to date there is no evidence that there is a strict hierarchy for the phosphorylations of TOH. Alternatively, the nicotine-activated kinase and PK-A may phosphorylate TOH independently, but the phosphorylations produced by the nicotine-activated kinase may only activate TOH if it has also been phosphorylated by PK-A. Previous studies have reported that cyclic AMP-dependent and Ca^{2+}-dependent activations of TOH are additive (Simon & Roth, 1979; Yanagihara *et al.*, 1987; George *et al.*, 1989), indicating that they are mediated by distinct mechanisms. However, these studies did not directly address the inter-dependence between these two mechanisms.

A second explanation for the dependence of nicotinic activation of TOH on PK-A is that basal PK-A activity might be required before nicotine can activate the kinase(s) that mediate the nicotinic activation of TOH. The nature of such a PK-A-dependent, nicotine-activated kinase is unknown. Nicotinic stimulation of bovine chromaffin cells is known to activate, *inter alia*, MAP-kinase (Ely *et al.*, 1990), PK-C (Haycock *et al.*, 1988a,b; TerBush *et al.*, 1988) and CAM-K-I and CAM-K-II (Haycock *et al.*, 1988a,b). A possible role of PK-A in nicotinic activation of MAP-kinase, PK-C or calmodulin-dependent kinases in chromaffin cells is not yet known.

Thirdly, nicotine may activate PK-A by a mechanism that does not involve increasing cyclic AMP levels. Such a novel mechanism has recently been reported for the activation of PK-A by PDGF in normal rat kidney cell membranes and intact Balb/c 3T3 cells (deBlaquiere *et al.*, 1994) and for PK-A activation by the nerve growth factor-activated kinase PK-N in PC12 cells (Volonté & Greene, 1994). In the latter case, PKN was found to phosphorylate the catalytic subunit of PK-A, increasing its V_{max} and reducing its K_m. Such a mechanism in chromaffin cells could explain the ability of nicotine to increase TOH activity additively with high concentrations of forskolin.

The present observations show that activation of TOH by nicotinic cholinoceptors requires PK-A activity but is not mediated by an increase in cyclic AMP levels and subsequent activation of PK-A. Further studies are needed to identify the site at which PK-A mediates its permissive role in the nicotinic activation of TOH and the nature of the protein kinases that do mediate this nicotinic response.

We thank Prof Peter Dunkley, Dr John Haycock, Dr Steve Bunn, Dr Julie deBlaquiere and Dr Cinzia Volonté for valuable and stimulating discussions. This work was supported by the Australian NH&MRC. P.D.M. is an NH&MRC Senior Research Fellow.

References

ANDERSON, K., ROBINSON, P.J. & MARLEY, P.D. (1992). Cholinergic regulation of cyclic AMP levels in bovine adrenal medullary cells. *Br. J. Pharmacol.*, **106**, 360–366.

BRALOW, R., THOMSON, K.A. & MARLEY, P.D. (1992). Nicotinic activation of tyrosine hydroxylase is dependent on protein kinase A in intact bovine adrenal medullary cells. *Proc. Austral. Physiol. Pharmacol.*, **23**, 211P.

BUTT, E., VAN BEMMELEN, M., FISCHER, L., WALTER, U. & JASTORFF, B. (1990). Inhibition of cGMP-dependent protein kinase by (Rp)-guanosine 3',5'-monophosphorothioates. *FEBS Lett.*, **263**, 47–50.

CHIJIWA, T., MISHIMA, A., HAGIWARA, M., SANO, M., HAYASHI, K., INOUE, T., NAITO, K., TOSHIOKA, T. & HIDAKA, H. (1990). Inhibition of forskolin-induced neurite outgrowth and protein phosphorylation by a newly synthesized selective inhibitor of cyclic AMP-dependent protein kinase, N-[2-(*p*-bromocinnamylamino)ethyl]-5-isoquinolinesulfonamide (H89), of PC12D pheochromocytoma cells. *J. Biol. Chem.*, **265**, 5267–5272.

DEBLAQUIERE, J., WALKER, F., MICHELANGELI, V.P., FABRI, L. & BURGESS, A.W. (1994). Platelet-derived growth factor stimulates release of protein kinase A from the cell membrane. *J. Biol. Chem.*, **269**, 4812–4818.

ELY, C.M., ODDIE, K.M., LITZ, J.S., ROSSOMANDO, A.J., KANNER, S.B., STURGILL, T.W. & PARSONS, S.J. (1990). A 42-kD tyrosine kinase substrate linked to chromaffin cell secretion exhibits an associated MAP kinase activity and is highly related to a 42-kD mitogen-stimulated protein in fibroblasts. *J. Cell. Biol.*, **110**, 731–742.

ERNEUX, C., VAN SANDE, J., JASTORFF, B. & DUMONT, J.E. (1986). Modulation of cyclic AMP action in dog thyroid by its agonist and antagonist S_p- and R_p-adenosine 3',5'-monophosphorothioate. *Biochem. J.*, **234**, 193–197.

GEORGE, R.J., HAYCOCK, J.W., JOHNSTON, J.P., CRAVISO, G.L. & WAYMIRE, J.C. (1989). In vitro phosphorylation of bovine adrenal chromaffin cell tyrosine hydroxylase by endogenous protein kinases. *J. Neurochem.*, **52**, 274–284.

GUIDOTTI, A. & COSTA, E. (1973). Involvement of adenosine 3',5'-monophosphate in the activation of tyrosine hydroxylase elicited by drugs. *Science*, **179**, 902–904.

GUIDOTTI, A. & COSTA, E. (1974). A role for nicotinic receptors in the regulation of adenylate cyclase of adrenal medulla. *J. Pharmacol. Exp. Ther.*, **189**, 665–675.

HAAVIK, J., SCHELLING, D.L., CAMPBELL, D.G., ANDERSSON, K.K., FLATMARK, T. & COHEN, P. (1989). Identification of phosphatase 2A as the major tyrosine hydroxylase phosphatase in adrenal medulla and corpus striatum: evidence from the effects of okadaic acid. *FEBS Lett.*, **251**, 36–42.

HAYCOCK, J.W. (1990). Phosphorylation of tyrosine hydroxylase *in situ* at serine 8, 19, 31, and 40. *J. Biol. Chem.*, **265**, 11682–11691.

HAYCOCK, J.W. (1993). Multiple signalling pathways in bovine chromaffin cells regulate tyrosine hydroxylase phosphorylation at Ser^{19}, Ser^{31} and Ser^{40}. *Neurochem. Res.*, 15–26.

HAYCOCK, J.W., AHN, N.G., COBB, M.H. & KREBBS, E.G. (1992). ERK1 and ERK2, two microtubule-associated protein 2 kinases, mediate the phosphorylation of tyrosine hydroxylase at serine-31 *in situ*. *Proc. Natl. Acad. Sci. U.S.A.*, **89**, 2365–2369.

HAYCOCK, J.W., BENNETT, W.F., GEORGE, R.J. & WAYMIRE, J.C. (1982a). Multiple site phosphorylation of tyrosine hydroxylase. Differential regulation *in situ* by 8-bromo-cAMP and acetylcholine. *J. Biol. Chem.*, **257**, 13699–13703.

HAYCOCK, J.W., BROWNING, M.D. & GREENGARD, P. (1988a). Cholinergic regulation of protein phosphorylation in bovine chromaffin cells. *Proc. Natl. Acad. Sci. U.S.A.*, **85**, 1677–1681.

HAYCOCK, J.W., GREENGARD, P. & BROWNING, M.D. (1988b). Cholinergic regulation of protein III phosphorylation in bovine adrenal chromaffin cells. *J. Neurosci.*, **8**, 3233–3239.

HAYCOCK, J.W., MELIGENI, J.A., BENNETT, W.F. & WAYMIRE, J.C. (1982b). Phosphorylation and activation of tyrosine hydroxylase mediate the acetylcholine-induced increase in catecholamine biosynthesis in adrenal chromaffin cells. *J. Biol. Chem.*, **257**, 12641–12648.

HAYCOCK, J.W. & WAKADE, A.R. (1992). Activation and multiple-site phosphorylation of tyrosine hydroxylase in perfused rat adrenal glands. *J. Neurochem.*, **58**, 57–64.

HIDAKA, H., WATANABE, M. & KOBAYASHI, R. (1991). Properties of the H-series of compounds as protein kinase inhibitors. *Methods Enzymol.*, **201**, 328–339.

JIANG, H., SHABB, J.B. & CORBIN, J.D. (1992). Cross-activation: overriding cAMP/cGMP selectivities of protein kinases in tissues. *Biochem. Cell. Biol.*, **70**, 1283–1289.

LIVETT, B.G., MARLEY, P.D., MITCHELHILL, K.I., WAN, D.C.C. & WHITE, T.D. (1987a). Assessment of adrenal chromaffin cell secretion: presentation of four techniques. In In Vitro *Techniques for Studying Secretion.* ed. Poisner, A.M. & Trifaro, J.-M., pp. 177–204. Amsterdam: Elsevier Science Publishers.

LIVETT, B.G., MITCHELHILL, K.I. & DEAN, D.M. (1987b). Adrenal chromaffin cells – their isolation and culture. In In Vitro *Techniques for Studying Secretion.* ed. Poisner, A.M. & Trifaro, J.-M., pp. 171–175. Amsterdam: Elsevier Science Publishers.

MARLEY, P.D. & THOMSON, K.A. (1992). Regulation of cyclic AMP metabolism in bovine adrenal medullary cells. *Biochem. Pharmacol.*, **44**, 2105–2110.

MARLEY, P.D., THOMSON, K.A. & BRALOW, R. (1993). Role of protein kinase A in nicotinic activation of tyrosine hydroxylase in bovine adrenal chromaffin cells. *J. Neurochem.*, **61**, Suppl., S135B.

MARLEY, P.D., THOMSON, K.A., JACHNO, K. & JOHNSTON, M.J. (1991). Histamine-induced increases in cyclic AMP levels in bovine adrenal medullary cells. *Br. J. Pharmacol.*, **104**, 839–846.

MELIGENI, J.A., HAYCOCK, J.W., BENNETT, W.F. & WAYMIRE, J.C. (1982). Phosphorylation and activation of tyrosine hydroxylase mediate the cAMP-induced increase in catecholamine biosynthesis in adrenal chromaffin cells. *J. Biol. Chem.*, **257**, 12632–12640.

MOELLER, I., BUNN, S.J. & MARLEY, P.D. (1989). Actions of somatostatin on perfused bovine adrenal glands and cultured bovine adrenal medullary cells. *Brain Res.*, **484**, 192–202.

POCOTTE, S.L., HOLZ, R.W. & UEDA, T. (1986). Cholinergic receptor-mediated phosphorylation and activation of tyrosine hydroxylase in cultured bovine adrenal chromaffin cells. *J. Neurochem.*, **46**, 610–622.

ROACH, P.J. (1991). Multisite and hierarchal protein phosphorylation. *J. Biol. Chem.*, **266**, 14139–14142.

ROSKOSKI, R. & ROSKOSKI, L.M. (1987). Activation of tyrosine hydroxylase in PC12 cells by the cyclic AMP and cyclic GMP second messenger systems. *J. Neurochem.*, **48**, 236–242.

SIMON, J.R. & ROTH, R.H. (1979). Striatal tyrosine hydroxylase: comparison of the activation produced by depolarization and dibutyryl-cAMP. *Mol. Pharmacol.*, **16**, 224–233.

TERBUSH, D.R., BITTNER, M.A. & HOLZ, R.W. (1988). Ca^{2+} influx causes rapid translocation of protein kinase C to membranes. Studies of the effects of secretagogues in adrenal chromaffin cells. *J. Biol. Chem.*, **263**, 18873–18879.

THOMSON, K.A., BRALOW, R. & MARLEY, P.D. (1993). Nicotinic activation of tyrosine hydroxylase in bovine chromaffin cells is not mediated by protein kinase A. *Proc. Austral. Neurosci. Soc.*, **4**, 156.

VOLONTÉ, C. & GREENE, L.A. (1994). Nerve growth factor-activated protein kinase N modulates the cAMP-dependent protein kinase. *J. Neurosci. Res.*, (in press).

WAYMIRE, J.C., JOHNSTON, J.P., HUMMER-LICKTEIG, K., LLOYD, A., VIGNY, A. & CRAVISO, G.L. (1988). Phosphorylation of bovine adrenal chromaffin cell tyrosine hydroxylase. Temporal correlation of acetylcholine's effect on site phosphorylation, enzyme activation, and catecholamine synthesis. *J. Biol. Chem.*, **263**, 12439–12447.

WU, J., FILER, D., FRIEDHOFF, A.J. & GOLDSTEIN, M. (1992). Site-directed mutagenesis of tyrosine hydroxylase. Role of serine 40 in catalysis. *J. Biol. Chem.*, **267**, 25754–25758.

YAMAUCHI, T. & FUJISAWA, H. (1979). *In vitro* phosphorylation of bovine adrenal tyrosine hydroxylase by adenosine-3',5'monophosphate-dependent protein kinase. *J. Biol. Chem.*, **254**, 503–507.

YAMAUCHI, T. & FUJISAWA, H. (1981). Tyrosine 3-monooxygenase is phosphorylated by Ca^{2+} calmodulin-dependent protein kinase, followed by activation by an activator protein. *Biochem. Biophys. Res. Commun.*, **100**, 807–813.

YANAGIHARA, N., UEZONO, Y., KODA, Y., WADA, A. & IZUMI, F. (1987). Activation of tyrosine hydroxylase by micromolar concentrations of calcium in digitonin-permeabilized adrenal medullary cells. *Biochem. Biophys. Res. Commun.*, **146**, 530–536.

ZIGMOND, R.E., SCHWARZSCHILD, M.A. & RITTENHOUSE, A.R. (1989). Acute regulation of tyrosine hydroxylase by nerve activity and by neurotransmitters via phosphorylation. *Annu. Rev. Neurosci.*, **12**, 415–461.

(Received August 18, 1994
Revised December 19, 1994
Accepted January 4, 1995)

British Journal of Pharmacology (1995) 114, 1694-1702 © 1995 Stockton Press All rights reserved 0007-1188/95 $12.00

NPC 15669-modulated human polymorphonuclear neutrophil functional responsiveness: effects on receptor-coupled signal transduction

[1]Robert J. Smith, James M. Justen, *John E. Bleasdale & Laurel M. Sly

Cell Biology and Inflammation Research and *Metabolic Diseases Research, The Upjohn Company, 301 Henrietta Street, Kalamazoo, MI 49001, U.S.A.

1 The effect of NPC 15669, N-carboxy-L-leucine, N-[(2,7-dimethylfluoren-9-yl)methyl]ester), an inhibitor of human polymorphonuclear neutrophil (PMN) adhesion, on granule exocytosis and the oxidative burst was investigated in PMN activated with receptor-specific pathophysiological stimuli.

2 NPC 15669 caused a concentration-dependent (1-30 μM) inhibition of the extracellular release of azurophil (myeloperoxidase) and specific (vitamin B_{12}-binding protein) granule constitutents from PMN exposed to N-formyl-methionyl-leucyl-phenylalanine (FMLP), leukotriene B_4 (LTB_4), platelet activating factor (PAF), C5a and interleukin-8 (IL-8).

3 The receptor agonist-triggered PMN oxidative burst, measured as superoxide anion (O_2^-) production, was suppressed by NPC 15669.

4 Phorbol myristate acetate (PMA)-stimulated degranulation and O_2^-) production were unaffected by NPC 15669.

5 NPC 15669 (0.1-10 μM) inhibited receptor-triggered inositol 1,4,5-trisphosphate (IP_3) production and the IP_3-triggered increase in cytosolic-free calcium ($[Ca^{2+}]_i$) in FMLP-activated PMN, but not in cells exposed to the other receptor agonists.

6 NPC 15669 suppressed FMLP but not PMA-stimulated redistribution of protein kinase C (PKC) in PMN.

7 The specific binding of [^{3}H]-FMLP but not [^{125}I]-C5a to PMN was inhibited by NPC 15669.

8 NPC 15669 suppressed O_2^- production and the rise in $[Ca^{2+}]_i$ in PMN treated with the guanine nucleotide-binding protein (G-protein) activators, sodium fluoride (NaF) and mastoparan, respectively.

9 The results show that NPC 15669 inhibits PMN responsiveness to various receptor agonists, and suggest interference with receptor-coupled signal transduction in this inflammatory cell at both the receptor and post-receptor level in a stimulus-specific manner.

Keywords: Neutrophil; receptor agonists; leukocyte granule exocytosis; oxidative burst; inositol 1,4,5-trisphosphate; cytosolic-free calcium; protein kinase C; guanine nucleotide-binding protein; cyclic AMP production

Introduction

The adherence of polymorphonuclear neutrophils (PMN) to vascular endothelium and subsequent transmigration to extravascular tissue is a hallmark of the inflammatory process, and a common component of host defence. PMN adherent to endothelial cells or subendothelial matrix proteins generate reactive oxygen species (ROS) and release proteinases when activated by peptide chemoattractants and cytokines (Wright & Gallin, 1979; Nathan, 1987; Nathan *et al.*, 1989; Shappell *et al.*, 1990; Richter *et al.*, 1990). These secretory products and ROS are thought to cause tissue injury associated with respiratory disorders (Cochrane *et al.*, 1983), ischaemia/reperfusion (Mullane *et al.*, 1988) and other PMN-mediated disorders (Henson & Johnston, 1987). Thus, a selective inhibitor of PMN adhesion may be efficacious in certain inflammatory disorders. NPC 15669, a representative of a class of compounds designated 'leumedins', has been reported to suppress PMN adhesion to endothelial cells *in vitro* (Bator *et al.*, 1992), and to inhibit several adherent PMN-mediated animal models of inflammation (Burch *et al.*, 1991; 1992; 1993). Although the mechanisms of action of NPC 15669 *in vitro* is, in part, related to inhibition of the expression of adhesion receptor subunits on activated PMN (Bator *et al.*, 1992), little is known regarding the effects of this compound on other PMN responses. Therefore, the purpose of these studies was to investigate the effects of NPC 15669 on pathophysiological agonist-triggered ROS generation and granule exocytosis in PMN. Further, we examined several post-receptor components of signal transduction in NPC 15669-treated PMN.

[1] Author for correspondence.

Methods

Preparation of human PMN

Blood from normal human donors was drawn by venipuncture into 0.1 volume of 3.8% (v/v) trisodium citrate in conical plastic tubes. PMN were purified by standard techniques of dextran sedimentation, centrifugation on Hypaque-Ficoll, and hypotonic lysis of erythrocytes. Final cell suspensions contained a minimum of 98% PMN, and cell viability always exceeded 98% as determined by trypan blue exclusion.

Incubation conditions

PMN suspended in modified phosphate buffered saline (PBS), pH 7.4, containing mM: NaCl 138, Na_2HPO_4 8.1, KH_2PO_4 1.5, KCl 2, $CaCl_2$ 1.0, $MgCl_2$ 1.0 and 0.1% (w/v) glucose were incubated according to the various protocols described under Results. After incubation, the samples were centrifuged at 750 *g* (4°C) for 3 min, and the clear super-

natants were assayed for lactate dehydrogenase (LDH), myeloperoxidase (MPO) and vitamin B_{12}-binding protein (B_{12}-BP) activities. The net percentage release of granule consitutents (MPO, B_{12}-BP) was calculated by subtracting the percentage release in buffer or vehicle from that attributable to a given test agent. The release of granule constituents from PMN is expressed as the percentage of total activity release by 0.2% (v/v) Triton X-100 in simultaneously run duplicate reaction mixtures.

Enzyme and vitamin B_{12}-binding protein assays

MPO (EC 1.11.1.7), LDH (EC 1.1.1.27) and B_{12}-BP activities were determined as previously described (Bergmeyer *et al.*, 1965; Gottlieb *et al.*, 1965; Henson *et al.*, 1978).

Superoxide anion generation assay

Superoxide anion (O_2^-) production by resting and stimulated PMN was determined by a previously reported modification of the spectrophotometric assay of superoxide dismutase-inhibitable reduction of ferricytochrome c (Smith & Iden, 1981).

Measurement of IP_3 in PMN

Inositol 1,4,5-trisphosphate (IP_3) (mass) was measured with a competitive radiobinding assay (Amersham International) as previously described (Smith *et al.*, 1990).

Measurement of intracellular calcium mobilization

The mobilization of intracellular calcium as reflected in a rise in the $[Ca^{2+}]_i$ was monitored in Fura-2/AM (1 μM)-loaded PMN according to a modification (Smith *et al.*, 1988a) of a previously described method (Grynkiewicz *et al.*, 1985).

Protein kinase C redistribution assay

PKC activity and redistribution in PMN fractions was investigated by previously described methods (Smith *et al.*, 1988b; 1990).

Measurement of specific binding of FMLP and C5a to PMN

PMN suspended in modified PBS at a density of 2.5×10^7 cells ml^{-1} were treated for 5 min at 37°C with 1, 3, 5 and 10 μM NPC 15669 or vehicle (dimethylsulphoxide DMSO, 0.05%). The cells were chilled on ice for 30 min before measuring binding at 0°C. Binding was measured by transferring 0.7 ml cells to 1.5 ml polypropylene tubes that contained [^{3}H]-FMLP (0.5 nM, 76.6 Ci $mmol^{-1}$) and unlabelled FMLP at various concentrations (0.1 to 300 nM) in 2 μl DMSO. After mixing, the cells were maintained at 0°C for 60 min before transferring 200 μl aliquots in triplicate onto 200 μl of silicone oil. (GE SF-1250, R.H. Carlson Co., Greenwich, CT, U.S.A.). The tubes were centrifuged (9,000 *g* for 90 s at 4°C) and then placed in dry ice-ethanol bath. Tips of tubes containing frozen cell pellets were cut off with a razor and pellets were dispersed in 0.75 ml water in a glass scintillation vial. Ultima Gold scintillation fluid (Packard Instrument Co.) (10 ml) was added and ^{3}H measured. Binding data were analysed by a non-linear least squares programme (damping Gauss-Newton algorithm) (Yamaoka *et al.*, 1981). Binding data at 0°C were found to fit best to a single binding site model of binding. When the same data were analysed by a two binding site model of binding, conclusions regarding the influence of NPC 15669 on FMLP binding remained unchanged.

C5a binding to PMN was measured by a modification of a previously described method (Chenoweth & Hugli, 1978). PMN were suspended in modified PBS that contained 0.5% gelatin (Bacto grade, Difco) (approx. 6×10^6 PMN ml^{-1}) and preincubated for 5 min at 37°C with 1, 3, 10 and 30 μM NPC-15669 or vehicle (DMSO, 0.05% final). PMN were then rapidly cooled to room temperature and portions (0.35 ml) were mixed with 0.05 ml of modified PBS with gelatin that contained [^{125}I]-C5a (0.1 nM final, 2200 Ci $mmol^{-1}$) and non-radiolabelled C5a at various concentrations (0.1 to 100 nM). After 30 min at room temperature, aliquots of PMN (0.1 ml) were loaded onto 0.2 ml of silicone oil and centrifuged (9,000 *g* for 90 s). Tubes were then placed in a dry ice-ethanol bath and the tip of each tube containing [^{125}I]-C5a bound to PMN was removed for gamma spectrometry. Binding data were analysed as described above using a single binding site model.

Measurement of cyclic AMP production in PMN

Cyclic AMP in TCA extracts from resting and activated PMN was quantified using radioimmunoassay (RIA) as described previously (Bleasdale *et al.*, 1990).

Reagents

NPC 15669 was obtained from Nova Pharmaceutical Corporation (Baltimore, MD, U.S.A.) and prepared as a solution in DMSO. N-formyl-methionyl-leucyl-phenylalanine (FMLP, Sigma Chemical Co., St. Louis, MO, U.S.A.), leukotriene B_4 (LTB_4, The Upjohn Co., Kalamazoo, MI, U.S.A.), platelet activating factor (PAF, Calbiochem-Behring, LaJolla, CA, U.S.A.), recombinant human C5a (Sigma) and recombinant human monocyte-derived interleukin-8 (IL-8, Biosource International, Camarillo, CA, U.S.A.) were prepared in DMSO, methanol, 0.15 M NaCl containing 2.5 mg ml^{-1} of bovine serum albumin (BSA), PBS containing 1 mg ml^{-1} of BSA, and PBS containing 0.5 mg ml^{-1} of BSA, respectively. Cytochalasin B (Aldrich Chemical Co., Milwaukee, WI, U.S.A.) and Fura-2/M (Molecular Probes, Inc., Junction City, OR, U.S.A.) were dissolved in ethanol and DMSO, respectively. Sodium fluoride (NaF) and mastoparan (Sigma) were prepared in PBS and distilled H_2O, respectively. The small amounts of DMSO, ethanol and methanol (final concentration of 0.1%) employed as vehicle did not alter cell viability, degranulation, superoxide anion production, Fura-2 fluorescence or IP_3, cyclic AMP and LTB_4 production.

Data analysis

One-way analysis of variance was initially employed to test for differences between groups. Data were then analyzed with Student's *t* test.

Results

Effect of NPC 15669 on granule exocytosis from PMN stimulated with various agonists

NPC 15669 caused a concentration-dependent inhibition of FMLP-triggered MPO (Figure 1a) and B_{12}-BP (Figure 1b) release from cytochalasin B-treated PMN with greater than 90% suppression of degranulation observed with 10 μM NPC 15669. FMLP-induced degranulation (release of either MPO or B_{12}-BP) was inhibited 50% by NPC 15669 at concentrations <2 μM, but concentrations >10 fold greater were required for equivalent suppression of degranulation elicited by other agonists (C5a, LTB_4, PAF, or IL-8) (Figure 1). In contrast, PMA-elicited PMN degranulation was unaffected by NPC 15669, an observation also made by Pou *et al.* (1993).

Superoxide anion production by NPC 15669-treated PMN

NPC 15669 was also a potent inhibitor of O_2^- generation by FMLP-activated cytochalasin B-treated PMN causing 50% inhibition at approximately 3 μM with total suppression observed at 20 μM (Figure 2). NPC 15669 was less effective in suppressing the C5a and PAF-induced oxidative burst, and failed to affect PMA-stimulated O_2^- generation (Figure 2).

The inability of NPC 15669 to suppress O_2^- production by a cell-free xanthine/xanthine oxidase O_2^--generating system in the presence of ferricytochrome c (data not shown) indicated that NPC 15669 was not functioning as a free radical scavenger, but most likely was inhibiting a more proximal event in PMN activation.

The release of cytoplasmic LDH from NPC 15669 (1–30 μM)-treated PMN was insignificant (<5% of total cell activity). The mechanism of action of NPC 15669, therefore, is unlikely to involve nonselective cytolysis.

Effect of NPC 15669 on receptor agonist-stimulated IP_3 production in PMN

NPC 15669 caused a concentration-dependent inhibition of IP_3 production in FMLP activated PMN with maximal suppression (89%, $P<0.01$) of IP_3 production occurring with 10 μM NPC 15669 (Figure 3). NPC 15669 (30 μM) caused less than 15% suppression ($P>0.05$) of IP_3 production in C5a, LTB_4, PAF and IL-8 stimulated PMN (data not shown). In addition, stimulated but not basal levels of IP_3 were affected by NPC 15669.

Receptor agonist-induced changes in cytosolic-free calcium in PMN exposed to NPC 15669

NPC 15669 caused a concentration-dependent (1–15 μM) suppression of the FMLP-triggered rise in $[Ca^{2+}]_i$ in PMN (Figure 4). The IC_{50} for NPC 15669 was approximately 5 μM, and complete inhibition of intracellular calcium mobilization was achieved with 15 μM. NPC 15669 (30 μM) alone did not affect the resting $[Ca^{2+}]_i$ (Figure 4). The data in Figure 5 show NPC 15669 (30 μM) to have no effect on either the C5a, PAF, LTB_4 or IL-8-elicited rise in $[Ca^{2+}]_i$ in PMN.

Effect of NPC 15669 on specific binding of [^{3}H]-FMLP and [^{125}I]-C5a to PMN

At 0°C, NPC 15669 caused a concentration-dependent inhibition of FMLP specific binding to PMN with greater than 90% suppression of specific binding (Figure 6a) observed in cells treated with 10 μM NPC 15669. NPC 15669 also decreased FMLP receptor affinity in PMN with K_d values of 12.9 ± 1.7, 15.9 ± 3.2, 17.6 ± 3.3 and 21.8 ± 4.4 nM (mean ± s.e. mean) observed in the presence of 1, 3, 5 and 10 μM NPC 15669, respectively, compared to 10.6 ± 1.3 in the absence of NPC 15669.

NPC 15669 (1–30 μM) had no effect on the specific binding of [^{125}I]-C5a to PMN at 37°C (Figure 6b). The K_d values were

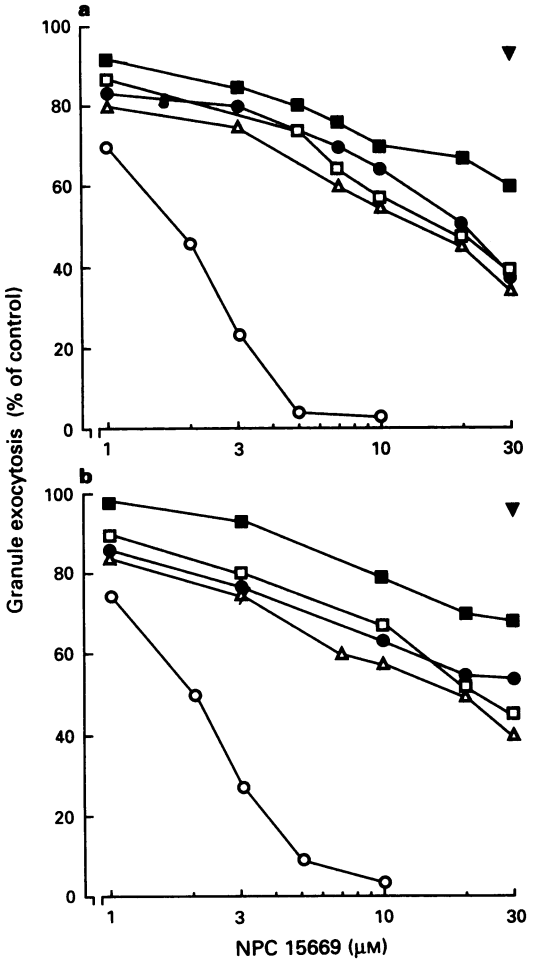

Figure 1 Concentration-dependence of the effects of NPC 15669 on granule exocytosis from PMN stimulated with receptor-specific agonists. PMN (5×10^6) were preincubated with or without the indicated concentrations of NPC 15669 for 15 min followed by a 5 min incubation with cytochalasin B (CB, 5 μg ml^{-1}). Cells were then exposed to either FMLP (○), C5a (△), PAF (●), LTB_4 (□), IL-8 (■) or PMA (▼) at 10 nM, 10 nM, 20 nM, 30 nM, 50 nM and 1.6 μM, respectively, for 5 min at 37°C. Total cell activities were (a) 0.977 ± 0.08 ΔABS 460 nM for MPO and (b) 2547 ± 486 ng B_{12}-BP per 5×10^6 cells for B_{12}-BP. Data are the means of three separate experiments peformed in duplicate (s.e. mean are within 10% of the mean). For abbreviations in this and subsequent legends, see text.

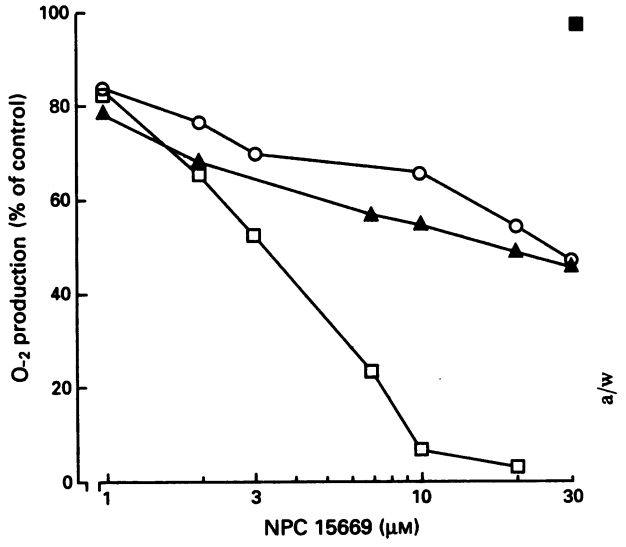

Figure 2 Concentration-dependence of the effects of NPC 15669 on the PMN oxidative burst elicited with receptor-specific agonists. PMN (5×10^6) were preincubated with or without the specified concentrations of NPC 15669 for 15 min followed by a 5 min incubation with CB. Cells were then exposed to either FMLP (□), C5a (○), PAF (▲) or PMA (■), at 100 nM, 100 nM, 1 μM and 10 nM, respectively, for 5 min at 37°C. The spontaneous generation of O_2^- in PMN exposed to buffer alone was 1.8 ± 0.3 mmol of ferricytochrome c reduced in 25 min per 5×10^6 cells. Data are the means of four separate experiments run in duplicate (s.e. mean are within 10% of the mean).

1.9 ± 0.6 nM and 1.7 ± 0.4 nM in the absence and presence of NPC 15669 (30 μM), respectively.

Effect of NPC 15669 on NaF-induced O_2^- production in PMN

NPC 15669 caused a concentration-dependent (3–30 μM) suppression of NaF-triggered O_2^- generation in PMN (50% inhibition at approximately 25 μM) (Figure 7).

Influence of NPC 15669 on mastoparan-stimulated intracellular calcium mobilization in PMN

Mastoparan induced a rapid rise in $[Ca^{2+}]_i$ in PMN that was inhibited in a concentration-dependent manner by NPC 15669 (Figure 8). Maximal suppression (80%, $P<0.01$) of the increase in $[Ca^{2+}]_i$ occurred with 30 μM NPC 15669.

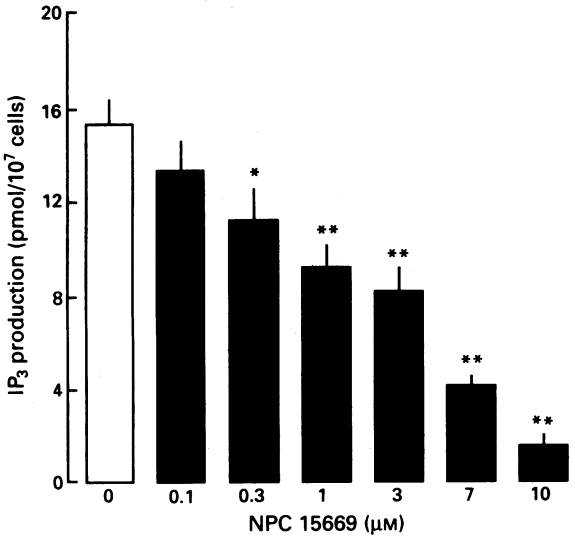

Figure 3 Effect of NPC 15669 on FMLP-stimulated IP_3 production in PMN. PMN (5×10^6) were preincubated with or without the specified concentrations of NPC 15669 for 3 min followed by a 5 s incubation with CB and FMLP (100 nM) at 37°C. Basal levels of IP_3 were 5.5 ± 1.7 pmol per 10^7 cells. Data are the means ± s.e. mean of three separate experiments performed in triplicate. $^*P<0.05$, $^{**}P<0.01$ compared with FMLP control.

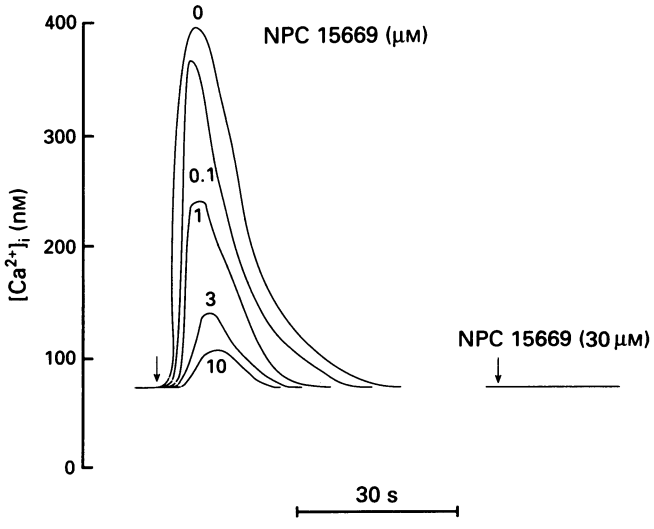

Figure 4 Receptor agonist-induced changes in cytosolic-free calcium in PMN exposed to NPC 15669. PMN (7.5×10^6) were preincubated with or without the specified concentrations of NPC 15669 for 3 min followed by incubation with FMLP (5 nM) at 37°C. The arrow indicates the time of FMLP addition. PMN were also challenged with NPC 15669 (30 μM) alone. The resting $[Ca^{2+}]_i$ was 68 ± 4.6 nM. Data are from a single experiment representative of at least four separate experiments.

FMLP and PMA-stimulated PKC redistribution in NPC 15669-treated PMN

Exposure of PMN to FMLP caused no change in the cytosolic PKC activity (Figure 9). However, a significant ($P<0.01$) decrease (78%) in PKC activity was demonstrated in the cytosol fraction of PMA activated cells. FMLP and PMA triggered significant ($P<0.01$) increases in the extractable particulate (membrane) fraction-associated PKC activity which was 257 and 193%, respectively, above the control value (Figure 9). NPC 15669 did not affect the cytosolic PKC activity in either FMLP- or PMA-treated PMN. However, NPC 15669 did inhibit the FMLP-stimulated redistribution of PKC to the membrane fraction of PMN (FMLP: 35.3 ± 8.1 vs. FMLP + NPC 15669: 15.7 ± 1.2 pmol min^{-1} mg^{-1} protein, $P<0.01$). In contrast, PMA-induced association of PKC with the PMN membrane fraction was unaffected by NPC 15669 (Figure 9). The PKC activity of the cytosolic and membrane fractions of unstimulated PMN was not affected by NPC 15669.

Cyclic AMP production in PMN exposed to NPC 15669

FMLP, C5a, LTB_4, PAF and IL-8, at 50 nM, elicted a rapid increase in adenosine 3′:5′-cyclic monophosphate (cyclic AMP) in PMN with peak concentrations observed at 20 s. NPC 15669 caused a concentration-dependent inhibition of FMLP-stimulated cyclic AMP production with maximum suppression (68%, $P<0.01$) occurring with 30 μM NPC 15669 (Figure 10). NPC 15669 (20 μM) exerted a 40% inhibitory effect ($P<0.05$) on cyclic AMP production in PAF-activated PMN, but this effect was markedly diminished (12%, $P>0.05$) at 30 μM. C5a, LTB_4 and IL-8-induced cyclic

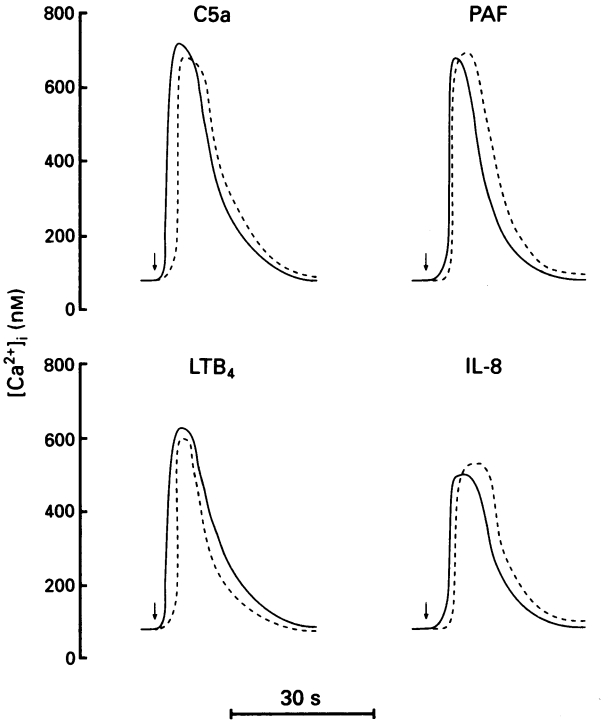

Figure 5 Effect of NPC 15669 on the C5a, PAF, LTB_4 and IL-8-stimulated rise in $[Ca^{2+}]_i$ in PMN. PMN (7.5×10^6) were preincubated with (continuous line) or without (dashed line) NPC 15669 (30 μM) for 3 min at 37°C followed by incubation with either C5a, PAF, LTB_4 or IL-8 at 5 nM. The arrows indicate the time of stimulus addition. Data are from a single experiment representative of at least three separate expermiments.

AMP production was inhibited by 25%, 15% and 12% ($P > 0.05$), respectively, with 30 μM NPC 15669 (Figure 10). Basal cyclic AMP levels were unaffected by NPC 15669.

Discussion

We have demonstrated that NPC 15669 inhibits human PMN responsiveness to receptor-specific pathophysiological agonists. The low micromolar concentrations of NPC 15669 required to suppress FMLP, C5a, LTB4, PAF and IL-8-stimulated granule exocytosis are either below or comparable to the concentrations reported previously to inhibit PMN adhesion (Bator *et al.*, 1992). We observed, however, that NPC 15669 was more potent in suppressing azurophil and specific granule exocytosis from FMLP-activated PMN compared to cells exposed to other receptor agonists. β_2-Integrins, such as MAC-1, which mediate PMN adhesion (Carlos & Harlan, 1994) are associated with specific granules (Miller *et al.*, 1987; Bainton *et al.*, 1987; Singer *et al.*, 1989). Thus, the suppression of Mac-1 expression and/or state of adhesiveness on activated PMN treated with NPC 15669, may be related to the inhibition of specific granule exocytosis. It is doubtful, however, that a major cause/effect relationship exists between degranulation and adhesion (Schleiffenbaum *et al.*, 1989; Richter *et al.*, 1990).

The oxidative burst is another major response of PMN to various agonists, and we have demonstrated that NPC 15669

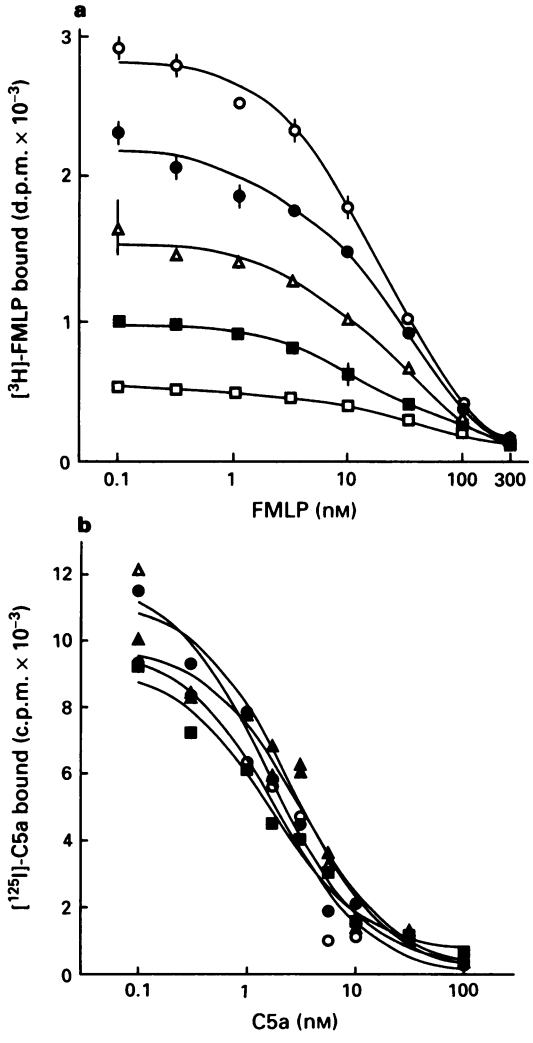

Figure 6 Influence of NPC 15669 on the specific binding of [^{3}H]-FMLP and [^{125}I]-C5a to PMN. PMN were preincubated with NPC 15669 at various concentrations for 5 min at 37°C and then used for measurement of specific cell surface binding of either FMLP (a) or C5a (b) as described in Methods. (a) Data are means ± s.e. mean for three determinations using one preparation of PMN and are typical of the results of two other experiments; NPC 15669: 0 (○); 1 (●); 3 (△); 5 (■) and 10 μM (□). (b) Data are mean values from triplicate determinations made using a single preparation of PMN and are typical of the results of two other experiments: NPC 15669: 0 (○); 1 (●); 3 (△); 10 (▲) and 30 μM (■): s.e. mean values were, in most cases, less than 10% of the mean and are omitted for clarity.

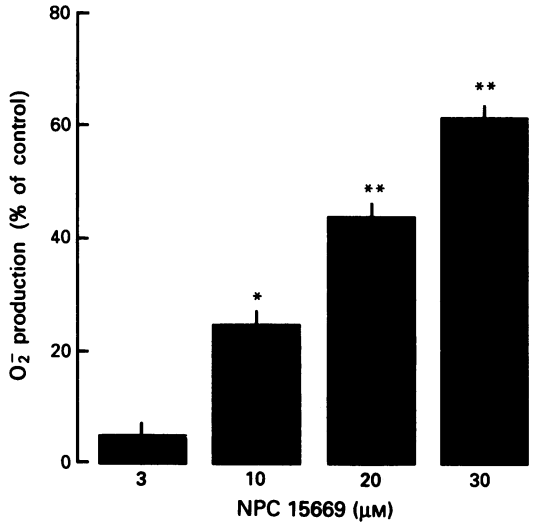

Figure 7 Effect of NPC 15669 on the NaF-stimulated oxidative burst in PMN. Cells (5 × 10^6) were preincubated in the presence and absence of the specified concentrations of NPC 15669 for 10 min at 37°C. PMN were then exposed to NaF (20 mM) for 20 min. Data are the means ± s.e. mean of four separate experiments run in duplicate. *$P < 0.05$ compared with NaF control, **$P < 0.01$ compared with NaF control.

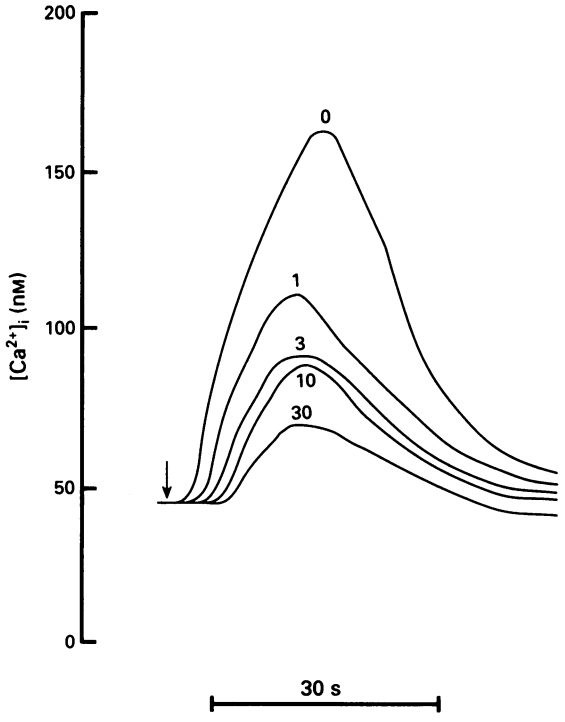

Figure 8 Influence of NPC 15669 on the mastoparan-triggered rise in $[Ca^{2+}]_i$ in PMN. Cells (5 × 10^6) were preincubated with or without NPC 15669 for 3 min followed by incubation with mastoparan (10 μM) at 37°C. The arrow indicates the time of mastoparan addition. The resting $[Ca^{2+}]_i$ was 48 ± 3.7 nM. The data are from a single experiment representative of at least four separate experiments.

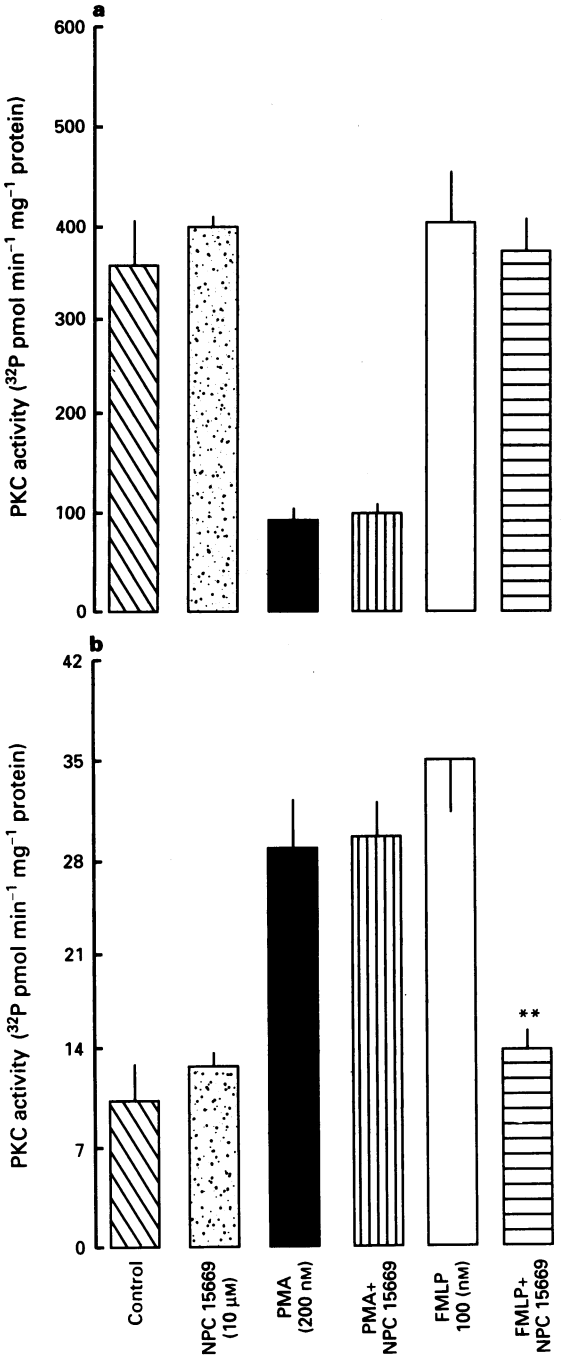

Figure 9 Effect of NPC 15669 on FMLP and PMA-stimulated PKC redistribution in PMN (a) cytosol fraction and (b) extractable particulate fraction. Cells (4×10^7) alone were incubated for 4 min at 37°C followed by a 4 min incubation with or without NPC 15669 (10 μM). Cells were preincubated for 4 min at 37°C followed by a 3 min incubation in either the presence or absence of NPC 15669. PMN were then incubated with PMA (200 nM) for 1 min. Cells were also preincubated for 2 min at 37°C followed by a 2 min incubation with CB and a 3 min incubation with or without NPC 15669 (10 μM). PMN were then incubated with FMLP (100 nM) for 1 min. Data are the means ± s.e. mean of four separate experiments performed in duplicate. $^{**}P<0.01$ compared with FMLP control.

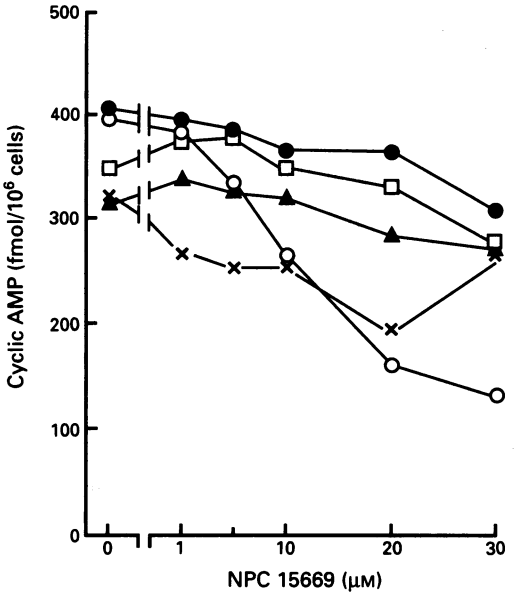

Figure 10 Receptor agonist-elicited cyclic AMP production in PMN exposed to NPC 15669. PMN (5×10^6) were preincubated with or without the specified concentrations of NPC 15669 for 10 min followed by a 20 s incubation with CB and C5a (●), IL-8 (□), LTB_4 (▲), PAF (X) or FMLP (○) at 37°C. Agonist concentration was 50 nM. Data are the means of three separate experiments run in triplicate (s.e. mean are within 10% of the mean).

inhibits FMLP, C5a, and PAF-induced ROS in PMN. Consistent with its effects on degranulation, NPC 15669 was also more potent in suppressing FMLP than either C5a or PAF-stimulated ROS production. The activation pathways which mediate expression of the respiratory burst and granule exocytosis are coupled to specific receptors for these agonists (Williams *et al.*, 1977; Chenoweth & Hugli, 1978; Valone & Goetzl, 1983; Kreisle & Parker, 1983); and the suppression of both functions by NPC 15669 suggests that this compound interferes with the transduction of signals common to these cell responses. NPC 15669 which did not affect PMA-elicted degranulation was also inactive against ROS production in PMA activated PMN.

NPC 15669 inhibited phospholipase C (PLC)-catalyzed IP_3 production in FMLP-activated PMN in the absence of any effect on basal IP_3 levels. Thus, NPC 15669 appeared to inhibit directly only the receptor-coupled IP_3 production in PMN. The IP_3-mediated rise in $[Ca^{2+}]_i$ (Berridge & Irvine, 1984; Smith *et al.*, 1990) was also suppressed by NPC 15669. NPC 15669 suppressed the receptor agonist-stimulated increase in $[Ca^{2+}]_i$ in the presence and absence of extracellular calcium (R.J. Smith, unpublished observation) suggesting that NPC 15669 inhibits the rise in $[Ca^{2+}]_i$ at the level of IP_3 production. In contrast, NPC 15669 caused marginal inhibition of IP_3 production and did not affect the IP_3-triggered rise in $[Ca^{2+}]_i$ in C5a, LTB_4, PAF or IL-8-activated PMN.

Although NPC 15669 exerted significant inhibitory effects on granule exocytosis and the oxidative burst by PMN exposed to structurally diverse receptor-specific agonists, this compound suppressed IP_3 production and the rise in $[Ca^{2+}]_i$ only in FMLP activated cells. Further, NPC 15669 is a more potent inhibitor of FMLP-triggered PMN responsiveness (degranulation and O_2^- production), than of PMN activation by C5a, LTB_4, PAF or IL-8. Thus, the possibility existed that NPC 15669 was interfering with the specific binding of FMLP and perhaps other agonists to their cell surface receptors. We show here, for the first time, that NPC 15669 inhibited the specific binding of FMLP to PMN at concentrations which potently suppressed cell function, IP_3 production and the rise in $[Ca^{2+}]_i$ elicited with this agonist. The specific binding of C5a, a receptor agonist whose capacity to elicit IP_3 production and a rise in $[Ca^{2+}]_i$ was unaffected by NPC 15669, was not influenced by NPC 15669. These findings not only explain, in part, the mechanism by which NPC 15669 suppresses PMN responsiveness to FMLP, but also suggested that the inhibition of PMN activation by C5a

as well as PAF, LTB_4 and IL-8 was at a post-receptor level.

PLC activity in stimulated PMN is regulated by a receptor-coupled G-protein at the plasma membrane (Berridge & Irvine, 1984; Snyderman *et al.*, 1986; Verghese *et al.*, 1986). The possibility that NPC 15669 interferes with receptor-coupled signal transduction at the level of the G-protein was investigated with a G-protein activator, NaF (Howlett *et al.*, 1979), that stimulates IP_3 production (Strnad *et al.*, 1986), intracellular calcium mobilization (English *et al.*, 1987), and an oxidative burst in PMN (Curnutte *et al.*, 1979). NPC 15669 suppressed NaF-stimulated ROS production in PMN at concentrations which interfered with cell responsiveness to C5a, LTB_4, PAF and IL-8. Further evaluation of the effects of NPC 15669 on signal transduction at the level of the G-protein revealed this compound to inhibit the rapid rise in $[Ca^{2+}]_i$ in PMN exposed to another G-protein activator, mastoparan (Higashijima *et al.*, 1988). The ability of NPC 15669 to inhibit PMN activation under conditions where the requirement of cell surface receptors is bypassed, further supported a post-receptor level of inhibition of signal transduction. It is important to note that whereas PMN responsiveness to NaF is pertussis toxin-resistant (Strnad *et al.*, 1986), IP_3 production (Perianin & Snyderman, 1989), a rise in $[Ca^{2+}]_i$ (Perianin & Snyderman, 1989), as well as granule exocytosis and the oxidative burst (Norgauer *et al.*, 1992) in mastoparan-activated PMN is pertussis toxin-sensitive. Thus, the inability of NPC 15669 to inhibit IP_3 production and the IP_3-triggered rise in $[Ca^{2+}]_i$ in C5a, LTB_4, PAF and IL-8 activated cells is surprising, in view of its capacity to suppress PMN responsiveness to mastoparan. With respect to mastoparan, however, an extracellular calcium-dependent component is associated with the stimulated rise in $[Ca^{2+}]_i$ (Perianin & Snyderman, 1989). We have found, however, that NPC 15669 inhibits the mastoparan-induced rise in $[Ca^{2+}]_i$ as well as the ionomycin-elicited oxidative burst in PMN in the absence of extracellular calcium (R.J. Smith, unpublished observations). Therefore, NPC 15669 does not appear to interfere with receptor agonist-triggered degranulation and ROS production at the level of extracellular calcium influx. Pertussis toxin-resistant G-proteins have been identified in inflammatory cells (Amatruda *et al.*, 1991; Simon *et al.*, 1991), and PMN responses to various receptor agonists are differentially sensitive to pertussis toxin (Verghese *et al.*, 1987). Accordingly, NPC 15669 may also target receptor-coupled PLC-independent/pertussis toxin-resistant G-proteins as a mechanism for suppressing PMN responsiveness to a variety of receptor agonists. The inhibition of receptor agonist-induced tyrosine phosphorylation in PMN by NPC 15669 (Naccache *et al.*, 1994), albeit at higher NPC 15669 concentrations than those used in our studies, may speak to this issue.

Cyclic AMP production is another G-protein-dependent event in PMN (Verghese *et al.*, 1985), and cyclic AMP and agents that stimulate its synthesis inhibit PMN activation (Zurier *et al.*, 1974; Ignarro *et al.*, 1974). Accordingly, cyclic AMP may function as an autoregulator of PMN responsiveness. NPC 15669, however, did not increase but markedly inhibited FMLP and modestly suppressed PAF-induced cyclic AMP production, in PMN; whereas this compound caused either weak or essentially no suppression of cyclic AMP production in C5a, LTB_4, and IL-8 activated cells. These data indicate that the inhibition of receptor-coupled PMN responsiveness by NPC 15669 is not a cyclic AMP-mediated process. It is becoming apparent that receptor occupancy triggers the activation of signal-response pathways in PMN that may be regulated by multiple G-proteins (Lackie, 1988; Simon *et al.*, 1991), and the possibility that NPC 15669 affects other G-proteins cannot be precluded.

Receptor agonists and PMA stimulate PKC redistribution from a cytosolic to membrane compartment (Wolfson *et al.*, 1985; Pike *et al.*, 1986; Smith *et al*, 1990; 1992) where it catalyzes the phosphorylation of proteins critical to PMN responsiveness. NPC 15669 suppressed FMLP but not PMA-induced redistribution of PKC to the PMN membrane. These data may explain the inability of NPC 15669 to affect PMA-triggered PMN activation.

We have shown that NPC 15669 inhibits PMN activation by receptor agonists in a stimulus-specific manner at both the receptor and post-receptor level of signal transduction. These studies reveal new effects of NPC 15669 on PMN and provide insight into potentially novel G-protein-regulated effector systems that control granule exocytosis, the oxidative burst and perhaps other receptor-specific pathophysiological agonist-triggered functions in the PMN, a major effector cell in various inflammatory diseases.

References

AMATRUDA III, T.T., STEELE, D.A., SLEPAK, V.Z. & SIMON, M.I. (1991). Gα16, a G protein α subunit specifically expressed in hematopoietic cells. *Proc. Natl. Acad. Sci. U.S.A.*, **88**, 5587–5591.

BAINTON, D.F., MILLER, L.J., KISHIMOTO, T.K. & SPRINGER, T.A. (1987). Leukocyte adhesion receptors are stored in peroxidase-negative granules of human neutrophils. *J. Exp. Med.*, **166**, 1641–1653.

BATOR, J.M., WEITZBERG, M. & BURCH, R.M. (1992). N-[9H-(2,7-dimethylfluorenyl-9-methoxy) carbonyl]-L-leucine, NPC 15669, prevents neutrophil adherence to endothelium and inhibits CD11b/CD18 upregulation. *Immunopharmacol.*, **23**, 139–149.

BERGMEYER, H.V., BERNT, E. & HESS, B. (1965). Lactic dehydrogenase. In *Methods of Enzymatic Analysis*, ed. Bergmeyer, H.U. pp. 736–743. New York: Academic Press.

BERRIDGE, M.J. & IRVINE, R.F. (1984). Inositol trisphosphate, a novel second messenger in cellular signal transduction. *Nature*, **312**, 315–321.

BLEASDALE, J.E., THAKUR, N.R., GREMBAN, R.S., BUNDY, G.L., FITZPATRICK, F.A., SMITH, R.J. & BUNTING, S. (1990). Selective inhibition of receptor-coupled phospholipase C-dependent processes in human platelets and polymorphonuclear neturophils. *J. Pharmacol. Exp. Ther.*, **255**, 756–768.

BURCH, R.M., CONNOR, J.R., BATOR, J.M., WEITZBERG, M., LAEMONT, K., NORONHA-BLOB, L., SULLIVAN, JP. & STERANKA, L.R. (1992). NPC 15669 inhibits the reversed passive arthus reaction in rats by blocking neutrophil recruitment. *J. Pharmacol. Exp. Ther.*, **263**, 933–937.

BURCH, R.M., NORONHA-BLOB, L., BATOR, J.M., LOWE, V.C. & SULLIVAN, J.P. (1993). Mice treated with a leumedin or antibody to MAC-1 inhibit leukocyte sequestration survive endotoxin challenge. *J. Immunol.*, **150**, 3397–3403.

BURCH, R.M., WEITZBERG, M., BLOK, N., MULHAUSER, R., MARTIN, D., FARMER, S.G., BATOR, J.M., CONNOR, J.R., KO, C., KUHN, W., MCMILLAN, B.A., RAYNOR, M., SHEARER, B.G., TIFFANY, C. & WILKINS, D.E. (1991). N-(Fluorenyl-9-methoxycarbonyl) amino acids, a class of antiinflammatory agents with a different mechanism of action. *Proc. Natl. Acad. Sci. U.S.A.*, **88**, 355–359.

CARLOS, T.M. & HARLAN, J.M. (1994). Leukocyte-endothelial adhesion molecules. *Blood*, **84**, 2068–2101.

CHENOWETH, D.E. & HUGLI, T.E. (1978). Demonstration of specific C5a receptor on intact polymorphonuclear leukocytes. *Proc. Natl. Acad. Sci. U.S.A.*, **75**, 3943–3947.

COCHRANE, C.G., SPRAGG, R. & REVAK, S.D. (1983). Pathogenesis of the adult respiratory distress syndrome: evidence of oxidant activity in the bronchoalveolar lung fluid. *J. Clin. Invest.*, **71**, 754–761.

CURNUTTE, J.T., BABIOR, B.M. & KARNOVSKY, M.L. (1979). Fluoride-mediated activation of the respiratory burst in human neutrophils. *J. Clin. Invest.*, **63**, 637–647.

ENGLISH, D., DEBONO, D.J. & GABIG, T.G. (1987). Relationship of phosphatidylinositol bisphosphate hydrolysis to calcium mobilization and functional activation in fluoride-treated neutrophils. *J. Clin. Invest.*, **80**, 145–153.

GOTTLIEB, C., LAU, K.S., WASSERMAN, L.R. & HERBERT, V. (1965). Rapid charcoal assay for intrinsic factor (IF), gastric juice unsaturated B_{12} binding capacity, antibody to IF, and serum unsaturated B_{12} binding capacity. *Blood*, **25**, 875–884.

GRYNKIEWICZ, G., POENIC, M. & TSIEN, R. (1985). A new generation of Ca^{2+} indicators with greatly improved fluorescence properties. *J. Biol. Chem.*, **260**, 3440–3450.

HENSON, P.M. & JOHNSTON, JR., R.B. (1987). Tissue injury in inflammation. Oxidants, proteases, and cationic proteins. *J. Clin. Invest.*, **79**, 669–674.

HENSON, P.M., ZANOLARI, B., SCHWARTZMAN, N.A. & HONG, S.R. (1978). Intracellular control of human neutrophil secretion: C5a-induced stimulus-specific desensitization and the effects of cytochalasin B. *J. Immunol.*, **131**, 851–855.

HIGASHIJIMA, T., UZU, S., NAKAJIMA, T. & ROSS, E.M. (1988). Mastoparan, a peptide toxin from wasp venom, mimics receptors by activating GTP-binding regulator proteins (G proteins). *J. Biol. Chem.*, **263**, 6491–6494.

HOWLETT, A.C., STERNWEIS, P.C., MACRIK, B.A., VAN ARSDALE, P.M. & GILMAN, A.G. (1979). Reconstitution of catecholamine-sensitive adenylate cyclase: Association of a regulatory component of the enzyme with membranes containing the catalytic protein and β-adrenergic receptors. *J. Biol. Chem.*, **254**, 2287–2295.

IGNARRO, L.J., LINT, T.F. & GEORGE, W.J. (1974). Hormonal control of lysosomal enzyme release from human neutrophils: Effects of autonomic neurohormones on enzyme release, phagocytosis, and cyclic nucleotide levels. *J. Exp. Med.*, **139**, 1395–1414.

KREISLE, R.A. & PARKER, C.W. (1983). Specific binding of leukotriene B_4 to a receptor on human polymorphonuclear leukocytes. *J. Exp. Med.*, **157**, 628–634.

LACKIE, J.M. (1988). The behavioural repertoire of neutrophils requires multiple signal transduction pathways. *J. Cell Sci.*, **89**, 449–452.

MILLER, L.J., BAINTON, D.F., BORREGAARD, N. & SPRINGER, T.A. (1987). Stimulated mobilization of monocyte MAC-1 and p150, 95 adhesion proteins from an intracellular vesicular compartment to the cell surface. *J. Clin. Invest.*, **80**, 535–544.

MULLANE, K.M., WESTLIN, W. & KRAMER, R. (1988). Activated neutrophils release mediators that may contribute to myocardial dysfunction associated with ischemia and reperfusion. *Ann. N.Y. Acad. Sci.*, **524**, 103–121.

NACCACHE, P.H., JEAN, N., LIAO, N.W., BATOR, J.M., MCCOLL, S.R. & KUBES, P. (1994). Registration of stimulated integrin surface expression in human neutrophils by tyrosine phosphorylation. *Blood*, **84**, 616–624.

NATHAN, C.F. (1987). Neutrophil activation on biological surfaces: Massive secretion of hydrogen peroxide in response to products of macrophages and lymphocytes. *J. Clin. Invest.*, **80**, 1550–1560.

NATHAN, C., SRIMAL, S., FARBER, C., SANCHEZ, E., KABBASH, L., ASCH, A., GAILIT, J. & WRIGHT, S.D. (1989). Cytokine-induced respiratory burst of human neutrophils: Dependence on extracellular matrix proteins and CD11/CD18 integrins. *J. Cell Biol.*, **109**, 1341–1349.

NORGAUER, J., EBERLE, M., LEMKE, H-D. & AKTORIES, K. (1992). Activation of human neutrophils by mastoparan: Reorganization of the cytoskeleton, formation of phosphatidyl 3,4,5-trisphosphate, secretion, up-regulation of complement receptor type 3 and superoxide anion production are stimulated by mastoparan. *Biochem. J.*, **282**, 393–397.

PERIANIN, A. & SNYDERMAN, R. (1989). Mastoparan, a wasp venom peptide, identifies two discrete mechanisms for elevating cytosolic calcium and inositol trisphosphates in human polymorphonuclear leukocytes. *J. Immunol.*, **143**, 1669–1673.

PIKE, M.C., JAKOI, L., MCPHAIL, L.C. & SNYDERMAN, R. (1986). Chemoattractant-mediated stimulation of the respiratory burst in human polymorphonuclear leukocytes may require appearance of protein kinase activity in the cells' particulate fraction. *Blood*, **67**, 909–913.

POU, S., GUNTHER, M.R., POU, W.S., CAO, G.L., BATOR, J.M., COHEN, M.S., BURCH, R.M. & ROSEN, G.M. (1993). Effect of NPC 15669, an inhibitor of neutrophil recruitment and neutrophil-mediated inflammation, on neutrophil function *in vitro*. *Biochem. Pharmacol.*, **45**, 2123–2127.

RICHTER, J., NG-SIKORSKI, J., OLSSON, I. & ANDERSSON, T. (1990). Tumor necrosis factor-induced degranulation in adherent neutrophils is dependent on CD11b/CD18-integrin-triggered oscillations of cytosolic free Ca^{2+}. *Proc. Natl. Acad. Sci. U.S.A.*, **87**, 9472–9746.

SCHLEIFFENBAUM, B., MOSER, R., PATARROYO, M. & FEHR, J. (1989). The cell surface glycoprotein Mac-1 (CD11b/CD18) mediates neutrophil adhesion and modulates degranulation independently of its quantitative cell surface expression. *J. Immunol.*, **142**, 3537–3545.

SHAPPELL, S.B., TOMAN, C., ANDERSON, D.C., TAYLOR, A.A., ENTMAN, M.L. & SMITH, C.W. (1990). Mac-1 (CD11b/CD18) mediates adherence-dependent hydrogen peroxide production by human and canine neutrophils. *J. Immunol.*, **144**, 2702–2711.

SIMON, M.I., STRATHMANN, M.P. & GAUTAM, N. (1991). Diversity of G proteins in signal transduction. *Science*, **252**, 802–808.

SINGER, I.I., SCOTT, S., KAWKA, D.W. & KAZAZIS, D.M. (1989). Adhesomes: specific granules containing receptors for laminin, C3bi/fibrinogen, fibronectin and vitronectin in human polymorphonuclear leukocytes and monocytes. *J. Cell Biol.*, **109**, 3169–3182.

SMITH, R.J. & IDEN, S.S. (1981). Modulation of human neutrophil superoxide anion generation by the calcium antagonist 8-(N-,N-diethylamino)-octyl-(3,4,5-trimethoxy) benzoate hydrochloride. *J. Reticuloendothel. Soc.*, **29**, 215–225.

SMITH, R.J., JUSTEN, J.M. & SAM, L.M. (1988a). Function and stimulus-specific effects of phorbol 12-myristate 13-acetate on human polymorphonuclear neturophils: autoregulatory role for protein kinase C in signal transduction. *Inflammation*, **12**, 597–611.

SMITH, R.J., SAM, L.M. & JUSTEN, J.M. (1988b). Diacylglycerols modulate human polymorphonuclear neutrophil responsiveness: Effects on intracellular calcium mobilization, granule exocytosis, and superoxide anion production. *J. Leuk. Biol.*, **43**, 411–419.

SMITH, R.J., SAM, L.M., JUSTEN, J.M., BUNDY, G.L., BALA, G.A. & BLEASDALE, J.E. (1990). Receptor-coupled signal transduction in human polymorphonuclear neutrophils: Effects of a novel inhibitor of phospholipase C-dependent processes on cell responsiveness. *J. Pharmacol. Exp. Ther.*, **253**, 688–697.

SMITH, R.J., SAM, L.M., LEACH, K.L. & JUSTEN, J.M. (1992). Post-receptor events associated with human neutrophil activation by interleukin-8. *J. Leuk. Biol.*, **52**, 17–26.

SNYDERMAN, R., SMITH, C.D. & VERGHESE, M.W. (1986). Model for leukocyte regulation by chemoattractant receptors: Roles of a guanine nucleotide regulatory protein and polyphosphoinositide metabolism. *J. Leuk. Biol.*, **40**, 785–800.

STRNAD, C.F., PARENTE, J.E. & WONG, K. (1986). Use of fluoride ion as a probe for the guanine nucleotide-binding protein involved in the phosphoinositide-dependent neutrophil transduction pathway. *FEBS Lett.*, **206**, 20–24.

VALONE, F.H. & GOETZL, E.J. (1983). Specific binding by human polymorphonuclear leucocytes of the immunological mediator 1-0-hexadecyl/octadecyl-2-acetyl-sn-glycero-3-phosphorylcholine. *Immunology*, **48**, 141–149.

VERGHESE, M.W., CHARLES, L., JAKOIM, L., DILLON, S.B. & SNYDERMAN, R. (1987). Role of a guanine nucleotide regulatory protein in the activation of phospholipase C by different chemoattractants. *J. Immunol.*, **138**, 4374–4380.

VERGHESE, M.W., FOX, K., MCPHAIL, L.C. & SNYDERMAN, R. (1985). Chemoattractant-elicited alterations of cAMP levels in human polymorphonuclear leukocytes require a Ca^{2+}-dependent mechanism which is independent of transmembrane activation of adenylate cyclase. *J. Immunol.*, **260**, 6769–6775.

VERGHESE, M.W., SMITH, C.D. & SNYDERMAN, R. (1986). Role of guanine nucleotide regulatory protein in polyphosphoinositide degradation and activation of phagocytic leukocytes by chemoattractants. *J. Cell. Biochem.*, **32**, 59–69.

WILLIAMS, L.T., SNYDERMAN, R., PIKE, M.C. & LEFKOWITZ, R.J. (1977). Specific receptor sites for chemotactic peptides on human polymorphonuclear leukocytes. *Proc. Natl. Acad. Sci. U.S.A.*, **74**, 1204–1208.

WOLFSON, M., MCPHAIL, L.C., NASRALLAH, V.N. & SNYDERMAN, R. (1985). Phorbol myristate acetate mediates redistribution of protein C in human neutrophils: Potential role in the activation of the respiratory burst. *J. Immunol.*, **135**, 2057–2062.

WRIGHT, D. & GALLIN, J. (1979). Secretory responses of human neutrophils: Exocytosis of specific (secondary) granules by human neutrophils during adherence *in vitro* and during exudation *in vivo*. *J. Immunol.*, **123**, 285–294.

YAMAOKA, T., TANIGAWARA, Y., NAKAGAWA, T. & UNO, T. (1981). A pharmacokinetic analysis program (MULTI) for microcomputer. *J. Pharm. Dyn.*, **4**, 879–885.

ZURIER, R.B., WEISSMAN, G., HOFFSTEIN, S., KAMMERMAN, S. & TAI, H.H. (1974). Mechanisms of lysosomal enzyme release from human leukocytes: II. Effects of cAMP and cGMP, autonomic agonists, and agents which affect microtubule function. *J. Clin. Invest.*, **53**, 297–309.

(Received October 14, 1994
Revised December 9, 1994
Accepted January 4, 1995)

British Journal of Pharmacology (1995) 114, 1703–1709 © 1995 Stockton Press All rights reserved 0007–1188/95 $12.00

Mechanism of action of the inhibitory effect of nifedipine on the growth of cultured aortic cells from spontaneously hypertensive and normotensive rats

Thierry Hérembert, Ding-Liang Zhu & [1]Pierre Marche

CNRS URA 1482, Groupe de Signalisation, Université René Descartes, UFR des Saints Pères, 45 rue des Saints Pères, 75270 Paris Cedex 06, France

1 To gain insight into the parameters which control vascular structure, we investigated the mechanisms whereby nifedipine, and other dihydropyridines, inhibit the growth of cultured fibroblasts isolated from the adventitia of the aorta of spontaneously hypertensive (SHR) and normotensive Wistar Kyoto (WKY) rats.

2 The effects of nifedipine on cell proliferation and on serum-induced DNA synthesis were determined by measuring the cell number and the incorporation of [^{3}H]-thymidine, respectively. The mechanism of action of nifedipine was studied by adding the drug either to randomly growing cells or to quiescent, G_0/G_1 arrested and synchronized cells. The effects of varying the duration of drug treatment were also examined.

3 In randomly growing cultures nifedipine, like other dihydropyridines concentration-dependently inhibited cell proliferation; the rank order of effect (measured at a concentration of 10 μM) was nifedipine> nisoldipine> nitrendipine~ nimodipine.

4 In G_0/G_1 arrested cell cultures, nifedipine concentration-dependently inhibited serum-induced [^{3}H]-thymidine incorporation. In this respect it had similar effects in cell cultures from WKY and SHR. In both SHR and WKY cultures, nifedipine delayed the transition from G_0/G_1 to S phase, and inhibited serum-induced DNA synthesis possibly by acting on the early G_1 phase.

5 In cell cultures from both SHR and WKY, serum-induced DNA synthesis was similarly (~40%) inhibited after a 1 day treatment with 10 μM nifedipine. In contrast, after 5 days treatment with the drug, the inhibition of DNA synthesis was ~65% and ~10% in SHR and WKY cultures, respectively. The inhibitory effects of nifedipine against proliferation of fibroblasts were ~25% and 60%, respectively, after 1 and 5 days of treatment, and were similar in cells derived from SHR and WKY. This indicates that 5 days treatment with nifedipine inhibited the proliferation of SHR and WKY fibroblasts by acting mostly on the early G_1 phase and the M phase, respectively.

6 Irrespective of the duration of treatment (1 or 5 days) with 10 μM nifedipine, the inhibition of DNA synthesis could be abolished and partially reduced by Bay K 8644 (1 μM) in WKY and SHR fibroblasts, respectively. In cell cultures from both SHR and WKY the inhibitory effects of a short term and of a long term treatment with nifedipine against cell proliferation were reduced and unaffected, respectively by Bay K 8644.

7 These results indicate that nifedipine inhibited cell proliferation and serum-induced DNA synthesis by altering the cell cycle through different mechanisms in SHR and WKY fibroblasts. They also suggest the existence in aortic fibroblasts of interactions between calcium channel blockers of the dihydropyridine series and the mitogenic signalling pathways of growth factors contained in serum.

Keywords: Dihydropyridines; rat aortic fibroblasts; antimitotic effect; vascular hypertrophy; DNA synthesis; cell proliferation; hypertension

Introduction

In primary hypertension, an abnormally high vascular resistance can be explained in terms of an alteration in vascular wall architecture (Folkow, 1982). In the blood vessels of the spontaneously hypertensive rat (SHR), structural changes are associated with functional changes such as increased vascular smooth muscle reactivity (Mulvany *et al.*, 1978; Owens & Schwartz, 1982). Smooth muscle cell hypertrophy and/or hyperplasia have been implicated as playing a central role in the vascular abnormalities noted in hypertension (Mulvany *et al.*, 1978; Folkow, 1982; Owens & Schwartz, 1982; Schwartz *et al.*, 1990; Jackson & Schwartz, 1992). Cultured arterial cells may provide a model for studying *in vitro* the mechanisms whereby cells originating from hypertensive subjects exhibit hyperproliferation and/or hyperresponsiveness. Since the intracellular concentration of free Ca^{2+} plays an important role in the control of cell growth, many studies have focused on the influence of calcium channel blockers on arterial smooth muscle cell proliferation *in vitro*. Drugs that inhibit L-type voltage-sensitive membrane Ca^{2+} channels decrease the DNA synthesis and/or proliferation of cultured arterial smooth muscle cells (see Jackson & Schwartz, 1992 for a recent review). The mechanisms underlying the inhibitory effect of calcium channel blockers on cell growth nevertheless have still to be clarified.

The importance of adventitial fibroblasts in the abnormal vascular growth of hypertensive subjects is still unclear. Increased DNA replication and hyperplasia of fibroblasts of arterial adventitia have been reported in rats rendered hypertensive by aortic ligation or deoxycorticosterone-salt treatment (Chatelain & Dardik, 1988; Todd, 1992). Moreover, collagen synthesis has been shown to be elevated in the arterial wall of the SHR (Ooshima *et al.*, 1974; Gilligan & Spector, 1984; Deyl *et al.*, 1987) and the activity of fibro-

[1] Author for correspondence.

blasts together with that of smooth muscle cells can account for this change. In addition, cultures of adventitial fibroblasts from SHR aorta behave similarly to those of smooth muscle cells in that both cell types from SHR proliferate more rapidly and exhibit hyperresponsiveness to a variety of activators compared with the corresponding cells of normotensive WKY rats (Berk *et al.*, 1989; Hadrava *et al.*, 1989; Scott-Burden *et al.*, 1989; Zhu *et al.*, 1990; 1991; 1992; Bukoski *et al.*, 1991; Venance *et al.*, 1993). Also, fibroblasts are one of the most commonly used cells in the study of cell growth and they have been demonstrated to possess dihydropyridine-sensitive calcium channels (Chen *et al.*, 1988).

To gain insight into the parameters involved in the control of vascular structure, and in an attempt to unravel the role played by the calcium channels in this phenomenon in hypertension, we have investigated the mechanisms whereby calcium channel blockers such as the dihydropyridines can affect the growth of cultured aortic fibroblasts isolated from SHR and WKY.

Methods

Cell culture and cell number determination

Fibroblasts were isolated from the adventitia of thoracic aortae of 10 week-old male SHR and WKY rats (Iffa-Credo, Les Oncins, France) by an explant method and cultured as previously detailed (Zhu *et al.*, 1991). They were passaged and cultured in minimum essential medium (MEM) containing 10% newborn calf serum (NCS). Examination of cell morphology by scanning electron microscopy provided evidence that the cultured cells were indeed fibroblasts. Throughout the experiments, cultures were protected from the light. In the present study, cells between the third and the tenth passage were used. The viability of cells was assessed by the trypan blue exclusion method. Cell number was determined by haemocytometer in 24-well plates or by crystal violet staining technique (Kueng *et al.*, 1989) in 96-well plates, as previously described (Zhu *et al.*, 1991). For the latter method, the optical density in each well was measured with a Dynatech MR 5000 microplate reader (Dynatech Labs Inc., Alexandria, VA, U.S.A.) at 570 nm.

DNA synthesis assay

Serum-induced DNA synthesis was determined by measuring the incorporation of [^{3}H]-thymidine into fibroblasts that had been treated with nifedipine (or one of the other dihydropyridines) or ethanol (control) for the period specified in the text. If not otherwise specified, fibroblasts were plated in 24-well dishes at a concentration of 2×10^4 cells/well in 0.5 ml MEM containing 10% NCS and cultured for 3 days, the time at which the cells were in the exponential growth phase (Zhu *et al.*, 1991). The cells were then synchronized in G_0/G_1 phase (hence rendered quiescent) by serum deprivation for 48 h and then exposed for 24 h to 10% NCS (or to diluent for baseline) in MEM containing 1 μmol l^{-1} thymidine and 0.5 μCi ml^{-1} [^{3}H]-thymidine. Thymidine incorporation was stopped by removing the labelling medium and washing cells twice with 1 ml/well cold phosphate buffered saline. Cells were then lysed with 1 ml/well 1% sodium dodecyl sulphate and the determination of the radioactivity incorporated into cells was carried out as already detailed (Zhu *et al.*, 1991). All measurements were corrected for cell number. The effect of dihydropyridines on serum-induced [^{3}H]-thymidine incorporation was expressed as % inhibition and was calculated from the following formula: % inhibition = 100 [1-(S'-B')/(S-B)], where B and S are the c.p.m./10^5 cells in unstimulated and stimulated cells, respectively in the absence of drug; B' and S' are the c.p.m./10^5 cells in unstimulated and stimulated cells, respectively in the presence of drug.

Materials

Cell culture materials and media were obtained from Costar and Gibco BRL (Cergy-Pontoise, France) respectively. Newborn-calf serum (NCS) was from Boehringer-Mannheim (Meylan, France). [^{3}H]-thymidine (666 GBq mmol^{-1}) was from Amersham International plc (Aylesbury, UK). Nifedipine, nisoldipine, nitrendipine and nimodipine were from Bayer AG (Wuppertal, Germany). The calcium channel activator, Bay K 8644 (methyl 1,4-dihydro-2,6-dimethyl-3-nitro-4-(2-trifluoromethylphenyl)-pyridine-5-carboxylate) was purchased from Calbiochem (San Diego, CA, U.S.A.). All other chemicals used in this study were from Sigma (St Louis, MO, U.S.A.). The dihydropyridines used were dissolved in absolute ethanol; the maximum ethanol concentration in cultures was 0.2% and was without effect on the cells.

Statistical analysis

Values are given as the means ± s.e.mean of n experiments. Each experiment involved one culture of each of SHR- and WKY-derived fibroblasts at the same passage number; within each experiment, cell number determination was made in triplicate (3 wells) and [^{3}H]-thymidine incorporation in duplicate (2 wells). Unless otherwise specified, tests of significance were performed by Student's paired t test.

Results

Nifedipine and cell proliferation

In the first series of experiments, nifedipine was tested for its ability to alter the proliferation of randomly cycling adventitial fibroblasts. Under the experimental conditions used, adventitial fibroblasts from SHR grew more rapidly than those from WKY (Figure 1), as already reported by Zhu *et al.* (1991). In the presence of 10 μM nifedipine, the cell numbers after 3, 5 or 7 days of culture were significantly reduced in both WKY- and SHR-derived cultures compared to the respective cultures grown in the absence of drug (Figure 1a and b). This inhibitory effect of nifedipine appeared to be concentration-dependent since, in the presence of 1 μM nifedipine, the cell numbers after 3, 5 or 7 days were significantly reduced by 8 ± 3, 5 ± 2 and 6 ± 2% respectively ($P < 0.05$ for each). Likewise, the inhibitory effect of 10 μM nifedipine (~35%) did not differ significantly between SHR and WKY when the cell number was determined 3 days after plating (Table 1). However, after 5 or 7 days of culture, the inhibitory effect of 10 μM nifedipine on cell number was significantly greater in WKY-derived cultures than in SHR-derived ones (Table 1). The inhibition of cell growth could also be observed with other calcium channel blockers of the dihydropyridine series such as nisoldipine, nitrendipine, and nimodipine. These agents (tested at a concentration of 10 μM) each reduced the cell number to a similar extent in the SHR- and WKY-derived cultures, irrespective of the day at which cell count was determined (Table 1). Comparison between the drugs (each at 10 μM), using ANOVA, clearly indicated that the rank order of effect was nifedipine > nisoldipine > nitrendipine ~ nimodipine, for both SHR- and WKY fibroblasts, irrespective of the day considered. Nifedipine-induced cell number decrease was also observed in cells synchronized in the G_0/G_1 boundary and allowed to grow for 1, 3 and 5 days in the presence or absence of nifedipine (Table 2). In these experiments the cell counts in the absence of nifedipine were: 8639 ± 1588, 20756 ± 2764 and 30254 ± 5894 after 1, 3 and 5 days, respectively, for WKY fibroblasts and 14789 ± 2781, 35710 ± 5172 and 52336 ± 7299 after 1, 3 and 5 days, respectively for SHR fibroblasts. Nifedipine (10 μM) inhibited the cell proliferation by 20–40%, according to the allowed growth period and no significant difference could be observed between SHR and

WKY (Table 2); 1 μM nifedipine also significantly reduced (by ~5–10%) the cell number (data not shown).

Effect of nifedipine on serum-induced [^{3}H]-thymidine incorporation

The observed inhibitory effect of nifedipine on cell proliferation could have resulted from an inhibition of DNA synthesis. To test this hypothesis, cells synchronized in G_0/G_1 phase were used. Control values representing serum-induced [^{3}H]-thymidine incorporation in the absence of nifedipine were 12463 ± 933 and 31178 ± 3183 c.p.m./10^5 cells ($P<0.01$) for WKY and SHR, respectively. Nifedipine (1–10 μM) concentration-dependently inhibited [^{3}H]-thymidine incorporation into adventitial fibroblasts and cultures from both SHR and WKY were similarly affected by the drug (Figure 2). These results clearly indicate that nifedipine reduced DNA synthesis. To ascertain that nifedipine indeed affected the transition of cells from G_0/G_1 to S phase, [^{3}H]-thymidine incorporation was measured at various times following stimulation by serum of quiescent cells in the absence or presence of nifedipine. The results of these experiments showed that entry of cells in the S phase occurred between 10 and 12 h after serum stimulation and appeared to be earlier in SHR- than in WKY-derived cells (Figure 3; note that the scales in the two panels differ). Figure 3 also shows that in both cell strains, nifedipine clearly delayed the entry of cells

Table 1 Inhibition by various dihydropyridines of adventitial fibroblast proliferation

		% inhibition at day 3	day 5	day 7
Nifedipine (10 μM)	WKY	36 ± 3	42 ± 3	37 ± 3
	SHR	33 ± 5	35 ± 3**	29 ± 2*
Nisoldipine (10 μM)	WKY	18 ± 1	19 ± 3	13 ± 2
	SHR	14 ± 2	20 ± 3	16 ± 5
Nitrendipine (10 μM)	WKY	7 ± 2	12 ± 2	8 ± 2
	SHR	7 ± 1	15 ± 2	11 ± 5
Nimodipine (10 μM)	WKY	7 ± 2	9 ± 1	6 ± 1
	SHR	8 ± 1	12 ± 3	10 ± 3

Cells were seeded in 96-well plates at a density of 2×10^3 cells/well. One day after plating, the dihydropyridine (or the solvent for control) was added to the culture medium and cells were grown for 3, 5 or 7 days, the times at which the cell number was determined. Results (mean ± s.e.mean of 8 experiments) are expressed as % inhibition, calculated from the formula: 100[1-(N'/N)] where N' and N represent the cell number in the presence and absence of dihydropyridine, respectively. SHR versus WKY: *$P<0.05$; **$P<0.02$.

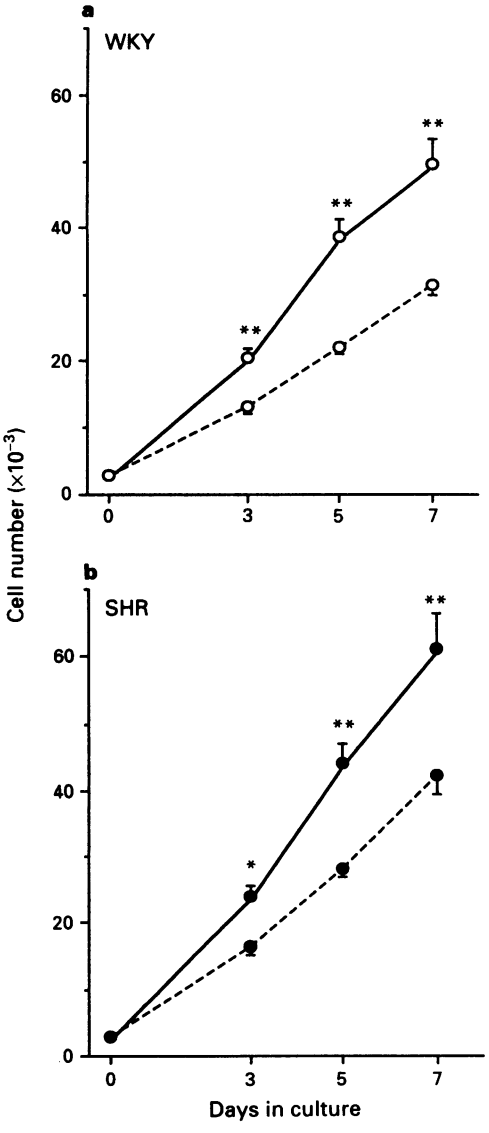

Figure 1 Growth kinetics of adventitial fibroblasts from SHR (●) and WKY (○) rat aortae. Effect of nifedipine. Fibroblasts were plated at a concentration of 2×10^3 cells/well in MEM containing 10% newborn calf serum and grown for 3, 5 or 7 days, times at which the cell numbers were determined. When present (dashed lines), nifedipine (10 μM) was added to cultures one day after plating. The culture medium was changed every other day. Results are the mean ± s.e.mean of 8 experiments. Within strain comparison (effect of nifedipine): *$P<0.02$; **$P<0.01$.

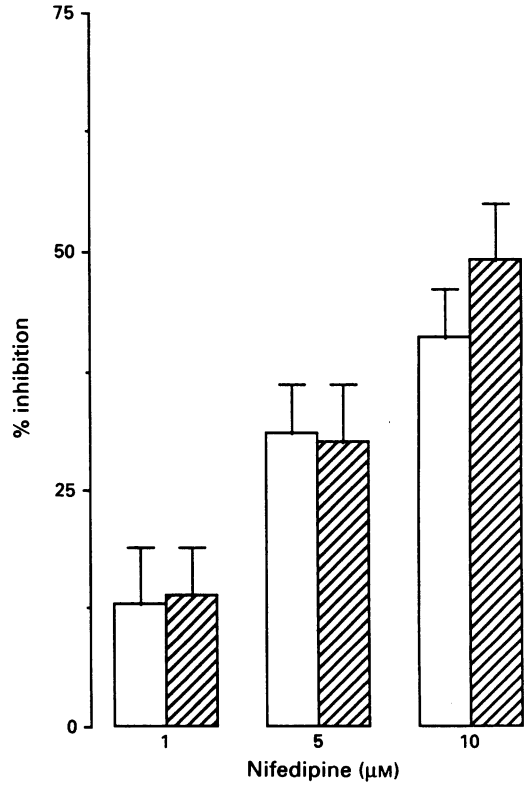

Figure 2 Effect of nifedipine on serum-induced [^{3}H]-thymidine incorporation. After 3 days of culture in 10% newborn calf serum (NCS), fibroblasts were made quiescent by serum deprivation for 2 days. Quiescent fibroblasts were then exposed to 5% NCS with either nifedipine (1–10 μM) or vehicle (control) for 24 h for measurement of [^{3}H]-thymidine incorporation. Results (mean ± s.e.mean of 5–6 experiments) are expressed as % inhibition (calculated as detailed in Methods). WKY fibroblasts (open columns); SHR fibroblasts (hatched columns).

into S phase. In another series of experiments, nifedipine (10 μM) was added at various times after serum stimulation of quiescent cells and [^{3}H]-thymidine incorporation was measured. Under these conditions, the inhibitory effect of nifedipine (10 μM) was maximal when the drug was added together with the stimulus but was abolished if the drug was added 16 h after the stimulus (Table 3). Moreover, the addition of nifedipine (10 μM) 4 h after cell stimulation, had a markedly reduced inhibitory effect, demonstrating that nifedipine must act on the early phase(s) of cell cycle to be fully effective against DNA synthesis. The kinetic studies depicted in Figure 2 and Tables 2 and 3 also show that nifedipine similarly affected both SHR and WKY fibroblasts.

Influence of the length of treatment with nifedipine

To investigate further the inhibitory effect of nifedipine, we measured serum-induced [^{3}H]-thymidine incorporation in cells exposed to the drug for various periods. Thus cultures were treated with nifedipine at time of stimulation (treatment duration of 1 day), during the serum deprivation period (treatment duration of 3 days) or as soon as one day after plating (treatment duration of 5 days). In these experiments, the values of [^{3}H]-thymidine incorporation in the absence of nifedipine were those mentioned above. As shown in Figure 4a the inhibitory effect of 10 μM nifedipine on [^{3}H]-thymidine incorporation increased in SHR and decreased in WKY fibroblasts with duration of treatment. Thus, when cells were treated for one day, the inhibitory potency of nifedipine did not significantly differ between SHR and WKY cells (34 ± 6 vs 42 ± 8%). When nifedipine was present for 3 days its inhibitory effect was significantly ($P<0.05$) higher in SHR than in WKY cells, the percentage inhibition being 40 ± 6 and 14 ± 9% in SHR and WKY cells, respectively (Figure 4a). When nifedipine was present for 5 days, its inhibitory effect was higher still in SHR than in WKY cells, the percentage inhibition being 66 ± 5 and 18 ± 9 ($P<0.001$) in SHR and WKY cells, respectively (Figure 4a); in some cultures of WKY fibroblasts, nifedipine had little or no inhibitory effect. Under these experimental conditions, the cell numbers per well at 1, 3 and 5 days in the absence of nifedipine were 14428 ± 2265, 15079 ± 2369 and 18718 ± 2553 (all NS) for SHR and 8250 ± 1566, 7478 ± 1058 and 9512 ± 1698 (all NS) for WKY. Nifedipine (10 μM) treatment for 1, 3 and 5 days decreased the cell number in SHR and WKY fibroblasts to a similar extent (20–30, 20 and 60%, respectively; Figure 4b).

Antagonistic effect of Bay K 8644

We next examined whether the calcium channel activator, Bay K 8644, could prevent the effect of nifedipine on serum-induced DNA synthesis. Since in the preceding experiments, the effect of nifedipine was dependent upon its cell contact time, we used the experimental protocol described in the preceding paragraph to investigate whether Bay K 8644 could alter the inhibitory effect of nifedipine on serum-induced DNA synthesis. When present, Bay K 8644 (1 μM) was added to cultures at the time of stimulation with 5% NCS. [^{3}H]-thymidine incorporation was determined 24 h later. Preliminary experiments showed that the addition of Bay K 8644 to cultures that were not treated with nifedipine did not significantly modify serum-induced [^{3}H]-thymidine incorporation (data not shown). Figure 5, which summarizes the results obtained with SHR and WKY cultures, shows

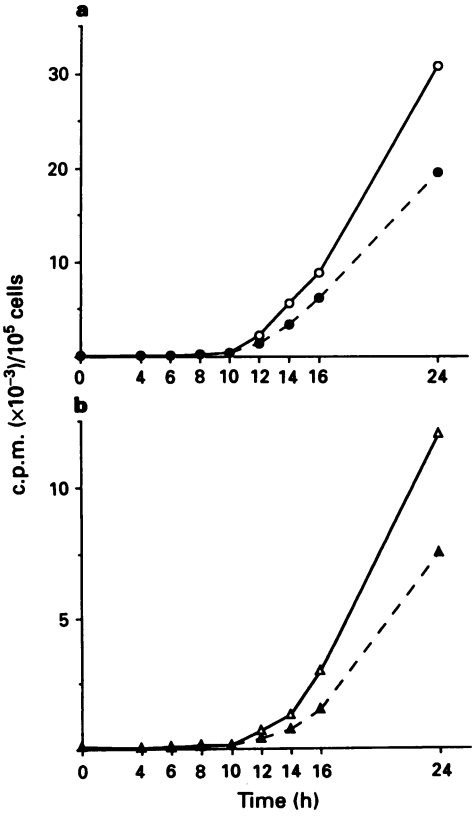

Figure 3 Effect of nifedipine on the transition from G_0/G_1 to S phase of aortic adventitial fibroblasts stimulated by serum. Quiescent fibroblasts from SHR (a) and WKY (b) were stimulated at time zero by the addition of 5% newborn calf serum with (closed symbols) or without (open symbols) 10 μM nifedipine and [^{3}H]-thymidine incorporation was measured at times indicated. Results shown are the means of duplicate determinations from a single experiment representative of two different cultures.

Table 2 The Inhibitory effect of nifedipine (10 μM) against cell number in G_0/G_1 synchronized cells

	% inhibition after		
	1 day	*3 days*	*5 days*
WKY	27.4 ± 3.1	36.7 ± 2.9	38.2 ± 2.3*
SHR	20.8 ± 3.7	32.1 ± 3.4*	29.1 ± 4.0

Cells were seeded in 96-well plates at a density of 1×10^3 cells/well and were grown for 3 days in MEM containing 10% newborn calf serum (NCS). Medium was then removed and replaced by serum-free MEM for 2 days, to synchronize cells at the G_0/G_1 boundary. Cells (8282 ± 1470 and 4979 ± 486 per well, for SHR and WKY, respectively) were then stimulated by 10% NCS in MEM, in the presence or absence (controls) of 10 μM nifedipine, for 1, 3 or 5 days, the times at which the cell number was measured. Results (mean ± s.e.mean of 5–9 experiments) are expressed as % inhibition due to the presence of nifedipine. Within strain comparison, versus value at day 1 (ANOVA): *$P<0.05$.

Table 3 Effect of delayed addition of nifedipine (10 μM) on serum-induced DNA synthesis in cultured aortic adventitial cells

	Time of addition (h following stimulation)			
	0	*4*	*8*	*16*
SHR	44.0 ± 5.7	29.3 ± 8.1	14.3 ± 3.9	2.0 ± 3.1
WKY	45.7 ± 1.5	27.3 ± 7.1	13.0 ± 10.7	−0.7 ± 4.6

Subconfluent cells, arrested in G_0/G_1 by serum deprivation for 2 days, were stimulated at time 0 by 5% newborn calf serum and [^{3}H]-thymidine incorporation was measured 24 h later. When present, 10 μM nifedipine was added at times indicated. Values (mean ± s.e.mean of 3 experiments) are expressed as % inhibition induced by nifedipine (10 μM).

that, irrespective of the length of treatment with nifedipine, Bay K 8644 partially but significantly reduced the inhibitory effect of nifedipine. Indeed, with a treatment duration of 1 day, while serum-induced [^{3}H]-thymidine incorporation was inhibited by 27 ± 6 and 32 ± 8% by nifedipine in WKY and SHR cultures, respectively, the addition of Bay K 8644 reduced the inhibitory effect of nifedipine to 6 ± 4 and 11 ± 6% in these cultures (Figure 5a). Essentially similar results were obtained when nifedipine was present for 5 days (Figure 5b).

Using the same experimental design as above, we then studied whether Bay K 8644 could also antagonize the inhibitory effect of nifedipine on cell proliferation, as measured with nifedipine treatment of varying duration. Figure 6 clearly shows that the addition of Bay K 8644 (1 μM) to both SHR and WKY cultures antagonized the effect of nifedipine (10 μM) when the drug was present for 1 or 3 days (Figure 6a and b). However, Bay K 8644 was without effect when nifedipine was present for 5 days (Figure 6c). Bay K 8644 added alone, in the absence of nifedipine, did not modify cell numbers (data not shown).

Discussion

Uehara *et al.* (1992) observed that the dihydropyridine, OPC-13340, attenuated the growth of cultured aortic smooth muscle cells from SHR and WKY and examined the underlying mechanisms. The present study has extended such observations to other dihydropyridine derivatives and to another cell type of the aortic wall, namely the adventitial fibroblasts from SHR and WKY.

The present results clearly showed that nifedipine, taken as a representative of these drugs, concentration-dependently reduced the cell number in randomly cycling cells as well in G_0/G_1 synchronized cells. A similar effect of nifedipine – and of the calcium channel blockers – has been documented in cultured aortic smooth muscle cells from various species (see

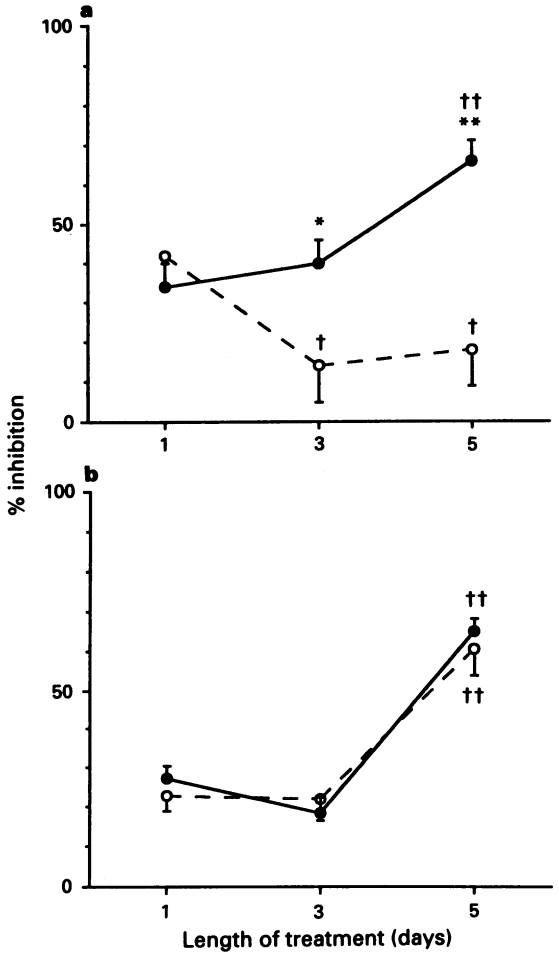

Figure 4 Effect of the duration of drug treatment on the inhibitory effects of nifedipine (10 μM) in aortic adventitial fibroblasts. Inhibition of serum-induced [^{3}H]-thymidine incorporation (a); inhibition of proliferation (b). Cells were plated at day zero; at day three they were placed in serum-free medium and at day five they were stimulated with 5% newborn calf serum. Twenty four hours later [^{3}H]-thymidine incorporation and cell number were measured. In these experiments, nifedipine (or vehicle in the case of controls) was added to cultures at the time of stimulation, at the time of serum deprivation or 1 day after plating, respectively, for the points designated 1, 3, or 5 days. Results (mean ± s.e.mean of 5–7 experiments) are percentage inhibitions calculated as described in Methods for [^{3}H]-thymidine incorporation and as detailed in the legend of Table 1 for cell number. SHR (solid symbols) and WKY (open symbols). SHR versus WKY: $*P<0.05$; $**P<0.001$. Within strain comparison versus the values at day 1: $\dagger P<0.05$; $\dagger\dagger P<0.001$.

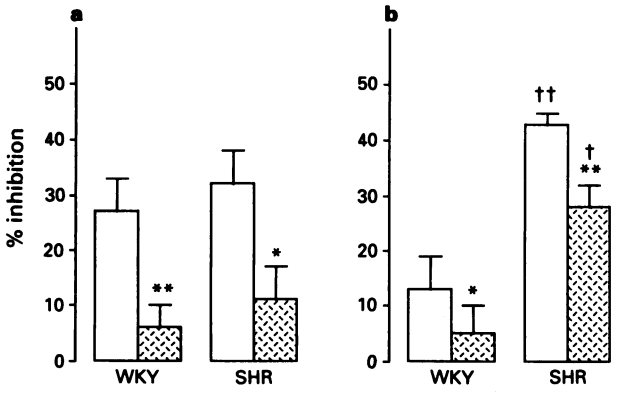

Figure 5 Effect of Bay K 8644 against the inhibitory effect of nifedipine on serum-stimulated DNA synthesis. In (a), quiescent cells were stimulated with 5% newborn calf serum (NCS) alone or with NCS and nifedipine (10 μM) or with NCS plus nifedipine plus Bay K 8644 (1 μM). [^{3}H]-thymidine incorporation was determined 24 h later. In (b), nifedipine was added 1 day after plating and was present throughout the experiment; quiescent cells were then stimulated as above. Results (mean ± s.e.mean of 5 experiments) are percentage inhibitions calculated as described in Methods. Open and stippled columns represent the inhibitory effect of nifedipine in the absence and in the presence of Bay K 8644, respectively. Within strain comparison (versus nifedipine alone): $*P<0.05$; $**P<0.01$. Between strain comparison: $\dagger P<0.05$; $\dagger\dagger P<0.002$.

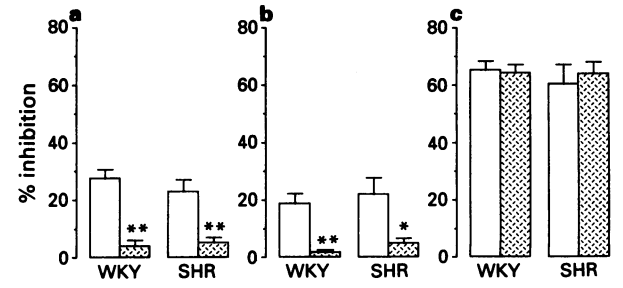

Figure 6 Effect of Bay K 8644 (1 μM) on the inhibitory effect of nifedipine (10 μM) against serum-induced cell proliferation. Cells were treated with nifedipine as described in the legend to Figure 4. The duration of nifedipine (10 μM) treatment was 1 day, 3 days and 5 days for data represented in (a), (b) and (c), respectively. When present, Bay K 8644 (1 μM) was added at the time of stimulation with 5% newborn calf serum. Cell number was determined 24 h after stimulation. Results (mean ± s.e.mean of 4–6 experiments) are expressed as percentage inhibitions calculated as described in the footnote to Table 1. Open and stippled columns represent the inhibitory effect of nifedipine in the absence and in the presence of Bay K 8644, respectively. Within strain comparison (versus nifedipine alone): $*P<0.05$; $**P<0.01$.

Jackson & Schwartz, 1992 for review). It is worth noting that the drug effect was of similar magnitude in SHR and WKY aortic fibroblasts or was slightly but significantly greater in WKY fibroblasts, according to conditions (Tables 1 and 2). By measuring serum-induced [^{3}H]-thymidine incorporation into adventitial fibroblasts, we have demonstrated that nifedipine concentration-dependently reduced DNA synthesis, to the same extent in SHR- and WKY-derived cultures (Figure 2, Table 3). This effect on DNA synthesis is likely to have resulted from the fact that nifedipine delayed the entry of fibroblasts into the S phase (Figure 3), since the drug acts in early G_0/G_1 phases (Table 3). In cultured and G_0/G_1 arrested vascular smooth muscle cells, nifedipine and other calcium channel antagonists of the dihydropyridine series also inhibited serum-induced DNA synthesis (Nilsson *et al.*, 1985; Jackson & Schwartz, 1992 for review). However, analysing the effect of OPC-13340 (a dihydropyridine calcium channel blocker) on aortic smooth muscle cell cycle, Uehara *et al.* (1992) reported that the drug reduced [^{3}H]-thymidine incorporation in randomly cycling SHR-cells but did not affect the transition from G_0/G_1 to S phase in both SHR and WKY cells. This observation as well as our finding that nimodipine and nitrendipine exhibited little effect in inhibiting cell proliferation (Table 1) indicate that each dihydropyridine possesses specific characteristics. Our results also suggested that SHR adventitial fibroblasts initiated DNA synthesis earlier than did WKY ones. A similar finding has been reported in cultured aortic smooth muscle cells from SHR and WKY (Hadrava *et al.*, 1992; Uehara *et al.*, 1992). Taken together these observations indicate that arterial cells from SHR, compared to those from WKY, exhibit hyperresponsiveness to serum, in agreement with preceding reports (Berk *et al.*, 1989; Zhu *et al.*, 1991; Saltis & Bobik, 1992; Uehara *et al.*, 1992).

The present results also demonstrate that the effect of nifedipine on DNA synthesis and cell number was dependent upon the length of treatment with the drug (Figure 4). The inhibitory effect of nifedipine on DNA synthesis differed in SHR and WKY fibroblasts in a manner indicating that SHR fibroblasts become progressively more sensitive to nifedipine whereas WKY fibroblasts become refractory (Figure 4a); a similar observation has already been made for fibroblast growth factor-induced DNA synthesis of rat aortic fibroblasts (Zhu *et al.*, 1994). However the inhibitory effect of nifedipine on cell proliferation was similar to SHR and WKY fibroblasts (Figure 4b). Thus, in SHR fibroblasts, the inhibition by nifedipine of cell number is likely to reflect the inhibition by the drug of DNA synthesis. In contrast, our finding that WKY cell number was considerably inhibited after 5 days of nifedipine treatment while such a drug treatment only weakly inhibited DNA synthesis, suggests that under this experimental condition, nifedipine reduced the proliferation of WKY fibroblasts by acting on a step distal to DNA synthesis, e.g. the M phase. Consistent with this hypothesis, an effect of the dihydropyridine calcium channel blocker OPC-13340 during the G_2/M period has been reported in cultured vascular smooth muscle cells (Uehara *et al.*, 1992). Irrespective of the length of treatment of cells with nifedipine (1–5 days), the inhibitory effect of the drug on DNA synthesis was abolished by the calcium channel agonist, Bay K 8644 in WKY fibroblasts and only partially reduced in SHR fibroblasts (Figure 5). Likewise, the inhibition of cell proliferation by nifedipine treatment for 1 or 3 days could be abolished (or almost) by Bay K 8644 (Figure 6a and b). In contrast, when the drug treatment lasted 5 days, Bay K 8644 could not antagonize the inhibitory effect of nifedipine on cell number (Figure 6c).

At the concentrations used in this study nifedipine may exert, besides its calcium channel blocker activity, various other effects that could be also antagonized by Bay K 8644 (Zernig, 1990). Nevertheless, from the present findings, one cannot rule out that the observed antimitotic effect of nifedipine involves L-type calcium channels at least partially. Differences may exist between SHR and WKY fibroblasts in the number of nifedipine binding sites, as has been reported for the binding of nitrendipine to membranes of various tissues in various models of hypertension (Ishii *et al.*, 1986) and for the number of calcium channels in cultured muscle cells or whole aortae (Rusch & Hermsmeyer, 1988; Lograno *et al.*, 1993). In addition, differences in the dihydropyridine binding capacity of proliferating cells might account for the observations reported since, under the conditions used for varying the length of nifedipine treatment, cells were exhibiting different growth characteristics (i.e. randomly growing in the presence of serum or quiescent in serum-free medium). Such characteristics have been described as affecting the binding of dihydropyridines (Dudkin *et al.*, 1988; Rampe *et al.*, 1988).

From the present data it can be concluded that nifedipine could inhibit the proliferation and serum-induced DNA synthesis by different mechanisms in SHR and WKY adventitial fibroblasts. The inhibition may occur at early G_0/G_1 phases and/or M phase. In addition our results strongly suggest the existence in aortic fibroblasts of interactions between Ca^{2+} channel blockers of the dihydropyridine series and the receptor signalling pathways of growth factors contained in serum, as documented in vascular smooth muscle cells for other mitogens (Nilsson *et al.*, 1985; Block *et al.*, 1989; Roe *et al.*, 1989; Ko *et al.*, 1992; Uehara *et al.*, 1992). Since the data showed that nifedipine could differentially affect SHR (vs WKY) cells, one may envisage that dihydropyridine-related mechanisms play a role in the abnormal vascular growth associated with hypertension.

This study was supported in part by the Fondation pour la Recherche Médicale and the research grant Bayer-Pharma/CNRS No. 67010300. The calcium channel blockers studied were a gift from Dr A. Knorr (Bayer AG, Wuppertal, Germany).

References

BERK, B.C., VALLEGA, G., MUSLIN, A.J., GORDON, H.M., CANESSA, M. & ALEXANDER, R.W. (1989). Spontaneously hypertensive rat vascular smooth muscle cells in culture exhibit increased growth and Na^+/H^+ exchange. *J. Clin. Invest.*, **83**, 822–829.

BLOCK, L.H., EMMONS, L.R., VOGT, E., SACHINIDIS, A., VETTER, W. & HOPPE, J. (1989). Ca^{2+}-channel blockers inhibit the action of recombinant platelet-derived growth factor in vascular smooth muscle cells. *Proc. Natl. Acad. Sci. U.S.A.*, **86**, 2388–2392.

BUKOSKI, R.D, DEWAN, P. & BO, J. (1991). Mechanism of the enhanced epidermal growth factor-induced growth response of genetically hypertensive rat vascular myocytes. *Circ. Res.*, **69**, 757–764.

CHATELAIN, R.E. & DARDIK, B.N. (1988). Increased DNA replication in the arterial adventitia after aortic ligation. *Hypertension*, **11** (suppl 1), 30–34.

CHEN, C., CORBLEY, M.J., ROBERTS, T.M. & HESS, P. (1988). Voltage-sensitive calcium channels in normal and transformed 3T3 fibroblasts. *Science*, **239**, 1024–1026.

DEYL, Z., JELINEK, J., MACEK, K., CHALDAKOV, G. & VANKOV, V.N. (1987). Collagen and elastin synthesis in the aorta of spontaneously hypertensive rats. *Blood Vessels*, **24**, 313–320.

DUDKIN, S.M., GNEDOJ, S.N., CHERNYUK, N.N. & SOLDATOV, N.M. (1988). 1,4 dihydropyridine receptor associated with Ca^{2+} channels in human embryonic fibroblasts. *FEBS Lett.*, **233**, 352–354.

FOLKOW, B. (1982). Physiological aspects of primary hypertension. *Physiol. Rev.*, **62**, 347–504.

GILLIGAN, J.P. & SPECTOR, S. (1984). Synthesis of collagen in cardiac and vascular walls. *Hypertension*, **6** (suppl 3), 44–49.

HADRAVA, V., TREMBLAY, J. & HAMET, P. (1989). Abnormalities in growth characteristics of aortic smooth muscle cells in spontaneously hypertensive rats. *Hypertension*, **13**, 589–597.

HADRAVA, V., TREMBLAY, J., SEKALY, R.P. & HAMET, P. (1992). Accelerated entry of aortic smooth muscle cells from spontaneously hypertensive rats into the S phase of the cell cycle. *Biochem. Cell. Biol.*, **70**, 599–604.

ISHII, K., KANO, T., ANDO, J. & YOSHIDA, H. (1986). Binding of [^{3}H]-nitrendipine to cardiac and cerebral membranes from normotensive and renal, deoxycorticosterone/NaCl and spontaneously hypertensive rats. *Eur. J. Pharmacol.*, **123**, 271–278.

JACKSON, C.L. & SCHWARTZ, S.M. (1992). Pharmacology of smooth muscle cell replication. *Hypertension*, **20**, 713–736.

KO, Y.D., SACHINIDIS, A., GRAACK, G.H., APPENHEIMER, M., WIECZOREK, A.J., DÜSING, R. & VETTER, H. (1992). Inhibition of angiotensin II and platelet-derived growth factor-induced vascular smooth muscle cell proliferation by calcium entry blockers. *Clin. Investig.*, **70**, 113–117.

KUENG, W., SILBER, E. & EPPENBERGER, U. (1989). Quantification of cells cultured on 96-well plates. *Anal. Biochem.*, **182**, 16–19.

LOGRANO, M.D., DANIELE, E., VULPIS, V. & PIRRELLI, A. (1993). Calcium channels in the vascular smooth muscle of spontaneously hypertensive rats. *J. Hypertens.*, **11** (suppl 5), S124–S125.

MULVANY, M.J., HANSEN, P.K. & AALKJAER, C. (1978). Direct evidence that the greater contractility of resistance vessels in spontaneously hypertensive rats is associated with a narrowed lumen, a thickened media, and an increased number of smooth muscle cell layers. *Circ. Res.*, **43**, 854–864.

NILSSON, J., SJÖLUND, M., PALMBERG, L., VON EULER, A.M., JONZON, B. & THYBERG, J. (1985). The calcium antagonist nifedipine inhibits arterial smooth muscle cell proliferation. *Atherosclerosis*, **58**, 109–122.

OOSHIMA, A., FULLER, G.C., CARDINALE, G.J., SPECTOR, S. & UNDENFRIEND, S. (1974). Increased collagen synthesis in blood vessels of hypertensive rats and its reversal by antihypertensive agents. *Proc. Natl. Acad. Sci. U.S.A.*, **71**, 3019–3023.

OWENS, G.K. & SCHWARTZ, S.M. (1982). Alterations in vascular smooth muscle mass in the spontaneously hypertensive rat. *Circ. Res.*, **51**, 280–289.

RAMPE, D., CAFFEY, J.M., SCHNEIDER, M.D. & BROWN, A.M. (1988). Control of expression of the 1,4-dihydropyridine receptor in BC_3H cells. *Biochem. Biophys. Res. Commun.*, **152**, 769–775.

ROE, M.W., HEPLER, J.R., HARDEN, T.K. & HERMAN, B. (1989). Platelet-derived growth factor and angiotensin II cause increases in cytosolic free calcium by different mechanisms in vascular smooth muscle cells. *J. Cell. Physiol.*, **139**, 100–108.

RUSCH, N.J. & HERMSMEYER, K. (1988). Calcium currents are altered in the vascular muscle cell membrane of spontaneously hypertensive rats. *Circ. Res.*, **63**, 997–1002.

SALTIS, J. & BOBIK, A. (1992). Vascular smooth muscle growth in genetic hypertension: evidence for multiple abnormalities in growth regulatory pathways. *J. Hypertens.*, **10**, 635–643.

SCOTT-BURDEN, T., RESINK, T.J. & BÜHLER, F.R. (1989). Enhanced growth and growth factor responsiveness of vascular smooth muscle cells from hypertensive rats. *J. Cardiovasc. Pharmacol.*, **14** (suppl 6), S16–S21.

SCHWARTZ, S.M., HEIMARK, R.L. & MAJESKY, M.W. (1990). Developmental mechanisms underlying pathology in arteries. *Physiol. Rev.*, **70**, 1177–1209.

TODD, M.E. (1992). Hypertensive structural changes in blood vessels: do endothelial cells hold the key? *Can. J. Physiol. Pharmacol.*, **70**, 536–551.

UEHARA, Y., KAWABATA, Y., HIRAWA, N., TAKADA, S., NUMABE, A., MATSUOKA, H., IKEDA, T., TAKABATAKE, Y., YAGI, S. & SUGIMOTO, T. (1992). OPC-13340, a new dihydropyridine calcium channel blocker attenuates rapid vascular smooth muscle cell growth in spontaneously hypertensive rats. *J. Cardiovasc. Pharmacol.*, **20**, 408–415.

VENANCE, S.L., WATSON, M.H., WIGLE, D.A., MAK, A.S. & PANG, S.C. (1993). Differential expression and activity of $p34^{cdc2}$ in cultured aortic adventitial fibroblasts derived from spontaneously hypertensive and Wistar-Kyoto rats. *J. Hypertens.*, **11**, 483–489.

ZERNIG, G. (1990). Widening potential for Ca^{2+} antagonists: non-L-type Ca^{2+} channel interaction. *Trends Pharmacol. Sci.*, **11**, 38–44.

ZHU, D.L., DURANT, S. & MARCHE, P. (1990). Phospholipase C activity in cultured aortic fibroblasts of hypertensive and normotensive rats. *J. Vasc. Med. Biol.*, **2**, 26–31.

ZHU, D.L., HÉREMBERT, T. & MARCHE, P. (1991). Increased proliferation of adventitial fibroblasts from spontaneously hypertensive rat aorta. *J. Hypertens.*, **9**, 1161–1168.

ZHU, D.L., HÉREMBERT, T. & MARCHE, P. (1992). Protein kinase C and cell proliferation in spontaneously hypertensive rats. *Clin. Exp. Hypertens.*, **14**, 875–887.

ZHU, D.L., HÉREMBERT, T. & MARCHE, P. (1994). Involvement of calcium channels in fibroblast growth factor-induced activation of arterial cells in spontaneously hypertensive rats. *J. Cardiovasc. Pharmacol.*, **23**, 395–400.

(Received June 20, 1994
Revised December 12, 1994
Accepted January 6, 1995)

British Journal of Pharmacology (1995) 114, 1710–1716 © 1995 Stockton Press All rights reserved 0007–1188/95 $12.00

Prejunctional facilitatory α_1-adrenoceptors in the rat urinary bladder

[1]G.T. Somogyi, M. Tanowitz & W.C. de Groat

Department of Pharmacology, University of Pittsburgh, Pittsburgh, PA 15261, U.S.A.

1 The effect of activation of α_1-adrenoceptors on acetylcholine (ACh) release and neurally evoked contractile responses induced by electrical field stimulation was investigated in smooth muscle strips from the rat urinary bladder.

2 Neurogenic contractions were facilitated by the α_1-adrenoceptor agonists, phenylephrine (PE) (2–128 μM) and methoxamine (2–128 μM) in a dose-dependent manner. These agents also increased small amplitude spontaneous contractions of bladder strips and in 10% of strips increased basal tone. However, contractions elicited by exogenous ACh (1–10 μM) were not affected by α_1-agonists.

3 The magnitude of the PE facilitation was higher at lower frequencies (1–5 Hz) or at submaximal intensities of stimulation and at lower Ca^{2+} concentrations (0.5–1 mM). The selective α_1-adrenoceptor antagonist, terazosin (TRZ) (0.05–1 μM), competitively inhibited (pA_2 value: 8.6) the PE facilitation of the neurally evoked contractions but not the PE induced increase of spontaneous contractions.

4 [^{3}H]-noradrenaline (NA) and [^{14}C]-ACh release evoked by electrical field stimulation were increased (140% and 173%, respectively) by 2 μM PE. TRZ (0.05–0.1 μM) blocked the PE facilitation of ACh release but not the facilitation of NA release. TRZ alone did not alter the release of ACh or NA nor the amplitude of the neurogenic contractions.

5 PE (2 μM) did not alter the basal release of ACh but did increase (by 180%) the basal release of NA. Desipramine (2 μM) blocked this effect of PE and also the PE-facilitation of evoked ACh and NA release.

6 It is concluded that cholinergic terminals in the rat urinary bladder exhibit α_1-adrenoceptors which can facilitate the release of transmitter. However, under the conditions of our experiments it appears that cholinergic transmission is not modulated by α_1 adrenergic mechanisms. Further studies are necessary to determine whether these receptors can be activated by endogenous noradrenaline released within the bladder.

Keywords: α_1-Adrenoceptors; prejunctional facilitation; urinary bladder

Introduction

Adrenergic modulation of autonomic transmission has been detected at various sites in the peripheral nervous system. For example, activation of α_1-adrenoceptors inhibits acetylcholine (ACh) release from the cholinergic nerve terminals in the ileum (Kapocsi *et al.*, 1986; Starke, 1987) and in autonomic ganglia (Paton & Thompson, 1953; Dawes & Vizi, 1973; de Groat & Booth, 1980) and inhibits noradrenaline (NA) release from adrenergic nerve terminals in the heart (Ledda & Mantelli, 1984), vas deferens (cf. Vizi, 1979) and urinary bladder (Somogyi & de Groat, 1990). α_1-Adrenoceptors which are prominent at postjunctional sites (Langer, 1974), have also been detected at the adrenergic and cholinergic nerve terminals in some peripheral tissues. However, the function of prejunctional α_1-adrenoceptors is more variable. Inhibitory α_1-adrenoceptors were detected on adrenergic nerves in the kidney (Rump & Majewski, 1987) and on adrenergic and cholinergic nerves in the heart (Ledda & Mantelli, 1984; Wetzel *et al.*, 1985). In addition, a facilitatory effect of certain α_1-agonists on ACh release in the heart has been described (Bognar *et al.*, 1990). α_1-Adrenoceptor facilitation of cholinergic transmission has also been reported at nicotinic synapses at the neuromuscular junction (Vizi, 1991) and in parasympathetic ganglia of the cat urinary bladder, where the α_1-adrenoceptors are located on the cell body (Akasu *et al.*, 1985; Keast *et al.*, 1990). In the cat bladder ganglia the facilitation is associated with a slow postsynaptic depolarization (de Groat & Booth, 1980; Akasu *et al.*, 1985). Recent patch clamp studies have revealed that α-adrenoceptor agonists also depolarize bladder parasympathetic neurones isolated from the major pelvic ganglion of the rat (Yoshimura & de Groat, 1992).

The presence of excitatory α_1-adrenoceptors on the soma of bladder parasympathetic neurones raises the possibility that similar receptors might be present at the axon terminals of these neurones in the urinary bladder. This was evaluated in the present experiments by examining the effects of α_1-adrenoceptor agonists on neurally evoked smooth muscle contractions and on ACh and NA release in strips of the rat urinary bladder. The results indicate that activation of α_1-adrenoceptors can facilitate ACh release and excitatory transmission in the bladder. These observations coupled with previous reports of muscarinic receptor (M_2) inhibition (D'Agostino *et al.*, 1986; Somogyi & de Groat, 1992) and muscarinic receptor (M_1) facilitation (Somogyi & de Groat, 1992; Somogyi *et al.*, 1994) of ACh release in the rat bladder indicate that cholinergic transmission in this organ is potentially complex and dependent upon the interaction of a variety of prejunctional modulatory mechanisms.

A preliminary report of some of these results has appeared as an abstract (Somogyi *et al.*, 1992).

Methods

Preparation

The urinary bladder was removed from male Sprague Dawley rats (250–300 g) following decapitation and circular slices were cut from the middle part of the bladder body.

[1] Author for correspondence.

Contractile experiments

The bladder strips weighing 20–30 mg were mounted in a double jacketed organ bath at 35°C in Krebs solution (mmol l^{-1}: NaCl 113, KCl 4.7, $CaCl_2$ 2.5, $MgSO_4$ 1.2, $NaHCO_3$ 25, KH_2PO_4 1.2, glucose 11.5) and constantly bubbled with a mixture of 95% O_2 and 5% CO_2. The initial tension was set at 1 g and isometric contractions were measured with strain-gauge transducers and recorded on a Grass polygraph. Electrical field stimulation with a Grass 88 stimulator was delivered through platinum electrodes inserted from the top and bottom of the organ bath and separated by 4 cm. Stimulation intensity-response curves were constructed in order to determine the voltage required to elicit a maximal contraction. The preparations were then stimulated at a maximal voltage at 10 Hz with 0.25 ms stimulus duration for 1 s at 1 min intervals. These stimulus parameters yielded contractions at a consistent amplitude over long periods of time (4–6 h). In some preparations the voltage was set to produce 50% of the maximal effect. However, unless otherwise stated, maximal stimulation was applied. When the frequency-response relationships were studied, a frequency-response curve was constructed before and after the addition of drugs by applying stimulus trains consisting of 10 shocks at frequencies ranging from 0.1 to 50 Hz.

The α_1-agonists were added to the bath at 6–8 min intervals in increasing concentrations to construct cumulative dose-response curves. The ED_{50} values for each agonist were calculated. The dose-response relationships were also examined in the presence of different concentrations of the α_1-antagonist, terazosin. Terazosin was added to the bath 20 min before each test.

Experiments on NA and ACh release

A double labelled isotopic technique was used to measure simultaneous release of NA and ACh from the same strip. Strips were incubated consecutively with 10 μCi ml^{-1} (−)-[7-^{3}H]-NA (specific activity: 17 Ci $mmol^{-1}$) for 30 min and after a wash-out, incubated with 0.5 μCi ml^{-1} [methyl-^{14}C]-choline (specific activity: 50 mCi $mmol^{-1}$) for another 30 min at 36°C. After the incubation each strip was suspended in a bath and superfused at a rate of 0.3 ml min^{-1} with oxygenated Krebs solution containing 10 μM hemicholinium-3. After a 60 min washing period, 3 min effluents were collected for 75 min with a fraction collector.

Stimulation and drug administration

Electrical field stimuli were applied through platinum plate electrodes positioned 2.5 cm apart on the top and the bottom of the perfusion bath. Two continuous electrical stimulations (100 shocks, 10 Hz, 100 V and 0.25 ms) were applied consecutively in the 66th (S_1) and 114th min (S_2) of the superfusion. Drugs were added to the perfusion solution 20 min before S_2; and the effects of the drugs were expressed as the S_2/S_1 ratio compared to that of controls.

Calculation of the experimental results

The radioactivity in the effluent was measured by using Optifluor scintillation reagent (Packard Industries) with a Beckman Beta Spectrometer. The measured counts were corrected to absolute activity both for ^{14}C and ^{3}H using the computer programme supplied with the scintillation counter. The acid soluble radioactive content of the tissue slices for both isotopes was determined after the experiments by placing the tissue in 1 ml of 10% trichloro-acetic acid for 16 h before counting. The released amounts of ^{3}H and ^{14}C are expressed as the fraction of the tissue ^{3}H and ^{14}C content, respectively (fractional release). The evoked release of NA and ACh was computed by calculating the area below the increased efflux curve of ^{3}H and ^{14}C, respectively, from the fractional release values as described earlier (Somogyi *et al.*, 1994). For characterization of the effect of treatments on basal release of radioactivity, we calculated the ratio of the basal release (B_2/B_1) of ^{3}H and ^{14}C before starting S_1 and S_2. This value is usually lower than one, unless the basal release of transmitter is increased by the treatment (Somogyi & de Groat, 1993).

Drugs

Atropine sulphate, desipramine hydrochloride, phenylephrine hydrochloride, methoxamine hydrochloride, tetrodotoxin and all constituents of the Krebs solution were purchased from Sigma Chemical Co. (St. Louis, Mo, U.S.A.). Terazosin was provided by Abbott Labs (Chicago, Ill, U.S.A.). (−)-[7-^{3}H]-noradrenaline and [methyl-^{14}C]-choline were purchased from NEN-Du Pont (Boston, MA, U.S.A.).

Statistical analysis

Student's *t* test and the non parametric Rank Sum test, or Kruskall-Wallis one way analysis of variance were used as appropriate. A level of $P<0.05$ was considered as statistically significant. The E_{max} as well as the ED_{50} and the pA_2 values were calculated with a computer programme (Tallarida & Murray, 1987).

Results

Effect of activation of α_1-adrenoceptors on the contractile response of the bladder strips

Phenylephrine (PE) added in increasing concentrations (0.2–128 μM) to the organ bath at 10 min intervals elicited three effects: (1) a concentration-dependent increase in the amplitude of the contractile response induced by electrical stimulation (Figure 1a), (2) increased basal tone in approximately 10% of the bladder strips; the maximal increase usually did not exceed 5–7% of the amplitude of the electrically evoked contractions, but the increase was concentration-dependent (Figure 1b), (3) increased low amplitude spontaneous activity (approximately 20% of the preparations). Similar effects were elicited by methoxamine (0.5–50 μM). Neither the spontaneous contractile activity nor the enhancement of the activity induced by α_1 agonists was inhibited by 1 μM tetrodotoxin or 0.1–1 μM atropine.

Tachyphylaxis did not occur when multiple cumulative dose-response curves were constructed at intervals of 20 min. The maximal effect of each concentration occurred within 4 min after administration of PE or methoxamine. In these experiments the effects of the highest concentration of PE were eliminated within 5–10 min after wash out of the drug.

To measure the direct postjunctional effect of PE on the contractile response of the bladder smooth muscle, dose-response curves for ACh were constructed in the absence and presence of various concentrations of PE (0.5–8 μM). In 3 experiments PE added to the bath 10 min before ACh did not significantly change the ACh dose-response curves (Figure 2). The slight shift of ACh dose-response curves to the right may be due to a weak desensitization of the postsynaptic muscarinic receptors to the high concentrations of ACh (up to 1 mM).

Effect of stimulus intensity and frequency on the PE-induced facilitation

Bladder strips were stimulated (10 Hz, 10 shocks) at an intensity producing 50% of the maximal contractions. As shown in Table 1 the contractions evoked by submaximal stimula-

tion exhibited a greater facilitation (85% ± 10 increase; $n = 13$) than those evoked by maximal stimulation (45% ± 9.2 increase, $n = 27$). Although the magnitudes of these effects were significantly different; $P < 0.01$, (Student's t test) there was no significant difference between the ED_{50} values for PE (1.44 ± 0.3 μM versus 1.1 ± 0.13 μM) during the two types of stimulation. The maximal facilitation produced by methoxamine, another selective α_1-agonist, during submaximal stimulation was in the same range (112 ± 24% increase, $n = 7$; $P > 0.1$ Student's t test) as that of PE; however, the ED_{50} value for methoxamine (Table 1) was significantly higher than that of PE.

The effect of PE was tested at different frequencies (0.1 to 50 Hz) with maximal intensities of stimulation and trains of 10 shocks. The magnitude of the facilitation correlated inversely with the stimulation frequency; the facilitatory effect of PE being more prominent at lower frequencies (0.1–5 Hz) than at higher frequencies (10–50 Hz) (Figure 3).

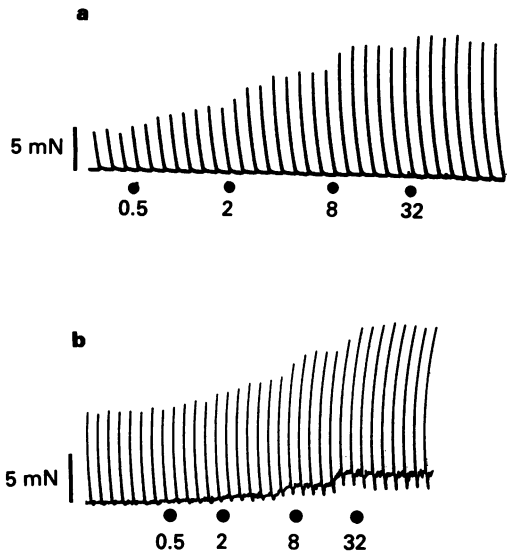

Figure 1 Facilitation by various concentrations of phenylephrine (PE) of the contractile response of a rat urinary bladder strip induced by submaximal electrical field stimulation of 10 Hz, 10 shocks at one minute intervals. (a) A typical tracing showing the facilitatory effect of PE. The concentration of PE was progressively increased at 6–10 min intervals. Note that there is minimal spontaneous activity of the strip, and the baseline is stable even at higher concentrations of PE. (b) In 10% of the bladder strips examined the basal tone and the spontaneous activity were increased by PE in addition to enhancement of the neurogenic contractions. Otherwise, the experiment was done in the same way as (a).

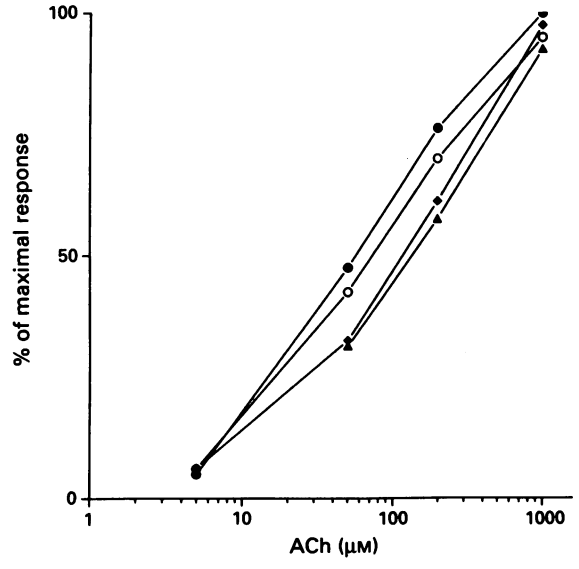

Figure 2 Effect of phenylephrine (PE) on the acetylcholine (ACh)-evoked contractile responses of the circular strips of rat urinary bladder. ACh was washed out after each addition. Increasing concentrations of PE were added 10 min before each ACh dose-response curve and were kept in the washing solution. The concentration of ACh is plotted against the contractile response expressed as the maximal response to ACh. The maximal response was extrapolated from the double reciprocal plot of the dose-response curve (Tallarida & Murray, 1987). The symbols represent (●) control; (○) 0.5 μM PE; (◆) 2 μM PE; (▲) 8 μM PE. Every point is the mean of 3 experiments. The s.e.mean was between 12–17%.

Effect of the extracellular Ca^{2+} concentration on the PE-induced facilitation

Since the M_1 muscarinic receptor mediated facilitation of cholinergic transmission in the bladder was positively correlated with the extracellular Ca^{2+} concentration (Somogyi *et al.*, 1994), the Ca^{2+}-dependence of the α_1 facilitation of the neurally evoked contractions was also examined. In these studies the extracellular Ca^{2+} concentration in the bath was changed in a stepwise fashion from 0 to 2.5 mM while the preparations were electrically stimulated. Then, the Ca^{2+} dose-response curve was repeated in the presence of various PE concentrations (0.5–8 μM). The amplitudes of the contractions at different Ca^{2+} concentrations in the presence and absence of PE are compared in Figure 4. PE was more effective ($P < 0.05$) in facilitating the neurogenic contractions at lower Ca^{2+} concentrations (0.5–1 mM), than at higher concentrations (1.5–2.5 mM).

Effect of terazosin (TRZ) on the PE response

The α_1-adrenoceptor antagonist, terazosin (TRZ), was added to the bath 20 min before constructing cumulative dose-response curves for PE and was present while PE was added to the bath. Experiments were begun with the lowest concentration of TRZ (10 nM) and when the maximal PE facilitation was reached, both PE and TRZ were washed out, and immediately a higher concentration of TRZ was added to the bath. The dose-response curve to PE was shifted to the right by TRZ in a dose-dependent manner (Figure 5). The pA_2 value for TRZ calculated according to Arunlakshana &

Table 1 The facilitatory effect of α_1-agonists on neurogenic contractions of the rat urinary bladder induced by maximal and submaximal intensities of electrical field stimulation (EFS)

	Maximal EFS		*Submaximal EFS*	
Drugs	ED_{50} (μM)	*Max. resp.* (%)	ED_{50} (μM)	*Max. resp.* (%)
PE	1.07 ± 0.13 $n = 27$	145 ± 9.2	1.44 ± 0.3 $n = 13$	185 ± 10
MTX			6.11 ± 1.7 $n = 7$	212 ± 24

The ED_{50} values were determined by calculating the concentrations of α_1-agonists which induce 50% of the maximal increase in electrically evoked contractions. The maximal facilitatory responses (max. resp.) to phenylephrine (PE) and methoxamine (MTX) were calculated as the percentage of the control contractions in strips stimulated with voltages producing a maximal contractile response or a voltage producing 50% of the maximal response (submaximal stimulation).

Schild (1959) was 8.26 and the slope of the Schild plot (1.13 ± 0.18) was not significantly different ($P>0.1$) from unity (Figure 6); indicating that TRZ inhibited the α_1-receptors in a competitive manner. TRZ (20–100 nM) inhibited the PE-induced increase in basal tone; however, it did not change the increased spontaneous activity evoked by PE.

Effect of PE and TRZ on the basal and evoked release of [^{3}H]-NA and [^{14}C]-ACh

The bladder tissues were incubated with [^{3}H]-NA and [^{14}C]-choline, so that the release of NA and ACh could be measured simultaneously. Two successive electrical stimulations using parameters (10 Hz, 100 shocks), which induce facilitation of ACh release via M_1 muscarinic receptors (Somogyi *et al.*, 1994) were applied in the 66th and 105th min of the superfusion (S_1 and S_2). The first stimulation markedly enhanced the efflux of both [^{3}H]-NA and [^{14}C]-ACh above the level of resting efflux. However, the amount of transmitter released was significantly lower during the second stimulation (S_2) producing an S_2/S_1 ratio of 0.49 ± 0.09 for [^{3}H]-NA and 0.3 ± 0.04 for [^{14}C]-ACh. The α_1-agonist, PE applied between S_1 and S_2 at a concentration of 2 μM (which is twice the ED_{50} value for facilitating neurally evoked contractions) significantly ($P<0.05$) facilitated the release of both NA (140.8 ± 47% increase) and ACh (173 ± 37% increase) elicited by the second stimulation. The α_1-antagonist, TRZ (0.1 μM) blocked the PE-induced facilitation of ACh release (53 ± 36% increase; not significantly different from the release in the absence of drugs; $P>0.05$). TRZ did not

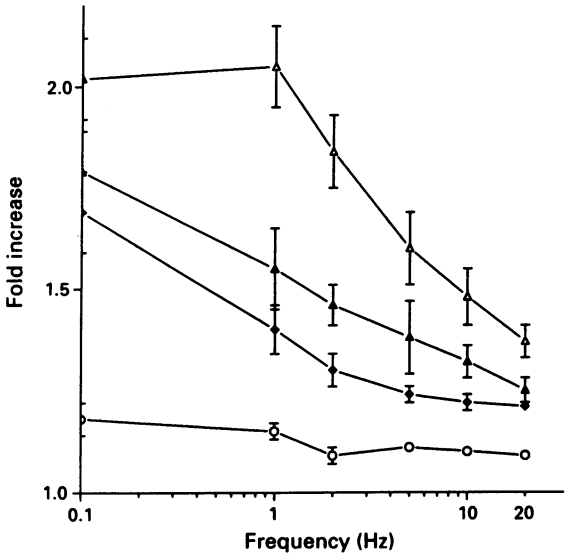

Figure 3 Frequency-dependence of phenylephrine (PE)-induced facilitation of the contractions of rat urinary bladder strips elicited by supramaximal electrical field stimulation. The ratio of the contractions in the presence and absence of various concentrations of PE is plotted against the stimulation frequency. Note that the lower frequencies of stimulation were more sensitive to the PE facilitation than the higher frequency of stimulation. The symbols represent (○) 0.1 μM, (◆) 0.5 μM, (▲) 2 μM and (△) 8 μM PE. Every point is an average of 4 experiments.

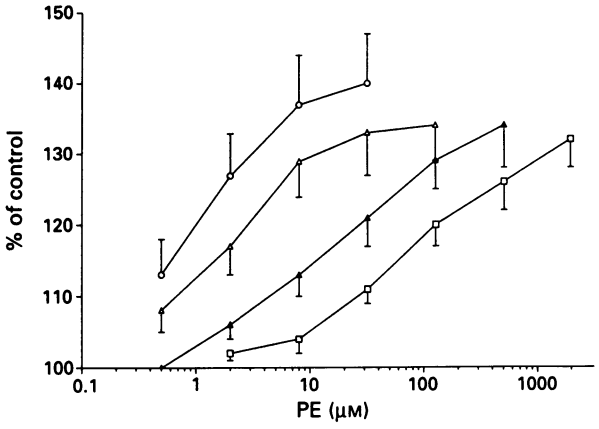

Figure 5 The effect of various concentrations of the α_1-adrenoceptor antagonist, terazosin, on phenylephrine (PE)-induced facilitation of the neurally evoked contractions of rat urinary bladder strips. The facilitatory effect of PE, expressed as a percentage of the control, was plotted against the concentrations of PE in μM. The symbols represent: no terazosin (○), 50 nM (△), 100 nM (▲), and 200 nM (□) terazosin. Every point is the mean ± s.e.mean of 7 experiments.

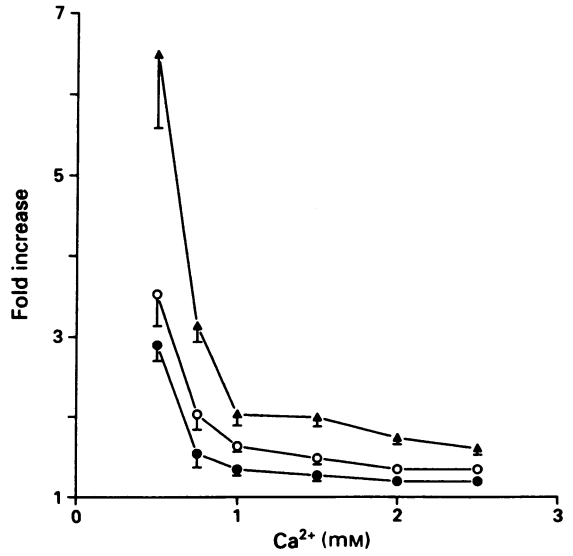

Figure 4 The influence of Ca^{2+} concentrations on the phenylephrine (PE)-facilitation of neurally evoked contractions of rat urinary bladder strips. The ratio of PE facilitated contractile responses to control (fold increase) is plotted against the Ca^{2+} concentration. The symbols represent: (●) 0.5 μM; (○) 2 μM; (▲) 8 μM PE. Every point is the mean (±s.e.mean) of 7 experiments.

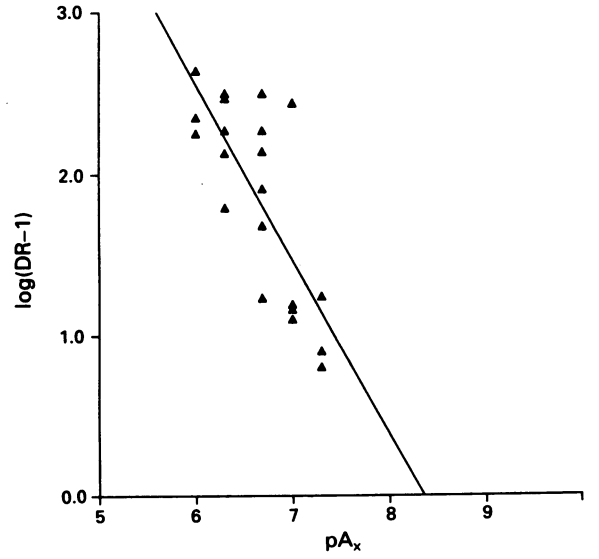

Figure 6 Schild plot showing the effect of the α_1-adrenoceptor antagonist, terazosin, on phenylephrine (PE) facilitation of neurally evoked contractions of rat urinary bladder strips. (pA_2 value: 8.27; slope: 1.13 ± 0.14; *r*: −0.81, $n=21$) where 'r' is the correlation coefficient. The slope is not significantly different from unity ($P>0.2$, paired *t* test).

Table 2 Effect of phenylephrine and terazosin on the basal release of [^{14}C]-acetylcholine ([^{14}C]-ACh) and [^{3}H]-noradrenaline ([^{3}H]-NA) in the presence and absence of desipramine

	ACh release		*NA release*	
Treatment	*Normal*	*Desipramine*	*Normal*	*Desipramine*
Control	0.72 ± 0.06 (6)	0.71 ± 0.04 (4)	0.77 ± 0.03 (6)	0.78 ± 0.01 (4)
PE (2 μM)	0.79 ± 0.06 (6)	0.64 ± 0.04 (4)	2.16 ± 0.17 (6)*	0.79 ± 0.02 (4)
TRZ + PE	0.82 ± 0.07 (6)	0.72 ± 0.11 (4)	2.05 ± 0.22 (6)*	0.92 ± 0.11 (4)
TRZ (0.1 μM)	0.79 ± 0.08 (6)	0.79 ± 0.08 (4)	0.91 ± 0.06 (6)	0.79 ± 0.03 (4)

The numbers in the table represent the B_2/B_1 ratio which was computed from the basal release values of [^{3}H]-NA and [^{14}C]-ACh before S_1 and S_2. Desipramine was present in a concentration of 2 μM. Normal values represent the basal release in preparations not treated with desipramine. The drugs (PE = phenylephrine; TRZ = terazosin and TRZ + PE) were added to the perfusion solution 20 min before S_2.

*Indicates values significantly different from the control in the same column ($P<0.05$, Kruskall-Wallis non-parametric one way analysis of variance combined with Rank Sum test). Note that desipramine blocked the effect of PE and PE + TRZ treatment on basal release of [^{3}H]-NA ($P<0.05$; Rank Sum test).

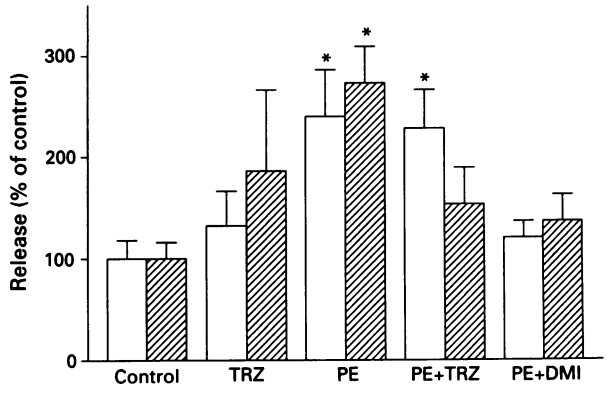

Figure 7 The effect of phenylephrine (PE) and/or terazosin (TRZ) on the stimulation evoked release of [^{14}C]-acetylcholine ([^{14}C]-ACh) and [^{3}H]-noradrenaline ([^{3}H]-NA) in normal and in desipramine (2 μM)-treated rat urinary bladder strips. Two supramaximal electrical field stimulations (100 V, 10 Hz, 100 shocks) were applied in the 66th (S_1) and 114th min (S_2) of superfusion and PE, TRZ or PE + TRZ were administered 20 min before S_2. When desipramine (2 μM) was applied, it was present throughout the experiments. Drug effects are expressed as % of the S_2/S_1 ratios in control experiments. Open columns denote NA release, hatched columns ACh release and the vertical lines denote s.e.mean.

alter the facilitation of [^{3}H]-NA release (128 ± 38% increase; not significantly different from the control PE facilitation of release; $P>0.05$). TRZ alone added to the perfusion solution 20 min before S_2 had no significant effect ($P>0.05$) either on [^{3}H]-NA (33 ± 34% increase) or on [^{14}C]-ACh release (86 ± 80% increase).

PE (2 μM) did not change the basal release of ACh but significantly increased the basal release of [^{3}H]-NA (181 ± 22% increase, $P<0.05$). In the presence of TRZ (0.1 μM) PE produced a similar increase in basal [^{3}H]-NA release (166 ± 28% increase; $P>0.05$) (Table 2), indicating that the effect of PE is not mediated by activation of α_1-receptors. However, desipramine (2 μM) treatment before S_2 completely inhibited (1 ± 2.5% increase; $P>0.05$) the PE-evoked increase of basal release demonstrating that an amine transport mechanism is involved in the basal release of NA (Vizi *et al.*, 1986b). The PE-induced increase in the electrically evoked [^{3}H]-NA and [^{14}C]-ACh release was completely abolished in the presence of desipramine (Figure 7).

Discussion

The present experiments revealed that PE, an α_1-adrenoceptor agonist, increased neurally evoked contractions as well as ACh and NA release in rat urinary bladder strips but did not change ACh-induced bladder contractions. It is concluded that at least part of the facilitatory effect of exogenous α_1-adrenoceptor agents on excitatory transmission in the rat bladder is mediated by prejunctional receptors on the cholinergic nerve terminals.

A review of the literature has not identified other studies which evaluated the effect of α_1-adrenoceptor agonists on neurally evoked bladder contractions; however, there are numerous reports of the direct effects of these agents on the bladder smooth muscle. Experiments in several species revealed that α_1-agonists elicited contractions of the smooth muscle in the bladder base but evoked variable effects on the bladder body (Downie *et al.*, 1975), ranging from no response to prominent excitatory responses (Ordway *et al.*, 1986). Some of this variation could be due to the age of the animals, since Ordway *et al.* (1986) reported that α_1-agonists produced more prominent excitatory responses in older (29 months) than in younger rats (7 months). In the young animals (3–4 months) which were used in the present study only 10% of the preparations exhibited a detectable rise in baseline tone following PE or methoxamine. However, these agents commonly increased the frequency of spontaneous contractions. Since the latter effect of PE or methoxamine was not blocked either by TRZ, tetrodotoxin or atropine, it seems reasonable to conclude that this effect is due to a direct postjunctional action on the smooth muscle. However, several observations indicate that this weak postjunctional action is unlikely to account for the facilitation of neurally evoked bladder contractions. Thus, the α_1-adrenoceptor facilitation of neurogenic contractions is most reasonably attributed to a prejunctional action.

To evaluate the contribution of the putative postjunctional α_1-adrenoceptor activation to the PE-induced increase of neurogenic contractions in the rat bladder, dose-response curves to ACh were constructed in the presence and absence of facilitatory concentrations of PE. Since the contractions evoked by ACh were not enhanced by PE the activation of the postjunctional α_1-adrenoceptors may not contribute significantly to the facilitation of neurogenic contractions. However, it is also possible that α_1-agonists could enhance the postjunctional action of non-cholinergic excitatory transmitters, since it is known that the rat bladder receives a noncholinergic-nonadrenergic excitatory innervation from parasympathetic (Alm & Elmér, 1975; Lincoln & Burnstock, 1993) as well as from afferent nerves (Maggi, 1993). This will be tested in future experiments by examining the effects of PE on the bladder contractions induced by ATP or substance P.

The possibility that a postjunctional action of PE might contribute to the facilitation of neurally evoked bladder contractions is also diminished by two other observations. First, PE elicited a direct effect on bladder smooth muscle baseline tension in only 10% of the preparations; whereas it consistently enhanced the neurally evoked contractions.

Secondly, the effect of PE in enhancing the amplitude of the intrinsic rhythmic activity of the smooth muscle strips was not altered by TRZ in concentrations that blocked the facilitation of neurally evoked contractions.

The present experiments also provided direct evidence that ACh release is facilitated by PE and that this effect of PE is blocked by an α_1-antagonist. This supports the conclusions based on measurements of contractile responses that the facilitatory α_1-adrenoceptors are located prejunctionally in the bladder. Earlier studies revealed facilitatory α_1-adrenoceptors on the cholinergic neurones in the vesical ganglia of the cat (de Groat & Booth, 1980; Akasu *et al.*, 1985; Keast *et al.*, 1990) and on dissociated bladder neurones from the rat major pelvic ganglion (Yoshimura & de Groat, 1992). Thus both the cell body and the nerve terminals of bladder cholinergic neurones exhibit facilitatory α_1-adrenoceptors. In contrast, at the cholinergic nerve terminals in the heart, prejunctional α_1-adrenoceptors are generally thought to inhibit ACh release (Wetzel *et al.*, 1985). One study has indicated that the α_1-agonist, oxymethazone, can facilitate ACh release in the heart; however, other α_1-adrenoceptor agonists did not mimic the effect of oxymethazone (Bognar *et al.*, 1990). Thus, the present demonstration of PE facilitation of neural input to the bladder is the clearest example in the peripheral nervous system of prejunctional α_1-adrenoceptor facilitation.

The α_1-blocker, TRZ, competitively inhibited the PE-induced facilitation of the contractile response of bladder strips to nerve stimulation yielding a pA_2 value of 8.3. Prazosin, another α_1-antagonist, which is generally equiactive with terazosin on α_1-adrenoceptors, has a similar pA_2 value for blocking α_1-receptors in the rat detrusor muscle (8.57; Ordway *et al.*, 1986) and in the rabbit pulmonary artery (8.76; Vizi *et al.*, 1986a). These results indicate that both the postjunctional and prejunctional α_1-receptors bind the non-selective α_1-antagonists with high affinity.

The degree of α_1-facilitation of the contractile response was inversely related to the magnitude of the contractions, being greater at low frequencies or submaximal intensities of stimulation or at low extracellular Ca^{2+}. Previously, we described a marked facilitation of ACh release in the urinary bladder through activation of prejunctional M_1 muscarinic receptors (Somogyi & de Groat, 1992; Somogyi *et al.*, 1994). In contrast to α_1-facilitation, M_1 facilitation was positively correlated with the stimulation strength, stimulation frequency and with the extracellular Ca^{2+} levels. Thus M_1 and α_1-facilitation have very different properties, possibly related to activation of different signal transduction pathways.

PE also enhanced the evoked and basal release of NA. However, the mechanisms involved in the PE-facilitation of ACh and NA release are clearly different. The facilitatory effect on ACh release was blocked by TRZ; whereas, the facilitation of NA release was not blocked. Thus PE could influence the outflow of NA by altering NA reuptake into the nerve terminals. This is consistent with the finding that desipramine, a NA uptake blocker, abolished the PE facilitation of NA release. In addition, PE enhanced basal release of NA but not the basal release of ACh; and this effect of PE was also blocked by desipramine. Thus it seems likely that the effect of PE on NA release is related to an effect on the amine transport system and not mediated by activation of α_1-receptors on the adrenergic terminals. Similar effects of NA uptake blockers on the carrier mediated release of NA have been described in other tissues (Vizi *et al.*, 1986b; Somogyi & Perel, 1991). One unusual observation which was not evaluated in detail was the effect of desipramine in blocking the PE-induced facilitation of ACh release. This might be mediated by a desipramine block of α_1-receptors, an effect that has been noted in other tissues with high concentrations of the drug (Hall & Ögren, 1981).

Although exogenous PE facilitated neurally evoked release of ACh, the physiological significance of this observation is uncertain since we could not detect a similar effect of endogenously released NA. If endogenous NA were exerting a facilitatory effect on the cholinergic nerve terminals, then it would be expected that blockade of α_1-adrenoceptors with TRZ would reduce neurally evoked release of ACh or the neurally evoked bladder contractions. However, neither response occurred.

Thus under the conditions of our experiments it appears that cholinergic transmission is not modulated by α_1-adrenoceptor mechanisms. However, this modulation may be prominent under more physiological conditions *in vivo* or in the presence of pathology. For example in the chronically decentralized bladder of the cat (Sundin *et al.*, 1977) or in human neurogenic bladders (Seiferth, 1976; Swierzewski *et al.*, 1993) it has been reported that excitatory α_1-adrenoceptors are upregulated and that these receptors can contribute to bladder hyperactivity. It is possible that both prejunctional and postjunctional receptor upregulation may occur in this condition. Similarly, the upregulation of α_1-adrenoceptors which occurs postjunctionally in the old rat (Ordway *et al.*, 1986) may occur prejunctionally as well. In future experiments α_1-adrenoceptor modulation of ACh release will be tested in the urinary bladder strips from older animals. Postjunctional α_1-adrenoceptors may also be important in pathological conditions such as benign prostatic hypertrophy (BPH). α_1-Adrenoceptor blocking agents have been used in the treatment of the symptoms of BPH. Although the rationale for the use of these agents in prostate disease is to reduce adrenergic tone in the urethra and thereby reduce urethral resistance and increase urine flow, it has been reported that there is no significant direct correlation between the drug-induced changes of bladder symptoms and urinary flow rates (Lepor *et al.*, 1990). This could occur if the adrenoceptor blocking agents act on neural (prejunctional) receptors as well as on postsynaptic receptors in the smooth muscle of the lower urinary tract. Thus the adrenergic facilitatory mechanism at cholinergic terminals in the urinary bladder may be an important target for drug therapy in the treatment of bladder hyperactivity.

This work was supported by a small grant from Abbott Labs as well as by NSF grant BNS-890-8934 and NIDDK Grants DK-45741 and DK-4930.

References

AKASU, T., GALLAGHER, J.P., NAKAMURA, T., SHINNICK-GALLAGHER, P. & YOSHIMURA, M. (1985). Noradrenaline hyperpolarization and depolarization in cat vesical parasympathetic neurones. *J. Physiol.*, **361**, 165–184.

ALM, P. & ELMÉR, M. (1975). Adrenergic and cholinergic innervation of the rat urinary bladder. *Acta Physiol. Scand.*, **94**, 36–45.

ARUNLAKSHANA, O. & SCHILD, H.O. (1959). Some quantitative uses of drug antagonists. *Br. J. Pharmacol. Chemother.*, **14**, 48–58.

BOGNAR, T.I., BARETTI, R., FISCHER, S., VELDET, C. & FUDER, H. (1990). Alpha adrenoceptor mediated facilitation of acetylcholine release in rat perfused heart. *J. Pharmacol. Exp. Ther.*, **254**, 702–710.

D'AGOSTINO, G., KILBINGER, H., CHIARI, C.M. & GRANA, E. (1986). Presynaptic inhibitory muscarinic receptors modulating ^{3}H-ACh release in rat urinary bladder. *J. Pharmacol. Exp. Ther.*, **239**, 522–528.

DAWES, P.M. & VIZI, E.S. (1973). Acetylcholine release from the rabbit isolated superior cervical ganglion preparation. *Br. J. Pharmacol.*, **48**, 225–232.

DE GROAT, W.C. & BOOTH, A.M. (1980). Inhibition and facilitation in parasympathetic ganglia. *Fed. Proc.*, **39**, 2990–2996.

DOWNIE, J.W., DEAN, D.M., CARRO-CIAMPI, G. & AWAD, S.A. (1975). A difference in sensitivity to alpha-adrenergic agonists exhibited by detrusor and bladder neck of rabbit. *Can. J. Physiol. Pharmacol.*, **53**, 525–530.

HALL, H. & ÖGREN, S.O. (1981). Effects of antidepressant drugs on different receptors in the brain. *Eur. J. Pharmacol.*, **70**, 393–407.

KAPOCSI, J., SOMOGYI, G.T., LUDVIG, N., SERFOZO, P., HARSING, L.G.Jr., WOODS, R.J. & VIZI, E.S. (1986). Neurochemical evidence for two types of presynaptic alpha$_2$ adrenoceptors. *Neurochem. Res.*, **12**, 141–147.

KEAST, J.R., KAWATANI, M. & DE GROAT, W.C. (1990). Sympathetic modulation of cholinergic transmission in cat vesical ganglia is mediated by α_1- and α_2-adrenoceptors. *Am. J. Physiol.*, **258**, R44–R50.

LANGER, S.Z. (1974). Presynaptic regulation of catecholamine release. *Biochem. Pharmacol.*, **23**, 1793–1800.

LEDDA, F. & MANTELLI, L. (1984). Differences between the prejunctional effects of phenylephrine and clonidine in guinea-pig isolated atria. *Br. J. Pharmacol.*, **81**, 491–497.

LEPOR, H., KNAP-MALONEY, G. & SUNSHINE, H. (1990). A dose titration study evaluating terazosin, a selective, once-a-day α_1 blocker for the treatment of symptomatic benign prostatic hyperplasia. *J. Urol.*, **144**, 1393–1398.

LINCOLN, J. & BURNSTOCK, G. (1993). Autonomic innervation of the urinary bladder and urethra. In *Nervous Control of the Urogenital System*, Vol. 3. ed. Maggi, C.A. pp. 33–68. London: Harwood Academic Publisher.

MAGGI, C.A. (1993). The dual sensory and 'efferent' function of the capsaicin-sensitive primary sensory neurons in the urinary bladder and urethra. In *Nervous Control of the Urogenital System*, Vol. 3. ed. Maggi, C.A. pp. 383–422. London: Harwood Academic Publisher.

ORDWAY, G.A., KOLTA, M.G., GERALD, M.C. & WALLACE, L.J. (1986). Age related change in α-adrenergic responsiveness of the urinary bladder of the rat is regionally specific. *Neuropharmacol.*, **25**, 1335–1340.

PATON, W.D.M. & THOMPSON, J.W. (1953). The mechanism of action of adrenaline on the superior cervical ganglion of the cat. In *Proc. Intl. Physiol. Cong.*, **19**, 664.

RUMP, L.C. & MAJEWSKI, H. (1987). Modulation of norepinephrine release through α_1 and α_2 adrenoceptors in rat isolated kidney. *J. Cardiovasc. Pharmacol.*, **9**, 500–507.

SEIFERTH, J. (1976). Type of neurogenic bladder in children with spina bifida and response to treatment with phenoxybenzamine. *Dev. Med. Child Neurol.*, Suppl. **18**, 94–96.

SOMOGYI, G.T. & DE GROAT, W.C. (1990). Modulation of the release of ^{3}H-norepinephrine from the base and body of the rat urinary bladder by endogenous adrenergic and cholinergic mechanisms. *J. Pharmacol. Exp. Ther.*, **255**, 204–210.

SOMOGYI, G.T. & DE GROAT, W.C. (1992). Evidence for inhibitory nicotinic and facilitatory muscarinic receptors on cholinergic nerve terminals of the rat urinary bladder. *J. Auton. Nerv. Syst.*, **37**, 89–98.

SOMOGYI, G.T. & DE GROAT, W.C. (1993). Modulation of the release of ^{3}H-acetylcholine in the major pelvic ganglion of the rat. *Am. J. Physiol.*, **264**, R1084–R1088.

SOMOGYI, G.T. & PEREL, J.M. (1991). Biphasic effect of tricyclic anti-depressants on the release of norepinephrine from the adrenergic nerves of the rabbit heart. *Psychopharmacology*, **104**, 237–243.

SOMOGYI, G.T., TANOWITZ, M. & DE GROAT, W.C. (1992). Evidence for facilitatory α_1 adrenoceptors on nerve terminals of the rat urinary bladder. *Soc. Neurosci. Abstr.*, **18**, 252.

SOMOGYI, G.T., TANOWITZ, M. & DE GROAT, W.C. (1994). M-1 muscarinic receptor mediated facilitation of acetylcholine release in the rat urinary bladder. *J. Physiol.*, **480**, 81–89.

STARKE, K. (1987). Presynaptic α-autoreceptors. *Rev. Physiol. Biochem. Pharmacol.*, **107**, 73–146.

SUNDIN, T., DAHLSTRÖM, A., NORLÉN, L. & SVEDMYR, N. (1977). The sympathetic innervation and adrenoceptor function of the human lower urinary tract in normal state and parasympathetic denervation. *Inv. Urol.*, **14**, 322–328.

SWIERZEWSKI, S.J.III, GORMLEY, E.A., BELVILLE, W.D., SWEETSER, P., WAN, J. & MCGUIRE, E.J. (1993). The effect of terazosin on bladder function in the spinal cord injured. *J. Urol.*, **149**, 265A.

TALLARIDA, R.J. & MURRAY, R.B. (1987). *Manual of Pharmacologic Calculations with Computer Programs*. Second edition. New York: Springer Verlag.

VIZI, E.S. (1979). Presynaptic modulation of neurochemical transmission. *Prog. Neurobiol.*, **12**, 181–290.

VIZI, E.S. (1991). Evidence that catecholamines increase acetylcholine release from neuromuscular junction through stimulation of alpha-1 adrenoceptors. *Naunyn-Schmied. Arch. Pharmacol.*, **343**, 435–438.

VIZI, E.S., HARSING, L.G.Jr., GAAL, J., KAPOCSI, J., BERNATH, S. & SOMOGYI, G.T. (1986a). CH-38083, a selective, potent antagonist of alpha$_2$ adrenoceptors. *J. Pharmacol. Exp. Ther.*, **238**, 701–706.

VIZI, E.S., SOMOGYI, G.T., HARSING, L.G.Jr. & ZIMANYI, I. (1986b). Release of ^{3}H-noradrenaline by α_1-adrenoceptor agonists. *Neurochem. Res.*, **11**, 71–84.

WETZEL, T.G., GOLDSTEIN, D. & BROWN, J.H. (1985). Acetylcholine release from atria can be regulated through an α_1-adrenergic receptor. *Circ. Res.*, **56**, 763–766.

YOSHIMURA, N. & DE GROAT, W.C. (1992). Patch clamp analysis of afferent and efferent neurons that innervate the urinary bladder of the rat. *Soc. Neurosci. Abstr.*, **18**, 126.

(Received October 3, 1994
Revised December 29, 1994
Accepted January 6, 1995)

British Journal of Pharmacology (1995) 114, 1717–1723 © 1995 Stockton Press All rights reserved 0007–1188/95 $12.00

Contrasting effects of the imidazol(in)e α_2-adrenoceptor agonists, medetomidine, clonidine and UK 14,304 on extraneuronal levels of noradrenaline in the rat frontal cortex: evaluation using *in vivo* microdialysis and synaptosomal uptake studies

J.W. Dalley & [1]S.C. Stanford

Department of Pharmacology, University College London, Gower Street, London WC1E 6BT

1 *In vivo* microdialysis in halothane-anaesthetized rats and synaptosomal [^{3}H]-noradrenaline uptake studies *in vitro* were used to evaluate the effects of imidazole (medetomidine) and imidazoline (clonidine and UK 14,304) α_2-adrenoceptor agonists on extraneuronal levels of noradrenaline in the frontal cortex.

2 Levels of noradrenaline in the dialysate were increased by a depolarizing concentration of K^+ (60 mM for 20 min) and substantially attenuated by reducing Ca^{2+} supply in the perfusate. These results suggest that spontaneous efflux of noradrenaline in the cortex is regulated predominantly by cation-dependent exocytotic mechanisms.

3 At a low perfusion concentration (0.5 μM), medetomidine, clonidine and UK 14,304 all reduced the level of noradrenaline in cortical dialysates. Continuous perfusion of the selective α_2-adrenoceptor antagonist, atipamezole (0.5 μM) caused a sustained increase in noradrenaline efflux and reversed the inhibitory effects of medetomidine. All these changes are consistent with drug actions at presynaptic α_2-adrenoceptors.

4 Higher concentrations of medetomidine (5–50 μM), but not clonidine or UK 14,304, evoked a non-desensitizing increase in noradrenaline efflux. This effect was not antagonized by 0.5 μM atipamezole.

5 The tricyclic noradrenaline reuptake inhibitor, desmethylimipramine (0.5–50 μM), increased noradrenaline efflux in a concentration-dependent manner.

6 The specific uptake of [^{3}H]-noradrenaline into cortical synaptosomes was inhibited by medetomidine and desmethylimipramine with IC_{50} values of approximately 7 μM and 8 μM respectively. Neither clonidine nor UK 14,304 inhibited [^{3}H]-noradrenaline uptake.

7 These results indicate that micromolar concentrations of the selective α_2-adrenoceptor agonist, medetomidine, can augment extraneuronal levels of noradrenaline in the rat frontal cortex; this effect seems to involve an inhibition of noradrenaline reuptake rather than an action at α_2-adrenoceptors.

Keywords: Atipamezole; clonidine; cortical synaptosomes; desmethylimipramine; frontal cortex; medetomidine; microdialysis; UK 14,304

Introduction

It is widely accepted that presynaptic α_2-adrenoceptors modulate noradrenaline release in the brain. Evidence to support this view stems from experiments *in vitro* studying transmitter release from synaptosomes (de Langen *et al.*, 1979; Maura *et al.*, 1992) and brain slices (Reichenbacher *et al.*, 1982; Raiteri *et al.*, 1992), and from experiments using *in vivo* microdialysis (L'Heureux *et al.*, 1986; Thomas & Holman, 1991; van Veldhuizen *et al.*, 1993). In all of these studies, noradrenaline efflux was reduced by α_2-adrenoceptor agonists and increased by α_2-adrenoceptor antagonists.

The imidazole derivative, (±)-4-[1-(2,3-dimethylphenyl) ethyl]-1H-imidazole (medetomidine), is a potent α_2-adrenoceptor agonist with an α_2/α_1 selectivity ratio of over 1600 (Virtanen *et al.*, 1988). In recent experiments, we used *in vivo* microdialysis to test the effects of this compound on noradrenaline efflux in the rat frontal cortex. The drug was administered directly into the terminal field *via* the dialysis probe. We found that the effects of medetomidine were strongly concentration-dependent. At a low perfusion concentration (0.5 μM), medetomidine reduced noradrenaline levels in the dialysate but higher concentrations evoked a non-desensitizing increase in noradrenaline efflux. These preliminary findings have been reported to the British Pharmacological Society (Dalley & Stanford, 1994). The aim of the present study was to eliminate the possibility that this increase in noradrenaline efflux involves α_2-adrenoceptors. To achieve this, we first tested whether the increase could be prevented by the selective α_2-adrenoceptor antagonist, atipamezole. In further studies the effects of medetomidine on noradrenaline efflux were compared with those of the imidazoline α_2-adrenoceptor agonists, clonidine and 5-bromo-*N*-(4,5-dihydro-1*H*-imidazol-2-yl)-6-quinoxalinamine (UK 14,304).

One limitation of *in vivo* microdialysis is that levels of noradrenaline in the dialysate reflect the net influence of both neurotransmitter release from the nerve terminals and its neuronal and non-neuronal reuptake from the extracellular fluid. Spontaneous changes in noradrenaline efflux are highly Ca^{2+}-dependent (L'Heureux *et al.*, 1986; van Veldhuizen *et al.*, 1990), suggesting that it is mainly transmitter release which determines the levels of noradrenaline in the dialysate under basal conditions. However, drug-induced changes in noradrenaline efflux could reflect changes in release and/or

[1] Author for correspondence.

reuptake. For this reason, further studies were carried out to compare the effects of medetomidine, clonidine and UK 14,304 on synaptosomal uptake of [^{3}H]-noradrenaline, using the potent noradrenaline reuptake inhibitor, desmethylimipramine, as an active control. We show that, whereas medetomidine and desmethylimipramine both increase noradrenaline efflux in the rat frontal cortex and inhibit cortical synaptosomal uptake of [^{3}H]-noradrenaline *in vitro*, neither of these effects is apparent with clonidine or UK 14,304.

Methods

Intracerebral microdialysis

Animals Male Sprague-Dawley rats (250–310 g) were obtained either from University College London (U.K.), or from Charles River (U.K.). Rats were maintained in groups of 4 at 21–24°C with a light/dark schedule of 12 h (lights on at 08 h 00 min) and allowed access to food and water *ad libitum*.

Surgical procedures Intracerebral microdialysis probes were constructed with a 5 mm conducting zone of semipermeable membrane (i.d. 200 μm, o.d. 300 μm, mol.wt. cut-off 20 kD; Filtral 12, Hospal Industrie, France) essentially as described by Sandberg *et al.* (1986). Under halothane anaesthesia, a tracheal cannula was inserted and used to deliver freely inspired halothane (1–1.5%) mixed in 95% O_2 and 5% CO_2 at 400 ml min^{-1}. The core body temperature was maintained at 37°C with a thermostatically controlled heating blanket in conjunction with a rectal probe (Harvard Instruments).

Rats were secured in a Kopf stereotaxic frame and the skull exposed to reveal bregma. After a craniotomy and removal of the dural membrane, a Ringer-primed microdialysis probe was inserted vertically into either the left or right frontal cortex (A 3.5, L 1.5, V 5.5 mm) according to published stereotaxic coordinates (Paxinos & Watson, 1986). At the conclusion of the experiment the location of the probe was verified histologically. For this purpose the brain was removed, fixed in 10% formaldehyde in normal saline, cryostatically sectioned, and examined under a low-power binocular microscope.

Dialysis procedure The dialysis probe was perfused with Ringer solution (composition mM: NaCl 150, KCl 4, $CaCl_2$ 1.2, pH 6.1) at 1.0 μl min^{-1}. *In vitro* calibration studies, carried out before experimentation, revealed that the relative recovery of noradrenaline was approximately 35% at 1.0 μl min^{-1}. Cortical dialysates were collected every 20 min into 5 μl 0.01 M perchloric acid. Experiments commenced, at the same time each day, 2.5 h after probe implantation.

Analysis of noradrenaline in dialysates Dialysates were analysed for noradrenaline content by reverse-phase high pressure liquid chromatography with electrochemical detection. Noradrenaline was separated at room temperature (maintained at 24°C) on a Hypersil ODS 5 μm cartridge column (25 cm × 4.6 mm; Fisons) protected by an Aquapore (7 μm) guard column (30 mm × 4.6 mm; Applied Biosystems). The filtered and degassed mobile phase, which contained sodium dihydrogen orthophosphate (83 mM), sodium (−)-octanesulphonic acid (2.77 mM), EDTA (0.85 mM), methanol (12%), and adjusted to pH 3.4 with orthophosphoric acid, was recycled at 1.275 ml min^{-1} (ESA model 580 solvent delivery module). Pressure fluctuations were buffered with a pulse dampener.

Electrochemical detection of noradrenaline was achieved with a dual electrode Coulochem II system (ESA) in redox mode. At the first analytical electrode a reducing potential of −275 mV was applied and, at the second (noradrenaline detecting) electrode, an oxidising potential of +275 mV was applied. A pre-injection guard cell set at +325 mV was used to condition the mobile phase. Standards and dialysates were injected manually into the loading port (Rheodyne 7125) with a loop volume of 20 μl. Chromatograms were relayed to an integrator (Spectra-Physics) and peak height used to quantitate noradrenaline levels. The detection limit for noradrenaline was approximately 2 fmol.

Drug treatment Drug solutions were perfused after 3 stable basal dialysates had been collected. Each drug was administered in increasing concentrations (0.5 μM, 5.0 μM and 50 μM) and each concentration was perfused for 3 sampling periods of 20 min. Atipamezole (0.5 μM) was continuously perfused, either alone, or in combination with increasing concentrations of medetomidine. In studies designed to confirm a neuronal origin of noradrenaline, either KCl was added to the perfusate (final concentration 60 mM) for 20 min, or $CaCl_2$ removed for 80 min. In these experiments the tonicity of the perfusate was maintained by adjusting the concentration of NaCl. The dead volume between the drug injection switch and the dialysis probe outlet was 10–15 μl. The following drugs were used: medetomidine hydrochloride (Orion-Farmos, Finland), clonidine hydrochloride (Boehringer Ingelheim, Germany), UK 14,304-18 (Pfizer, U.K.), atipamezole hydrochloride (Norden Laboratories), desmethylimipramine hydrochloride (Sigma).

Uptake of (−)-[^{3}H]-noradrenaline into cortical synaptosomes

Preparation of synaptosomes Male Sprague-Dawley rats (175–225 g) were killed by stunning and cervical dislocation and their brains removed. Crude synaptosomes were prepared essentially as described by Redfern *et al.* (1993). The cerebral cortex was dissected on ice and gently homogenized in 2 ml of 0.32 M sucrose in a glass homogenizer fitted with a Teflon pestle. The homogenizer was washed twice with 2 ml sucrose and the wash added to the homogenate which was then centrifuged at 650 *g* for 10 min at 4°C. The supernatant was then spun at 12,000 *g* for 20 min at 4°C and the final pellet resuspended in 0.32 M sucrose at a concentration of 1 g wet weight of the original tissue per 2 ml sucrose.

Measurement of uptake of (−)-[^{3}H]-noradrenaline To 100 μl of the synaptosomal suspension were added 200 μl of Tris-Krebs buffer (containing mM: NaCl 136, KCl 5, $MgCl_2$ 12, $CaCl_2$ 2.5, (+)-glucose 10, (−)-ascorbate 1, Tris base 20, pargyline hydrochloride 0.25). The buffer was gassed with 95% O_2 and 5% CO_2 for 30 min and the pH adjusted to 7.4 with 0.1 M HCl before use; 100 μl aliquots containing dissolved test compounds were added to give a final concentration of 0.5 μM, 5 μM or 50 μM. Buffer (100 μl) was added to remaining samples to standardize the total volume. All samples were prepared in duplicate and preincubated for 3 min at either 37°C or 4°C; the latter served as a blank for non-specific uptake. The assay was started by addition of 100 μl [^{3}H]-noradrenaline to all samples to give a final concentration of 50 nM. The [^{3}H]-noradrenaline solution was prepared from a stock of (−)-[ring-2,5,6-^{3}H]-noradrenaline of specific activity 71.7 Ci mmol^{-1}, diluted 10 fold with unlabelled (−)-noradrenaline. After 3 min the incubation was terminated by filtration of the samples over Whatman GF/B filter discs. These were washed twice with 2 ml Tris-Krebs buffer and counted for tritium content in 9 ml scintillation fluid (Packard 'Ultima Gold'). The d.p.m. in each sample was generated from a standard quench curve.

The [^{3}H]-noradrenaline content of the samples is expressed as pmol mg^{-1} protein. Active uptake of [^{3}H]-noradrenaline was calculated as the difference in uptake at 37°C and 4°C; this typically accounted for 80% of the total. The protein content of the samples was measured in duplicate aliquots using the method of Lowry *et al.* (1951).

Statistical analysis The noradrenaline content of the dialysates is expressed as fmol 20 μl^{-1} ± s.e.mean, without correction for recovery. Statistical analyses were carried out on the raw data. Analysis of the effect of each drug treatment on noradrenaline efflux was carried out on orthonormalised data (*i.e.* on orthogonal contrasts: Norusis, 1990), with time as a within-subjects factor, using the MANOVA facility on SPSS PC$^+$. Averaged *F*-tests were used to assess the level of statistical significance of any changes in noradrenaline efflux. Comparison of drug effects at different doses used MANOVA, with time and drug concentration as within subjects factors. Again averaged *F*-tests were used to assess the level of significance when multivariate tests indicated significant changes in main effects of time or drug concentration. When these indicated statistically significant main effects, MANOVA was used on relevant clusters of data to compare the effects of specific drug concentrations. Again, concentration and time were used as within-subjects factors. A significant multivariate test was the criterion for using averaged *F*-tests to assess the level of significance of any differences.

Effects of individual drugs on [^{3}H]-noradrenaline uptake were evaluated from orthonormalised raw data using the one-way ANOVA facility on SPSS PC$^+$. When the ANOVA indicated a significant drug effect, a *post hoc* Tukey multiple range test was used to test for the significance of differences between means; the criterion for significance was set at $P<0.05$. Two-way ANOVA was used to compare the effects of different drugs on [^{3}H]-noradrenaline uptake with drug and concentration as the main factors.

Results

Effects of increased [K^+] or reduced [Ca^{2+}] on noradrenaline levels in cortical dialysates

Typical chromatograms showing the elution times, separation and content of noradrenaline, 3,4-dihydroxyphenylacetic acid and 5-hydroxyindole-3-acetic acid in an external standard and basal cortical dialysate are given in Figure 1. Spontaneous efflux of noradrenaline in the frontal cortex was approximately 20 fmol 20 μl^{-1}. This remained constant throughout the entire time course of the experiment: a sequence of 14 consecutive samples showed no significant change with respect to time ('extended basals' $F=0.89$; d.f. 14,56; $P=0.578$) (Figure 2).

In experiments designed to assess whether the basal level of noradrenaline in the dialysate was derived from exocytotic release of transmitter, its sensitivity to the ionic composition of the perfusion medium was assessed (Figure 2). Perfusion of K^+ (60 mM) for 20 min increased noradrenaline efflux by 82%; this was statistically significant compared with the noradrenaline efflux in three basal dialysates.

Removal of Ca^{2+} from the perfusion medium produced a significant reduction (by 66%) in the dialysate concentration of noradrenaline. The basal levels of noradrenaline were restored when Ca^{2+} was reintroduced in the perfusion medium. Collectively, these results confirm the mainly neuronal origin of noradrenaline in cortical dialysates.

Effects of medetomidine, UK 14,304, clonidine and desmethylimipramine on noradrenaline levels in cortical dialysates

When medetomidine was perfused *via* the dialysis probe, there were main effects of drug concentration ($F=37.83$; d.f. 3,12; $P<0.001$) and time ($F=53.25$; d.f. 2,8; $P<0.001$) as well as a concentration × time interaction ($F=31.11$; d.f. 6,24; $P<0.001$) (Figure 3). Specific comparisons exposed a reduction in noradrenaline efflux induced by 0.5 μM medetomidine with respect to basal efflux. This reached a maximum reduction of 25% after 1 h, but was not statistically significant ($F=1.41$; d.f. 1,4; $P=0.301$). In contrast, increasing the concentration of medetomidine to 5 μM increased noradrenaline efflux (Figure 3). Overall, levels of noradrenaline during perfusion with 5 μM medetomidine were significantly higher than those measured after 0.5 μM medetomidine ($F=10.86$; d.f. 1,4; $P=0.03$) but were not significantly different from basal levels ($F=0.89$; d.f. 1,4; $P=0.398$). Increasing the concentration of medetomidine to

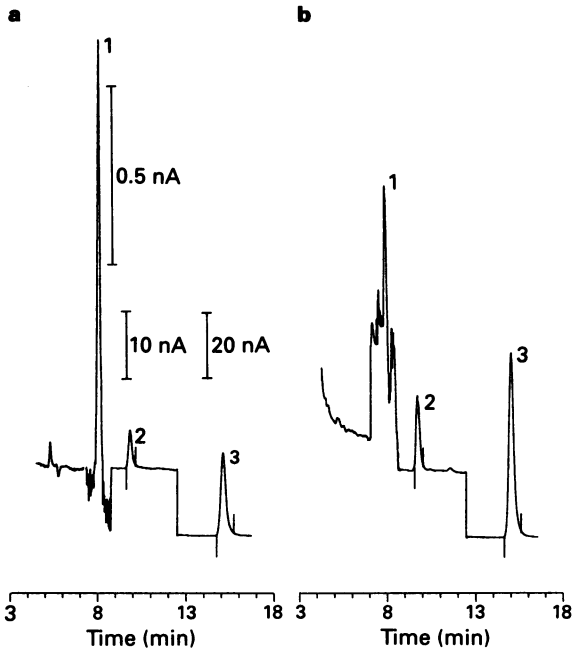

Figure 1 Representative chromatograms of (a) an external standard containing 50 fmol noradrenaline (1), 500 fmol, 3,4-dihydroxyphenylacetic acid (2), and 2 pmol 5-hydroxyindole-3-acetic acid (3), and (b) a dialysate from the frontal cortex, during Ringer perfusion which contains 22.7 fmol noradrenaline.

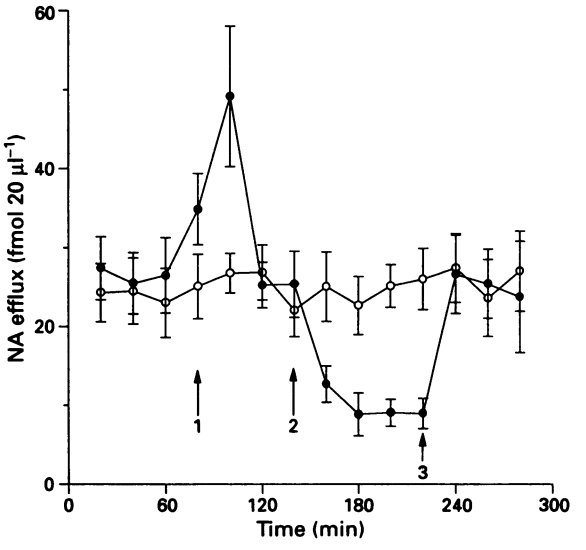

Figure 2 Extended time course of basal noradrenaline (NA) efflux in dialysates of the rat frontal cortex (○) and changes in noradrenaline efflux evoked by modification of the cation composition of the perfusion medium (●). Across all time points, there was a significant main effect of cation treatment ($F=19.69$; d.f. 3,12; $P<0.001$). K^+ (60 mM for 20 min) added at (1), significantly increased noradrenaline efflux ($F=48.95$ d.f. 1,4 $P=0.002$) relative to the three basal samples. Ca^{2+} removal for 80 min (2) significantly reduced noradrenaline efflux ($F=16.26$ d.f. 1,4 $P=0.016$) which returned to basal levels when Ca^{2+} was reinstated at 3 ($F=0.58$ d.f. 1,4 $P=0.58$).

50 μM produced a greater increase in noradrenaline efflux: at this concentration, noradrenaline efflux was significantly greater than both basal efflux ($F = 29.68$; d.f. 1,4; $P = 0.006$) and that induced by 5 μM medetomidine ($F = 170.1$; d.f. 1,4; $P < 0.001$).

Perfusion of clonidine *via* the dialysis probe reduced noradrenaline efflux with main effects of concentration ($F = 121.9$; d.f. 3,9; $P < 0.001$) and time ($F = 11.91$; d.f. 2,6; $P < 0.008$) (Figure 3). At 0.5 μM clonidine, noradrenaline efflux was reduced when compared with that in the basal samples ($F = 121.85$; d.f. 1,3; $P < 0.003$) (Figure 3). This reached a maximum of 36% after 1 h. There was a further reduction in noradrenaline levels in the dialysate when the concentration of clonidine was increased to 5 μM; this reduction was significantly greater than that caused by 0.5 μM clonidine ($F = 162.09$; d.f. 1,3; $P < 0.001$). Increasing the concentration of clonidine to 50 μM did not further reduce noradrenaline efflux ($F = 0.69$; d.f. 1,3; $P = 0.467$ *cf.* efflux with 5 μM clonidine).

UK 14,304 also reduced noradrenaline efflux (Figure 3) but main effects of concentration (multivariate analysis: $P = 0.106$) and time (multivariate analysis: $P = 0.095$) across all samples were not statistically significant. This is because the effects of this drug on noradrenaline efflux rapidly attained maximal inhibition at 0.5 μM and subsequent samples showed no appreciable change. Notwithstanding a reduction in efflux of 37% after 1 h, this reduction was not statistically significant when compared with basal efflux ($F = 6.27$; d.f. 1,3; $P = 0.087$) (Figure 3). However, increasing the concentration of UK 14,304 to 5 μM reduced noradrenaline efflux by a maximum of 42%; this reduction was significant when compared with basal efflux ($F = 27.19$; d.f. 1,3; $P = 0.014$). There was no further reduction in noradrenaline levels when the concentration of UK 14,304 was increased to 50 μM ($F = 1.92$; d.f. 1,3; $P = 0.26$ *cf.* 5 μM UK 14,304).

Perfusion of 0.5–50 μM desmethylimipramine caused a progressive increase in levels of noradrenaline in the dialysate (Figure 3). Whereas 0.5 μM desmethylimipramine had no effect on noradrenaline levels in the dialysate, both 5 μM ($F = 8.67$; d.f. 1,4; $P = 0.042$) and 50 μM ($F = 13.57$; d.f. 1,4; $P = 0.021$) drug concentrations caused a significant increase with respect to basal efflux. Moreover, the increase induced by 50 μM desmethylimipramine was significantly greater than that at 5 μM ($F = 18.62$; d.f. 1,4; $P < 0.05$).

Effects of atipamezole alone, or in combination with medetomidine, on changes in noradrenaline efflux induced by medetomidine

Continuous perfusion of 0.5 μM atipamezole caused a progressive (time-dependent) increase in noradrenaline concentration in the dialysate which stabilized after 1 h ($F = 11.47$; d.f. 11,44; $P < 0.001$) (Figure 4). Overall, this increase was significant when compared with basal samples collected before drug administration ($F = 150.7$; d.f. 1,8; $P < 0.001$).

Noradrenaline efflux during continuous infusion of 0.5 μM atipamezole was compared with that in parallel samples collected in the presence of increasing concentrations of medetomidine alone (Figure 4). Although there was no main effect of drug ($F = 0.03$; d.f. 1,8; $P = 0.878$), there was a main effect of concentration ($F = 61.69$; d.f. 3,24; $P < 0.001$) and a drug × concentration interaction ($F = 17.29$; d.f. 3,24; $P < 0.001$). Noradrenaline efflux for each cluster of 3 samples at each concentration of medetomidine was therefore compared with that in time-matched samples collected during perfusion of 0.5 μM atipamezole. At 0.5 μM medetomidine, the main effect of drug (0.5 μM medetomidine *versus* 0.5 μM atipamezole) just failed to reach significance ($F = 4.84$; d.f. 1,8; $P = 0.059$). This is because the effects of atipamezole did not reach maximum until 1 h after the start of its perfusion. However, with this dose of medetomidine, there was a significant drug × time interaction ($F = 11.36$; d.f. 2,16; $P < 0.001$). Noradrenaline levels increased during perfusion of 5 μM medetomidine but they remained significantly lower than those in parallel samples taken during perfusion of

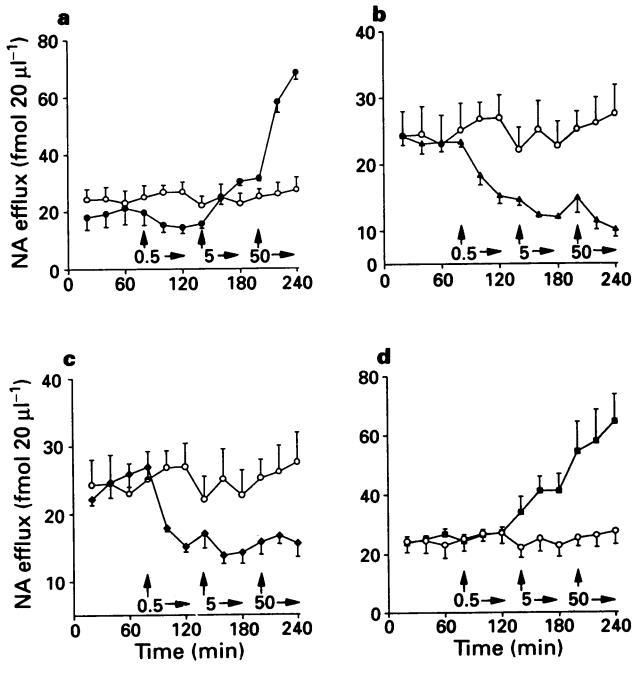

Figure 3 Effects of the imidazol(in)e α_2-adrenoceptor agonists (a) medetomidine (●), (b) clonidine (▲) and (c) UK 14,304 (◆) and the noradrenaline uptake inhibitor, (d) desmethylimipramine (■) on noradrenaline efflux in dialysates of the rat frontal cortex. Drugs were added to the perfusion medium in increasing concentrations (0.5 μM, 5.0 μM and 50 μM) and perfused for 60 min at the times indicated; (○) represents extended basal controls. Univariate ANOVA and multivariate statistical analyses are detailed in the Results section. Basal noradrenaline efflux (fmol 20 μl^{-1}; $n = 4$–5) was 21.2 ± 5.5 (●), 23.3 ± 1.4 (▲), 25.9 ± 2.0 (◆) and 26.6 ± 2.0 (■).

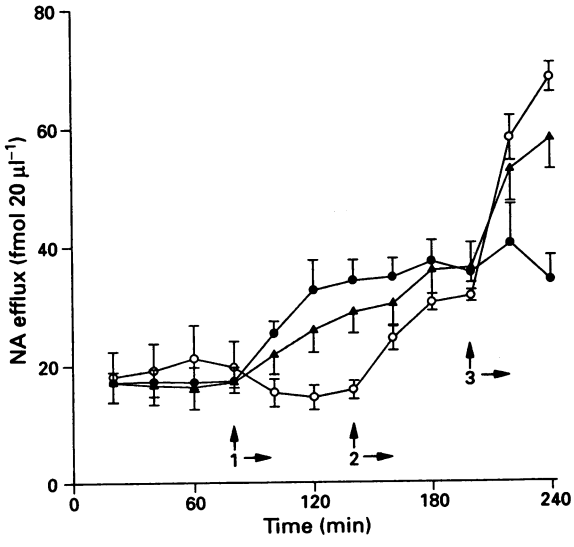

Figure 4 Effects of the selective α_2-adrenoceptor antagonist, atipamezole, on medetomidine-induced changes in cortical noradrenaline efflux (○). Atipamezole (0.5 μM) was continuously perfused from time (1), either alone (●), or combined with increasing concentrations of medetomidine (▲) as described in Figure 3 and indicated by arrows at (1) (0.5 μM), (2) (5.0 μM) and (3) (50 μM). Basal noradrenaline efflux was 17.2 ± 2.5 fmol 20 μl^{-1} ($n = 5$) (●), 16.3 ± 3.8 fmol 20 μl^{-1} ($n = 5$) (▲) and 21.2 ± 5.5 ($n = 5$) (○).

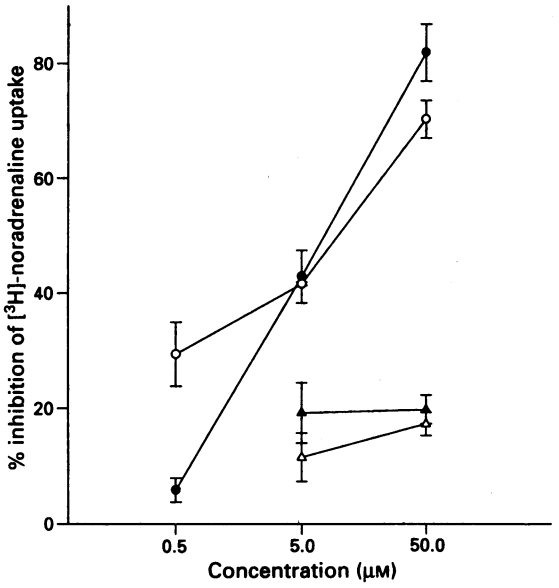

Figure 5 Concentration-dependent inhibition of [^{3}H]-noradrenaline uptake into cortical synaptosomes by medetomidine (●) and desmethylimipramine (○). Clonidine (▲) and UK 14,304 (△) were also tested. Each data point represents mean ± s.e.mean % inhibition of specific [^{3}H]-noradrenaline uptake ($n = 6-9$). Statistical analyses of the raw data are described in the text.

0.5 μM atipamezole alone ($F = 11.92$; d.f. 1,8; $P = 0.009$). In contrast, noradrenaline efflux during perfusion of 50 μM medetomidine was significantly greater than that in equivalent samples collected with atipamezole alone ($F = 13.64$; d.f. 1,8; $P = 0.006$).

Atipamezole (0.5 μM) was then co-administered with medetomidine (5–50 μM). When compared with medetomidine alone there was no main effect of drug ($F = 0.22$; d.f. 1,8; $P = 0.065$) over all samples, but there was a main effect of concentration ($F = 93.62$; d.f. 3,24; $P < 0.001$) and a significant drug × concentration interaction ($F = 3.39$; d.f. 3,24; $P = 0.034$) (Figure 4). Noradrenaline efflux was therefore compared between specific drug treatments. Comparison of noradrenaline efflux with 0.5 μM medetomidine and 0.5 μM medetomidine plus 0.5 μM atipamezole failed to expose a main effect of drug ($F = 2.21$; d.f. 1,8; $P = 0.175$). Multivariate tests also failed to show any drug treatment × time interaction ($P = 0.129$). Since comparison of medetomidine alone and atipamezole alone did expose a drug × time interaction (see above), it seems that changes in noradrenaline efflux induced by 0.5 μM medetomidine or 0.5 μM atipamezole are diminished when these drugs are given in combination. This suggests an additive interaction between these drugs at these concentrations. In contrast, there was no effect of atipamezole on noradrenaline efflux when this was co-administered with either 5.0 μM ($F = 4.44$; d.f. 1,8; $P = 0.068$) or 50 μM medetomidine ($F = 0.65$; d.f. 1,8; $P = 0.444$ *cf.* medetomidine alone).

Effects of medetomidine, UK 14,304, clonidine and desmethylimipramine on uptake of (−)-[^{3}H]-noradrenaline by cortical synaptosomes in vitro

Specific synaptosomal uptake of [^{3}H]-noradrenaline at 37°C was 1.02 ± 0.10 pmol mg^{-1} protein ($n = 9$). This uptake was inhibited by medetomidine with an IC_{50} of approximately 7 μM ($F = 11.15$; d.f. 3,35; $P < 0.001$) (Figure 5). Compared with the uptake in the absence of drug, *post hoc* tests exposed significant uptake inhibition at both 5 and 50 μM drug concentrations. Similar results were obtained with desmethylimipramine: this produced a significant, concentration-dependent reduction in synaptosomal uptake ($F = 6.52$; d.f. 3,42; $P = 0.01$) with *post hoc* tests exposing significant inhibition at both 5 and 50 μM concentrations. The IC_{50} for uptake inhibition was approximately 8 μM. In contrast, neither clonidine ($F = 0.11$; d.f. 2,11; $P = 0.896$) nor UK 14,304 ($F = 0.04$; d.f. 2,11; $P = 0.954$) produced any changes in synaptosomal uptake of [^{3}H]-noradrenaline.

Discussion

Systemic administration of medetomidine produces sedation, hypotension (Savola & Virtanen, 1991), antinociception (reviewed by Pertovaara, 1993), hypothermia (MacDonald *et al.*, 1988) and a reduction in general anaesthetic requirement (Bloor *et al.*, 1992). These effects have been attributed to activation of α_2-adrenoceptors since they are shared by other α_2-adrenoceptor agonists and are prevented by α_2-adrenoceptor antagonists. This is consistent with evidence from binding studies *in vitro* showing that medetomidine has a greater selectivity for α_2- *versus* α_1-adrenoceptors, and a higher affinity for binding to α_2-adrenoceptors than either clonidine or UK 14,304 (Virtanen *et al.*, 1988). In view of this binding profile, systemic administration of medetomidine should reduce noradrenaline release in the brain by activating both somatodendritic α_2-autoreceptors in the locus coeruleus and presynaptic α_2-adrenoceptors in the terminal field. Attenuated release of noradrenaline is suggested by a decline in brain levels of the noradrenaline metabolite, 3-methoxy-4-hydroxyphenylethylene glycol (MHPG) after systemic administration of a low dose of medetomidine (MacDonald *et al.*, 1991). Also, in the present study, a low micromolar concentration of medetomidine reduced noradrenaline efflux, whereas the α_2-adrenoceptor antagonist, atipamezole, increased it.

Despite this receptor selectivity, the main finding of the present study was that, at higher concentrations (5–50 μM), medetomidine markedly increased the levels of noradrenaline in cortical dialysates. Although unlikely to contribute to its clinical actions, this effect could be relevant to published reports that medetomidine has a biphasic effect on brain MHPG content: after an initial reduction, MHPG levels show a dose-dependent recovery (MacDonald *et al.*, 1991). It might also explain the reversal of sedation as the drug dose is increased beyond that recommended in anaesthesia (Doze *et al.*, 1989). It is also unlikely that the increase in noradrenaline efflux induced by medetomidine is related to its agonist action at α_2-adrenoceptors. This is because both clonidine and UK 14,304 were devoid of this effect, yet both these compounds are regarded as relatively potent and selective α_2-adrenoceptor agonists. More importantly, the increase in noradrenaline efflux was not prevented by co-administration of the α_2-adrenoceptor antagonist, atipamezole.

Attenuation of noradrenaline efflux by low, and increased efflux at high, drug concentrations could suggest that medetomidine has a lower efficacy at presynaptic α_2-adrenoceptors than noradrenaline. There are several reasons for discounting this possibility. First, the large increase in efflux caused by 50 μM medetomidine would indicate that α_2-adrenoceptors experience considerable tonic activation by spontaneously released noradrenaline. Yet, this is at variance with our results: the increase was no greater after treatment with atipamezole, either alone or in conjunction with medetomidine, than after medetomidine alone. Others have shown that, even high concentrations (100 μM) of selective α_2-antagonists, piperoxan and yohimbine, have little or no effect on noradrenaline levels in dialysates of the rat frontoparietal cortex (van Veldhuizen *et al.*, 1993). Interestingly, the imidazoline α_2-adrenoceptor antagonist, idazoxan

(100 μM), does cause an appreciable increase in efflux (150% with respect to basal: Dennis *et al.*, 1987), but this is considerably less than that reported here with medetomidine. Secondly, high concentrations of clonidine did not increase noradrenaline efflux despite evidence that this compound may act as a partial α_2-agonist (Medgett *et al.*, 1978). Finally, the presence of a large presynaptic α_2-adrenoceptor reserve in the cortex (Adler *et al.*, 1987) should lessen the impact of partial α_2-agonist activity on extraneuronal levels of noradrenaline.

An alternative explanation is that medetomidine inhibits uptake of noradrenaline from the extracellular fluid. To test this, the effects of medetomidine, clonidine and UK 14,304 on synaptosomal uptake of [^{3}H]-noradrenaline were compared with those of the uptake inhibitor, desmethylimipramine. Medetomidine inhibited [^{3}H]-noradrenaline uptake with a potency comparable with that of desmethylimipramine. This effect further distinguished medetomidine from clonidine and UK 14,304 which were both devoid of this activity. The high (micromolar) concentration of desmethylimipramine required to cause appreciable inhibition of [^{3}H]-noradrenaline uptake suggests that this mainly involved uptake into dopaminergic synaptosomes (Wood & Wyllie, 1983; Michel *et al.*, 1984). A similar action for medetomidine might therefore be inferred. Since both drugs inhibited synaptosomal uptake *in vitro* and increased efflux *in vivo* at the same concentrations, it is likely that these effects are related. This would indicate that much of the noradrenaline released in the cerebral cortex is sequestered by dopaminergic nerve terminals. This is entirely consistent with evidence that uptake of transmitter into noradrenergic neurones has a minor role in determining basal extracellular levels of noradrenaline in this brain area (Thomas & Holman, 1991).

An important finding of this study was that atipamezole did not modify the increase in noradrenaline efflux produced by medetomidine. In the presence of an uptake inhibitor, an α_2-autoreceptor antagonist like atipamezole should potentiate extracellular levels of noradrenaline through disinhibition of α_2-autoregulatory function. Presumably, these results reflect a competitive interaction between these two compounds at the α_2-autoreceptor.

To our knowledge, there are no previous reports of an α_2-adrenoceptor agonist inhibiting noradrenaline reuptake. Assuming structural differences to be important, it may be relevant that medetomidine is an imidazole derivative, whereas both clonidine and UK 14,304 are imidazolines. Whether this is the key distinguishing feature can only be resolved by structure-activity analyses, comparing the effects of a range of these compounds on noradrenaline efflux and synaptosomal uptake.

It is widely recognized that imidazol(in)es, as well as binding to α_2-adrenoceptors, share high affinity for non-adrenoceptor imidazoline/idazoxan binding sites (I-receptors: Wikberg *et al.*, 1991). These receptors, which seem to be anatomically, and possibly functionally, unrelated to α_2-adrenoceptors (Michel *et al.*, 1990; de Vos *et al.*, 1994), are selectively labelled by idazoxan in the presence of phenylethylamines or synthetic α_2-adrenoceptor ligands (Miralles *et al.*, 1993; Olmos *et al.*, 1993). Autoradiography studies have revealed a moderate density of I-receptors in the rabbit (Renouard *et al.*, 1993) and human (de Vos *et al.*, 1994) cerebral cortex. However, functional implications of I-receptor binding are poorly understood. Whilst there is no obvious link between the I-receptor binding affinities of medetomidine, clonidine and UK 14,304 in the rat brain (Miralles *et al.*, 1993) and their respective effects on synaptosomal noradrenaline uptake, it is evident that [^{3}H]-idazoxan binding in the cortex can be resolved into at least two components (Renouard *et al.*, 1993). Consequently, an I-receptor involvement in our results cannot be ruled out until agonist efficacies and full binding profiles to putative I-receptor subtypes have been characterized more fully.

One possible target linking transmitter uptake and I-receptor binding is the Na^+ -H^+ exchange pump of the neurolemma. I-receptors in the renal tubule, at least, modulate this proton pump (Bidet *et al.*, 1990) and changes in [Na^+] modify the affinity of the noradrenaline transporter protein for its substrate (Sammet & Graefe, 1979). This sequence of events could influence outward transport, as well as uptake, of noradrenaline (Langeloh & Trendelenburg, 1987). An extension of this mechanism involves the possible intracellular localisation of I-receptors (Tesson *et al.*, 1991) and their reported association with monamine oxidase (Olmos *et al.*, 1993; Renouard *et al.*, 1993). Modulation of monoamine oxidase activity by I-receptor ligands could indirectly affect neuronal uptake by altering axoplasmic concentrations of noradrenaline (Langeloh & Trendelenburg, 1987; Trendelenburg, 1989). This suggestion, that a receptor target for imidazol(in)es might be functionally coupled to the transmitter uptake transporter, is not new. An early scheme also proposed an imidazol(in)e site on the α_2-adrenoceptor which was coupled to the noradrenaline transporter (Gothert *et al.*, 1983; Starke, 1987) but results of recent investigations have not supported this theory (Zier *et al.*, 1988; Limberger *et al.*, 1990). Nevertheless, in the light of the present findings, the possibility that imidazol(in)e α_2-adrenoceptor ligands bind to a second, functionally distinct receptor which, albeit indirectly, influences noradrenaline uptake merits further consideration.

In summary, our results show that the selective α_2-adrenoceptor agonist, medetomidine, at micromolar concentrations, augments, rather than reduces, extraneuronal levels of noradrenaline in the rat frontal cortex. This effect appears to be largely due to inhibition of noradrenaline reuptake rather than any action at α_2-adrenoceptors. It remains to be determined whether medetomidine produces this effect *via* desmethylimipramine recognition sites on the uptake carrier complex.

We are indebted to Orion-Farmos, Boehringer Ingelheim and Pfizer for their generous gifts of drugs. We wish to thank Dr R. Virtanen for his helpful comments on the manuscript. This study was funded in part by the MRC (Great Britain).

References

ADLER, C.H., MELLER, E. & GOLDSTEIN, M. (1987). Receptor reserve at the alpha-2-adrenergic receptor in the rat cerebral cortex. *J. Pharmacol. Exp. Ther.*, **240**, 508–515.

BIDET, M., POUJEOL, P. & PARINI, A. (1990). Effect of imidazolines on Na^+ transport and intracellular pH in renal proximal tubule cells. *Biochem. Biophys. Acta*, **1024**, 173–178.

BLOOR, B.C., FRANKLAND, M., ALPER, G., RAYBOULD, D., WEITZ, J. & SHURTLIFF, M. (1992). Hemodynamic and sedative effects of dexmedetomidine in dog. *J. Pharmacol. Exp. Ther.*, **263**, 690–697.

DALLEY, J.W. & STANFORD, S.C. (1994). Paradoxical effects of an α_2-adrenoceptor agonist on cortical noradrenaline efflux: comparison in halothane-anaesthetised and freely-moving rats using dialysis. *Br. J. Pharmacol.*, **112**, 154P.

DENNIS, T., L'HEUREUX, R., CARTER, C. & SCATTON, B. (1987). Presynaptic *alpha*-2 adrenoceptors play a major role in the effects of idazoxan on cortical noradrenaline release (as measured by *in vivo* dialysis) in the rat. *J. Pharmacol. Exp. Ther.*, **241**, 642–649.

DOZE, V.A., CHEN, D.-X. & MAZE, M. (1989). Dexmedetomidine produces a hypnotic-anaesthetic action in rats *via* activation of central alpha$_2$ adrenoceptors. *Anaethesiology*, **71**, 75–79.

GOTHERT, M., SCHLICKER, E & KOSTERMANN, F. (1983). Relationship between transmitter uptake inhibition and effects of α-adrenoceptor agonists on serotonin and noradrenaline release in the rat brain cortex. *Naunyn-Schmied. Arch. Pharmacol.*, **322**, 121–128.

LANGELOH, A. & TRENDELENBURG, U. (1987). The mechanism of the ^{3}H-noradrenaline releasing effect of various substrates of uptake$_1$: role of monoamine oxidase and of vesicularly stored ^{3}H-noradrenaline. *Naunyn-Schmied. Arch. Pharmacol.*, **336**, 611–620.

DE LANGEN, C.D.J., HOGENBOOM, F. & MULDER, A.H. (1979). Presynaptic noradrenergic α-receptors and modulation of ^{3}H-noradrenaline release from rat brain synaptosomes. *Eur. J. Pharmacol.*, **60**, 79–89.

L'HEUREUX, R., DENNIS, T., CURET, O. & SCATTON, B. (1986). Measurement of endogenous noradrenaline release in rat cerebral cortex *in vivo* by transcortical dialysis: effects of drugs affecting noradrenergic transmission. *J. Neurochem.*, **46**, 1794–1801.

LIMBERGER, N., STARKE, K. & SINGER, E.A. (1990). Serotonin uptake blockers influence serotonin autoreceptors by increasing the biophase concentration of serotonin and not through a 'molecular link'. *Naunyn-Schmied. Arch. Pharmacol.*, **342**, 363–370.

LOWRY, O.H., ROSEBROUGH, N.J., FARR, A.L. & RANDALL, R.J. (1951). Protein measurement with the Folin Phenol reagent. *J. Biol. Chem.*, **193**, 265–275.

MACDONALD, E., SCHEININ, H. & SCHEININ, M. (1988). Behavioural and neurochemical effects of medetomidine, a novel veterinary sedative. *Eur. J. Pharmacol.*, **158**, 119–127.

MACDONALD, E., SCHEININ, M., SCHEININ, H. & VIRTANEN, R. (1991). Comparison of the behavioural and neurochemical effects of the two optical enantiomers of medetomidine, a selective alpha-2-adrenoceptor agonist. *J. Pharmacol. Exp. Ther.*, **259**, 848–854.

MAURA, G., BONANNO, G. & RAITERI, M. (1992). Presynaptic α_2-adrenoceptors mediating inhibition of noradrenaline and 5-hydroxytryptamine release in rat cortex: further characterization as different α_2-adrenoceptor subtypes. *Naunyn-Schmied. Arch. Pharmacol.*, **345**, 410–416.

MEDGETT, I.C., MCCULLOCH, M.W. & RAND, M.J. (1978). Partial agonist action of clonidine on prejunctional and postjunctional α-adrenoceptors. *Naunyn-Schmied. Arch. Pharmacol.*, **304**, 215–221.

MICHEL, M., HIEMKE, C. & GHRAF, R. (1984). Preferential uptake of norepinephrine into dopaminergic terminals of a synaptosomal preparation from rat cortex. *Brain Res.*, **301**, 149–152.

MICHEL, M.C., REGAN, J.W., GERHARDT, M.A., NEUBIG, R.R., INSEL, P.A. & MOTULSKY, H.J. (1990). Nonadrenergic [^{3}H]-idazoxan binding sites are physically distinct from α_2-adrenergic receptors. *Mol. Pharmacol.*, **37**, 65–68.

MIRALLES, A., OLMOS, G., SASTRE, M., BARTUREN, F., MARTIN, I. & GARCIA-SEVILLA, J.A. (1993). Discrimination and pharmacological characterization of I_2-imidazoline sites with [^{3}H]idazoxan and alpha-2-adrenoceptors with [^{3}H]RX821002 (2-methoxy idazoxan) in the human and rat brains. *J. Pharmacol. Exp. Ther.*, **264**, 1187–1197.

NORUSIS, M.J. (1990). *SPSS Advanced Statistics User's Guide*. Chicago, U.S.A.: SPSS Inc.

OLMOS, G., GABILONDO, A.M., MIRALLES, A., ESCRIBA, P.V. & GARCIA-SEVILLA, J.A. (1993). Chronic treatment with the monoamine oxidase inhibitors clorgyline and pargyline down-regulates non-adrenoceptor [^{3}H]-idazoxan binding in the rat brain. *Br. J. Pharmacol.*, **108**, 597–603.

PAXINOS, G. & WATSON, C. (1986). *The Rat Brain in Stereotaxic Coordinates*. Sydney, Australia: Academic Press.

PERTOVAARA, A. (1993). Antinociception induced by alpha-2-adrenoceptor agonists, with special emphasis on medetomidine studies. *Prog. Neurobiol.*, **40**, 691–709.

RAITERI, M., BONANNO, G., MAURA, G., PENDE, M., ANDRIOLI, G.C. & RUELLE, A. (1992). Subclassification of release-regulating α_2-autoreceptors in human brain cortex. *Br. J. Pharmacol.*, **107**, 1146–1151.

REDFERN, W.S., MACKINNON, A.C., BROWN, C.M., MARTIN, A.B., KILPATRICK, A.T., CLAGUE, R.U. & SPEDDING, M. (1993). Modulation of central noradrenergic function by RS-15385-197. *Br. J. Pharmacol.*, **108**, 526–533.

REICHENBACHER, D., REIMANN, W. & STARKE, K. (1982). α-Adrenoceptor-mediated inhibition of noradrenaline release in rabbit brain cortex slices. Receptor properties and role of the biophase concentration of noradrenaline. *Naunyn-Schmied. Arch. Pharmacol.*, **319**, 71–77.

RENOUARD, A., WIDDOWSON, P.S. & CORDI, A. (1993). [^{3}H]-idazoxan binding to rabbit cerebral cortex recognises multiple imidazoline I_2-type receptors: pharmacological characterization and relationship to monoamine oxidase. *Br. J. Pharmacol.*, **109**, 625–631.

SAMMET, S. & GRAEFE, K.H. (1979). Kinetic analysis of the interaction between noradrenaline and Na^+ in neuronal uptake: kinetic evidence for co-transport. *Naunyn-Schmied. Arch. Pharmacol.*, **309**, 99–107.

SANDBERG, M., BUTCHER, S.P. & HAGBERG, H. (1986). Extracellular overflow of neuroactive amino acids during severe insulin-induced hypoglycemia: in vivo dialysis of the rat hippocampus. *J. Neurochem.*, **47**, 178–184.

SAVOLA, J.-M. & VIRTANEN, R. (1991). Central α_2-adrenoceptors are highly stereoselective for dexmedetomidine, the dextro enantiomer of medetomidine. *Eur. J. Pharmacol.*, **195**, 193–199.

STARKE, K. (1987). Presynaptic α-autoreceptors. *Rev. Physiol. Biochem. Pharmacol.*, **107**, 73–146.

TESSON, F., PRIP-BUUS, C., LEMOINE, A., PEGORIER, J.-P. & PARINI, A. (1991). Subcellular distribution of imidazoline-guanidinium receptive sites in human and rabbit liver. *J. Biol. Chem.*, **266**, 155–160.

THOMAS, D.N. & HOLMAN, R.B. (1991). Regulation of endogenous noradrenaline release in rat hippocampus and frontal cortex: *in vivo* microdialysis. *Br. J. Pharmacol.*, **102**, 5P.

TRENDELENBURG, U. (1989). The uptake and metabolism of ^{3}H-catecholamines in rat cerebral cortex slices. *Naunyn-Schmied. Arch. Pharmacol.*, **339**, 293–297.

VAN VELDHUIZEN, M.J.A., FEENSTRA, M.G.P., BOER, G.J. & WESTERINK, B.H.C. (1990). Microdialysis studies on cortical noradrenaline release: basic characteristics, significance of extracellular calcium and massive post-mortem increase. *Neurosci. Lett.*, **119**, 233–236.

VAN VELDHUIZEN, M.J.A., FEENSTRA, M.G.P., HEINSBROEK, R.P.W. & BOER, G.J. (1993). *In vivo* microdialysis of noradrenaline overflow: effects of α-adrenoceptor agonists and antagonists measured by cumulative concentration-response curves. *Br. J. Pharmacol.*, **109**, 655–660.

VIRTANEN, R., SAVOLA, J.-M., SAANO, V. & NYMAN, L. (1988). Characterization of the selectivity, specificity and potency of medetomidine as an α_2-adrenoceptor agonist. *Eur. J. Pharmacol.*, **150**, 9–14.

DE VOS, H., BRICCA, G., DE KEYSER, J., DE BACKER, J.-P., BOUSQUET, P. & VAUGUELIN, G. (1994). Imidazoline receptors, non-adrenergic idazoxan binding sites and α_2-adrenoceptors in the human central nervous system. *Neuroscience*, **59**, 589–598.

WIKBERG, J.E.S., UHLEN, S. & CHHAJLANI, V. (1991). Medetomidine stereoisomers delineate two closely related subtypes of idazoxan (imidazoline) I-receptors in the guinea-pig. *Eur. J. Pharmacol.*, **193**, 335–340.

WOOD, M.D. & WYLLIE, M.G. (1983). Critical assessment of noradrenaline uptake in synaptosomal preparations. *Naunyn-Schmied. Arch. Pharmacol.*, **322**, 129–135.

ZIER, G., DROBNY, H., VALENTA, B. & SINGER, E.A. (1988). Evidence against a functional link between noradrenaline uptake mechanisms and presynaptic alpha-2 adrenoceptors. *Naunyn-Schmied. Arch. Pharmacol.*, **337**, 118–121.

(Received October 6, 1994
Revised January 9, 1995
Accepted January 11, 1995)

British Journal of Pharmacology (1995) 114, 1724–1730 © 1995 Stockton Press All rights reserved 0007–1188/95 $12.00

The role of α_2-adrenoceptors in the vasculature of the rat tail

[1]William S. Redfern, *Margaret R. MacLean, Ruth U. Clague & *John C. McGrath

Department of Pharmacology, Syntex Research Centre, Heriot-Watt University Research Park, Riccarton, Edinburgh EH14 4AP and *Clinical Research Initiative in Heart Failure Laboratories, Division of Neuroscience and Biomedical Systems, Institute of Biomedical and Life Sciences, West Medical Building, Glasgow University, Glasgow G12 8QQ

1 The effects of α_2-adrenoceptor agonists and antagonists on rat tail skin temperature (t_{ts}), an indicator of local cutaneous blood flow, were studied in conscious and anaesthetized rats and in the isolated, Krebs perfused, vascular bed of the rat tail.

2 In conscious rats, at an ambient temperature of 18.5–20°C, t_{ts} was 21.0 ± 0.2°C and core (rectal) temperature (t_c) was 38.2 ± 0.04°C ($n = 126$). The α_2-adrenoceptor antagonist, delequamine (RS-15385-197; 1 mg kg^{-1}, s.c., $n = 6$), produced a rapid elevation in t_{ts} to 29.1 ± 0.7°C ($P < 0.001$ *vs.* saline-treated control group), attained 10 min after injection. t_c fell slightly, by 1.0 ± 0.1°C. The t_{ts} response was dose-related over the dose-range tested (0.01–1 mg kg^{-1}, s.c.), with an ED_{50} of 17 μg kg^{-1}, s.c. ($n = 6$ per dose).

3 The maximum increases in t_{ts} in response to a dose of 1 mg kg^{-1}, s.c. of α_2-adrenoceptor antagonists were as follows ($n = 6$ per drug): delequamine (+ 9.6 ± 0.8°C) > yohimbine (+ 9.0 ± 1.0°C) > WY-26703 (+ 7.9 ± 1.3°C) > piperoxan (+ 5.6 ± 1.7°C) > idazoxan (+ 4.6 ± 1.3°C) > imiloxan (+ 4.1 ± 1.3°C) > SKF 104078 (+ 2.0 ± 1.9°C) > BDF-6143 (+ 1.3 ± 0.8°C).

4 Prazosin (0.3 mg kg^{-1}, s.c.), hydralazine (10 mg kg^{-1}, s.c.) and nifedipine (3 mg kg^{-1}, s.c.) did not increase t_{ts}, whereas propranolol (10 mg kg^{-1}, s.c.) evoked a small increase in t_{ts} (+ 2.9 ± 1.0°C). Pentolinium (2–10 mg kg^{-1}, s.c.) elicited a dose-related increase in t_{ts}, which was elevated by 4.4 ± 1.3°C after a dose of 10 mg kg^{-1}; t_c was reduced in a dose-related manner. Drug vehicles (1 ml kg^{-1}, s.c.) had no effect on t_{ts} or t_c.

5 In anaesthetized rats, idazoxan (300 μg, i.v.) produced a rapid increase in t_{ts} which was detectable 2 min after beginning the injection, reaching a peak after 7 min. When the same dose was administered i.c.v., t_{ts} also rose, but more slowly. The peak response (+ 3.6 ± 0.7°C, $n = 5$) was significantly smaller than when idazoxan was administered intravenously (+ 6.3 ± 1.2°C, $n = 5$), which suggests that the increase in t_{ts} following systemic administration of α_2-adrenoceptor antagonists is not due to a central effect. The change in t_{ts} was not secondary to changes in blood pressure.

6 In the isolated, Krebs perfused, tail vascular bed of the rat, at an ambient temperature of 20–21°C, under *constant flow* conditions (3.5–4.0 ml min^{-1}; $n = 4$), baseline perfusion pressure was 57 ± 4 mmHg. 5-Hydroxytryptamine (5-HT; 70–150 nM) increased perfusion pressure by 56 ± 9 mmHg. The α_2-adrenoceptor agonist, UK-14,304 (10 nmol), elicited a further increase in perfusion pressure by 27.5 ± 15 mmHg but had no effect in the absence of 5-HT; this response to UK-14,304 was abolished by rauwolscine (1 μM).

7 Under *constant pressure* conditions (~100 mmHg; $n = 9$), baseline mean perfusion flow was 2.1 ± 0.2 ml min^{-1}, and mean tail skin temperature was 31.6 ± 0.6°C. 5-HT (119 ± 28 nM) decreased t_{ts} by 3.3 ± 2.0°C and reduced flow by 1.2 ± 0.3 ml min^{-1}. UK-14,304 (10 nmol) further reduced t_{ts} by 3.0 ± 0.3°C without significant effect on flow; this effect was also abolished by 1 μM rauwolscine.

8 We conclude that post-junctional α_2-adrenoceptors in the vasculature of the rat tail have a major vasoconstrictor role, controlling both the flow and distribution of blood within the tail and thereby thermoregulatory heat loss from its surface.

Keywords: α_2-Adrenoceptors; rat tail; thermoregulation; cutaneous vasoconstriction; delequamine; RS-15385-197

Introduction

The highly vascularized tail of the rat is an important organ of thermoregulation in this species (Rand *et al.*, 1965). The resting temperature of the tail skin is normally only a degree or so above the ambient air temperature, but if body core temperature rises above a critical threshold (approximately 39°C; Thomson & Stevenson, 1965; Little & Stoner, 1968), the tail skin temperature is rapidly elevated to within 3–4°C of the body core temperature (Grant, 1963; O'Leary *et al.*, 1985), and up to 20% of the total heat production of the rat may thereby be dissipated via the tail (Rand *et al.*, 1965). This is indicative of an active process of thermoregulatory heat loss, and is known to be under the control of the hypothalamus (Thomson & Stevenson, 1965; Young & Dawson, 1982). The most comprehensive study of the vascularity of rodent tails was carried out by Thorington (1966), who noted many similarities to other mammalian extremities, including human digits, particularly in the complex arrangement of both arterial and venous shunts. Thus, the increase in tail skin temperature during thermoregulatory heat loss could be brought about by generalized vasodilatation of arterial and/or venous vessels within this organ, preferential vasodilatation of surface vessels, redistribution of blood flow from core vessels to surface vessels by the opening of shunt vessels, or opening of arterio-venous anastomoses within the tail.

The pharmacological basis of the control of blood flow through and within the rat tail is unclear. In intact, conscious

[1] Author for correspondence.

rats, a variety of systemically-administered agents have been shown to raise the tail skin temperature, usually in studies on central neurotransmitters involved in thermoregulation (e.g. Cox & Lee, 1977). Few of these studies addressed the question of the local pharmacology of the rat tail vasculature. During *in vivo* testing of the potent, selective α_2-adrenoceptor antagonist, delequamine (RS-15385-197; Brown *et al.*, 1993; Redfern *et al.*, 1993), we casually observed an apparent warming of the tail following its administration to conscious rats. We therefore set out to study this phenomenon more systematically, addressing such questions as to whether it was a general feature of α_2-adrenoceptor antagonists and whether this was a local or central effect.

There are few examples *in vitro* of isolated blood vessels that possess a functional population of post-junctional α_2-adrenoceptors. In the isolated vascular bed of the rat tail, however, it has been shown that raising the vascular tone with vasopressin or endothelin can uncover responses to the α_2-adrenoceptor agonist, UK-14,304 (Templeton *et al.*, 1989; MacLean & McGrath, 1990). This preparation was, therefore, modified to study the effects of UK-14,304 on the skin temperature of the rat isolated tail. 5-Hydroxytryptamine (5-HT) was used to raise the basal vascular tone.

Preliminary accounts of part of this work have been presented to the British Pharmacological Society (Redfern & Clague, 1991; Redfern *et al.*, 1994).

Methods

Studies in unanaesthetized rats

Male Sprague-Dawley rats weighing 200–330 g were used. They were housed in pairs in standard wire cages at an ambient temperature of 18–20°C from arrival in the animal unit 2–6 days before the experiment. The experiments were conducted between 10 h 00 min–16 h 00 min at an ambient temperature of 18.5–20.0°C. The rats were placed in well-ventilated perspex holders (length 18 cm, width 12 cm, height 10 cm) and lightly restrained by passing the tail through an aperture at the rear of the cage and taping it to a perspex rod which protruded from the rear wall above the opening. Rectal core temperature was monitored by a thermocouple which was inserted 5 cm past the anal sphincter and taped to the tail. A flat disc thermocouple (diameter 7 mm; RS Components Ltd) was affixed to the dorsal skin of the tail, 7 cm from the tip, using two layers of surgical tape (Elastoplast fabric tape; Smith & Nephew Ltd). The rats were able to move their head limbs easily, and usually became settled within a few minutes. Readings of ambient temperature (t_a), rectal core temperature (t_c) and dorsal tail skin temperature (t_{ts}) were taken at 5 min intervals for 75 min, beginning 60 min after first placing the rats in the holders. Immediately after the fourth reading the rats received drug or vehicle by subcutaneous injection (1 ml kg^{-1}) into the nape of the neck.

Studies in anaesthetized rats

Male Sprague-Dawley rats weighing 260–330 g were anaesthetized with sodium pentobarbitone (60 mg kg^{-1}, i.p.). Core temperature was monitored from the rectum and maintained at 36–38°C with a heating lamp. Cannulae were inserted in the trachea, to facilitate respiration, the left jugular vein, to permit injections of drug and supplementary injections of anaesthetic, and the left carotid artery, to record arterial blood pressure. Recordings of blood pressure and heart rate were displayed on a Lectromed Multitrace 4 chart recorder. Tail skin temperature was measured from the dorsal surface 7 cm from the tip as described above. The thermocouple was connected to a custom-built thermocouple amplifier, and the measurement displayed on a Lectromed Multitrace 4 chart recorder. The tail was shielded from the heating lamp by a sheet of aluminium foil. Air temperature beneath the shield was monitored close to the tail by means of a thermometer, and remained within the range 22.5 to 25°C; within any individual experiment it remained within 1°C of the pre-drug value.

I.c.v. injections The head was fixed in a stereotaxic frame in the orientation of Paxinos & Watson's (1982) atlas. The skull was exposed and cleared of connective tissue, and a small burr-hole drilled 1.6 mm lateral to the mid-line and 0.8 mm caudal to bregma. The injection system consisted of a 30G steel injection cannula connected via a length of polythene cannula to a 50 µl Hamilton syringe; the injection cannula was held inside a 22G guide cannula mounted in a micromanipulator, such that the tip of the injection cannula protruded 1.5 mm beyond the tip of the guide cannula. The injection assembly was lowered into the brain so that the tip of the injection cannula was 3 mm below the brain surface. When the records had stabilized, a single injection of idazoxan (300 µg) was made in a volume of 10 µl injected over 60 s. After completing the experiment the location of the cannula tip in the ventrical was confirmed by injection of 10 µl Indian ink. In each case, the ink was distributed throughout the ventricular system as far as the spinal canal.

I.v. injection The rat was placed in a prone position with its head raised by supporting the upper incisors, to facilitate respiration. When the records had stabilized, a single injection of idazoxan (300 µg) was made in a volume of 0.05 ml flushed in over 60 s with 0.1 ml saline. The cannula dead space was 0.05 ml. The responses were followed over 1 h.

In vitro *studies*

Male Wistar rats weighing 275–325 g were killed by stunning followed by cervical dislocation. The ventral surface of the tail was shaved at the base before amputation by cutting through an intervertebral disc. The skin was reflected around the proximal first 3–5 cm of the tail, and a longitudinal incision made through the midline of the fascia on the underside of the tail. The tail artery was exposed using blunt forceps and cleaned of fat and connective tissue. Following insertion of a polyethylene cannula (o.d. 0.75 mm) into the tail artery, the tail was placed on a perspex platform and the arterial cannula attached to a perfusion circuit. The tail was perfused with modified physiological salt solution (gassed with 95% O_2: 5% CO_2), the temperature of which was altered to ensure that the perfusate entering the tail was at 37°C (measured with a thermocouple (RS Components Ltd)). The ambient temperature was 20–21°C.

Constant flow experiments Flow was held at 3.5–4.0 ml min^{-1}. After the start of perfusion, blood filled drops were observed from the cut end of the tail, indicating a successful cannulation. A flat disc thermocouple (diameter 7 mm; RS Components Ltd) linked to a digital thermometer (Digitron Instrumentation Ltd) was taped to the dorsal surface of the rat tail some 13–16 cm from the tip, just below the point of cannulation. This was connected to a flat-bed recorder to give continuous temperature measurements. In one preparation, after setting up under constant flow conditions, t_{ts} was measured with the flat disc thermocouple, at 1 cm distances from the tip of the tail.

Constant pressure experiments A reservoir, open to the pressure transducer, was situated on a shelf at a fixed distance above the tail to give a constant pressure of approximately 100 mmHg. Blood flow out of the tail was determined by collection of perfusate into a measuring cylinder. The temperature of the perfusate leaving the tail was also measured with the thermocouple.

Experiments were initially conducted under constant flow

conditions to investigate the effect of 5-HT and UK-14,304 on perfusion pressure and then the preparation was set up under constant pressure. UK-14,304 (10 nmol) was administered as a 10 µl bolus injection into an injection port situated just prior to the inflow cannula. 5-HT and rauwolscine were included in the perfusate at the required concentration.

Statistical analysis

For the *in vivo* studies, differences between groups were tested by repeated measures analysis of variance; if there was a significant interaction between treatments over time, the groups were compared at each time point with two-tailed *t* test (using the residual variance). For *in vitro* studies, differences between groups were tested with a two-tailed *t* test.

Drugs used

Pentobarbitone sodium ('Sagatal') and pentolinium tartrate (M & B); clonidine HCl, guanethidine sulphate, hydralazine, nifedipine, prazosin HCl and yohimbine HCl (Sigma); 5-hydroxytryptamine creatinine sulphate (BDH biochemicals); UK-14,304 (5-bromo-6-[2-imidazolin-2-ylamino]-quinoxaline bitartrate (Pfizer); rauwolscine HCl (Roth); BDF 6143 (4-chloro-2-[2-imidazoline-2-ylamino]-isoindoline hydrochloride), dipropyl 5-carboxamido tryptamine (DP5-CT), idazoxan HCl, imiloxan HCl, piperoxan HCl, delequamine (RS-15385-197), SKF 104078 (6-chloro-9-(3-methyl-2-butenyl)oxyl-3-methyl-1*H*-2,3,4,5-tetrahydro-3-benzazepine maleate) and WY26703 (N-methyl-N-(1,3,4,6,7,11 bα-hexahydro-2H-benzo (a)-quinolizin-2β-yl) isobutane sulphonamide) were synthesized by Dr R. Clark, Syntex, Palo Alto, California, U.S.A. In the studies in anaesthetized rats, idazoxan HCl was dissolved in saline at a concentration of 6 mg (base) ml^{-1} (i.v. dosing) or 30 mg (base) ml^{-1} (i.c.v. administration); higher concentrations could not be achieved.

In the *in vitro* studies, the composition of the physiological salt solution was (in mM): NaCl 118.4, $NaHCO_3$ 25, KCl 4.7, KH_2PO_4 1.2, $MgSO_4$ 1.2, $CaCl_2$ 2.5, glucose 11, Na_2EDTA 0.023. Ficoll 2% (molecular weight approximately 70,000) was included to prevent excessive oedema within the tail.

Results

Unanaesthetized rats

In conscious rats, lightly restrained at an ambient temperature of 18.5–20°C, t_{ts} was 21.0 ± 0.2°C and core (rectal) temperature (t_c) was 38.2 ± 0.04°C ($n = 126$).

α_2-Adrenoceptor antagonist At a dose of 1 mg kg^{-1}, s.c., delequamine (RS-15385-197) evoked a rapid and prolonged increase in t_{ts} to a peak of 29.1 ± 0.7°C ($n = 6$) with a small (<1°C) decrease in t_c (Figure 1). The threshold dose for evoking an increase in t_{ts} was 0.01 mg kg^{-1}, s.c. Yohimbine (1 mg kg^{-1}, s.c.) and idazoxan (1 mg kg^{-1}, s.c.) also produced a rapid increase in t_{ts} (Figure 2); however, the response to idazoxan (1 mg kg^{-1}, s.c.) was only slightly larger than that evoked by a low dose of delequamine (0.01 mg kg^{-1}, s.c.). The order of apparent potency for the α_2-adrenoceptor antagonists in elevating tail skin temperature at a dose of 1 mg kg^{-1}, s.c., was as follows (peak increases in t_{ts} in parentheses; $n = 6$ for each): delequamine (+9.6 ± 0.8°C) > yohimbine (+9.0 ± 1.0°C) > WY-26703 (+7.9 ± 1.3°C) > piperoxan (+5.6 ± 1.7°C) > idazoxan (+4.6 ± 1.3°C) > imiloxan (+4.1 ± 1.3°C) > SKF 104078 (+2.0 ± 1.9°C) > BDF-6143 (+1.3 ± 0.8°C).

Other agents (n = 6 for each) The α_2-adrenoceptor agonist, clonidine (0.3 mg kg^{-1}, s.c.), produced a small, transient in-

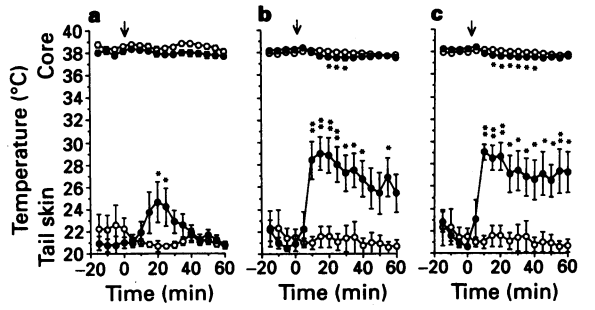

Figure 1 Effects of the selective α_2-adrenoceptor antagonist, delequamine, on core (rectal) temperature and dorsal tail skin temperature (measured 7 cm from the tip) in conscious, lightly restrained rats. (○), Saline 1 ml kg^{-1}, s.c.; (●) delequamine at doses of (a) 0.01 mg kg^{-1}, s.c.; (b) 0.1 mg kg^{-1}, s.c.; (c) 1 mg kg^{-1}, s.c. Injection at arrow. Values are mean ± s.e.mean, $n = 6$. $^*P<0.05$; $^{**}P<0.01$, drug-treated *vs.* vehicle-treated group, *t* test at each point using residual variance following repeated measures ANOVA.

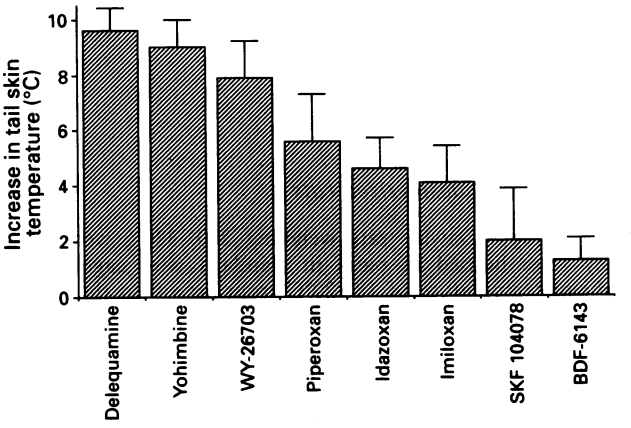

Figure 2 Maximal increases in tail skin temperature evoked by a range of α_2-adrenoceptor antagonists administered to conscious rats at a dose of 1 mg kg^{-1}, s.c. ($n = 6$ per group). The data are the mean of maximal increases in t_{ts} (maximum t_{ts} attained following drug administration (regardless of latency) minus t_{ts} immediately before drug administration) for each individual within a treatment group.

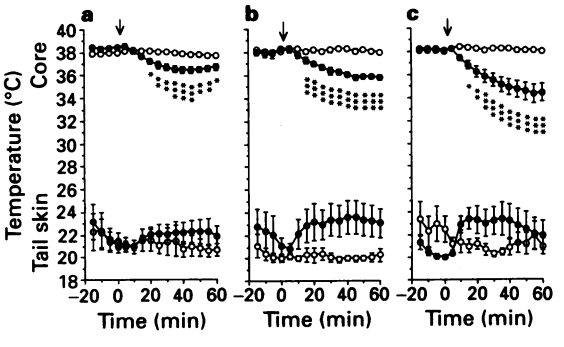

Figure 3 Effects of the ganglion blocking agent, pentolinium, on t_c and t_{ts} in conscious rats. (○), Saline 1 ml kg^{-1}, s.c.; (●) pentolinium at doses of (a) 2 mg kg^{-1} s.c.; (b) 5 mg kg^{-1}, s.c.; (c) 10 mg kg^{-1}, s.c. Injection at arrow. Values are mean ± s.e.mean, $n = 6$. $^*P<0.05$; $^{**}P<0.01$; $^{***}P<0.001$, drug-treated *vs.* vehicle-treated group, *t* test at each time point using residual variance following repeated measures ANOVA. In (b), there was a significant overall treatment effect on t_{ts} averaged over time ($P = 0.0387$); in (c) there was a significant interaction between treatment and time in the t_{ts} data ($P = 0.204$). *Post-hoc t* tests did not reveal any significant differences in t_{ts} for any individual time point, for any of the three doses.

crease in t_{ts} (+ 1.9 ± 0.6°C) accompanied by a large decrease in t_c and piloerection. The ganglion blocking agent pentolinium (2 and 5 mg kg^{-1}, s.c.) evoked a small increase in t_{ts} and a 2°C decrease in t_{ts} (Figure 3). At a higher dose (10 mg kg^{-1}, s.c.) pentolinuim elevated t_{ts} by 4.4 ± 1.3°C, with a concomitant decrease in core temperature (− 3.8 ± 0.8°C; Figure 3). The α_1-adrenoceptor antagonist, prazosin (0.3 mg kg^{-1}, s.c.; Figure 4) and the adrenergic neurone blocking agent, guanethidine (10 mg kg^{-1}, s.c.), had no effect on t_{ts} or t_c. The β-adrenoceptor antagonist, propranolol (10 mg kg^{-1}, s.c.), produced a small increase in tail skin temperature (+ 2.0 ± 1.0°C) accompanied by a small (~1°C) fall in core temperature (Figure 4). The vasodilator agent, hydralazine (10 mg kg^{-1}, s.c.), lowered t_c (− 3°C), which was delayed in onset by some 20 min, but did not affect t_{ts}, whereas the calcium antagonist, nifedipine (3 mg kg^{-1}, s.c.), was inactive. The 5-HT$_{1A}$ receptor agonist, dipropyl 5-carboxamido tryptamine (DP5-CT; 1 mg kg^{-1}, s.c.), produced a large decrease in t_c (− 4°C) without changing t_{ts}. The injection of an equivalent volume of water or saline (1 ml kg^{-1}, s.c.) had no effect on either parameter.

Anaesthetized rats

Tail skin temperature The tail skin temperature (t_{ts}) of each animal was very stable (23.3 ± 0.2°C; n = 10) until administration of idazoxan. Whereas blood pressure fluctuated before drug administration, this had no effect on t_{ts}. Core temperature began to fall after injection of idazoxan, but this was arrested by use of the heating lamp, and was maintained within 1°C of the pre-drug value. Idazoxan (300 μg, i.v.) produced a rapid increase in t_{ts} which was detectable 2 min after beginning the injection, reaching a peak 7 min after beginning the injection (Figure 5a). When the same dose was administered i.c.v., t_{ts} also rose, but more slowly: no detectable effect was seen until 4 min after injection, and the response reached a peak 10 min after injection (Figure 5a). Also, the peak response (+ 3.6 ± 0.7°C; n = 5) was substantially smaller than when idazoxan was administered intravenously (+ 6.3 ± 1.2°C; n = 5). Statistically significant differences between the responses elicited by the two routes of administration were seen from 3–15 min after injection (Figure 5a).

Mean arterial blood pressure Before injection of idazoxan, mean arterial blood pressure in this group of rats was 118.4 ± 7.2 mmHg (n = 10). Changes in blood pressure which followed the administration of idazoxan were small but complex. After the i.v. dose, there appeared to be a biphasic response: MAP appeared to fall slightly (by 6.5 ± 7.3 mmHg) during the injection and then rose, reaching a peak (+ 8.5 ± 2.3 mmHg) 1.5 min after beginning the injection. With i.c.v. injection, there was no change in MAP during the injection period, but MAP rose gradually by 3.9 ± 2.3°C (6 min after beginning the injection). MAP then fell below the pre-drug level by 7.3 ± 1.7 mmHg (Figure 5b). With either route of administration, the changes in t_{ts} did not merely follow the changes in blood pressure.

Heart rate Before injection of idazoxan, heart rate in this group of rats was 397.6 ± 12.7 b.p.m. (n = 10). Upon i.v. administration of idazoxan there was an immediate tachycar-

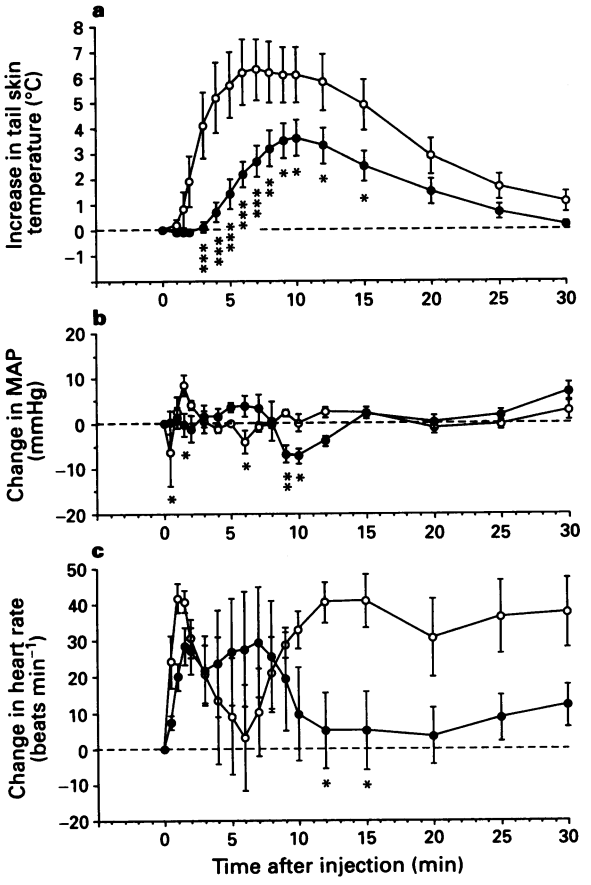

Figure 5 Comparison of effects of i.v. (○) and i.c.v. administration (●) of the α_2-adrenoceptor antagonist, idazoxan (300 μg), on (a) tail skin temperature, (b) mean arterial blood pressure and (c) heart rate, in pentobarbitone-anaesthetized rats. Values are mean ± s.e.mean, n = 5. *P<0.05; **P<0.01; ***P<0.001, i.v. *vs.* i.c.v. treated group, t test at each time point using residual variance following repeated measures ANOVA.

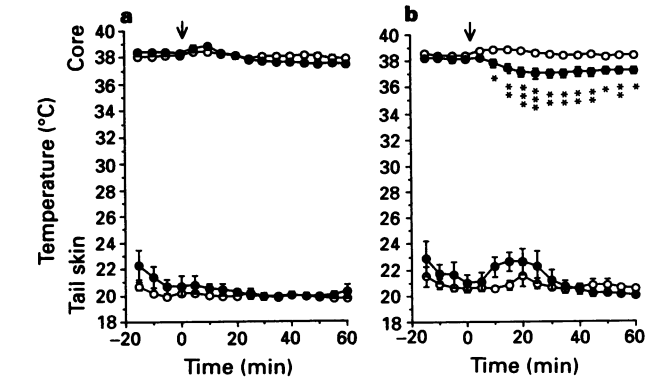

Figure 4 Effects of (a) the selective α_1-adrenoceptor antagonist, prazosin (0.3 mg kg^{-1}, s.c.), and (b) the selective β-adrenoceptor antagonist, propranolol (10 mg kg^{-1}, s.c.) on t_c and t_{ts} in conscious, lightly restrained rats. Values are mean ± s.e.mean, n = 6. *P<0.05; **P<0.01; ***P<0.001, drug-treated *vs.* vehicle-treated group t test at each time point using residual variance following repeated measures ANOVA.

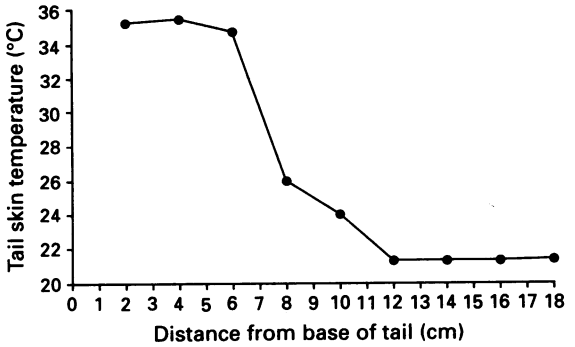

Figure 6 Dorsal skin temperatures at different points along an isolated tail of rat perfused with Krebs solution at constant flow (0.8 ml min^{-1}), with perfusate entering the base of the tail at 37°C. The ambient temperature was 20°C.

dia which began within seconds of commencing the 60 s injection, reaching a peak of $+41.8 \pm 4.0$ b.p.m. at the end of the 1 min injection period, and descending to the pre-drug level 6 min after injection. Heart rate then rose again, and was still elevated by some 35–40 b.p.m. 60 min after injection. Following i.c.v. injection there was also a very rapid tachycardia. However, this did not reach the same peak although it was sustained for about 10 min. There was no secondary increase in heart rate (Figure 5c).

In vitro *studies*

Under constant flow conditions (3.5–4.0 ml min^{-1}), perfusion pressure was 57 ± 4 mmHg ($n = 4$). In each preparation, we established a concentration of 5-HT which approximately doubled perfusion pressure. In four preparations, 5-HT (119 ± 28 nM) raised perfusion pressure by 56 ± 9 mmHg. A bolus injection of UK-14,304 (10 nmol in 10 µl) caused an increase of perfusion pressure of 27.5 ± 15 mmHg in the presence of 5-HT but did not have an effect in its absence. Inclusion of 1 µM rauwolscine in the perfusate abolished responses to UK-14,304 ($P<0.05$). Figure 6 shows the rat tail skin temperature at 1 cm distances from the tip of the tail under constant flow conditions. It shows that, in this preparation, the t_{ts} was reduced by ~14°C from the base of the tail to the tip.

In nine preparations, under constant pressure conditions, the temperature of the perfusate entering the tail was 37.0 ± 0.4°C and the temperature of the perfusate leaving the tail was 26.5 ± 0.3°C. The fixed perfusion pressure was 99.4 ± 3.5 mmHg, the skin temperature was 31.6 ± 0.6°C and mean perfusate flow through the tail was 2.1 ± 0.2 ml min^{-1}. 5-HT (119 ± 28 nM) decreased t_{ts} by 3.3 ± 2°C and reduced flow by 1.2 ± 0.3 ml min^{-1} ($n = 4$). Under these conditions, UK-14,304 (10 nmol in 10 µl) further reduced t_{ts} by 3.0 ± 0.3°C but flow was not significantly altered, increasing by 0.6 ± 0.5 ml min^{-1} ($n = 4$). The effects of UK-14,304 were abolished by inclusion of 1 µM rauwolscine in the perfusate ($P<0.05$).

Discussion

In the present study, a variety of α_2-adrenoceptor antagonists were shown to elevate tail skin temperature in the conscious rat. This was not secondary to an increase in core temperature, as this actually fell slightly. Apart from an incidental observation by Wilson & Fregly (1985) relating to yohimbine, this is the first systematic study of this phenomenon. Several questions arose following our initial observations: was the increase in tail skin temperature due to blockade of α_2-adrenoceptors *per se*; was it unique to blockade of α_2-adrenoceptors; was it a centrally, systemically or locally-mediated effect; was it secondary to changes in blood pressure; was it merely part of a generalized vasodilatation; and was it brought about by generalized vasodilatation of arterial and/or venous vessels within this organ, preferential vasodilatation of superficial vessels, shunting of blood flow from core vessels to surface vessels, or opening of arterio-venous anastomoses within the tail?

The increase in t_{ts} seen with delequamine (RS-15385-197) was most probably related to α_2-adrenoceptor blockade as it was also evoked by a range of other α_2-adrenoceptor antagonists. The putative receptor involved appears to be an α_2-adrenoceptor rather than an imidazoline receptor, as the response was also evoked not only by idazoxan but also by delequamine and yohimbine, which, unlike idazoxan, do not interact with imidazoline binding sites (Brown *et al.*, 1990; 1993). However, the α_2-adrenoceptor antagonists tested at a dose of 1 mg kg^{-1} for effects on tail skin temperature produced a wide range of magnitude of response. This was poorly correlated with their i.v. ED_{50} either for peripheral (UK-14,304 pressor responses in pithed rats) or central (UK-14,304 mydriasis) α_2-adrenoceptor antagonism (Brown *et al.*, 1993). These data may hint at the involvement of an α_2-adrenoceptor sub-type, or differential selectivity for prejunctional α_2-adrenoceptors, in that increased transmitter release could compensate for blockade of post-junctional α_2-adrenoceptors. Alternatively, this broad range of response could be a result of differences in absorption from the subcutaneous injection site.

The question of whether the increase in t_{ts} was centrally mediated was addressed by comparing responses to the same dose of idazoxan (300 µg) given either by intravenous or intracerebroventricular injection, in anaesthetized rats. This agent elicited an increase in tail skin temperature by both routes of administration. However, following i.c.v. injection the response was both of a smaller magnitude and delayed in onset. Drugs administered into a lateral ventricle diffuse to distant brain regions, but are also absorbed into the general circulation. Thus, our data indicate either that the response is elicited from a site distant from the ventricles or else the drug is diffusing out of the brain to effect its response from a peripheral site. If the former were true it would be expected that the response would be of the same magnitude, if not larger, than that elicited by the same dose given intravenously. As this was not the case, absorption into the general circulation seems a more likely explanation. The blood pressure responses were different following the two routes of administration, but in both cases were small and complex. It is, however, worth noting that in neither case did the change in tail skin temperature follow the change in blood pressure. The initial tachycardia was immediate by either route, suggesting that idazoxan given centrally elicited tachycardia by a central action, and confirming that the i.c.v. injections were successful. These experiments with idazoxan pointed to a peripheral site of action for the α_2-adrenoceptor antagonists in elevating tail skin temperature. The suggestion that α_2-adrenoceptors located in the tail vasculature were responsible for such thermoregulatory changes was confirmed by the results of the *in vitro* studies. These data showed a direct cooling effect of an α_2-adrenoceptor agonist in the rat isolated tail. This effect was inhibited by a selective α_2-adrenoceptor antagonist, verifying that the response was α_2-adrenoceptor-mediated. Prior to introduction of 5-HT and UK-14,304, the temperature of the perfusate was decreased by more than 10°C on passage through the tail, indicating that the vasculature was markedly dilated.

The most straightforward hypothesis to emerge from these studies was that the α_2-adrenoceptors involved were located post-junctionally within the tail vasculature, and were responsible for mediating tonic sympathetic vasoconstriction within this vascular bed. Therefore, interruption of sympathetic vasoconstrictor tone with a ganglion blocking agent would be expected to result in responses of a similar magnitude to those elicited by antagonists at α_2-adrenoceptors. The ganglion-blocking agent, pentolinium (10 mg kg^{-1}, s.c.), elevated t_{ts} by 4.4°C, which was greater than the response at 5 mg kg^{-1} (+3.4°C), but was only approximately 45% of the largest response evoked by an α_2-adrenoceptor antagonist (+9.6°C, delequamine). However, core temperature (and therefore blood temperature) fell rapidly after pentolinium, which would limit the maximum attainable tail skin temperature. Also, blood pressure (and therefore tail blood flow) would be greatly reduced by pentolinium. These two effects would combine to offset any increase in tail skin temperature evoked by ganglionic blockade. Moreover, it is known that in anaesthetized rats, abdominal sympathectomy produces an elevation in t_{ts} to the same level as that observed during body heating (O'Leary *et al.*, 1985).

As to whether post-junctional α_2-adrenoceptors provide the major mechanism of ongoing sympathetic vasoconstriction in the tail vasculature, propranolol (10 mg kg^{-1}, s.c.) produced only a small (+2.9°C) increase in tail skin temperature accompanied by a 1°C fall in core temperature, arguing against a major role of β-adrenoceptors in the control of tail

blood flow in this species. Perhaps surprisingly, prazosin (0.3 mg kg^{-1}, s.c.) had no effect, indicating that α_1-adrenoceptors do not play a major role in sympathetic vasomotor control within the tail. Early attempts to determine the relative contribution of post-junctional α_1- *vs.* α_2-adrenoceptors to vasoconstriction in the tail vasculature used proximal segments of the main ventral tail artery *in vitro*; whereas Itoh *et al.* (1983) clearly demonstrated an α_2-adrenoceptor component, Medgett *et al.* (1984) were able to demonstrate an α_2-adrenoceptor component only in tail arteries taken from hypertensive rats. The conclusions drawn by subsequent authors on the role of α_2-adrenoceptors in the tail artery ranged from mere facilitation of the α_1-adrenoceptor mediated response (Xiao & Rand, 1989) to a complete denial of their existence in this vessel (Marwood *et al.*, 1986). However, Medgett (1985) looked beyond the proximal tail artery and found that the contribution made by α_2-adrenoceptors was greater in more distal segments of the vessel; our present data illustrate this in the intact, entire tail vascular bed, both *in vivo* and, under appropriate conditions, *in vitro*. It is also known that, in rings prepared from the rat tail artery, α_2-adrenoceptor-mediated contractions are enhanced when the temperature is reduced from 37°C to 24°C (Harker *et al.*, 1991), which is close to the baseline tail skin temperatures in our experiments (where the ambient temperature was the standard housing temperature for laboratory rats).

The α_2-adrenoceptor agonist, clonidine, itself produced a small increase in t_{ts} with a pronounced hypothermia; clearly this hypothermia was not due entirely to heat loss from the tail, as much larger increases in tail skin temperature were evoked by α_2-adrenoceptor antagonists, associated with only modest decreases in core temperature. This suggests either cutaneous vasodilatation elsewhere or an inhibition of heat production as the cause of the clonidine hypothermia: a centrally mediated decrease in thermogenesis has previously been ascribed to this agent in the rat (Lin *et al.*, 1984). The small increase in t_{ts} may have been secondary to an initial increase in blood pressure. A similar hypothermia occurred after administration of the 5-HT_{1A} agonist, DP5-CT, without any change in t_{ts}, again serving to emphasize the specificity of the response to the α_2-adrenoceptor antagonists. The finding that hydralazine did not increase t_{ts} suggests that α_2-adrenoceptor antagonists do not cause generalized arterial vasodilatation within the tail. If their effect was mediated by opening arteriovenous anastomoses, which are known to be present in this vascular bed in the rat (Gemmel & Hales, 1977), hydralazine might be expected to do the same, as it does open arteriovenous anastomoses, at least in the rabbit (Bolt & Saxena, 1984). Alternatively, it is possible that the tail arterioles are insensitive to hydralazine, although it is known that the proximal tail artery does relax to hydralazine *in vitro* (Ebeigbe & Aloamala, 1985). The most likely explanation is that the α_2-adrenoceptor antagonists effect a redistribution of blood flow from the core of the tail to the surface either by an action on the arterial or venous side of the tail vasculature. It is known that such a redistribution of blood flow occurs in the rat tail *in vivo* as a local response to changes in the ambient temperature to which the tail is exposed (Raman *et al.*, 1983); perhaps the increased effectiveness of α_2-adrenoceptor-mediated vasoconstriction as temperature is lowered (Harker *et al.*, 1991) contributes to this local thermal autoregulation.

In summary, blockade of α_2-adrenoceptors within the rat tail *in vivo* elevates tail skin temperature, whereas activation of α_2-adrenoceptors within the rat tail *in vitro* reduces tail skin temperature. We conclude that post-junctional α_2-adrenoceptors in the vasculature of the rat tail play a major role in sympathetic vasoconstriction within this organ, controlling the flow and distribution of blood within the tail, and thereby thermoregulatory heat loss from its surface. This is analogous to their apparent role in the vascular beds of some human extremities, such as the fingertips (Coffman, 1991).

The authors wish to thank Dr Robin Clark of the Institute of Organic Chemistry, Syntex, Palo Alto for synthesizing delequamine, BDF 6143, DP5-CT, idazoxan, imiloxan, piperoxan, SKF 104078 and WY26703, Dr Michael Spedding for his encouragement during the course of these studies, and Drs Peter Hicks and Alison Templeton for their helpful comments during the preparation of this manuscript.

References

BOLT, G.R. & SAXENA, P.R. (1984). Interaction of atenolol with the systemic and regional hemodynamic effects of hydralazine in conscious renal hypertensive rabbits. *J. Pharmacol. Exp. Ther.*, **230**, 205–213.

BROWN, C.M., MACKINNON, A.C., MCGRATH, J.C. SPEDDING, M. & KILPATRICK, A.T. (1990). α_2-Adrenoceptor subtypes and imidazoline-like binding sites in the rat brain. *Br. J. Pharmacol.*, **99**, 803–809.

BROWN, C.M., MACKINNON, A.C., REDFERN, W.S., HICKS, P.E., KILPATRICK, A.T., SMALL, C., RAMCHARAN, M., CLAGUE, R.U., CLARK, R.D., MACFARLAND, C.B. & SPEDDING, M. (1993). The pharmacology of RS-15385-197, a potent and selective α_2-adrenoceptor antagonist. *Br. J. Pharmacol.*, **108**, 516–525.

COFFMAN, J.D. (1991). Raynaud's phenomenon: an update. *Hypertension*, **17**, 593–602.

COX, B. & LEE, T.F. (1977). Do central dopamine receptors have a physiological role in thermoregulation? *Br. J. Pharmacol.*, **61**, 83–86.

EBEIGBE, A.B. & ALOAMAKA, C.P. (1985). Mechanism of hydralazine-induced relaxation of arterial smooth muscle. *Cardiovasc. Res.*, **19**, 400–405.

GEMMELL, R.T. & HALES, J.R.S. (1977). Cutaneous arteriovenous anastomoses present in the tail but absent from the ear of the rat. *J. Anat.*, **124**, 355–358.

GRANT, R.T. (1963). Vasodilatation and body warming in the rat. *J. Physiol.*, **167**, 311–317.

HARKER, C.T., OUSLEY, P.J., BOWMAN, C.J. & PORTER, J.M. (1991). Cooling augments α_2-adrenoceptor-mediated contractions in rat tail artery. *Am. J. Physiol.*, **260**, H1166–H1171.

ITOH, T., KITAMURA, K. & KURIYAMA, H. (1983). Roles of extrajunctional receptors in the response of guinea-pig mesenteric and rat tail arteries to adrenergic nerves. *J. Physiol.*, **345**, 409–422.

LIN, M.T., SHIAN, L.R. & LEU, S.Y. (1984). Clonidine-induced hypothermia: possible involvement of cholinergic and serotonergic mechanisms. *Naunyn-Schmied. Arch. Pharmacol.*, **326**, 124–128.

LITTLE, R.A. & STONER, H.B. (1968). The measurement of heat loss from the rat's tail. *Q.J. Exp. Physiol.*, **53**, 76–83.

MACLEAN, M.R. & MCGRATH, J.C. (1990). Effects of pre-contraction with endothelin-1 on α_2-adrenoceptor- and (endothelium-dependent) neuropeptide Y-mediated contractions in the isolated vascular bed of the rat tail. *Br. J. Pharmacol.*, **101**, 205–211.

MARWOOD, J.F., CHAPMAN, K.L. & STOKES, G.S. (1986). Studies that question the existence of alpha-2 adrenoceptors in tail arteries of normotensive Sprague-Dawley rats. *J. Pharmacol. Exp. Ther.*, **238**, 267–272.

MEDGETT, I.C. (1985). α_2-Adrenoceptors mediate sympathetic vasoconstriction in distal segments of rat tail artery. *Eur. J. Pharmacol.*, **108**, 281–287.

MEDGETT, I.C., HICKS, P.E. & LANGER, S.Z. (1984). Smooth muscle alpha-2 adrenoceptors mediate vasoconstrictor responses to exogenous norepinephrine and to sympathetic stimulation to a greater extent in spontaneously hypertensive than in Wistar Kyoto rat tail arteries. *J. Pharmacol. Exp. Ther.*, **231**, 159–165.

O'LEARY, D.S., JOHNSON, J.M. & TAYLOR, W.F. (1985). Mode of neural control mediating rat tail vasodilatation during heating. *J. Appl. Physiol.*, **59**, 1533–1538.

PAXINOS, G. & WATSON, C. (1982). *The Rat Brain in Stereotaxic Coordinates*. Sydney: Academic Press.

RAYMAN, E.R., ROBERTS, M.F. & VANHUYSE, V.J. (1983). Body temperature control of rat tail blood flow. *Am. J. Physiol.*, **245**, R426–R432.

RAND, R.P., BURTON, A.C. & ING, T. (1965). The tail of the rat, in temperature regulation and acclimatization. *Can. J. Physiol. Pharmacol.*, **43**, 257–267.

REDFERN, W.S. & CLAGUE, R.U. (1991). Effects of RS-15385-197 and other α_2-adrenoceptor antagonists on tail skin temperature in unanaesthetized rats. *Br. J. Pharmacol.*, **104**, 50P.

REDFERN, W.S., MACLEAN, M.R. & MCGRATH, J.C. (1994). α-Adrenoceptor antagonists elevate tail skin temperature in the rat by an action within the tail, not the brain. *Br. J. Pharmacol.*, **113**, 101P.

REDFERN, W.S., MACKINNON, A.C., BROWN, C.M., MARTIN, A.B., KILPATRICK, A.T., CLAGUE, R.U. & SPEDDING, M. (1993). Modulation of central noradrenergic function by RS-15385-197. *Br. J. Pharmacol.*, **108**, 526–533.

TEMPLETON, A.G.B., MACMILLAN, J., MCGRATH, J.C., STOREY, N.D. & WILSON, V.G. (1989). Evidence for prazosin-resistant, rauwolscine-sensitive α-adrenoceptors mediating contractions in the isolated vascular bed of the rat tail. *Br. J. Pharmacol.*, **97**, 563–571.

THOMSON, G.E. & STEVENSON, J.A.F. (1965). The temperature response of the male rat to treadmill exercise, and the effect of anterior hypothalamic lesions. *Can. J. Physiol. Pharmacol.*, **43**, 279–287.

THORINGTON, R.W. (1966). *The Biology of Rodent Tails: A Study of Form and Function.* Report of Project 823, Document Number AAL-TR-65-8 from Arctic Aeromedical Laboratory, Fort Wainwright, Alaska.

WILSON, K.M. & FREGLY, M.J. (1985). Factors affecting angiotensin II-induced hypothermia in rats. *Peptides*, **6**, 695–701.

YOUNG, A.A. & DAWSON, N.J. (1982). Evidence for on-off control of heat dissipation from the tail of the rat. *Can. J. Physiol. Pharmacol.*, **60**, 392–398.

XIAO, X.-H. & RAND, M.J. (1989). α_2-Adrenoceptor agonists enhance responses to certain other vasoconstrictor agonists in the rat tail artery. *Br. J. Pharmacol.*, **96**, 539–546.

(Received August 25, 1994
Revised December 23, 1994
Accepted January 12, 1995)

British Journal of Pharmacology (1995) 114, 1731-1737 © 1995 Stockton Press All rights reserved 0007-1188/95 $12.00

Effects of 8-bromo cyclic GMP and verapamil on depolarization-evoked Ca^{2+} signal and contraction in rat aorta

Salvatore Salomone, Nicole Morel & [1]Théophile Godfraind

Laboratoire de Pharmacologie, Université Catholique de Louvain, FARL 5410, Avenue Hippocrate, 54, B-1200 Bruxelles, Belgium

1 The pharmacological action of NO donors is usually attributed to a cellular rise in guanosine 3':5'-cyclic monophosphate (cyclic GMP), but this hypothesis is based only on indirect evidence. Therefore, we have studied the effects of cyclic GMP on Ca^{2+} movements and contraction in rat isolated endothelium-denuded aorta stimulated by KCl depolarizing solution using the permeant analogue 8-bromo cyclic GMP (BrcGMP). Isometric contraction and fura-2 Ca^{2+} signals were measured simultaneously in preparations treated with BrcGMP and with verapamil. The activation of calcium channels was estimated by measuring the quenching rate of the intracellular fura-2 signal by Mn^{2+} and by the depolarization-dependent influx of $^{45}Ca^{2+}$.

2 Stimulation with 67 mM KCl-solution evoked an increase in cytosolic Ca^{2+} concentration ($[Ca^{2+}]_{cyt}$) and a contractile response which were inhibited by pretreatment with verapamil (0.1 μM) or BrcGMP (0.1–1 mM). However, the inhibition of the fura-2 Ca^{2+} signal was significantly higher with verapamil than with BrcGMP, whereas the contraction was inhibited to a similar extent.

3 When preparations were exposed to K^+-depolarizing solution in which the calcium concentration was cumulatively increased, the related increase in fura-2 Ca^{2+} signal was barely affected by BrcGMP, whereas the contractile tension was strongly and significantly inhibited.

4 Cellular Ca^{2+} changes were also estimated with $^{45}Ca^{2+}$. $^{45}Ca^{2+}$ influx in resting preparations was significantly reduced by BrcGMP (0.1 mM) but not by verapamil (0.1 μM); $^{45}Ca^{2+}$ influx in KCl-depolarized preparations was reduced by verapamil but was unaffected by BrcGMP.

5 Measurements of Mn^{2+}-induced quenching of the intracellular fura-2 signal showed that BrcGMP did not affect divalent cation entry in K^+-stimulated preparations, whereas verapamil concentration-dependently inhibited Mn^{2+} entry stimulated by K^+-depolarization.

6 The present results indicate that BrcGMP did not affect voltage-dependent Ca^{2+} channel gating in the rat aorta. For a given fura-2 Ca^{2+} signal, the contraction was lower in preparations exposed to BrcGMP than in the untreated ones, suggesting that the activation of cyclic GMP-dependent kinases reduced the contractile efficacy of calcium. Furthermore, the reduction of depolarization-dependent $^{45}Ca^{2+}$ uptake reported with sodium nitroprusside, a NO donor, was not observed with biologically active concentrations of BrcGMP, suggesting that this drug could have additional mechanisms of action, unrelated to activation of protein G-kinase.

Keywords: Rat aorta; cyclic GMP; fura-2; verapamil; $^{45}Ca^{2+}$ influx; Mn^{2+}; L-type calcium channel

Introduction

Guanosine 3':5'-cyclic monophosphate (cyclic GMP) is involved in the signal transduction mechanism activated by several hormones and drugs. Recently, the recognition of the activation of the soluble guanylate cyclase by nitric oxide (NO) has extended the importance of the role played by cyclic GMP in many cells, particularly vascular smooth muscle cells. It is established that endothelium-dependent vasorelaxations are largely mediated by NO or a closely related compound (Palmer *et al.*, 1987; Ignarro, 1989) and that endothelium-derived NO stimulates the soluble guanylate cyclase in smooth muscle cells, leading to an increase in cyclic GMP (Rapoport & Murad, 1983). However, the mechanism by which cyclic GMP induces vasorelaxation is not known. It has been suggested that vasorelaxation is related to a lowering of cytosolic Ca^{2+} concentration ($[Ca^{2+}]_{cyt}$, for review see Schmidt *et al.*, 1993) but other studies have demonstrated that cyclic GMP (Pfitzer *et al.*, 1986) or endothelium-derived NO (Dietrich *et al.*, 1994) regulate vascular tone by a $[Ca^{2+}]_{cyt}$-independent mechanism. The effect of cyclic GMP also depends on the nature of the stimulation applied to the artery: in the rat aorta, removal of the endothelium enhances the contractile response and the Ca^{2+} influx evoked by α-adrenergic agonists, whereas it does not affect the contraction or the $^{45}Ca^{2+}$ influx stimulated by high K^+ solution (Godfraind, 1986).

Nitrocompounds are known to release NO and to increase cellular cyclic GMP levels (Feelisch & Kelm, 1991). The latter property is usually considered to be responsible for the cellular actions of these compounds so that they are often used to study the action of cyclic GMP in vascular smooth cells. For example, it has been reported that sodium nitroprusside decreases the cytosolic Ca^{2+} concentration in vascular smooth muscle and the sensitivity of contractile elements to Ca^{2+} (Karaki *et al.*, 1988), and that it uncouples the development of active stress from myosin phosphorylation (McDaniel *et al.*, 1992). These effects were attributed to the increase in cyclic GMP levels. However, not all studies support a role for cyclic GMP in mediating the vasorelaxant effects of nitrocompounds. Some effects of sodium nitroprusside could be due to the generation of cyanide (McDaniel *et al.*, 1992). Moreover, some of the effects of NO itself are independent of cyclic GMP production and could be related either to the marked reactivity of the nitric oxide free radical

[1] Author for correspondence.

(Braughler *et al.*, 1979) or to a direct effect of NO (Gupta *et al.*, 1994; Bolotina *et al.*, 1994).

The purpose of the present study was to characterize the effect of cyclic GMP on the $[Ca^{2+}]_{cyt}$ and the Ca^{2+}-tension relationship in rat aorta contracted by high KCl. We used 8-bromo cyclic GMP (BrcGMP), a lipophilic and non-hydrolysable analogue of cyclic GMP, which enters smooth muscle cells and activates cyclic GMP-dependent kinases (Sekhar *et al.*, 1992). Experiments were carried out in the presence of N^{ω}-nitro-L-arginine (L-NOARG), an inhibitor of NO synthase (Moore *et al.*, 1990; Mulsch & Busse, 1990), in order to avoid interference by nitric oxide. Isometric contraction has been measured simultaneously with front-surface fluorometry of fura-2 loaded rings of aorta. Furthermore, the activation of calcium channels was estimated by measuring the rate of quenching of the intracellular fura-2 signal by Mn^{2+} simultaneously with muscle tone. In separate experiments, $^{45}Ca^{2+}$ influx through voltage-dependent Ca^{2+} channels was estimated by measuring the K^+ depolarization-evoked fast change in the specific activity of cellular calcium resistant to lanthanum (Godfraind, 1976).

The results show that BrcGMP decreases fura-2 Ca^{2+} signals in the rat aorta depolarized by KCl without affecting voltage-dependent Ca^{2+} influx, indicating that this could be due to increased rate of Ca^{2+} sequestration or efflux. Moreover, the inhibition of contractile tension by BrcGMP cannot be entirely related to the lowering of $[Ca^{2+}]_{cyt}$, but also to a modification of the relationship between $[Ca^{2+}]_{cyt}$ and contraction. Furthermore, since biologically active concentrations of BrcGMP did not modify depolarization-dependent $^{45}Ca^{2+}$ influx, reduction of this influx by sodium nitroprusside, as reported by Karaki *et al.* (1984), is likely to occur by a mechanism that is independent of the rise in cyclic GMP evoked by this drug.

Methods

Measurement of contractile tension and $[Ca^{2+}]_{cyt}$

Aortic rings (mean length 3.28 ± 0.02 mm) were inverted and lightly rubbed to remove the endothelium. They were incubated for 3–5 h at room temperature in a physiological solution (composition, mM: NaCl 122, KCl 5.9, $NaHCO_3$ 15, $MgCl_2$ 1.25, $CaCl_2$ 1.25, glucose 11) containing 5 μM fura-2 acetoxymethyl ester (fura-2 AM) and 0.05% Cremophor EL, and further incubated for 30 min with 0.1 mM L-NOARG and with or without BrcGMP and/or verapamil. L-NOARG was used in order to avoid interference by nitric oxide which could possibly be produced by the inducible NO synthase activity of smooth muscle; this enzymatic activity could be induced by bacterial contamination during the long lasting fura-2 loading period. Rings were mounted between two hooks under a tension of 2 g in a 5 ml organ bath filled with physiological solution at 37°C gassed with 95% O_2 and 5% CO_2. This bath was part of a fluorimeter (CAF 110, JASCO, Tokyo) which allows us to estimate the calcium signal. The muscle tone was measured by an isometric lever connected to an isometric force transducer. The luminal face of the aortic ring was alternatively illuminated (128 Hz) with two excitation wavelengths (340 ± 10 nm and 380 ± 10 nm) obtained from a xenon high pressure lamp (75 W) coupled to two monochromators. The emitted light from the muscle was collected by a photomultiplier through a 500 ± 12 nm filter. The time constant for the optical channel was 0.26 s. The ratio of the fluorescence due to excitation at 340 nm (F340) to that at 380 nm (F380) was calculated from successive illumination periods. The fluorescence signals, F340, F380 and the ratio F340/F380 were measured simultaneously with contractile tension and recorded on a computer, by using data acquisition hardware (MacLab) and data recording software (Chart v3.2, AD Instruments Pty Ltd., Castle Hill, Australia). At the end of the experiment, the fura-2-Ca^{2+} signal was calibrated. The maximal ratio ($R_{max} = 1.497 \pm 0.038$, $n = 50$) was measured in calcium saturating medium by adding ionomycin (14 μM) in high KCl solution (KCl, 128 mM), while the minimal ratio ($R_{min} = 0.318 \pm 0.03$, $n = 50$) was obtained in calcium-free medium in the presence of ethylene glycol-*bis* (β-aminoethyl ether) *N,N,N',N'*-tetraacetic acid (EGTA, 8 mM). The autofluorescence was finally measured at 340 nm and 380 nm by quenching the fura-2 fluorescence with $MnCl_2$ (10 mM) and it was subtracted from the experimental values for the calculation of the cytosolic calcium concentration ($[Ca^{2+}]_{cyt}$). R_{max}, R_{min} and autofluorescence were determined in each preparation. $[Ca^{2+}]_{cyt}$ was calculated by the application of the following equation (Grynkiewicz *et al.*, 1985):

$$[Ca^{2+}]_{cyt} = \frac{R - R_{min}}{R_{max} - R} \quad \beta \times K_D$$

where K_D is the apparent dissociation constant of the fura-2/Ca^{2+} complex and is assumed to be equal to 224 nM; β (1.510 ± 0.038, $n = 50$) is a correcting factor equal to the ratio of the fluorescence intensities of the free dye (measured with EGTA) and the calcium saturated dye (measured with ionomycin), at 380 nm; the β value was calculated for each preparation according to the fluorescence intensities of the free dye and of the calcium-saturated dye which were measured in the same preparation. R is the ratio of the fluorescence intensities emitted at 500 nm at the two excitation wavelengths 340 nm and 380 nm for each experimental value.

Measurement of $^{45}Ca^{2+}$ influx

Calcium influx was estimated by measuring changes in the specific activity of the calcium fraction resistant to displacement by lanthanum (Godfraind, 1976). After an equilibration period of 60 min in physiological solution maintained at 37°C and aerated with a gas mixture of 95% O_2 and 5% CO_2, aortic segments were further incubated, for 30 min, in the same solution in the presence of 0.1 mM L-NOARG, and in the absence or presence of BrcGMP (0.1 mM–1 mM) and/or verapamil (0.1 μM). Thereafter, the aortic segments were transferred, for 2 min, either in a physiological solution, or in a 100 mM KCl depolarizing solution, both containing $^{45}Ca^{2+}$ (4 μCi ml^{-1}). After this 2 min-incubation, they were washed for 5 min in 500 ml of La^{3+} solution (composition, mM: NaCl 122, KCl 5.9, $MgCl_2$ 1.25, $LaCl_3$ 50, glucose, 11 and Tris-maleate buffer, 15; pH 6.8) to remove extracellular Ca^{2+}. The aortic segments were then dried on filter paper, weighed and dissolved in 0.1 ml of a mixture of perchloric acid: H_2O_2 (1:1). The radioactivity bound to the tissue was counted in 4 ml of Pico-fluor 30 by liquid scintillation.

Measurement of contractile tension and quenching rate of fura-2 evoked by Mn^{2+}

The Mn^{2+}-induced quenching of fura-2 fluorescence was estimated at 363 ± 10 nm excitation wavelength, which represented the fura-2 isosbestic wavelength in our system. This was determined by recording fura-2 excitation spectra at different Ca^{2+} concentrations, according to Grynkiewicz *et al.* (1985). The fluorescence signal F363 and contractile tension were measured simultaneously, at 2 s intervals. Mechanically endothelium-denuded aortae were loaded with fura-2 AM and preincubated with 0.1 mM L-NOARG which was present in all bathing solutions during the experiment. Rings were mounted between two hooks under a tension of 2 g in a 5 ml organ bath filled with a zero Ca^{2+} physiological solution (containing 0.1 mM EGTA) at 37°C, gassed with 95% O_2 and 5% CO_2. After 5 min incubation, 0.1 mM $MnCl_2$ was added to the bath and the fluorescence, as well as the muscle tone were measured. After 3 min the rings were

stimulated by a 67 mM KCl solution which produced an increase in the quenching rate and a contractile response. After 15 min, 10 mM $MnCl_2$ was added to the organ bath to quench rapidly the remaining fluorescence. The minimum value measured in the presence of 10 mM $MnCl_2$ was considered as background (autofluorescence) and subtracted from the values recorded during the experiment. Experimental values were normalized by dividing all fluorescence values by the fluorescence measured before the addition of 0.1 mM $MnCl_2$, such that the maximum value was 1 and the minimum value was 0. The quenching rate was estimated from the slope of the change in the normalized fluorescence (fluorescence units s^{-1}). It was calculated by linear regression of the data obtained during the 60 s preceding (Mn^{2+} influx in resting preparation) and the 60 s following (Mn^{2+} influx in depolarized preparation) the change to the 67 mM KCl solution.

Drugs

Fura-2 acetoxymethyl ester (Fura-2 AM) and ionomycin were obtained from Boehringer Mannheim. Verapamil was obtained from Sigma, a millimolar stock solution was prepared in water. N^{ω}-nitro-L-arginine and 8-bromo-cyclic GMP were from Sigma, they were dissolved directly in physiological or depolarizing solutions.

Statistical analysis

Results of the experiments are expressed as means ± standard error (s.e.mean). Tests of significance have been made using Student's paired or unpaired *t* test, or by analysis of variance (ANOVA), when comparisons involved more than two groups. *P* values smaller than 0.05 were considered significant.

Results

Effects of verapamil and BrcGMP on contractile tension and $[Ca^{2+}]_{cyt}$

The $[Ca^{2+}]_{cyt}$ of fura-2 loaded rat aortae was measured in rings without endothelium (mechanically rubbed), in the presence of L-NOARG. The preparations were mounted in the organ chamber, in physiological solution. After 3 min they were stimulated with a 67 mM KCl solution for 3 min. The physiological solution was then readmitted in the bath and, after 7 min, the fluorescence was measured; the $[Ca^{2+}]_{cyt}$ estimated from this fluorescence value was considered as resting $[Ca^{2+}]_{cyt}$. The rings were then further stimulated by the 67 mM KCl solution and fluorescence as well as contractile tension were measured up to 5 min after the beginning of this second stimulation. Matched preparations had been pretreated for 30 min at the end of the fura-2 loading period with verapamil (0.1 μM) and/or BrcGMP (0.1 mM–1 mM).

The resting $[Ca^{2+}]_{cyt}$ measured in physiological solution after the first KCl-stimulation of the muscle was not significantly different between untreated rings and rings treated either with verapamil (0.1 μM), BrcGMP (0.1 and 1 mM) or both (Table 1). Stimulation of the artery rings with the 67 mM KCl solution evoked an increase in $[Ca^{2+}]_{cyt}$ ($\Delta[Ca^{2+}]_{cyt}$) and in contractile tension. As illustrated in Figure 1, the increase in $[Ca^{2+}]_{cyt}$ reached a maximum value after 46 ± 4 s ($n = 50$). The development of muscle tone typically showed a fast and a slow component. In order to quantify the action of the various treatments, Ca^{2+} signals and muscle tone were measured at two time points: (1) the time of the first peak of the Ca^{2+} signal, usually occurring between 20 and 70 s after exposure to the high K^+ solution; (2) 5 min after exposure to the high K^+ solution, a time needed to reach the steady state of the contractile response. As shown in Figure 1, verapamil (0.1 μM) similarly inhibited the increase in $[Ca^{2+}]_{cyt}$ and in tension evoked by the KCl-solution. BrcGMP (0.1 mM–1 mM) produced a marked inhibition of the contractile response evoked by the high KCl solution and only a slight depression of the Ca^{2+} signal.

When preparations were treated with both 0.1 mM BrcGMP and 0.1 μM verapamil, the contractile tension was almost completely abolished while the $\Delta[Ca^{2+}]_{cyt}$ was not significantly different from the response measured in the presence of verapamil alone (Table 1).

These observations suggested that BrcGMP decreased the contractile response without markedly affecting the increase in $[Ca^{2+}]_{cyt}$, and thus could change the $[Ca^{2+}]_{cyt}$/tension relationship. We further tested this hypothesis by measuring the contractile tension and the $[Ca^{2+}]_{cyt}$ in preparations exposed to increasing concentrations of extracellular Ca^{2+} in 100 mM KCl solution, which maintains the membrane potential at a constant depolarized level. Figure 2 illustrates the relationship between $[Ca^{2+}]_o$ and either the contractile tension or $[Ca^{2+}]_{cyt}$. In 0.1 mM BrcGMP-treated rings, the $[Ca^{2+}]_o$-contraction curve was significantly shifted to the right compared to untreated rings. The threshold of $[Ca^{2+}]_o$ needed to obtain a contraction was increased by a factor of ten and 3 mM $CaCl_2$ in the bath produced a contraction equal to only 25% of the response recorded in the absence of BrcGMP. In contrast, the increase in $[Ca^{2+}]_{cyt}$ evoked by increasing $[Ca^{2+}]_o$ was hardly affected by BrcGMP. As a result, the $[Ca^{2+}]_{cyt}$-tension relation was clearly depressed by BrcGMP (0.1 mM), as illustrated in Figure 3.

Effects of verapamil and BrcGMP on $^{45}Ca^{2+}$ influx

Aortic segments were incubated for 30 min in physiological solution in the presence of 0.1 mM L-NOARG, and in the absence or presence of verapamil and/or BrcGMP. Thereafter, they were transferred, for 2 min, either in a physiological solution, or in a 100 mM KCl depolarizing solution, both containing $^{45}Ca^{2+}$. Figure 4 shows the effects of 0.1 μM verapamil and 0.1 mM BrcGMP on $^{45}Ca^{2+}$ influx. In aortic rings bathed in physiological solution, $^{45}Ca^{2+}$ influx

Table 1 Effects of BrcGMP and verapamil on resting $[Ca^{2+}]_{cyt}$, on $\Delta[Ca^{2+}]_{cyt}$ and contraction evoked by 67 mM KCl-solution

	Resting $[Ca^{2+}]_{cyt}$ (nM)	*$\Delta[Ca^{2+}]_{cyt}$* (nM)		*Contraction* (mN)	
		Peak	*5 min*	*Peak*	*5 min*
Untreated ($n = 16$)	98.0 ± 11.6	110.2 ± 7.4	100.9 ± 5.0	12.2 ± 1.1	19.9 ± 1.3
BrcGMP 0.1 mM ($n = 8$)	85.5 ± 9.6	81.5 ± 9.7*	88.0 ± 10.2	5.8 ± 1.1**	7.8 ± 1.1**
BrcGMP 1 mM ($n = 10$)	84.2 ± 8.1	85.4 ± 8.5*‡‡	82.5 ± 8.8*‡	4.0 ± 0.6**	4.5 ± 0.6**
Verapamil 0.1 μM ($n = 8$)	92.0 ± 12.0	53.2 ± 5.3**†	54.6 ± 4.4**††	3.1 ± 0.5**	7.1 ± 1.2**
Verapamil 0.1 μM + BrcGMP 0.1 mM ($n = 8$)	95.3 ± 14.1	37.2 ± 5.9**††	45.8 ± 5.8**††	0.3 ± 0.2**††	0.7 ± 0.3**††‡‡

$\Delta[Ca^{2+}]_{cyt}$ and contraction were measured simultaneously at the peak time of $[Ca^{2+}]_{cyt}$ (46 ± 4 s, see also text) and at 5 min after the stimulation with the KCl-solution. The number of preparations for each group is given in parentheses.
*$P<0.05$, **$P<0.01$, vs. untreated; †$P<0.05$, ††$P<0.01$, vs. BrcGMP 0.1 mM; ‡$P<0.05$, ‡‡$P<0.01$, vs. verapamil 0.1 μM; ANOVA.

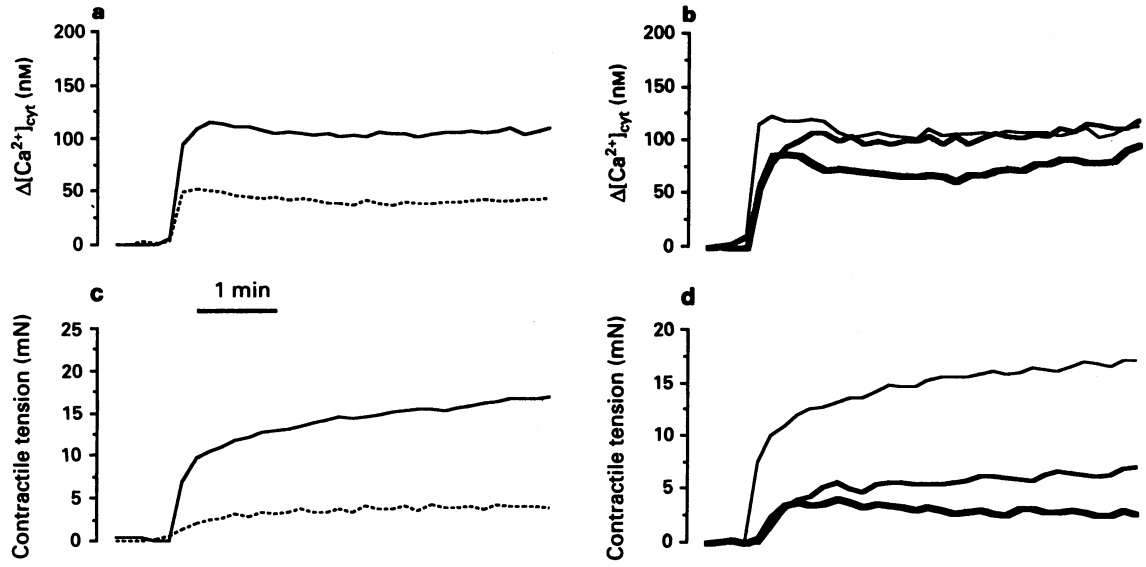

Figure 1 Effects of verapamil (0.1 μM) and BrcGMP (0.1–1 mM) on 67 mM KCl-stimulated calcium signals ($\Delta[Ca^{2+}]_{cyt}$; a, b) and contractile tension (c, d). (a, c) Solid line: untreated preparation; dashed line: 0.1 μM verapamil-treated preparation. (b, d) Thin line: untreated preparation; thicker line: 0.1 mM BrcGMP-treated preparation; thickest line: 1mM BrcGMP-treated preparation. Corresponding averaged values (from 8–16 different preparations) are shown in Table 1.

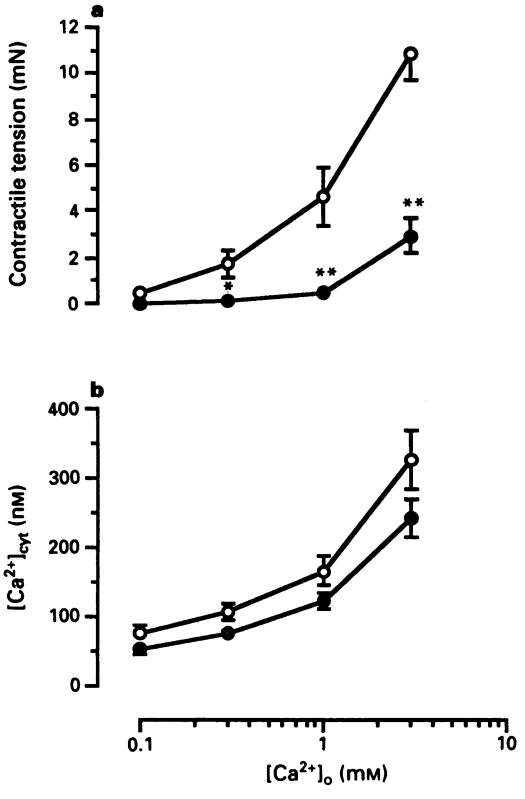

Figure 2 Effects of cumulative increases of extracellular calcium concentrations ($[Ca^{2+}]_o$) on contractile tension (a) and $[Ca^{2+}]_{cyt}$ (b), in untreated (○) and 0.1 mM BrcGMP-treated (●) rings. The preparations were incubated in Ca^{2+}-free solution for 15 min at room temperature, followed by 10 min at 37°C in a Ca^{2+}-free 100 mM KCl solution, before increasing the extracellular Ca^{2+} concentration. Values are expressed as mean ± s.e.mean from 7 rings. In some cases s.e.mean did not exceed the size of the symbol. $*P<0.05$, $**P<0.01$; Student's unpaired t test.

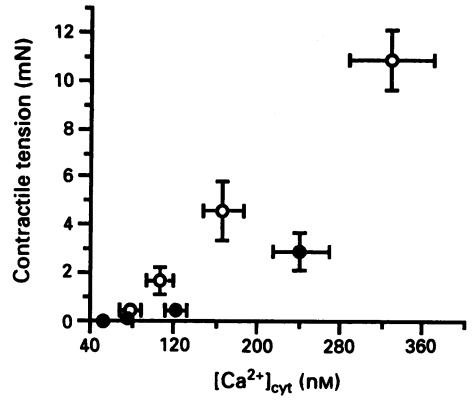

Figure 3 $[Ca^{2+}]_{cyt}$-tension relationship in untreated (○) and 0.1 mM BrcGMP-treated (●) rings, from data of Figure 2.

was slightly but significantly reduced in the presence of BrcGMP to 77.7 ± 6.4% of its value in untreated rings ($P<0.01$, ANOVA). $^{45}Ca^{2+}$ influx in physiological solution was unaffected by 0.1 μM verapamil (89.5 ± 7.7% of the value in untreated preparations; $P=0.28$). The combination of verapamil and BrcGMP reduced $^{45}Ca^{2+}$ influx to 74.9 ± 11.9% of its value in untreated rings ($P<0.05$). Incubation of aortic rings in 100 mM KCl-solution markedly increased the $^{45}Ca^{2+}$ influx. In KCl-depolarized aortic rings, verapamil significantly inhibited the total $^{45}Ca^{2+}$ influx to 76.6 ± 4.4% of the value measured in untreated preparations ($P<0.01$), which corresponds to an inhibition of 44.6% of the KCl-evoked stimulation of $^{45}Ca^{2+}$ influx, obtained after subtraction of the basal $^{45}Ca^{2+}$ influx measured in physiological solution. BrcGMP did not affect $^{45}Ca^{2+}$ influx in the KCl-solution, in the presence or in the absence of verapamil. Increasing the concentration of BrcGMP to 1 mM did not induce an inhibition of the K^+-stimulated $^{45}Ca^{2+}$ influx which was equal to 103.1 ± 8.7% ($n=5$) of the value obtained in the absence of BrcGMP.

Effects of verapamil and BrcGMP on the quenching rate of fura-2 and the contractile response evoked by Mn^{2+}

Fura-2 loaded aortic rings were first incubated for 5 min in a zero Ca^{2+} physiological solution (containing 0.1 mM EGTA). The addition of 0.1 mM $MnCl_2$ to the bath slightly enhanced the quenching rate of fura-2 fluorescence. When the K^+ concentration in the bath was increased to 67 mM, the quen-

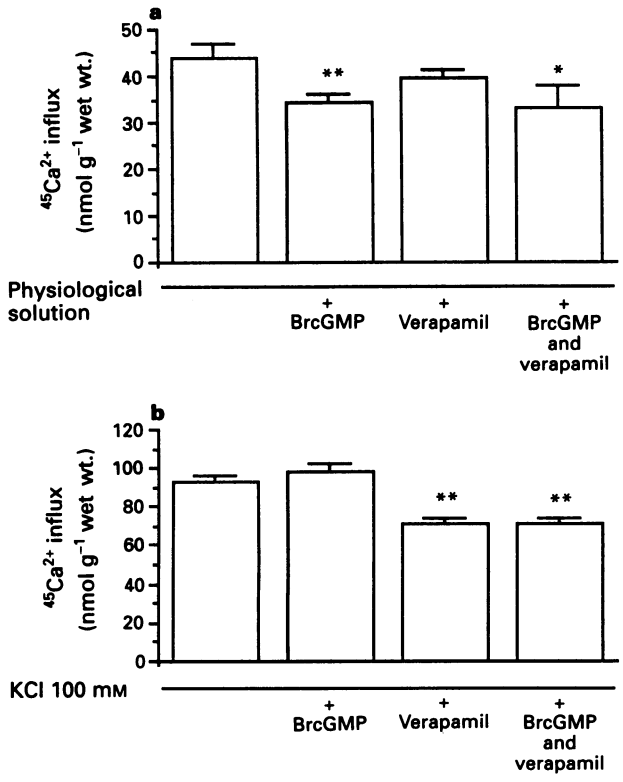

Figure 4 Effects of 0.1 mM BrcGMP and 0.1 μM verapamil on $^{45}Ca^{2+}$ influx in rat aorta. Aortic segments were incubated for 30 min in physiological solution in the presence of 0.1 mM N^{ω}-nitro-L-arginine (L-NOARG) and in the absence or in the presence of 0.1 mM BrcGMP and/or 0.1 μM verapamil. Thereafter, they were transferred, for 2 min, either in a physiological solution (a), or in a 100 mM KCl depolarizing solution (b), both containing $^{45}Ca^{2+}$. Each value is the mean with s.e.mean from 6–17 aortic segments. *$P<0.05$, **$P<0.01$ vs. untreated preparations; ANOVA.

ching rate of the fluorescence rapidly increased and a contractile response was recorded. As shown in Figure 5, BrcGMP (1 mM) did not affect the slope of the fluorescence decay in 67 mM KCl, whereas it strongly inhibited the contractile response. Verapamil concentration-dependently inhibited both the KCl-evoked increase in the rate of fluorescence decay and the contractile response evoked by $MnCl_2$ in KCl-solution (Figure 6). A high concentration of verapamil (10 μM) abolished both responses. Figure 7 illustrates the mean effect of BrcGMP and verapamil on the quenching rate and on the contractile response evoked by Mn^{2+} in several K^+-depolarized preparations. Those treatments did not significantly affect the quenching rate measured in physiological solution.

Discussion

The present results show that the inhibitory effect of BrcGMP on K^+-evoked contraction was stronger than its effect on the fura-2 Ca^{2+} signal; moreover, the lowering of $[Ca^{2+}]_{cyt}$ resulting from BrcGMP-treatment in K^+-depolarized preparations was neither associated with an inhibition of $^{45}Ca^{2+}$ influx nor with an inhibition of Mn^{2+} entry, while they were inhibited by verapamil, an inhibitor of voltage-dependent L-type calcium channels (Godfraind *et al.*, 1986), suggesting that BrcGMP does not affect voltage-dependent calcium channel gating. Various cyclic GMP-dependent mechanisms affecting $[Ca^{2+}]_{cyt}$ have been reported: (1) phosphorylation of phospholamban with consequent activation of the Ca^{2+}-ATPase of the endoplasmic reticulum (Cornwell *et al.*, 1991); (2) phosphorylation of the PI-kinase (Vrolix *et al.*, 1988) or of a 240 kDa protein (Yoshida *et al.*, 1991) with consequent activation of the Ca^{2+}-ATPase of plasma membrane; (3) activation of the Na^+/Ca^{2+} exchange (Furukawa *et al.*, 1991); (4) inhibition of voltage-dependent L-type calcium channels (Ishikawa *et al.*, 1993; Lorenz *et al.*, 1994). The measurement of the rate of fura-2 quenching by Mn^{2+} is a direct estimate of Mn^{2+} influx, which has been

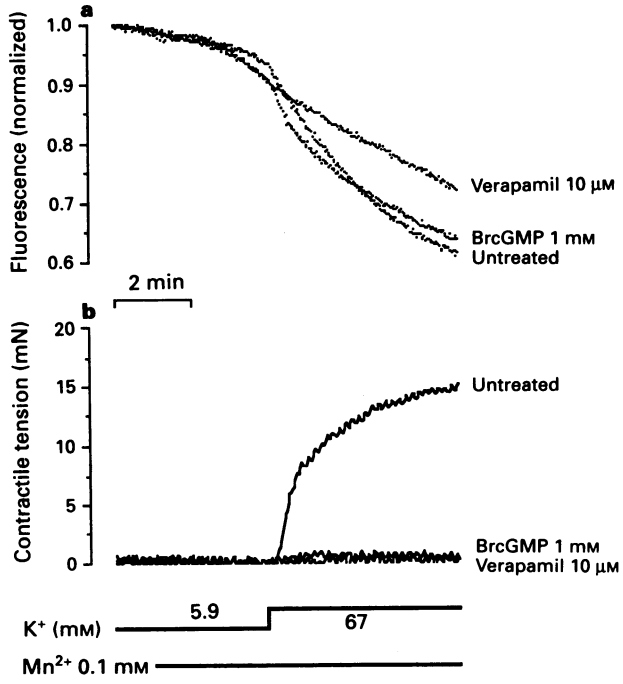

Figure 5 Effects of 1 mM BrcGMP and 10 μM verapamil on Mn^{2+}-induced quenching of 363 nm fura-2 fluorescence (a; ordinate scale: normalized fluorescence units) and Mn^{2+}-induced contraction (b) after 67 mM KCl-stimulation. Fluorescence was normalized by subtracting the autofluorescence from each measurement and dividing by the fluorescence value measured before the addition of $MnCl_2$.

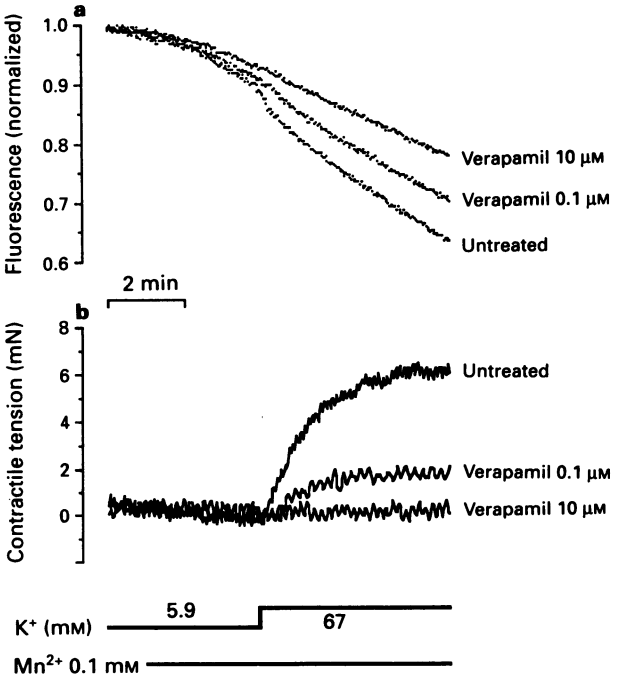

Figure 6 Effects of verapamil (0.1 μM and 10 μM) on Mn^{2+}-induced quenching of 363 nm fura-2 fluorescence (a; ordinate scale: normalized fluorescence units) and Mn^{2+}-induced contraction (b) after 67 mM KCl-stimulation. Fluorescence was normalized by subtracting the autofluorescence from each measurement and dividing by the fluorescence value measured before the addition of $MnCl_2$.

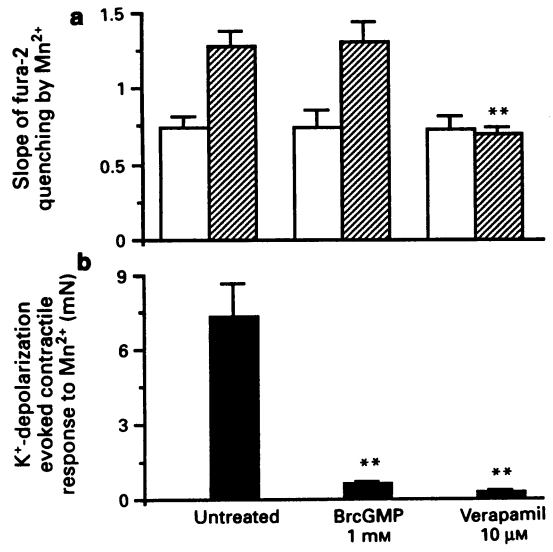

Figure 7 Effects of verapamil and BrcGMP on the quenching rate of fura-2 and the contractile response evoked by Mn^{2+}. Means ± s.e.mean (from 4–8 different preparations) of slopes of fura-2 quenching by Mn^{2+} (a; ordinate scale: 10^{-3} normalized fluorescence units/s) and of contractile responses to Mn^{2+} (b), in preparations depolarized by 67 mM KCl and treated or not with BrcGMP (1 mM) or verapamil (10 μM). After addition of 0.1 mM $MnCl_2$ to the bath, 363-nm fluorescence was measured at 2 s intervals; it was then normalized by subtracting from each measurement the autofluorescence and dividing by the fluorescence value measured before the addition of $MnCl_2$. Slope of change in normalized fluorescence was calculated by linear regression of data from the 60 s preceding (open columns: Mn^{2+} influx in resting preparation) and the 60 s following (hatched columns: Mn^{2+} influx in depolarized preparation) the change to the 67 mM KCl solution. $^{**}P<0.01$ vs. untreated preparations; ANOVA.

reported to occur through voltage-dependent Ca^{2+} channels (Chen & Van Breemen, 1993). Mn^{2+} influx was sensitive to verapamil but not to BrcGMP. Thus, the reduction of the fura-2 Ca^{2+} signal observed in BrcGMP-treated preparations depolarized by KCl cannot be ascribed to an inhibition of Ca^{2+} influx through voltage-dependent Ca^{2+} channels, but it is likely to result from a stimulation of Ca^{2+} sequestration into sarcoplasmic reticulum (SR) by cyclic GMP-dependent kinases activated processes, a view consistent with the absence of effect of BrcGMP on $^{45}Ca^{2+}$ uptake.

The present observations confirm the results reported earlier by Godfraind (1986) and by Collins *et al.* (1988) showing that BrcGMP does not affect $^{45}Ca^{2+}$ influx stimulated by high K^+ solution in the rat aorta, but are at variance with the inhibition of the L-type Ca^{2+} current by BrcGMP observed in rabbit portal vein (Ishikawa *et al.*, 1993) and in A7r5 cells (Lorenz *et al.*, 1994; Blatter & Wier, 1994). This difference may be related to experimental conditions. For example, the enzymatic dispersion of cells has been shown to affect the properties of calcium channels (Feron *et al.*, 1992). Differences in the sensitivity to cyclic GMP could also arise from the existence of different subtypes of L-type Ca^{2+} channels, which are differentially expressed in dispersed and cultured cells and differentially regulated (Neveu *et al.*, 1994).

It has been reported (Karaki *et al.*, 1984) that sodium nitroprusside inhibits KCl-stimulated $^{45}Ca^{2+}$ influx in rat aorta; such an effect was not reproduced with BrcGMP in the present study, suggesting that it is unrelated to the stimulation of guanylate cyclase. This is consistent with the view that effects of NO and nitrocompounds (which are NO-donors) are only in part mediated by the increase of cellular cyclic GMP, and that some of them could be supported by direct interactions of NO with ionic channels (Bolotina *et al.*, 1994).

We observed that in resting tissues, deprived of functional endothelium, BrcGMP slightly reduced both the $^{45}Ca^{2+}$ influx and the $[Ca^{2+}]_{cyt}$ estimated by the fura-2 technique (with the latter technique, however, the effect of BrcGMP did not reach statistical significance). These effects could result from either a hyperpolarization (which decreases the probability of opening of voltage-dependent Ca^{2+} channels and so the $^{45}Ca^{2+}$ influx in resting preparations) or from an increase of Ca^{2+} sequestration and/or extrusion, by the mechanisms mentioned above. Krippeit-Drews *et al.* (1992) indeed showed that the spontaneous release of endothelium-derived relaxing factor (EDRF) hyperpolarizes rat aortic smooth muscle cells by 4–6 mV and that the blockade of the NO-synthase activity by L-NOARG, which lowers membrane potential in resting aortic rings, induces an increase in the basal $^{45}Ca^{2+}$ influx. The hyperpolarizing effect of NO could be mediated by a cyclic GMP-dependent protein kinase activation of Ca^{2+}-dependent K^+ channels (Robertson *et al.*, 1993; Taniguchi *et al.*, 1993). However, at variance with the effect of NO, a hyperpolarizing effect of BrcGMP has not been detected in rat aortic smooth muscle with intact functional endothelium (Vanheel *et al.*, 1994). Thus, the cause of the reduction of $^{45}Ca^{2+}$ influx in physiological solution by BrcGMP remains to be elucidated.

The major finding of the present study was that the effect of BrcGMP on the contraction evoked by high KCl solution was not related to its effect on $[Ca^{2+}]_{cyt}$ and that BrcGMP modified the relationship between $[Ca^{2+}]_{cyt}$ and contraction. In contrast, verapamil produced an inhibition of the KCl-induced contraction and a decrease in $[Ca^{2+}]_{cyt}$ that were of the same level. This can be explained by a cyclic GMP-dependent decrease in the sensitivity of the contractile elements to Ca^{2+}, a conclusion consistent with the report by Nishimura & Van Breemen (1989) in α-toxin permeabilized mesenteric artery. These findings are also consistent with the report by Karaki *et al.* (1988) who showed that sodium nitroprusside, a NO donor that stimulates cyclic GMP production, affects the $[Ca^{2+}]_{cyt}$-tension relationship for KCl-induced contractions in rat aorta.

It is noteworthy that, in depolarized preparations, BrcGMP inhibited Mn^{2+}-evoked contraction (in zero Ca^{2+}, 0.1 mM EGTA) as well as it did with Ca^{2+}-evoked contraction. The mechanism of Mn^{2+}-evoked contraction in smooth muscle has not been completely elucidated. It seems to involve the direct stimulation of actomyosin ATPase activity and acts independently of myosin light chain phosphorylation (Hoar & Kerrick, 1988). Thus, the inhibitory effect of BrcGMP on Mn^{2+}-evoked contraction could probably not be accounted for by an effect on myosin light chain phosphorylation. Whether or not such a conclusion could also be extended to Ca^{2+}-evoked contraction remains a matter of speculation.

In summary, the present results show that in contrast to verapamil, the inhibition of contractile tension by BrcGMP cannot be related to a calcium channel blocking mechanism, but to a modification of the relationship between $[Ca^{2+}]_{cyt}$ and contraction. Furthermore, because the reduction of K^+ depolarization-dependent $^{45}Ca^{2+}$ influx reported by Karaki *et al.* (1984) with sodium nitroprusside was not observed with BrcGMP, it is likely that this drug has additional mechanisms of action, unrelated to a rise in cyclic GMP.

This work was supported by a grant of the Fonds National de la Recherche Scientifique (FRSM No. 3.4546.92 and No. 3.4597.93), a grant of the Bekales Fundation (1994) and by the Ministère de l'Education et de la Recherche Scientifique (grant Action Concertée No. 89/95-135). S.S. is Fellow of the Fonds du Développement Scientifique de l'Université Catholique de Louvain. The authors thank Dr M. Wibo for reading the manuscript and Mrs M. Leonardy and N. Bussy for their technical assistance.

References

BLATTER, L.A. & WIER, W.G. (1994). Nitric oxide decreases $[Ca^{2+}]_i$ in vascular smooth muscle by inhibition of the calcium current. *Cell Calcium*, **15**, 122–131.

BOLOTINA, V.M., NAJIBI, S., PALACINO, J.J., PAGANO, P.J. & COHEN, R.A. (1994). Nitric oxide directly activates calcium-dependent potassium channels in vascular smooth muscle. *Nature*, **368**, 850–853.

BRAUGHLER, J.J., MITTAL, C.K. & MURAD, F. (1979). Effects of thiols, sugars, and proteins on nitric oxide activation of guanylate cyclase. *J. Biol. Chem.*, **254**, 12450–12454.

CHEN, Q.C. & VAN BREEMEN, C. (1993). The superficial buffer barrier in venous smooth muscle: sarcoplasmic reticulum refilling and unloading. *Br. J. Pharmacol.*, **109**, 336–343.

COLLINS, P., HENDERSON, A.H., LANG, D. & LEWIS, M.J. (1988). Endothelium-derived relaxing factor and nitroprusside compared in noradrenaline- and K^+-contracted rabbit and rat aortae. *J. Physiol.*, **400**, 395–404.

CORNWELL, T.L., PRYZWANSKY, K.B., WYATT, T.A. & LINCOLN, T.M. (1991). Regulation of the sarcoplasmic reticulum protein phosphorylation by localized cyclic GMP-dependent protein kinase in vascular smooth muscle cells. *Mol. Pharmacol.*, **40**, 923–931.

DIETRICH, H.H., KIMURA, M. & DACEY, JR, R.G. (1994). N^{ω}-nitro-L-arginine constricts cerebral arterioles without increasing intracellular calcium levels. *Am. J. Physiol.*, **266**, H1681–H1686.

FEELISCH, M. & KELM, M. (1991). Biotransformation of organic nitrates to nitric oxide by vascular smooth muscle and endothelial cells. *Biochem. Biophys. Res. Commun.*, **180**, 286–293.

FERON, O., WIBO, M., CHRISTEN, M.O. & GODFRAIND, T. (1992). Interaction of pinaverium (a quaternary ammonium compound) with 1,4-dihydropyridine binding sites in rat ileum smooth muscle. *Br. J. Pharmacol.*, **105**, 480–484.

FURUKAWA, K.I., OHSHIMA, N., TAWADA-IWATA, Y. & SHIGEKAWA, M. (1991). Cyclic GMP stimulates Na^+/Ca^{2+} exchange in vascular smooth muscle cells in primary culture. *J. Biol. Chem.*, **266**, 12337–12341.

GODFRAIND, T. (1976). Calcium exchange in vascular smooth muscle, action of noradrenaline and lanthanum. *J. Physiol.*, **260**, 21–35.

GODFRAIND, T. (1986). EDRF and cyclic GMP control gating of receptor-operated calcium channels in vascular smooth muscle. *Eur. J. Pharmacol.*, **126**, 341–343.

GODFRAIND, T., MILLER, R.C. & WIBO, M. (1986). Calcium antagonisms and calcium entry blockade. *Pharmacol. Rev.*, **38**, 321–416.

GRYNKIEWICZ, G., POENIE, M. & TSIEN, R.Y. (1985). A new generation of Ca^{2+} indicators with greatly improved fluorescence properties. *J. Biol. Chem.*, **260**, 3440–3450.

GUPTA, S., MCARTHUR, C., GRADY, C. & RUDERMAN, N.B. (1994). Stimulation of vascular Na^+-K^+-ATPase activity by nitric oxide: a cGMP-independent effect. *Am. J. Physiol.*, **266**, H2146–H2151.

HOAR, P.E. & KERRICK, W.G.L. (1988). Mn^{2+} activates skinned smooth muscle cells in the absence of myosin light chain phosphorylation. *Pflügers Arch.*, **412**, 225–230.

IGNARRO, L.J. (1989). Endothelium-derived nitric oxide: actions and properties. *FASEB J.*, **3**, 31–36.

ISHIKAWA, T., HUME, J.R. & KEEF, K.D. (1993). Regulation of Ca^{2+} channels by cAMP and cGMP in vascular smooth muscle cells. *Circ. Res.*, **73**, 1128–1137.

KARAKI, H., NAKAGAWA, H. & URAKAWA, N. (1984). Comparative effects of verapamil and sodium nitroprusside on contraction and ^{45}Ca uptake in the smooth muscle of rabbit aorta, rat aorta and guinea-pig taenia coli. *Br. J. Pharmacol.*, **81**, 393–400.

KARAKI, H., SATO, K., OZAKI, H. & MURAKAMI, K. (1988). Effects of sodium nitroprusside on cytosolic calcium level in vascular smooth muscle. *Eur. J. Pharmacol.*, **156**, 259–266.

KRIPPEIT-DREWS, P., MOREL, N. & GODFRAIND, T. (1992). Effect of nitric oxide on membrane potential and contraction of rat aorta. *J. Cardiovasc. Pharmacol.*, **20**, S72–S75.

LORENZ, J.N., BIELEFELD, D.R. & SPERELAKIS, N. (1994). Regulation of calcium channel current in A7r5 vascular smooth muscle cells by cyclic nucleotides. *Am. J. Physiol.*, **266**, C1656–C1663.

MCDANIEL, N.L., CHEN, X.L., SINGER, H.A. MURPHY, R.A. & REMBOLD, C.M. (1992). Nitrovasodilators relax arterial smooth muscle by decreasing $[Ca^{2+}]_i$ and uncoupling stress from myosin phosphorylation. *Am. J. Physiol.*, **263**, C461–C467.

MOORE, P.K., AL-SWAYE, O.A., CHONG, N.W.S., EVANS, R.A. & GIBSON, A. (1990). L-N^G nitroarginine (L-NOARG), a novel, L-arginine-reversible inhibitor of endothelium-dependent vasodilatation *in vitro*. *Br. J. Pharmacol.*, **99**, 408–412.

MULSCH, A. & BUSSE, R. (1990). N^G-nitro-L-arginine (N5-[imino (nitroamino) methyl]-L-ornithine) impairs endothelium-dependent dilations by inhibiting cytosolic nitric oxide synthesis from L-arginine. *Naunyn-Schmied. Arch. Pharmacol.*, **341**, 143–147.

NEVEU, D., QUIGNARD, J.F., FERNANDEZ, A., RICHARD, S. & NARGEOT, J. (1994). Differential β-adrenergic regulation and phenotypic modulation of voltage-gated calcium currents in rat aortic myocytes. *J. Physiol.*, **479**, 171–182.

NISHIMURA, J. & VAN BREEMEN, C. (1989). Direct regulation of smooth muscle contractile elements by second messengers. *Biochem. Biophys. Res. Commun.*, **163**, 929–935.

PALMER, R.M.J., FERRIGE, A.G. & MONCADA, S. (1987). Nitric oxide release accounts for the biological activity of endothelium-derived relaxing factor. *Nature*, **327**, 524–526.

PFITZER, G., MERKEL, L., RÜEGG, J.C. & HOFMANN, F. (1986). Cyclic GMP-dependent protein kinase relaxes skinned fibers from guinea-pig taenia coli but not from chicken gizzard. *Pflügers Arch.*, **407**, 87–91.

RAPOPORT, R.M. & MURAD, F. (1983). Agonist induced endothelium-dependent relaxation in rat thoracic aorta may be mediated through cGMP. *Circ. Res.*, **52**, 352–357.

ROBERTSON, B.E., SCHUBERT, R., HESCHELER, J. & NELSON, M.T. (1993). cGMP-dependent protein kinase activated Ca-activates K channels in cerebral artery smooth muscle cells. *Am. J. Physiol.*, **265**, C299–C303.

SCHMIDT, H.H.H.W., LOHMANN, S.M. & WALTER, U. (1993). The nitric oxide and cGMP signal transduction system: regulation and mechanism of action. *Biochim. Biophys. Acta*, **1178**, 153–175.

SEKHAR, K.R., HATCHETT, R.J., SHABB, J.B., WOLFE, L., FRANCIS, S.H., WELLS, J.N., JASTORFF, B., BUTT, E., CHAKINALA, M.M. & CORBIN, J.D. (1992). Relaxation of pig coronary arteries by new and potent cGMP analogs that selectively activate type Iα, compared with type Iβ, cGMP-dependent protein kinase. *Mol. Pharmacol.*, **42**, 103–108.

TANIGUCHI, J., FURUKAWA, K.I. & SHIGEKAWA, M. (1993). Maxi K^+ channels are stimulated by cyclic guanosine monophosphate-dependent protein kinase in canine coronary artery smooth muscle cells. *Pflügers Arch.*, **423**, 167–172.

VANHEEL, B., VAN DE VOORDE, J. & LEUSEN, I. (1994). Contribution of nitric oxide to the endothelium-dependent hyperpolarization in rat aorta. *J. Physiol.*, **475**, 277–284.

VROLIX, M., RAEYMAEKERS, L., WUYTACK, F., HOFMANN, F. & CASTEELS, R. (1988). Cyclic GMP-dependent protein kinase stimulates the plasmalemmal Ca^{2+} pump of smooth muscle via phosphorylation of phosphatidylinositol. *Biochem. J.*, **255**, 855–863.

YOSHIDA, Y., SUN, H.T., CAI, J.Q. & IMAI, S. (1991). Cyclic GMP-dependent protein kinase stimulates the plasma membrane Ca^{2+} pump ATPase of vascular smooth muscle via phosphorylation of a 240 kDa protein. *J. Biol. Chem.*, **266**, 19819–19825.

(Received October 14, 1994
Revised January 11, 1995
Accepted January 13, 1995)

British Journal of Pharmacology (1995) 114, 1738–1744 © 1995 Stockton Press All rights reserved 0007–1188/95 $12.00

Actions of the novel neuroprotective agent, lifarizine (RS-87476), on voltage-dependent sodium currents in the neuroblastoma cell line, N1E-115.

Joseph G. McGivern, Leslie Patmore & [1]Robert D. Sheridan

Department of Pharmacology, Syntex Research Centre, Research Avenue South, Edinburgh EH14 4AP

1 The actions of the neuroprotective agent, lifarizine (RS-87476-190), on voltage-dependent Na^+ currents have been examined in the neuroblastoma cell line, N1E-115, using the whole-cell variant of the patch clamp technique.

2 At a holding potential of −80 mV, lifarizine reduced the peak Na^+ current evoked by a 10 ms depolarizing step with an IC_{50} of 1.3 μM. At holding potentials of −100 and −60 mV the IC_{50} concentrations of lifarizine were 7.3 μM and 0.3 μM, respectively.

3 At a holding potential of −100 mV, most channels were in the resting state and the IC_{50} value for inhibition of Na^+ current should correspond to the dissociation constant of lifarizine for resting channels (K_R). K_R was therefore estimated to be 7.3 μM.

4 In the absence of lifarizine, recovery from inactivation following a 20 s depolarization from −100 mV to 0 mV was complete within 2 s. However, in the presence of 3 μM lifarizine recovery took place in a biexponential fashion with time constants of 7 s and 79 s.

5 Lifarizine (1 μM) had no effect on steady-state inactivation curves when conditioning pre-pulses of 1 s duration were used. However, when pre-pulse durations of 1 min were used the curves were shifted to the left by lifarizine by about 10 mV. Analysis of the shifts induced by a range of lifarizine concentrations revealed that the apparent affinity of lifarizine for the inactivated state of the channel (K_I) was 0.19 μM.

6 Lifarizine (1 μM) had no effect on chloramine-T-modified Na^+ currents, suggesting no significant open channel interaction.

7 Taken together, these data show that lifarizine is a potent voltage-dependent inhibitor of Na^+ currents in N1E-115 cells and that the voltage-dependence arises from an interaction of the compound with the inactivated state of the channel. The possible contribution of Na^+ current inhibition to the neuroprotective actions of lifarizine is discussed.

Keywords: Sodium currents; sodium channels; neuroblastoma; ion channels; neuroprotection; cerebral ischaemia; chloramine-T; lifarizine; RS-87476; N1E-115 cell line

Introduction

Considerable effort has been expended in recent years in the search for pharmacological interventions which might help to improve the clinical outcome following stroke (Alps, 1992; Lees, 1992). This search has led to a wide variety of chemically diverse agents which appear to exert neuroprotective actions in animal models of brain ischaemia, including, *N*-methyl-D-aspartate receptor/channel antagonists, inhibitors of glutamate release, 21-aminosteroids, gangliosides, nitric oxide synthase inhibitors, enhancers of GABA-ergic and adenosinergic neurotransmission and calcium entry blockers. Despite this variety, there is still no clinically proven treatment for acute stroke.

The diphenylpiperazine derivative, lifarizine (RS-87476-190; Figure 1), displays marked neuroprotective activity in both focal and global models of central nervous system ischaemia: rat 4-vessel occlusion (B.J. Alps, personal communication), rat 2-vessel occlusion (McBean *et al.*, 1995a), gerbil unilateral carotid artery occlusion (Brown *et al.*, 1993), mouse middle cerebral artery occlusion (C.M. Brown *et al.*, 1994), cat middle cerebral artery occlusion (Kucharczyk *et al.*, 1991) and rat rose Bengal model of focal cortical infarct (McBean *et al.*, 1995b). At the mechanistic level there is good evidence that the compound interacts with the voltage-dependent Na^+ channel. Thus, lifarizine antagonizes contractures induced by the Na^+ channel activator, veratrine, in chick cardiomyocytes ($IC_{50} = 1.6 \times 10^{-6}$ M; Patmore *et al.*, 1991) and inhibits rat neocortical neuronal cell death *in vitro* induced by exposure to the site 2 Na^+ channel toxin, veratridine ($IC_{50} = 3 \times 10^{-7}$ M; May *et al.*, 1995). Furthermore, lifarizine potently displaces the Na^+ channel ligand, [^{3}H]-batrachotoxin, from rat cortical synaptosomes ($IC_{50} = 5.5 \times 10^{-8}$ M; C.M. Brown *et al.*, personal communication). The present experiments were therefore performed in an effort to characterize the actions of lifarizine directly on voltage-dependent Na^+ currents. The mouse neuroblastoma clonal cell line, N1E-115, was used as the test system. Some of this work has already appeared in abstract form (Sheridan *et al.*, 1991; McGivern *et al.*, 1994a,b).

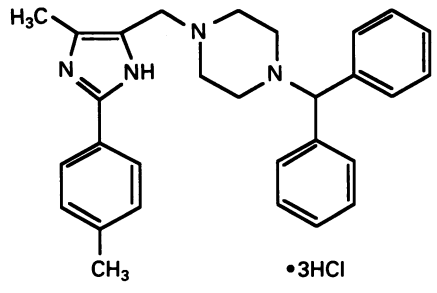

Figure 1 Structure of lifarizine: 1-[(2-(4-methylphenyl)-5-methyl)-1H-imidazol-4-yl-methyl]-4-diphenylmethyl-piperazine trihydrochloride.

[1] Author for correspondence.

Methods

Cell culture

N1E-115 mouse neuroblastoma cells (obtained from the European Collection of Animal Cell Cultures) were grown in 35 mm cell culture dishes. Cells were used between passages 20–45.

Electrophysiology

Voltage-dependent sodium currents were recorded from undifferentiated N1E-115 cells by use of conventional whole-cell voltage clamp techniques (Hamill *et al.*, 1981). Cells were clamped with an EPC-7 or EPC-7B patch clamp amplifier (List-electronic, Germany). Following attainment of the whole-cell configuration cells were clamped at the appropriate V_{hold} (see below) and Na^+ currents were evoked by 10 ms depolarizing steps to 0 mV at a frequency of 0.1 Hz. The currents usually took about 10 min to stabilize, during which time the series resistance compensation was optimized (achieving greater than 70% compensation in the majority of cases). Uncompensated series resistance was typically about 3 MΩ. The voltage clamp protocols used in these experiments were generated by computer (CED Voltage Clamp Software, Cambridge Electronic Design, U.K.) controlling a CED 1401 Laboratory Interface (Cambridge Electronic Design, U.K.). Whole-cell currents were low-pass filtered (5 kHz Bessel), digitized at 20 kHz (CED 1401) and stored on magnetic media for off-line analysis. Leak and capacitative current correction was performed by the voltage clamp software and consisted of subtracting the appropriately scaled current waveform produced by a 10 mV depolarizing step (from V_{hold}) from the current to be corrected. The experiments were conducted at room temperature (19 to 21°C).

Data analysis

The curve fitting procedures were performed by the method of least squares regression using KaleidaGraph (version 2.1; Abelbeck Software). Statistical comparisons of data groups were made using Student's paired or unpaired, 2-tailed *t* test. Concentration-effect curves describing the inhibition of Na^+ current by lifarizine were fitted to the following relation (Hill equation):

$$\text{normalized } Na^+ \text{ current} = 1 - \{1/(1 + (IC_{50}/[Lif])^{n_H})\} \quad (1)$$

where IC_{50} is the concentration of lifarizine ([Lif]) required to inhibit Na^+ current by 50%, and n_H is the Hill coefficient.

Affinity of lifarizine for resting Na^+ channels

The equilibrium dissociation constant of lifarizine for resting channels (K_R) was assumed to be the same as the IC_{50} concentration of lifarizine inhibiting Na^+ current at a V_{hold} of −100 mV (at which most channels are in the resting state).

Affinity of lifarizine for inactivated Na^+ channels

The shifts in the steady-state inactivation curves induced by a series of lifarizine concentrations were used to estimate the equilibrium dissociation constant of lifarizine for inactivated channels (K_I). A modification of the method of Bean *et al.* (1983) was employed. Bean *et al.* (1983) used the following relationship to derive K_I:

$$\Delta V_{half} = k.\ln\{(1 + [Lif]/K_R)/(1 + [Lif]/K_I)\} \quad (2)$$

where ΔV_{half} is the shift in the half-maximum inactivation point (i.e., $V_{half(control)} - V_{half(lifarizine)}$), k is the slope factor of the curve (taken as the 'global average' k from all experiments) and the other terms are as defined above. Thus, when the affinity of lifarizine for the resting state is very low (K_R very high) and lifarizine is present at its K_I concentration, then $\Delta V_{half} = k.\ln\{0.5\} = k. - 0.693$ mV (curve shifted to the left). Conversely, when K_I is very high (low affinity for the inactivated state) and lifarizine is present at its K_R concentration, then $\Delta V_{half} = k.\ln\{2\} = k. + 0.693$ mV (curve shifted to the right). By rearranging equation (2) and incorporating the Hill coefficient (n_H) we obtained the following relation:

$$\exp\{\Delta V_{half}/k\} = \{1 + ([Lif]/K_R)^{n_H}]/\{1 + ([Lif]/K_I)^{n_H}\} \quad (3)$$

This rearrangement allows the shift induced by lifarizine in each cell to be normalized by the slope of the steady-state inactivation curve obtained from that cell, thereby reducing the variability and enhancing the accuracy of the K_I determination. Inclusion of the Hill coefficient (n_H) was designed to improve the flexibility of the model.

Drug application

Lifarizine (dissolved in water) was added to the superfusate from concentrated stock solutions of either 10^{-2} or 10^{-3} M. In pilot experiments it was established that the response to lifarizine achieved equilibrium within 4–6 min superfusion. A drug application time of 10 min was therefore used throughout these experiments. Chloramine-T (0.5 M dissolved in water) was added to the superfusate to achieve a final concentration of 1 mM.

Drugs and solutions

All chemicals were obtained from Sigma (UK) unless otherwise specified. Lifarizine trihydrochloride (RS-87476-190; Figure 1) was synthesized by Syntex Discovery Research. The following solutions were used to isolate I_{Na} in the patch clamp experiments: pipette (in mM)–CsF 120, tetraethylammonium Cl 10, NaCl 10, $CaCl_2$ 1, $MgCl_2$ 1, EGTA 11, HEPES (free acid) 10, adjusted to pH 7.3. with CsOH (Aldrich-Chemie, Germany); extracellular–NaCl 145, KCl 3, $CaCl_2$ 1, $MgCl_2$ 1, $CdCl_2$ 0.5, HEPES (free acid) 10, D-glucose 5, adjusted to pH 7.3 with NaOH. Glass for the patch pipettes was obtained from the Garner Glass Co. (Claremont, CA, U.S.A.) and had tip diameters of about 2 μm after pulling, and resistances of about 1 MΩ after filling.

Results

Influence of V_{hold} on inhibition of Na^+ currents by lifarizine

The effect of lifarizine on Na^+ currents was investigated at 3 different holding potentials: −100, −80 and −60 mV. Currents were generated by 10 ms depolarizing steps to membrane potentials more positive than V_{hold}. A family of control sodium currents from a single N1E-115 cell held at −80 mV is shown in Figure 2a. In this cell 1 μM lifarizine reduced the peak current by nearly 50% (Figure 2b). The effect of 1 μM lifarizine on the average current/voltage relationship ($n = 3$ cells) at a V_{hold} of −80 mV is summarized Figure 2c.

The inhibitory potency of lifarizine could be altered by manipulating the potential at which the cells were held. The effects of lifarizine on the normalized current/voltage relationship for cells held at −100 mV ($n = 4$) and −60 mV ($n = 3$) are illustrated in Figure 3a and 3b, respectively.

The concentration-response curves shown in Figure 4 summarize the effects of lifarizine on the normalized peak Na^+ current obtained at the 3 different holding potentials. It was apparent that as the holding potential became increasingly less negative so the inhibitory potency of lifarizine increased ($IC_{50} = 7.3$, 1.3 and 0.3 μM at V_{hold}s of −100, −80 and −60 mV, respectively). This observation suggested that lifarizine interacted with the inactivated state of the Na^+ channel, and this was studied in more detail in subsequent experiments.

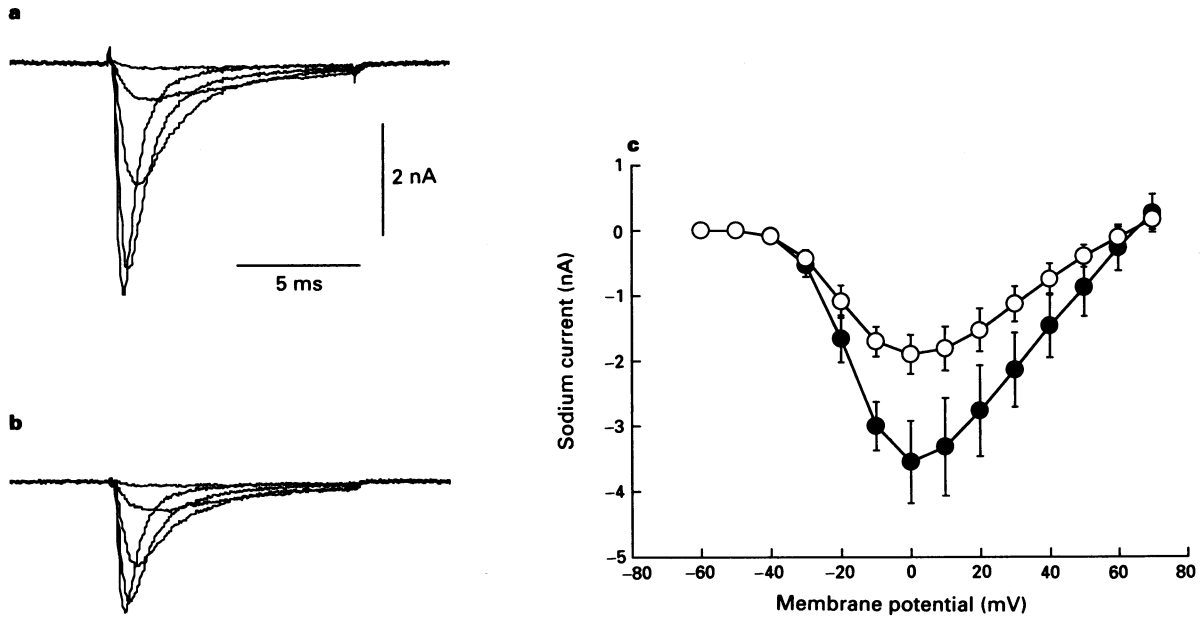

Figure 2 Families of Na^+ currents generated by a single N1E-115 cell from a holding potential of −80 mV in the absence (a) and presence (b) of 1 μM lifarizine applied for 10 min. (c) Current-voltage relationships in the absence (●) and presence (○) of 1 μM lifarizine (data points show the means ± s.e.mean for 3 N1E-115 cells).

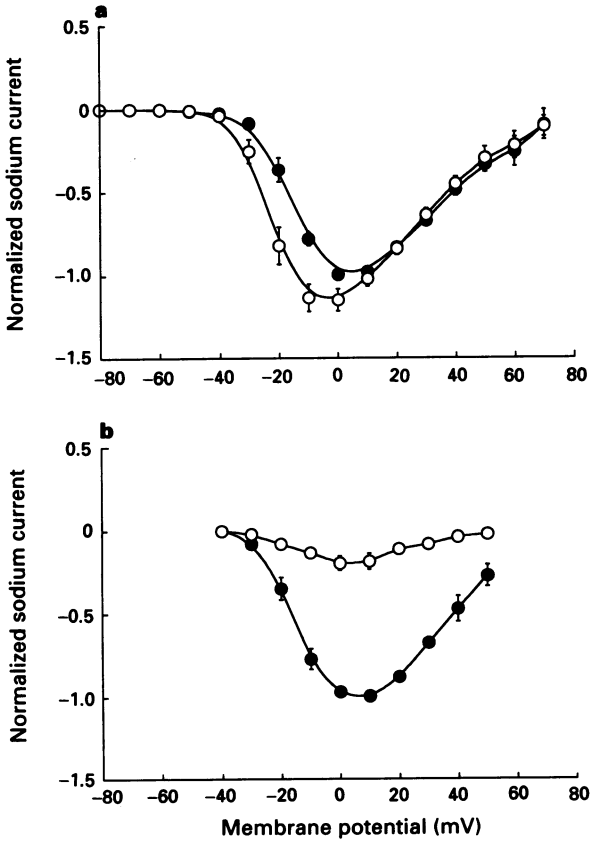

Figure 3 Current-voltage relationships generated by N1E-115 cells held at −100 mV (a; $n = 4$) and −60 mV (b; $n = 3$) in the absence (●) and presence (○) of 1 μM lifarizine applied for 10 min. The data points for each cell have been normalized to the peak control current amplitude for that cell and then averaged for all cells studied (data points are means ± s.e. mean). The slight increase in peak current and small leftward shift of the current/voltage recorded from a holding potential of −100 mV was artefactual, and was established in separate experiments (data not shown) to result from holding the cell at a very negative membrane potential for a prolonged period of time (about 30 min).

K_R *of lifarizine for the resting state*

The affinity of lifarizine for resting channels was estimated directly from experiments examining the inhibitory effects of lifarizine on Na^+ currents in cells held at −100 mV. At this very negative holding potential it may be assumed that most channels are in the resting state since the steady-state inactivation curve in untreated cells has apparently plateaued (see Figure 6). If a linear relationship is assumed between the occupancy by lifarizine of its binding site on the resting state channel and the degree of inhibition of the Na^+ current, then the IC_{50} value for inhibition of the current should be identical to the dissociation constant for resting channels (K_R). The value of K_R was therefore estimated to be 7.3 μM (i.e. the IC_{50} for lifarizine at a V_{hold} of −100 mV).

Voltage-dependent block by lifarizine

In cells held at −100 mV, application of 3 μM lifarizine for 10 min reduced the Na^+ current (evoked by 10 ms depolarizing steps to 0 mV at 0.1 Hz) to about 85% of the pre-drug control current. When the membrane potential was now clamped to a conditioning potential of 0 mV for 20 s, a test current evoked 2 s later by a 10 ms depolarization to 0 mV was reduced to about 10% of the pre-conditioning control current (averaged data from 2 cells shown in Figure 5). Furthermore, during subsequent test depolarizations at 0.1 Hz, the Na^+ current gradually recovered to the pre-conditioning control level with a biexponential time-course: $\tau_{fast} = 7$ s (representing 27% of the total) and $\tau_{slow} = 79$ s (representing 73%). In control cells recovery from inactivation was complete within 2 s (data not shown). These experiments (summarized in Figure 5) provided further evidence for an interaction of lifarizine with the inactivated state of the Na^+ channel.

Effect of lifarizine on steady-state inactivation

Steady-state inactivation curves were constructed by stepping the membrane potential from a V_{hold} of −80 mV to a series of pre-pulse potentials ranging from −100 to −20 mV. Immediately after the pre-pulse a 10 ms test pulse to 0 mV was made to probe the degree of channel inactivation induc-

ed during the pre-pulse. Steady-state inactivation curves were drawn by plotting the current evoked by the test pulse (normalized to the peak current amplitude) against the pre-pulse potential and fitting the data points to the Boltzmann function:

$$\text{normalized } I_{Na} = 1/\{1 + \exp[(V_{pre\text{-}pulse} - V_{half})/k]\}$$

where V_{half} is the membrane potential (mV) at which 50% of the channels are inactivated and k is the slope factor of the steady-state inactivation curve (mV per e-fold change in I_{Na}).

When pre-pulse durations of 1 s were used, lifarizine (1 μM) failed to affect either the V_{half} or k of the steady-state inactivation curve (Figure 6a; $V_{half(control)} = -64.2 \pm 3.7$ mV, $V_{half(lifarizine)} = -66.1 \pm 4.0$ mV ($P > 0.05$); $k_{(control} = 6.9 \pm 0.6$ mV/e-fold, $k_{(lifarizine)} = 7.0 \pm 0.4$ mV/e-fold ($P > 0.05$); $n = 3$ cells). However, when pre-pulse durations of 1 min were used, lifarizine (1 μM) induced a hyperpolarizing shift of the steady-state inactivation curve of about 10 mV (Figure 6b; $V_{half(control)} = -71.8 \pm 2.1$ mV, $V_{half(lifarizine)} = -81.1 \pm 1.4$ mV ($P < 0.002$); $k_{(control)} = 6.2 \pm 0.3$ mV/e-fold, $k_{(lifarizine)} = 6.4 \pm 0.1$ mV/e-fold ($P > 0.05$); $n = 5$ cells). This finding indicates either that lifarizine binds to a slowly inactivating state of the Na^+ channel or that the rate of association of lifarizine with the inactivated state is somewhat slow.

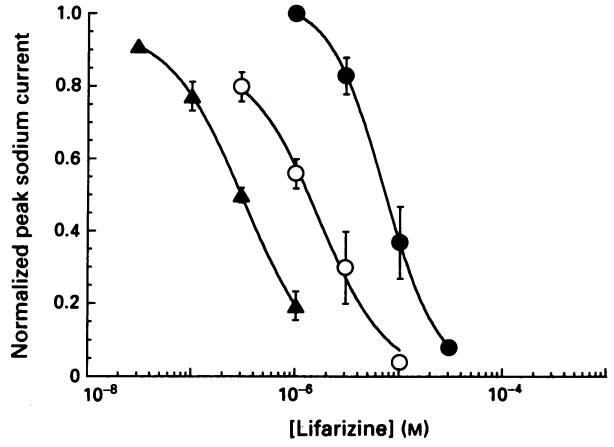

Figure 4 Concentration-response curves showing the effects of lifarizine on Na^+ currents generated from holding potentials of −60 mV (▲), −80 mV (○) and −100 mV (●). The IC_{50}s for inhibition of Na^+ currents at these three holding potentials were 0.3, 1.3 and 7.3 μM, respectively. Each data point represents the mean ± s.e. mean for 3 or more cells. Smooth curves were fitted according to the logistic function: $1-[1/(1 + (IC_{50}/[\text{lifarizine}])^{n_H})]$, where n_H is the Hill coefficient and IC_{50} is the concentration of lifarizine required to inhibit the normalized sodium current by 50%.

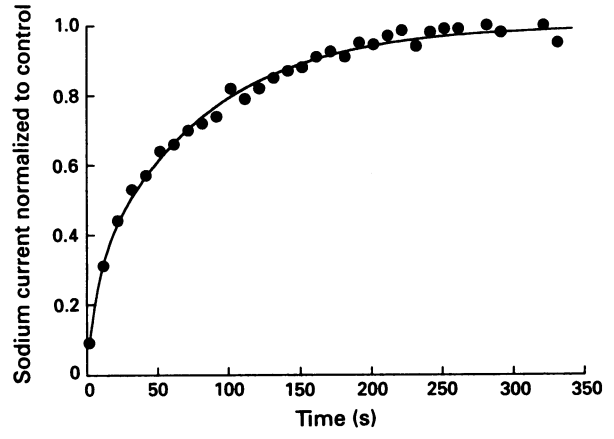

Figure 5 Recovery from voltage-dependent block in the presence of 3 μM lifarizine (average data from 2 N1E-115 cells). The data points were generated by stepping the membrane potential from the holding potential (−100 mV) to 0 mV for 20 s, returning to the holding potential and then evoking test currents by 10 ms steps to 0 mV. The first test current was evoked at 2 s, with subsequent test currents generated at intervals of 10 s. The data points were best described by a biexponential function (smooth curve) of the form: $n^*[a + b^*\{1 - \exp(-t/\tau_1)\}] + m^*[c + d^*\{1 - \exp(-t/\tau_2)\}]$, where a and c are the y axis intercepts of the two exponentials having time constants of τ_1 and τ_2, respectively, $(a + b)$ and $(c + d)$ give the respective asymptotes, and n and m give the relative proportions of τ_1 and τ_2. The times constants generated from a fit to this expression were: $\tau_1 = 7$ s (27%) and $\tau_2 = 79$ s (73%).

K_I of lifarizine for the inactivated state

The K_I of lifarizine for the inactivated state of the Na^+ channel was estimated by a modification of the method described by Bean et al. (1983). The estimation was based on quantification of the shifts in the steady-state inactivation curves (using 1 min pre-pulse durations) induced by different concentrations of lifarizine. Pre-pulse durations of 1 min were used to ensure equilibrium conditions as in pilot experiments the effects of lifarizine (0.1–3 μM) achieved apparent steady-state in less than 20 s.

Figure 7 shows a plot of $\exp(\Delta V/k)$ against the concentration of lifarizine (see Methods). A fit of the data points to eq. 3 generated a K_I of 0.19 μM (Figure 7), a value slightly less than the IC_{50} concentration of lifarizine inhibiting I_{Na} at a V_{hold} of −60 mV (0.3 μM; Figure 4). The Hill coefficient (n_H) corresponding to this fit was 0.51.

Interaction of lifarizine with open Na^+ channels

Due to the transient nature of the open state and because estimation of the affinity of lifarizine for open Na^+ channels

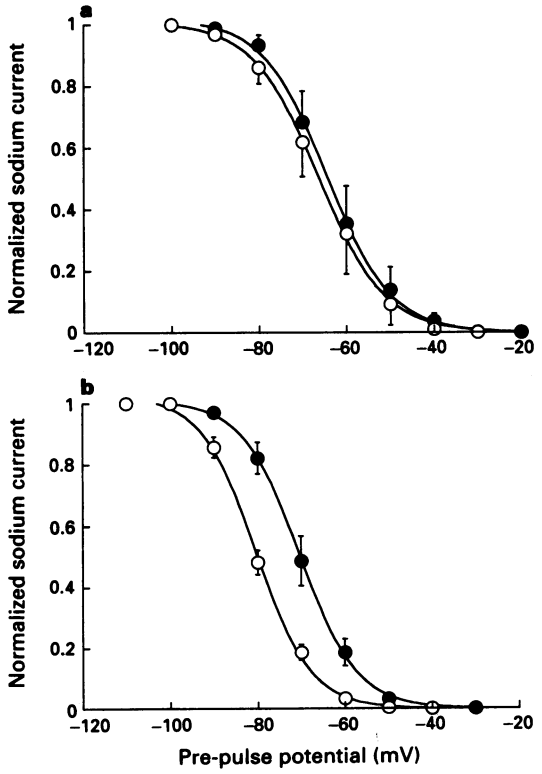

Figure 6 Steady-state inactivation curves in N1E-115 obtained using 1 s (a) or 1 min (b) pre-pulse durations in the absence (●) and presence (○) of 1 μM lifarizine. The data points show the mean ± s.e. mean for 3 cells (a) and 5 cells (b). The smooth curves were obtained by a least squares regression fit to the Boltzmann function (see Results).

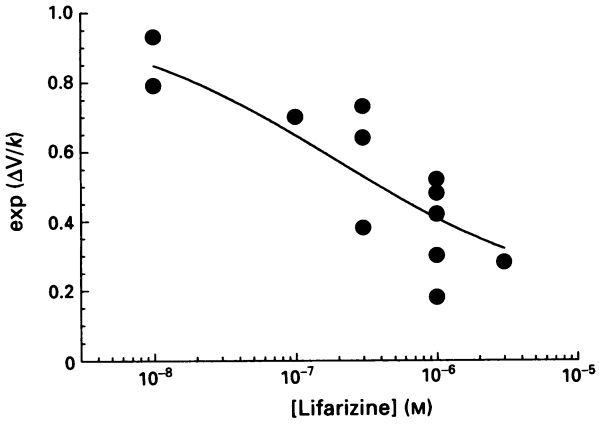

Figure 7 Estimation of the dissociation constant of lifarizine for the inactivated state of the sodium channel (K_I). The data points were obtained by examining the shifts in the steady-state inactivation curves (ΔV), normalized by the slope of the curves (k), produced by lifarizine applied at 0.01 μM ($n = 2$ cells), 0.1 μM ($n = 1$), 0.3 μM ($n = 3$), 1 μM ($n = 5$) and 3 μM ($n = 1$). The smooth curve is a least squares regression fit to the mean values at each concentration using Eq.3 (see Methods) and generated a K_I of 0.19 μM (using an estimated K_R of 7.3 μM).

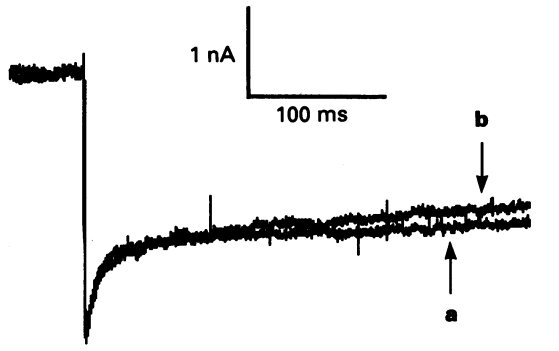

Figure 8 Effect of lifarizine on chloramine-T-modified currents. (a) Control Na^+ current generated in a single N1E-115 cell following treatment with 1 mM chloramine-T. (b) Na^+ current generated in the same chloramine-T-treated cell in the presence of 1 μM lifarizine. Neither the peak nor the sustained phase of the current was reduced, indicating that this concentration of lifarizine does not interact significantly with resting or open Na^+ channels, respectively.

would have required equilibrium conditions to be met, we could not obtain an estimate of K_O. However, to gain some insight into a possible open channel interaction of lifarizine we used the oxidizing agent, chloramine-T, to produce currents which decayed very slowly (Figure 8). This slow decay is due to a chloramine-T-induced prolongation of channel open time in combination with bursts of channel openings during the entire pulse duration (Niemann *et al.*, 1991). The effect of lifarizine on chloramine-T-modified currents (generated by a depolarization to 0 mV from a V_{hold} of −80 mV) was examined in 5 cells. An example from a single cell is shown in Figure 8. Lifarizine (1 μM, 10 min) had very little effect on either the amplitude of the initial peak of the modified current (4.4 ± 2.0% reduction) or on the amplitude of the persistent current (12.6 ± 3.6% reduction at 250 ms). The reduction in amplitude of the persistent current, after taking into account the reduction in the amplitude of the initial peak, was not statistically significant. In contrast the local anaesthetic, (±)-bupivacaine, applied at a concentration of 10 μM to chloramine-T-treated cells, induced decreases of 12.5 ± 3.9% in the peak and 39.8 ± 4.6% in the persistent phase of the modified current (both $P<0.05$; $n = 4$ cells), consistent with the known interaction of this agent with open and resting Na^+ channels (Wang & Wang, 1992).

Discussion

The present experiments were undertaken in order to provide a functional electrophysiological correlate to the ligand binding data and pharmacological data suggesting an interaction of lifarizine with the voltage-dependent Na^+ channel (see Introduction). The findings demonstrate that lifarizine potently inhibits Na^+ currents in N1E-115 cells.

The experiments investigating the effects of lifarizine on Na^+ currents generated by cells clamped at three different holding potentials (−100, −80 or −60 mV) provided the initial suggestion that lifarizine interacts with the inactivated state of the Na^+ channel to exert its inhibitory actions. The concentration of lifarizine required to inhibit the peak sodium current by 50% varied by 24 fold over this range of holding potentials: 0.3 μM at −60 mV compared to 7.3 μM at −100 mV. Since the proportion of channels in the inactivated state increases with depolarization (see the steady-state inactivation curves in Figure 6), these data provided direct evidence that the inhibitory potency of lifarizine varies commensurately with the number of channels in the inactivated state. This observation serves to underline the point that quoting an IC_{50} concentration at a single V_{hold} for a Na^+ current inhibitor that has a significant interaction with the inactivated state of the channel is inappropriate since the potency varies with the proportion of channels in the inactivated state and, therefore, with the holding potential. Nevertheless, a recent study (N.A. Brown *et al.*, 1994) has reported that the IC_{50} concentration of lifarizine required to inhibit Na^+ currents generated from a V_{hold} of −80 mV in the human neuroblastoma cell line, SH-SY5Y, is around 0.8 μM, a value not very different from the 1.3 μM obtained in the present study.

That lifarizine interacts with the inactivated state of the Na^+ channel was further supported by the experiments investigating voltage-dependent block by lifarizine. In these experiments cells were clamped to a conditioning potential of 0 mV for 20 s in the presence of 3 μM lifarizine. Immediately after the conditioning depolarization, the membrane potential was returned to −100 mV and a series of 10 ms test depolarizations was performed to probe recovery from voltage-dependent block. The first test depolarization was made 2 s after the long conditioning pulse and this invariably evoked a current much smaller than the pre-conditioning control current (in untreated cells recovery from inactivation was complete within 2 s). The most likely explanation for this phenomenon is that during the conditioning depolarization all of the channels are shifted from the resting state (at −100 mV) to the inactivated state (at 0 mV), thus allowing lifarizine to bind. The degree of inhibition of the current generated by the first post-conditioning test depolarization is presumably dependent on the affinity of lifarizine for the inactivated state of the Na^+ channel. During subsequent test depolarizations the current gradually returned to the pre-conditioning level following a recovery process having fast and slow time constants of 7 s (27%) and 79 s (73%), respectively. This finding suggests that lifarizine may bind to 2 inactivated states of the channel. Evidence for fast and slow inactivated states of the Na^+ channel in N1E-115 cells has been obtained by Quandt (1987).

To obtain an estimate of the affinity (rather than just the potency) of lifarizine for the inactivated state of the Na^+ channel we next looked at the effects of the compound on the steady-state inactivation relationship in N1E-115 cells. It has been shown consistently by others that drugs which inhibit Na^+ currents by interacting with the inactivated state of the channel consistently induce leftward shifts of the steady-state inactivation curve (Hille, 1977; Hondeghem & Katzung,

1977; Matsuki *et al.*, 1984). Surprisingly, lifarizine, applied at a concentration of 1 μM, failed to induce a leftward shift of the steady-state inactivation curve when pre-pulses of 1 s duration were used. A similar finding has been reported by N.A. Brown *et al.* (1994), who also failed to find an effect of 1 μM lifarizine on the steady-state inactivation relation in SH-SY5Y cells (using 200 ms pre-pulse durations). However, when we used pre-pulse durations of 1 min, 1 μM lifarizine induced a leftward shift of about 10 mV. This finding can be interpreted in one of two ways. As stated above, Na^+ channels in N1E-115 cells are known to develop two inactivated states, fast and slow (Quandt, 1987). The present findings are consistent with the need fully to develop the slow inactivated state before the effects of lifarizine on the steady-state inactivation curve can be observed. However, an equally plausible explanation may be that lifarizine requires a relatively long period of time to associate with inactivated channels. This latter possibility is currently being investigated in ligand binding studies using [^{3}H]-lifarizine.

To estimate the affinity of lifarizine for the inactivated state we used a modification of the method developed by Bean *et al.* (1983), which involved looking at shifts in the steady-state inactivation curves induced by a range of lifarizine concentrations. Our modifications were designed to improve the accuracy and flexibility of the method and involved incorporation of the Hill coefficient into the original equation and taking into account the slope factor (k) of the steady-state inactivation curve from each cell individually, rather than using a 'global average' value for the slope factor (see Methods for more detail). When examined in this way (using eq. 3 to fit the data in Figure 7), the apparent dissociation constant (K_I) of lifarizine for the inactivated state of the Na^+ channel was estimated to be 0.19 μM. This value was only slightly less than the IC_{50} value for inhibition of Na^+ currents from a holding potential of −60 mV ($IC_{50} = 0.3$ μM). That this should be the case is intuitively reasonable, as −60 mV is close to the foot of the steady-state inactivation curve for Na^+ channels in these cells (see Figure 6). It is apparent, then, that when an inhibitor exerts its effects primarily by an interaction with the inactivated state of the channel, the IC_{50} concentration for Na^+ current inhibition approaches K_I as the membrane potential becomes progressively less negative and an increasing proportion of the channels move from the resting to the inactivated state.

However, the Hill coefficient corresponding to the fit to eq. 3 was extremely low ($n_H = 0.51$). One possible explanation for this low value is that lifarizine interacts with more than one site to induce the shifts in the steady-state inactivation curves, and this interpretation may be consistent with the bi-exponential recovery from voltage-dependent block discussed earlier. However, it is also possible that the low Hill coefficient is generated by a mechanism unrelated to the molecular interaction between lifarizine and its binding site. For example, if the concentration of lifarizine seen by the binding site is less than the concentration in the medium (due to, say, partitioning of drug into membrane lipid) then this could influence the Hill slope by making it appear shallower than it actually is. It is therefore important not to be too dogmatic with regard to the significance of the low n_H value until more biochemical data are available.

In the final series of experiments we examined the ability of lifarizine to block open channels. Estimation of the affinity of lifarizine for the resting and inactivated state is, as has been demonstrated, a relatively straightforward matter, since these channel states achieve membrane potential-dependent equilibria. In contrast, open state channels appear only transiently, with most channels opening only once during a depolarizing pulse and, even then, only very briefly (0.6 ms at 15–16°C in N1E-115 cells; Niemann *et al.*, 1991). Therefore, in order to study the interaction of lifarizine with open channels it was necessary to modify chemically the function of the Na^+ channel with the oxidizing agent, chloramine-T. Brief extracellular application of chloramine-T converts the transient whole-cell Na^+ current into one lasting many hundreds of milliseconds. Studies at the single channel level in N1E-115 cells (Niemann *et al.*, 1991) indicate that the persistent Na^+ current after treatment with chloramine-T results from an extended average channel open time (2.0 ms) in combination with bursts of channel openings during the entire pulse duration. The local anaesthetic agents, benzocaine (Meeder & Ulbricht, 1987), cocaine and bupivacaine (Wang & Wang, 1992), accelerate the decay of the chloramine-T-modified Na^+ current by selectively binding to open channels and blocking them. In contrast to these agents, lifarizine, applied to chloramine-T-treated cells held at −80 mV at a concentration sufficient to inhibit unmodified Na^+ currents by 40%, did not accelerate the decay of the modified current. This result suggests that lifarizine has a low affinity for open Na^+ channels, although the possibility that lifarizine may require a longer time to associate with open channels (as may be the case with the inactivated channel interaction discussed above) cannot be excluded. That the initial peak of the chloramine-T-modified Na^+ current was also unaffected by lifarizine, provides further evidence to support the contention that lifarizine has low affinity for resting Na^+ channels (see earlier).

In summary, the present experiments have shown that lifarizine is a highly potent voltage-dependent inhibitor of Na^+ currents in N1E-115 cells and that the voltage-dependence derives from an interaction of the compound with one or more inactivated state(s) of the Na^+ channel. Whether this spectrum of action underlies the neuroprotective activity of lifarizine in animal models of global and focal cerebral ischaemia (see Introduction) cannot be stated with certainty at present. However, such a mechanism may be expected to attenuate the inappropriate and uncontrolled excitation of metabolically-compromised neurones in the ischaemic penumbra (Siesjö, 1988) and, as such, would be consistent with a neuroprotective action. A number of studies have highlighted the involvement of neuronal Na^+ channel activation in the events occurring in hypoxia and ischaemia. Prenen *et al.* (1988) described an inhibitory effect of tetrodotoxin, applied focally into the rat striatum, on the extracellularly recorded d.c. potential following induction of cardiac arrest. Yamasaki *et al.* (1991) have reported a protective effect of tetrodotoxin, injected focally into rat hippocampus, on the histologically-assessed outcome following four-vessel occlusion. Systemically-administered lignocaine has been shown to limit infarct size in a cat middle cerebral artery occlusion model (Shokunbi *et al.*, 1990) and to promote the recovery of electrical activity (EEG and evoked potentials) in a rabbit model of incomplete global ischaemia (Rasool *et al.*, 1990). Interestingly, it has recently been reported that another neuroprotective drug, riluzole, inhibits sodium currents generated by *Xenopus* oocytes expressing the α subunit of the rat brain IIA sodium channel, and that this inhibition, like that exerted by lifarizine in the present experiments, arises from a preferential interaction of the drug with the inactivated state of the channel (Hebert *et al.*, 1994).

In conclusion, the ability of lifarizine to block inactivated Na^+ channels in a potent and selective way lends credence to the idea that lifarizine will selectively dampen the hyperactivity of ischaemic neurones that have become excessively depolarized through reduction or loss of metabolic support, while Na^+ channels in non-ischaemic areas (both central and peripheral) would remain unaffected.

We are grateful to Mr Greig P. Duncan and Mr William S. Rowand for provision of the cell cultures.

References

ALPS, B. (1992). Drugs acting on calcium channels: potential treatment for ischaemic stroke. *Br. J. Clin. Pharmacol.*, **34**, 199–206.

BEAN, B.P., COHEN, C.J. & TSIEN, R.W. (1983). Lidocaine block of cardiac sodium channels. *J. Gen. Physiol.*, **81**, 613–642

BROWN, C.M., CALDER, C., ALPS, B.J. & SPEDDING, M. (1993). The effect of lifarizine (RS-87476), a novel sodium and calcium channel modulator, on ischaemic dopamine depletion in the corpus striatum of the gerbil. *Br. J. Pharmacol.*, **109**, 175–177.

BROWN, C.M., SMALL, C., CALDER, C. & PATMORE, L. (1994). Neuroprotective properties of lifarizine (RS-87476) in a mouse model of focal ischaemia. *Can. J. Physiol. Pharmacol.*, **72** (Suppl. 1), 435.

BROWN, N.A., KEMP, J.A. & SEABROOK, G.R. (1994). Block of human voltage-sensitive Na^+ currents in differentiated SH-SY5Y cells by lifarizine. *Br. J. Pharmacol.*, **113**, 600–606.

HAMILL, O.P., MARTY, A., NEHER, E., SAKMANN, B. & SIGWORTH, F.J. (1981). Improved patch-clamp techniques for high-resolution current recording from cells and cell-free membrane patches. *Pflügers Arch.*, **391**, 85–100.

HEBERT, T., DRAPEAU, P., PRADIER, L. & DUNN, R.J. (1994). Block of the rat brain IIA sodium channel α subunit by the neuroprotective drug riluzole. *Mol. Pharmacol.*, **45**, 1055–1060.

HILLE, B. (1977). Local anesthetics: hydrophilic and hydrophobic pathways for the drug-receptor reaction. *J. Gen. Physiol.*, **69**, 497–515.

HONDEGHEM, L.M. & KATZUNG, B.G. (1977). Time- and voltage-dependent interactions of antiarrhythmic drugs with cardiac sodium channels. *Biochim. Biophys. Acta*, **472**, 373–398.

KUCHARCZYK, J., MINTOROVITCH, J., MOSELEY, M.E., ASGARI, H.S., SEVICK, R.J., DERUGIN, N. & NORMAN, D. (1991). Ischemic brain damage: reduction by sodium-calcium ion channel modulator RS-87476. *Radiology*, **179**, 221–227.

LEES, K.R. (1992). Therapeutic interventions in acute stroke. *Br. J. Clin. Pharmacol.*, **34**, 486–493.

MATSUKI, N., QUANDT, F.N., TEN EICK, R.E. & YEH, J.Z. (1984). Characterization of the block of sodium channels by phenytoin in mouse neuroblastoma cells. *J. Pharmacol. Exp. Ther.*, **228**, 523–530.

MAY, G.R., ROWAND, W.S., MCCORMACK, J.G. & SHERIDAN, R.D. (1995). Neuroprotective profile of lifarizine (RS-87476) in rat cerebrocortical neurones in culture. *Br. J. Pharmacol.*, (in press).

MCBEAN, D.E., WINTERS, V., WILSON, A.D., OSWALD, C.B. & ARMSTRONG, J.M. (1995a). Neuroprotective efficacy of the ion channel modulator lifarizine (RS-87476) in a rodent model of global cerebral ischaemia. *Br. J. Pharmacol.*, (Proceeding), (in press).

MCBEAN, D.E., WINTERS, V., WILSON, A.D., OSWALD, C.B. & ARMSTRONG, J.M. (1995b). The ion channel modulator lifarizine (RS-87476) reduces the size of the infarct produced in the rat by the rose Bengal photochemical focal model of cerebral ischaemia. *Br. J. Pharmacol.*, (Proceeding), (in press).

MCGIVERN, J.G., PATMORE, L. & SHERIDAN, R.D. (1994a). Voltage-dependent inhibition of sodium currents (I_{Na}) in N1E-115 by the neuroprotective agent, lifarizine (RS-87476-190). *Can. J. Physiol. Pharmacol.*, **72** (Suppl. 1), 522.

MCGIVERN, J.G., SHERIDAN, R.D. & PATMORE, L. (1994b). The neuroprotective agent, lifarizine (RS-87476), inhibits sodium currents via an interaction with the slowly inactivating state of the channel. *Br. J. Pharmacol.*, **112**, 485P.

MEEDER, T. & ULBRICHT, W. (1987). Action of benzocaine on sodium channels of frog nodes of Ranvier treated with chloramine-T. *Pflügers Arch.*, **409**, 265–273.

NIEMANN, P., SCHMIDTMAYER, J. & ULBRICHT, W. (1991). Chloramine-T effect on sodium conductance of neuroblastoma cells as studied by whole-cell clamp and single-channel analysis. *Pflügers Arch.*, **418**, 129–136.

PATMORE, L., DUNCAN, G.P., KENNY, B.A. & SPEDDING, M. (1991). RS-87476, a novel neuroprotective agent, inhibits veratrine-induced calcium overload in embryonic chick cardiac myocytes. *Br. J. Pharmacol.*, **104**, 175P.

PRENEN, G.H., GO, K.G., POSTEMA, F., ZUIDERVEEN, F. & KORF, J. (1988). Cerebral cation shifts in hypoxic-ischemic brain damage are prevented by the sodium channel blocker tetrodotoxin. *Exp. Neurol.*, **99**, 118–132.

QUANDT, F.N. (1987). Burst kinetics of sodium channels which lack fast inactivation in mouse neuroblastoma cells. *J. Physiol.*, **392**, 563–585.

RASOOL, N., FAROQUI, M. & RUBINSTEIN, E.H. (1990). Lidocaine accelerates neuroelectrical recovery after incomplete global ischemia in rabbits. *Stroke*, **21**, 929–935.

SHERIDAN, R.D., PATMORE, L. & SPEDDING, M. (1991). The novel neuroprotective agent, RS-87476, potently inhibits sodium currents in mouse neuroblastoma. *Br. J. Pharmacol.*, **104**, 25P.

SHOKUNBI, M.T., GELB, A.W., WU, X.M. & MILLER, D.J. (1990). Continuous lidocaine infusion and focal feline cerebral ischemia. *Stroke*, **21**, 107–111.

SIESJÖ, B.K. (1988). Historical overview: calcium, ischemia and death of brain cells. *Ann. N.Y. Acad. Sci.*, **522**, 638–661.

WANG, G.K. & WANG, S-Y. (1992). Altered stereoselectivity of cocaine and bupivacaine isomers in normal and batrachotoxin-modified Na^+ channels. *J. Gen. Physiol.*, **100**, 1003–1020.

YAMASAKI, Y., KOGURE, K., HARA, H., BAN, H. & AKAIKE, N. (1991). The possible involvement of tetrodotoxin-sensitive ion channels in ischemic neuronal damage in the rat hippocampus. *Neurosci. Lett.*, **121**, 251–254.

(Received October 17, 1994
Revised December 23, 1994
Accepted January 18, 1995)

British Journal of Pharmacology (1995) 114, 1745–1749 © 1995 Stockton Press All rights reserved 0007–1188/95 $12.00

Electrocardiographic interactions between pinacidil, a potassium channel opener and class I antiarrhythmic agents in guinea-pig isolated perfused heart

Quan Yang, [1]Roberto Padrini, Sergio Bova, *Donatella Piovan & *Gianna Magnolfi

Department of Pharmacology and *Institute of Clinical Medicine, University of Padua, Padua, Italy

1 Drugs that shorten action potential duration could decrease the Na-channel blocking effect of class I antiarrhythmic agents by reducing the availability of Na channel in the inactivated state.

2 This hypothesis was tested in guinea-pig perfused heart, measuring the surface ECG effects of three class I drugs endowed with different binding kinetics (15 μM mexiletine, 10 μM quinidine and 3 μM flecainide) in the presence of increasing concentrations of pinacidil (10 μM, 30 μM, 50 μM), a potassium channel opener that shortens action potential duration.

3 The ECG parameters measured were: the QRS interval, i.e. the intraventricular conduction time; the JT interval, which reflects the duration of ventricular repolarization; the ratio between JTpeak (the time from the end of QRS and the peak of T wave) and JT interval, which quantifies changes in the morphology of the T wave.

4 At the concentrations tested all the antiarrhythmic drugs widened the QRS complex by 55–60%. Flecainide did not significantly change JT interval, but quinidine prolonged and mexiletine shortened it. Mexiletine also decreased the JTpeak/JT ratio. Pinacidil by itself decreased the JT interval and the JT peak/JT ratio in a dose-dependent way, but did not affect QRS duration.

5 In the presence of fixed antiarrhythmic drug concentrations, however, pinacidil decreased the QRS prolongation induced by mexiletine (−17%) and quinidine (−8%), but not that induced by flecainide: this effect was already maximal at the lower concentration tested (10 μM) and there was no relationship between pinacidil-induced JT shortening and QRS changes. To explain this unexpected result it has been supposed that, at the driving frequency used (4 Hz), myocardial cells were partially depolarized and that pinacidil could repolarize them, thus decreasing the number of inactivated Na channels and the effects of drugs that (mainly or partly) block the channels in the inactivated state. In agreement with this hypothesis, an additional series of experiments carried out with 15 μM mexiletine at a lower stimulation rate (2 Hz) showed only a negligible loss of QRS effect (−2.3%) at any pinacidil concentration.

6 Flecainide, but not quinidine and mexiletine, antagonized the JT shortening induced by pinacidil; furthermore, no drug modified the JTp/JT decrease induced by pinacidil.

7 These results indicate that: (a) an antagonism between class I antiarrhythmic drugs and pinacidil is possible; (b) mexiletine is the most involved among the drugs tested; (c) the interaction is not related to pinacidil-induced repolarization shortening, but probably to changes in membrane resting potential. The possible clinical implications need to be defined.

Keywords: Pinacidil; mexiletine; quinidine; flecainide; interaction; class I antiarrhythmic agents; guinea-pig isolated heart

Introduction

Potassium channel openers (KCO), as a class of drugs, have been widely studied in the last decade because of their wide-spectrum pharmacological effects (Cook, 1988) and clinical applications (Andersson, 1992). Recently, some papers (Wollenbreg *et al.*, 1989; Chi *et al.*, 1990; Padrini *et al.*, 1992) pointed out the potential proarrhythmic effect of these drugs both in acute ischaemia and in normoxic conditions. However, the effect of K channel openers on heart rhythmicity is not unequivocal. On the one hand, these drugs favour re-entry arrhythmias by shortening action potential duration (APD) and increasing refractoriness dispersion (Di Diego & Antzelevitch, 1993). On the other hand, however, they have proved to be effective, even at low concentrations, in suppressing arrhythmias triggered by early afterdepolarizations (Fish *et al.*, 1990). The interplay between KCO and arrhythmias, may be further complicated by a potential interaction between KCOs and the class I antiarrhythmic drugs (Na channel blockers). On the basis of the 'modulated receptor' (Hondeghem & Katzung, 1977) or 'guarded receptor' (Starmer *et al.*, 1984) hypotheses, shortening of APD is expected to reduce the availability of sodium channels in the inactivated state and, hence, to decrease the electrophysiological effects of those antiarrhythmic agents that predominantly block the inactivated sodium channels.

Since there is little information about this interaction, we studied the influence of pinacidil on the electrophysiological actions of three commonly used class I antiarrhythmic drugs, which differ as to receptor binding kinetics and channel state preferentially blocked (Campbell, 1983; Kodama *et al.*, 1987; Weirich & Antoni, 1990): mexiletine (fast kinetics, inactivated channel blocked), flecainide (slow kinetics, open channel blocked) and quinidine (intermediate kinetics, open channel blocked).

The electrophysiological effects were evaluated in terms of surface ECG changes, in guinea-pig Langendorff perfused hearts. This experimental model, as well as providing physiological perfusion conditions, has also been shown in several studies (Gillis & Kates, 1988; Bova *et al.*, 1989; Nielsen *et al.*, 1989; Gillis & Keashly, 1991; Padrini *et al.*, 1992) to be suitable for measuring the effects of drugs on ventricular repolarization (QT interval) and on intraventricular conduction time (QRS).

[1] Author for correspondence at: Department of Cardiological Sciences, St. George's Hospital Medical School, Cranmer Terrace, London SW17 0RE (until September 1995).

Methods

Guinea-pigs of either sex (body weight 250–350 g) were stunned by a blow to the neck and exsanguinated. The heart was rapidly removed, put in ice-cold buffer solution and perfused retrogradely at a constant flow rate (10 ml min^{-1}) with a Gilson peristaltic micropump. The perfusion medium was a modified Krebs-Henseleit solution (mM: NaCl 118, KCl 4.7, $CaCl_2$ 2.5, $MgSO_4$ 1.2, $NaCO_3$ 25, KH_2PO_4 1.2, glucose 11.1 and pyruvate 2) bubble with O_2:CO_2 gas mixture (95%:5%) and maintained at 37°C (pH 7.46 ± 0.01). Atrial free walls and septum were removed and platinum electrodes were fitted over the upper border of the interventricular septum to by-pass the AV node and stimulate the His bundle. A driving frequency of 4 Hz was chosen in order to magnify the effect of class I antiarrhythmic drug on the QRS interval (use-dependent effect) (Grant *et al.*, 1984). In some experiments frequency was set at 2 Hz to investigate the influence of rate on drug interaction (see Results). The stimulation parameters (S88 Grass stimulator) were: amplitude 2–5 V (= × 1.5 threshold value); duration 0.5 ms.

ECG measurements

Surface ECG was recorded by means of two electrodes, one placed on the crux cordis and the other on the left ventricle free wall. The signal was monitored with a storage oscilloscope (Tektronix Mod. 5115) and, when required, the ECG tracing was 'frozen' on the screen and photographed with a polaroid camera. The following time intervals were measured (Figure 1): (1) The intraventricular conduction time (QRS interval), i.e. the interval from the stimulus artifact (corresponding to the His bundle activation) to the end of ventricular activation. (2) The duration of ventricular repolarization (QT interval): the interval from the stimulus artifact to the end of T wave. (3) The time from the stimulus artifact to the T wave peak (QTpeak interval). In order to improve the accuracy of the ECG interval measurements, two different recording speeds were used, according to the duration of the interval to be measured: 0.2 mm ms^{-1} for the QT and QTpeak intervals; 0.5 mm ms^{-1} for the QRS interval.

Using the values of QRS, QT and QTpeak other parameters were calculated: the JT interval (QT minus QRS interval), which reflects more specifically than QT pure repolarization changes; the JTpeak interval (QTpeak minus QRS interval); JTpeak/JT ratio, which is an index of changes in the T wave shape. This ratio has already been shown to decrease following exposure to pinacidil (Padrini *et al.*, 1992). Since changes in the QT interval, at constant frequency, induce the opposite changes in the duration of the electrical diastole, the diastolic interval (DI) was also measured as the difference between cycle length (250 ms) and QT.

Drug treatment

Hearts were first exposed to 15 μM mexiletine hydrochloride, 10 μM quinidine sulphate or 3 μM flecainide hydrochloride. Preliminary experiments have shown that these concentrations produced a similar QRS enlargement (about 55–60%). After reaching steady state ECG effects, pinacidil monohydrate was added in steps to obtain a concentration of 10, 30 and 50 μM. In a separate series of experiments the effects of the same pinacidil concentrations were evaluated without antiarrhythmic drugs.

Statistical analysis

All data are expressed as mean ± s.e. The ECG changes from the baseline induced by pinacidil, mexiletine, quinidine and flecainide were analysed by means of Student's paired *t* test. Comparisons of the effect of pinacidil alone and in the presence of antiarrhythmic drugs were carried out by two-way analysis of variance (ANOVA) followed by multiple Student's *t* test with the Bonferroni correction. Possible correlations between QRS and other ECG parameters were tested by means of linear regression analysis. The statistical analysis was carried out on a PC (SuntaQ AC-486) using the 'Excel' statistical package. Statistical significance was set at $P<0.05$.

Results

The effects of 10 μM quinidine, 15 μM mexiletine and 3 μM flecainide observed on the QRS interval and the JT interval were consistent with their cellular electrophysiological effects. All the drugs widened the QRS interval (quinidine = +54.3%, $P<0.001$; mexiletine = +56.4%, $P<0.001$; flecainide = +59.2%, $P<0.005$). In addition, quinidine prolonged the JT interval by +7.2% ($P<0.05$), mexiletine shortened it by −2.4% ($P<0.05$), while flecainide induced non significant changes (+4.2%, NS). The JTp/JT ratio was not changed by quinidine and flecainide, but was significantly decreased by mexiletine ($P<0.05$).

The mean values (± s.e) of the ECG parameters given above, measured in control conditions and at steady state of drug effects are shown in Table 1.

The ECG effects of 10–30–50 μM pinacidil, both alone and in the presence of a fixed concentration of quinidine (10 μM), mexiletine (15 μM) and flecainide (3 μM), are shown in Figures 2–4.

Pinacidil alone shortened the JT interval (Figure 3, ●), decreased JTp/JT (Figure 4, ●) but did not affect the QRS interval duration (Figure 2, ●).

Although it had no direct effect on QRS, when in the presence of fixed antiarrhythmic drug concentrations pinacidil concentrations were increased stepwise (10–30–50 μM), the QRS prolongation induced by quinidine and mexiletine was curtailed, on average, by −17% and −8%, respectively; however, the QRS effect of flecainide was

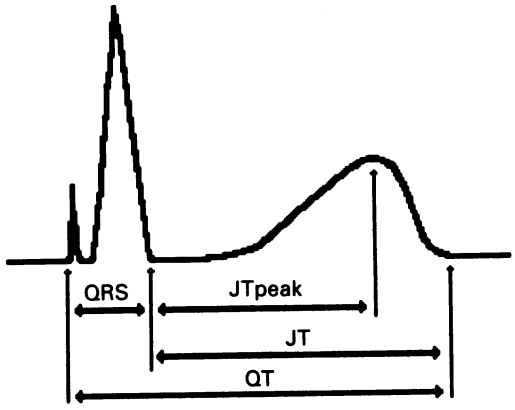

Figure 1 Schematic drawing of the ECG signal, with the indication of the basic intervals measured (QRS, QT, JT and JTpeak).

Table 1 Electrocardiography parameters in control and treated hearts

		QRS (ms)	*JT* (ms)	*JTp/JT*
Quinidine	C	35.9 ± 2.0	143.2 ± 4.1	0.83 ± 0.03
	T	55.4 ± 3.3***	153.7 ± 5.8*	0.84 ± 0.01 NS
Mexiletine	C	33.6 ± 2.5	143.3 ± 5.2	0.84 ± 0.02
	T	52.5 ± 1.4***	139.9 ± 4.1*	0.81 ± 0.01*
Flecainide	C	36.0 ± 2.5	140.5 ± 2.9	0.85 ± 0.01
	T	58.6 ± 1.4**	146.5 ± 3.8 NS	0.84 ± 0.02 NS

Significance levels: ***$P<0.001$; **$P<0.005$; *$P<0.05$; NS = not significant. C: control; T: treated.

not modified (Figure 2). The antagonism of the QRS effect of quinidine and mexiletine by pinacidil was not concentration-dependent but it did appear to be an all-or-nothing response, at least in the range of concentrations tested. In fact, the QRS decrease observed was virtually the same at both the lowest and at the highest concentrations. Furthermore, there was no correlation either between the pinacidil-induced QRS changes and the corresponding JT (Figure 5) or QT shortening, or between QRS changes and diastolic interval (data not shown). To obtain more information on the mechanism of the interaction we carried out another set of experiments at a lower stimulation frequency (2 Hz). The new hypothesis being tested was that the high frequency formerly used (4 Hz) partially depolarized cardiac myocytes and that pinacidil could repolarize cell membrane and decrease the number of inactivated Na channels (see Discussion). Mexiletine was chosen for these experiments because it showed the most marked interaction with pinacidil.

At 2 Hz, mexiletine increased the QRS duration by 17.2 ± 2.0% (as compared with 56.4 ± 3.4% at 4 Hz). In contrast with 4 Hz results, at the 2 Hz driving rate pinacidil induced only a negligible loss in the mexiletine effect at any concentration considered (−2.3%, on average) (Figure 6). Since the maximum JT shortening induced by pinacidil at 2 Hz was virtually the same (−26.7 ± 4.3%) as that obtained at 4 Hz (−24.8 ± 5.2%), it is likely that the resting membrane potential increase (rather than repolarization shortening) was responsible for the drug interaction.

The typical effects of quinidine and mexiletine on ventricular repolarization were also modified by pinacidil and the results of the interaction was the simple algebraic sum of the effect of each drug. However, in the presence of flecainide the JT shortening induced by pinacidil was significantly smaller (Figure 3). These results indicate that some class I antiarrhythmic drugs can, in their turn, interfere with the repolarization effects of pinacidil. The JTp/JT ratio decrease induced by pinacidil was not significantly modified by any of the antiarrythmic drugs tested (Figure 4).

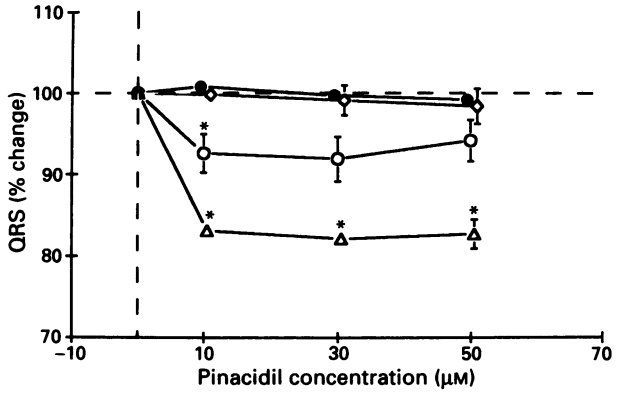

Figure 2 Relationship between pinacidil concentrations and mean percentage QRS changes obtained with pinacidil alone (control group: ●) and in the presence of 15 μM mexiletine (Δ), 10 μM quinidine (○) and 3 μM flecainide (◇). Each point is the mean ± s.e.mean of 5 experiments. Two-way analysis of variance (ANOVA) showed that the QRS effect was not different between the 3 concentration groups and that pinacidil significantly decreased QRS in the mexiletine and quinidine groups compared to the controls. The asterisks indicate significant differences when multiple *t* tests (with Bonferroni adjustment) were applied.

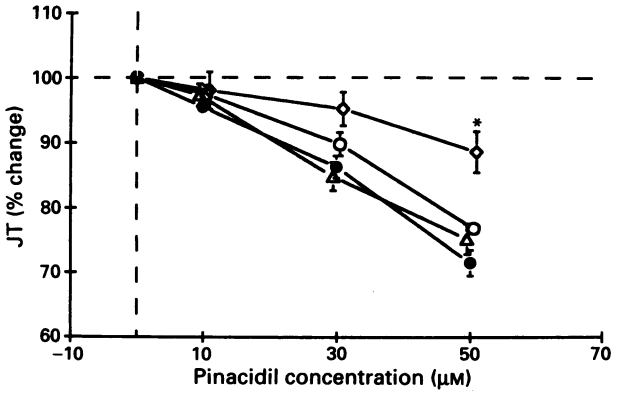

Figure 3 Relationship between pinacidil concentrations and mean percentage JT changes obtained with pinacidil alone (control group: ●) and in the presence of 15 μM mexiletine (Δ), 10 μM quinidine (○) and 3 μM flecainide (◇). Each point is the mean ± s.e.mean of 5 experiments. Two-way analysis of variance showed a significant concentration-dependent JT shortening in all groups, but the JT shortening was significantly less marked in the flecainide group than in the controls. The asterisks indicate significant differences when multiple t tests (with Bonferroni adjustment) were applied.

Discussion

QRS interval changes induced by class-I antiarrhythmic agents are believed to reflect changes in the Na inward current and a widely used clinical classification (Vaughan Williams, 1984) divides class-I drugs into three subgroups

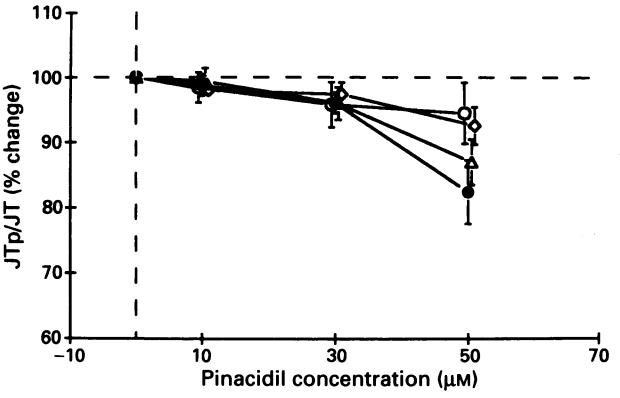

Figure 4 Relationship between pinacidil concentrations and mean percentage JTp/JT ratio changes obtained with pinacidil alone (control group: ●) and in the presence of 15 μM mexiletine (Δ), 10 μM quinidine (○) and 3 μM flecainide (◇). Each point is the mean ± s.e.mean of 5 experiments. Two-way analysis of variance showed a significant concentration-dependent JTp/JT shortening for all the three drug groups; the JTp/JT effect was not significantly different from the controls.

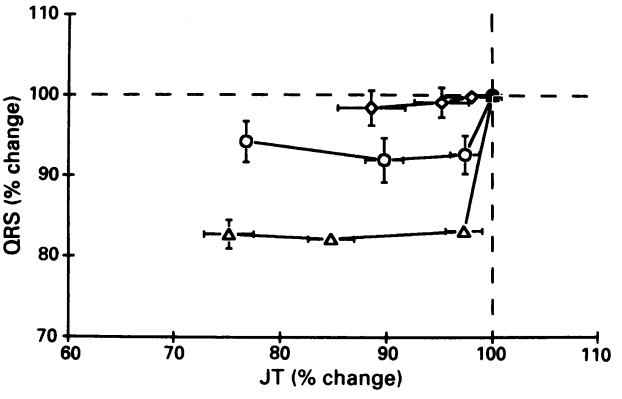

Figure 5 Relationships between pinacidil-induced decreases in JT interval and the corresponding QRS changes, in the presence of 15 μM mexiletine (Δ), 10 μM quinidine (○) and 3 μM flecainide (◇). Each point is the mean ± s.e.mean of 5 experiments.

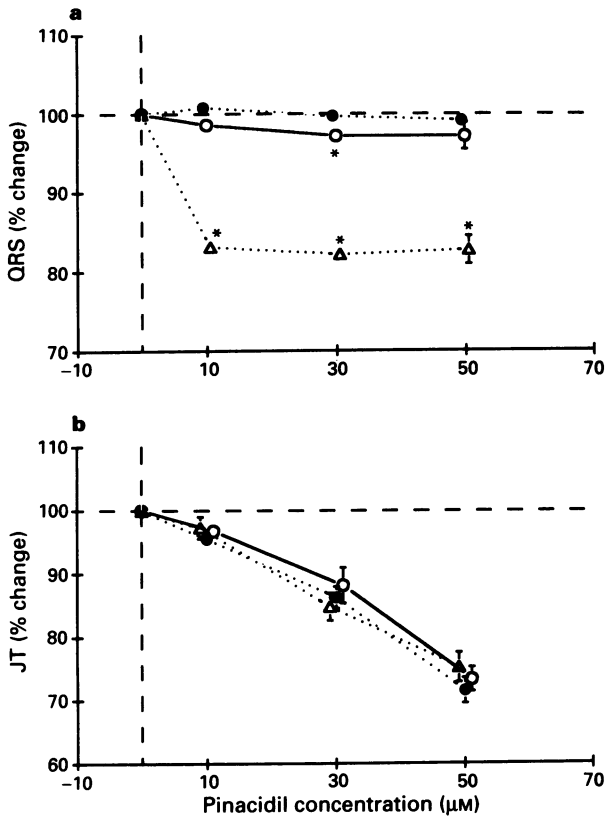

Figure 6 Pinacidil-mexiletine interaction at a 2 Hz stimulation frequency. (a) Relationships between pinacidil concentration and mean percentage changes in QRS interval (○). (b) Relationships between pinacidil concentration and mean percentage changes in JT interval (○). For comparison, the results obtained with mexiletine at 4 Hz stimulation frequency are also shown (dotted lines): controls (●) and 15 μM mexiletine (△). Two-way analysis of variance (ANOVA) showed that the QRS effect was not different between the 3 concentration groups and that pinacidil significantly decreased QRS compared to the control group. The asterisks indicate significant differences when multiple *t* tests (with Bonferroni adjustment) were applied.

(Ia, Ib, Ic) according to their ability to widen the QRS complex at sinus rhythm on surface ECG. Although theoretical and experimental evidence has indicated that the relationship between Na current and conduction velocity is not linear (Buchanan *et al.*, 1985), QRS interval is generally accepted as an approximate index of Na channel availability (provided that intraventricular conduction pathway remains constant).

Our results show that pinacidil can antagonize the typical QRS widening effect of class I antiarrhythmic drugs, with differences that seem related to the binding kinetics of each individual drug. Flecainide, which is believed to block the Na channel mainly in the open state and is characterized by a slow recovery from block (Anno & Hondeghem, 1990), fully maintained its QRS effect even at the highest pinacidil concentration tested. Mexiletine, which has fast recovery kinetics and mainly interacts with the inactivated Na channel (Kodama *et al.*, 1987), lost about 17% of its QRS effect. Quinidine, which mainly is an open channel blocker with intermediate rate kinetics (Snyders & Hondeghem, 1990), but also binds to Na-channels during the slow inactivation phase (Hondeghem & Matsubara, 1988), lost only a small part of its effect (8%). The different degrees of interaction between drugs can be at first sight explained in the framework of the 'modulated receptor' or 'guarded receptor' hypotheses. Both these hypotheses predict (Grant *et al.*, 1984) that APD shortening and/or diastolic interval (DI) prolongation would decrease the effect of the drugs that bind the Na channel in the inactivated state (i.e., during the plateau phase of AP), especially if the binding kinetics are fast. On the contrary, drugs that mainly block the open Na channel or drugs with slow binding kinetics, are not expected to feel the effect of APD/DI changes. However, in the case of mexiletine and quinidine, the lack of correlation between repolarization shortening (or DI increase) and QRS shortening does not fit into this model. One could speculate that as well as shortening APD, pinacidil may also hyperpolarize resting membrane potential (RMP), thus reducing the number of inactivated Na channels (Hondeghem, 1987). Wyse *et al.* (1993) have demonstrated that the effect of mexiletine on the maximum rate of depolarization is more affected by changes in RMP than is that of quinidine. The hyperpolarizing effect of pinacidil has been shown in smooth muscle cells (Southerton *et al.*, 1988; Weston, 1989), which have a much less negative RMP than the K equilibrium potential but it has not generally been seen in isolated ventricular myocytes (Imanishi *et al.*, 1984; Smallwood & Steinberg, 1988) where the RMP is more negative. It is, however, possible that in our experimental conditions, cardiac cells may be partially depolarized. In multicellular preparations high driving rates induce K accumulation in intercellular clefts and a negative shift in RMP (Attwell *et al.*, 1981). A similar mechanism was considered by Buchanan *et al.* (1985) to explain the progressive decrease in conduction velocity they observed in guinea-pig papillary muscle when driving frequency was increased in steps from 0.1 to 8 Hz.

To verify the hypothesis that cell hyperpolarization was the main mechanism underlying drug interaction, we repeated the experiments with mexiletine (the most sensitive among the drugs tested to pinacidil interaction) at a stimulation rate 50% lower (2 Hz) than that formerly used. At this frequency the QRS effect of mexiletine was diminished, but still present, (+17.2%). Although the ability of pinacidil to shorten repolarization was fully maintained, pinacidil only marginally antagonized the mexiletine effect (−2.3%). These findings strongly suggest that changes in RMP rather than in APD are responsible for the interaction.

Kojima & Ban (1988) studied the interaction between nicorandil (another KCO) and two antiarrhythmic agents, lignocaine (20 μM) and disopyramide (20 μM), in guinea-pig papillary muscles at different stimulation rates. They found that nicroandil reduced the V_{max} effect of lignocaine (an inactivated channel blocker with fast kinetics), but not that of disopyramide (an open channel blocker with slow kinetics) and that the interaction with lignocaine was evident only at driving frequencies higher than 2 Hz. In spite of the similarity with our results, the mechanism of the interaction was different in that RMP underwent little, non significant hyperpolarization while APD_{90} markedly shortened to about 30% of control. It could be speculated that the small size of the preparation used (2-3 × 1 mm) did not permit a marked interstitial K accumulation. Unfortunately, a full comparison with our data is prevented by the fact that only one, very high (1 mM), nicorandil concentration was tested.

Since the pinacidil hyperpolarizing effect occurs at lower concentrations than those required to shorten AP, assessment of the working mechanism of the interaction is a clinically relevant issue. If RMP hyperpolarization is the true mechanism, low (and possibly therapeutic) pinacidil concentrations would be enough to decrease the mexiletine antiarrhythmic effect during sustained high frequency arrhythmias; an important corollary is that pinacidil may induce a loss of mexiletine selectivity for pathologically depolarized myocardium (e.g. ischaemia), even at physiological heart rates.

In summary, an antagonism between pinacidil and class I antiarrhythmic agents is possible but considerable differences may exist between individual drugs. Mexiletine appears to be the most involved of all the drugs tested. The exact mechanism of such an interaction is not fully understood, but a high heart rate is essential for its occurrence. Since, at present, the only official therapeutic indication of pinacidil is

essential hypertension, it seems advisable that hypertensive patients requiring mexiletine treatment for ventricular arrhythmias are carefully checked for possible arrhythmic recurrences.

Financial support was given by the Ministero della Ricerca Scientifica e Tecnologica (MURST, 60% and 40% funds) and by the Consiglio Nazionale delle Ricerche (CNR, FATMA project).

References

ANDERSSON, K.E. (1992). Clinical pharmacology of potassium channel openers. *Pharmacol. Toxicol.*, **70**, 244–254.

ANNO, T. & HONDEGHEM, L.M. (1989). Interaction of flecainide with guinea pig cardiac sodium channels. Importance of activation unblocking to the voltage dependence of recovery. *Circ. Res.*, **66**, 789–803.

ATWELL, D., COHEN, I. & EISNER, D.A. (1981). The effects of heart rate on the action potential of guinea-pig and human ventricle muscle. *J. Physiol.*, **313**, 439–461.

BOVA, S., PADRINI, R., CARGNELLI, G., PIOVAN, D. & FERRARI, M. (1989). Influence of acidosis on myocardial uptake and electrocardiographic effects of disopyramide. *Eur. J. Pharmacol.*, **168**, 179–185.

BUCHANAN, J.W., SAITO, T. & GETTES, L.S. (1985). The effects of antiarrhythmic drugs, stimulation frequency, and potassium-induced resting membrane potential changes on conduction velocity and dV/dt_{max} in guinea pig myocardium. *Circ. Res.*, **56**, 696–703.

CAMPBELL, T.J. (1983). Importance of physico-chemical properties in determining the kinetics of the effects of Class I antiarrhythmic drugs on maximum rate of depolarization in guinea-pig ventricle. *Br. J. Pharmacol.*, **80**, 33–40.

CHI, L., UPRICHARD, A.C.G. & LUCCHESI, B.R. (1990). Profibrillatory actions of pinacidil in a conscious canine model of sudden coronary death. *J. Cardiovasc. Pharmacol.*, **15**, 452–464.

COOK, N.S. (1988). The pharmacology of potassium channels and their therapeutic potential. *Trends Pharmacol. Sci.*, **9**, 21–28.

DI DIEGO, J.M. & ANTZELEVITCH, C. (1993). Pinacidil-induced electrical heterogeneity and extrasystolic activity in canine ventricular tissues. Does activation of ATP-regulated potassium current promote phase 2 reentry? *Circulation*, **88**, 1177–1189.

FISH, F.A., PRAKASH, C. & RODEN, D.M. (1990). Suppression of repolarization-related arrhythmias *in vitro* and *in vivo* by low-dose potassium channel activators. *Circulation*, **82**, 1362–1369.

GILLIS, A.M. & KATES, R.E. (1988). Effects of pH on the mycardial uptake and pharmacodynamics of propafenone in the isolated rabbit heart. *J. Cardiovasc. Pharmacol.*, **12**, 526–534.

GILLIS, A.M. & KEASHLY, R. (1991). Myocardial uptake and pharmacodynamics of quinidine and propafenone in isolated rabbit hearts: metabolic versus respiratory acidosis. *J. Cardiovasc. Pharmacol.*, **17**, 532–538.

GRANT, A.O., STARMER, C.F. & STRAUSS, H.C. (1984). Antiarrhythmic drug action. Blockade of the inward sodium current. *Circ. Res.*, **55**, 427–439.

HONDEGHEM, L.M. (1987). Antiarrhythmic agents: modulated receptor applications. *Circulation*, **75**, 514–520.

HONDEGHEM, L.M. & KATZUNG, B.G. (1977). Time- and voltage-dependent interactions of antiarrhythmic drugs with cardiac sodium channels. *Biochim. Biophys. Acta*, **472**, 373–398.

HONDEGHEM, L.M. & MATSUBARA, T. (1988). Quinidine blocks cardiac sodium channels during opening and slow inactivation in guinea-pig papillary muscle. *Br. J. Pharmacol.*, **93**, 311–318.

IMANISHI, S., ARITA, M., AOMINE, M. & KIYOSUE, T. (1984). Antiarrhythmic effects of nicorandil on canine cardiac Purkinje fibres. *J. Cardiovasc. Pharmacol.*, **6**, 772–779.

KODAMA, I., TOYAMA, J., TAKANAKA, C. & YAMADA, K. (1987). Block of activated and inactivated sodium channels by Class-I antiarrhythmic drugs studied by using maximum upstroke velocity (Vmax) of action potential in guinea-pig cardiac muscles. *J. Mol. Cell. Cardiol.*, **19**, 367–377.

KOJIMA, M. & BAN, T. (1988). Nicorandil shortens action potential duration and antagonizes the reduction of Vmax by lidocaine but not by dispyramide in guinea-pig papillary muscle. *Naunyn-Schmied. Arch. Pharmacol.*, **337**, 203–212.

NIELSEN, C.B., MELLEMKJAER, S. & NIELSEN-KUDSK, F. (1989). Pinacidil uptake and effects in the isolated rabbit heart. *Pharmacol. Toxicol.*, **64**, 14–19.

PADRINI, R., BOVA, S., CARGNELLI, G., PIOVAN, D. & FERRARI, M. (1992). Effects of pinacidil on guinea-pig isolated perfused heart with particular reference to the proarrhythmic effect. *Br. J. Pharmacol.*, **105**, 715–719.

SMALLWOOD, J.K. & STEINBERG, M.I. (1988). Cardiac electrophysiological effects of pinacidil and related pyridylcyanoguanidines: relationship to antihypertensive activity. *J. Cardiovasc. Pharmacol.*, **12**, 102–109.

SNYDERS, D.J. & HONDEGHEM, L.M. (1990). Effects of quinidine on the sodium current of guinea-pig ventricular myocites. Evidence for drug-associated rested state with altered kinetics. *Circ. Res.*, **66**, 565–579.

SOUTHERTON, J.S., WESTON, A.H., BRAY, K.M., NEWGREEN, D.T. & TAYLOR, S.G. (1988). The potassium channel opening action of pinacidil; studies using biochemical, ion flux and microelectrode techniques. *Naunyn-Schmied. Arch. Pharmacol.*, **388**, 310–318.

STARMER, C.F., GRANT, A.O. & STRAUSS, H.C. (1984). Mechanisms of use-dependent block of sodium channels in excitable membranes by local anaesthetics. *Biophys. J.*, **46**, 15–27.

VAUGHAN WILLIAMS, E.M. (1984). A classification of antiarrhythmic actions reassessed after a decade of new drugs. *J. Clin. Pharmacol.*, **24**, 129–147.

WEIRICH, J. & ANTONI, H. (1990). Differential analysis of the frequency-dependent effects of class I antiarrhythmic drugs according to periodical ligand binding: implications for antiarrhythmic and proarrhythmic efficacy. *J. Cardiovasc. Pharmacol.*, **15**, 998–1009.

WESTON, A.H. (1989). Smooth muscle K^+ channel openers; their pharmacology and clinical potential. *Pflügers Arch.*, **414** (suppl 1), S99–S105.

WOLLENBERG, C.D., SANGUINETTI, M.C. & SIEGEL, P.K.S. (1989). Influence of ATP-potassium channel modulators on ischemia-induced fibrillation in isolated rat hearts. *J. Mol. Cell. Cardiol.*, **21**, 783–788.

WYSE, K.R., YE, V. & CAMPBELL, T.J. (1993). Effects of hyperkalaemia on the depression of maximum rate of depolarization by class I antiarrhythmic agents in guinea-pig myocardium. *Br. J. Pharmacol.*, **108**, 255–261.

(Received October 27, 1994
Revised January 11, 1995
Accepted January 17, 1995)

British Journal of Pharmacology

VOLUME 114 (8) APRIL 1995

SPECIAL REPORTS

A.A. Rodrigues, F.P. Jansen, R. Leurs, H. Timmerman & G.D. Prell. Interaction of clozapine with the histamine H_3 receptor in rat brain 1523

R.A. Borman & D.E. Burleigh. Functional evidence for a 5-HT_{2B} receptor mediating contraction of longitudinal muscle in human small intestine 1525

PAPERS

S.A. Douglas, G.R. Beck Jr, J.D. Elliott & E.H. Ohlstein. Pharmacological evidence for the presence of three distinct functional endothelin receptor subtypes in the rabbit lateral saphenous vein 1529

V. Ralevic. Modulation by nicotinamide adenine dinucleotide of sympathetic and sensory-motor neurotransmission via P_1-purinoceptors in the rat mesenteric arterial bed 1541

D.A. Cabrini, A.M. Silva & J.B. Calixto. Mechanisms of bradykinin-induced contraction of the guinea-pig gallbladder *in vitro* 1549

C. Bolego, C. Pinna, M.P. Abbracchio, F. Cattabeni & L. Puglisi. The biphasic response of rat vesical smooth muscle to ATP 1557

P. Picard, L. Chrétien & R. Couture. Functional interaction between losartan and central tachykinin NK_3 receptors in the conscious rat 1563

B.W. McFerran & S.B. Guild. The effects of calyculin A upon calcium-, guanine nucleotides- and phorbol 12-myristate 13-acetate-stimulated ACTH secretion from AtT-20 cells 1571

V. Sexl, G. Mancusi, S. Baumgartner-Parzer, W. Schütz & M. Freissmuth. Stimulation of human umbilical vein endothelial cell proliferation by A_2-adenosine and β_2-adrenoceptors 1577

S.-M. Yu & S.-C. Kuo. Vasorelaxant effect of isoliquiritigenin, a novel soluble guanylate cyclase activator, in rat aorta 1587

S. Guimarães, A. Albino-Teixeira & M.Q. Paiva. Hypertension and enhanced β-adrenoceptor-mediated facilitation of noradrenaline release produced by chronic blockade of adenosine receptors 1595

L. Chen, J.R. McNeill, T.W. Wilson & V. Gopalakrishnan. Differential effects of phosphoramidon on contractile responses to angiotensin II in rat blood vessels 1599

H. Bohn, J. Brendel, P.A. Martorana & K. Schönafinger. Cardiovascular actions of the furoxan CAS 1609, a novel nitric oxide donor 1605

K. Seuwen & H.G.W.M. Boddeke. Heparin-insensitive calcium release from intracellular stores triggered by the recombinant human parathyroid hormone receptor 1613

U.N. Westfelt, G. Benthin, S. Lundin, O. Stenqvist & Å. Wennmalm. Conversion of inhaled nitric oxide to nitrate in man 1621

A.J. Cross, J.A. Jones, M. Snares, K.-G. Jostell, U. Bredberg & A.R. Green. The protective action of chlormethiazole against ischaemia-induced neurodegeneration in gerbils when infused at doses having little sedative or anticonvulsant activity 1625

S.G. Sydserff, A.J. Cross, K.J. West & A.R. Green. The effect of chlormethiazole on neuronal damage in a model of transient focal ischaemia 1631

K.M.L. Cross, R.C. Foreman & J.E. Chad. Enhancement by 5-hydroxytryptamine and analogues of desensitization of neuronal and muscle nicotinic receptors expressed in *Xenopus* oocytes 1636

D.L. Downie, A.G. Hope, D. Belelli, J.J. Lambert, J.A. Peters, K.R. Bentley, L.J. Steward, C.-Y. Chen & N.M. Barnes. The interaction of trichloroethanol with murine recombinant 5-HT_3 receptors 1641

A.C. Newby, K. Lim, M.A. Evans, N.P.J. Brindle & R.F.G. Booth. Inhibition of rabbit aortic smooth muscle cell proliferation by selective inhibitors of protein kinase C 1652

H. Zhang & T.B. Bolton. Effect of UK-84149 on voltage-activated calcium currents of single smooth muscle cells from guinea-pig and rabbit jejunum and rabbit coronary artery 1657

C.-C. Wu, S.-J. Chen, C. Szabó, C. Thiemermann & J.R. Vane. Aminoguanidine attenuates the delayed circulatory failure and improves survival in rodent models of endotoxic shock 1666

C.E. Bryant, G.H. Allcock & T.D. Warner. Comparison of effects of chronic and acute administration of N^G-nitro-L-arginine methyl ester to the rat on inhibition of nitric oxide-mediated responses 1673

A.A. Laniyonu & M.D. Hollenberg. Vascular actions of thrombin receptor-derived polypeptides: structure-activity profiles for contractile and relaxant effects in rat aorta 1680

P.D. Marley, K.A. Thomson & R.A. Bralow. Protein kinase A and nicotinic activation of bovine adrenal tyrosine hydroxylase 1687

R.J. Smith, J.M. Justen, J.E. Bleasdale & L.M. Sly. NPC 15669-modulated human polymorphonuclear neutrophil functional responsiveness: effects on receptor-coupled signal transduction 1694

T. Hérembert, D.-L. Zhu & P. Marche. Mechanism of action of the inhibitory effect of nifedipine on the growth of cultured aortic cells from spontaneously hypertensive and normotensive rats 1703

G.T. Somogyi, M. Tanowitz & W.C. de Groat. Prejunctional facilitatory α_1-adrenoceptors in the rat urinary bladder 1710

J.W. Dalley & S.C. Stanford. Contrasting effects of the imidazol(in)e α_2-adrenoceptor agonists, medetomidine, clonidine and UK 14,304 on extraneuronal levels of noradrenaline in the rat frontal cortex: evaluation using *in vivo* microdialysis and synaptosomal uptake studies 1717

W.S. Redfern, M.R. MacLean, R.U. Clague & J.C. McGrath. The role of α_2-adrenoceptors in the vasculature of the rat tail 1724

S. Salomone, N. Morel & T. Godfraind. Effects of 8-bromo cyclic GMP and verapamil on depolarization-evoked Ca^{2+} signal and contraction in rat aorta 1731

J.G. McGivern, L. Patmore & R.D. Sheridan. Actions of the novel neuroprotective agent, lifarizine (RS-87476), on voltage-dependent sodium currents in the neuroblastoma cell line, N1E-115 1738

Q. Yang, R. Padrini, S. Bova, D. Piovan & G. Magnolfi. Electrocardiographic interactions between pinacidil, a potassium channel opener and class I antiarrhythmic agents in guinea-pig isolated perfused heart 1745

STOCKTON

BRITISH JOURNAL OF PHARMACOLOGY

The *British Journal of Pharmacology* welcomes contributions in all fields of experimental pharmacology including neuroscience, biochemical, cellular and molecular pharmacology. The Board of Editors represents a wide range of expertise and ensures that well-presented work is published as promptly as possible, consistent with maintaining the overall quality of the journal.

Edited for the British Pharmacological Society by

A.T. Birmingham
(Chairman)

R.W. Horton **W.A. Large**
(Secretaries)

Editorial Board

P.I. Aaronson *London*
J.A. Angus *Melbourne, Australia*
G.W. Bennett *Nottingham*
T.P. Blackburn *Harlow*
W.C. Bowman *Glasgow*
N.G. Bowery *London*
S.D. Brain *London*
K.D. Butler *Horsham*
M. Caulfield *London*
R. Chess-Williams *Sheffield*
T. Cocks *Melbourne, Australia*
S.J. Coker *Liverpool*
R.A. Coleman *Ware*
Helen M. Cox *London*
A.J. Cross *London*
V. Crunelli *Cardiff*
T.C. Cunnane *Oxford*
F. Cunningham *London*
A. Dickenson *London*
J.R. Docherty *Dublin*
A. Dray *London*
L. Edvinsson *Lund, Sweden*
G. Edwards *Manchester*
J.M. Edwardson *Cambridge*
R.M. Eglen *Palo Alto, USA*
P.C. Emson *Cambridge*
A.C. Foster *San Diego, USA*
J.R. Fozard *Basle, Switzerland*
Allison D. Fryer *Baltimore, USA*
J.P. Gallagher *Galveston, USA*
Sheila M. Gardiner *Nottingham*
C.J. Garland *Bristol*
A. Gibson *London*
M.A. Giembycz *London*
W.R. Giles *Calgary, Canada*
R.G. Goldie *Perth, Australia*
R.J. Griffiths *Connecticut, USA*
R.W. Gristwood *Cambridge*
Judith M. Hall *London*
D.W.P. Hay *Philadelphia, USA*
P.G. Hellewell *London*
P.E. Hicks *Edinburgh*
K. Hillier *Southampton*
S.J. Hill *Nottingham*
S.M.O. Hourani *Guildford*
J.C. Hunter *Palo Alto, USA*
E.J. Johns *Birmingham*
R.S.G. Jones *Oxford*
C.C. Jordan *Ware*
P.A.T. Kelly *Edinburgh*
D.A. Kendall *Nottingham*
C. Kennedy *Glasgow*
P. Leff *Loughborough*
A.T. McKnight *Cambridge*
C.A. Maggi *Florence, Italy*
Janice M. Marshall *Birmingham*
G. Martin *Beckenham*
W. Martin *Glasgow*
A. Mathie *London*
D.N. Middlemiss *Harlow*
P.K. Moore *London*
C.D. Nicholson *Oss, The Netherlands*
H. Osswald *Tübingen, Germany*
F.L. Pearce *London*
J.D. Pearson *London*
A.G. Renwick *Southampton*
P.J. Roberts *Bristol*
G.J. Sanger *Harlow*
W.C. Sessa *Connecticut, USA*
P. Sneddon *Glasgow*
K. Starke *Freiburg, Germany*
R.J. Summers *Melbourne, Australia*
P.V. Taberner *Bristol*
J. Tamargo *Madrid, Spain*
C. Thiemermann *London*
M.D. Tricklebank *Basle, Switzerland*
T.J.N. Verbeuren *Suresnes, France*
R.R. Vollmer *Pittsburgh, USA*
K.J. Watling *Boston, USA*
A.H. Weston *Manchester*
J. Westwick *Bath*
Eileen Winslow *Riom, France*
B. Woodward *Bath*
E.H.F. Wong *California, USA*

Corresponding Editors

P.R. Adams *Stony Brook, U.S.A.*
C. Bell *Melbourne, Australia*
F.E. Bloom *La Jolla, U.S.A.*
A.L.A. Boura *Newcastle, Australia*
N.J. Dun *Toledo, U.S.A.*
R.F. Furchgott *New York, U.S.A.*
T. Godfraind *Brussels, Belgium*
S.Z. Langer *Paris, France*
R.J. Miller *Chicago, U.S.A.*
R.C. Murphy *Denver, U.S.A.*
E. Muscholl *Mainz, Germany*
R.A. North *Geneva, Switzerland*
M. Otsuka *Tokyo, Japan*
M.J. Rand *Melbourne, Australia*
S. Rosell *Södertalje, Sweden*
P. Seeman *Toronto, Canada*
L. Szekeres *Szeged, Hungary*
B. Uvnas *Stockholm, Sweden*
P.A. Van Zwieten *Amsterdam, Netherlands*
V.M. Varagič *Belgrade, Yugoslavia*
G. Velo *Verona, Italy*
Wang Zhen Gang *Beijing, China*
M.B.H. Youdim *Haifa, Israel*

Submission of manuscripts: Manuscripts (two copies) should be sent to The Editorial Office, British Journal of Pharmacology, St. George's Hospital Medical School, Cranmer Terrace, London SW17 0RE.

Authors should consult the Instructions to Authors and the Nomenclature Guidelines for Authors in Vol. **114**, 245–255. These Instructions and Guidelines also appear with the journal Index for Volumes **111–113**, 1994. A checklist of the essential requirements is summarised in each issue of the journal, or as the last page of the issue.

Whilst every effort is made by the publishers and editorial committee to see that no inaccurate or misleading data, opinion or statement appears in this Journal, they and the *British Pharmacological Society* wish to make it clear that the data and opinions appearing in the articles and advertisements herein are the responsibility of the contributor or advertiser concerned. Accordingly, the *British Pharmacological Society*, the publishers and the editorial committee and their respective employees, officers and agents accept no liability whatsoever for the consequences of any such inaccurate or misleading data, opinion or statement.

The *British Journal of Pharmacology* is published by Stockton Press, a division of Macmillan Press Ltd. It is the official publication of the British Pharmacological Society.

Scope The *British Journal of Pharmacology* is published twice a month. It welcomes contribution in all field of experimental pharmacology including neuroscience, biochemical, cellular and molecular pharmacology. The Board of Editors represents a wide range of expertise and ensures that well-presented work is published as promptly as possible, consistent with maintaining the overall quality of the journal

This journal is covered by Current Contents, Excerpta Medica, BIOSIS and Index Medicus.

Editorial Manuscripts (plus two copies) and all editorial correspondence should be sent to: The Editorial Office, British Journal of Pharmacology, St George's Hospital Medical School, Cranmer Terrace, London SW17 0RE, UK. Tel: +44 (0)181 767 6765; Fax: +44 (0)181 767 5645.

Advertisements Enquiries concerning advertisements should be addressed to: Michael Rowley, Hasler House, High Street, Great Dunmow, Essex CM6 1AP, UK. Tel: +44 (0)1371 874613; Fax: +44 (0)1371 872273.

Publisher All business correspondence, supplement enquiries and reprint requests should be addressed to British Journal of Pharmacology, Stockton Press, Houndmills, Basingstoke, Hampshire RG21 2XS, UK. Tel: +44 (0)1256 29242; Fax: +44 (0)1256 810526. Publisher: Marija Vukovojac. Editorial Assistant: Alice Ellingham. Production Controller: Karen Stuart.

Subscriptions – EU/Rest of World Subscription price per annum (3 volumes, 24 issues) £620, rest of world £820 (Airmail), £685 (Surface mail) or equivalent in any other currency. Orders must be accompanied by remittance. Cheques should be made payable to Macmillan Magazines and sent to: The Subscription Department, Macmillan Press Ltd, Houndmills, Basingstoke, Hampshire RG21 2XS, UK. Where appropriate, subscribers may make payments into UK Post Office Giro Account No. 519 2455. Full details must accompany the payment. Subscribers from EU territories should add sales tax at the local rate.

Subscriptions – USA USA subscribers call toll free 1-800-221-2123 or send check/money order/credit card details to: Stockton Press, 49, West 24th Street, New York, NY 10010; Tel: 212 627 5757, Fax: 212 627 9256. USA annual subscription rates: $1230 Airmail; $1030 Surface (Institutional/Corporate); $225 (Individual making personal payment).

British Journal of Pharmacology (ISSN 0007–1188) is published twice a month by Macmillan Press Ltd, c/o Mercury Airfreight International Ltd, 2323 Randolph Avenue, Avenel, NJ 07001, USA. Subscription price for institutions is $1030 per annum (surface). 2nd class postage is paid at Rahway NJ. Postmaster: send address corrections to Macmillan Press Ltd, c/o Mercury Airfreight International Ltd, 2323 Randolph Avenue, Avenel NJ 07001.

Reprints of any article in this journal are available from Stockton Press, Houndmills, Basingstoke, Hampshire RG21 2XS, UK. Tel: +44 (0)1256 29242; Fax: +44 (0)1256 810526.

Copyright © 1995 Stockton Press
ISSN 0007–1188

All rights of reproduction are reserved in respect of all papers, articles, illustrations, etc., published in this journal in all countries of the world.

All material published in this journal is protected by copyright, which covers exclusive rights to reproduce and distribute the material. No material published in this journal may be reproduced or stored on microfilm or in electronic, optical or magnetic form without the written authorisation of the Publisher.

Authorisation to photocopy items for internal or personal use of specific clients, is granted by Stockton Press, for libraries and other users registered with the Copyright Clearance Center (CCC) Transaction Reporting Service, provided that the base fee of $12.00 per copy is paid directly to CCC, 21 Congress St., Salem, MA 01970, USA. 0007-1188/95 $12.00+$0.00.

Apart from any fair dealing for the purposes of research or private study, or criticism or review, as permitted under the Copyright, Designs and Patent Act 1988, this publication may be reproduced, stored or transmitted, in any form or by any means, only with the prior permission in writing of the publishers, or in the case of reprographic reproduction, in accordance with the terms of licences issued by the Copyright Licensing Agency.

KNOW YOUR COPY RIGHTS

RESPECT OURS

The publication you are reading is protected by copyright law. This means that the publisher could take you and your employer to court and claim heavy legal damages if you make unauthorised photocopies from these pages.

Photocopying copyright material without permission is no different from stealing a magazine from a newsagent, only it doesn't seem like theft.

The Copyright Licensing Agency (CLA) is an organisation which issues licences to bring photocopying within the law. It has designed licensing services to cover all kinds of special needs in business, education, and government.

If you take photocopies from books, magazines and periodicals at work your employer should be licensed with CLA.

Make sure you are protected by a photocopying licence.

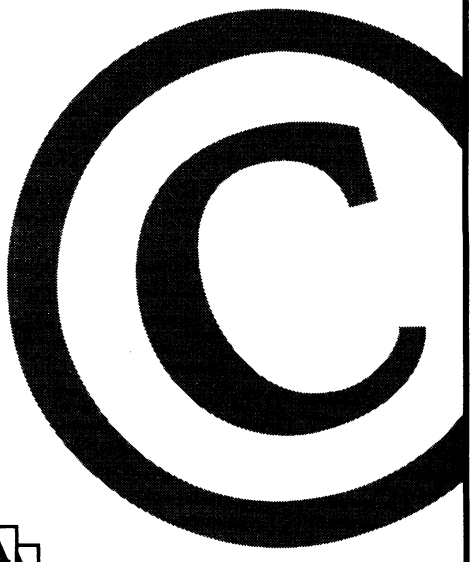

CLA

The Copyright Licensing Agency Limited
90 Tottenham Court Road, London W1P 0LP

Telephone: 0171 436 5931
Fax: 0171 436 3986

PREPARATION OF MANUSCRIPTS

Authors are strongly recommended to read the full *Instructions to Authors* and *Nomenclature Guidelines for Authors* (*Br. J. Pharmacol.* 1995, **114,** 245–255) before submitting a manuscript for publication in the *British Journal of Pharmacology*. The manuscript and cover letter should be checked against the following list before mailing.

The original and one copy of the manuscript must be supplied. Manuscripts must be typed in double-line spacing on one side of A4 paper, in type not smaller than 12 characters per inch or 10 point. Both copies to include Tables and a set of labelled Figures. One set of Figures without numbers or letters is also to be included. The text to be arranged in the following subsections:

1. **Title**—To have no more than 150 characters on a separate page, which should also include a Short Title (50 characters maximum) and the name and address of the author for correspondence.

2. **Summary**—To be arranged in numbered paragraphs (Full Papers) or a single paragraph (Special Reports).
   —to include aims, principal results and conclusions.
   —to include Key words (10 maximum) at end of summary.

3. **Introduction**—To contain concise statements of the problem and the aims of the investigation.

4. **Methods**—To have brief but adequate account of the procedures; *full names of drugs* (*including those referred to by manufacturer's code*), sources of drugs and statistical tests to be stated.

5. **Results**—To have no repetition of data in Figures, Tables and text.

6. **Discussion**—Findings and conclusions to be placed in context of other relevant work.
   NB Simple repetition of results and unwarranted speculation are not acceptable.

7. **Acknowledgements**—Sources of support. Sources of drugs not widely available commercially.

8. **References**—All references in the text to be included in the Reference List and *vice versa*. References in alphabetical order with complete citations; Journals publishing 'in press' papers identified.
   References to manuscripts submitted to other journals but not yet accepted are not allowed.

9. **Tables**—Each on a separate page and prepared in accordance with current requirements of the Journal.

10. **Figures**—Both labelled and non-labelled Figures to be prepared in accordance with current requirements of the Journal (see *Instructions to Authors*, 1995, **114,** 245–251) and provided with Figure Number and Authors' names on back (*in pencil*).
    —each legend to be typed on a separate page and carrying keys to symbols.
    —keys to symbols and histograms must not appear on the figures themselves, but in the respective legends.
    —'box style' figures are not in keeping with the Journal style; line drawings etc must have only left-hand and bottom axes.

11. **Manuscripts**—To be accompanied by a declaration signed by each author that
    (a) results are original
    (b) approval of all persons concerned has been given to submit manuscripts for consideration (see also 12b)
    (c) the same material is neither 'in press' (i.e. is in proof or has definitely been accepted for publication) nor under consideration elsewhere. Furthermore it will not be submitted or published elsewhere before a decision has been reached by the Editorial Board of the *British Journal of Pharmacology* and will not be submitted elsewhere if accepted by the *British Journal of Pharmacology*.
    (d) Copyright assignment is included.

12. **Cover letter**—To state clearly
    (a) Corresponding author's full postal address, telephone, telex or Fax number
    (b) where appropriate, that *either* ethical approval has been given for investigation *or* Company or Institutional permission to publish work has been received.

13. **Reminder**—Packaging to be sufficiently robust to protect Figures and to withstand mailing.

Failure to comply with *Instructions to Authors* may lead to substantial delays in processing, review and publication and may even jeopardize acceptance of the manuscript.

NOMENCLATURE

Authors are reminded that accepted receptor and associated terminology is laid out in *Nomenclature Guidelines for Authors*, as published in the *British Journal of Pharmacology*, *Br. J. Pharmacol.*, 1995, **114,** 253–255.

SPECIAL REPORTS

The purpose of *Special Reports* is to provide rapid publication for **new** and **important** results which the Editorial Board considers are likely to be of special pharmacological significance. *Special Reports* will have publication priority over all other material and so authors are asked to consider carefully the status of their work before submission.

In order to speed publication there is normally no revision allowed beyond very minor typographical or grammatical corrections. If significant revision is required, the Board may either invite rapid re-submission or, more probably, propose that it be re-written as a Full Paper and be re-submitted for consideration. In order to reduce delays, proofs of *Special Reports* will be sent to authors but **essential corrections must reach the Production Office within 48 hours of receipt.** Authors should ensure that their submitted material conforms exactly to the following requirements.

Special Reports should normally occupy no more than two printed pages of the Journal; two illustrations (Figures or Tables, with legends) are permitted. As a guideline, with type face of 12 pitch and double-line spacing, a page of A4 paper could contain about 400 words. The absolute maximum length of the *Special Report* is 1700 words. For each Figure or Table, please deduct 200 words. The manuscript should comprise a Title page with key words (maximum of 10), a Summary consisting of a single short paragraph, followed by Introduction, Methods, Results, Discussion and References (maximum of 10). In all other respects, the requirements are the same as for Full Papers (see current 'Instructions to Authors').

BRITISH JOURNAL OF PHARMACOLOGY VOLUME 114 (8) 1995

SPECIAL REPORTS

A.A. Rodrigues, F.P. Jansen, R. Leurs, H. Timmerman & G.D. Prell. Interaction of clozapine with the histamine H_3 receptor in rat brain 1523

R.A. Borman & D.E. Burleigh. Functional evidence for a 5-HT_{2B} receptor mediating contraction of longitudinal muscle in human small intestine 1525

PAPERS

S.A. Douglas, G.R. Beck Jr, J.D. Elliott & E.H. Ohlstein. Pharmacological evidence for the presence of three distinct functional endothelin receptor subtypes in the rabbit lateral saphenous vein 1529

V. Ralevic. Modulation by nicotinamide adenine dinucleotide of sympathetic and sensory-motor neurotransmission via P_1-purinoceptors in the rat mesenteric arterial bed 1541

D.A. Cabrini, A.M. Silva & J.B. Calixto. Mechanisms of bradykinin-induced contraction of the guinea-pig gallbladder *in vitro* 1549

C. Bolego, C. Pinna, M.P. Abbracchio, F. Cattabeni & L. Puglisi. The biphasic response of rat vesical smooth muscle to ATP 1557

P. Picard, L. Chrétien & R. Couture. Functional interaction between losartan and central tachykinin NK_3 receptors in the conscious rat 1563

B.W. McFerran & S.B. Guild. The effects of calyculin A upon calcium-, guanine nucleotides- and phorbol 12-myristate 13-acetate-stimulated ACTH secretion from AtT-20 cells 1571

V. Sexl, G. Mancusi, S. Baumgartner-Parzer, W. Schütz & M. Freissmuth. Stimulation of human umbilical vein endothelial cell proliferation by A_2-adenosine and β_2-adrenoceptors 1577

S.-M. Yu & S.-C. Kuo. Vasorelaxant effect of isoliquiritigenin, a novel soluble guanylate cyclase activator, in rat aorta 1587

S. Guimarães, A. Albino-Teixeira & M.Q. Paiva. Hypertension and enhanced β-adrenoceptor-mediated facilitation of noradrenaline release produced by chronic blockade of adenosine receptors 1595

L. Chen, J.R. McNeill, T.W. Wilson & V. Gopalakrishnan. Differential effects of phosphoramidon on contractile responses to angiotensin II in rat blood vessels 1599

H. Bohn, J. Brendel, P.A. Martorana & K. Schönafinger. Cardiovascular actions of the furoxan CAS 1609, a novel nitric oxide donor 1605

K. Seuwen & H.G.W.M. Boddeke. Heparin-insensitive calcium release from intracellular stores triggered by the recombinant human parathyroid hormone receptor 1613

U.N. Westfelt, G. Benthin, S. Lundin, O. Stenqvist & Å. Wennmalm. Conversion of inhaled nitric oxide to nitrate in man 1621

A.J. Cross, J.A. Jones, M. Snares, K.-G. Jostell, U. Bredberg & A.R. Green. The protective action of chlormethiazole against ischaemia-induced neurodegeneration in gerbils when infused at doses having little sedative or anticonvulsant activity 1625

S.G. Sydserff, A.J. Cross, K.J. West & A.R. Green. The effect of chlormethiazole on neuronal damage in a model of transient focal ischaemia 1631

K.M.L. Cross, R.C. Foreman & J.E. Chad. Enhancement by 5-hydroxytryptamine and analogues of desensitization of neuronal and muscle nicotinic receptors expressed in *Xenopus* oocytes 1636

D.L. Downie, A.G. Hope, D. Belelli, J.J. Lambert, J.A. Peters, K.R. Bentley, L.J. Steward, C.-Y. Chen & N.M. Barnes. The interaction of trichloroethanol with murine recombinant 5-HT_3 receptors 1641

A.C. Newby, K. Lim, M.A. Evans, N.P.J. Brindle & R.F.G. Booth. Inhibition of rabbit aortic smooth muscle cell proliferation by selective inhibitors of protein kinase C 1652

H. Zhang & T.B. Bolton. Effect of UK-84149 on voltage-activated calcium currents of single smooth muscle cells from guinea-pig and rabbit jejunum and rabbit coronary artery 1657

C.-C. Wu, S.-J. Chen, C. Szabó, C. Thiemermann & J.R. Vane. Aminoguanidine attenuates the delayed circulatory failure and improves survival in rodent models of endotoxic shock 1666

C.E. Bryant, G.H. Allcock & T.D. Warner. Comparison of effects of chronic and acute administration of N^G-nitro-L-arginine methyl ester to the rat on inhibition of nitric oxide-mediated responses 1673

A.A. Laniyonu & M.D. Hollenberg. Vascular actions of thrombin receptor-derived polypeptides: structure-activity profiles for contractile and relaxant effects in rat aorta 1680

P.D. Marley, K.A. Thomson & R.A. Bralow. Protein kinase A and nicotinic activation of bovine adrenal tyrosine hydroxylase 1687

R.J. Smith, J.M. Justen, J.E. Bleasdale & L.M. Sly. NPC 15669-modulated human polymorphonuclear neutrophil functional responsiveness: effects on receptor-coupled signal transduction 1694

T. Hérembert, D.-L. Zhu & P. Marche. Mechanism of action of the inhibitory effect of nifedipine on the growth of cultured aortic cells from spontaneously hypertensive and normotensive rats 1703

G.T. Somogyi, M. Tanowitz & W.C. de Groat. Prejunctional facilitatory α_1-adrenoceptors in the rat urinary bladder 1710

J.W. Dalley & S.C. Stanford. Contrasting effects of the imidazol(in)e α_2-adrenoceptor agonists, medetomidine, clonidine and UK 14,304 on extraneuronal levels of noradrenaline in the rat frontal cortex: evaluation using *in vivo* microdialysis and synaptosomal uptake studies 1717

W.S. Redfern, M.R. MacLean, R.U. Clague & J.C. McGrath. The role of α_2-adrenoceptors in the vasculature of the rat tail 1724

S. Salomone, N. Morel & T. Godfraind. Effects of 8-bromo cyclic GMP and verapamil on depolarization-evoked Ca^{2+} signal and contraction in rat aorta 1731

J.G. McGivern, L. Patmore & R.D. Sheridan. Actions of the novel neuroprotective agent, lifarizine (RS-87476), on voltage-dependent sodium currents in the neuroblastoma cell line, N1E-115 1738

Q. Yang, R. Padrini, S. Bova, D. Piovan & G. Magnolfi. Electrocardiographic interactions between pinacidil, a potassium channel opener and class I antiarrhythmic agents in guinea-pig isolated perfused heart 1745

STOCKTON

Typeset by Elite Typesetting Techniques, Eastleigh, Hants
and printed in Great Britain by Unwin Brothers Ltd., The Gresham Press, Old Woking, Surrey